# GLACIAL HISTORY OF THE NASS RIVER REGION

by

Shirley J. McCuaig

M.Sc., Carleton University, 1994

THESIS SUBMITTED IN PARTIAL FULFILLMENT OF

THE REQUIREMENTS FOR THE DEGREE OF

DOCTOR OF PHILOSOPHY

in the Department

of

Geography

© Shirley McCuaig 2000

SIMON FRASER UNIVERSITY

March 2000

All rights reserved. This work may not be
reproduced in whole or in part, by photocopy
or other means, without permission of the author.

National Library of Canada
Acquisitions and Bibliographic Services
395 Wellington Street
Ottawa ON K1A 0N4
Canada

Bibliothèque nationale du Canada
Acquisitions et services bibliographiques
395, rue Wellington
Ottawa ON K1A 0N4
Canada

*Your file Votre référence*

*Our file Notre référence*

The author has granted a non-exclusive licence allowing the National Library of Canada to reproduce, loan, distribute or sell copies of this thesis in microform, paper or electronic formats.

The author retains ownership of the copyright in this thesis. Neither the thesis nor substantial extracts from it may be printed or otherwise reproduced without the author's permission.

L'auteur a accordé une licence non exclusive permettant à la Bibliothèque nationale du Canada de reproduire, prêter, distribuer ou vendre des copies de cette thèse sous la forme de microfiche/film, de reproduction sur papier ou sur format électronique.

L'auteur conserve la propriété du droit d'auteur qui protège cette thèse. Ni la thèse ni des extraits substantiels de celle-ci ne doivent être imprimés ou autrement reproduits sans son autorisation.

0-612-51898-1

Canada

## Abstract

Surficial geology mapping, section description, shallow seismic reflection, ground penetrating radar and drilling are used to determine the stratigraphy of the Nass Valley and the glacial history of the Nass River region. The glacial sediment package, most completely represented in the Nass Valley, comprises till, glaciomarine and glaciofluvial deposits. From the analysis of these deposits and their stratigraphic relationships, a complex sequence of glacial events is determined.

The most complete Quaternary stratigraphic sequence is found in the Nass Valley; less complete sequences occur elsewhere in the study area. Till is the most pervasive deposit, as it is found throughout the region, at all elevations. From oldest to youngest, the region's stratigraphy comprises bedrock, till, fluvial or lacustrine interstadial sediments, till, glaciomarine proximal deposits, glaciomarine distal deposits, glaciofluvial braidplain/braid delta deposits and Holocene deposits.

There is little evidence of glacial and nonglacial deposition prior to the last glaciation. A Middle Wisconsinan age was obtained from a section in a small valley near the Nass Valley. Palynology of this site shows that spruce forests with no modern analogues were the dominant vegetation at that time. Till and glaciofluvial deposits formed before the last glaciation were unequivocally identified at only one site; other such deposits may have been removed by highly erosive glaciers as glaciation progressed.

At the height of the last glaciation, ice flowed southwest over the entire region. It deposited a compact till called 'Kwinatahl till', which is derived from Bowser Lake Group metasedimentary bedrock that underlies the eastern part of the study area. Kwinatahl till deposits are locally more than 50 m thick.

As ice thinned during deglaciation, it became confined to valleys and fiords. 'Kinskuch till', a till containing rounded clasts and volcanic material, formed in the northeastern part of the study area at this time. Kinskuch till overlies Kwinatahl till and occurs in an area of drumlinized terrain. The drumlins are interpreted to have formed by deformation of Kinskuch till.

High sea levels at the onset of deglaciation likely caused calving and rapid retreat of glaciers in fiord areas. The maximum marine limit is 230 m above present sea level, and is thought to have been achieved around 10 500 radiocarbon years BP. Rapid deglaciation and rapid sea level fall occurred after this maximum was reached.

In the fiords, interbedded gravel, sand and silt were deposited subaqueously in ice-proximal glaciomarine environments during the early part of deglaciation. These deposits grade distally to massive silty clay. Apparently, the glaciers experienced no stillstands; proximal to distal depositional environments migrated, following rapidly retreating ice margins. Distal silty clay deposits in the Nass Valley are up to 25 m thick.

Eventually, ice became grounded as valley glaciers retreated and sea level dropped. Extensive meltwater braidplains formed in front of the glaciers, terminating in marine water and forming large braid deltas at their termini. Deltas without associated braidplains formed in more mountainous areas, where valleys are smaller and steeper. The deltas and braidplains record sea levels of 230, 185, 150 and 135 m above present sea level, of which the 150 m highstand was the longest lived.

In the upper Nass Valley, one such braidplain (the Nass Braidplain North) formed during the 185 m highstand. It was succeeded by the Aiyansh Braidplain, an extensive braidplain that formed northeast of the town of New Aiyansh when sea level had dropped to 150 m. The meltwater river occupied the western side of a bedrock ridge when the Nass Braidplain North formed, but it switched to the eastern side of the ridge to form the Aiyansh Braidplain. The river then moved back to its original location (on the western side) when sea level was at 135 m, forming a small braidplain southwest of the Nass Braidplain North. Sea level then fell to its present level. The meltwater river evolved into the modern Nass River and assumed its current course, which incises the 185 m and 135 m braidplains.

## Acknowledgments

Special thanks are due to Mike Roberts, my advisor and mentor, for all his input, guidance, suggestions and thesis revisions. I would like to thank him also for the time he spent in the field with me, running geophysics, driving the drill rig and being our driller.

I would like to thank my committee members John Clague, Ted Hickin and James MacEachern for help, advice and thesis revisions.

Lionel Jackson was my Geological Survey of Canada liaison. He was instrumental in securing GSC funding and provided much helpful advice and support.

Adrian Hickin, Edna Kaiser, Kevin Netherton and Mark Newman-Bennett provided able assistance in the field. Mike and Ev Roberts helped greatly with GPR and seismic field work in May 1997 and with drilling in May 1998. Carol Evenchick accommodated us at her Anyox camp in the summer of 1996 and provided helpful discussions on the area's bedrock geology. She also supplied several geology maps of the area, reviewed the bedrock geology section of the thesis and helped run seismic lines for a few days in 1997. John Clague visited Kevin and I in the field in 1996 and offered useful suggestions.

Kaz Shimamura showed me how to use ARC/INFO and helped immensely with map production; he also loaned me his own work station for use at the GSC in the evenings.

Marlow Pellatt (Dept. of Biological Sciences, SFU) analyzed five clay samples for pollen, dinoflagellates and acritarchs. Ian Hutchinson provided help with some diatom identifications. Tim Patterson of Carleton University did foraminiferal analyses of several clay samples.

Shannon Wood (Archeology Dept.) helped with x-radiography and x-ray developing. Ken Myrtle (Physics Dept.) ran the SEM and XRF; Albert Curzon (Physics Dept.) also helped with SEM.

Lisa Sankeralli reviewed the final draft of the manuscript. Dan Herold of Parallel Geoscience provided a good deal of technical support for Seismic Processing Workshop. Andrew Calvert helped with seismic processing. Graeme Comyn co-designed and created blueprints for the weight drop device. The Nisga'a Tribal Council kindly granted permission to drill in proposed Nisga'a lands. Julie Nguyen drafted most of Figure 8.2.

Financial support was provided by a Natural Sciences and Engineering Research Council (NSERC) Operating Grant awarded to Dr. Roberts. Field support for the mapping component (including 4 X 4 truck rental, trailer rental, helicopter time) was provided in 1996 by the Terrain Sciences Division of the Geological Survey of Canada. The Division loaned some field equipment for the 1997 and 1998 seasons and funded till and foraminiferal analyses, as well as several radiocarbon dates. Terrain Sciences also funded part of the 1998 field season.

Field support and equipment, including seismograph, GPR device and a van and trailer were provided by Dr. Roberts for the 1997 and 1998 field seasons. All other support, including radiocarbon dates and conference travel, was provided by Dr. Roberts' operating grant.

Funding was provided to the author in the form of an NSERC Postgraduate Scholarship, a Simon Fraser University Special Graduate Entrance Scholarship, a William and Ada Isabelle Steel Memorial Graduate Scholarship (SFU), two Graduate Fellowships (SFU), a President's Ph.D. Stipend (SFU) and several teaching assistantships (SFU).

## Table Of Contents


Title Page i
Approval ii
Abstract iii
Acknowledgments v
Table Of Contents vii
List of Tables xii
List of Figures xiii

CHAPTER ONE: INTRODUCTION 1
Introduction 1
Physical Setting 5
Physiography 5
Climate 8
Bedrock Geology 8
Objectives 11

CHAPTER TWO: PREVIOUS WORK 13
Regional Glacial History Studies 13
Introduction 13
Queen Charlotte Island/Dixon Entrance Region 13
Southeast Alaska Region 17
Terrace-Kitimat Region 18
Smithers-Bulkley Valley Region 19
Babine Lake Region 19
Stikine River Region 21
Regional Sea Level Studies 21
Local Glacial Studies 23

CHAPTER THREE: RESEARCH METHODS 25
Surficial Geology and Geomorphology Mapping 25
Mapping 25
Glacial Deposits 25
Ice Flow Directions 26
Subsurface Geology Techniques 29
Sections 29
Drilling 29
Subsurface Geophysical Methods 32
Downhole Geophysical Logs 32
Shallow Reflection Seismic Surveys 32
Limitations 34
Set-up Used in This Study 35
Seismic Source 37
Tests Conducted Prior to Data Acquisition 37
Noise Reduction in the Field 38
Data Processing (Noise Reduction in the Lab) 38
Line 1001 39
Ground Penetrating Radar (GPR) 41
Set-up Used in This Study 42
Microscopic and Other Investigations 44
Diatom Analysis 44
Foraminiferal Analysis 44
Palynological Analysis 45
Radiocarbon Dating 45
X-Radiography 45
Scanning Electron Microprobe (SEM) Analysis 45

CHAPTER FOUR: QUATERNARY DEPOSITS 46
Introduction 46
Glacial Phase Deposits 46
Kwinatahl till 46
Kinskuch till 49
Retreat-Phase Deposits and Erosional Features 53
Glaciofluvial Erosion 54
Glaciofluvial Deposits 54
Glaciofluvial Braidplains 56
Glaciofluvial Deltas 57
Glaciolacustrine Deposits 60
Glaciomarine Deposits 60
Ice Proximal Deposits 61
Ice Distal Deposits 61
Postglacial Deposits 65
Colluvial Deposits 65
Alluvial Deposits 66
Alluvial Fan Deposits 68
Neoglacial Deposits 72
Other Deposits 72

CHAPTER FIVE: LITHOSTRATIGRAPHY 74
Sections 74
Sections 96705-10 (West Hastings Arm), 96810-10 (Hoan Creek), 96805-10 (Shumal Creek) 74
Description 74
Interpretation 80
Section 97723-01 (Kinskuch Valley) 82
Description 82
Interpretation 82
Section 97621-01 (Kiteen River) 84
Description 84
Interpretation 87
Section 97613-03 (Tchitin River) 89
Description 89
Interpretation 89
Section 97530-01 (Irene Meadows Road) 92
Description 92
Interpretation 92
Section 97602-05 (Aiyansh Gravel Pit) 96
Description 96
Interpretation 100
Section 97609-01 (Tseax Creek) 101
Description 101
Interpretation 101
Section 97601-01 (near Aiyansh lava flow) 104
Description 106
Interpretation 106
Drill Hole and Geophysical Log Descriptions 106
Drill Hole 98-1-1007 108
Location 108
Description 108
Interpretation 110
Drill Hole 98-2-1005 110
Location 110
Description 110
Geophysical Log Description 112

Interpretation 114
Drill Hole 98-3-1013 114
Location 114
Description 116
Interpretation 116
Drill Hole 98-4-1014 116
Location 116
Description 116
Interpretation 117
Drill Hole 98-5-1008 117
Location 117
Description 117
Geophysical Log Description 119
Interpretation 119
Drill Hole 98-6-1001 119
Location 119
Description 120
Geophysical Log Description 124
Interpretation 124
Summary 125
Stratigraphy 125
History 126

CHAPTER SIX: SEISMIC STRATIGRAPHY 127
Introduction 127
Line 1001 128
Seismic Facies Analysis 128
Seismic Facies 1 128
Seismic Facies 2 128
Seismic Facies 3 132
Seismic Facies 4 132
Seismic Facies Interpretation 132
Seismic Facies 1: Bedrock 132
Seismic Facies 2: Glacial Sediments? 133
Seismic Facies 3: Till 133
Seismic Facies 4: Glaciomarine Deposits 133
Summary 134

CHAPTER SEVEN: RADAR STRATIGRAPHY 135
Introduction 135
Radar Facies 139
Radar Line Descriptions and Interpretations 140
Aiyansh Gravel Pit: Lines NV101 and NV102 140
Radar Facies Description 140
Radar Facies 3a 140
Radar Facies Interpretation 142
Radar Facies 3a: Braid Delta Foreset Beds 142
Aiyansh Gravel Pit: Lines NV108 and NV109 142
Radar Facies Description 144
Radar Facies 3d 144
Radar Facies 3b 144
Radar Facies Interpretation 144
Radar Facies 3d: Braidplain Channel Deposits 145
Radar Facies 3b: Braid Delta Topset Beds 145
Nass Camp Delta: Lines NV113 to NV118 145
Radar Facies Description 146
Radar Facies 3a 152
Radar Facies 3b 152

Radar Facies 3d 152
Radar Facies Interpretation 152
Radar Facies 3a and 3b: Braid Delta Foreset and Topset Beds 152
Radar Facies 3d: Braidplain Channel Deposits 153
Paleoflow 153
Irene Meadows: Lines NV124 and NV130 153
Radar Facies Description 157
Radar Facies 3a 157
Radar Facies 3c 157
Radar Facies 3e 157
Radar Facies Interpretation 158
Radar Facies 3a: Braid Delta Foreset Beds 158
Radar Facies 3c: Braidplain Horizontally Bedded Deposits 158
Radar Facies 3e: Slump Deposits 158
New Aiyansh Delta: Lines NV125, 126, 128, 129 159
Radar Facies Description 166
Radar Facies 1 166
Radar Facies 2 166
Radar Facies 3a 166
Radar Facies 3b 167
Radar Facies 3d 167
Radar Facies Interpretation 167
Radar Facies 1: Bedrock 167
Radar Facies 2: Glaciomarine Silty Clay 167
Radar Facies 3a: Braid Delta Foreset Beds 167
Radar Facies 3b: Braid Delta Topset Beds 168
Radar Facies 3d: Braidplain Channel Deposits 168
Dragon Lake: Line NV131 169
Radar Facies Description 169
Radar Facies 4a 169
Radar Facies 4b 169
Radar Facies Interpretation 171
Radar Facies 4a and 4b: Alluvial Fan Horizontally Bedded and Channel Deposits 171
Kiteen River: Lines NV132 and NV133 171
Radar Facies Description 173
Radar Facies 3c 173
Radar Facies 3d 173
Radar Facies Interpretation 176
Radar Facies 3c: Braidplain Horizontally Bedded Deposits 176
Radar Facies 3d: Braidplain Channel Deposits 176
Nass Braidplain South: Lines NV135 and NV136 176
Radar Facies Description 177
Radar Facies 1 177
Radar Facies 3c 177
Radar Facies 3d 177
Radar Facies Interpretation 181
Radar Facies 1: Bedrock 181
Radar Facies 3c and 3d: Braidplain Horizontally Bedded and Channel Deposits 181
Nass Braidplain North: Lines NV139 and NV140 182
Radar Facies Description 182
Radar Facies 2 182
Radar Facies 3a 182
Radar Facies 3e 182
Radar Facies Interpretation 185
Radar Facies 2: Glaciomarine Silty Clay 185
Radar Facies 3a: Braid Delta Foreset Beds 185

Radar Facies 3e: Slump Deposits 185
Radar Facies Summary 186
Glacial History Summary 187

CHAPTER EIGHT: ICE FLOW AND SEA LEVEL HISTORY 192
Ice Flow History 192
Early Ice Flow 192
Late Ice Flow 195
Streamlined Bedrock Features 195
Very Early Ice Flow 197
Summary 197
Till Fabric Analysis 202
White River area 202
Kinskuch/Nass Valley area 206
Drumlins 211
Air Photo Interpretation 211
Till Fabric Analysis 213
Drumlin Genesis Theories 223
Sea Level History 228

CHAPTER NINE: SUMMARY AND CONCLUSIONS 232
Quaternary Stratigraphy 232
Glacial History 235
Comparison of Regional Glacial History to Other
Parts of British Columbia 237
Pleistocene Deposits 237
Sea Levels 238
Recommendations for Future Work 239

REFERENCES 241

APPENDIX A: GEOCHEMISTRY 249
APPENDIX B: WEIGHT DROP 251
APPENDIX C: CMP DATA 254
APPENDIX D: APPLICATIONS 255
Engineering Properties of Glacial Sediments 255
Groundwater 255
Aggregate Resources 256
Potential Hazards 257
APPENDIX E: RADIOCARBON DATING AND MICROPALEONTOLOGICAL ANALYSES 261
Radiocarbon dating 261
Micropaleontological analyses 265
Diatom analysis 265
Foraminiferal analysis 269
Palynological analysis 271
X-Radiography 272
SEM and XRF analysis 273

## List of Tables


| | | |
|---|---|---|
| Table 2.1. | Timing of glacial events in the region. | 16 |
| Table 8.1. | Till fabric data. | 203 |
| Table E.1. | Radiocarbon dates. | 261 |
| Table E.2. | Locations and results of diatom analyses. | 267 |
| Table E.3. | Diatom ecology. | 267 |
| Table E.4. | Locations and results of foraminiferal analyses. | 269 |
| Table E.5. | Locations and results of pollen and palynomorph analysis. | 271 |
| Table E.6. | Percentages of pollen types at Kinskuch Valley section. | 272 |
| Table E.7. | Atomic percentage and mineral formulae of elements identified by XRF. | 273 |

## List of Figures


| | | |
|---|---|---|
| Figure 1.1. | Location map of the study area. | 2 |
| Figure 1.2. | Extent of the thesis area. | 4 |
| Figure 1.3. | Physiographic features of the Nass River region. | 6 |
| Figure 1.4. | Hanging valleys, cirques and arêtes. | 7 |
| Figure 1.5. | Generalized bedrock geology of the study area. | 9 |
| Figure 2.1. | Location map of other Quaternary investigation sites. | 14 |
| Figure 2.2. | Ice flow directions in northern B.C. | 15 |
| Figure 3.1. | Ice flow indicator measurements. | 27 |
| Figure 3.2. | a) Facet relationships. b) Fabric measurement. | 28 |
| Figure 3.3. | a) Mud rotary drilling. b) Solid stem augering. | 31 |
| Figure 3.4. | a) The Mt. Sopris geophysical logger. b) SP and R being recorded. | 33 |
| Figure 3.5. | a) Smartseis S12 seismograph. b) Buffalo gun seismic source. c) Weight drop seismic source. d) Stihl gas auger. | 36 |
| Figure 3.6. | Processing flow for seismic line 1001. | 40 |
| Figure 3.7. | Ground penetrating radar in the field. | 43 |
| Figure 4.1. | Kwinatahl Till. | 47 |
| Figure 4.2. | Kinskuch Till. | 50 |
| Figure 4.3. | Ternary plots of the matrix of Kwinatahl, Kinskuch and Neoglacial tills. | 52 |
| Figure 4.4. | a,b) Fluvially sculpted bedrock. c,d) Glaciofluvial gravel. | 55 |
| Figure 4.5. | Deltaic deposits. | 59 |
| Figure 4.6. | Glaciomarine sediments. | 62 |
| Figure 4.7. | Colluvial deposits. | 67 |
| Figure 4.8. | a) Alluvial fan deposits. b) Recent debris flow deposit. | 70 |
| Figure 4.9. | a) Fan deltas near Anyox, Hastings Arm. b) Marmot Glacier. | 71 |
| Figure 5.1. | Location of major sections. | 75 |
| Figure 5.2. | Legend for lithologic logs of sections and drill holes. | 76 |
| Figure 5.3. | Section 96805-10, Shumal Creek. | 77 |
| Figure 5.4. | Section 96705-10, West Hastings Arm. | 78 |
| Figure 5.5. | Section 96810-10, Hoan Creek. | 79 |
| Figure 5.6. | West Hastings Arm Section views. | 81 |
| Figure 5.7. | Section 97723-01, Kinskuch Valley. | 83 |
| Figure 5.8. | Kiteen River Section. a) Section log location. b) Bullet-shaped boulder. c) Normal fault and crossbeds. d) Coarsening-upward unit. | 85 |
| Figure 5.9. | Section 97621-01, Kiteen River. | 86 |
| Figure 5.10. | Horizontally bedded gravel, sand and silt overlying glaciomarine silty clay. | 90 |
| Figure 5.11. | Section 97613-03, Tchitin River. | 91 |
| Figure 5.12. | Section 97530-01, Irene Meadows Road. | 93 |
| Figure 5.13. | Irene Meadows Road Section. a) Normal fault. b) Horizontal bedding, current ripples and flaser/wavy bedding. | 94 |
| Figure 5.14. | Irene Meadows Road Section. a) Flaser bedding, ball and pillow structure and convolute lamination. b) Flame structure. c) Rip-up clast. | 95 |
| Figure 5.15. | Section 97602-05, Aiyansh Gravel Pit. | 97 |
| Figure 5.16. | Aiyansh Gravel Pit, panoramic view. | 98 |
| Figure 5.17. | Aiyansh Gravel Pit. a) Isolated boulder. b) Thinning and fining-upward beds. | 99 |
| Figure 5.18. | Section 97609-01, Tseax Creek. | 102 |
| Figure 5.19. | Upper part of Tseax Creek Section. | 103 |
| Figure 5.20. | Section 97601-01, near Aiyansh lava flow. | 105 |
| Figure 5.21. | Location of drill holes. | 107 |
| Figure 5.22. | Drill hole 98-1-1007. | 109 |
| Figure 5.23. | Drill hole 98-2-1005. | 111 |
| Figure 5.24. | Split spoon core samples. | 113 |
| Figure 5.25. | Drill holes 98-3-1013 and 98-4-1014 A-D. | 115 |
| Figure 5.26. | Drill hole 98-5-1008. | 118 |
| Figure 5.27. | Upper half of Drill hole 98-6-1001. | 121 |
| Figure 5.28. | Lower half of Drill hole 98-6-1001. | 122 |

Figure 5.29. Complete lithologic and geophysical logs for Drill hole 98-6-1001. 123
Figure 6.1. Seismic line 1001, uninterpreted profile. 129
Figure 6.2. Seismic line 1001, interpreted profile. 130
Figure 6.3. Relationship of drill hole 98-6-1001 to seismic line 1001. 131
Figure 7.1. Location of radar lines with respect to the Nass and Aiyansh braidplains. 136
Figure 7.2. Reflector terminology for radar facies interpretations. 137
Figure 7.3. Characteristics and visual examples of radar facies. 138
Figure 7.4. Radar lines NV101 and NV102, Aiyansh Gravel Pit. 141
Figure 7.5. Radar lines NV108 and NV109, Aiyansh Gravel Pit. 143
Figure 7.6. Nass Camp Delta: radar lines and section location. 147
Figure 7.7. Exposure 97708-01. 147
Figure 7.8. Line NV113, Nass Camp Delta, uninterpreted profile. 148
Figure 7.9. Line NV113, Nass Camp Delta, interpreted profile. 149
Figure 7.10. Radar lines NV114, NV115 and NV116, Nass Camp Delta. 150
Figure 7.11. Radar lines NV117 and NV118, Nass Camp Delta. 151
Figure 7.12. Fence diagram of radar lines NV113 to NV118. 154
Figure 7.13. Radar lines NV130 and NV 124, Irene Meadows Road, uninterpreted profiles. 155
Figure 7.14. Radar lines NV130 and NV 124, Irene Meadows Road, interpreted profiles. 156
Figure 7.15. Slump activity on the prodelta slope of a braid delta. 160
Figure 7.16. Location of radar lines and sections in New Aiyansh. 161
Figure 7.17. Sections 97602-04 and 96701-01. 161
Figure 7.18. Radar lines NV125 and NV126, New Aiyansh Delta, uninterpreted profiles. 162
Figure 7.19. Radar lines NV125 and NV126, New Aiyansh Delta, interpreted profiles. 163
Figure 7.20. Radar lines NV128 and NV129, New Aiyansh Delta, uninterpreted profiles. 164
Figure 7.21. Radar lines NV128 and NV129, New Aiyansh Delta, interpreted profiles. 165
Figure 7.22. Radar line NV131, near Dragon Lake. 170
Figure 7.23. Location of radar lines and section near Kiteen River. 172
Figure 7.24. Section 97519-04. 172
Figure 7.25. Radar line NV132, near Kiteen River. 174
Figure 7.26. Radar line NV133, near Kiteen River. 175
Figure 7.27. Orientation of radar lines NV135 and NV136. 178
Figure 7.28. Radar line NV135, Nass Braidplain South. 179
Figure 7.29. Radar line NV136, Nass Braidplain South. 180
Figure 7.30. Sloping surface in logged area that resembles a delta front. 183
Figure 7.31. Orientation of lines NV139 and NV140 on the Nass Braidplain North. 183
Figure 7.32. Radar lines NV139 and NV140, Nass Braidplain North. 184
Figure 7.33. Location of deltas as re-interpreted from GPR data. 188
Figure 7.34. Location of 152 m contour with respect to glaciofluvial deposits. 189
Figure 8.1. Ice flow directions superimposed on bedrock geology. 193
Figure 8.2. High elevation early ice flow indicators. 194
Figure 8.3. Streamlined bedrock ridges. 196
Figure 8.4. Stoss and lee relationships showing ice flow up the wall of a cirque. 198
Figure 8.5. Revised ice flow directions for the glacial maximum in northwestern B.C. 201
Figure 8.6. Confidence levels for S1/S3 values of till fabrics. 204
Figure 8.7. Location of drumlins in White River area. 205
Figure 8.8. White River area till fabrics, non drumlin areas. 207
Figure 8.9. Till fabrics from various localities. 208
Figure 8.10. Locations of various till fabric sites. 209
Figure 8.11. Locations of drumlins and bedrock ridges in Kinskuch Valley. 212
Figure 8.12. Possible relationships of Kinskuch till to Kwinatahl till. 214
Figure 8.13. Drumlin A. 216
Figure 8.14. Drumlin B. 217
Figure 8.15. Drumlin C. 218
Figure 8.16. Drumlin D. 220
Figure 8.17. Drumlin E. 221
Figure 8.18. Drumlin F. 221
Figure 8.19. Drumlin G. 222

Figure 8.20. Drumlin H. 222
Figure 8.21. Hairpin erosional marks. 226
Figure 8.22. a) Raised delta. b) Raised braidplain. 229
Figure 8.23. Apparent changes in sea level over time. 231

Figure A.1. Till geochemistry. 250
Figure B.1. Machining instructions for the weight drop device. 252
Figure B.2. Machining instructions for the weight drop weights. 253
Figure C.1. Examples of CMP data. 254
Figure D.1. Debris slide from till slope adjacent to logging road. 258
Figure D.2. Earthflow in glaciomarine sediments. 260
Figure E.1. Locations of samples taken for radiocarbon dating. 262
Figure E.2. Tree trunk within a lava flow tree mould. 264
Figure E.3. Location of clay samples for micropaleontological analyses. 266
Figure E.4. Scanning electron microprobe analyses. 274

# CHAPTER ONE

# INTRODUCTION

## Introduction

Glaciation in British Columbia has been extensive and its effects on the landscape profound. Most of the province's mountainous landscape shows evidence of glacial scouring and deposition. Much is known about the movements and deposits of the last known ice body, the Cordilleran Ice Sheet, but most of this information documents glacial history in southern B.C., the most populous and most accessible region of the province (*e.g.* Ryder et al., 1991). Vast tracts of northern B.C. have not been investigated and their glacial history is unknown, in part due to the inaccessibility of the region. Research in these northern areas is still needed, and the Nass River region of northwestern B.C. is an example of such an area. Prior to this work, very little was known about its glacial history. The Nass River region is located just east of the lower portion of the Alaskan panhandle (Figure 1.1).

Mineral deposits of silver, gold, lead, zinc, molybdenum and copper have attracted considerable attention in the region over the years (Sharp, 1980; Dawson and Alldrick, 1986) and gold is currently being mined at Red Mountain (Figure 1.1). Despite the area's mineral wealth, there have been only very limited bedrock or Quaternary studies, and no regional scale mapping.

The objectives of this dissertation are to determine the Quaternary geology, geomorphology and stratigraphy of the Nass River region, and to produce an overview of the glacial history of the area. This work helps fill part of the gap in our knowledge about glaciation in northern B.C.

The Geological Survey of Canada initiated the "Nass River Project" to address the paucity of geological data in the area through a specially funded program of regional bedrock and surficial geology mapping. The surficial geology mapping aspect of the project was undertaken as a component of this dissertation. Two 1:100 000 sheets were mapped: NTS sheets 103P/NW and 103P/SW. 103P/SW has been extended eastward somewhat, in order to include important

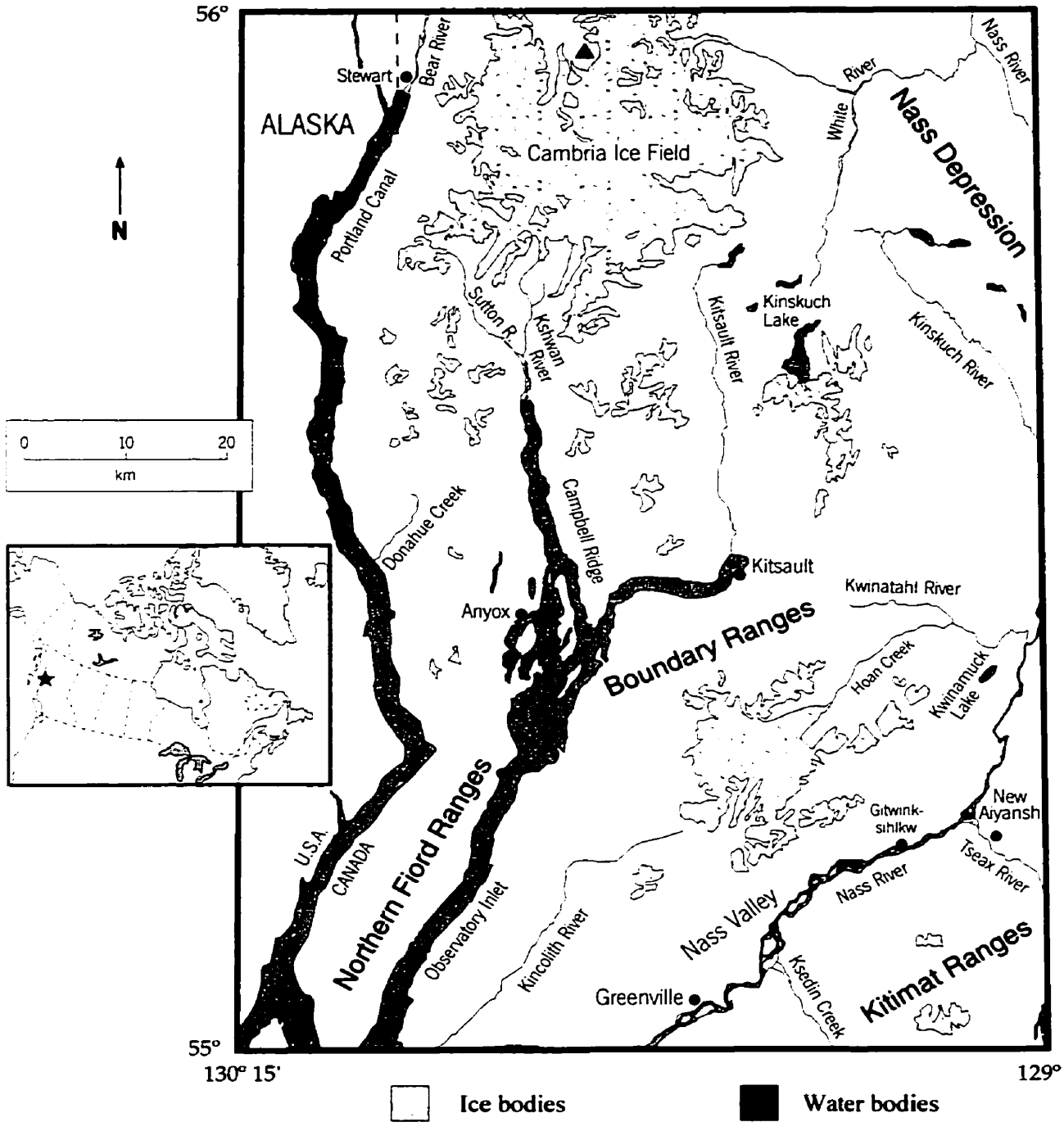


Figure 1.1. General location map of the study area. The small triangle is Red Mountain.

glacial features of the Nass Valley (Figure 1.2). These two map areas cover the western half of the 1:250 000 sheet 103P (as well as a small portion of the eastern half).

Reconnaissance level mapping was done in the first field season (1996). Most of the study area was covered at that time and a number of stratigraphic questions were identified. Sediments in the Nass Valley, a major feature of the study area, were found to be poorly exposed. Man-made and natural exposures were extremely rare. Massive, weathered clay is common, as are coarse gravel deposits. Sandy sediments are scarcer. Two large gravel plains flanking a low, valley-parallel bedrock rise, were mapped. Farther up-valley and in adjacent Kinskuch Valley, drumlins were found.

The relationship of these deposits to each other and the underlying bedrock, as well as the sequence of glacial events in the valley were unclear. The regional surficial geology mapping thus revealed that a more focussed approach would be required in order to understand the glacial history of the Nass Valley, which appears to have been a major depocentre. To this end, shallow seismic reflection, ground penetrating radar, section description, borehole drilling and geophysical downhole logging were employed in subsequent field seasons to investigate the sedimentary structures and the stratigraphic sequence in this area. The goal of these detailed studies was to extend the surficial geology into the third dimension, to better define the glacial sedimentary sequences.

In summary, this dissertation aims to provide an outline of regional glacial history for the entire region and to elucidate in more detail the sequence stratigraphy of the Nass Valley. Applied information arising out of the research includes the two surficial geology maps, the location and extent of aggregate resources and potential groundwater aquifers, and the location of areas of potential slope instability. The research thus has potential applications for civil engineering, water resources, aggregate resources, and the forestry and fisheries industries.

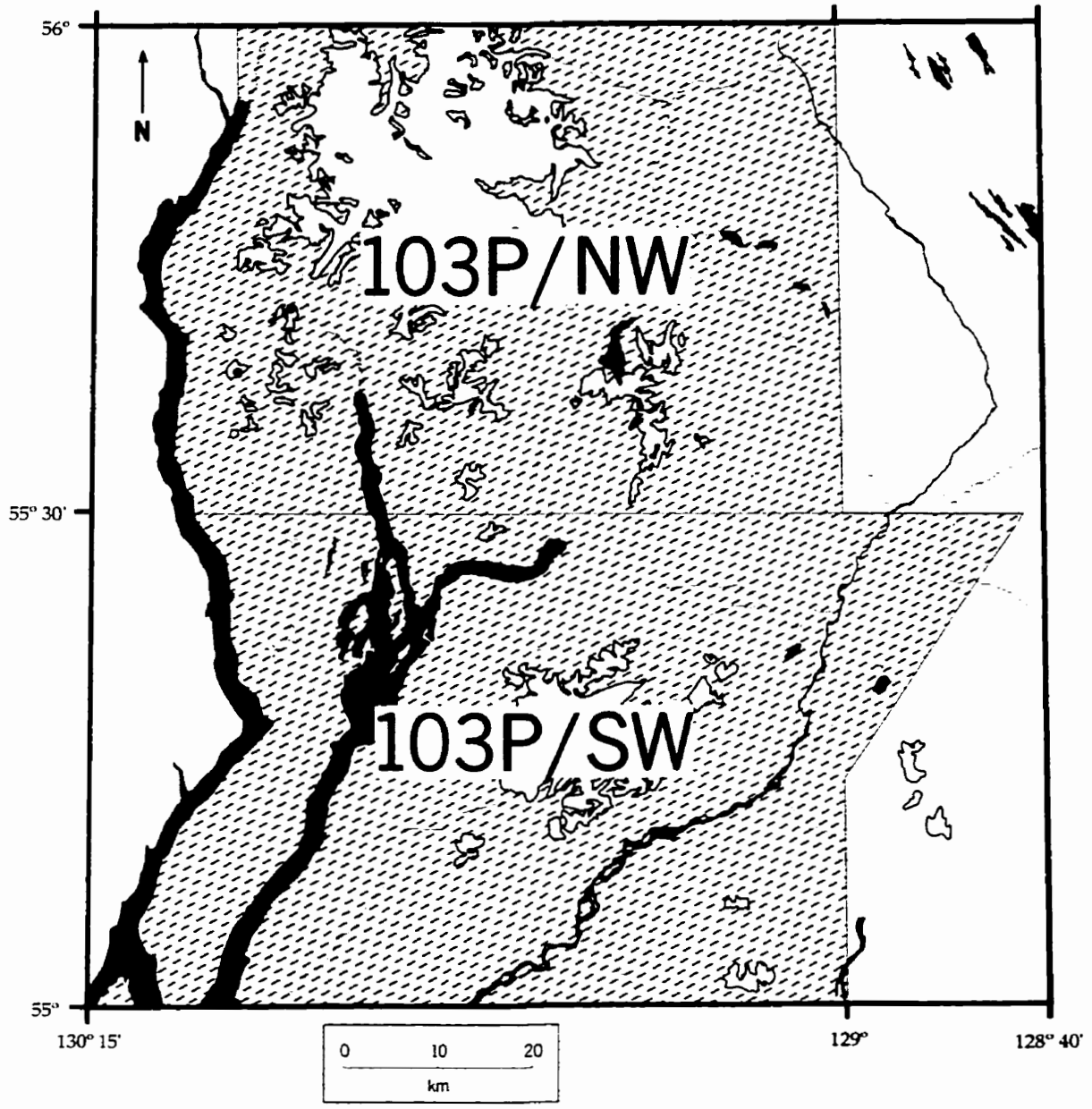


Figure 1.2. The extent of the thesis area (hatched) and the NTS sheet numbers of the surficial geology maps. Ice bodies are white with heavy border; water bodies are grey.

## Physical Setting

*Physiography*

The study area encompasses parts of the Coast and Skeena Mountain physiographic regions of the Canadian Cordillera (Mathews, 1986) and includes the Nass Depression and the Boundary, Northern Fiord and Kitimat Ranges. The Nass Depression is a wide, bedrock influenced lowland that trends southeastward in the northeastern part of the study area; it is part of the Skeena Mountain physiographic unit (Figure 1.1). The Coast Mountains are divided into the Boundary Ranges in the north and central parts of the study area, the Northern Fiord Ranges in the west and the Kitimat Ranges in the south (Figure 1.1). The southern Nass River Valley is considered to be part of the Nass Depression, but is referred to here as the Nass Valley to avoid confusion.

Mountain peaks range from 1100 to 2265 m asl and alpine ice caps such as the Cambria Ice Field are present at high elevations (Figure 1.1). Modern cirque and valley glaciers (Figure 1.3a) are also present, but none reach fiord waters today. Ice cover is common, but it is not as extensive as it is in other areas to the northwest (Henoch, 1967). In 1972, the glaciation level (critical elevation above which glaciers form) in coastal B.C. was about 900 m; this elevation increases linearly to the east (Østrem, 1972).

The montane landscape has been both carved and smoothed by glaciation. Jagged and rounded mountain peaks and ridges (Figure 1.3b, c) separate numerous U-shaped valleys. Horns, arêtes and cirques are prevalent at higher elevations, while rounded ridges are common at lower ones. Hanging valleys are characteristic features along the walls of the larger valleys and fiords (Figure 1.4).

Steep-sided coastal fiords in the western part of the study area extend for tens of kilometres, emphasizing the considerable vertical relief in this region (Figure 1.3c). The fiords tend to be v-shaped, rather than u-shaped, especially Hastings Arm and Observatory Inlet (Figure 1.3d). In the eastern part of the map area, relief is not as pronounced. Many of the mountains are flat-topped, and may be part of a former plateau.

Figure 1.3. Physiographic features of the Nass River region. a) Looking southwest down Sutton Glacier from Cambria Ice Field. Mountain peaks are jagged and many have small glaciers. b) Looking northeast up the Nass Valley near the river mouth. The valley is broad and flanked by jagged snow-capped peaks. The river has one to two channels here, and a wide floodplain. c) Looking northwest across Hastings Arm. Note the blue green water colour due to rock flour introduced by Kshwan River, which drains an alpine glacier. The water is muddier at the mouth of the river (upper right). Lower elevation mountain peaks are rounded in this area. d) V-shaped profile of Hastings Arm, looking south from a point at about the centre of c).

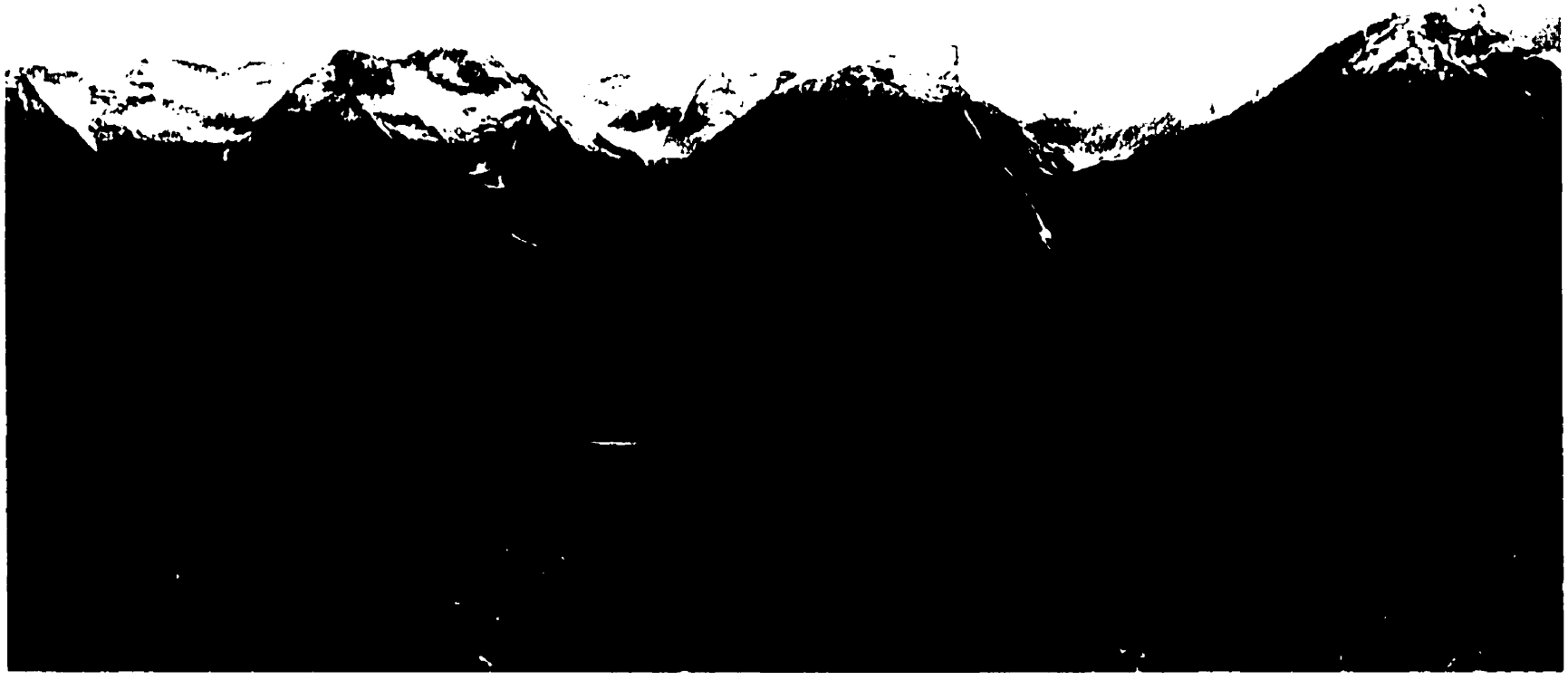

Figure 1.4. Looking northwest across Nass Valley from Ksedin Creek area. Hanging valleys, cirques and arêtes are common valley side features.

The Nass River is a single channeled, straight to sinuous river incised into bedrock in its upper reaches, where it flows southeastward along the Nass Depression. It flows southwest in the southern part of the study area, along the Nass Valley. The river has a more complex planform south of the mouth of Tseax River, forming a wandering gravel-bed river with generally one or two (less commonly three) active channels and a wide floodplain (Figure 1.3b).

*Climate*

The region has cold, wet winters and cool summers due to the influence of Polar Maritime air (Farley, 1979). Mean annual precipitation ranges from 150 to 350 cm, with higher mountain peaks receiving the most precipitation, mainly in the form of snow (Farley, 1979). January temperatures are between 0° and -15°C, while July temperatures average 14-16°C in the lowlands and less than 14°C in the mountains (Farley, 1979).

The biogeoclimatic zones of the map area include coastal western hemlock in valleys and fiords, as well as Engelmann spruce/subalpine fir, subalpine mountain hemlock and alpine tundra, listed in order of increasing elevation (Farley, 1979).

*Bedrock Geology*

Carter and Grove (1971) produced a preliminary geological map of the area that has been expanded upon by more recent studies. The bedrock in the study area is a mix of sedimentary, igneous and metamorphic rocks. Figure 1.5 is a compilation of geological data from Carter and Grove (1971) and the sources referred to below.

The Jura-Cretaceous Bowser Lake Group forms the bedrock in the eastern half of the study area. These rocks are slightly metamorphosed (hornfels grade), consisting of sandstone (lithic or arkosic arenite), siltstone and mudstone turbidite sequences (Evenchick and Mustard, 1996) that formed in open shelf and deep marine settings (Evenchick *et al.*, 1992). Bowser Lake Group rocks are grey or dark grey in the Nass Depression (Evenchick and Mustard, 1996) and blue grey elsewhere.

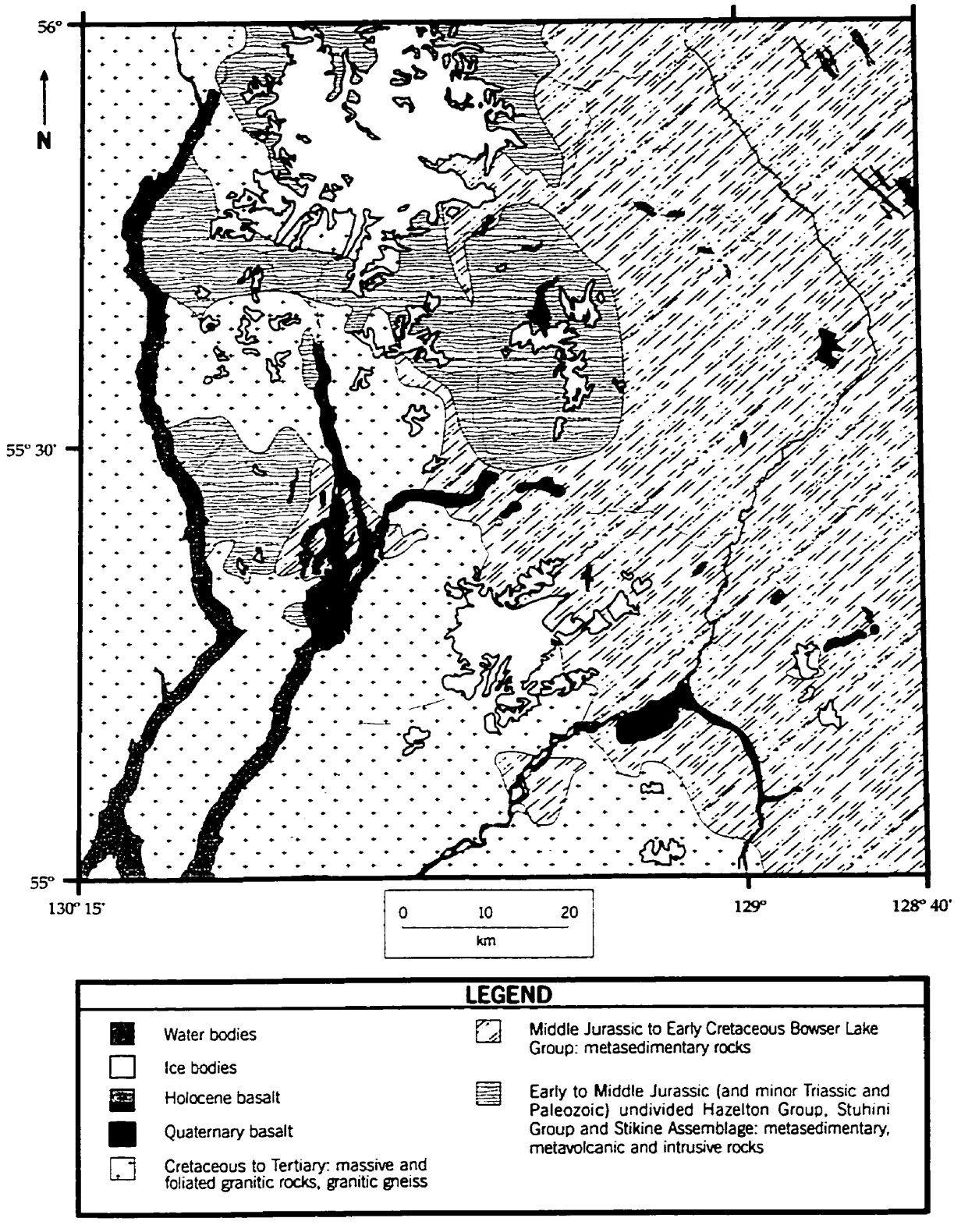


**Figure 1.5. Generalized bedrock geology of the study area.**

Cretaceous to Tertiary plutons are the major bedrock unit in the western part of the map area. They comprise quartz monzonite, quartz monzodiorite, granodiorite and granite (Greig and Gehrels, 1995, Evenchick and Mustard, 1996, Evenchick and Holm, 1997).

Interbedded metavolcanic and metasedimentary rocks of Triassic-Jurassic age are found in the north and northwest, as well as in the Anyox region. Detailed mapping of these units has been done in areas of mineral potential. Mudstone, siltstone, sandstone, wacke and conglomerate of the Kitsault Valley area are interbedded with porphyritic basalt, volcanic breccia and andesitic tuff (Dawson and Alldrick, 1986). Tertiary quartz monzonite and granodiorite intrusions and microdiorite to lamprophyre dykes are present locally. In the vicinity of Kinskuch Lake, siltstone, sandstone, limestone, and chert alternate with mafic pyroclastics, felsic tuff, felsic tuff-breccia and porphyritic dacite (Greig, 1992). These rocks are subdivided into the Stuhini and Hazelton Groups (Greig, 1992). Rhyolite dykes and sills intrude the youngest formations. Tertiary granite, Paleozoic (?) to Mesozoic folded plutonic, volcanic and sedimentary rocks make up the Anyox pendant, near Anyox (Evenchick and Holm, 1997). In this area, slightly metamorphosed Middle Jurassic Bowser Lake sandstone, siltstone and mudstone turbidites are underlain by Triassic to Middle Jurassic pillow basalt, tuff and breccia. A complex of igneous, volcanic and sedimentary rocks of uncertain age are found west of Anyox along Portland Canal. Gabbro dykes are common and quartz monzodiorite or quartz diorite dykes are found locally. Hazelton Group mudstone, siltstone, wacke, debris flow conglomerate, basalt, tuff and tuff-breccia are found to the north of the map area, in the vicinity of Meziadin and Bowser Lakes (north of the White River area).

Young lava flows of slightly vesicular columnar basalt with plagioclase phenocrysts are present locally in the Kwinatahl and Nass Valley areas (Evenchick and Mustard, 1996, Haggart, 1998). They are thought to be Pleistocene in age. A flow in Hoan Creek dated at 175 ± 50 ka BP, confirms this hypothesis (Evenchick *et al.*, 1997). A Holocene lava flow (the Aiyansh flow) occupies the lower Tseax River Valley and extends into the Nass River valley, near the town of New Aiyansh (for location of rivers, see Figure 1.1). It is an alkali basalt flow that occurred about

220 years ago and appears to have altered the course of the Nass River (Sutherland Brown, 1969).

## Objectives

The primary objectives of this study are to determine the glacial history and glacial geology of the Nass River area. These goals can be summarized as three distinct objectives:

1. *To determine and to map the Quaternary geology and geomorphology of the Nass River region. Emphasis is placed on deducing the depositional environments that produced the lithostratigraphic succession.*
2. *To determine the glacial history of the region.*
3. *To identify and define in more detail the sequence of events that created the Nass Valley basin fill.*

These objectives are expanded upon below.

1. *Quaternary geology of the Nass River region*

Surficial geology and geomorphic units are determined by air photo interpretation and field mapping. Details provided by surficial mapping include relative succession of the major units, marine limit, various types of till present, and the location of geomorphic features such as glaciofluvial deltas, alluvial fans, fan deltas, drumlins and landslides.

2. *Glacial history of the region*

Glacial history is determined by uncovering evidence of former ice flow directions, depositional processes and the style of glaciation and deglaciation. The ways in which the deposits formed, the regional sequence of events and the thickness of the Cordilleran Ice Sheet are investigated.

The timing of glacial events are determined by radiocarbon dating. Finally, correlations are made with glacial events in other areas of B.C.

*3. The sequence of events that created the Nass Valley basin fill*

By combining stratigraphic and glacial history information, the changing depositional environments that existed throughout the last glaciation is outlined. The chronology of glacial events, the speed of isostatic rebound, and the role of the currently incised Nass River in the postglacial history of the area are more difficult to define, as they hinge on the availability of radiocarbon datable material.

# CHAPTER TWO
# PREVIOUS WORK

## Regional Glacial History Studies

*Introduction*

There are only a few studies dealing with glaciation in northern British Columbia. Areas that have been investigated in the general vicinity of the study area include: 1) Stikine Valley, 2) southeast Alaska, 3) Terrace-Kitimat, 4) Queen Charlotte Island/Prince Rupert, 5) Smithers-Bulkley Valley and 6) Babine Lake (Figure 2.1). Ryder and Maynard (1991) produced a generalized map of ice flow directions in northern B.C. at the climax of the Fraser Glaciation (Figure 2.2). In general, the regions surrounding the study area show evidence of an interstadial period (probably the Olympia Nonglacial Interval), followed by the last glaciation and the current postglacial period (Table 2.1). In the thesis, dates are given as radiocarbon kiloyears before present.

The Olympia Nonglacial Interval started before 59 ka BP and continued until about 25 ka BP (Clague, 1981). It was followed by the last glaciation (Fraser Glaciation). The latter event spanned about 25 to 10 ka BP, but the time of deglaciation varies locally, so that some coastal areas were ice-free by 15 ka BP, while more interior locations were not deglaciated until about 10 ka BP (Table 2.1). Both the Fraser glaciation and the Olympia event are Wisconsinan in age. The current postglacial period spans the Holocene, from about 10 ka BP to present. Evidence of pre-Fraser Glaciation is rare in the region, due to scouring of earlier deposits during the Fraser event. Table 2.1 gives the few exceptions.

*Queen Charlotte Island/Dixon Entrance Region*

In the northern Queen Charlotte Islands at Cape Ball, the only regional evidence of a pre-Fraser event is a glaciomarine/till sequence of infinite radiocarbon age (Clague *et al.*, 1982a). It is overlain by nonglacial deposits of Olympia age (28-23 ka BP), glacial sediments of Late

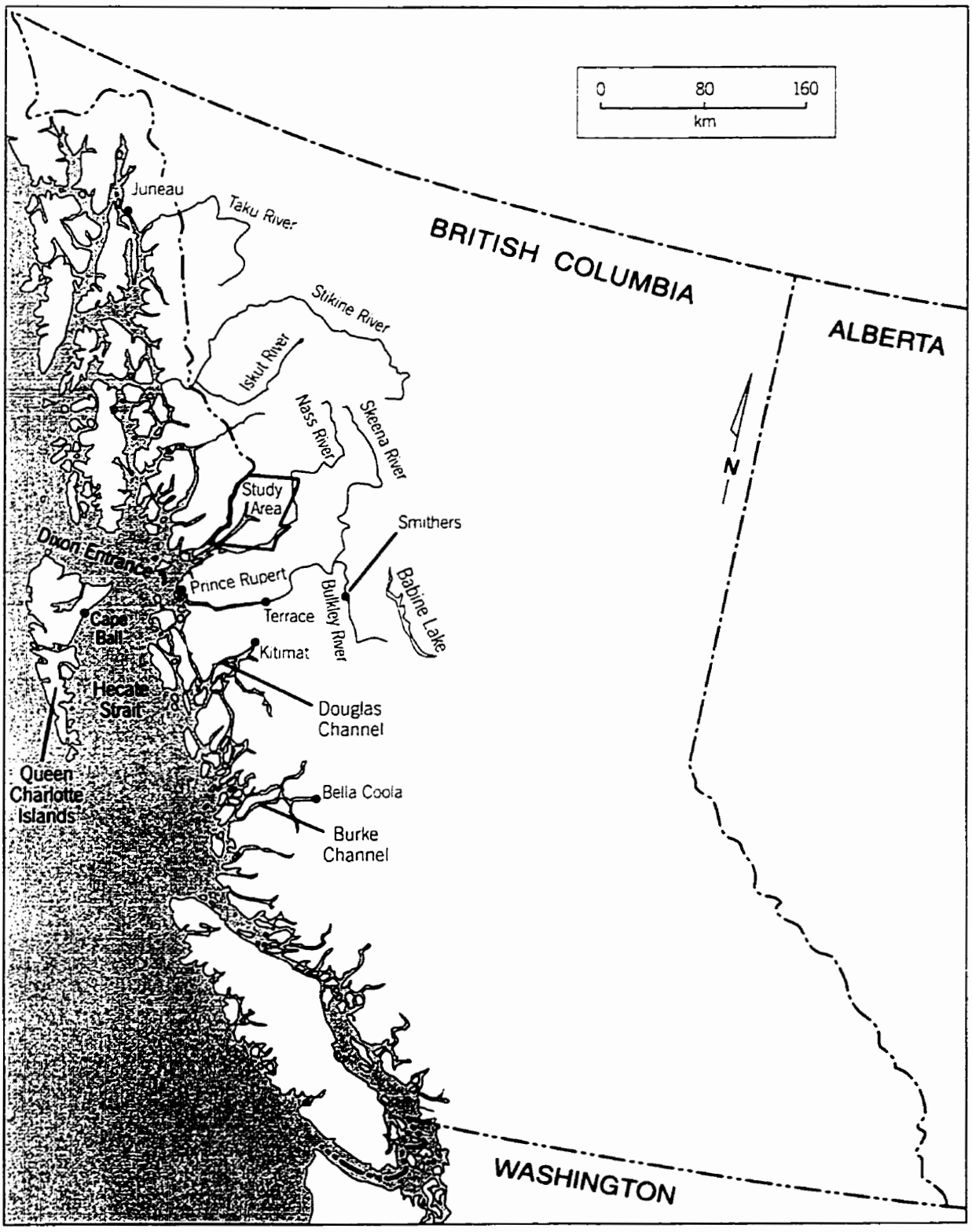


Figure 2.1. Location map of Quaternary investigation sites in the vicinity of the study area. The Stikine Valley, Queen Charlotte Islands, Terrace-Kitimat, Prince Rupert, Smithers-Bulkley Valley and Babine Lake regions are detailed study locales.

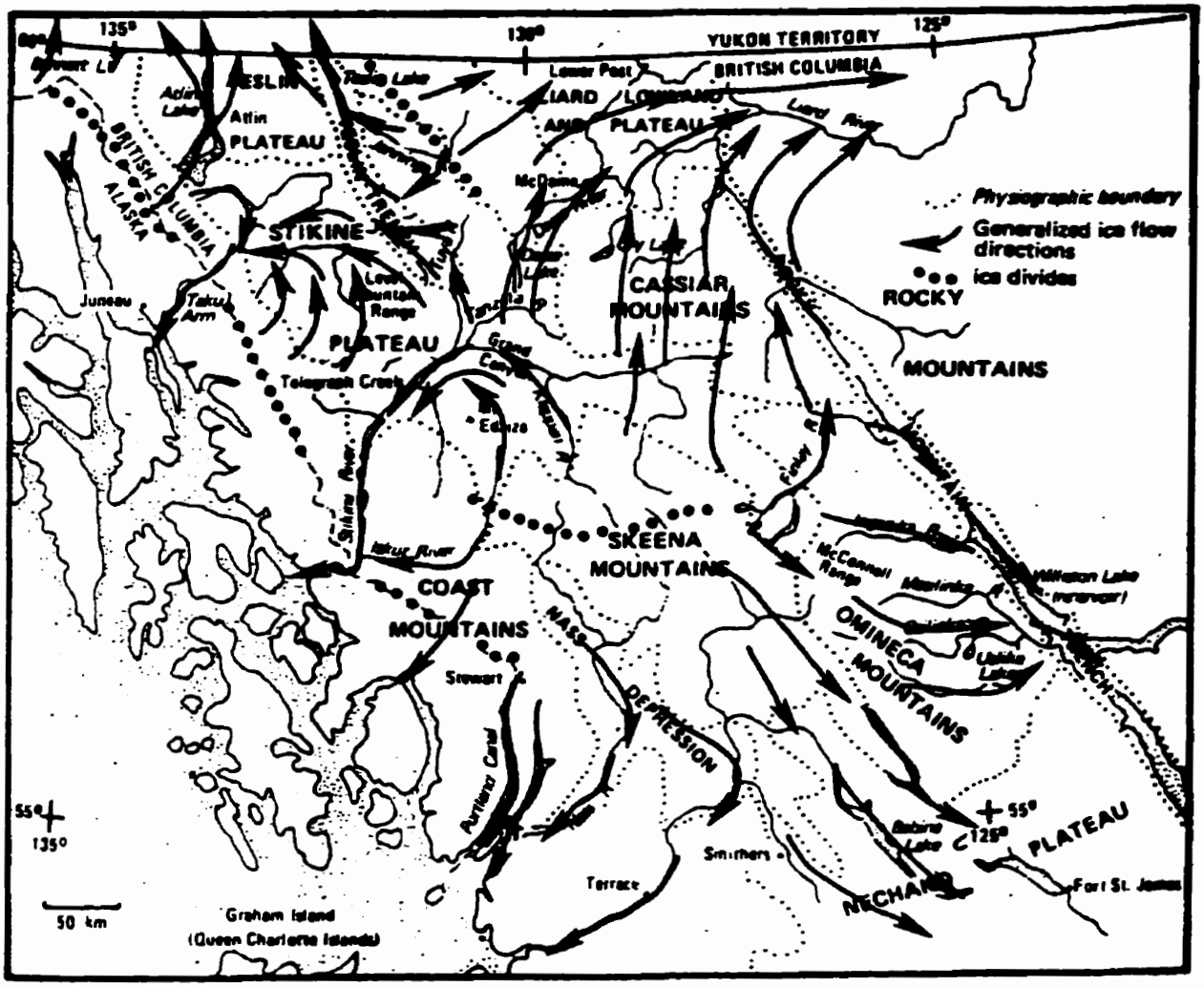


Figure 2.2. Ice flow directions in Northern B.C. at the climax of Wisconsinan Glaciation (from Ryder and Maynard, 1991).

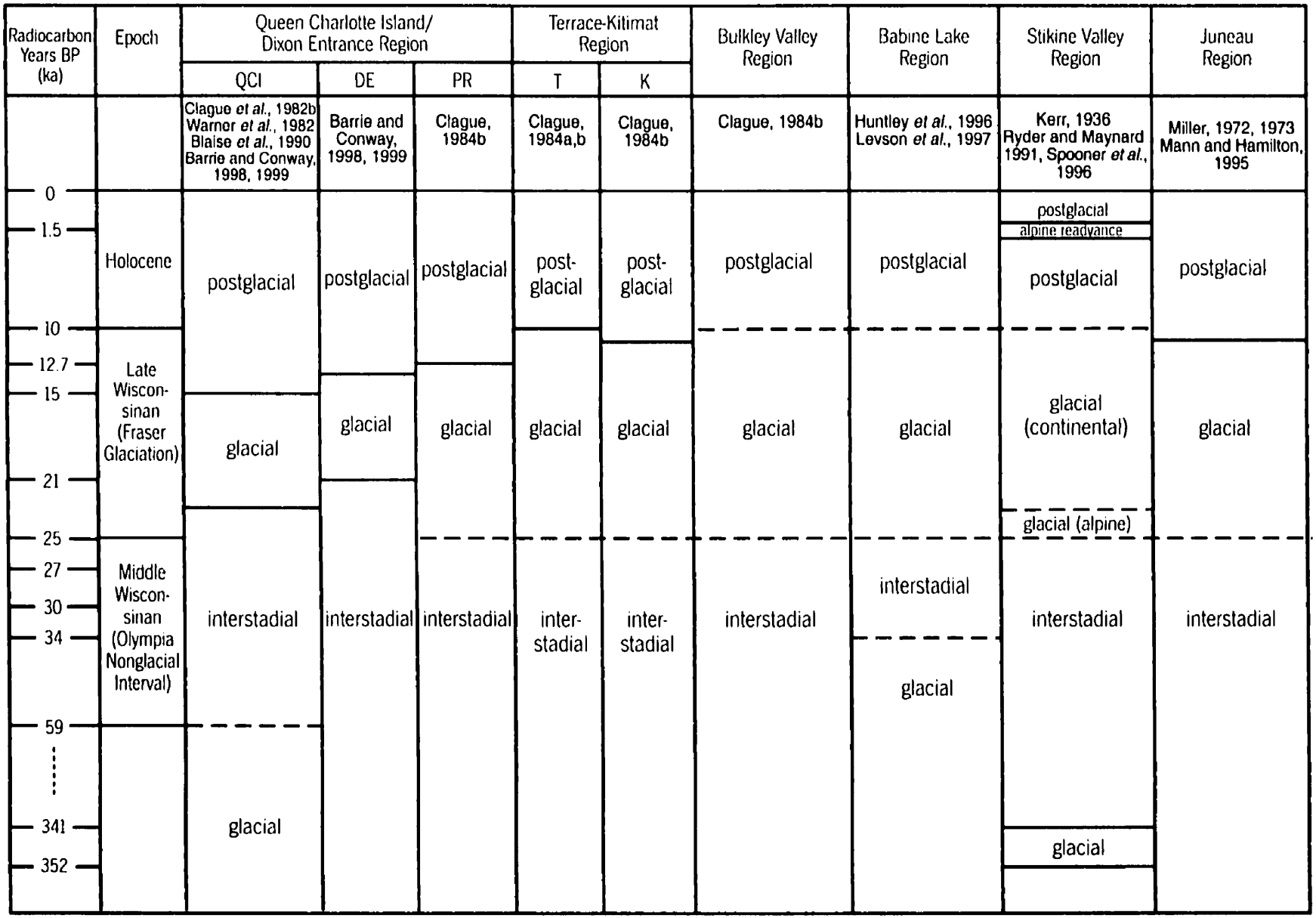


Table 2.1 Timing of glacial events in the region. Dashed lines indicate that exact timing is unknown. QCI = Queen Charlotte Islands; DE = Dixon Entrance; PR = Prince Rupert; T = Terrace; K = Kitimat.

Wisconsinan age and postglacial sediments dated at 15-16 ka BP (Table 2.1) (Clague *et al.*, 1982a , Blaise *et al.*, 1990). Further west at Mary Point, advance-phase outwash was deposited from 23 to 21 ka BP, followed by till deposition under advancing ice, which subsequently retreated from 16 to 15 ka BP (Blaise *et al.*, 1990). Flora was well established on the island by 16-15 ka BP (Warner *et al.*, 1982). Fraser ice was probably a complex of piedmont ice flowing southwest from the mainland coast and south from Alaska, which joined local Queen Charlotte ice caps and reached its maximum sometime after 21 ka (Clague *et al.*, 1982a, Barrie and Conway, 1998, 1999). Ice in Dixon Entrance was at least 350 m thick at this time (Barrie and Conway, 1999).

Deglaciation was rapid, starting at around 15 ka and finishing by 13.5 to 13 ka BP (Barrie and Conway, 1998, 1999). The Prince Rupert area, which has few glacial deposits, was deglaciated by 12.7 ka BP (Clague, 1984b).

The deglacial period was one of sea level lowstand near the Queen Charlotte Islands (Clague *et al.*, 1982a, Josenhans *et al.*, 1995, 1997), such that Hecate Strait formed a land bridge and Dixon Entrance was narrower (Barrie and Conway, 1999). Glaciofluvial outwash, fluvial, lacustrine and beach deposits formed on the land bridge and were later submerged (Barrie and Conway, 1999, Josenhans *et al.*, 1995). Sea level at Prince Rupert, however, was at least 11 m above present at 12.7 ka BP (Clague, 1984b), after which time it dropped.

*Southeast Alaska Region*

In the southern 'Alaskan Panhandle' region, reported evidence of glaciation is Late Wisconsinan in age. Most information is for deglacial time only. Ice retreat in the area was rapid due to abundant calving and deglaciation was complete by about 13.5 ka BP (Mann and Hamilton, 1995).

In the Juneau area, glaciomarine diamictons that pre-date 12.8 ka BP and that are found above 120 m asl, rarely contain fossils (Miller, 1973). This suggests that conditions were more turbid and sediment influx was high during the early stages of ice retreat (marine limit was 230 m asl; Miller, 1972). Fossils and foraminifera are common, however, in lower elevation deposits. The

highest dated marine deposit in this area is at 121 m asl (11.9 ka BP), while other deposits at elevations below 31 m asl have produced dates of 12.3 to 12.8 ka BP (Miller, 1973). The latter deposits would be interpreted today as fan deltas. It is possible that the fan delta material was reworked from glaciomarine diamicton of higher elevations, so it could be that these dates actually represent a time when sea level was above 121 m. It should be noted that the dates obtained by Miller are from marine shells and may be too old by about 600 years, due to the ocean reservoir effect.

A number of deltas formed in the Juneau area during deglaciation, at elevations of 75 and 150 m (Miller, 1972). There are none at the highest marine limit of 230 m. Extensive raised beaches are found at 185 and 150 m, as well as at lower elevations (Miller, 1972). The 185 m deposits are older than 8.3 ka BP. Deposits at 55 m are between 10.6 and 7.2 ka BP in age.

Neoglacial ice advances occurred from 3500 to 2000 years ago in the Juneau area. Modern glaciers reached their Little Ice Age maxima 230 years ago (Miller, 1972).

*Terrace-Kitimat Region*

Extensive glaciomarine, glaciofluvial and deltaic deposits have been mapped in the Skeena Valley and Terrace-Kitimat region, but till is rare in this area (Clague, 1984b). At the glacial maximum (about 18 ka BP), ice likely covered peaks up to 2000 m high and thinned toward the coast (Clague, 1984b).

A late glacial rise in sea level is thought to have triggered rapid retreat of ice in coastal areas, followed by slower retreat as ice became confined to fiords. South of Kitimat, fiord glaciers retreated rapidly (8-10 m/a between 12.7 and 12 ka) but at 12 ka, halted long enough to produce a submerged gravelly morainal sill in Douglas Channel (Bornhold, 1983). By 11 ka, ice had retreated to the Kitimat area. Large volumes of coarse, ice-proximal sediment were deposited in northern Kitimat Arm at this time (Bornhold, 1983).

Further south, slow initial retreat of fiord glaciers was followed by rapid retreat in Burke Channel near Bella Coola, but the exact timing of these events is not known (McCann and Kostaschuk, 1987).

Sometime between 12.7 and 10.5 ka BP, ice was flowing southwestward in the Skeena Valley past Terrace (Figure 2.2) and southward in the Kitimat-Terrace corridor (Clague, 1984b). An end moraine was constructed at Kitimat at about 11 ka BP. The Terrace-Kitimat region was not completely ice free until 10-10.5 ka BP (Table 2.1) (Clague, 1984b). Deglaciation occurred by downwasting and frontal retreat, resulting in a connected system of valley glaciers. When deglaciation began, sea level was approximately 200 m higher than present, and glaciomarine sediments were deposited in fiords. Deltas formed at the mouths of valleys that are tributary to the Skeena Valley and the Kitimat Terrace corridor; some have two deltas formed at different sea levels (Clague, 1984b). Large delta-sandur complexes graded to the 200 m marine limit formed at ice margins when retreating valley glaciers stabilized for short periods of time. (Sandurs and their deltas are referred to in the thesis as braidplains and braid deltas, after McPherson *et al.*, (1987). They are shown as 'glaciofluvial plain' and 'glaciofluvial delta' on the maps to comply with the GSC standard). At about 10.1 ka BP, a large glacial lake formed north of Terrace, dammed behind one such feature (Clague, 1984a,b).

*Smithers-Bulkley Valley Region*

Fluvial and lacustrine sediments of possible Olympia age underlie Fraser Till in Bulkley Valley (Table 2.1) (Clague, 1984b). As ice advanced to the southeast during the Fraser Glaciation (Figure 2.2), glaciolacustrine and glaciofluvial sediments were laid down in proglacial areas. Till was deposited over these sediments during the Fraser advance. Deglacial deposits are few, indicating relatively debris-free ice and active flow during retreat (Clague, 1984b).

*Babine Lake Region*

The earliest glaciation in the Babine Lake (Nechako Plateau) region is recorded solely by glaciated bedrock underlying the oldest nonglacial sediments, and therefore its age is unknown, although it is older than 34 ka (Table 2.1). Pre-Late Wisconsinan (Olympia?) fluvial and lacustrine environments were followed by proglacial glaciofluvial and glaciolacustrine settings as ice moved into the area.

Early work in the Babine Lake-Nechako Plateau region was done by Armstrong and Tipper (1948). They concluded that the main ice centre of the Cordilleran Ice Sheet in this area during the last glacial maximum was in the Coast Mountains, and that ice flowed eastward from the Coast Mountains across the Nechako Plateau and northwest up the Rocky Mountain Trench. Recent work, however, contradicts this conclusion (Levson *et al.*, 1997, Stumpf *et al.*, in press).

At the climax of the Fraser glaciation, ice actually flowed to the west from an ice divide in the Omineca Mountains (Stumpf *et al.*, in press). Ice was more than 2 km thick and it crossed topographic divides, even flowing upslope in many areas. Prior to and after the climax, ice flowed along valleys in various directions, originating from several smaller ice centres, including one in the Coast Mountains (Levson *et al.*, 1997, Stumpf *et al.*, in press).

During deglaciation, thinning ice became controlled by topography, and valley glaciers receded by frontal retreat and stagnation. Braidplains formed in front of retreating ice and glacial lakes formed locally (Huntley *et al.*, 1996; Levson *et al.*, 1997).

In the Nechako Plateau, glacially streamlined bedrock underlies massive till plains that are rolling, fluted or drumlinized. The lodgement and basal melt-out till is regional in extent and is overlain in places by supraglacial till and glaciogenic debris flows (Huntley *et al.*, 1996). Till veneer is common in upland areas. Till is overlain by glaciofluvial, fluvial, organic and colluvial deposits in all parts of the region (Levson *et al.*, 1997). Glaciofluvial deposits (esker, kame, braidplain and deltaic sediments) are abundant in both montane and valley settings, but are thickest in valleys. They are especially abundant in areas surrounding Babine Lake. Glaciolacustrine deposits are common in valleys, near modern lakes (*e.g.* Babine and Takla lakes). Organic deposits, the most abundant Holocene deposits, overlie till and glaciofluvial sediments (Huntley *et al.*, 1996, Levson *et al.*, 1997). Colluvial veneers that thicken toward valley floors are found on steep slopes. They commonly incorporate till as well as bedrock (Levson *et al.*, 1997). Alluvial fans, fan deltas and alluvial plains constitute the remainder of Holocene sediments in the region (Levson *et al.*, 1997).

*Stikine River Region*

An early glacial advance in the Stikine Valley between 341 and 352 ka BP (Figure 2.1, Table 2.1) deposited advance-phase glaciolacustrine and ice-contact deposits, as well as retreat-phase glaciofluvial or fluvial gravels (Spooner *et al.*, 1996). A similar advance-phase lake (Glacial Lake Stikine) also formed in Late Wisconsinan time (Ryder and Maynard, 1991). The lake was dammed by ice flowing out of the Coast Mountains, indicating that a long phase of alpine glaciation occurred before the Cordilleran Ice Sheet formed (Table 2.1). At the climax of Fraser glaciation, ice flowed radially from the Skeena Mountains (Figure 2.2), although at some time during the Pleistocene (earlier?), ice flowed southwestward across the Coast Mountains in the Stikine, Iskut and Taku River areas (Kerr, 1934).

Deglaciation occurred by frontal retreat and downwasting, with abundant meltwater production. The Stikine outlet glacier retreated and thinned rapidly, with glaciofluvial and localized glaciolacustrine deposits forming in front of it. The Grand Canyon of the Stikine is thought to have been initiated as a tunnel valley, since numerous eskers show that many subglacial channels fed into it and its morphology could be that of a very large subglacial conduit (Ryder and Maynard, 1991).

In the Holocene, a warm period occurred in the Stikine Valley from 5.5 to 1.5 ka BP, followed by a readvance of mountain glaciers (Kerr, 1936). Minor oscillations have marked the movement of alpine glaciers in the last 2 ka BP (Kerr, 1936).

## Regional Sea Level Studies

The decay of the Cordilleran Ice Sheet was much faster than its growth. As a result, isostatic rebound was quite rapid in all areas of coastal B.C. (Clague, 1983). The rate of uplift decreased exponentially with time, and uplift was generally complete by the Mid-Holocene. The associated relative sea level change was due to a combination of isostasy, eustasy and tectonic forces. Isostatic recovery was the dominant element causing sea level change, followed by eustasy (Clague *et al.*, 1982b).

Along the entire mainland coast, rapid emergence in the early Holocene resulted in 150 to 200 m of uplift (Clague *et al.*, 1982b). Less uplift occurred in outer coastal areas because ice was thinner and isostatic depression less dramatic (Clague, 1983). A sea level fall of 200 m, coupled with 100 m of eustatic sea level rise, resulted in a total isostatic rebound of 300 m along parts of the B.C. coast (Hutchinson, in press). Such a large degree of isostatic adjustment suggests that the coastal lithosphere is thin and the underlying mantle very responsive to ice loading and unloading. This is probably due to the fact that B.C. overlies a subducting plate margin (Hutchinson, in press).

The highest marine limit (230 m) was reached in the Juneau area (Figure 2.1) (Miller, 1973, Mann and Hamilton, 1995), but the time at which it was reached is not known. A maximum marine limit of 200 m was reached in Kitimat between 13 and 11 ka BP (Clague *et al.*, 1982b) and near Terrace at 10.2 ka (Clague, 1984b). In Kitimat, sea level fell 85 m from 10.1 to 9.3 ka BP (Clague, 1983). Sea level also dropped rapidly in the Prince Rupert area from 14.6 to 12.5 ka (Barrie and Conway, 1998). It reached its present level in the Prince Rupert area at about 5 ka (Clague *et al.*, 1982b).

The Queen Charlotte Islands, on the other hand, experienced low sea levels during deglaciation, as much as 150 m below present (Clague *et al.*, 1982a, Josenhans *et al.*, 1997, Barrie and Conway, 1999). Sea level changed rapidly between 12 and 9.3 ka BP, rising from 140 m below to 16 m above present sea level (Josenhans *et al.*, 1997). River, lake and beach deposits, as well as forested lands of the lowstand period became submerged at this time (Josenhans *et al.*, 1995). Sea level fell slowly until 6 ka BP, then fell more rapidly for a time; this slow sea level lowering continues today (Clague *et al.*, 1982a, Clague, 1983, Josenhans *et al.*, 1997).

The anomalous sea level history of the Queen Charlotte Islands is thought to be due to the rapid collapse and migration of a crustal forebulge during deglaciation (Clague, 1983; Josenhans *et al.*, 1997). The limited amount of ice cover and thin continental crust of the Queen Charlottes allowed this peripheral isostatic bulge to develop as "plastic" crustal material was pushed aside by the weight of ice over mainland B.C. (Josenhans *et al.*, 1995, 1997; Hutchinson, in press).

## Local Glacial Studies

Very little work has been done within the study area itself, but some information is available in scattered localities. The Nass River region has been terrain mapped for forestry purposes at 1:50 000 scale by Vold (1980) and Kowall and Daykin (1981). These maps were part of a preliminary air photo terrain mapping effort with no field checking. As a result, the maps are not of sufficient detail or precision to be incorporated into the mapping undertaken for this thesis. In addition, only a few of the unit types required in a surficial geology map are present and the differing criteria for their definitions result in boundaries that do not match those of a Quaternary geology map (e.g. glaciomarine clay in the Nass Valley is terrain mapped as fluvial deposits). For these reasons, the terrain maps were consulted, but were not used as a basis for the maps produced in the thesis.

Brief descriptions of Quaternary deposits and glacial geomorphology can be found in reports on the bedrock geology of some of the area's mineralized zones. Rounded mountain peaks, U-shaped tributary valleys, erratics and high elevation striations were identified in the Kitsault River Valley (Hanson, 1921). High elevation erratics and moraines were observed in the Bear River area near Stewart (McConnell, 1913). "Boulder clay" (till) was found in the Kitsault and Bear River valleys and "stratified blue clay" was seen near Anyox and in valleys near Kitsault and Stewart (Hanson, 1921, 1935). In an ore petrology investigation, Sharp (1980) noted till and gravel in valleys near Anyox. He also found stratified marine clay at 45 to 60 m asl and mentions that fossils from the clay were identified by an earlier investigator as the same as those currently found in Observatory Inlet. Because the fossils in the stratified clay were found to be similar to modern marine fauna, a glacial origin for these sediments is unlikely. They are probably Holocene deposits. Unfortunately, the exact sampling information and the locations of these sites are not known. A similar conclusion may be reached regarding marine fossils in blue clay deposits of the Bear River Valley that are similar to those currently found in Portland Canal (McConnell, 1913). Fossil-free blue clay deposits were identified farther up Bear Valley at an elevation of 150 m

(McConnell, 1913). Hanson (1935) described gravel terraces near Kitsault that are mapped as parts of a glaciomarine delta in this thesis (Nass Valley map). Raised gravel deposits in the Kitsault Valley, thought to be the product of modern fluvial processes (Hanson, 1935), are here considered to be glaciofluvial deposits, after examination in the field during the summer of 1996.

# CHAPTER THREE
# RESEARCH METHODS

The methods used to analyze the surficial and subsurface Quaternary geology of the study area include mapping of surficial geology and geomorphology, section description, drilling, seismic reflection, ground penetrating radar, borehole logging, radiocarbon dating, clay sampling, x-radiography and microscopic analyses.

## Surficial Geology and Geomorphology Mapping

### *Mapping*

Part of the process of determining regional Quaternary geology is mapping the glacial deposits of the study area. To this end, aerial photographic interpretation was carried out and was followed by ground truthing in the summer of 1996. Field work consisted of foot, boat, truck and helicopter reconnaissance, with approximately 30% of the mapped units ground checked. Field work included: 1) mapping, 2) section description, 3) collection of organic samples for radiocarbon dating and 4) collection of clay samples, mainly from the Nass Valley, for microfossil analysis. Till samples were also collected for the Geological Survey of Canada to determine regional background values of till geochemistry (Appendix A).

Eleven draft maps of surficial geology at 1:50 000 scale were produced in the fall of 1996. These were traced by hand, scanned, vectorized and imported into ARC/INFO at the Vancouver office of the Geological Survey of Canada. The drafts were compiled into two 1:100 000 scale sheets and edited. These maps are found in the map pocket at the back of the dissertation.

### *Glacial Deposits*

Sedimentary units were examined at exposures created by stream and river cuts, road cuts, gravel pits and hand auger holes. Exposures more than 3 m in height are extremely rare.

Till samples were obtained from unweathered parts of sections, from a point at least 1 m below the upper surface of the section (the C horizon). The outer 20-50 cm of weathered section material was removed with a shovel or rock hammer before sampling and description. Large cobbles and boulders were selectively removed before placing the samples in plastic bags.

*Ice Flow Directions*

Ice flow directions were determined by striation, groove (deep striation), chattermark and till fabric measurements. Although fine striations from later ice flow were difficult to locate on hard substrates like granite, grooves and chattermarks were identifiable on granitoid rocks in some areas (Figure 3.1a). Striations are best preserved on Bowser Lake Group siltstone, which was probably more heavily striated in the first place, due to its softness.

At striation sites, surface till and other debris was removed with a shovel or trowel. The site was scrubbed clean with a scrub brush and misted with water to bring out the striations. Ten individual striations were measured at each site and their average taken as the direction at that site, rounded to the nearest degree. Striae were not measured in areas where deflection was likely, such as around resistant bedrock knobs within softer rocks, or on steeply sloping surfaces. Where possible, crosscutting relationships or preservation of older striae within facets were used to establish the order of ice flow events (Figures 3.1b, c, 3.2a). Facets are generally till covered and had to be excavated for striae measurement. They are rock surfaces that preserve an earlier ice flow direction in the form of striae because they become covered with till and the till, rather than the bedrock, is striated by later ice flow.

Striations and grooves provide the best, most accurate evidence of ice flow history, but till fabrics can be used to infer general ice flow directions (Syverson, 1995). There was an abundance of high quality striations in the study area, so till fabrics were rarely needed. This was fortunate, because till fabrics should not be used as the sole directional criteria for a particular area due to within-site variability problems (Lian, 1997).

For till fabric measurements, the outer 50 cm of weathered till were removed before measuring began. The a-axes of 50 clasts were measured at each site (Figure 3.2b). Only

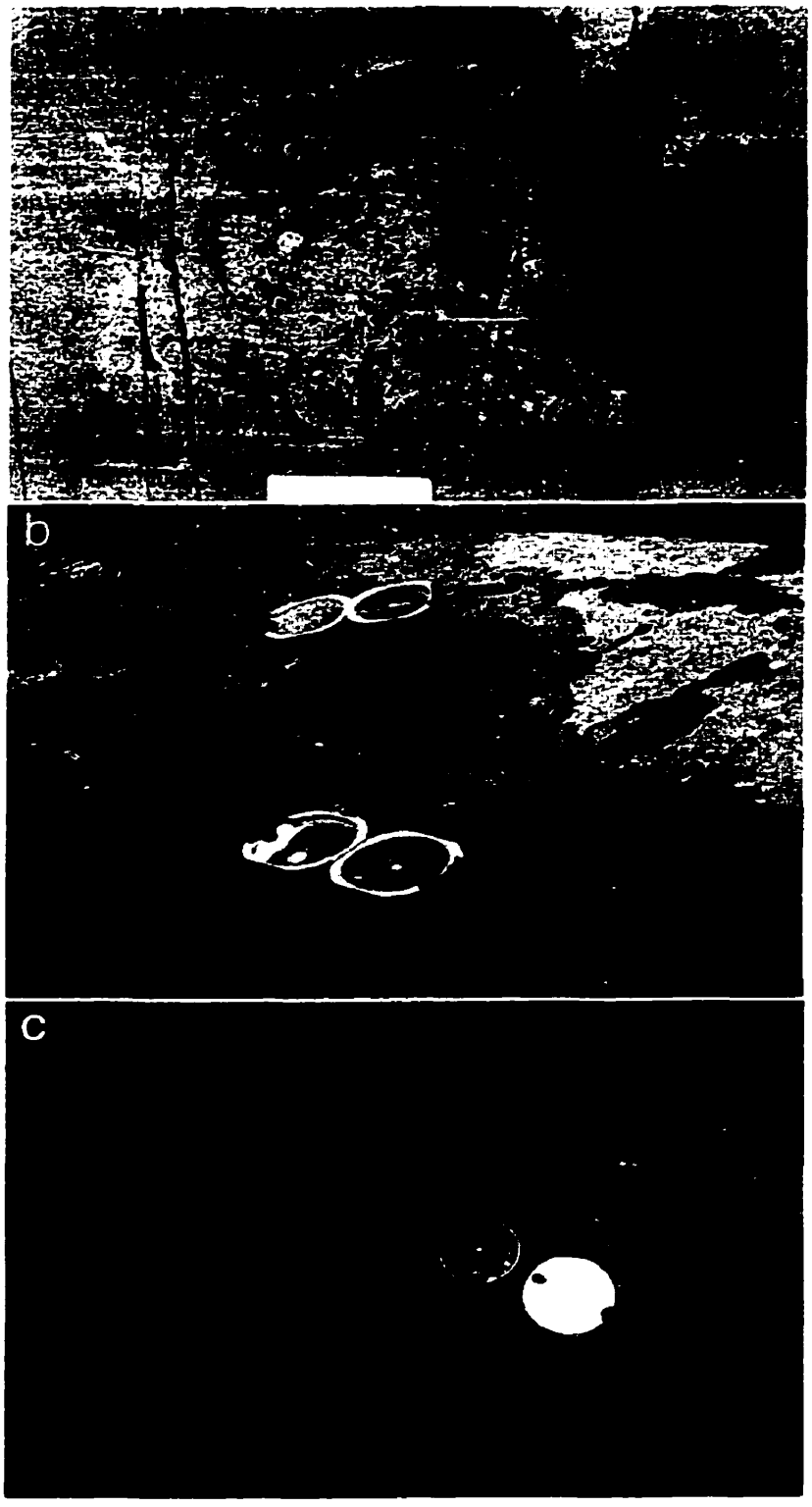


Figure 3.1. Ice flow indicator measurements. a) Grooves and chattermarks on granite. Ice flow from right to left. White scale bar is 18 cm long. b) Crosscutting relationships: older striations parallel to upper compass are almost completely obliterated by younger striations parallel to lower compass. c) Crosscutting relationships: striations parallel to pen crosscut those parallel to compass and are therefore younger. Till overlies the striated bedrock in b) and c).

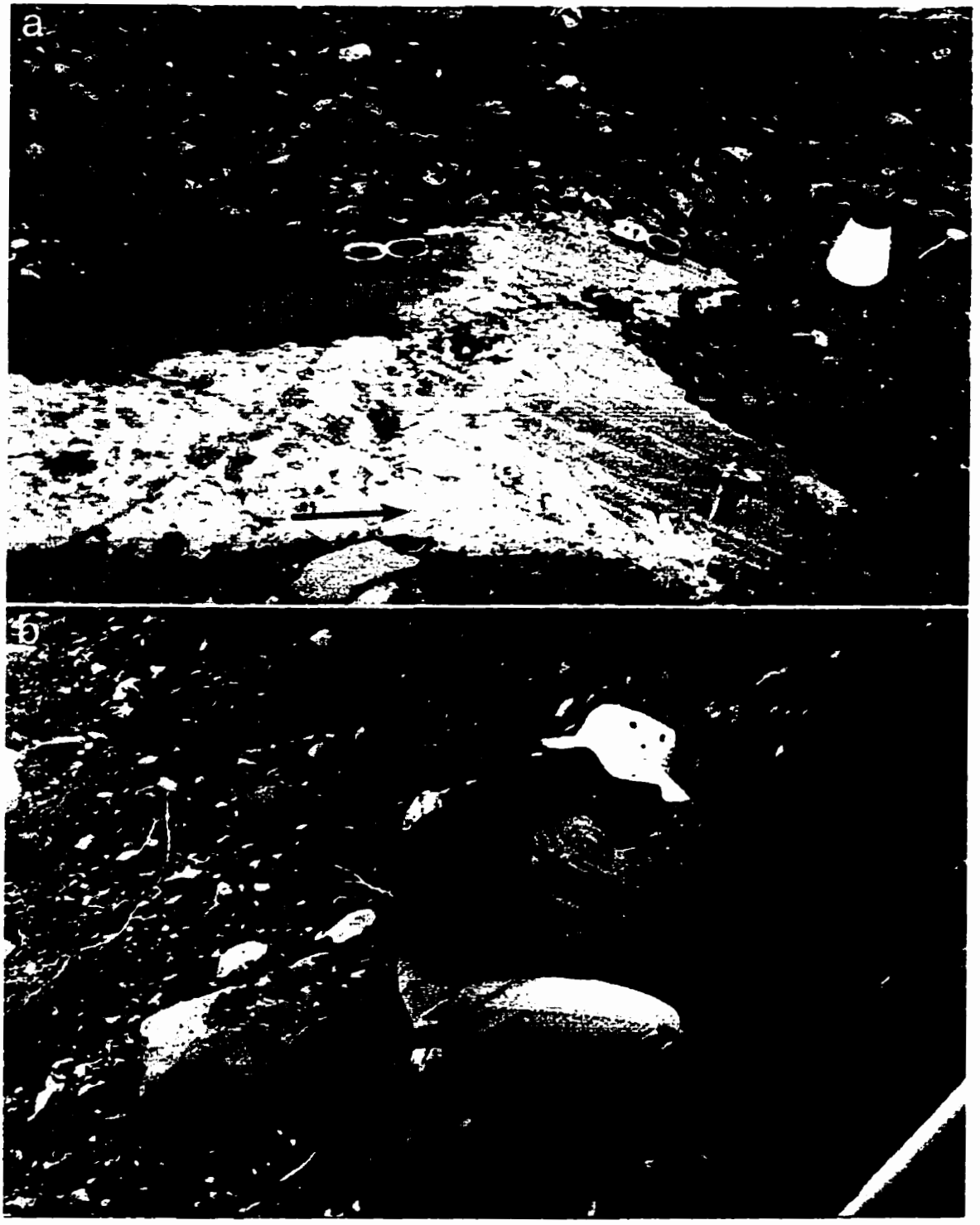


Figure 3.2. a) Facet relationships: heavily striated Bowser Lake Group siltstone in facet (parallel to compass on right) has been skipped over by later ice flow (striations parallel to upper compass and shown by arrow). Note that till rests directly on striated bedrock. b) Fabric measurement in thick till deposit.

pebbles whose a:c axis ratio was >1.5, that were larger than 1 cm long and were not located close to larger clasts were measured. Pebbles with triangular or round shapes were not measured as the a-axis was difficult to define accurately. Till fabric measurements thus took up to two hours to complete at each site. Data were collected by the author during each field season with the help of four different field assistants. Fabrics were plotted on Schmidt equal area stereonets by hand in the field, for quick analysis, and by computer in the lab using the program Spheri-Stat. Both striation and fabric orientations were recorded with a Brunton geological compass.

Streamlined bedrock ridges were also mapped, but are not used as flow indicators because they are highly variable in orientation and because they could have formed by water flow. These ridges are discussed in more detail under Streamlined Bedrock Features, Chapter 7.

## Subsurface Geology Techniques

*Sections*

Many small exposures were encountered and logged during the 1996 season. Thick exposures giving major insights into the subsurface geology of the area are rare, but several such exposures were identified and were logged in detail in the 1997 field season. Rappelling was required at sections exposed as precipitous cliffs.

Potential sections along the Nass River (visible in air photos) were inaccessible by foot or vehicle. A boat was rented in 1997 to check potential river sections, but they turned out to be bedrock cliffs.

Drumlin sections were analyzed in 1998 for clues as to their genesis. Tills were described and fabric analyses were done in logging road cuts and in pits dug in the drumlins.

*Drilling*

Drilling was carried out in the spring of 1998. Drill holes were located on or near previously shot seismic lines (described later). Drilling was accomplished with a Mobile B-53 mud-rotary drill rig mounted on a 5 ton International Harvester truck. An 8.4 cm (3.5 in) tri-cone drill bit was used

to drill the holes. Drilling was accomplished by adding 3 m (10 ft) drill pipes onto those already down hole. A 1.5 m (5 ft) pipe was added and removed before each 3 m length was added, due to limitations in how high the drill chuck could be raised above the hole. Cuttings from each drill hole were logged for grain size with the aid of a 1 mm grid sieve to catch coarser material (Figure 3.3a).

At sites where gravel or gravelly sand were encountered, augering with 15 cm solid stem or 20 cm hollow stem flight augers was substituted for mud rotary drilling (Figure 3.3b). These methods were also employed at each hole to drill through the extremely hard upper levels of weathered silty clay. Unfortunately, flight augers were not able to penetrate to great depths (20 m maximum) and drilling rates when using them were relatively slow (drilling speeds were fastest in unweathered silty clay with the mud rotary method). The large hollow stem augers were also used to case the upper 1.5 to 3 m of all mud rotary holes to provide constraint on drill angle.

Samples were taken at various intervals with a split-spoon core sampler. All drill rods were retrieved from the hole, the bit was removed and replaced with the sampler and the rods were then lowered into the hole again in 6.1 m (20 ft) sections. The sampler was then pushed into the sediment. Where sand was present, the sampler was hammered in using a manually operated rope and hammer assembly. Rods were then pulled again, the sampler removed, the drill bit replaced and the rods lowered back into the hole in 6.1 m sections. Drilling resumed after the core sample was described and wrapped in plastic.

Sedimentary structures are commonly difficult to define with mud rotary drilling because continuous core is not retrieved. However, since the upper part of all holes was augered, resulting in relatively undisturbed core acquisition, the sites will be referred to as drill holes instead of boreholes.

Vibracoring was attempted but was unsuccessful in this area, due to the tendency of the silty clays to liquefy when agitated. Pure sand deposits that are ideal for vibracoring are virtually nonexistent in the region.

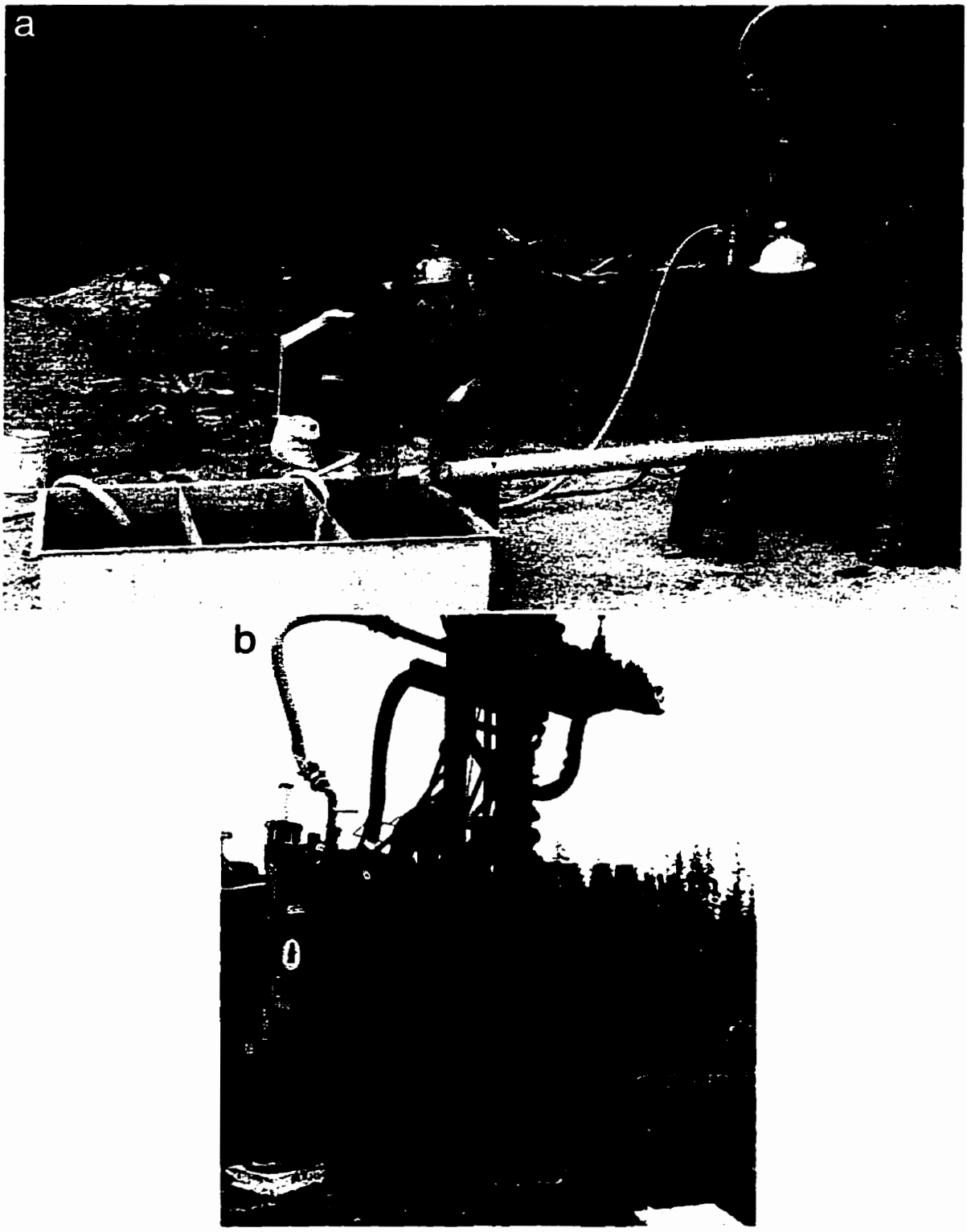


Figure 3.3. a) Mud rotary drilling with hollow stem auger casing. Cuttings were logged from the mud return and coarser grain sizes were caught with a sieve. b) Solid stem augering. Silty clay has been retrieved from this drill hole.

## Subsurface Geophysical Methods

Geophysical logs, seismic reflection and ground penetrating radar were used to collect data on subsurface bedding features and possible lithology changes. The advantage of these methods is that they are fairly inexpensive to run and give detailed stratigraphic information that is not available any other way in areas with little subsurface exposure.

### *Downhole Geophysical Logs*

Geophysical logs were taken at three of the drill holes to provide an aid in stratigraphic interpretations. Gamma ray ($\gamma$), spontaneous potential (SP) and resistivity (R) were measured simultaneously using a Mt. Sopris 1000-C logger (Figure 3.4a,b). This particular tool measures natural gamma radiation, electric current and relative resistance to an imposed electrical current of a given volume of sediment. Measurements were obtained as the tool was pulled upward inside the hole. The steel casing over the upper 3 m prevented collection of SP and R records at the top of the holes. Since SP and R require conductive fluid between the tool and the borehole wall, these logs are not reliable above the water table. Drill holes were not cased below the upper 3 m, but wall collapse was not a problem.

### *Shallow Reflection Seismic Surveys*

Shallow seismic reflection is a powerful tool for defining a subsurface stratigraphic framework in areas where exposures are limited. It is relatively inexpensive and provides high resolution results. A two-dimensional picture of Quaternary deposits that may include the bedrock-sediment interface is produced (Roberts *et al.*, 1992). Depth penetration can be as high as 700 m (Vanderburgh and Roberts, 1996), but a high penetration depth is achieved at the expense of resolution in the uppermost part of the sediment package.

Seismic reflection shows the location of acoustic contrasts (acoustic impedance) in sediments (Steeples and Miller, 1990). These contrasts commonly occur at geological contacts, due to sudden changes in density or seismic velocity. They also occur, however, where there are

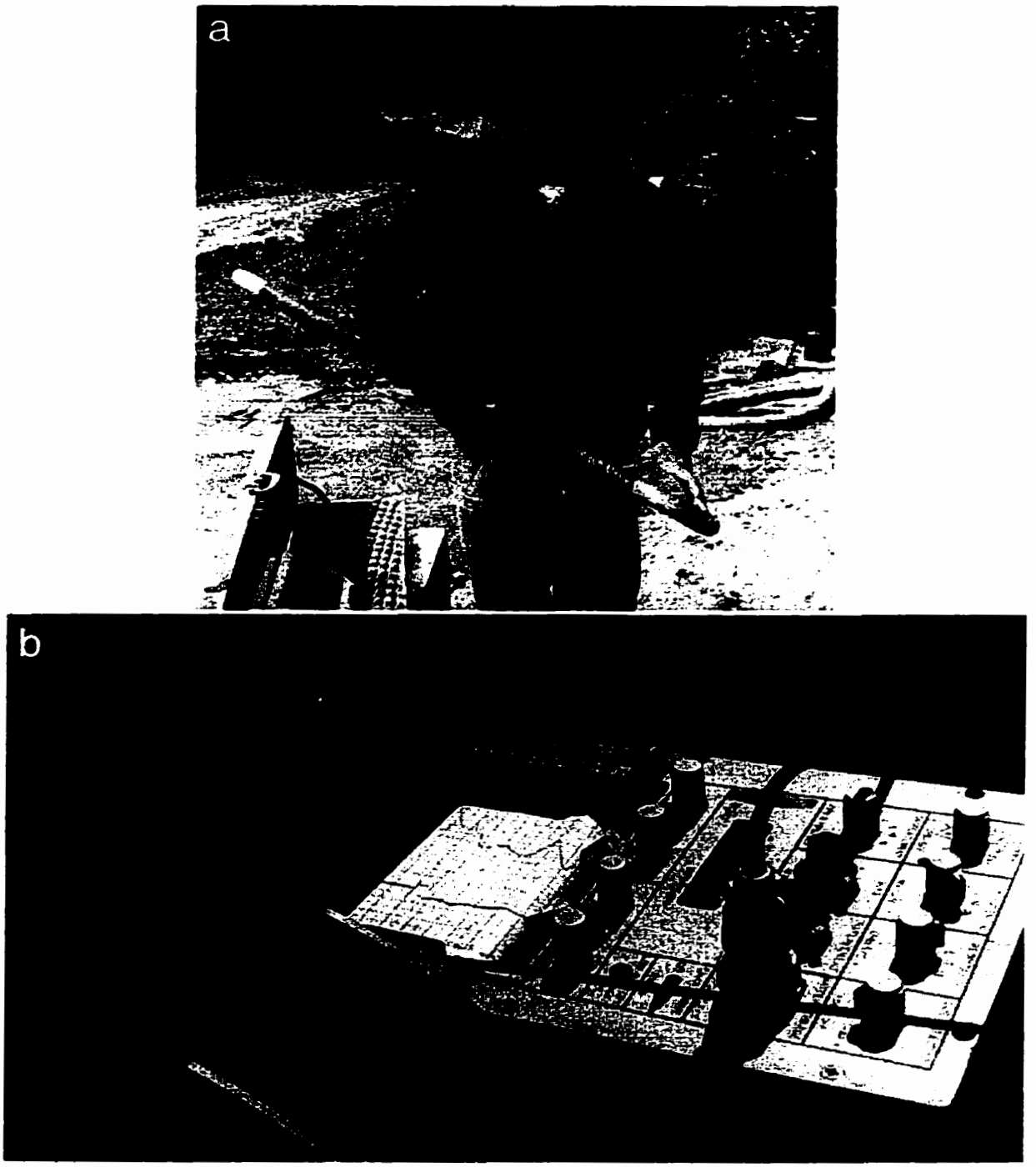


Figure 3.4. a) The Mt. Sopris geophysical logger. Field assistant is showing the length of the area of investigation covered by the tool at any given time. b) SP and R being recorded simultaneously as the tool is hoisted up the hole.

changes in pore fluid, compaction or texture (Roberts *et al.*, 1992). In Quaternary geology, acoustic contrasts are commonly related to lithology, because density and velocity changes between clay, silt, sand and gravel can be quite significant. The acoustic contrasts shown on the image are called reflections. Reflections represent stratal surfaces, which are defined as relict depositional surfaces such as bedding planes or unconformities (Brown and Fisher, 1985).

Seismic waves include compressional sound waves or p-waves. Waves produced by the seismic source travel through the ground, reflect off acoustic impedance surfaces (*e.g.* geological contacts) and return to the earth's surface, where they are measured by geophones. A straight line, two-dimensional image is the result. Fermat's principle of least time states that the point where a seismic wave is reflected off a horizontal subsurface layer is exactly half way between the source and the geophone (Steeples and Miller, 1990). The angle of incidence is thus equal to the angle of reflection, resulting in a subsurface sampling interval that is exactly half the geophone interval.

Each channel records one geophone measurement, producing a seismic trace on the seismograph. Seismic waves are recorded as a function of time on the seismograph (Roberts *et al.*, 1992) and the vertical axis on the image is time (t) in milliseconds. The horizontal axis is distance in metres from the initial geophone.

Limitations

Because sediments can strongly attenuate high frequency energy, the ability of a particular deposit to transmit energy is a major limiting factor in the final quality of the seismic profile (Pullan and Hunter, 1999). The best conditions are found in wet, fine grained surface sediments.

A number of subsurface contacts can be picked up with this method, but multiple reflections can also occur when a seismic wave bounces several times between beds before returning to the surface (Steeples and Miller, 1990). Waves that are refracted near the surface and then reflected are also recorded. Re-sampling the same reflection several times with a multiple channel seismograph minimizes these types of errors.

Reflection paths from very shallow beds are similar to the path of the direct wave which travels through the ground surface directly to the geophone. As a result, the shallowest beds cannot be determined (Roberts *et al.*, 1992), as they are drowned out by these early arrivals.

Set-up Used in This Study

In this study, a 24 channel EG&G Geometrics Smartseis S24 seismograph was used with a 36 geophone array shot end on (Figure 3.5a). High frequency 50 Hz geophones in marsh casings were used. The 36 geophones were arranged in linear array. The source was detonated and 24 channels were recorded at once. A rollalong switch was used to advance the 24 channels to phones 2 through 25. The next source was shot, the next 24 channels were recorded and the switch was rolled along again. The process was repeated until phones 13 through 36 had been recorded. The initial 12 geophones were then pulled up and tacked onto the end of the line for the next series of shots. This is known as the CMP (common midpoint) method (Roberts *et al.*, 1992). Depending on the length of a line, the recording of each line took 1 to 3 days to complete.

The advantage of a multi-channel system such as this one is that several points in the subsurface are sampled at once and each point is re-sampled 12 times. The 12 traces at each point are summed and averaged during computer processing to enhance the signal and to reduce noise (CMP stacking).

Lines were shot with a record length of 512 ms and a sampling interval of 250 μs, with a -10 μs delay. The geophone spacing was 3 or 5 m (typically 3 m) and both were tested at each site. One line was run with a 2.5 m spacing, before it was discovered that the processing program had difficulty dealing with spacings that were not whole numbers.

Waves made in the air by the ringing of the metal plate (weight drop and hammer source only) form a distinctive reflection on the seismic images called the ground-coupled air wave. Unfortunately, this could not be avoided, but the signature of this wave was easily recognizable. It was minimized by signal to noise reduction (summing and averaging traces) and muting. The frequency of the air wave was found to be unaffected by applying filters during recording.

Figure 3.5. a) Smartseis S12 seismograph in operation. b) Buffalo gun seismic source. One gun is loaded with a new blank while the other is set and triggered. The trigger held by the field asssistant in the background is dropped onto the shell from a safe distance. c) Weight drop seismic source. Hammer with attached trigger is dropped onto the steel base. The weight drop is moved with a heavy duty hand cart. d) A Stihl gas auger is used to drill holes for the buffalo gun.

Seismic Source

Two types of acoustic wave generation were used in this study: a 12 gauge "buffalo gun" (Figure 3.5b) (Pullan and MacAulay, 1987) and a weight drop (Figure 3.5c). For both sources, a trigger was used to tell the seismograph the timing of the shot.

Preliminary testing of each source was done at each site to determine which type of source produced the best data. The buffalo gun worked best in water-saturated, fine-grained sediments, as expected. These conditions were found only at line 1001. In all cases where the buffalo gun was used, a 0.5 to 1 m hole was drilled with a Stihl gas powered flight auger and filled with water before detonating 12 gauge Winchester Super-X black powder blanks (Figure 3.5d). Water fill was not required at line 1001, as the water table was almost at the surface.

In less ideal conditions, where sediments were coarse, loose and dry, the weight drop was found to be a better option. This method commonly (but not always) produced a ground coupled air wave on the record due to ringing of the metal plate after impact.

The weight drop was custom designed and created for the project (Appendix B). It consists of a heavy metal plate welded to a short cylindrical base into which a metal pipe is screwed. Disc weights of 10 or 20 kg fit over the pipe. These were dropped from heights notched into the pipe at 1 or 1.5 m. The trigger was screwed on to the top of the weight with a trigger attachment.

Tests Conducted Prior to Data Acquisition

A noise test was first conducted by letting the seismograph record background noise without a source shot. Individual traces (and hence geophone connections) were checked for function.

The second test determined the most effective source. The buffalo gun and weight drop were both tried at each line. Both weight sizes and both heights were tested on the weight drop. A hammer and plate source was also tested at a few sites, but the signal was found to be too weak for this environment.

The optimum offset (Hunter *et al.*, 1984), or distance between shot and geophones, was determined by testing several shot locations (walkaway tests) and geophone spacing was determined by making test runs of different spacings. The optimum offset varied between 18 and 42 m. Higher offsets did not produce a strong enough signal.

Spatial aliasing occurs when the geophones are spaced too far apart to pick up the targeted features. Tests for aliasing were done at each site by moving the source one half geophone interval closer to the spread and re-shooting. If the seismic signals of both were similar, the reflections were considered to be real. A series of trial spreads incorporating each of these tests were done before the seismic lines were recorded.

Noise Reduction in the Field

Vehicle noise was avoided by waiting for traffic to pass by before shooting. This was rarely a problem in this remote area, as most work occurred on deactivated logging roads. Wind noise was reduced by waiting for wind to die down, or in severe cases, by burying the geophones. Raindrop noise was a problem that could not be surmounted, so seismic work had to be halted until the rain ceased. Thunderstorms were a particular problem in the Nass Valley. Filter tests were conducted at each site by trying several low and high cut filters, but generally, no filters were applied, as the improvement of the record was not noticeable and filters could always be applied later, during data processing. An automatic gain control of 500 was applied to enhance reflections.

Data Processing (Noise Reduction in the Lab)

Seismic data were processed to enhance reflections and reduce noise, ground roll and multiples. Field records were stored on the seismograph hard drive and then transferred to 100 Mb Zip disks for storage.

Data were processed using Seismic Processing Workshop (SPW) software on a Power Macintosh G3 computer. This software package is extremely flexible and allows many processing options to be tried. It operates as a flow chart and is easy to use. However, a clear understanding

of each processing parameter is required in order to acquire the best final profile. The processing options generally used were static shifts, refractions statics, nmo correction, mute definition, cmp stack and a time variant Butterworth filter. Parameters were changed often to see if results could be improved. Reiterative testing of various parameters was required for every line. Ideal velocity functions were obtained by producing printouts of each line at about 15 different velocity values. The best value for each time interval was then chosen, the various values inserted, and the processing tests continued. Because of the ongoing testing of various parameters, the processing of a single seismic profile could take up to one month. Depths were calculated on the final stacked section using the two way travel time equation: d=vt/2, where v was the final velocity identified for each time interval.

Line 1001

One good seismic reflection profile was obtained. The processing flow for this line, Line 1001, is shown in Figure 3.6. Refraction statics were required to correct for refractions at the surface due to irregularities of geophone height. A separate flow was used to get the refraction statics information needed for the static shifts operation in the main flow. Static shifting was applied to data sorted by shot. One, two and zero refractor solutions were tested, with the two refractor solution producing the best results. Only this solution appears in the final flow. This means that two major refractions had to be accounted for with this data set. Datum statics were then done to accommodate topographic variances. The velocity function was determined by testing single values for the entire profile, as outlined in the last sub-section. The chosen velocities were used to calculate the normal moveout (nmo correction). Nmo correction straightens the hyperbolae of the reflections that are due to later wave arrival at more distal geophones. Spectral whitening was done to enhance reflections. Muting was applied to each shot gather to eliminate noise and refractions at the top of the gathers, as well as some significant ground roll noise. This resulted in a loss of data at the top of the profile. Trim statics helped resolve more of the irregularities not completely removed by the other statics processes. The data was then stacked to create the final profile, which reduces noise and enhances reflections

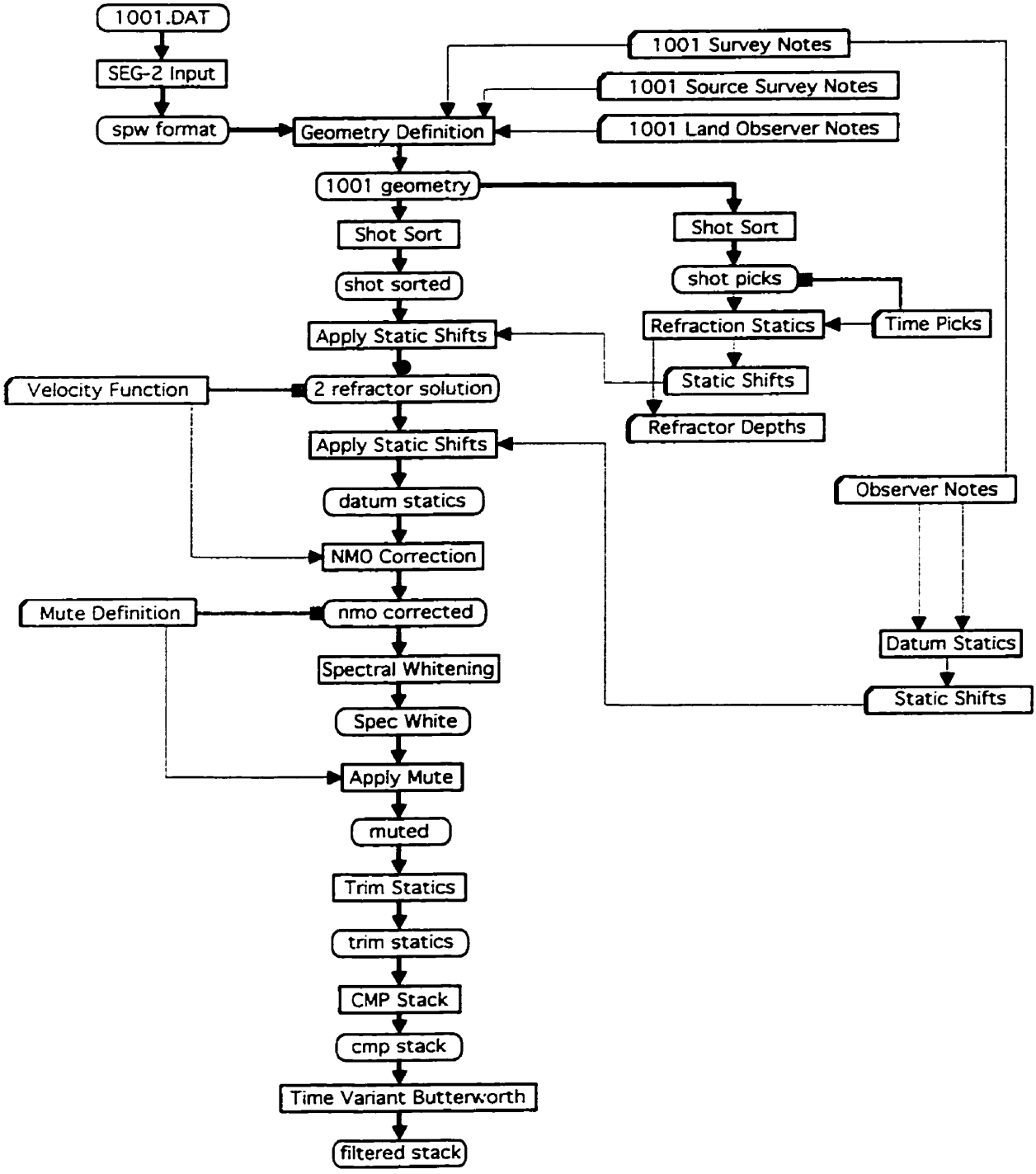


Figure 3.6. Processing flow for seismic line 1001.

by summing 12 gather traces to create one trace on the profile. Finally, the data was filtered to the 40-150 Hz range for the whole profile using a time variant Butterworth filter.

*Ground Penetrating Radar (GPR)*

Dry glaciofluvial sediments typically provide a good signal response for GPR (Jol *et al.*, 1996). GPR surveys were therefore done in parts of the Nass Valley where sand and gravel deposits were exposed at the surface. These deposits include two braidplains, an alluvial fan and other coarse units.

The GPR method examines the subsurface with radio waves in the 10 to 1000 MHz frequency range (Jol and Smith, 1991; Moorman *et al.*, 1991). Obtaining data with this method is much faster and much less expensive than with seismic reflection and provides higher resolution of the shallowest subsurface sediments (penetration depth is generally less than 30 m; Davis and Annan, 1989; Smith and Jol, 1995).

GPR produces results somewhat similar in appearance to those of seismic reflection. However, the GPR device sends and receives an electromagnetic signal, whereas in seismic reflection sound waves are generated. Changes in dielectric properties are measured, rather than changes in acoustic impedance (Davis and Annan, 1989). The dielectric constant is the sediment's capacity to store an applied electric charge, and electric conductivity is the sediment's ability to act as a conductor. Both parameters affect GPR signals. Grain size, porosity, salinity, moisture content and organic content all influence the electrical properties of sediments.

Although depth of penetration is much lower than that of seismic, the resulting data are generally more detailed. Two-way travel time is measured in nanoseconds, compared to milliseconds for shallow seismic reflection. Penetration depth is poor in saturated silt, clay and saline sediments because their conductivity and dielectric constants are high, which cause signal attenuation. Unsaturated coarse and organic deposits provide the best conditions for GPR analysis (Moorman *et al.*, 1991).

Set-up Used in This Study

The greatest depth penetration (about 50 m) has been achieved using a 1000 V transmitter with 25 MHz antennae (Smith and Jol, 1995) in ideal subsurface conditions. However, the SFU system has 50, 100 and 200 MHz antennae and a 400 V transmitter, so penetration depths were expected to be lower. Although the 50 MHz antenna did give greater depth penetration, as suggested by Smith and Jol (1995), it was decided that better resolution was more important for this study. The goal of this study was to resolve detailed stratigraphy in order to delineate deltaic and fluvial environments, rather than to try to determine their thicknesses. The thicknesses of these deposits are variable and possibly too great for complete penetration by radar in any case.

GPR surveys were conducted with a 400 V digital PulseEKKO IV radar system carried as a backpack or rolled on wheels (Figures 3.7a,b). The backpack assembly was most commonly used, as field conditions were commonly difficult (Figure 3.7c). Data were collected using the reflection survey mode, with 100 MHz antennae, a 0.5 m step size and an antenna separation of 1 m. Traces were vertically stacked 64 times, with a time sampling rate of 800 ps.

Profiles were plotted using PulseEKKO IV version 4.2 software. The processing parameters chosen were AGC of 500 (automatic gain control), signal saturation correction (dewow), a trace stacking parameter of 2 (horizontal average) and a point stacking parameter of 7 (running average). Profiles were topographically corrected where necessary. All of the profiles are vertically exaggerated.

Velocity and depth measurements were calculated from common midpoint (CMP) surveys with an initial antennae separation of 0.5 m. Two examples of CMP data are included in Appendix C. The average velocity value was 0.12 m/ns. As velocities were determined from best-fit lines to a reflection slope, depths must be considered as approximations only. In some areas, section data were used to achieve more accurate depth determinations.

The first two reflections on the profiles are the direct air wave and the direct ground surface wave. These do not show geological features and should be ignored. The horizontal scale of the profiles is distance in metres, while the vertical scale is expressed both as depth in metres and as two-way travel time in nanoseconds.

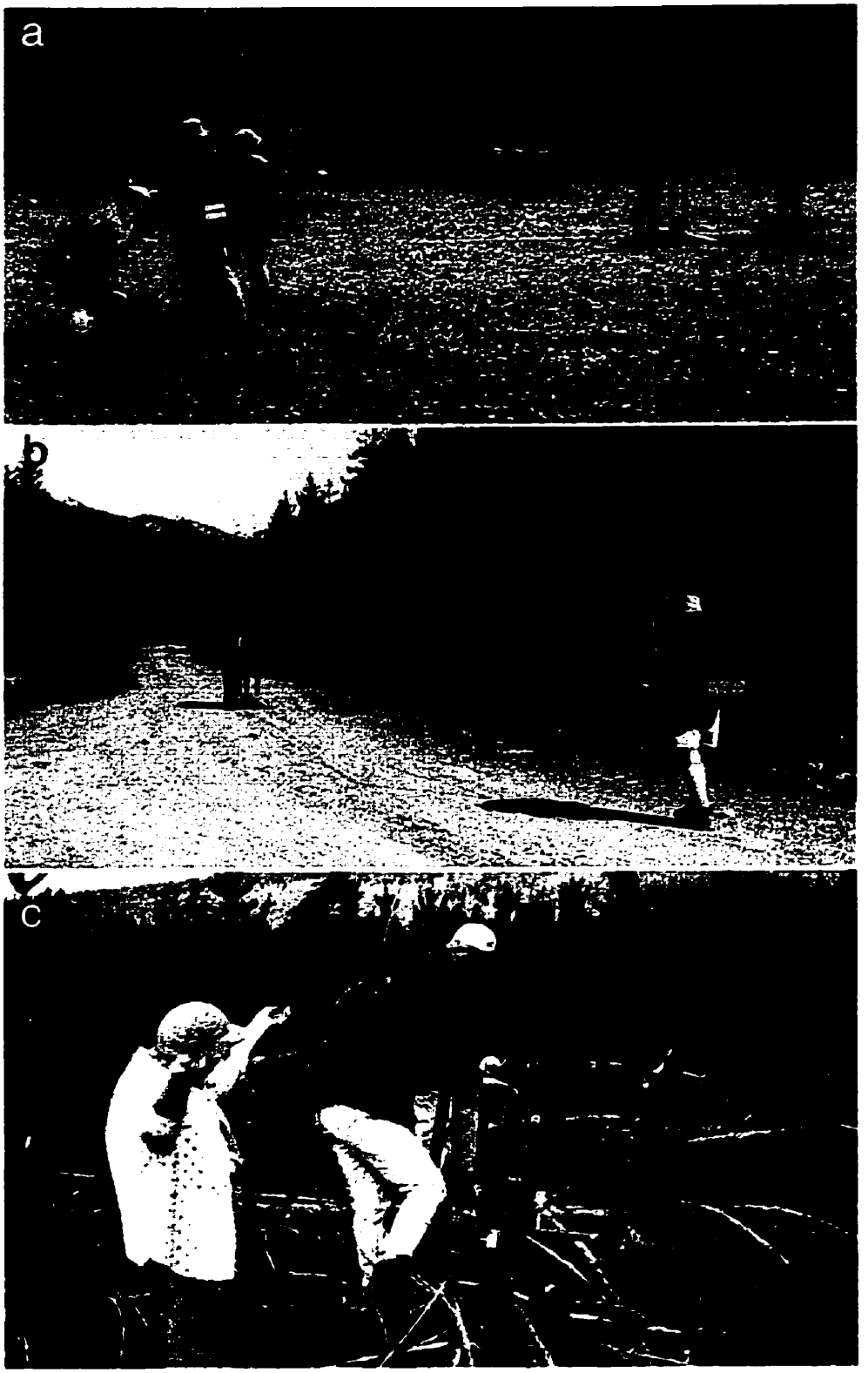


Figure 3.7. a) Testing the 50 MHz antennae in Aiyansh gravel pit. The cart assembly is shown. b) Using the backpack assembly on a logging road near Kiteen River. c) Conditions were locally difficult. Field assistant in foreground is keeping fiber optic cables from becoming tangled in the bramble.

## Microscopic and Other Investigations

A suite of clay samples for microfossil analyses was taken in the 1996 and 1997 field seasons. A pick or hammer was used to take samples, after removal of the outer 20-40 cm of weathered material. Depths below section surface varied from 1 to 7 m. Most of the samples were weathered to pale brown, but a few were fresh. Samples were stored in plastic bags for several months to a year in cool, but not refrigerated, conditions.

### *Diatom Analysis*

Diatom analysis was done on the above clay samples. Slides for diatom analysis were prepared in the SFU biogeography lab. Subsamples of each clay sample were placed in 250 ml beakers and boiled in hydrogen peroxide to remove organic components. Distilled water was added and the solution allowed to settle. After one hour, the clay in suspension was poured off. This decanting process was repeated several times, until the suspension was clear or translucent. The remaining solution was stirred and a drop of the suspension was placed on a cover slip and air dried. The cover slip was then mounted on a slide using Hyrax mounting medium and heated on a hot plate to drive off toluene. Slides were then cooled and analyzed under a light microscope at 10X, 40X and 100X magnification. 6 preparations of 13 samples were made, for a total of 78 slides.

A scan of the entire slide at 10X magnification was done initially to find diatoms, followed by examination at higher magnification to analyze individuals. Immersion oil was used to enhance features examined at 100X. Diatoms were compared to those in a number of taxonomy volumes for identification (*e.g.* Round *et al.*, 1996).

### *Foraminiferal Analysis*

The same set of clay samples were sent to Carleton University, Ottawa, for foraminiferal analysis by Tim Patterson. Samples were agitated for one hour using a Burrell wrist shaker and

then washed on a 63 μm sieve to eliminate fine sediments. Foraminifera were identified and counted using an Olympus binocular microscope, typically at 40X.

*Palynological Analysis*

Two of the samples from the clay sample suite and three from one of the sections were prepared according to the general pollen preparation procedure (Berglund, 1986, p. 456). The samples were analyzed by Marlow Pellatt of Biological Sciences, SFU.

*Radiocarbon Dating*

Several organic samples were taken from sections for radiocarbon dating. The outer 20-50 cm of section surface were removed before sampling. Samples were taken with a trowel and placed in plastic bags. Some samples were bulk dated at the Geological Survey of Canada in Ottawa, while others were dated by Accelerator Mass Spectrometry (AMS). AMS samples were wet sieved and individual faunal fragments picked out with tweezers.

*X-Radiography*

Core sample x-rays were taken to identify laminations and dropstones that may not have been visible to the naked eye. X-rays were done and the negatives developed in the Archeology Department Radiography Lab at SFU. 80 and 90 kV settings and x-ray duration times of 2 to 10 seconds were tested. The distance from the sample to the x-ray device was 91 cm.

*Scanning Electron Microprobe (SEM) Analysis*

SEM analysis was done to determine mineralogy of the Nass Valley silty clay deposits. A mineral content of primary silicates and nonswelling clay minerals is an important prerequisite for earthflow genesis (Torrance, 1988). One clay sample was sent to Vancouver Petrographics to prepare it for SEM analysis. It was dried slowly (to retain salts), impregnated with resin, and made into a thin section. The slide was thinly coated with carbon at the Physics Department of SFU and was analyzed with their SEM. Photographs were taken with Polaroid film.

# CHAPTER FOUR
# QUATERNARY DEPOSITS

## Introduction

One of the objectives of this thesis was to determine the surficial geology of the Nass River region. The mapping work provides a broad overview of the glacial deposits in the study area and the surficial geology maps are found in the map pocket of the thesis. What follows is a detailed explanation of the contents of these maps (glacial deposits).

Numerous glacial deposits were mapped in the study area. They include glaciofluvial, glaciomarine and glaciolacustrine deposits, as well as till. These are subdivided into glacial and retreat phase deposits: till makes up the former and the other three make up the latter.

## Glacial Phase Deposits

Holocene soils are well developed in low-lying areas, so glacial deposits can only be viewed beneath the 50-70 cm thick soil layer.

Two informally named tills of probable Pleistocene age were identified in the region: "Kwinatahl till" and "Kinskuch till". The latter is restricted in extent, whereas Kwinatahl till is common throughout the map area, occurring as thick valley fill (up to 50 m) that thins to a veneer on valley walls. It is present on some mountain peaks as a very patchy veneer. Both tills weather to a pale brown colour.

### *Kwinatahl till*

Kwinatahl till is a very poorly sorted, extremely compact, massive, clast-rich diamicton with angular to subangular or subrounded, granule- to boulder-sized clasts encased within a sandy, silty clay or silty sand matrix (Figure 4.1a). Clasts are commonly triangular or bullet shaped, heavily striated, and range from granule to boulder in size. Unweathered Kwinatahl till has a distinctive blue grey colour in most of the study area. Clast lithology is dominated by meta-sandstone and

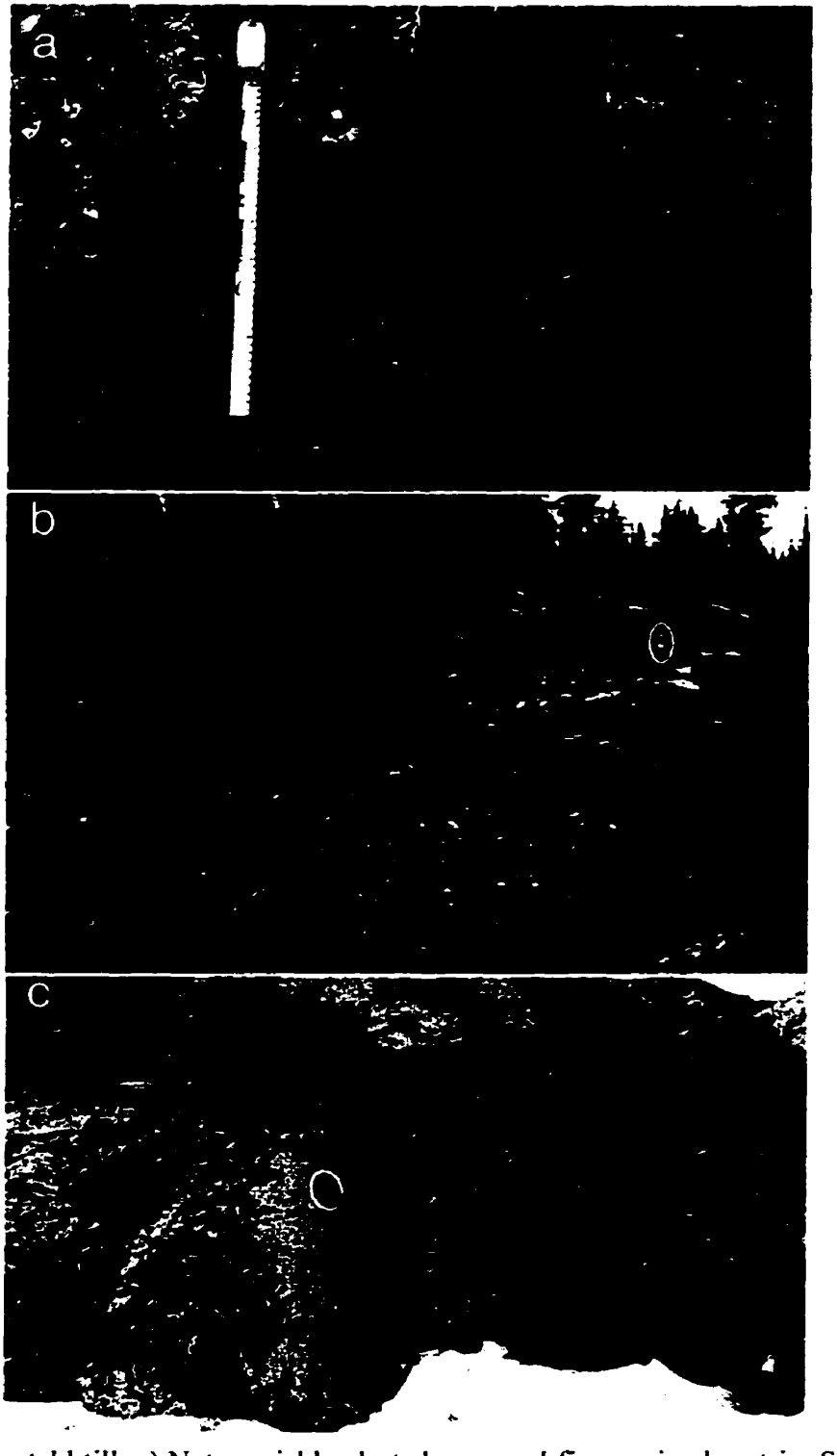


Figure 4.1. Kwinatahl till. a) Note variable clast shapes and fine-grained matrix. Scale in cm. b) Kwinatahl till exposed along Kwinatahl logging road. The till rests on heavily striated Bowser Lake Group bedrock, which is visible where figure (circled) is standing. c) Kwinatahl till at high elevation, forming a thin veneer over striated bedrock. Ice flow direction is away from viewer. Compass is circled.

meta-siltstone of the Bowser Lake Group, which give the till its characteristic colour. Bowser Lake rocks are a blue grey colour in most of the map area, but are dark grey and black in the Nass Depression, resulting in grey Kwinatahl till in this area. The softer siltstone clasts are more commonly and more heavily striated (contain many more striations) than the sandstone clasts, but in many areas all clasts are heavily striated. In the southwestern part of the study area, the till is slightly coarser textured, and is greyer or browner due to the incorporation of granitic clasts of local bedrock. These clasts tend to be better rounded. In the north, the till is grey brown due to the presence of local metavolcanic and metasedimentary rocks. However, Bowser Lake Group clasts are present in all regions. In high elevation areas, where it forms a thin, patchy cover over bedrock, the till is commonly less compact. This is probably due to weathering of the thin till layer, although it may be due to lower ice pressure at these heights. Kwinatahl till commonly lies directly upon striated bedrock (Figure 4.1b, c). Good exposures of this till can be found along Kwinatahl logging road in Kwinatahl Valley. An excellent section (Figure 4.1b) is located at UTM coordinates 480995, 6144800.

Large erratics are rare, perhaps due to the softness of Bowser Lake Group bedrock and resultant comminution to smaller grain sizes. Although the granitic bedrock of the southwestern part of the study area should theoretically favour the production of larger erratics, they are not abundant there either.

Kwinatahl till is interpreted to be a basal lodgement till, based on its massive texture, very poor sorting, striated angular to subangular clasts, high degree of compaction in most areas, lack of sand or gravel lenses, and overlying relationship with striated bedrock. There is no evidence of faulting of the till or of overlying sediments. Nor is there evidence of any draped or interbedded stratified sediments.

In the region, Kwinatahl till exhibits the same set of characteristics regardless of where it is found, making it readily identifiable. However, at a couple of sites, some differences from the norm were noted. A coarse-grained sand matrix is present at one site in the Nass Valley on the central bedrock ridge (the mainly till-covered area in the Nass Valley (Nass Valley map)). In this same area, lenses of silt and very coarse-grained gravel were seen within the till. Clasts range from

subrounded to very angular and soft ones are heavily striated. One exotic red tuff clast was identified. The till in these areas is interpreted as melt-out till. In the Hoan Creek Valley, a single location possessed visible laminations in the silty clay matrix of the till. A melt-out origin was also inferred for that till. At all other sites investigated in this study (more than 200), the till is interpreted as massive lodgement till. It is possible however, that in places it is a deformation till where structures have been eliminated, producing a massive till.

Bowser Lake Group bedrock crops out in the east and northeast parts of the study area (Figure 1.3). The presence of Kwinatahl till throughout the region is inferred to indicate that it was emplaced by western, southwestern or northwestern ice flow.

*Kinskuch till*

The Nass Depression is much flatter than the rest of the study area, and the deposits of this physiographic region are quite different. Two stratigraphically superimposed tills underlie drumlinized plains that occur between bedrock highs veneered with till. The stratigraphically lower till is Kwinatahl till (which is typically dark grey in this area), with angular clasts of Bowser Lake Group, a high degree of compaction, and a sandy, silty clay matrix. The upper till is informally named 'Kinskuch till'. It is grey brown, with an abundance of highly rounded clasts (in addition to angular ones) and a moderate degree of compaction. It is also massive, with pebble- to boulder-sized clasts and a clayey silty sand or silty sand matrix. The till ranges from 2 to 5 m in thickness. Most clasts are of Bowser Lake Group lithologies (grey, blue grey, and black meta-siltstone, -sandstone and -conglomerate in this area), but significant quantities of green, red, grey, black and maroon volcanic clasts are present as well (basalt, porphyritic rhyolite, porphyritic andesite, volcanic breccia, grey and white or beige and red tuff). Green meta-sandstone, green metasedimentary breccia, and red and olive green meta-siltstone are also present (Figure 4.2a). Clasts, even the rounded ones, can be heavily striated (Figure 4.2b), but in some places, clasts are less commonly or less heavily striated than that of Kwinatahl till.

At one section, 3 km east of the Niska Lakes (496750, 6181875), the till's matrix is horizontally bedded. Dispersed pebbles are aligned with the bedding but boulders are not.

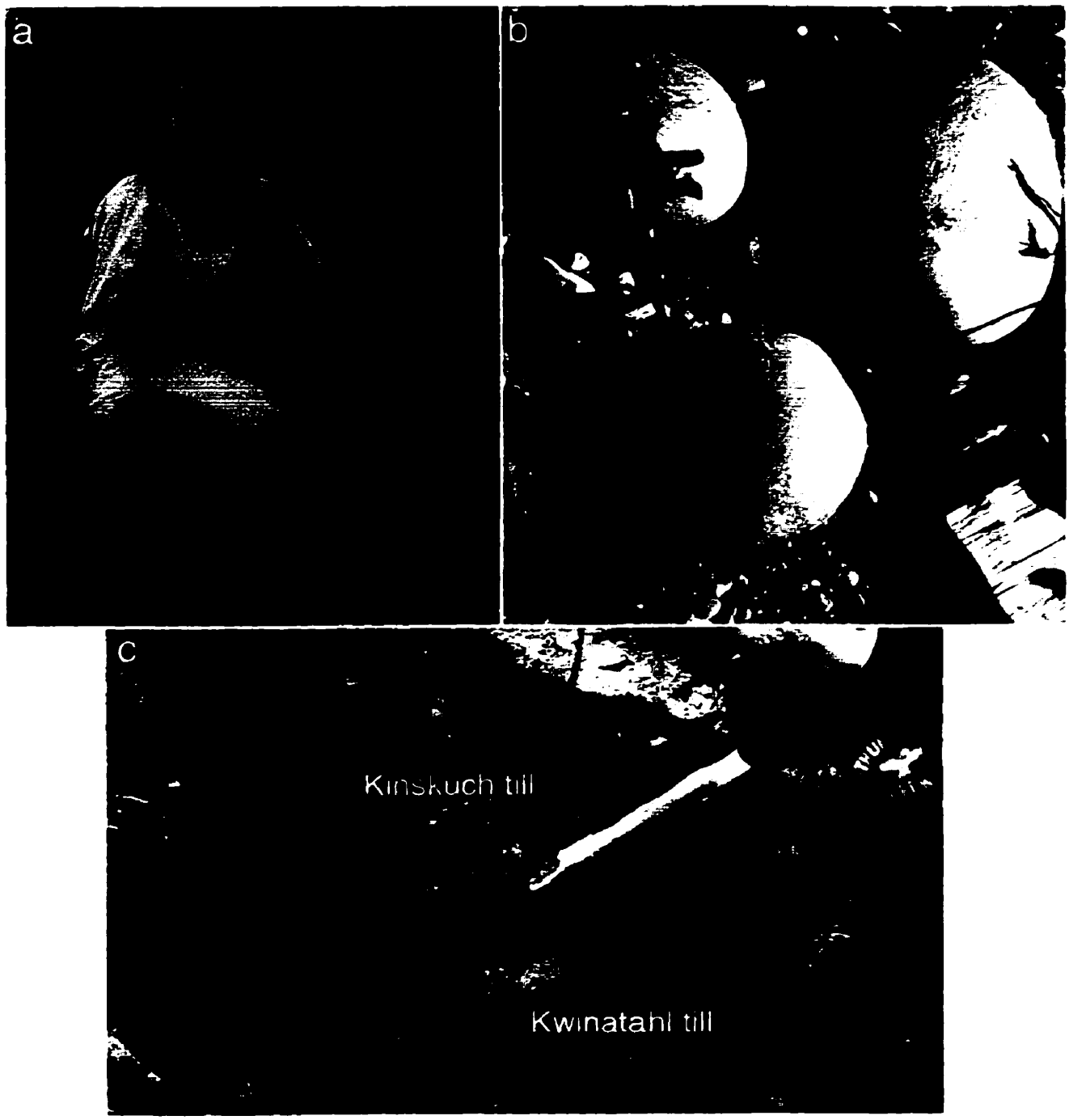


Figure 4.2. Kinskuch till. a) Author is holding green meta-sandstone clast from Kinskuch till, which overlies the Bowser Lake Group dominated Kwinatahl till. Note striated Bowser Lake meta-siltstone boulder below knee. Kinskuch till in the section is above and to right, just out of photo. b) Striated well rounded boulders of Kinskuch till. Note that angular clasts are also common. Hammer is 14 cm long. c) Assistant is pointing to irregular contact between brown Kinskuch and blue grey Kwinatahl tills.

Some of the matrix bedding is draped over the larger clasts. At another site, in the upper Kinskuch Valley, south of the gravel deposit, the till is weakly bedded and draped, showing similar bed-parallel clast alignment. This is similar to the debris flow deposits seen in colluvial fans elsewhere in the study area, so Kinskuch till is suggested to be a flow till at this location. At another site in the same area (496750, 6181875), an imbricate, 20 cm thick gravel lens was identified within Kinskuch till. The lens overlies Kinskuch till in which lodged boulders were observed. The upper part of the till (with the lens) is inferred to be a melt-out till, which overlies the lower lodgement till. Since these are two in about 30 sites where Kinskuch till was observed, Kinskuch till appears to be dominantly a lodgement till, although it is very rarely has a flow facies or a melt-out facies that overlies a lodged facies. Where lodged clasts are not visible (at the majority of sites), the till may be a deformation till that lacks any structure.

The matrices of Kwinatahl and Kinskuch tills are very similar in texture. Ternary plots show that most tills lie in the central portion of the diagram (equal parts sand, silt and clay) or toward the left, in the silty sand area (Figure 4.3). Generally, the lower contact of Kinskuch till is irregular but not particularly sharp (Figure 4.2c). The contact was gradational at several sites, (south of Paw Lake, 492310, 6192875; between Tchitin and Kinskuch Rivers, 498125, 6159850; 6 km east of the Niska Lakes, 499710, 6182350; and at Drumlin D, discussed in Chapter 8). The gradational change from Kwinatahl to Kinskuch till could mean that the change in ice flow direction, and hence source area, was gradual. The change to Kinskuch type compositions would lag somewhat behind the actual change in ice flow direction, because debris from new source areas would need time to arrive at each site. This means that in some areas, Kwinatahl till would show ice flow directions similar to that of Kinskuch till. This gradual change from one till to another suggests that there was no ice retreat between the deposition of the two tills. Ice cover and ice flow were continuous; ice flow simply changed directions.

The source area for the volcanic clasts of Kinskuch till is to the north in the Meziadin Lake area, just beyond the Kitsault Valley map sheet. It appears then that Kinskuch till formed during deglaciation, when ice flow directions were re-routed along major valleys. There is some evidence that Kwinatahl till was reworked in the late phase ice flow direction as suggested above. For

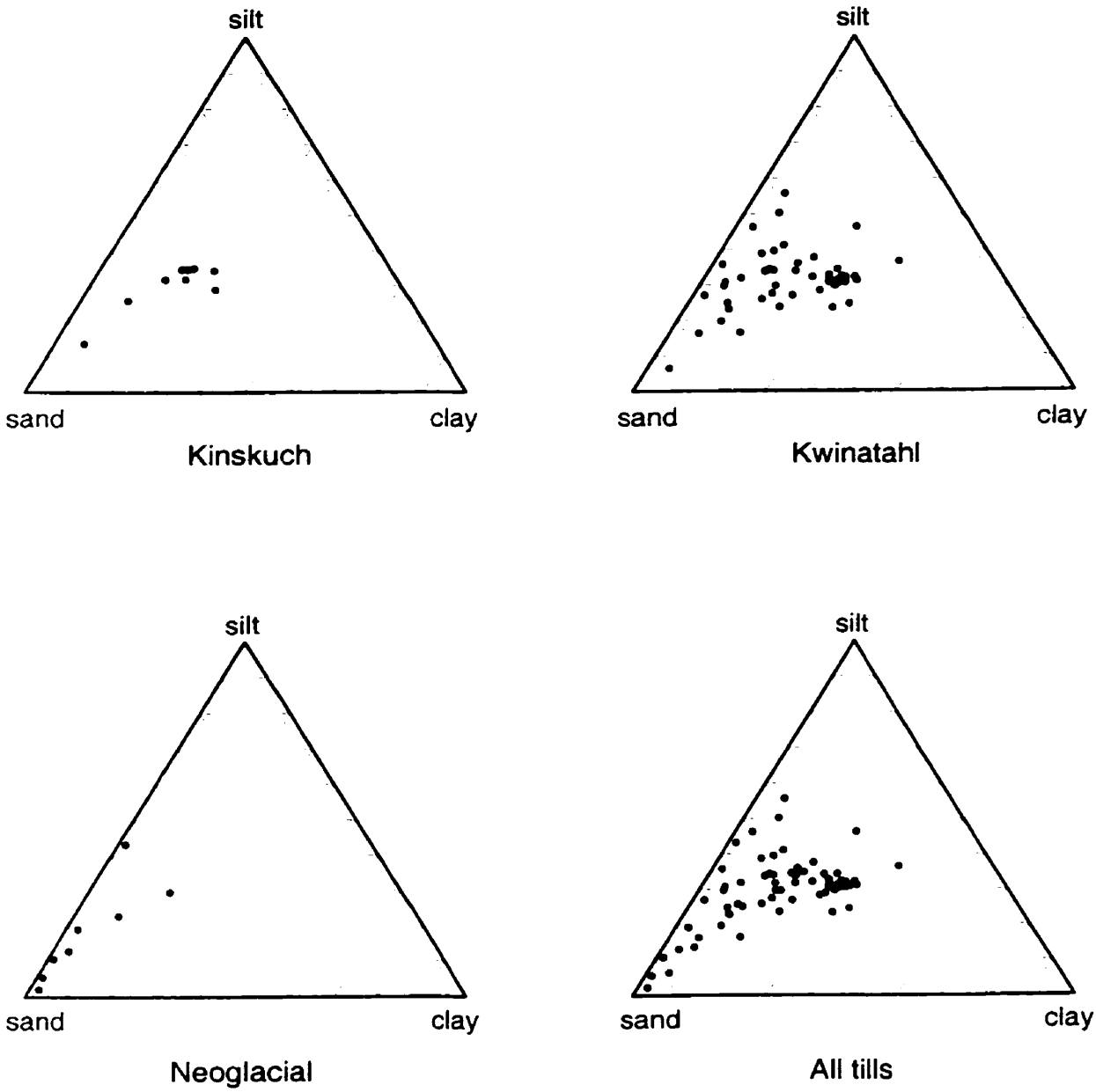


Figure 4.3. Ternary plots of the matrix of Kwinatahl, Kinskuch and Neoglacial tills. The fourth plot is all of the tills combined.

example, in the upper Kinskuch Valley near the Niska Lakes (485725, 6178475), Kwinatahl till lies directly on bedrock with striations parallel to the valley (150°).

The presence of rounded clasts in Kinskuch till implies water flow. However, ice cover was continuous, so water flow must have been subglacial (a subaerial braidplain source, for example, can be ruled out). Subglacial and englacial conduits probably existed throughout the late phase of ice flow, which was coincident with deglaciation. Subglacial sheet floods may also have occurred, but there is little evidence to support this contention. Debris entrained at all levels in the ice must have been fluvially reworked by these mechanisms and then frozen in place as conduits changed course or were abandoned (Kirkbride and Spedding, 1996), or when flooding ceased. Ongoing active ice flow then entrained both rounded fluvial and angular lodged debris in Kinskuch till, completely destroying the conduit shapes and eliminating any possibility of esker preservation. Clast interaction caused striation of all clast surfaces and the common breakage of rounded clasts.

The presence of subglacial conduits during ice retreat is proven by the style of glaciomarine deposition in the Nass Valley. Proximal glaciomarine deposition from subaqueous jets (see Drill Hole 98-5-1008 discussion, Chapter 5) certainly requires subglacial conduit drainage to have been present. The existence of subglacial flooding during late phase ice flow is harder to prove. This is elaborated on later, in Chapter 8.

### Retreat-Phase Deposits and Erosional Features

Deposits of the deglacial period are abundant. They include numerous glaciofluvial and glaciomarine deposits, and much rarer deposits of glaciolacustrine sediments. Glaciofluvial erosional features also formed during deglaciation and late phase ice flow.

There is little evidence of ice stagnation during deglaciation. In the entire map area, not a single esker has been preserved. Kettled deposits were not found anywhere in the study area. Retreat therefore must have occurred largely by calving, frontal retreat and downwasting.

*Glaciofluvial Erosion*

The main evidence of glaciofluvial activity in the study area is the presence of coarse-grained deposits. However, some fluvially scoured bedrock is present in Observatory Inlet (up to 150 m asl) and at the mouth of the Nass River (up to 40 m asl) (Nass Valley map). Cavettos, sinuous longitudinal furrows and irregular open spindles (Kor *et al.*, 1991) are found in places on vertical fiord walls (Figure 4.4a, b). There are no transverse morphologies. Water flow was parallel to ice flow down the fiords, and at the Nass River site, had a slight upward flow vector (Figure 4.4b). Modern fiord floors are under water, and no fluvially sculpted bedrock was noted on any valley floors in the region. In all cases, valley floors are heavily striated and commonly show flat bedrock surfaces (*e.g.* the medial ridge of the Nass Valley, Figure 7.1). Faceted and crosscutting striations showing both early and late phase ice flow (discussed in Chapter 8) are locally preserved on these low-lying bedrock surfaces. However, the deepest parts of the Nass Valley and the fiord floors are covered with sediment and/or water, it is not known whether or not they exhibit the same features.

*Glaciofluvial Deposits*

Glaciofluvial gravels and sands discontinuously overlie till, glaciomarine deposits and bedrock (which is locally striated) in all parts of the study area (Figure 4.4c, d). Exposures can be more than 40 m thick. The upper surfaces of braidplains in valleys are commonly boggy, a result of high water tables that are probably due to underlying glaciomarine silty clay or clay-rich till. Eskers and kame terraces are notably absent. Despite extensive braidplain deposits, there are no associated eolian deposits. This could be the result of rapid postglacial plant colonization which may have inhibited wind blown deposition. Alternatively, eolian sediments were small in volume or had limited opportunity to accumulate in basins.

Glaciofluvial sands and gravels are generally of more local provenance than tills, due to the confinement of glaciers to valley systems during ice retreat. This effect is particularly pronounced in tributary valleys of the southwest Nass Valley, where till dominated by Bowser Lake metasedimentary clasts contrasts sharply with granitic glaciofluvial deposits of local derivation.

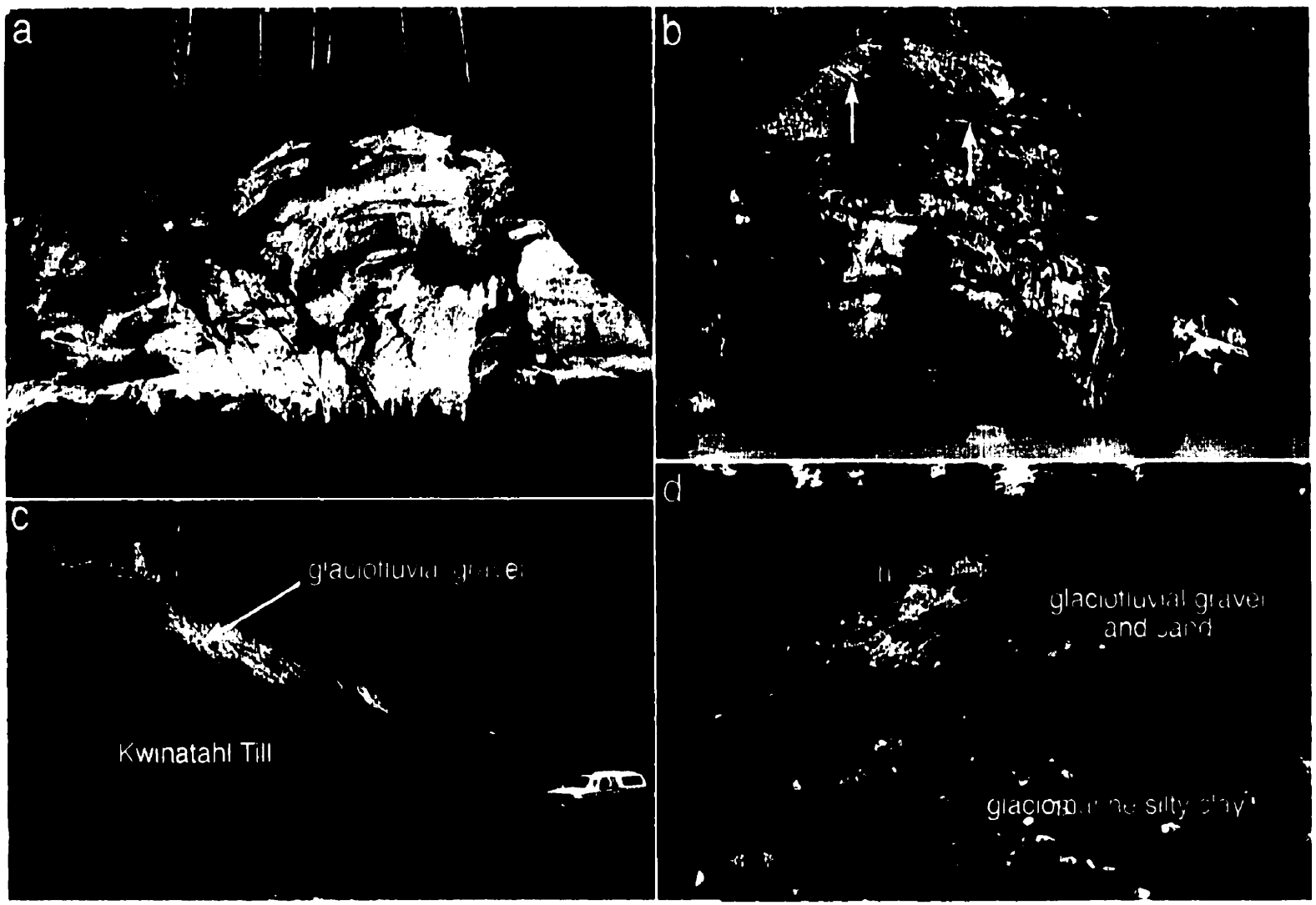


Figure 4.4. a) Fluvially sculpted granitic rock in Observatory Inlet. The locations of these sites are shown on the maps with a triple arrow symbol. Horizontal and slight upward flow formed these furrows. Flow was to the right. b) Cavetto (arrowed) and furrows near the mouth of the Nass River. A slight upward flow component was present in the down-valley flowing water. Flow was to the left. c) Glaciofluvial gravel overlying till. d) Glaciofluvial gravel overlying glaciomarine clay. Glaciofluvial deposits are typically massive, however some horizontal bedding (h) can be seen at this site. Gravel slump from above covers the silty clay in area where figure is standing.

Rare volcanic clasts from Kinskuch till were found in a glaciofluvial braidplain just south of Kinskuch Valley, but these are still of local derivation, since Kinskuch till occurs just up-valley.

Glaciofluvial deposits throughout the study area consist of moderately to poorly sorted fine-grained sand to boulder gravel. Cobble and boulder gravel are most common. Clasts are subrounded to well rounded and unstriated. Deposits are typically completely massive but vague horizontal bedding can be seen locally. Clasts may or may not be imbricate. Deposits of sand size and finer material are rare, and generally contain lenses or lags of pebble gravel. Fining-upward beds, planar tabular crossbedding, trough crossbedding and coarsening-upward sequences are extremely rare. Ripples, pebble or boulder lags and horizontal laminations are also rare. Finer-grained beds tend to have draped lower contacts while coarser-grained beds have erosive ones.

The region's meltwater rivers are interpreted as gravel dominated river systems, many of which were probably braided. The majority of glaciofluvial plain deposits were identifiable on air photographs as braidplains. Gravelly braided river systems are the main type of river in modern glacial settings (Rust and Koster, 1984). This is true for the study area, as braided rivers currently drain modern glaciers (*e.g.* Kshwan River, Kitsault Valley map). A braidplain interpretation for the flat, gently downvalley dipping gravel bodies in many valley bottoms is therefore deemed reasonable.

Glaciofluvial Braidplains

There are several glaciofluvial braidplains in the study area. The Sutton and Kshwan braidplains just south of the Cambria Ice Field are graded to 150-160 m asl. Two major braidplains are found in the Nass Valley, the Nass Braidplain and the Aiyansh Braidplain (Figure 7.1).

The Aiyansh Braidplain appears to be quite a thick deposit (more than 75 m) and it has remained largely unmodified since its emplacement. The Nass Braidplain, on the other hand, is over 40 m thick (Figure 5.11), has been heavily dissected by fluvial erosion since initial deposition, and has been further modified by earthflows (Nass Valley map). Both braidplains dip gently to the southwest, from about 210 m in their upper reaches to elevations between 135 and 150 m at their termini. Their flatness, continuity, and downvalley dip indicate subaerial deposition.

Clast size does not diminish downstream. Exposures larger than 1 or 2 m high are rare in these sediments.

In its upper reaches, the Nass Braidplain has a higher abundance of finer-grained sediments (fine-grained sand to pebble gravel) than in its lower reaches, where pebble/cobble/boulder gravel predominates. These deposits grade or change abruptly laterally to coarser beds. Braidplain deposits overlie glaciomarine silty clay, with which there is a sharp contact. In some places the contact is loaded, with load casts up to 40 cm deep. Paleoflow measurements on the upper braidplain range from 170° to 233°, indicating a general southwest flow direction, albeit one that is highly variable.

The Aiyansh Braidplain is generally composed of sandy pebble/cobble/boulder gravel, although it is finer-grained in its terminal areas. The contact with underlying glaciomarine sediments is visible at the Tseax Creek section (Figure 5.18) and at a section just south of the Kiteen River section (Figure 5.10). Both contacts are erosional.

Glaciofluvial Deltas

Many deltaic deposits have been identified and mapped in the study area. They are generally coarse-grained, poorly sorted, and composed of topset/foreset bedsets. Deltaic deposits have been used to determine various marine limits.

A large delta at Kitsault (Nass Valley map) is graded to 230 m, the highest marine limit in the region and in British Columbia. Coarsening-upward sediments indicate progradation of the delta. Deltaic sediments are interbedded with till in the delta's lowest reaches, suggesting an ice contact origin (subaqueous fan) that changed to a proglacial style of deposition as ice left the area. This is the only location where this change is recorded – ice proximal deposits probably did not develop into deltas elsewhere (unless the evidence for this is buried). The delta backs onto a mountain side, so there is no ice-contact face at the up flow end of the delta. A glaciofluvial plain may have existed in the past, but all that remains of it are irregular glaciofluvial deposits in the Illiance River Valley (Nass Valley Map). The interbedding of till and gravel results in a complex aquifer/aquitard relationship, evidence of which can be seen below the high tide line during low tide, where water

from the deltaic gravel seeps out over till. The deltaic gravel also overlies striated bedrock in places. Remnants of another delta graded to 230 m are found near the mouth of the Nass River, on the south slope of the Nass Valley (Nass Valley map).

At a delta graded to 150 m asl at Greenville (Nass Valley map), both topset and foreset beds are exposed. The foreset beds dip gently and become tangential down-dip. Silt, sand and gravel interbeds make up both the topset and foreset beds, but the uppermost topset beds are mainly pebble gravel (Figure 4.5a). Small outsized clasts are evident within the foreset beds.

A delta north of Ksedin Creek (Nass Valley map) has its highest level graded to 230 m. Foresets and bottomsets are visible in Figure 4.5b, but these have been erosionally truncated by a second generation of foresets. The bottomset beds are mostly sand, while the foresets are sand and gravel. At a lower elevation further down a forest road, gravel topset and sandy gravel foreset beds are present. This delta is a good example of the 'telescoping' that occurs when a delta forms in a setting of continued sea level drop and early delta deposits are incised with new ones forming at lower elevations. The elevation of Figure 4.5b is about 70 m, but topsets are not visible so sea level must have been higher. The topsets below are graded to about 50 m. Paleoflow is toward 290°, indicating flow towards the Nass basin from Ksemamaith Creek.

A small delta at 300 m in Hoan Valley (Nass Valley map) has a westward paleoflow direction. Since striation data is also westerly (up the valley), an ice body retreating eastward must have deposited at least part of the till that underlies the delta and later, an ice-dammed lake must have formed there. The lake may have been blocked up-valley by montane glaciers. This is a freshwater delta and thus is not an indicator of marine limit. The delta is composed of poorly sorted glaciofluvial deposits, with clasts that are parallel to bedding and beds that become less steep towards the top (Figure 4.5c). Some beds are wavy. This style of sedimentation is interpreted as an underwater conical delta, where the prodelta slope changed angles due to continued aggradation (Nemec, 1990). The delta did not complete its evolution into a Gilbert-type delta.

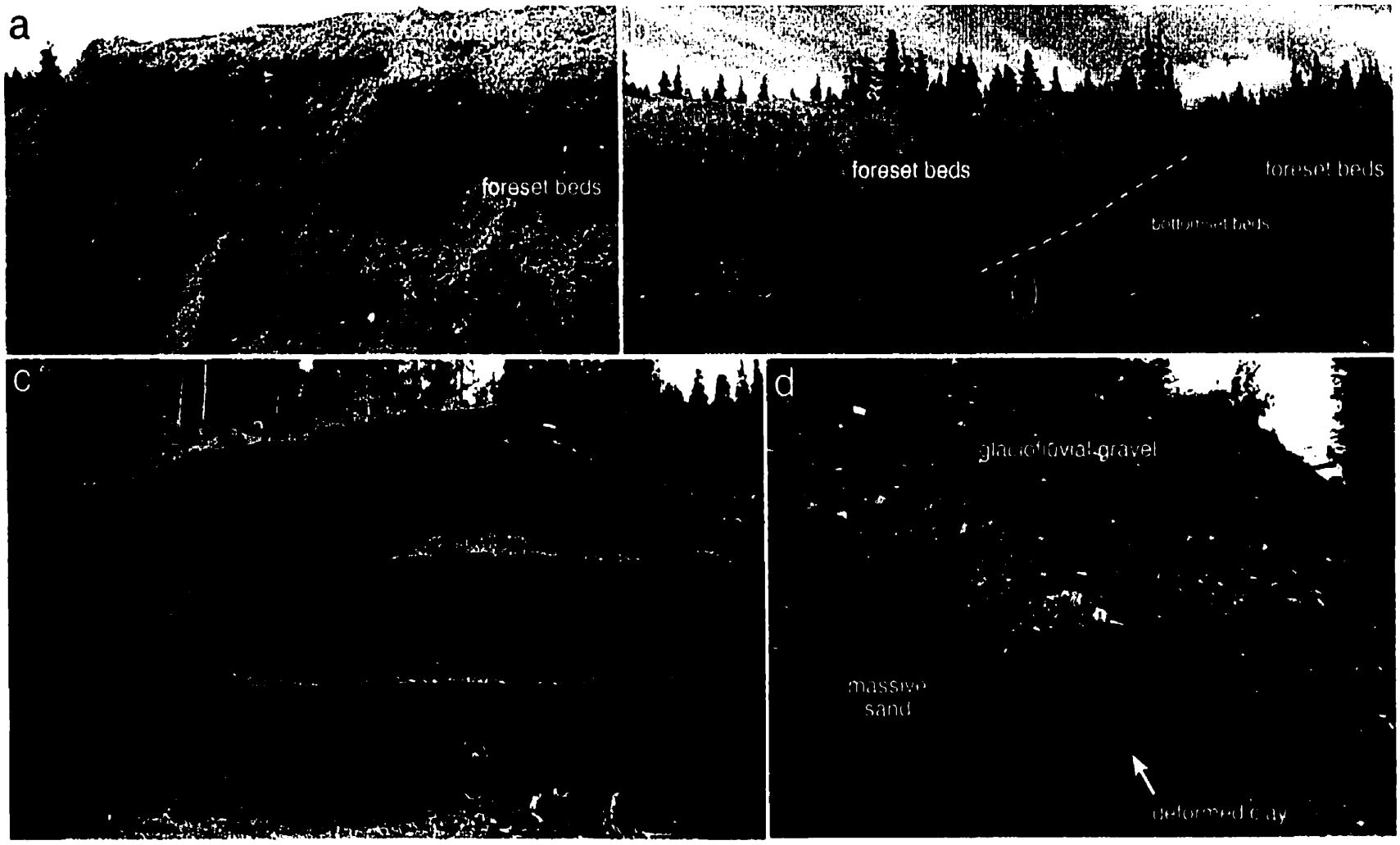


Figure 4.5. a) Delta near Greenville. Topset beds are coarser-grained than foreset beds. b) Delta north of Ksedin Creek. Foreset beds above figure's head erosionally truncate foresets and bottomsets to the right. b) Conical style delta near Hoan Creek. Figure in foreground is circled. d) Deformed clay within massive sand (just left of figure), overlain by horizontally bedded gravel and sand.

*Glaciolacustrine Deposits*

Glaciolacustrine deposits are extremely rare in the study area, indicating that ponding of fresh water was uncommon during deglaciation. Small deposits of laminated silt, clay and sand with dropstones were found at a few locations in Ksedin Valley, Hoan Valley, Kinskuch Valley, Nass Valley and the Nass Depression. These deposits are underlain and locally overlain by more extensive glaciofluvial gravels and sands. They are generally 1-10 m thick, but a 20 m thick deposit is present in Ksedin Valley. Most are above marine limit. A glaciolacustrine origin is therefore inferred for these isolated deposits.

At one site in the Nass Depression, (x in Figure 8.2) pebble/cobble/granule gravels fine-upward to granule/fine-grained sand/silt, and are sharply overlain by clay laminations. The fine-grained sediments in this locality may be an abandoned fluvial channel, but may also be glaciolacustrine.

The Hoan Valley delta described in the last section is evidence that a glacial lake existed in the valley, despite the lack of preserved fine-grained sediments in the area. Further down valley at elevations of 230 and 240 m asl, there are ice contact deposits of Kwinatahl till interbedded with gravel, sand and silty clay. Laminated silty clay and fine-grained sand contain dropstones, while the gravel and sand are massive or horizontally bedded. Clasts are aligned along bedding. Yellow brown massive clay is deformed within the massive sands. Rapid sedimentation of the coarse-grained upper beds may have caused the deformation (Figure 4.5d). These deposits are interpreted as subaqueous fans (ice proximal deposits) deposited in a glacial lake, because they are too high in elevation to be marine.

*Glaciomarine Deposits*

Glaciomarine sediments are extensive, especially in the Nass Valley. They can be divided into coarse-grained ice proximal and fine-grained ice distal deposits.

Ice Proximal Deposits

Ice proximal deposits are coarse-grained but well sorted, differentiating them from the majority of glaciofluvial sediments. They are rarely exposed in section.

At a 5 m high exposure near Gitwinksihlkw, dark grey, medium- to coarse-grained sand is interbedded with granule to pebble gravel that is not imbricate. Thin laminae of grey or yellow brown sand commonly cap fining-upward beds. Sediments are moderately to well sorted, with abundant unstriated dropstones. This is interpreted as an ice proximal subaqueous fan deposit (Figure 4.6a, b).

Silty very fine-grained sand with dropstones in a small bay at the mouth of Alice Arm, and sand/clay beds in the Kwinamuck Lake area that contain dropstones may be similar types of ice proximal deposits. At another site just west of the point where the Kwinatahl River meets the Nass River, extensive dropstone-free silty clay deposits are commonly interbedded with gravel and sand. Sandy deposits within the silty clay unit are also found up to 2 km south of this point. A nearby delta or subaqueous fan may also be indicated by these deposits.

Ice Distal Deposits

Thick (up to 30 m) blue grey silty clay deposits which weather to pale brown are extensive in the Nass Valley north of the Aiyansh lava flow. They are also present in the southwest Nass region near Greenville and at various low elevation locations along Observatory Inlet, Alice Arm and Hastings Arm, including the Anyox town site. These gullied deposits are generally massive (Figure 4.6c) and no macrofossils were found despite the large number of exposures visited (exposures are typically 1-2 m thick). Dropstones and/or weak lamination are present at about 50% of the sections. Rhythmic laminations with dropstones are present near Anyox, while simple laminations with granite dropstones are found at the Hastings Arm Section (Figure 5.4). The clays are highly cohesive, a common characteristic of glaciomarine clay. They all lie below the highest marine limit of 230 m asl.

The Nass Valley clay strata generally overlie Kwinatahl till and/or ice proximal glaciomarine deposits and locally underlie glaciofluvial gravel and sand.

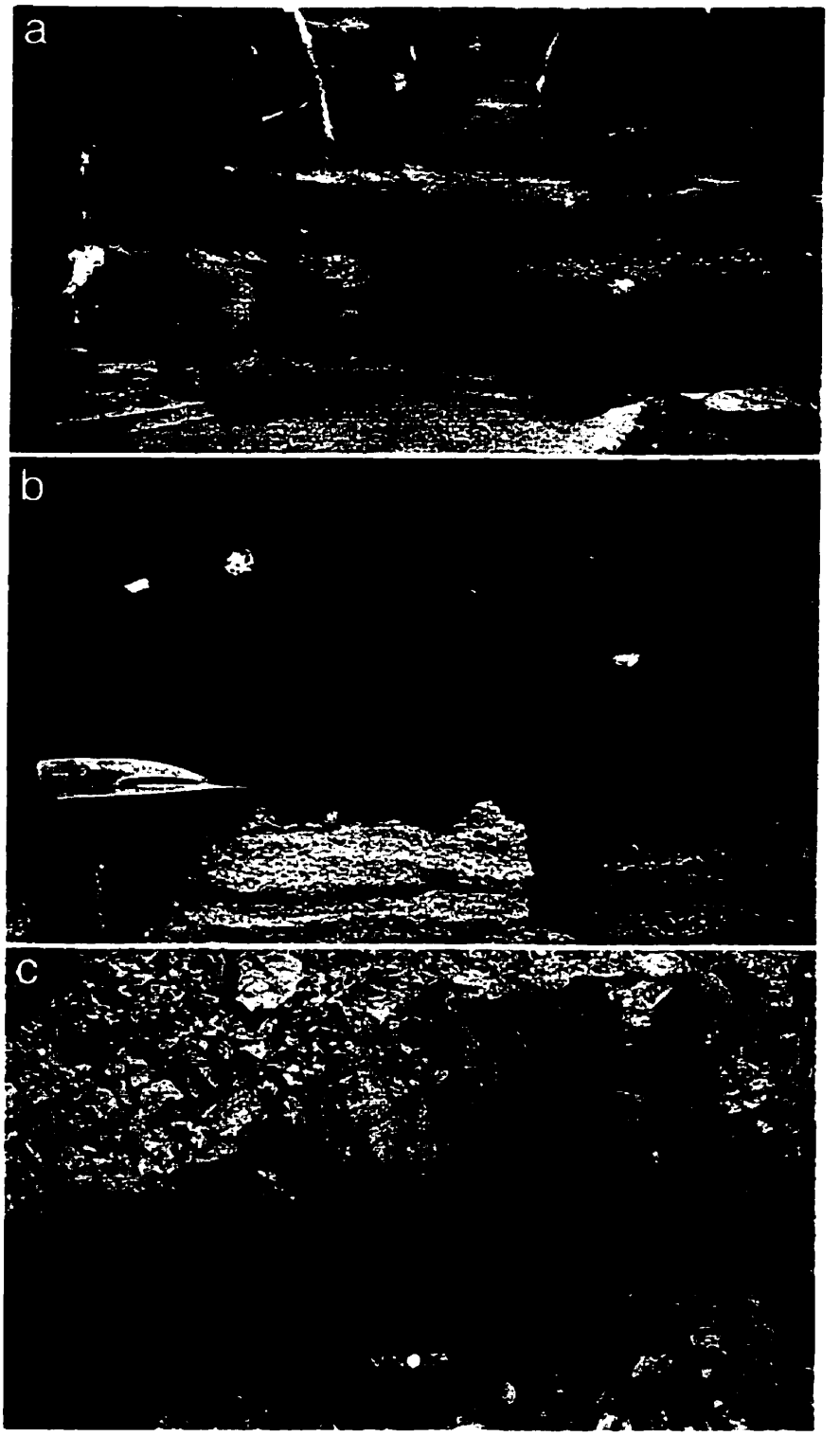


Figure 4.6. Glaciomarine sediments. a) Proximal glaciomarine deposit with dropstones. Sand beds are dark toned, while silt beds are light toned and very thin. Gravelly beds are also light toned but are not thin. Hammer is 14 cm long. b) Close up of a), in vicinity of hammer. Note the very thin silt beds and the dropstones. c) Massive glaciomarine silty clay. Light and dark toned variations are due to weathering and root casts (not bedding). Lens cap is 49 mm in diameter.

Fossil marine shells have been found in low elevation clay deposits near Anyox and Stewart (Hanson, 1935, Sharp, 1980), but their glacial context is uncertain. It is possible that these sediments are Holocene in age (see Previous Work, Chapter 2). No shells were found by the author in any glaciomarine deposits in the region.

Glaciomarine sediments in the Nass Valley (and elsewhere) are interesting in that they appear to contain no fossils (Appendix E), in contrast to the fossiliferous glaciomarine deposits to the south (Clague, 1984b). Something made the area a hostile environment for life forms. When no fossils were found in the silty clay, the question arose as to whether these deposits were laid down beneath an ice shelf (no light for photosynthesis) or whether they were deposited in a glacial lake.

The ice shelf theory can be immediately discounted, because pollen that accumulated on the ice surface would be released to the fiord floor upon melting of the shelf. There is no pollen in the silty clay (Appendix E), so a quiet ice shelf environment probably did not exist.

The deposits are inferred to be glaciomarine as opposed to glaciolacustrine for several reasons. Since marine limit is 230 m asl and silty clay deposits are common below 230 m asl, but never occur above this height, it is a logical assumption that they are marine deposits. Also, one of the 230 m deltas is found at a tributary valley near the mouth of the Nass River, so the valley was certainly inundated by marine water to a height of 230 m, although the location of the ice front at that time is not known.

Dropstones are present at about 50% of the silty clay exposures in the Nass Valley, but are not abundant at any of these sites. The dropstone paucity, the great thickness of clay and the lack of fossils (including pollen) together suggest that sedimentation rates were very high and that basinal waters were turbid. Areas with more dropstones were probably sites farther removed from the ice front, where sedimentation rates were lower.

Biologically barren sediment of this type is common in modern tidewater glacier fiords in Alaska (Cowan *et al.*, 1997), where sedimentation rates are high and photosynthesis cannot occur due to insufficient light penetration through the turbid water. However, fossils are common in glacial sediments of the Juneau (Miller, 1973) and Terrace areas (Clague, 1984b). In Arctic

fiords, burrowing organisms are only found in areas of lower sedimentation rates (Syvitski and Hein, 1991). I suggest then, that an extremely high sedimentation rate is responsible for the lack of fossils in the Nass Valley. The Juneau and Terrace areas have much more complex bedrock geology and different styles of deglaciation (*e.g.* punctuated by readvances and stillstands), so sedimentation rates were probably lower. The Nass area's soft Bowser Lake Group lithologies allowed a higher amount of glacial erosion and deposition to occur, resulting in the voluminous glaciomarine deposits of the Nass Valley.

It is argued that earthflows, common in marine sediments near Terrace (Clague, 1984b) and in Nass Valley silty clay deposits, provide postdepositional evidence of a glaciomarine origin for the silts. The shear strengths of Nass Valley clays are extremely low (Geertsema, 1998), a common characteristic of marine quick clays (clays that liquefy easily). The SEM analysis of this study (Appendix E) and the liquefaction of the clay by our vibracoring further indicate a quick clay tendency.

Finally, fiords in northern B.C. generally show the same depositional sequence as that seen here: till overlain by interbedded ice contact deposits and capped by glaciomarine mud (McCann and Kostaschuk, 1987).

It is concluded, therefore, that the Nass Valley silty clays are distal glaciomarine deposits related to the 230 m and lower sea level stands. Coarser sediments are proximal glaciomarine deposits that formed prior to the distal silty clay deposits that overlie them. Some silty and sandy interbeds may have been deposited as distal facies of fan deltas in basinal areas near the valley edge.

Considering the great width of the valley (10-15 km), deposition of 25-35 m of fine-grained sediment is taken to indicate an immense amount of clastic influx. Since most of silty clay deposits are massive, it is possible that deposition was continuous. However, the presence of laminations at some locations indicates at least some minor fluctuations in deposition. It is also possible that the massive nature of Nass Valley clays is due to liquefaction, since laminated structures are absent at most sites and the clays are known to be readily liquifiable (SEM Analysis, Appendix E).

All evidence points to continuous, rapid retreat of ice in the Nass Valley. Morainal banks or subaqueous fan ridges indicative of a stillstand were not revealed by drilling, although more drilling might reveal such morphologies. Extremely rapid retreat of tidewater glaciers terminating in deep water is common in Alaska (Paterson, 1994) and is probably what happened in the Nass Valley. In fact, Powell's (1981) "Facies Association I: Facies of rapidly retreating tidewater glaciers with ice fronts actively calving in deep water" best describes the sediment package of the Nass Valley. In this scenario, till, gravel and sand are deposited at the ice front. Subglacial meltwater jets deposit gravel and sand that fine distally to laminated sand and mud. Mud (possibly with dropstones) is deposited beyond this zone, but intertongues with it. The input of coarse debris by fan deltas and valley-side talus is also common in fiord settings, but the main clastic input source is the ice front (Syvitski *et al.*, 1986).

The Nass Valley basin is quite different from that of the Terrace-Kitimat-Skeena area to the south, but fiord depositional processes are affected by a number of parameters, including length and depth of the fiord (Paterson, 1994), climate and glacial history. It is not uncommon for basin fills to be unique to individual fiords (Syvitski, 1993). Stillstands occurred in the Terrace-Kitimat area where bedrock ridges and narrowing of the valleys to 3-5 km wide provided pinning points (Clague, 1984b). The Nass Valley is wide; there are no pinning points. Constrictions do occur east of the medial bedrock ridge north of New Aiyansh and down valley near the mouth of the Nass River, but any sediment accumulations indicating stillstands that may have formed at these locations are now covered by glaciofluvial and fluvial deposits, respectively.

## Postglacial Deposits

### *Colluvial Deposits*

Colluvial deposits are the most abundant postglacial deposits of this predominantly mountainous region. Along with bedrock, they comprise the majority of the mapped units on both maps. Debris flow scars and avalanche tracks are abundant on steeper slopes. On steep valley sides, colluvial debris consists of a mixture of reworked till, glaciofluvial or marine deposits,

and local bedrock, and most commonly occurs as a thin veneer over bedrock (drift veneer of Clague, 1984b). Colluvium generally lacks a silt/clay fraction (except where glaciomarine silty clay is a major constituent), or contains only a small proportion of silt. Clasts are almost entirely of local derivation (>95%) and are mainly angular; subrounded clasts are common in debris flow deposits. Colour is typically brown, clasts are unstriated, and the deposit is loose (easily dislodged with a pick).

Rockfalls can produce abundant debris that includes huge angular boulders (>2 m in diameter). Colluvial aprons or scree slopes are formed mainly by rockfall processes on steep mountain slopes (Figure 4.7a).

Colluvial fans (debris flow cones) are mainly composed of debris flow sediments and form cones at the foot of mountains (Figure 4.7b). Granule- to boulder-sized unstriated clasts are set in a medium- to coarse-grained sand or silty sand matrix. Clasts are highly angular to subrounded, with angular clasts generally dominant. The deposits are very poorly sorted, massive to vaguely bedded, with clasts commonly protruding into overlying beds (Figure 4.7c). The finer-grained beds can be locally foliated, indicating shear plane formation within a slowing debris flow.

Landslides include localized rockfalls and earthflows in fine-grained glaciomarine sediments. Undercutting by streams seems to be an important factor in earthflow initiation.

*Alluvial Deposits*

Alluvial plains (river floodplains) are found throughout the region. Alluvial plains have been formed by the Nass, Kshwan, White, Kiteen and Kinskuch rivers. The Nass River, the largest river, is incised into bedrock in the White River and upper Nass Valley areas. It has incised through glacial sediments and into underlying bedrock. As a result, it is straight to sinuous and has a single channel. In the lower Nass Valley, the river cuts into glacial sediments alone. In this locality, it takes the form of a wandering gravel bed river, with up to three channels flowing past forested medial and lateral bars. This form persists into in its sandy lower reaches. The Aiyansh lava flow has modified the river's planform by forcing the river against a bedrock ridge in the vicinity of Gitwinksihlkw. At this locality, the river flows rapidly through a narrow gorge, temporarily becoming

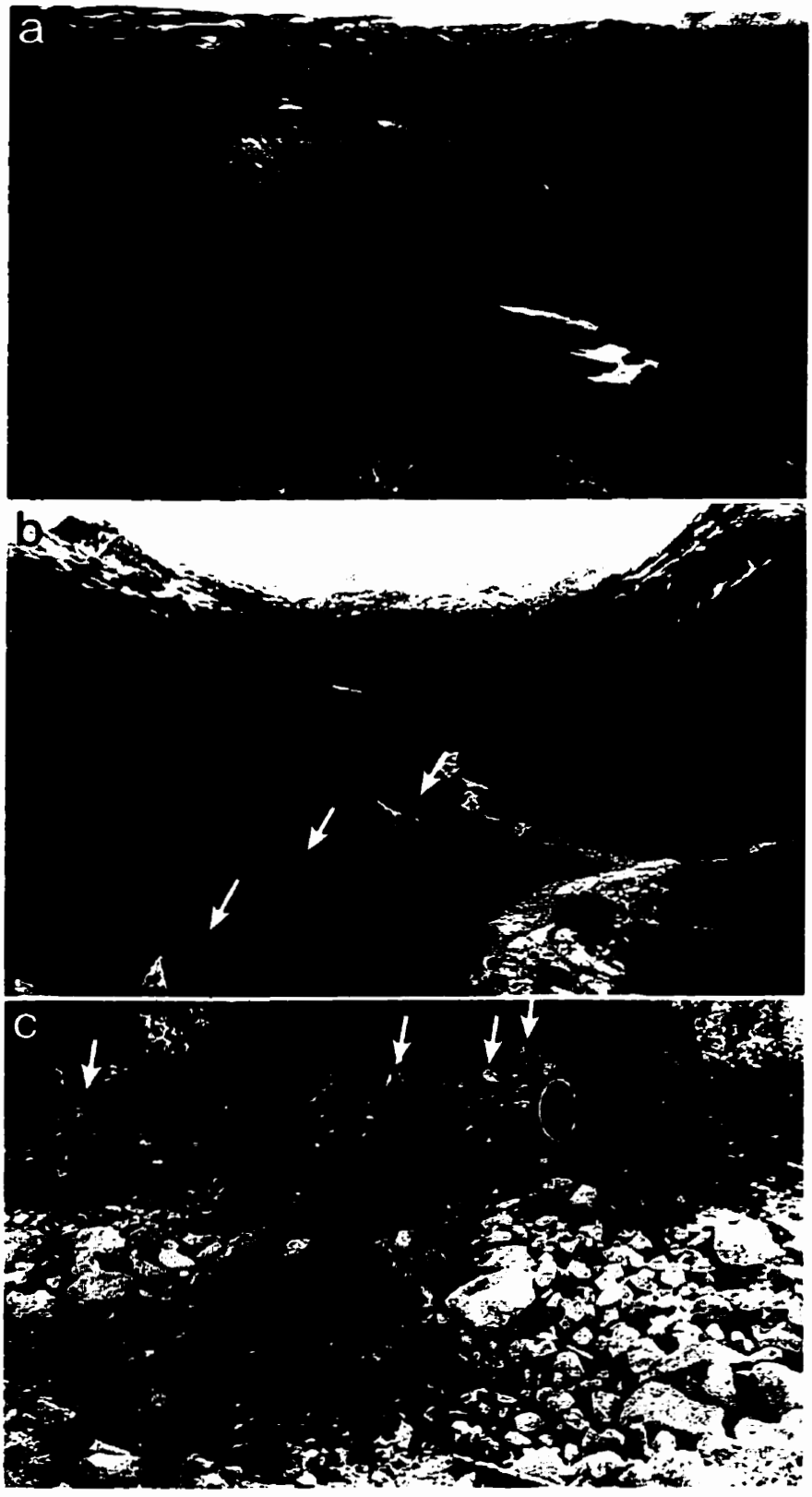


Figure 4.7. Colluvial deposits. a) Colluvial apron, formed mainly by rockfall. b) Typical colluvial fans or debris flow cones (arrowed). c) Colluvial fan debris flow sediments, with protruding clasts arrowed. Figure for scale circled.

single channeled again. An alluvial floodplain just southwest of the lava flow is forested and was probably abandoned when the lava flow formed. Grey to dark grey clayey silt and clay that may contain woody debris or other organics are present in some of the abandoned and slower flowing channels of the Nass River. Units can be massive or laminated. Heavy mineral concentrations (small placers) are present in areas of granitic bedrock. All of the other rivers have a braided planform over at least part of their alluvial plains, changing to wandering gravel bed rivers in places.

Stable and unstable bars are common components of alluvial plains. The former are forested. Clasts are subrounded to well rounded (commonly discoid), imbricate, and sediments range from fine-grained sand to cobble gravel. Beds are poorly to well sorted, and sorting across bar surfaces is common (fining downstream). Vague and obvious horizontal beds are locally visible. Lower contacts of coarse beds are erosive or sharp. Fines are common in abandoned and slow flowing channels of all alluvial deposits. Bowser Lake Group rocks are common constituents of the coarser fraction, but granite and syenite clasts are more abundant in the west, as these lithologies withstand fluvial transport better. Metavolcanics are present near the source terrane.

*Alluvial Fan Deposits*

Alluvial fans form where rivers from small valleys enter major valleys, a common occurrence in a region with an abundance of hanging and tributary valleys as in the Nass region. Most alluvial fans are active, probably due to the high rainfall and high relief of the area. It is possible that the majority of each fan deposit is paraglacial (Ryder, 1970), but the surface portions are definitely Holocene in age. These units are good aggregate sources, but are neither as extensive nor as thick as the glaciofluvial deposits. Alluvial fans are made up of poorly to very poorly sorted pebble to boulder gravel with a sandy matrix. Clasts are subrounded to angular, but are generally more rounded than those of Kwinatahl till or colluvial fans. Clasts are mostly of local provenance (>95%), so granitic lithologies dominate in the west, while Bowser Lake Group rocks dominate in the east. The debris flow component of the deposit consists of beds of massive, matrix-supported diamicton that commonly drape underlying beds. Outsized clasts commonly project

into overlying beds. Clasts can be >1 m in diameter. Pebbles and cobbles are aligned parallel to the horizontal or draped bedding in the beds that have a sand matrix. The fluvial component is most commonly clast-supported, with localized imbrication showing down-fan paleoflow directions. Subhorizontal bedding that varies from well defined to indistinct is common, dipping gently down-fan. Crossbedded gravel sets are rare. In steeply sloping areas (proximal fan regions), beds can be contorted by downslope movement (Figure 4.8a). In distal fan areas, sandy deposits are common.

A very recent debris flow deposit was observed on the Dragon Lake alluvial fan complex. A series of three stream and debris flow fed fans have coalesced at this location (Figure 7.1, Nass Valley map). On the southernmost fan, a new channel has been cut by a large debris flow. The creek has been relocated to this new channel. Levees 3 m high are visible down each side of the channel (Figure 4.8b) and there is also one in the channel centre. Gravel flowed into parts of the surrounding forest floor without disturbing tree growth. A fabric bed blanket wrapped around a log caught in the flow shows that this was a very recent event. Logs and other woody debris are common within the bouldery flow.

A little further south, deposits of the old channel of this fan are present. Both old and new flows exhibit angular to subrounded boulders up to 70 cm in diameter. Sand and gravel are also present and the deposit is poorly sorted. Granite from the mountain side is the dominant lithology, but Bowser Lake Group sedimentary rocks are also incorporated.

Fan deltas are alluvial fans that have built out into water (Figure 4.9a). Their sediments are moderately to well sorted, with subrounded to round clasts of local bedrock. At one site in Hastings Arm, sand, pebbles, cobbles and boulders are sorted by size on the fan surface. Boulders are found near the high tide line, cobbles form beaches at lower levels, and sand-dominated areas are found in the central area near low tide line. Presumably, sand and finer-grained sediments are present beneath the water surface.

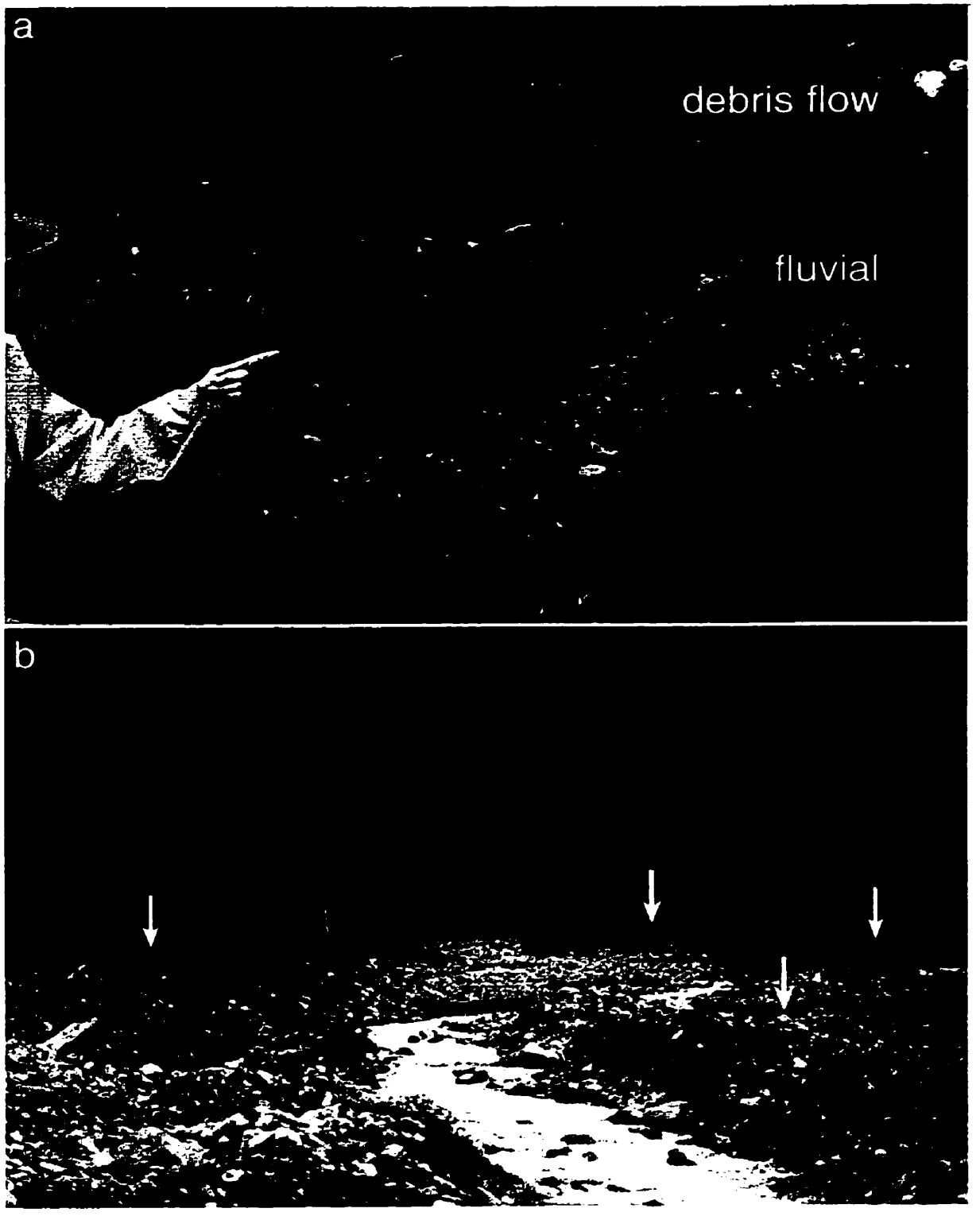


Figure 4.8. a) Deformed fluvial beds of sand and clast-supported sandy gravel overlain by matrix-supported debris flow bed with somewhat aligned clasts in proximal fan region (finger is pointing to fluvial sediments). b) Recent debris flow deposit in the Dragon Lake area. Large levees (arrowed) can be seen on either side of the flow as well as in the centre.

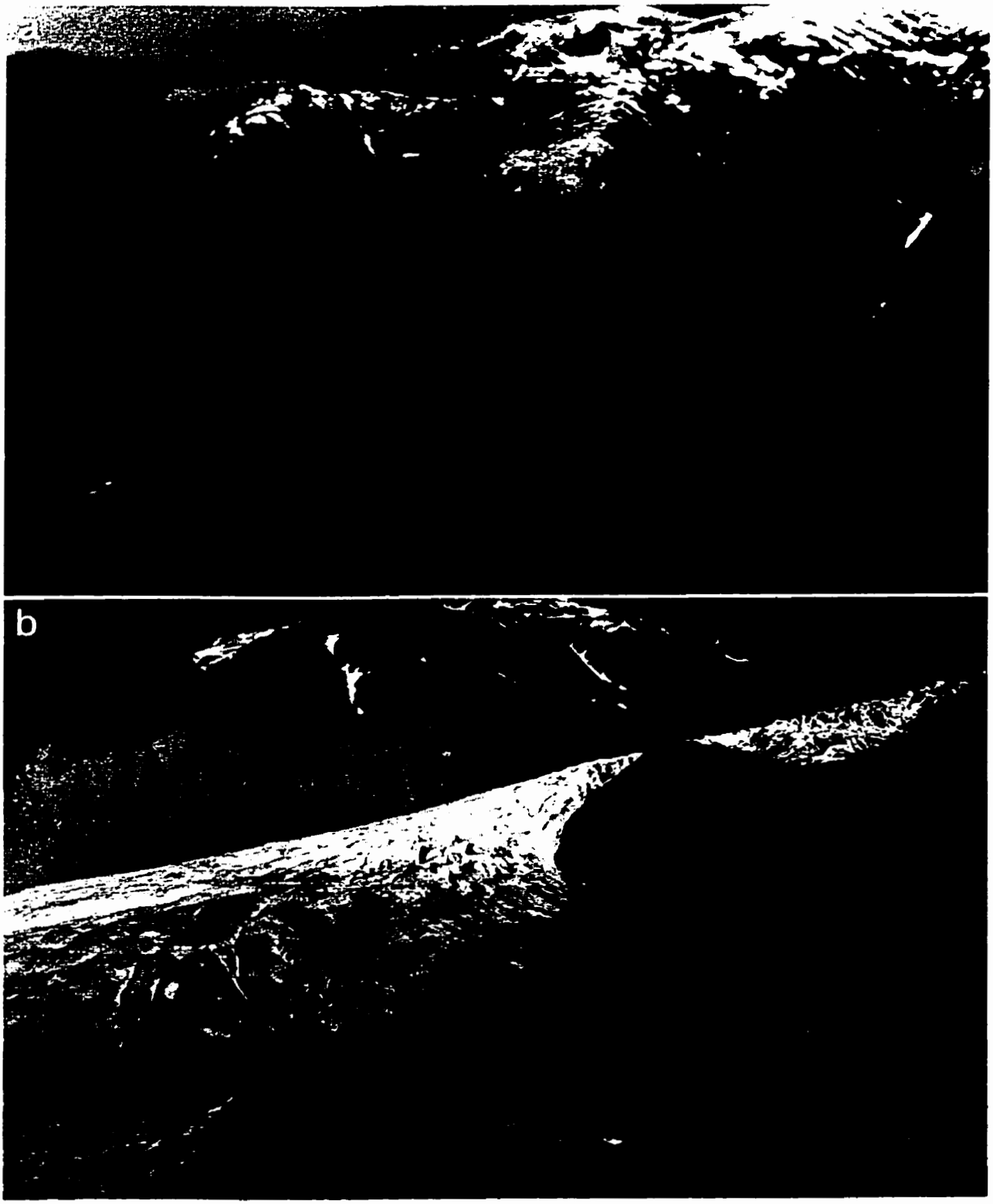


Figure 4.9. a) Fan deltas near Anyox, Hastings Arm. b) Marmot Glacier. Note large, gullied lateral moraine in the distance.

*Neoglacial Deposits*

Neoglacial till is present at the margins of modern glaciers, all of which are currently retreating from their recent maxima, which were probably attained during the Little Ice Age. These loose, poorly sorted, massive diamictons contain granule- to boulder-sized clasts set in a medium- to coarse-grained sand matrix. Neoglacial till has a significantly coarser matrix than the two Pleistocene tills (Figure 4.8), because Bowser Lake Group rocks comprise only a minor component. Clasts, predominantly soft ones, are striated, and the unweathered colour is grey to dark grey or brown. Clasts are subangular (rarely subrounded) to very angular and are entirely of local provenance. Flights of recessional and lateral moraines are common, contrasting with the complete absence of terminal and lateral moraines in Pleistocene deposits (Figure 4.9b). The oldest moraines are more weathered and plants have begun to colonize a few of them. Moraines are commonly gullied and cut by streams and debris flows. Debris flow and talus cones have formed along the base of the moraines; the cones commonly coalesce to form aprons. Many modern glaciers have a frontal complex of till and glaciofluvial deposits (*e.g.* Sutton Glacier, Kitsault Valley map).

Neoglacial glaciofluvial deposits consist of subangular to subrounded pebble to cobble gravel. Strong imbrication, moderate sorting and indistinct horizontal bedding are characteristic. Colour is variable due to the presence of many local volcanic and sedimentary lithologies in the Cambria Ice Field region.

There are no glacier-dammed lakes within the thesis area, but some do exist on the north side of the Cambria Ice Field, just beyond the northern limit of the study area.

*Other Deposits*

Organic deposits are abundant throughout the study area. They consist of peat bogs developed locally on bedrock or glacial deposits. They are common features on braidplains, probably due to high water tables caused by underlying clay or till deposits.

Felsenmeer, which locally obscures striations, is present at high altitudes, both in granite and siltstone/sandstone successions.

The Aiyansh Lava Flow is also a postglacial feature. It has infilled parts of the Tseax and Nass Valleys. The flow dammed lakes, reoriented rivers and covered alluvial fans. It filled a major part of the Nass River floodplain, forcing the river to the edge of the flow. A major alluvial fan was overrun, and it has continued its deposition on top of the flow.

R12 was a sample of wood from the Aiyansh lava flow (Appendix E). It came from a lava-encased tree trunk in growth position (Figure E.2). Moss growing on the top of the stump was avoided when sampling. Since 8 cm of trunk was missing at the edge of the tree mould and there was an average of 5 rings/cm in the sample collected, the date is about 40 calendar years too old. As this was a bulk date - several rings were pulverized - it is probably another 10 years older. The calendar dates for the 280 ± 50 radiocarbon years BP date are 1526-1557 or 1629-1663 A.D. Subtracting 50 years, the new calendar ages are 1476-1507 or 1579-1613 A.D.

McCullagh (1918) discussed the native Nisga'a story that says that a 'seven-told human age' (seven lifetimes of 21 years) had passed since the flow, putting the age of the flow at about 1770 A.D. In 1898, trees were cut that were involuted from bark stripping 128 years earlier, at a site where the Nisga'a people are said to have made a temporary camp after the destruction of their villages (McCullagh, 1918). The 1770 A.D. age is not in agreement with the radiocarbon date, so the timing of the oral history appears to be incorrect. The seven lifetimes would each have to be at least 43 years long, and the bark stripping must not have been due to rebuilding after the flow.

# CHAPTER FIVE

# LITHOSTRATIGRAPHY

This chapter reviews information gathered from natural and man-made exposures (sections) of the entire study area, as well as from holes drilled in the Nass Valley. In addition to lithological data, downhole geophysical logs of the drill holes are also discussed.

## Sections

Major sections are rare in the study area. In the area covered by the two 1:100 000 map sheets, only ten sections were identified; the locations of these are shown in Figure 5.1. Since several sections show similar stratigraphy, they are discussed as a group. The remaining sections are discussed individually, from north to south.

The section diagrams contain detailed lithological descriptions of the sections, so discussions in the text are kept brief. The legend for the sections and drill holes is shown in Figure 5.2. The elevations at the top of each section are approximate, as they were determined from the topographic maps.

### *Sections 96705-10 (West Hastings Arm), 96810-10 (Hoan Creek), 96805-10 (Shumal Creek)*

Description

These sections are located near West Hastings Arm, Hoan Creek and Shumal Creek (Figure 5.1) at 60 m, 335 m and 183 m asl elevations, respectively. Only the Hoan Creek section is above marine limit, which is 230 m (Chapter 4). The sections are all natural river-cut exposures and each is a good example of thick diamicton overlain by finer sorted sediments. Detailed descriptions and lithologic logs of these sections are shown in Figures 5.3, 5.4 and 5.5. The diamicton in these sections is 25 to 43 m thick and may be thicker, because bedrock was not

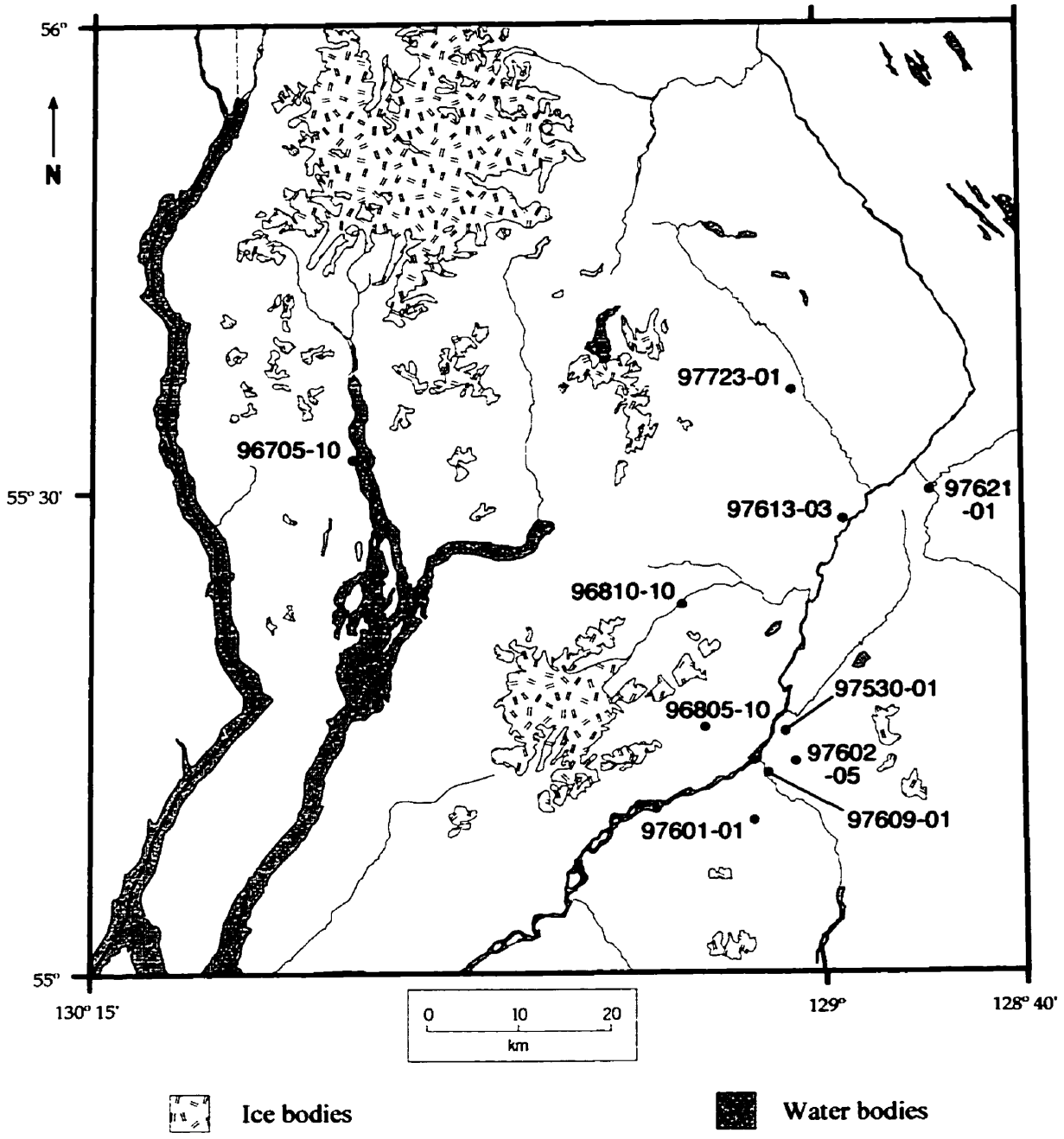


Figure 5.1. Location of major sections described in the text.

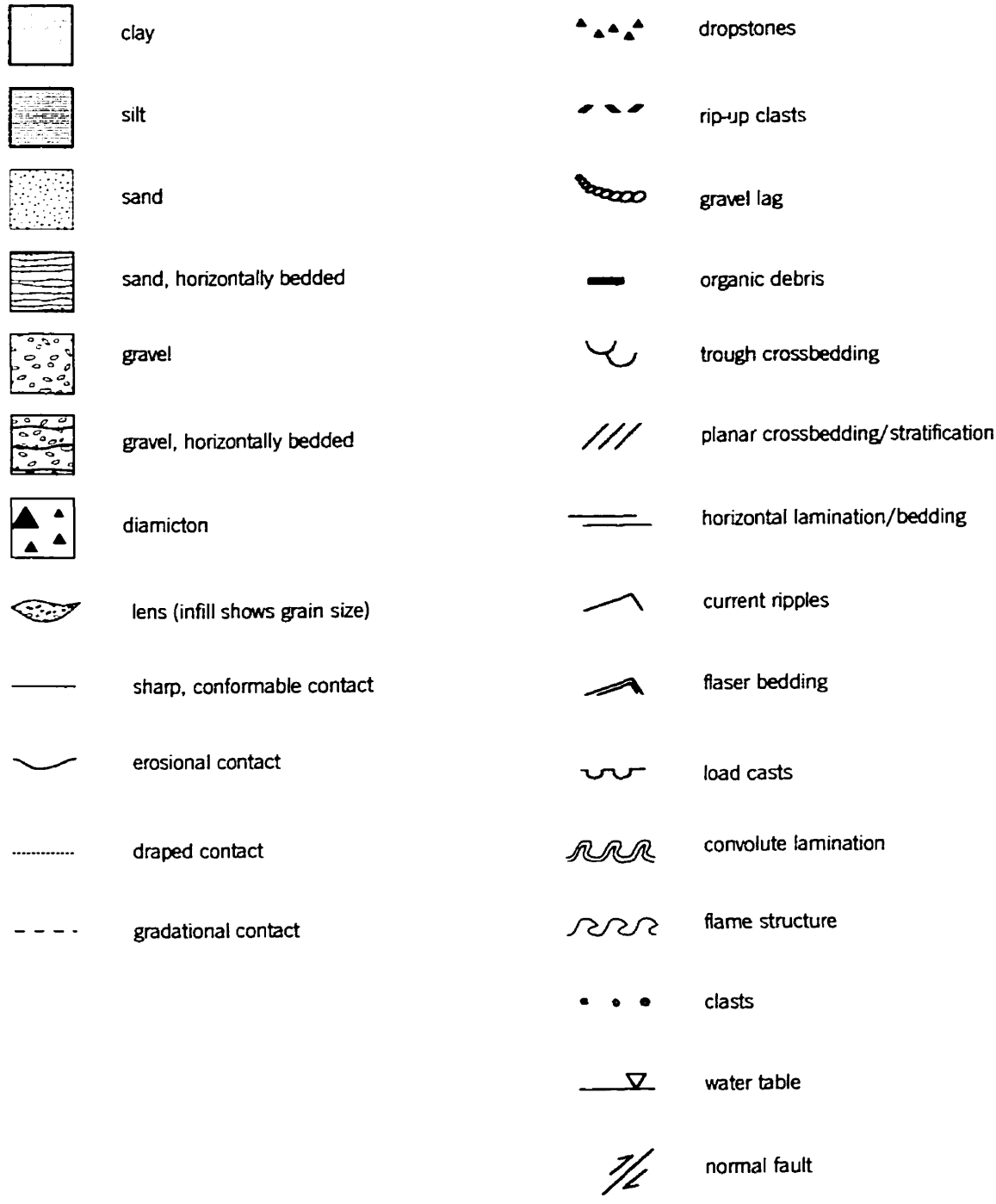


**Figure 5.2. Legend for lithologic logs of sections and drill holes.**

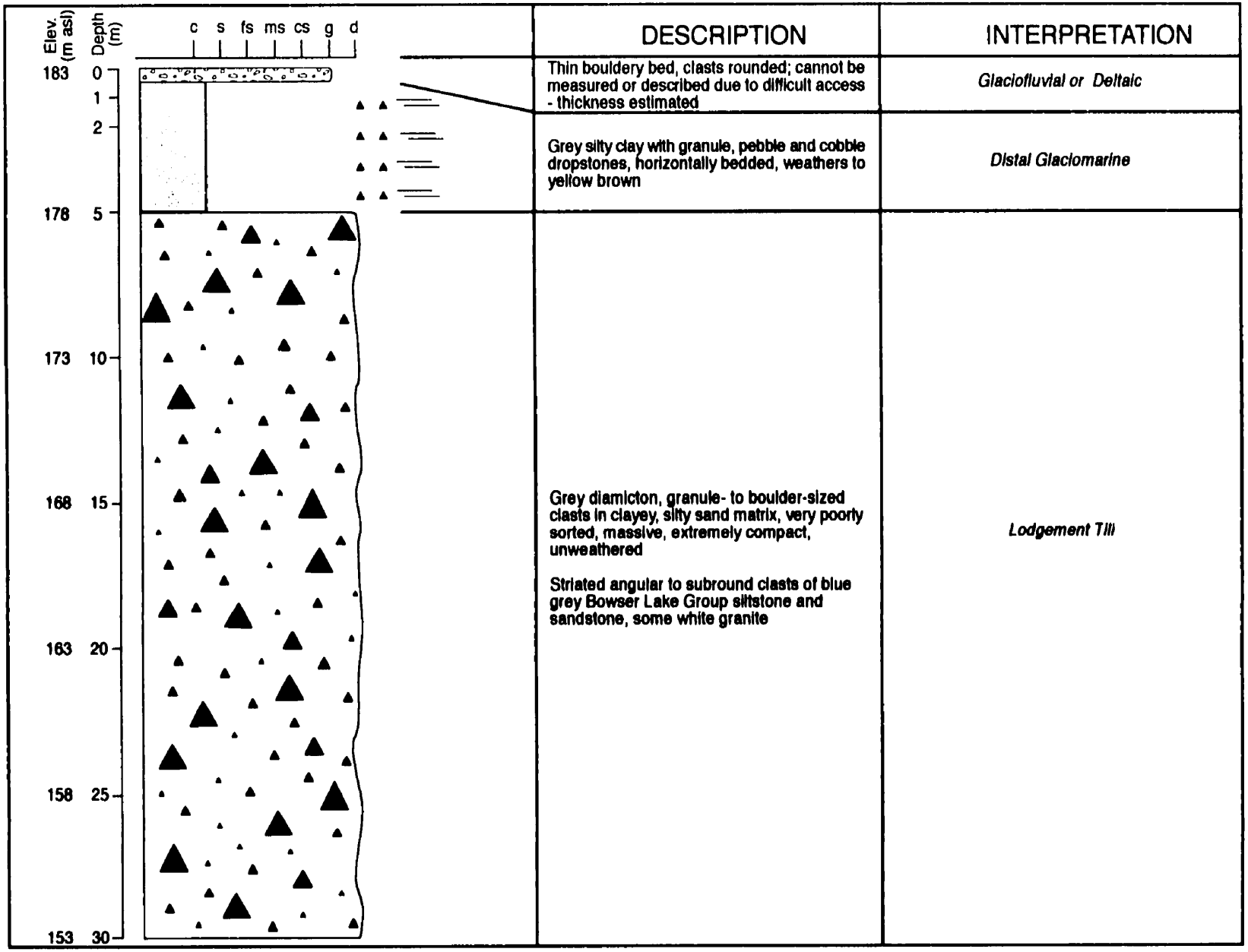


Figure 5.3. Section 96805-10, Shumal Creek, detailed lithological log, description and interpretation.

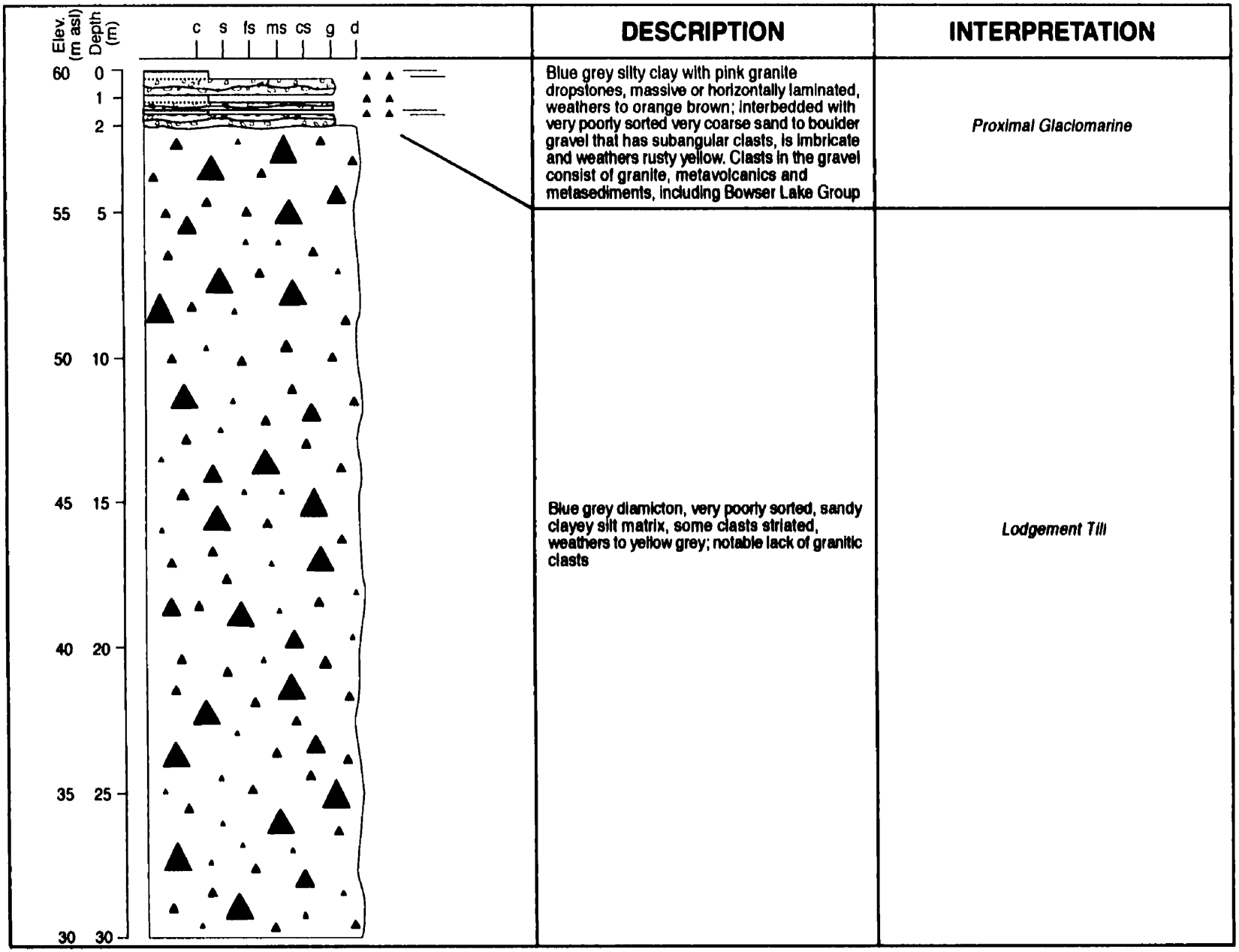


Figure 5.4. Section 96705-10, West Hastings Arm, detailed lithological log, description and interpretation.

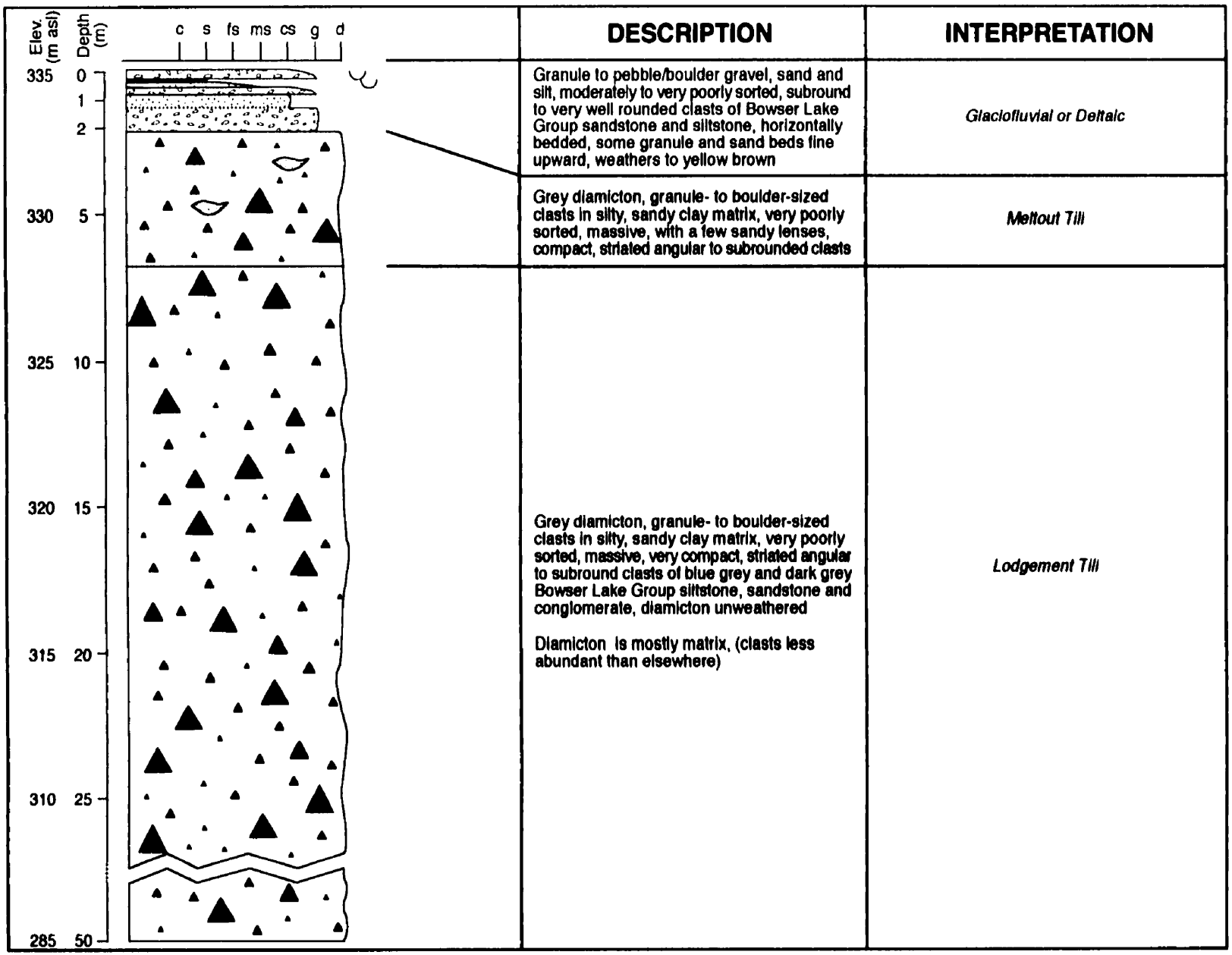


Figure 5.5. Section 96810-10, Hoan Creek, detailed lithological log, description and interpretation.

encountered at the base of the sections. The diamicton is overlain by gravel and/or silty clay that may contain dropstones.

Interpretation

The diamictons are interpreted as lodgement till due to their very poor sorting, clast angularity, compactness, massive texture and striated clasts. The till is dominated by Bowser Lake Group clasts and will be referred to by the informal name 'Kwinatahl till' in the dissertation. At Hoan Creek (Section 97810-10), the lodgement till is overlain by a till (also Kwinatahl till) that is inferred to be a melt-out till due to its less compact nature and the presence of sandy lenses.

At Shumal Creek, horizontally bedded silty clay with dropstones is interpreted to have formed in a distal glaciomarine environment. The presence of dropstones indicates that it formed in either a glaciomarine or a glaciolacustrine environment. The possibility that the silty clay could have been deposited in a glaciolacustrine environment is discounted for reasons outlined earlier (Chapter 4).

At West Hastings Arm (Section 96705-10), interbedded coarse-grained sand to boulder gravel and horizontally laminated silty clay with dropstones (Figure 5.6a, b) is interpreted to reflect proximal glaciomarine deposition. The presence of dropstones and the site's location adjacent to a major fiord support this interpretation. The presence of granitic bedrock clasts of local provenance in the glaciomarine deposit, but not in the till, indicates that the till is of distal provenance, while the glaciomarine sediments are of local provenance. A major change in source areas appears to have occurred between these two depositional events.

Glaciofluvial or deltaic deposition is inferred for the uppermost packages of the Hoan Creek section and the Shumal Creek section, due to the coarse-grained nature and rounding of clasts in these units. This bed was not accessible at Shumal Creek, but these characteristics were visible from the middle portion of the section. At Hoan Creek, moderate to poor sorting and horizontal bedding support this interpretation (see Glaciofluvial Deposits, Chapter 4).

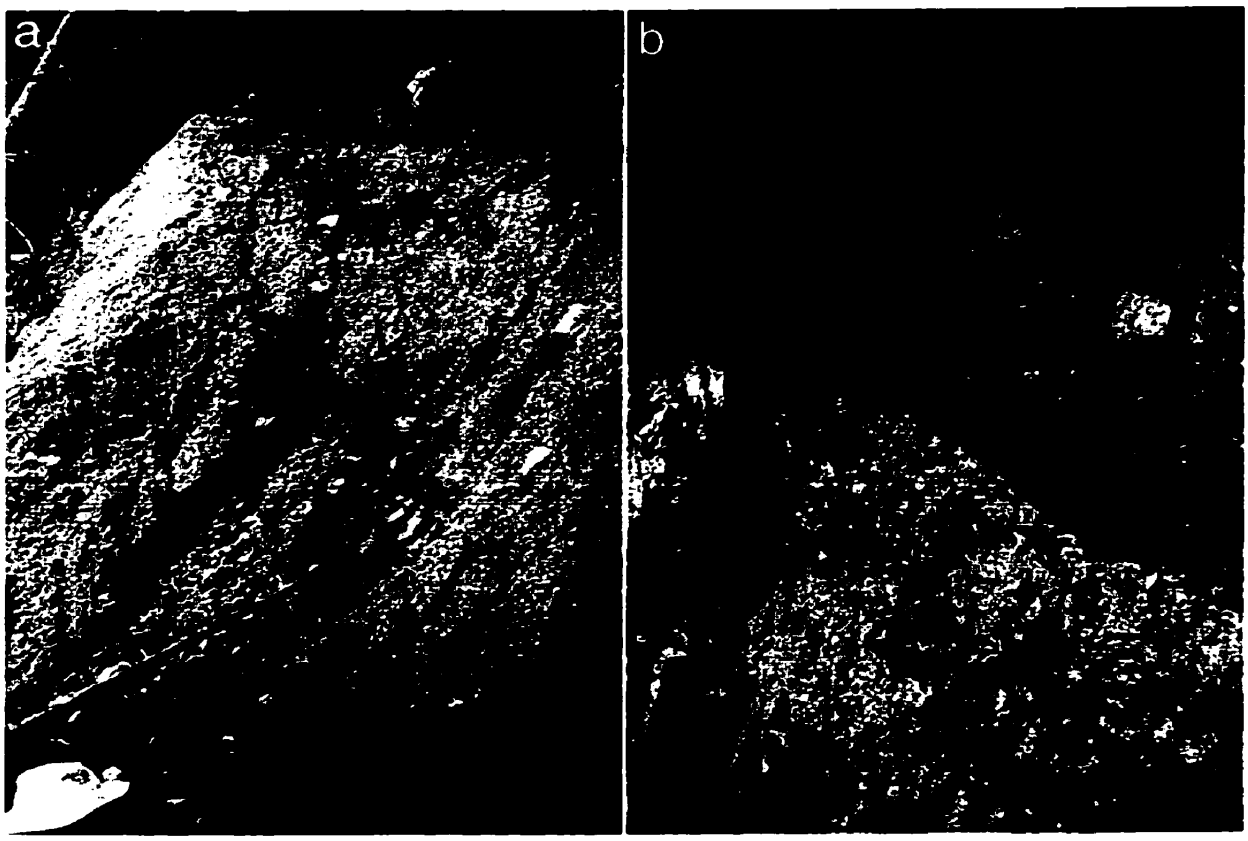


Figure 5.6. Section 96705-10, West Hasting Arm. a) Entire section, which consists mostly of diamicton. Coarse bedded sediments are visible at the top of the photo. b) Close-up of upper part of section. Note the sharp, erosive contact between the diamicton and overlying interbeds of gravel and silt. Hammer is about 30 cm long.

*Section 97723-01 (Kinskuch Valley)*

This exposure is the only major section from which a radiocarbon dating sample was obtained (Figure 5.7). For details on the sample and the dates, see Appendix E. Pollen samples were also analyzed (Appendix E). The exposure is at an elevation of 274 m asl, which is above marine limit (Chapter 4).

Description

A horizontally laminated clay layer is overlain and underlain by horizontally bedded fine-grained sand, coarse-grained sand, and granule, pebble and cobble gravel at this site. The lower contact of the clay unit drapes the underlying sediments, while the upper contact is erosive. The whole section is only about 2 m wide, so lateral relationships could not be determined. See Figure 5.7 for a more detailed description.

Sample R7 was taken from a road cut in Kinskuch Valley. It is the same sample as 97723-31, Kinskuch Valley Section, Figure 5.7. The organic sample was actually taken a year before the section was described, hence the different sample number. Terrestrial moss (identified by R. Mathews, Biological Sciences Dept., SFU) was initially AMS dated (TO-6354). It was considered *in situ* as it formed mats of a single species. When this age turned out to be interstadial, a second age was obtained from flattened stems of *Equisetum* sp. in the same sample (Beta-124778). This age is slightly older, possibly due to the different labs at which the samples were dated. The site is interglacial, correlative to the Olympia Nonglacial Interval of southern B.C.

Interpretation

The radiocarbon dates obtained from sample 97723-31 are 27 130 ± 280 and 30 080 ± 170 a BP, indicating that the laminated clay unit is interstadial in age. The section is interpreted to represent fluvial and possibly lacustrine or deltaic environments of the Olympia Nonglacial Interval. Coarse fluvial or deltaic sedimentation was responsible for the deposition of gravel from 6.9 to 7.8 m. This type of deposition halted at some point, and lake or abandoned

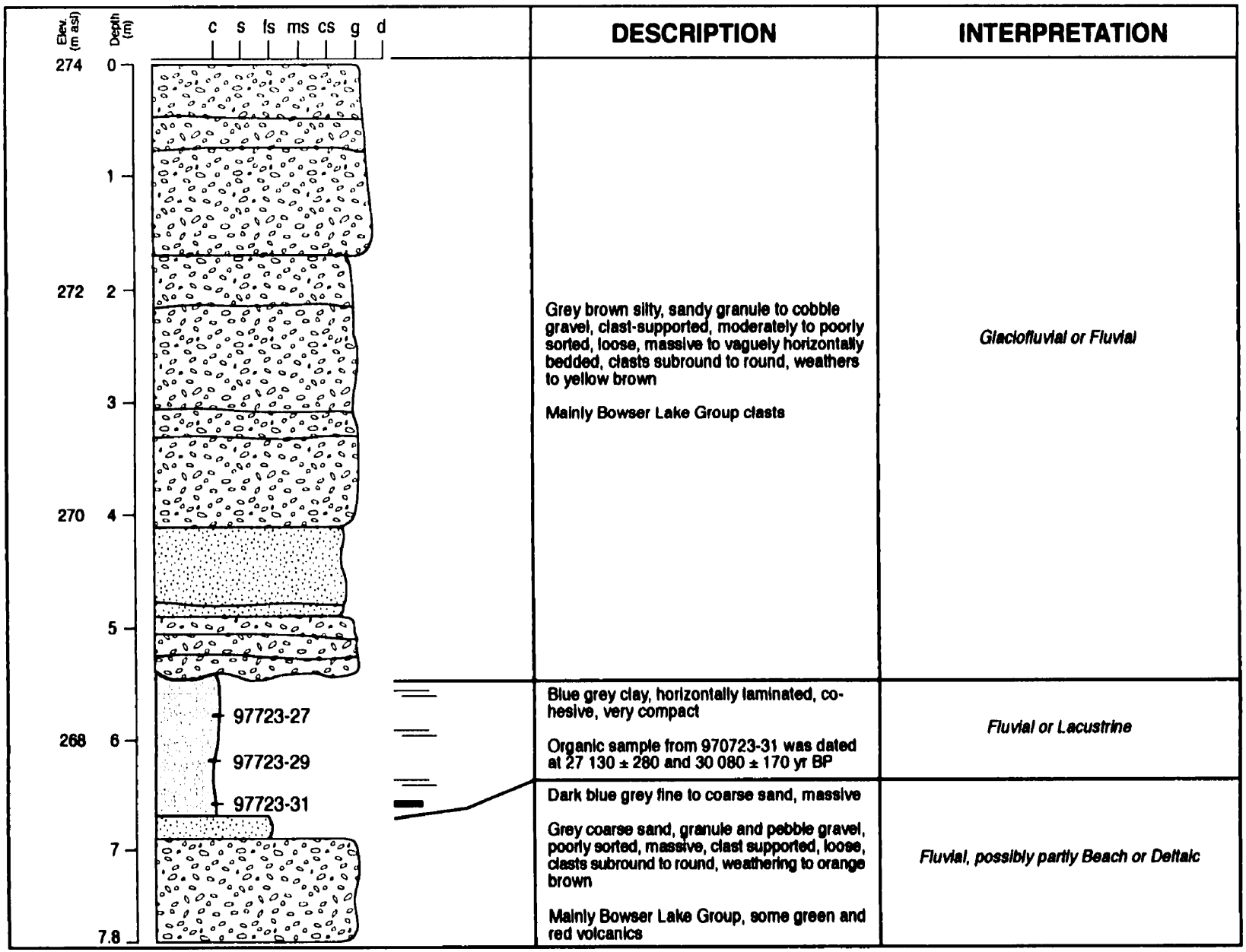


Figure 5.7. Section 97723-01, Kinskuch Valley, detailed lithological log, description and interpretation. Pollen analysis samples were taken at sites 97723-27, 29 and 31.

channel sedimentation ensued with the onset of fine-grained sand deposition which could be from a beach (freshwater), deltaic or fluvial setting. Unfortunately, the exposure is too narrow to determine lateral continuity and the sand deposit is massive. The actual depositional environment of the sand and gravel is thus difficult to define. Deepening of the lake or slowing of channel flow allowed the deposition of laminated clay, including an organic layer which may have washed in from a nearby lake or stream margin. The organic debris in the laminated clay consists of fine leaves and stems, all well preserved, but completely flattened by the weight of overlying sediments and/or ice. The lake or channel later drained, and fluvial erosion followed by gravel and sand deposition occurred. The horizontally bedded gravel and sand from 5.4 to 0 m is interpreted to have been deposited in a river due to its clast support, moderate to poor sorting, massive to weak bedding and loose nature, but it is not certain whether the depositional environment was a glacial meltwater river or an interstadial river.

The pollen analysis of this site is detailed in Appendix E. The three samples show that a spruce forest with no modern analogues existed in the region in interstadial time. Climate must have been cooler than present at that time.

*Section 97621-01 (Kiteen River)*

This section is a natural exposure cut by the Kiteen River (Figure 5.8a). The top of the section is at 140 m asl. Its location is just north of the mapped area of 103P/SW and just east of 103P/NW, so it does not appear on either of the Quaternary geology maps. However, its location is shown on Figure 5.1.

Description

The detailed log and section description are shown in Figure 5.9. At the base of the section is a gravel unit (34-32 m depth) in which 15% of the clasts are striated. The gravel is overlain by interbedded fine- and medium-grained sand.

The unit from 25 to 30 m is a diamicton with a sand matrix. It is massive, very poorly sorted, and has striated clasts. Bullet-shaped boulders are present in the lower part of the diamicton

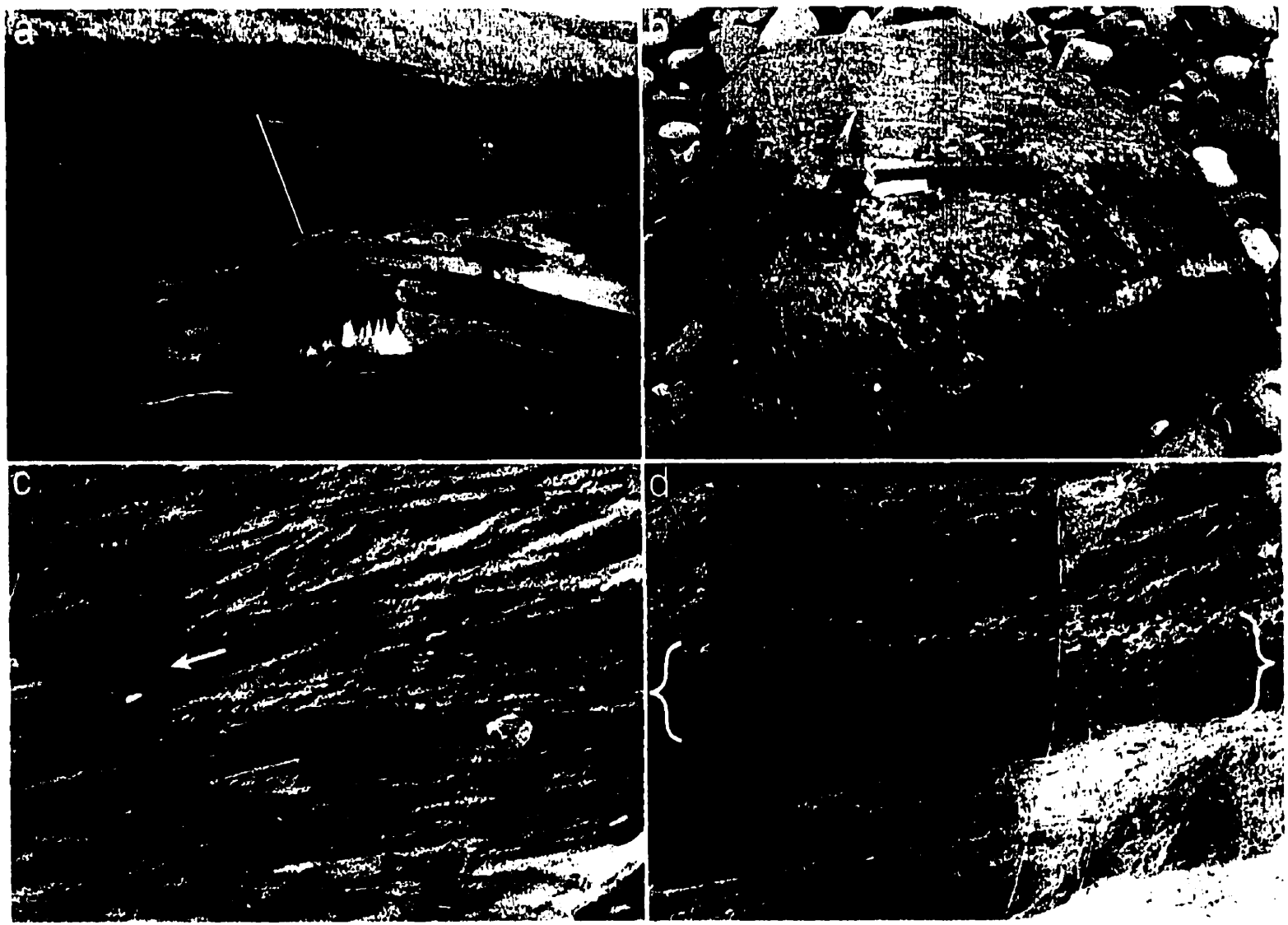


Figure 5.8. Kiteen River Section (97621-01). a) The vertical cliff exposes coarse-grained deposits that overlie till. Solid line shows where section was measured. b) Bullet-shaped boulder weathered out of lower diamicton. Striae are parallel on the top and bottom planes of the boulder. Hammer is about 30 cm long. c) Normal fault (arrowed), planar tabular crossbeds and rare pebbles in coarse-grained sand, at about 20 m depth. Lens cap is 49 mm wide. d) Coarsening upward unit (within brackets).

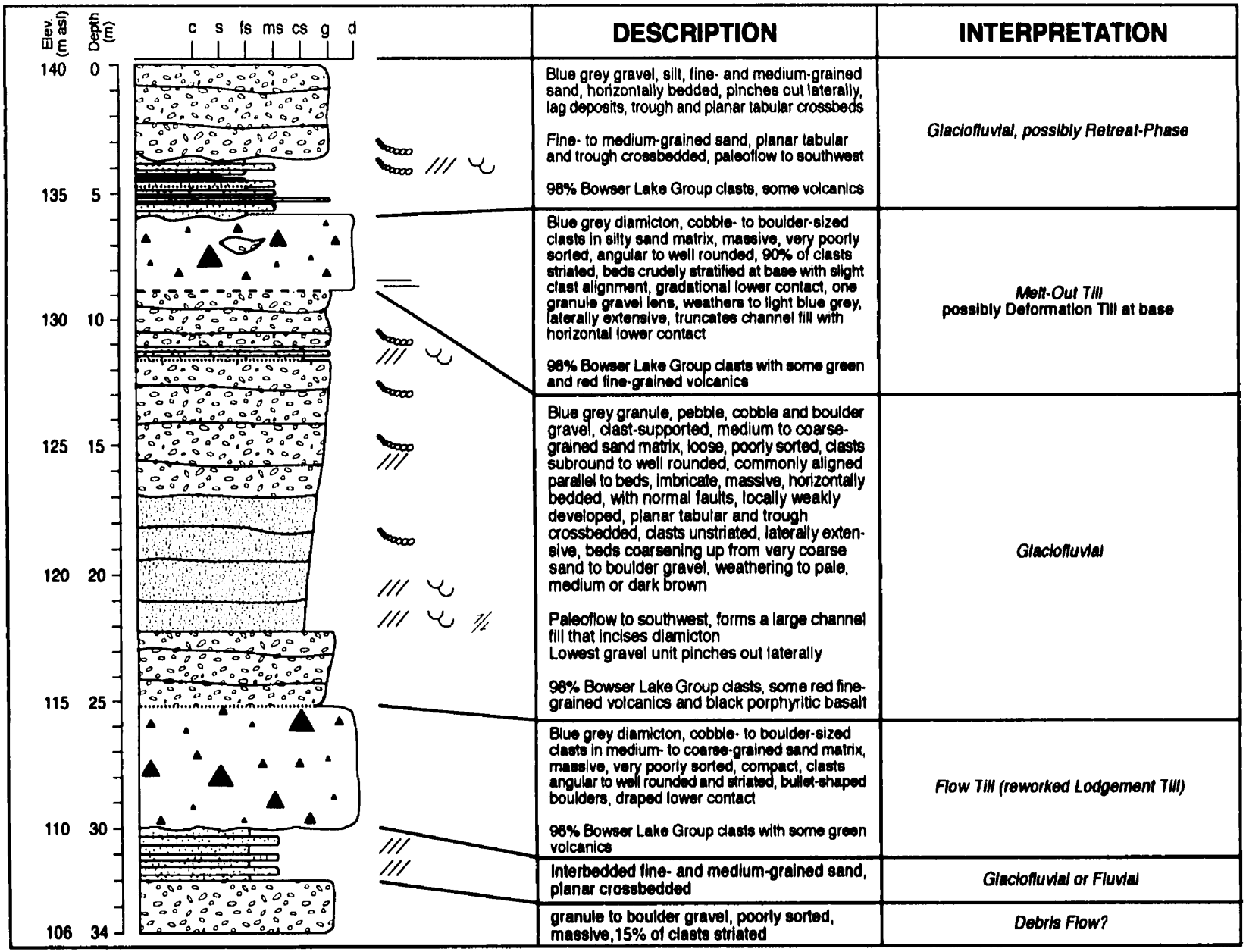


Figure 5.9. Section 97621-01, Kiteen River, detailed lithological log, description and interpretation.

(Figure 5.8b) and its lower contact is draped. The presence of meta-volcanic clasts, well rounded clast shapes and the sand matrix distinguish it as a diamicton that is different from Kwinatahl till.

Overlying the diamicton is a horizontally bedded coarse-grained sand to boulder gravel unit, with a southwest paleoflow direction. This flow direction is exactly opposite the northeastern flow direction of the modern Kiteen River at this location. Numerous gravel lags, planar tabular crossbeds, trough crossbeds, and normal faults can be seen (Figure 5.8c) and the beds coarsen upward, although they are individually massive (Figure 5.8d). A normal fault is visible in Figure 5.8c. The erosive lower contact is part of a large channel feature cut into the underlying diamicton. The diamicton is a thicker unit where the channel cut is less deep. To the north, horizontally bedded boulder gravel is visible in the distance, but its relationship to the diamicton is unclear as it is inaccessible.

From 6 to 9 m is a very poorly sorted diamicton with a silty sand matrix, massive texture and a single granule gravel lens. The percentage of striated clasts in the diamicton is about 90%. The basal contact is gradational and beds are crudely stratified, especially near the base of the unit. The stratified beds also display slight clast alignment.

The uppermost unit, from 6-0 m, consists of interbedded silt, fine-grained sand, medium-grained sand and gravel. Lags and crossbedding are present in places.

The abundance of sedimentary structures sets this section apart from the majority of structureless glaciofluvial deposits in the regain.

Interpretation

The gravel and sand at the base of the log (34-30 m) are interpreted as glaciofluvial or fluvial deposits and a possible debris flow that may have reworked a till deposit (striated clasts). The diamicton above them is very poorly sorted, compact, and contains striated and bullet shaped clasts. However, it has a coarse-grained matrix and a draped lower contact, so it could be a melt-out till or a flow till. It is more likely the latter because striated and bullet shaped clasts imply that it was originally a lodgement till. Since the diamicton overlies laterally extensive gravel and sand, the underlying sediments could be subglacial fluvial deposits.

The planar tabular and trough crossbedded coarse-grained sand to boulder gravel from 25 to 8.8 m is interpreted as a glaciofluvial deposit. It contains the gravel lags and crossbedding common in fluvial environments and is part of the infill of the paleochannel cut into the till. The succession also coarsens upwards, which is consistent with an approaching ice front, so it may represent an advance-phase deposit. The river's paleoflow direction is southwest, down the Nass Valley. An alternative hypothesis is that these are deposits of one subglacial flood. However, individual beds are thin and exhibit no grading, which might be expected in a surging flood type environment. Also, the coarsening-upward of numerous beds indicates a gradual change in flow regime. The beds could also be interpreted as channel deposits that received higher velocity flow over time, possibly due to adjacent channel abandonment. If this is the case, they may not be advance-phase deposits. For these reasons, the unit is simply interpreted as glaciofluvial.

The diamicton overlying the coarsening-upward sequence is likely a melt-out till, as it has a silty sand matrix, a granule gravel lens and indistinct stratification. It is not a debris flow, as 90% of its clast are striated. It is similar to the Kwinatahl till of the region. The lower contact may actually be an erosive contact. Underlying gravels may have been entrained as a deformable bed, creating the illusion of a gradational contact at this location. The till may be a deformation till at its base if this is the case.

The coarse, horizontally bedded deposits from 6 to 0 m are interpreted as glacial river deposits. In this stratigraphic position, they are probably deglacial sediments, since they overlie glaciofluvial sediments and till. Any glaciomarine deposits that may have existed between the till and glaciofluvial sediments was likely eroded away by fluvial activity.

The glacial history of this site is one of ice advance and retreat, followed by a second advance and retreat. An ice advance deposited the lodgement till that was reworked by flow and possibly the fluvial and debris flow sediments beneath it. This ice retreated and glaciofluvial sediments were later deposited. These may be either advance- or retreat-phase sediments. There was a major erosive event which formed the channel in which the fluvial sediments lie. The channel is cut into thick till deposits that are represented by the thin diamicton at the base of the section. Lateral relationships between this till and horizontally bedded gravel some distance to

the north are uncertain. Melt-out and possibly deformation till (Kwinatahl till) was deposited when a second glacier advanced across the site. When this glacier retreated, more glaciofluvial deposits were laid down in its wake. Two major ice advances are thus recorded at this site, with associated intervening fluvial deposition.

A year after this section was described, a major earthflow, visible in the foreground of Figure 5.8a, occurred to the south of it. Here, about 30 m of glaciomarine massive silty clay is exposed, with about 6 m of fluvial gravels erosively overlying the clay (Figure 5.10). No evidence of till deposition was seen. It is interesting that such a different depositional record could be preserved at a site so close to the Kiteen River Section. The Kiteen River Section area must have been protected from the deeper erosion that the southern section experienced prior to glaciomarine deposition. Neither section is protected by nearby bedrock outcrops, so protection must have been provided in the form of glacial sediments.

*Section 97613-03 (Tchitin River)*

This section is a natural exposure within the Nass Braidplain at 158 m asl (Figure 5.11), formed by the incision of a small tributary of the Nass River called Tchitin River (Figure 5.1). Much of the section is covered by slumped material, but it was able to be logged by the clearing of small sections at various intervals. The exposure is actually more than 40 m thick, but lower levels on the other side of the overgrown logging road were inaccessible.

Description

The detailed log and description of the 40 m section are shown in Figure 5.11. Most of the section comprises granule to boulder gravel that is poorly sorted, horizontally bedded and planar tabular crossbedded. A few silt rip-up clasts and silt, clay or sand beds are present locally.

Interpretation

Clast supported gravels, poor sorting, horizontal bedding, planar tabular crossbedding, clast roundness, imbrication, and the presence of rip-up clasts point to a glaciofluvial origin for this

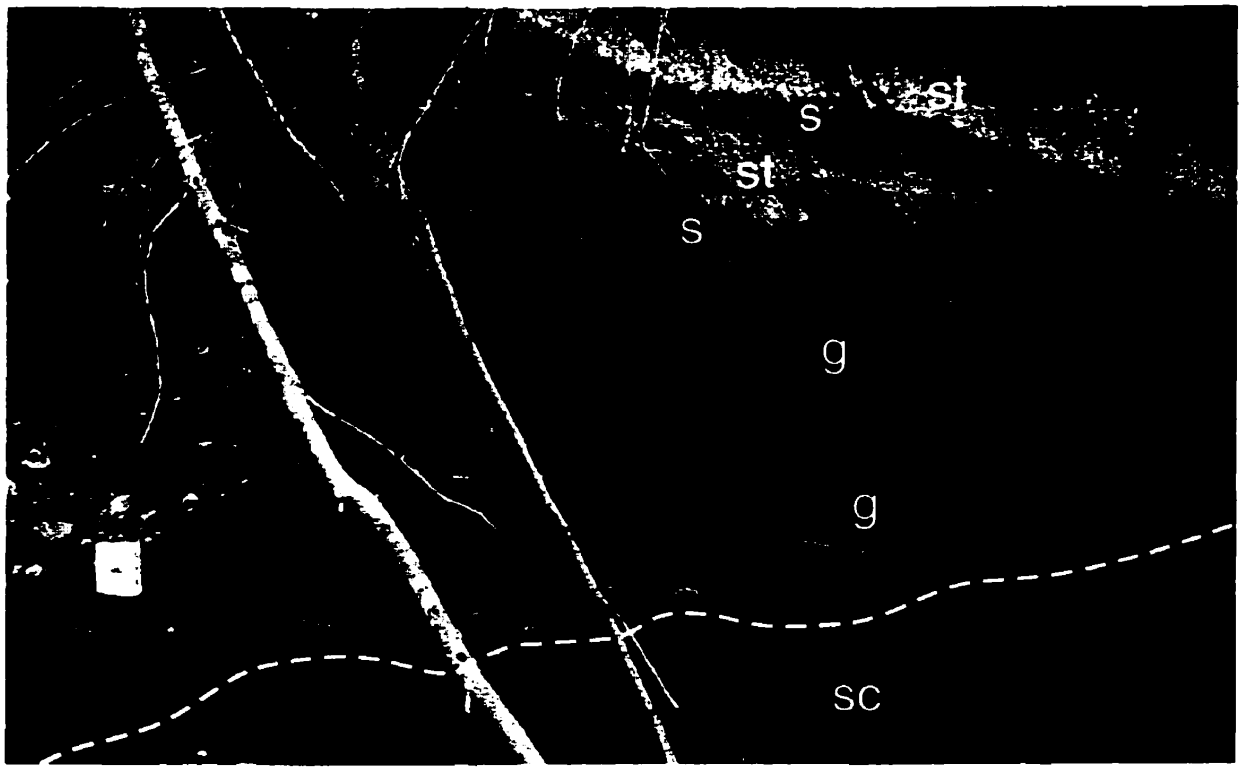


Figure 5.10. Horizontally bedded gravel (g), sand (s) and silt (st) overlie a thick deposit of glaciomarine silty clay (sc) just south of the Kiteen River Section. Note erosive contact (dashed). Notebook is 18 cm long.

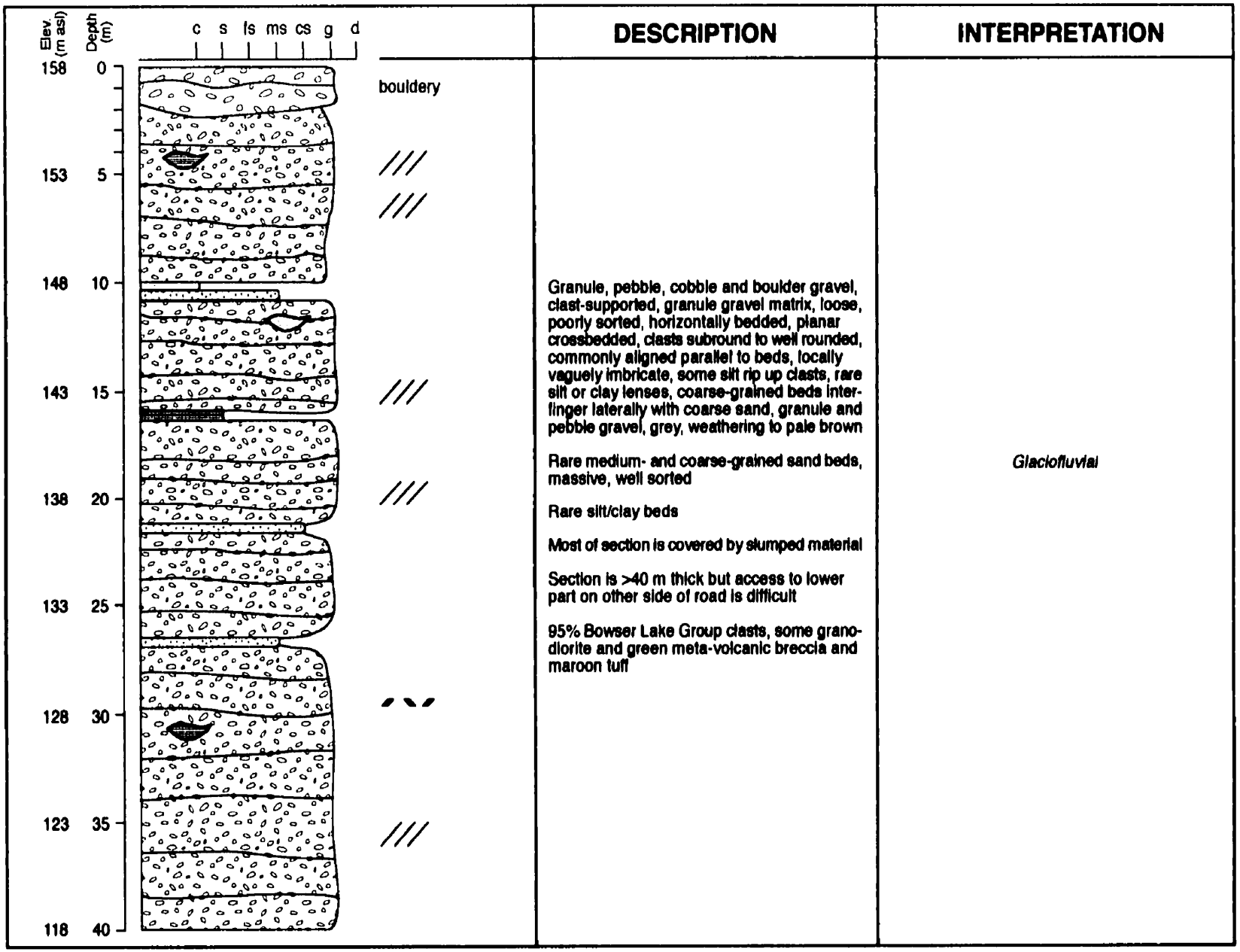


Figure 5.11. Section 97613-03, Tchitin River, detailed lithological log, description and interpretation.

site. Additional geomorphic information from the surficial geology mapping shows that the area surrounding the section is a braidplain. The section is thus interpreted to be a glaciofluvial braidplain deposit. This section provides an insight into the late glacial (retreat-phase) glaciofluvial environment of the Nass Valley: deposits are locally more than 40 m thick, indicating that aggradation was rapid if these features were short-lived.

*Section 97530-01 (Irene Meadows Road)*

This section is an exposure in a road cut within the Aiyansh Braidplain that had to be extensively cleared of slumped material (Figure 5.1). Several offset vertical sections were measured to complete the lithological log and description of Figure 5.12. The elevation at the top of the section is 85 m asl.

Description

The section consists of well sorted, horizontally interbedded silt, fine- and medium-grained sand. Most beds are massive but some are normally graded. Current ripples, type B climbing current ripples, flame structures, flaser bedding, wavy bedding, normal faults, soft sediment deformation structures and clay rip-up clasts are common (Figures 5.13a,b and 5.14a,b,c). Flaser bedding commonly passes upward into wavy bedding. Paleoflow direction was indicated by ripple orientations, which all show flow to the southwest. Laminations dip 10° to the southwest as well.

Interpretation

The excellent sorting, generally finer grain sizes, 10° dip of laminae, normal faults, flaser beds, ripples, horizontal bedding, normally graded beds, flame structure, rip up clasts, convolute lamination and ball and pillow structures indicate that these sediments were likely deposited in a deltaic setting. The section is interpreted to be lower delta slope deposits. The alternation of sand and silt (*e.g.* flaser bedding, horizontal interbeds) is a common feature of deltaic (and other) environments. Normal faults occurred when parts of the rapidly accumulated deltaic deposit failed and shifted slightly down slope. Sand was likely deposited during higher river flows. Normal

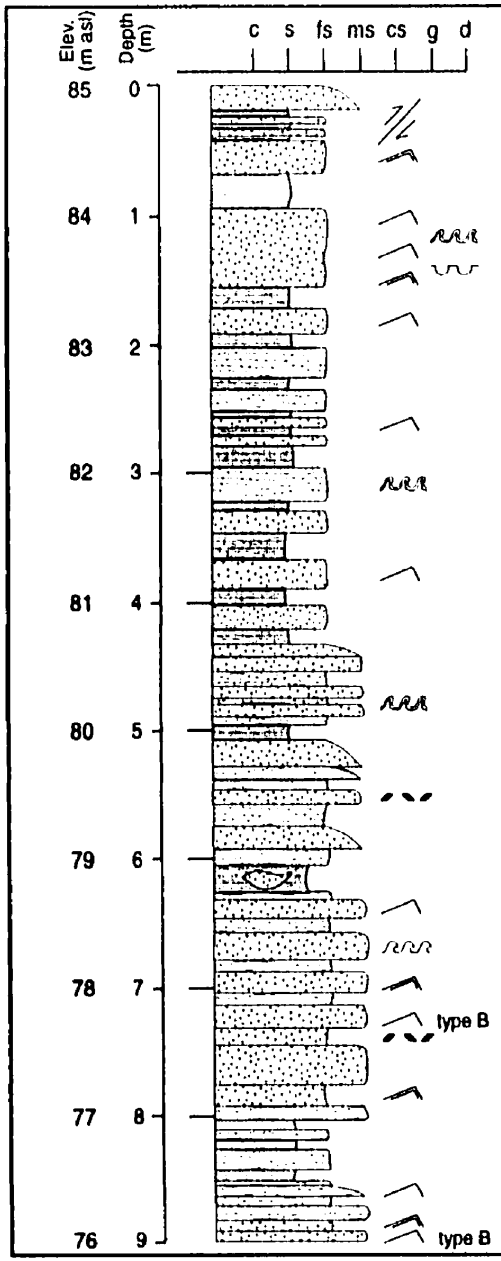


| DESCRIPTION | INTERPRETATION |
|---|---|
| Brown and grey fine- to medium-grained sand, well sorted, massive, horizontally bedded, interbedded with horizontally laminated brown silt, some beds normally graded, laminae dip 10° toward southwest<br><br>Current ripples, type B climbing ripples, flame structures, flaser lamination<br><br>Soft sediment deformation: convolute lamination, ball and pillow load structures, normal faults, rip-up clasts<br><br>Paleoflow direction: 237° (from ripple cross lamination) | *Glaciofluvial Delta* |

Figure 5.12. Section 97530-01, Irene Meadows Road, detailed lithological log, description and interpretation.

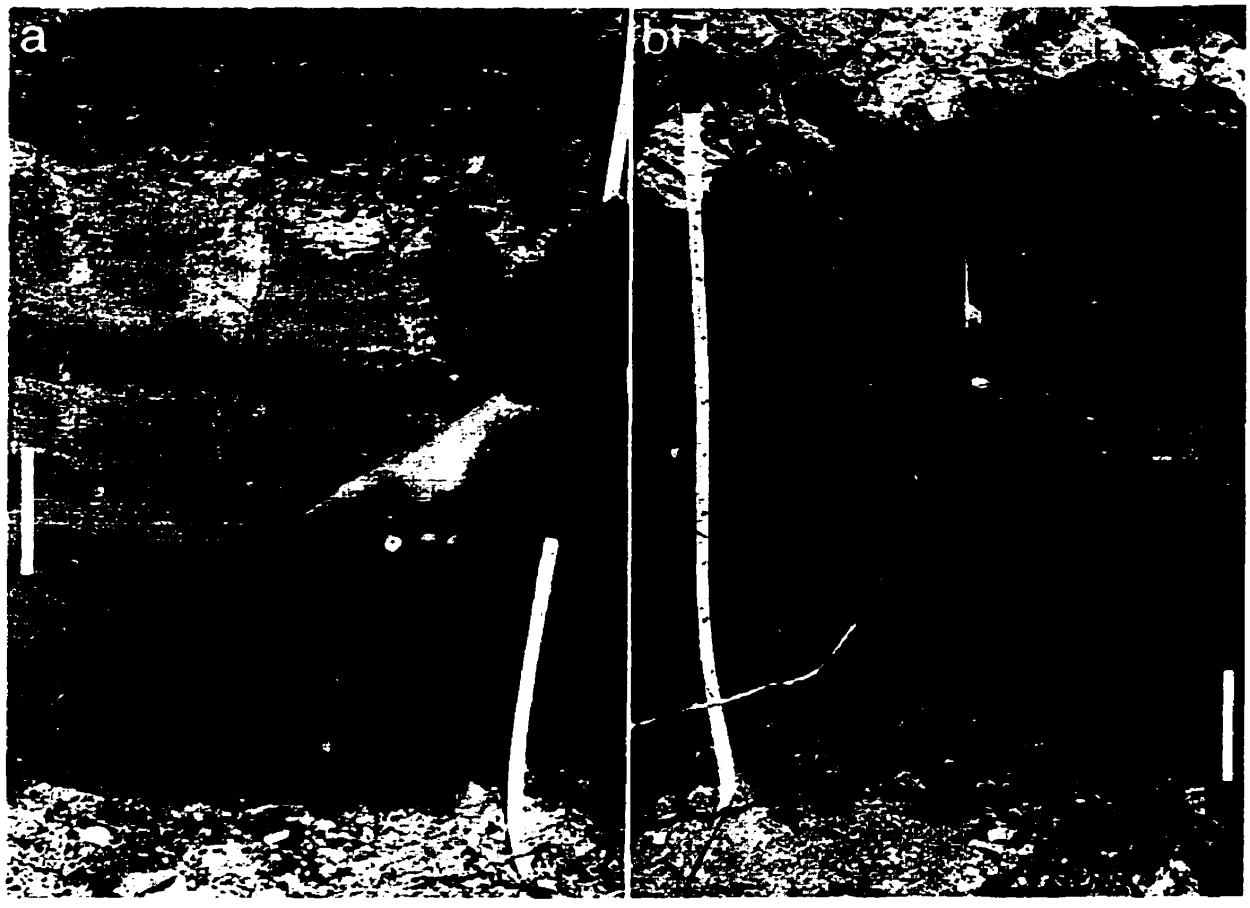


Figure 5.13. Irene Meadows Road Section. a) Person is pointing to a normal fault in horizontally laminated and current rippled silt and sand. Vertical scale bar is 10 cm long. b) Horizontal bedding, current ripples and flaser/wavy bedding in dark toned sand and light toned silt. Vertical scale bar is 10 cm long.

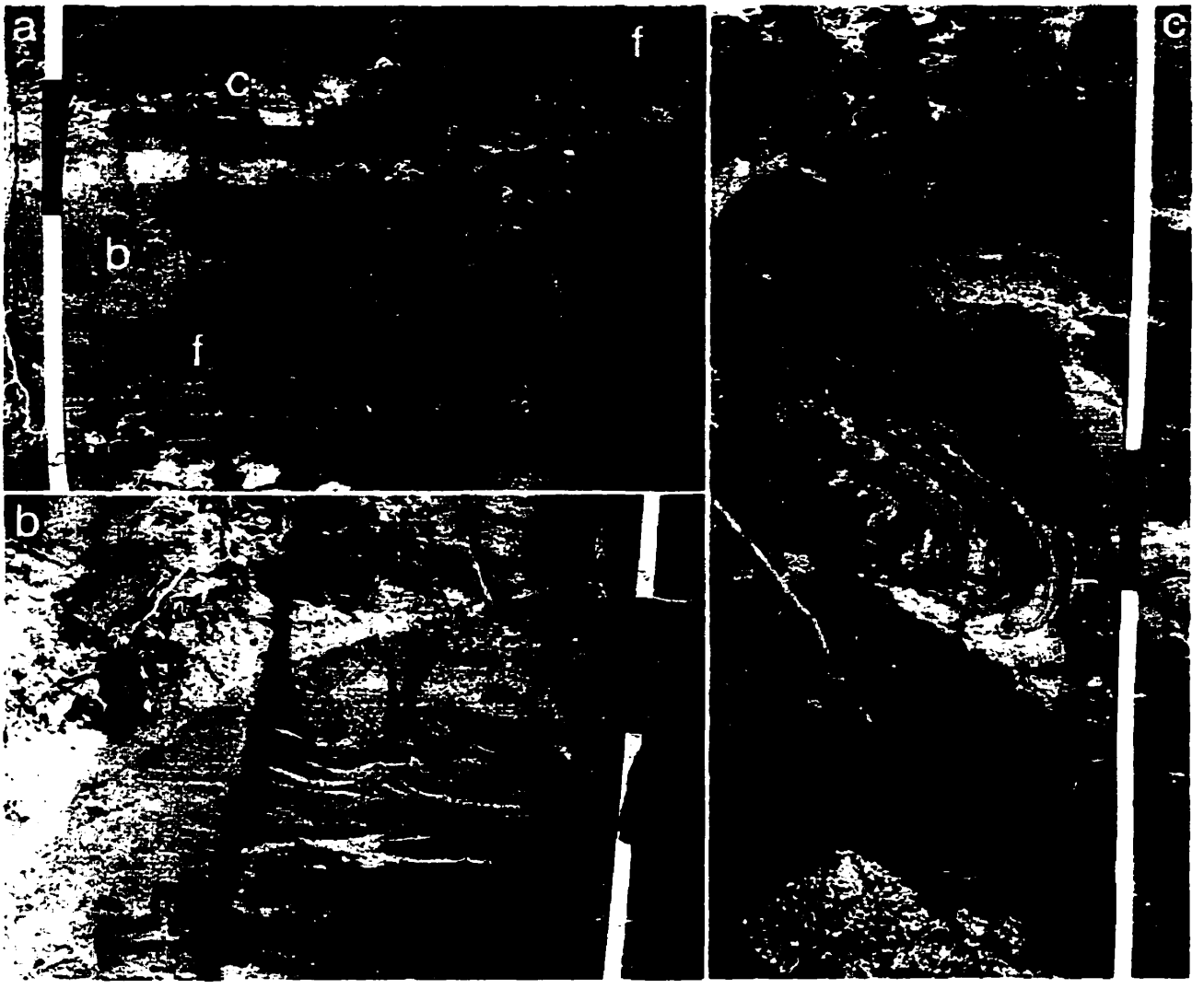


Figure 5.14. Section 97530-01, Irene Meadows Road. a) Flaser bedding (f), ball and pillow structure (b) and convolute lamination (c) in dark toned sand and light toned silt beds. b) Flame structure in sand, highlighted by lighter toned silt. c) Large silt and sand rip-up clast within dark toned sand bed. Black bars on measuring tapes are 10 cm long in all photographs.

grading, rip-up clasts and ripple cross stratification indicate that flow velocity was variable. Ball and pillow and flame structures formed when sand was rapidly deposited over water-saturated silt and sank into it. Convolute laminations also indicate rapid deposition, which is a common feature of deltas. The surficial geology mapping shows this section to be near the terminus of a large braidplain (Nass Valley map). This geomorphic locality is one where a delta would be likely to form and the southwest paleoflow direction is consistent with this interpretation. Similar sediments are interpreted as having formed near a delta front in a glacial lake environment in the Okanagan Valley (Shaw, 1977).

*Section 97602-05 (Aiyansh Gravel Pit)*

The most accessible and extensive section in the study area is the Aiyansh Gravel Pit (Figure 5.1). Its well sorted gravel makes ideal aggregate for road building and maintenance. There are three levels to the pit, so the lithologic log is a composite of information obtained at three different locations. The top of the section is 152 m asl, and the pit is located in the terminal zone of a large braidplain (Nass Valley map).

Description

The lower part of the section consists of laterally extensive pebble/cobble gravel interbeds, thinning and fining up to pebble/granule gravel beds (Figure 5.15). Individual beds are moderately sorted, do not fine upward and have sharp and planar contacts. Clasts are unstriated. subangular to well rounded and aligned or imbricate. One normal fault was observed (Figure 5.16).

From 10 to 6.8 m, cobble gravel thins and fines upward to coarse-grained sand (Figure 5.17b). A few gravel lags and planar tabular crossbeds are present. From 5.5 to 6.8 m, there are well sorted, fining-upward beds of granule gravel to coarse-grained sand, that contain some planar crossbedding and one flaser bedded unit. Sigmoid (epsilon) crossbeds in the uppermost part of the section indicate a southwesterly paleoflow direction. There are local outsized clasts

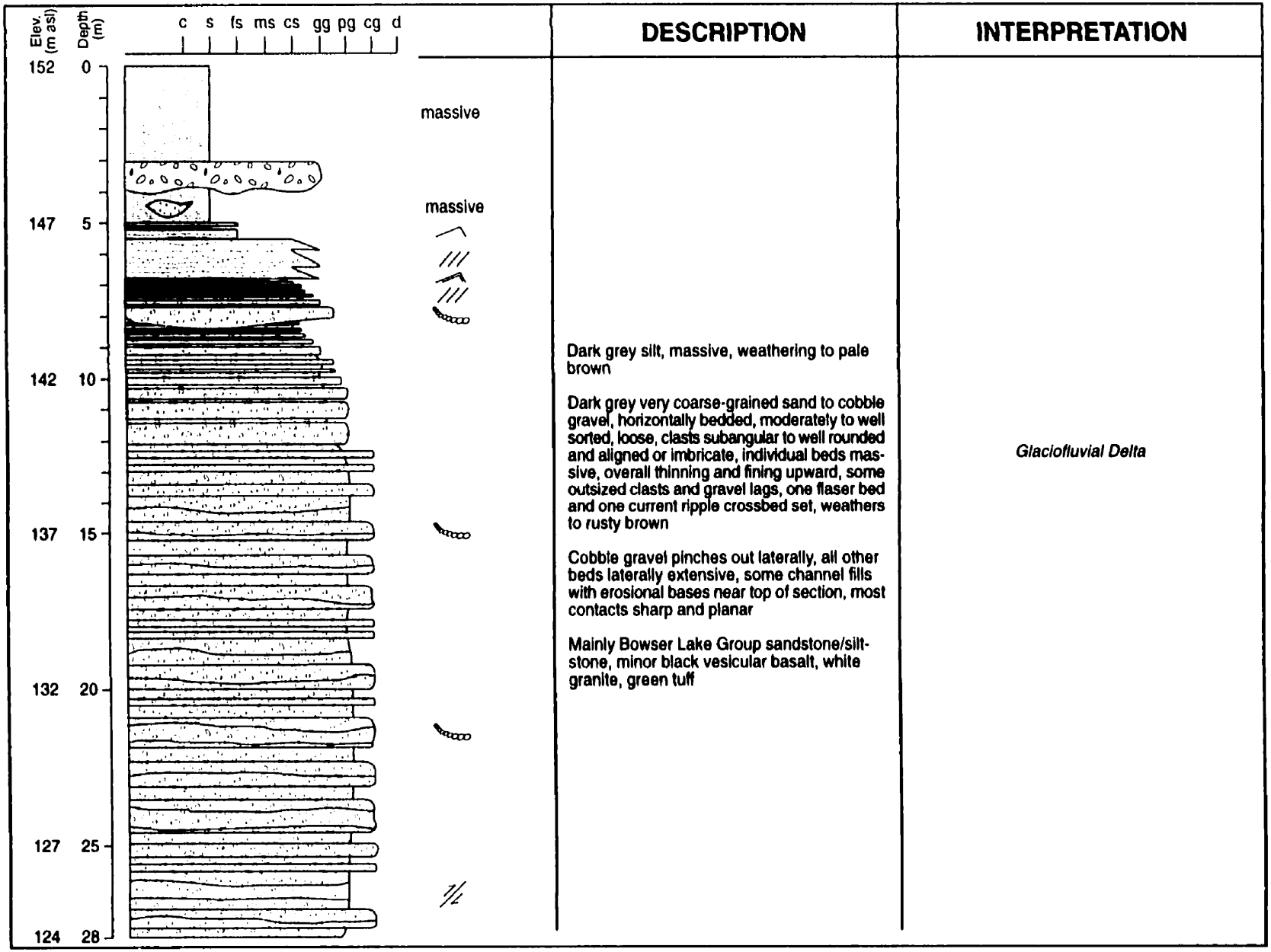


Figure 5.15. Section 97602-05, Aiyansh Gravel Pit, detailed composite lithological log, description and interpretation. Note expanded gravel divisions.

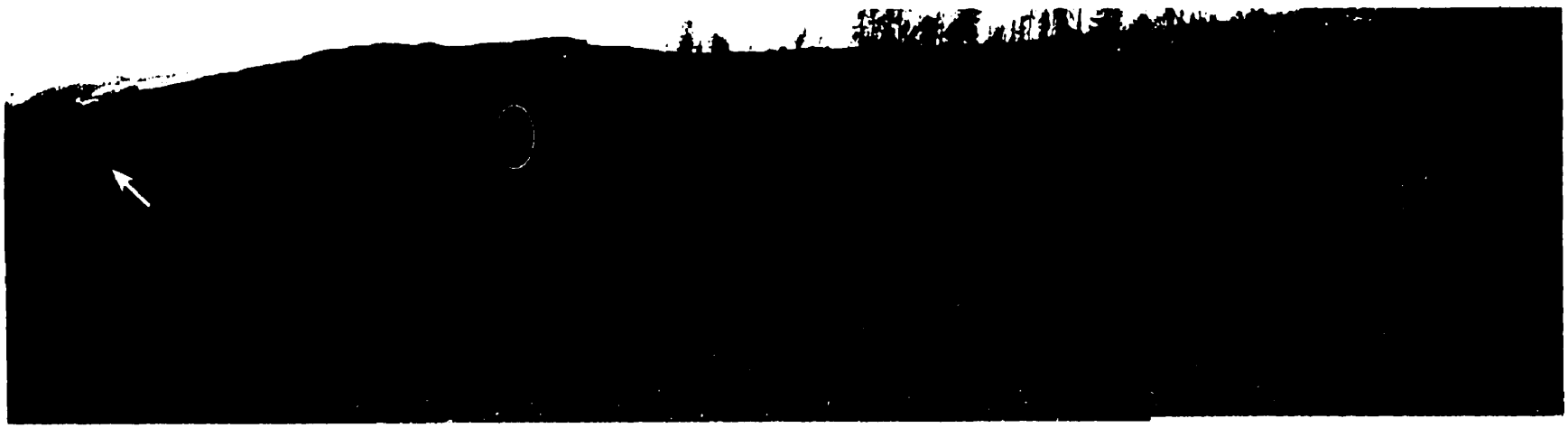

Figure 5.16. Section 97602-05, Aiyansh Gravel Pit. Laterally extensive, horizontally bedded gravel. Note normal fault (arrowed) and figure for scale (circled). The lower 15 m of the section was logged at sites to the left (where fault is located) and right of the figure.

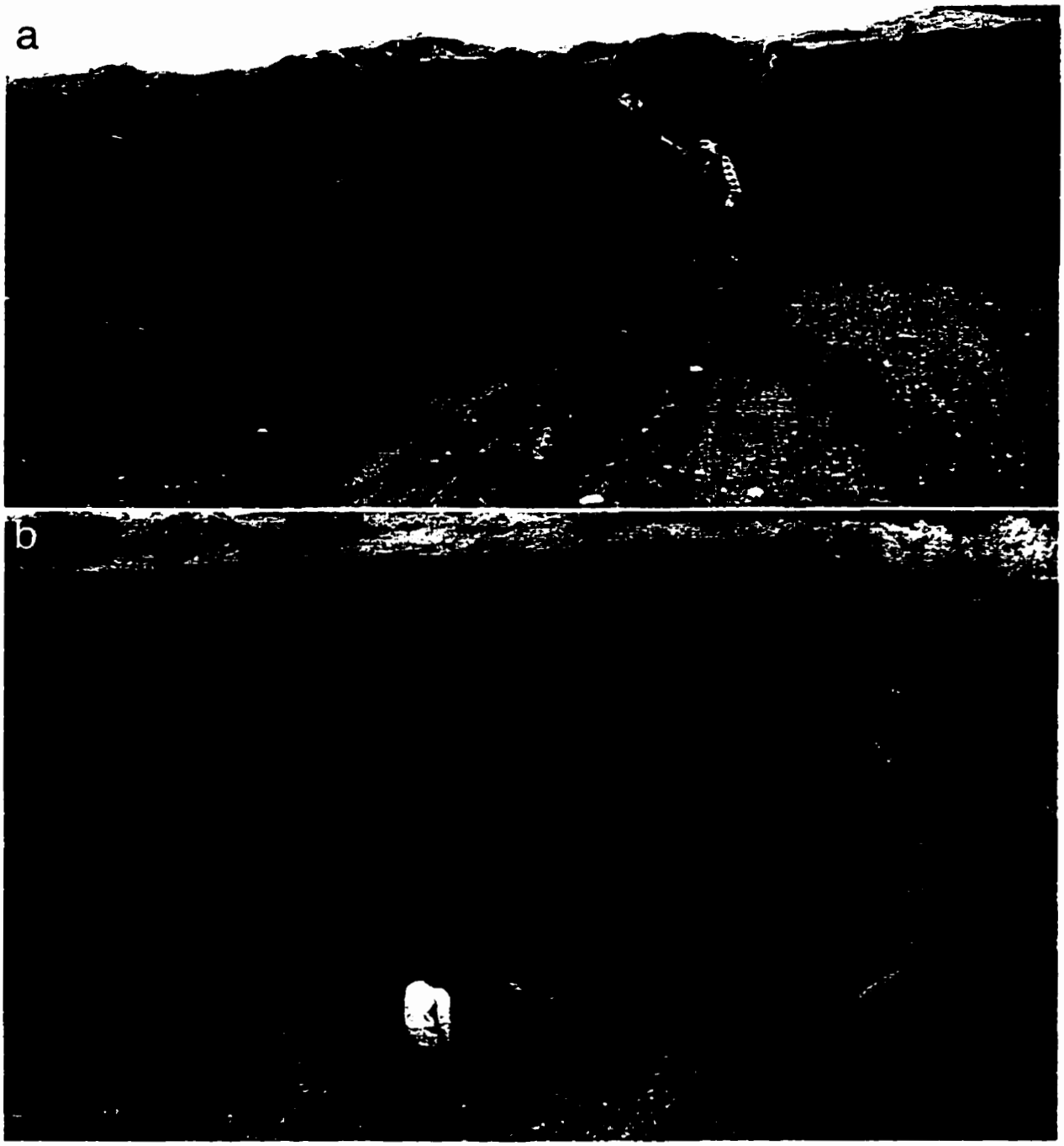


Figure 5.17. Aiyansh Gravel Pit. a) Figure is pointing to an isolated boulder within gravel beds. b) Upper part of section. Thinning and fining upward of massive beds is indicated by a change from light toned gravel to dark toned sand. Note erosive basal contact of granule gravel bed near top of section. Light toned sediment overlying dark toned sand at top of photo is silt.

and gravel lags (Figure 5.17a). The fining-upward beds are overlain by a few silt and fine-grained sand interbeds that show ripple cross lamination.

The upper part of the section comprises massive silt, interrupted by an erosive granule gravel bed and some sand lenses. Soft sediment deformation is common at both the upper and lower silty clay contact. Elsewhere in the gravel pit, the silt unit is overlain by about 2 m of coarse-grained sand and granule gravel interbeds.

Interpretation

The section is located in the terminal zone of the Aiyansh Braidplain, which was determined to be a braidplain from surficial mapping. The coarse, clast-supported gravel, fining-upward beds, planar crossbedding, gravel lags, trough crossbedding and erosive basal contacts indicate deposition in a fluvial environment. However, the laterally extensive beds are not what might be expected in a fluvial or migrating delta distributary channel environment, one where cut and fill features would be common. Outsized clasts within the beds could be interpreted as the remainder of colluvial or alluvial fan debris flow deposits that overran the deposit from the steep valley sides. Smaller clasts were easily removed by water flow, but the river was not able to move the larger clasts. The deposit is interpreted as a glaciofluvial delta. Its location at the terminal zone of a large braidplain suggests that it is a braid delta. The silt at the top of the section may be the final product of waning flow, which is indicated by the thinning and fining-upward beds. The waning flow suggests that the ice front was receding and meltwater production was abating (or was re-directed). The Irene Meadows Road section (Figure 5.12) is stratigraphically lower than the Aiyansh Pit Section, which is near the surface of the braidplain. This site appears to be in an upper delta plain location, while the Irene Meadows section is in a more distal delta slope setting. This basinward fining further supports a deltaic interpretation. Further investigation at this site by ground penetrating radar was carried out and will be discussed in Chapter 7.

*Section 97609-01 (Tseax Creek)*

The Tseax Creek section is northwest of a bridge over Tseax Creek on the Nisga'a Highway at an elevation of 61 m asl (Figure 5.1). Prior to the emplacement of the Aiyansh lava flow, the section was probably eroded by the Nass River, but after the flow, Tseax Creek alone eroded the section. The lava flow overlies former Nass River fluvial gravel, sand and clay on the opposite bank of Tseax Creek.

Description

Figure 5.18 shows the detailed log and description, while Figure 5.19 is a photo of the entire section. From 48 to 17.5 m depth, a very poorly sorted, slightly compact, indistinctly horizontally bedded, blue grey diamicton is interbedded with local beds of granule gravel. The individual diamicton beds are massive and laterally continuous. Clasts within the diamicton vary from very angular to well rounded, and are heavily striated. The matrix is a silty fine-grained sand. A few lenses of normally graded sand are present (*e.g.* 20 m, 27.5 m).

In the central part of the section (17.5 to 7.5 m), gravel, sand, silt and diamicton are interbedded and interfinger laterally with each other. Horizontal bedding, imbrication and massive beds are common. Clasts are angular to subrounded and unstriated, except for the diamicton clasts, which are angular to well rounded, and 10% of which are striated. Dropstones are abundant in the silt and fine-grained sand beds.

In the upper part of the section (6.4 to 7.5 m), massive, unfossiliferous blue silty clay is interbedded with brown silt and some fine-grained sand and gravel beds. These beds are jointed and horizontally laminated, with a few dropstones and some small lenses of very fine-grained sand. They are overlain by well rounded pebble gravel.

Interpretation

The lowest unit, a 30 m thick diamicton, with indistinct horizontal bedding and local interbeds of granule gravel and sand lenses, is interpreted as a melt-out till. The poor bedding preserves some of the original texture of the till in ice, and has been preserved by melt out rather

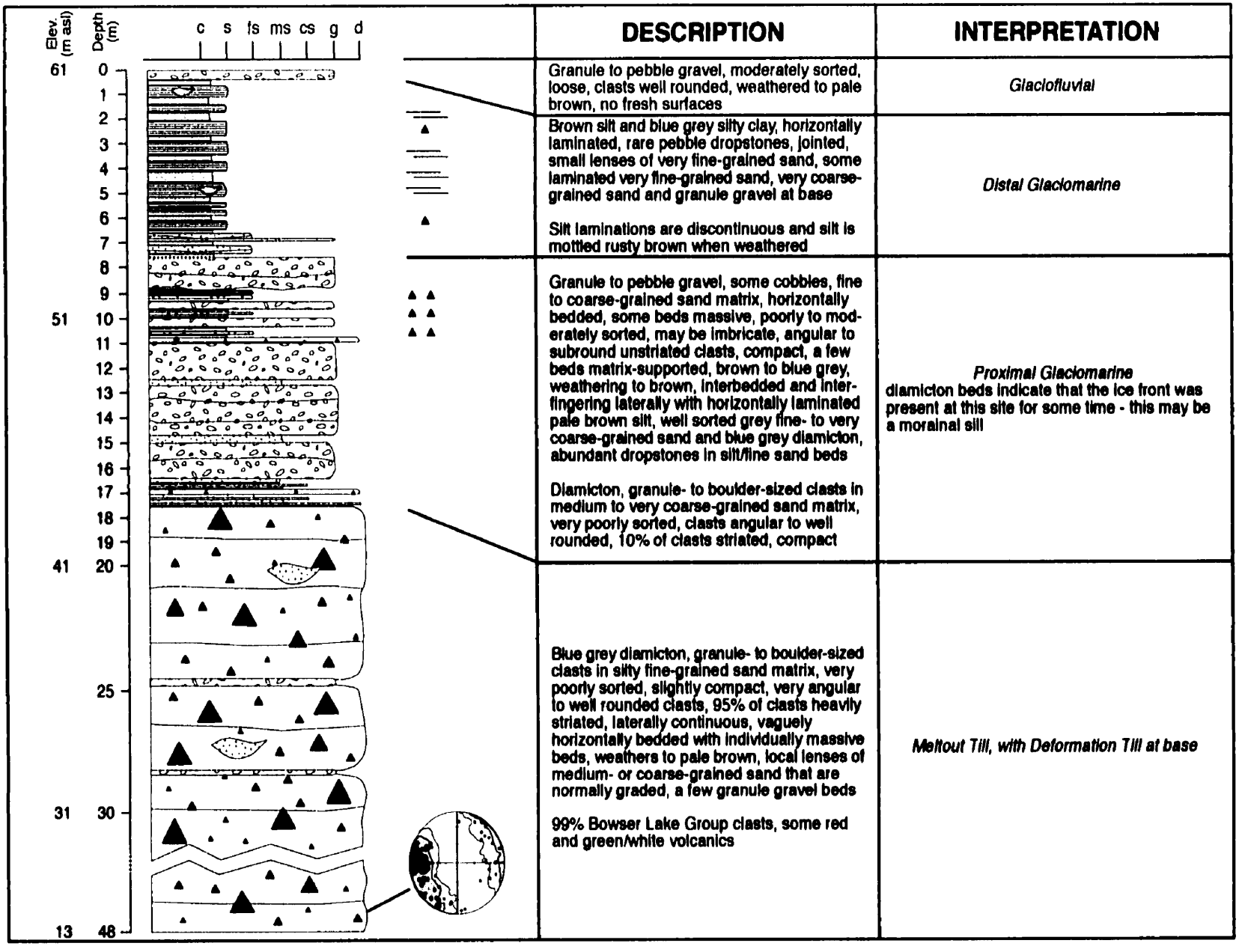


Figure 5.18. Section 97609-01, Tseax Creek, detailed lithological log, description and interpretation. A till fabric from the base of the section is shown.

Figure 5.19. Upper part of section 97609-01, Tseax Creek. Brackets show fine-grained interbeds (f), coarse-grained interbeds (c) and diamicton (d).

than obliterated by lodgement, deformation or post-depositional flow. Small englacial channel deposits are also preserved (normally graded sand lenses, granule gravel beds). A till fabric from the base of the section is not particularly strong, and shows an approximate southwest ice flow direction (ice flow down the Nass Valley) (Figure 5.18). Its spread nature suggests that the till at the base of the section is actually a deformation till. The diamicton is not interpreted as a rain out till, because that type of till would have no discernible fabric or bedding.

The overlying interfingering beds of coarse- and fine-grained sediments and diamicton (17.5 to 7.5 m) are typical of a very ice proximal glaciomarine environment (Powell and Molnia, 1989). None of the beds is particularly thick, and the high variability and lateral pinch outs are distinctive of a subaqueous fan deposit. As a subglacial jet changes position, coarse-grained sedimentation also changes position, resulting in beds that pinch out laterally. However, the group of beds is laterally extensive, so it does not seem to have an actual fan shape that is discernible at the section scale. This section is large, though (50 m high and about 200 m wide), so a fan shaped morphology is likely to be visible if present. The ice front may have been too mobile for a complete subaqueous fan to develop. The fan shape that develops as a subaqueous jet sweeps back and forth at a stationary ice front would not have had enough time to form if the ice front was retreating rapidly.

The finer-grained overlying beds are interpreted as distal glaciomarine deposits. The fining up at the base of this unit (7.7 to 6.7 m) is interpreted to reflect the retreat of the ice front. The interbedded silt and silty clay show that flow fluctuations reached distal areas. Very fine-grained sand lenses probably represent distal parts of channelized flows that reached distal glaciomarine areas. The uppermost gravel bed is probably glaciofluvial or deltaic, as inferred from its well rounded clasts, coarse-grained and loose nature, as well as its proximity to a major braidplain (Nass Valley map).

*Section 97601-01 (near Aiyansh lava flow)*

This section is a logging road cut exposure just south of the Aiyansh lava flow, at 155 m asl (Figure 5.1). A detailed log and description are given in Figure 5.20.

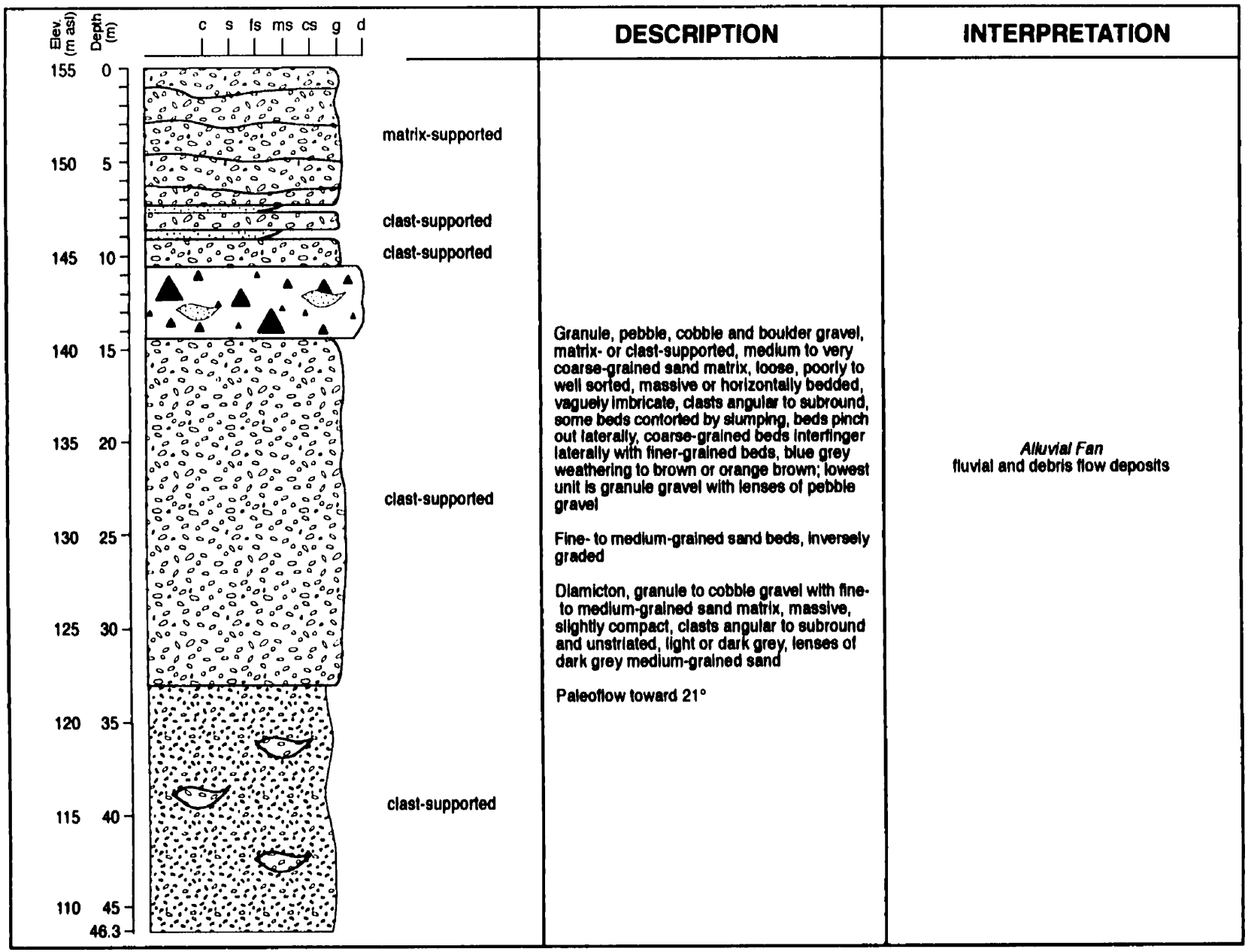


Figure 5.20. Section 97601-01, near Aiyansh lava flow, detailed lithological log, description and interpretation.

Description

Most of the section exposes clast-supported, vaguely imbricate, poorly to well sorted, granule to boulder gravel. Local interbeds of coarsening-upward fine- to medium-grained sand and lenses of massive pebble gravel within granule gravel occur in this unit. There are also some matrix supported, horizontally bedded gravels and a diamicton bed. The latter is a massive deposit of granule to cobble gravel with a sand matrix, containing angular to subround clasts and sand lenses.

Paleoflow direction, based on imbricate clast orientations, is to the north-northeast at 21°.

Interpretation

The mix of clast- and matrix-supported gravel, diamicton and sand lenses is consistent with an alluvial fan interpretation. This interpretation is also supported by surficial geology mapping (see Nass Valley map), as the area surrounding the section is mapped as an alluvial fan deposit. The diamicton and matrix-supported gravels are interpreted as debris flow sediments, while the clast supported gravels are fluvial deposits. The alluvial fan shown on the Nass Valley map has formed from a northward flowing river and debris flows. The paleoflow direction of 21° is thus consistent with the alluvial fan's direction of progradation.

## Drill hole and Geophysical Log Descriptions

Drilling was carried out in areas of the Nass Valley where there were no section exposures and at sites on or close to seismic line locations. For the most part, surface sediments were either massive silty clay, sand or gravel. Drill sites were spaced at intervals along the Nass Valley to obtain good down valley coverage (Figure 5.21). All holes were drilled in areas of expected glaciomarine deposits, but a few were near or on braidplain and alluvial fan deposits.

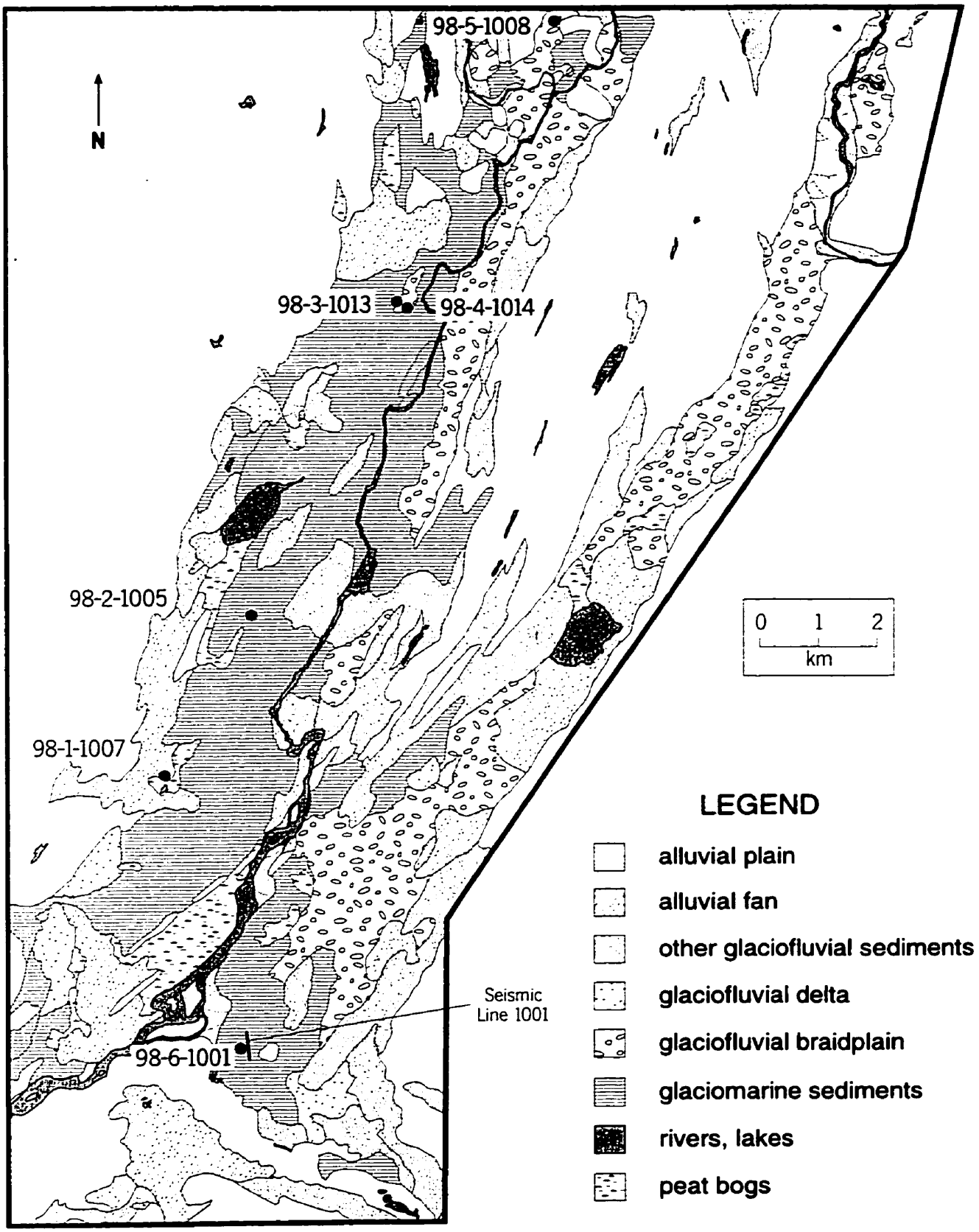


Figure 5.21. Location of drill holes with respect to glaciomarine and other deposits.

*Drill Hole 98-1-1007*

Location

This drill hole was located at the eastern edge of a modern alluvial fan on the valley's western edge, at 125 m asl (Figure 5.21). The site was chosen for its proximity to the fan, in order to examine possible fan contributions to the glaciomarine environment. A small section is exposed 800 m to the east, on the same logging road as the drill hole. The section shows silty clay overlain by and grading laterally to yellow brown weathering sand and gravel. The gravels are indistinctly horizontally bedded.

The hole was drilled at the roadside, and therefore a thin layer of road gravel was encountered at the surface. This gravel is not included in either the log or the description, as it does not add to the understanding of glacial history.

Description

The detailed lithology of the drill hole is shown in Figure 5.22. The lower portion of the log (14.9 to 3 m) is dominated by massive, sticky, blue grey silty clay. Silt, very fine-grained sand and medium-grained sand are found at the base of this unit. There appears to be a slight fining-upward trend in these beds. The overlying silty clay unit is interrupted in places by very fine-grained sand beds, some of which have clast-rich bases. The upper clast-rich layer (at 6.9 m) consists of granules whereas the lower one (9.9 m) contains subangular to angular pebbles and cobbles.

A silty, sandy pebble/cobble gravel bed with subangular clasts is found from 3 to 0.7 m. It is poorly sorted and loose.

Overlying the gravel is more silty clay.

All of the coarser-grained beds are dark blue grey in colour, and the gravels are of Bowser Lake Group provenance. The blue grey clay is probably of the same provenance.

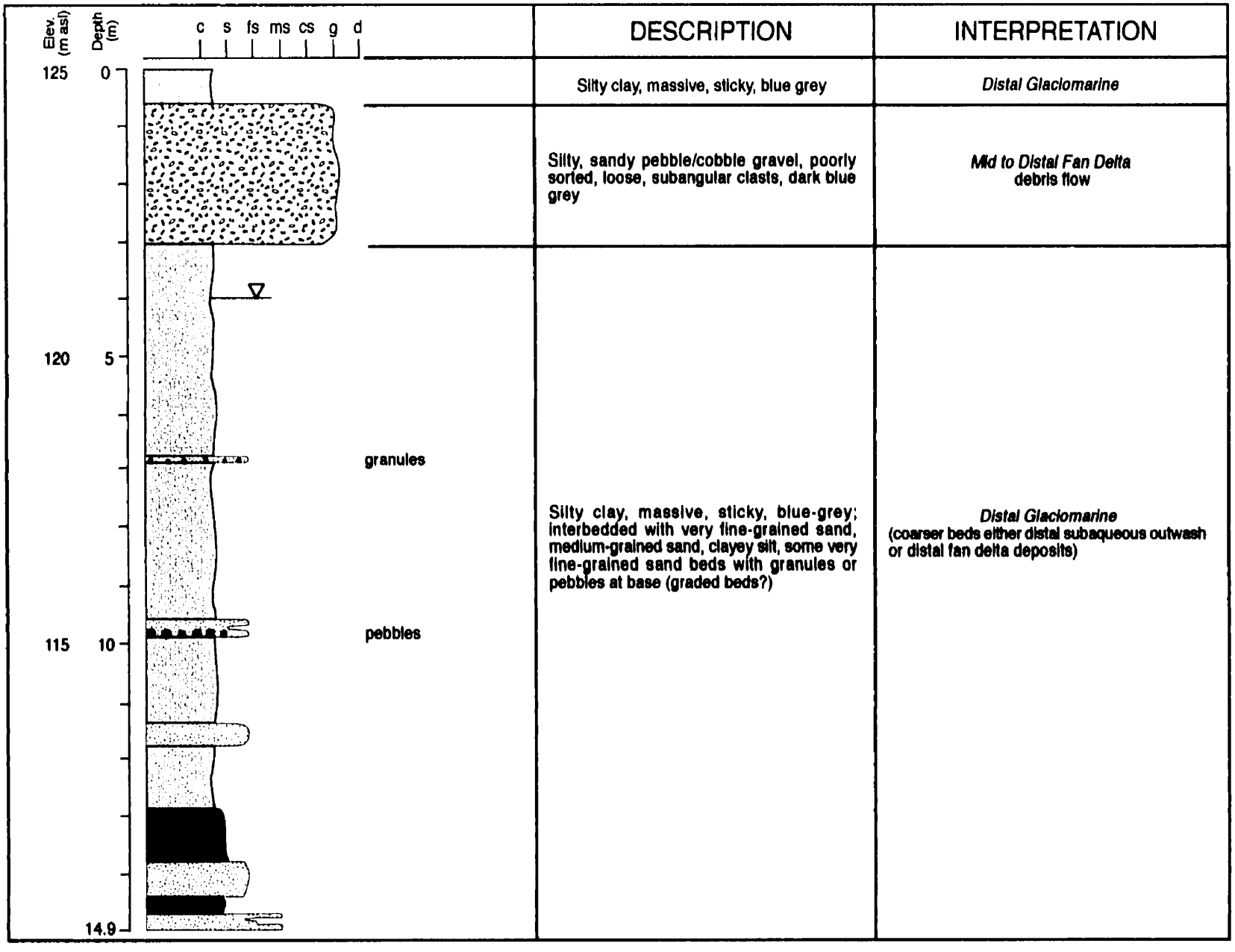


Figure 5.22. Drill hole 98-1-1007, detailed lithological log, description and environmental interpretation.

Interpretation

The silty clay, silt and sand beds are interpreted as distal glaciomarine deposits. The coarse interbeds from 14.9 to 6.7 m may be distal deposits of subaqueous outwash from a receding ice front. This interpretation is supported by the upward thinning and less common occurrence of coarse interbeds toward the top of the record. The sand beds with clast-rich bases might correspond to graded beds of turbidite deposits formed by subaqueous underflows, but it is impossible to be certain of this without a good section exposure.

The poorly sorted gravel near the top of the hole is interpreted as a subaqueous debris flow deposit. The modern alluvial fan visible at the surface may have been present as a fan delta during the deposition of the glaciomarine silty clay. Talus cones and fan deltas are common minor sediment sources in modern fiords (Syvitski and Hein, 1991). If this was the case, the fan was much smaller initially, contributing only local coarse beds, such as this one, to the distal glaciomarine environment. Immediately prior to the end of marine deposition, the fan grew considerably. It was at this time that the thick debris flow bed found near the top of the interval was deposited. Quiet silty clay deposition followed, signaling a return to glaciomarine conditions. Fan deposition halted temporarily or the depositional zone moved to a different location at this time.

*Drill Hole 98-2-1005*

Location

This drill hole was drilled in an area of extensive surficial clay deposits, 2 km east of two modern alluvial fans, at 163 m asl (Figure 5.21). The site was chosen because it was the closest point to the centre of the western part of the Nass basin that could be accessed with the drill rig. A long record (about 36 m) was obtained at this location.

Description

A detailed description accompanies the lithologic and geophysical logs in Figure 5.23. Poorly sorted clay to pebble gravel diamicton with striated clasts was encountered at the base of the hole. This unit was extremely hard, and it plugged the drill bit twice. Although it was very hard

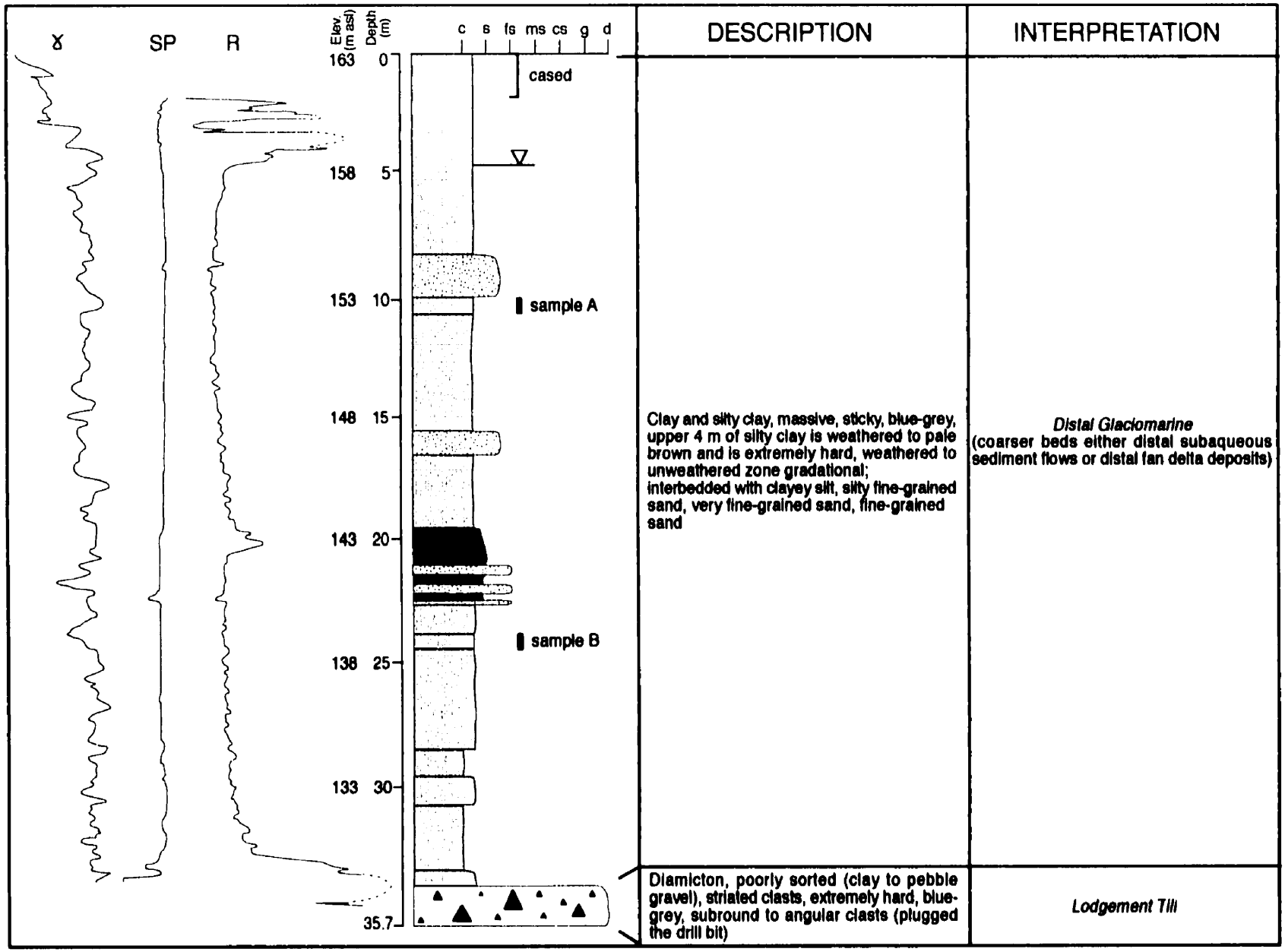


Figure 5.23. Drill hole 98-2-1005, geophysical logs, lithological log and interpretation. Note the marked deviation in the logs at the diamicton bed. Split spoon sample intervals are shown with black bars.

to drill, some of the diamicton came up with the drill bit due to the plugging, which allowed a better description of the diamicton. The matrix of the diamicton was blue grey in colour.

Sticky, blue grey clay and silty clay overlie the diamicton. The upper 3 to 4 m of silty clay is weathered to pale brown and is extremely hard. The weathered to unweathered zone is gradational and the unweathered silty clay is quite soft. Localized incursions of silty sand, sand and clayey silt are also present, but overall, the drill core is dominated by silty clay.

Samples A and B were taken at 9.9 and 23.8 m respectively. Both samples revealed massive, sticky silty clay over a 50-55 cm interval (Figure 5.24a).

Geophysical Log Description

The three geophysical logs are fairly uniform throughout the drill hole, but there are deviations in places. The logs deviate or disappear entirely at the contact with the diamicton (Figure 5.23), indicating that the diamicton bed must be distinctly different from the strata above. The gamma log does not parallel the lithologic log, although it must be detecting variations in gamma radiation. In some places (e.g. 22 m, 9 m) it does reflect sandier beds, but in others, perhaps the change was too subtle to recognize with the method used (logging cuttings rather than retrieving core). Alternatively, the deflections could be showing areas enriched in illite, a potassium-bearing clay mineral. Small deviations in the R log at 8, 20 and 22.5 m are related to the fine-grained sand, very fine-grained sand and silt beds. The latter of these deflects the opposite way and may indicate a pure clay bed at the location that was too thin to pick up with the cuttings analysis method. One of the very fine-grained sand beds (16 m) was not detected; it is not clear why it was not. The deflections in the upper part of the R log indicate that the water table was encountered at 5 m, thus the electrical logs above this point are unreliable. There is no SP or R response over the cased interval. All of the logs are more or less uniform, indicating that there are no major upward fining or coarsening trends in the sequence.

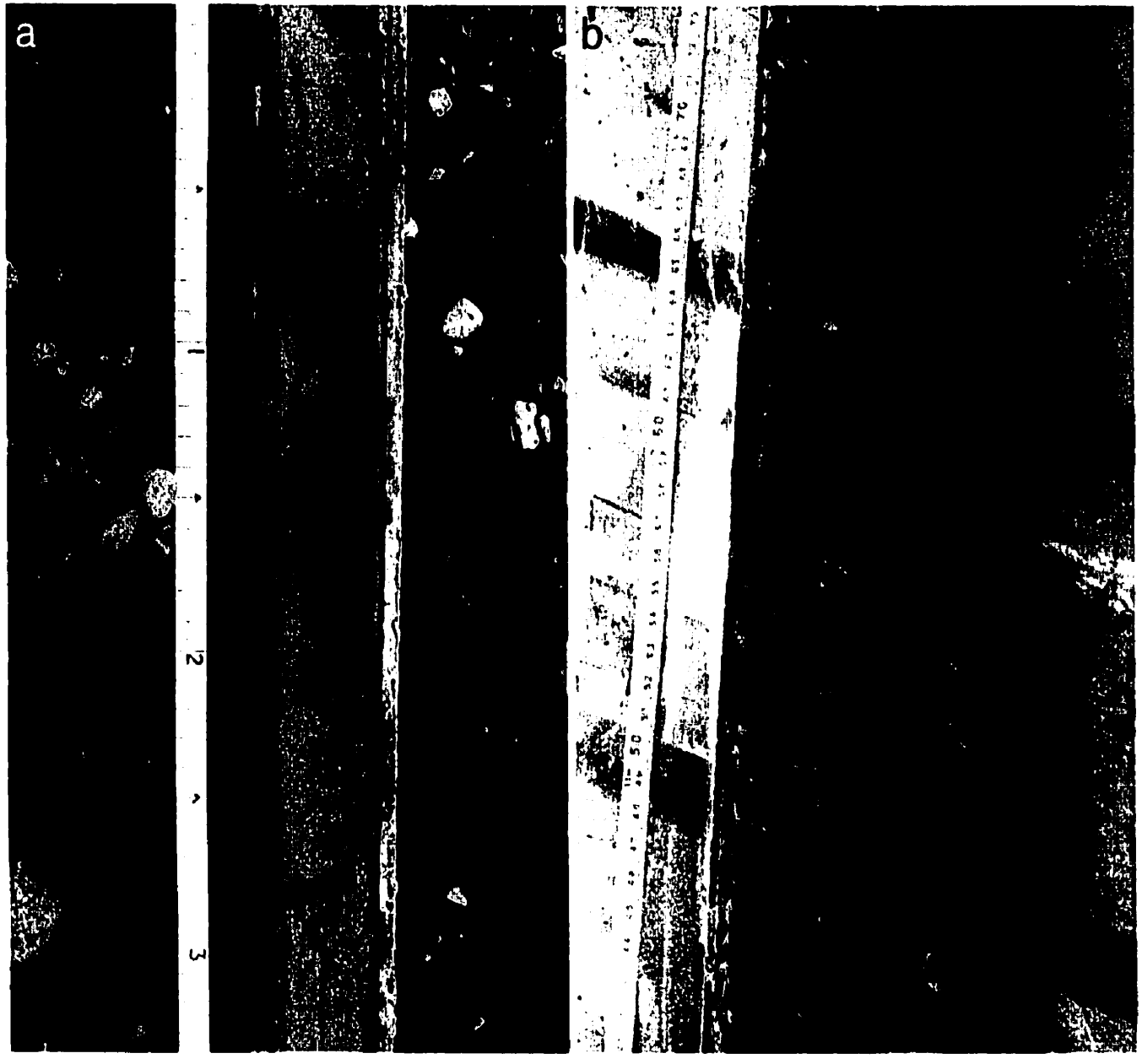


Figure 5.24. Split spoon core samples. a) Sample A from Drill Hole 98-2-1005, massive, sticky blue grey silty clay. b) Sample D from Drill Hole 98-6-1001. The silty clay is finely laminated. Scales for both photos are in cm.

*Interpretation*

Actively flowing ice deposited the compact diamicton, which is interpreted as lodgement till due to its compact nature, poor sorting and striated clasts (all visible in the plugged drill bit). Its blue grey colour suggests a Bowser Lake Group provenance. Formation of the diamicton by rain-out is possible, but is considered unlikely due to the high matrix to clast ratio of the till.

The massive nature of the silty clay itself indicates continuous and fairly rapid deposition of rock flour and possibly clay minerals that settled from suspension in deep water as meltwater plumes lost energy in locations distal to the ice front. It is similar to the homogeneous "bergstone mud" environment distal to the tidewater front in fiord systems (Powell and Molnia, 1989). However, dropstone influx is not evident here and it is better termed a homogeneous silty clay deposited in a distal glaciomarine environment. This type of deposition occurred for a sufficient period of time to accumulate 35 m of fine sediment.

The silty fine-grained sand and fine-grained sand beds within the silty clay are interpreted as the tail end of sediment flows from either valley side fan deltas or from subglacial meltwater influx at a grounded ice margin. The beds do not show any upward fining, thinning or coarsening trend, based on drill hole and geophysical log evidence, so it is difficult to say which source area interpretation is correct.

*Drill Hole 98-3-1013*

Location

This drill hole is at the edge of a significant clay/gravel contact at the surface (Figure 5.21), and the purpose of drilling this hole and the following one (98-4-1014) was to delineate the subsurface nature of this contact. Drill hole 98-4-1014 actually comprises a series of four drill holes, which along with 98-3-1013, form a transect across the gradational surficial contact. The transect is at an elevation of about 165 m asl. From surficial mapping work, the western portion of the transect was determined to be an extensive surficial clay unit, whereas the eastern portion was defined as a glaciofluvial braidplain (Nass Valley map). It was suspected that this braidplain

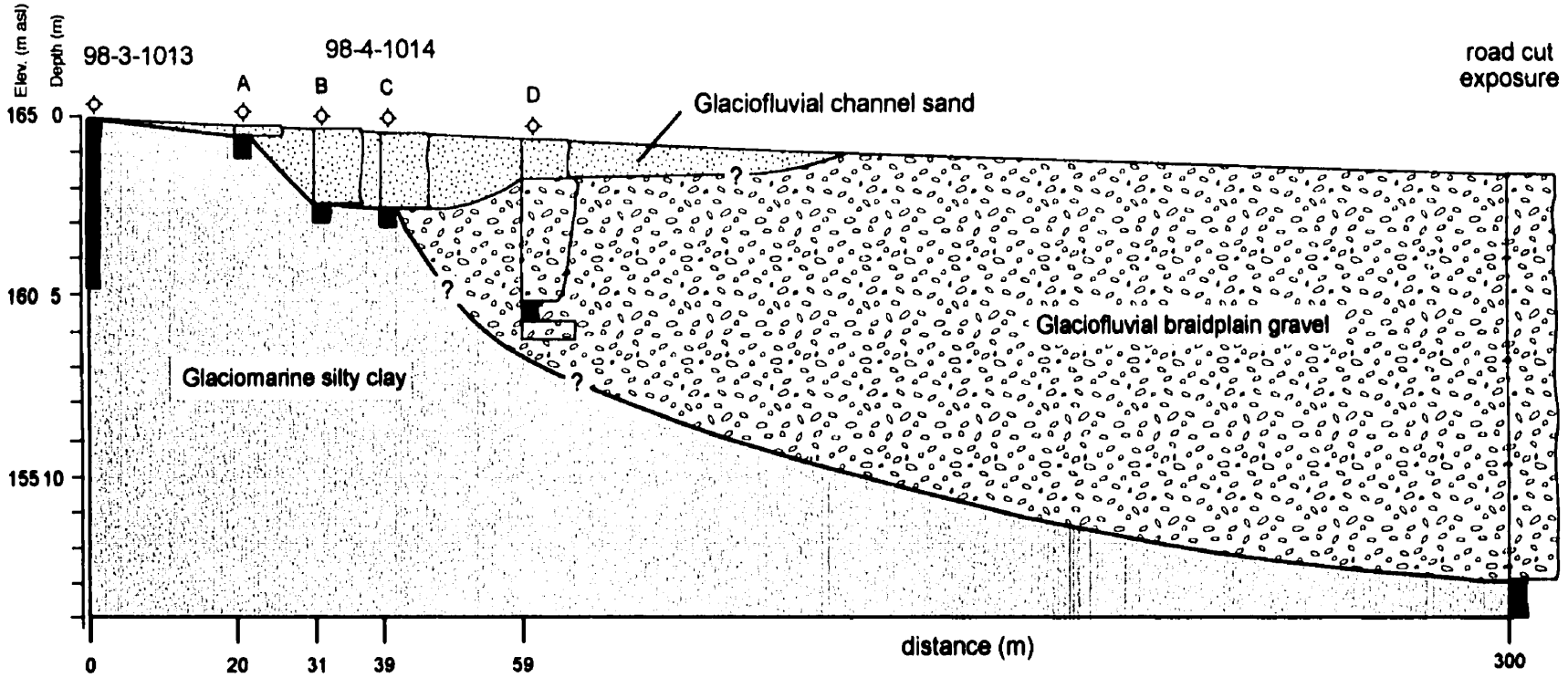


Figure 5.25. Drill holes 98-3-1013 and 98-4-1014 A-D, from clay contact to glaciofluvial gravel area. The lithologic log on the right is a road cut exposure. The holes (identified by the circular drillhole symbol) penetrate the western edge of the glaciofluvial plain and delineate the extent of the subsurface contact of glaciofluvial gravel/sand and underlying glaciomarine clay. The approximate location of the channel edge is shown. Clay is shown darker on logs than in legend.

was part of the Nass Braidplain to the east (Figure 5.21) and that earthflow activity and fluvial incision had isolated it and made it a remnant.

Description

The core from this hole revealed massive silty clay to almost 5 m depth (Figure 5.25). The blue grey silty clay was weathered to pale brown down to 3 m. The contact between weathered and unweathered clay was gradational.

Interpretation

The silty clay at this site represents the same distal glaciomarine environment as that of the previous drill hole (98-2-1005).

*Drill Hole 98-4-1014*

Location

Four closely spaced holes (labelled A to D) were drilled to continue the transect started with Drill Hole 98-3-1013. A road cut exposure completes the transect (Figure 5.25). Since they are very close together, the holes and exposure are shown as a single point on Figure 5.21. The hollow stem auger was used at these sites as the sandy gravels at the surface were difficult to penetrate, even with the solid stem auger.

Description

The exposure and all of the holes, except hole D, bottomed out in silty clay. Sand and gravel overlie the clay in each hole (Figure 5.25). Very coarse-grained sand with pebbles and granules was found at the top of holes A to D. Hole D, however, also had an inversely graded unit of coarse-grained sand to pebble gravel and a pebble gravel unit. The road cut exposure is dominated by sandy pebble gravel. The area surrounding the road cut is a small gravel plateau that has been eroded on all sides by earthflow activity. The earthflows may have been induced by bank erosion along the nearby Nass River.

Interpretation

From air photo interpretation and field work, the sand and gravel deposits were determined to be part of a small braidplain. The coarse-grained sediments are interpreted as glaciofluvial deposits. Drill core evidence shows that the gravel is incised into the marine clay. The coarse-grained sand in the upper levels and near the edge of the transect may be a deposit from a slower flowing channel. Further reconnaissance in the area revealed the presence of thin, localized, fine-grained sand overlying glaciomarine clay just west and also south of hole 98-3-1013. Clearly, the glaciofluvial gravel and sand were deposited after the glaciomarine sediments and the lower erosive contact is a major discontinuity, since subaerial exposure of the clay must have occurred prior to fluvial incision.

*Drill Hole 98-5-1008*

Location

This drill hole was situated near the edge of a large earthflow, just west of the Nass River, at 185 m asl (Figure 5.21). Its location on a more northern part of the Nass Braidplain was aimed at establishing the relationship of the braidplain to the underlying sediments in this area.

Description

A detailed description, the lithologic log and the geophysical logs are shown in Figure 5.26. The drill hole bottomed out in gravel at 17.7 m. Clasts were crushed and it was difficult to tell whether the lowest bed was gravel or whether it was diamicton.

The gravelly bed is overlain by fine-grained sand, medium-grained sand and silty clay interbeds. The succession thins and fines upward, but individual beds are not normally graded. The sand and clay beds are overlain by silty clay which is weathered gradationally down to 4.3 m. The uppermost unit consists of interbedded fine-, medium- and coarse-grained sand.

Sample C, taken at 15.5 m, is unfortunately very thin (4 cm) (Figure 5.26). However, medium-grained sand, silt and fine-grained sand interbeds with sharp contacts are present in the

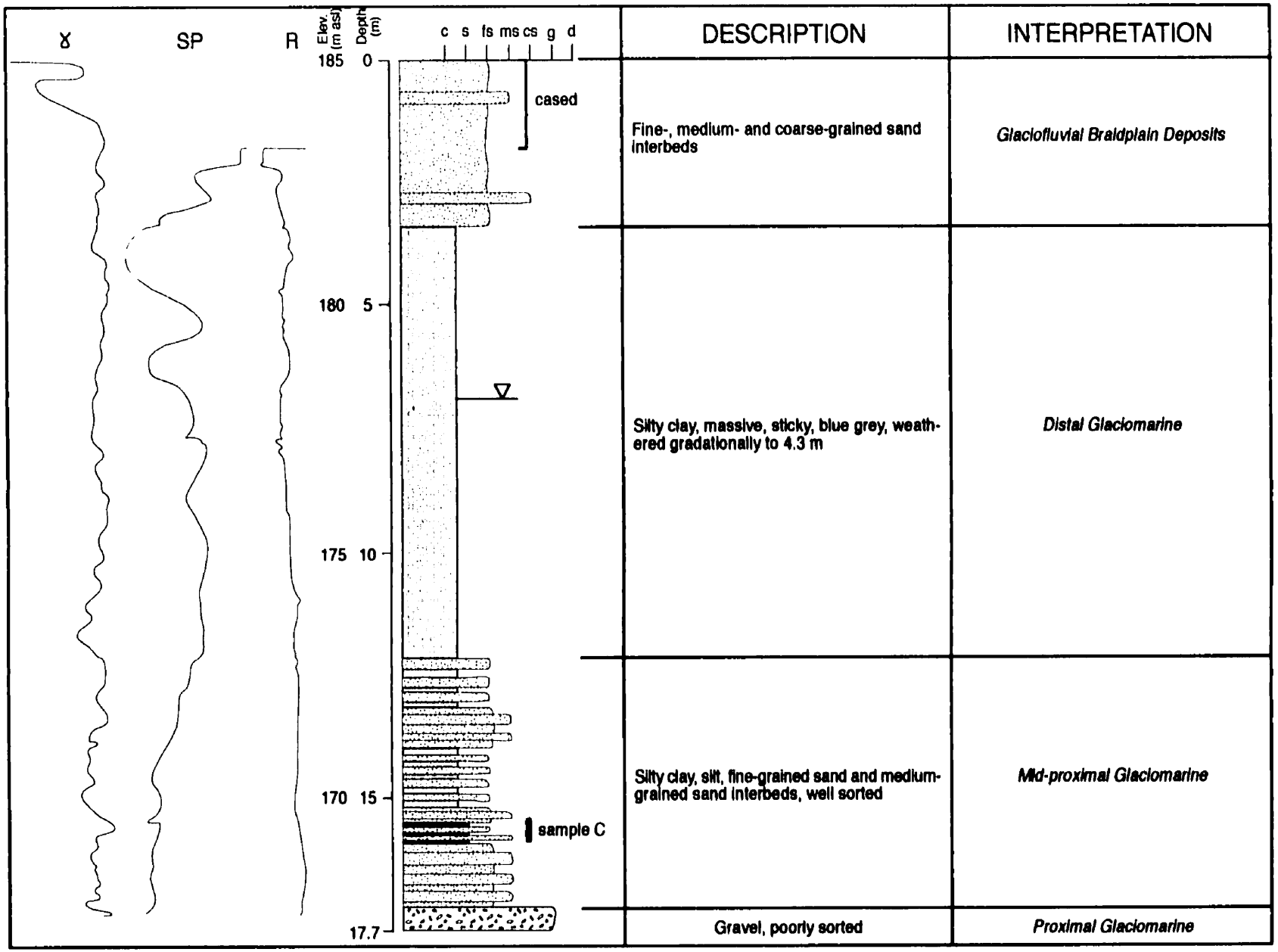


Figure 5.26. Drillhole 98-5-1008, geophysical logs, lithological log and interpretation. Split spoon sample interval is shown with a black bar.

sample. Each bed is 1 cm thick. Beds are well sorted but lack obvious primary sedimentary structure.

Geophysical Log Description

The geophysical logs are not very informative at this site, except for the SP log, which shows a general upward fining from 17.2 m to 12.2 m (Figure 5.26). The deviations in the upper part of the SP log are probably due to the location of the water table at about 6.5 m and are considered unreliable. The R log is therefore unreliable to this depth as well. These logs start below the cased interval.

Interpretation

It was difficult to tell with certainty whether the lowermost unit was diamicton or poorly sorted gravel, due to clast crushing during drilling. The geophysical logs do not deviate significantly enough to suggest that the unit is a till (as they do at 98-2-1005), so it is considered to be a gravel. Overlying beds become progressively finer, leading to the inference that the ice margin was initially nearby but gradually withdrew, until only silty clay was deposited. The source for these sediments was probably one or more subaqueous fluvial jets. This unit is therefore interpreted as a proximal glaciomarine deposit, while the upper unit is more distal. The lack of gravelly sediments in the proximal unit suggests that it can be further refined. It is interpreted as a mid-proximal glaciomarine environment.

Later, glaciofluvial (braidplain) sands were deposited over the glaciomarine clay when sea level dropped and the ice front had retreated even further. The contact between the upper two units is thus a major discontinuity.

*Drill Hole 98-6-1001*

Location

This site is located in an extensive clay unit near the town of New Aiyansh, southwest of the Aiyansh Braidplain (Figure 5.21) and is at an elevation of 90 m. The drill hole is not far from the

location of seismic line 1001 (Nass Valley map). This site completes the down valley cross section obtained by the drilling program.

The silty clay was very dry and hard compared to that of sites west of the Nass River. Coherent pieces of clay came up in the mud return, possibly due to this hardness. The diamicton at the base of the hole eventually plugged the drill bit.

Description

In order to show the lithologic details, the lithologic log, geophysical logs and descriptions of the drill hole have been split into two figures, comprising the upper and lower portion of the drill hole (Figures 5.27 and 5.28). The complete drill hole is shown in Figure 5.29 for reference, but some of the details are lost due to the larger scale.

The lowest unit is a diamicton, a pebbly deposit which plugged the drill bit. The plugged 'sample' was a stiff, blue grey, compact, poorly sorted diamicton. Drilling progress halted when the bit encountered a boulder.

The unit overlying the diamicton consists of a series of beds from silt to granule gravel interfingered with silty clay (24.2 m to 41.5 m). Pebble gravel beds were rare and no fining-upward trend was evident.

Completely uniform, structureless silty clay makes up the remainder of the drill hole log (above 24.2 m).

Samples D and E were taken at 11.3 and 25 m, respectively (Figures 5.27 to 5.29). Sample E required considerable hammering. Sample D is a finely laminated silty clay (Figure 5.24b). It is a rare laminated example of the ubiquitous silty clay in the Nass Valley. The same silty clay is massive across the upper 6 m of the hole, as determined by augering. From bottom to top, sample E consists of 24 cm of very well sorted, fine-grained sand with one 2 mm silt lamination, 10 cm of silt and 6 cm of angular (crushed?) granule gravel. The silt is blue grey and is also finely laminated, whereas the fine-grained sand is massive and dark grey.

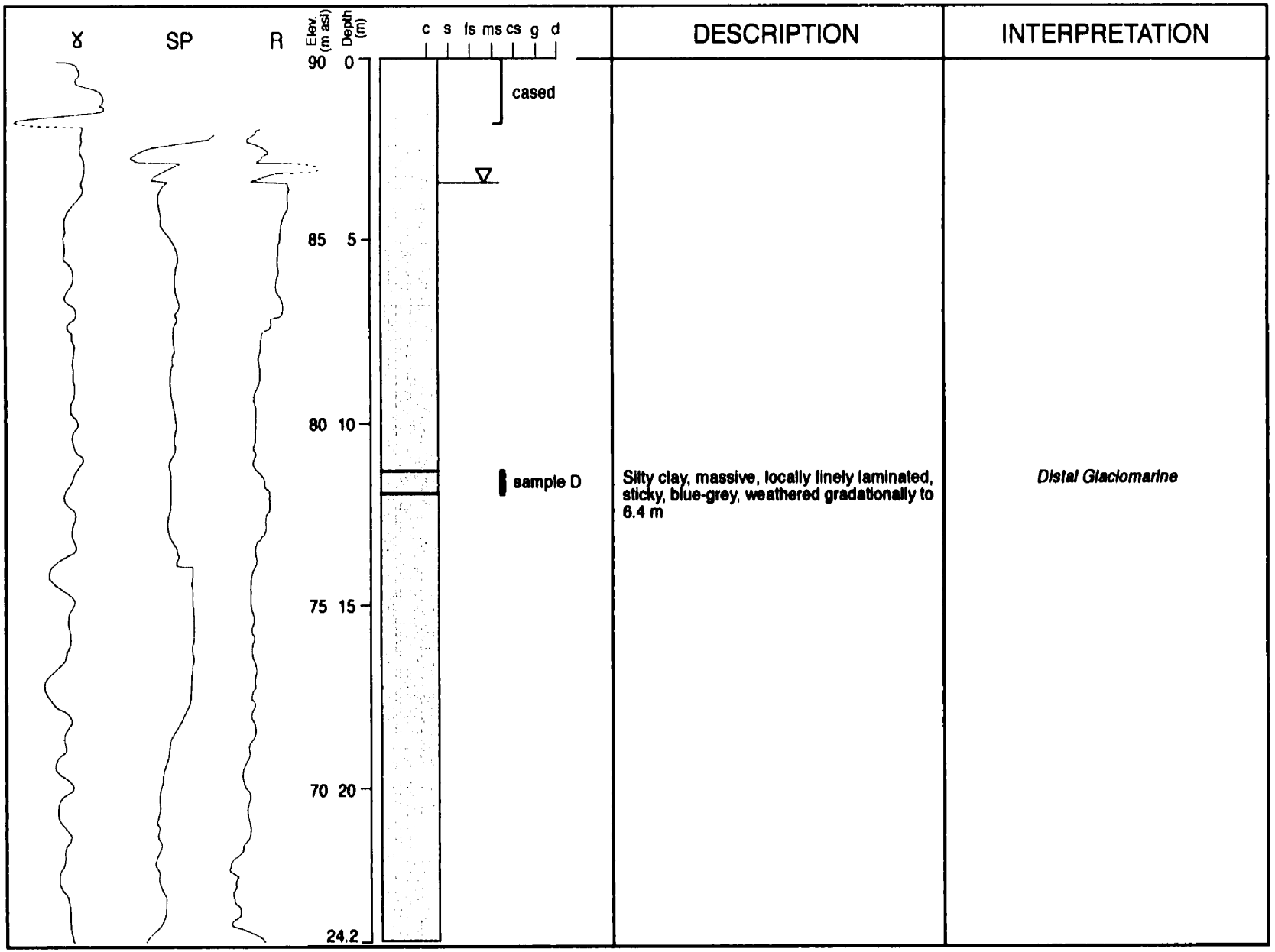


Figure 5.27. Upper half of Drillhole 98-6-1001, geophysical logs, lithological log and interpretation; split spoon sample interval is shown with a black bar.

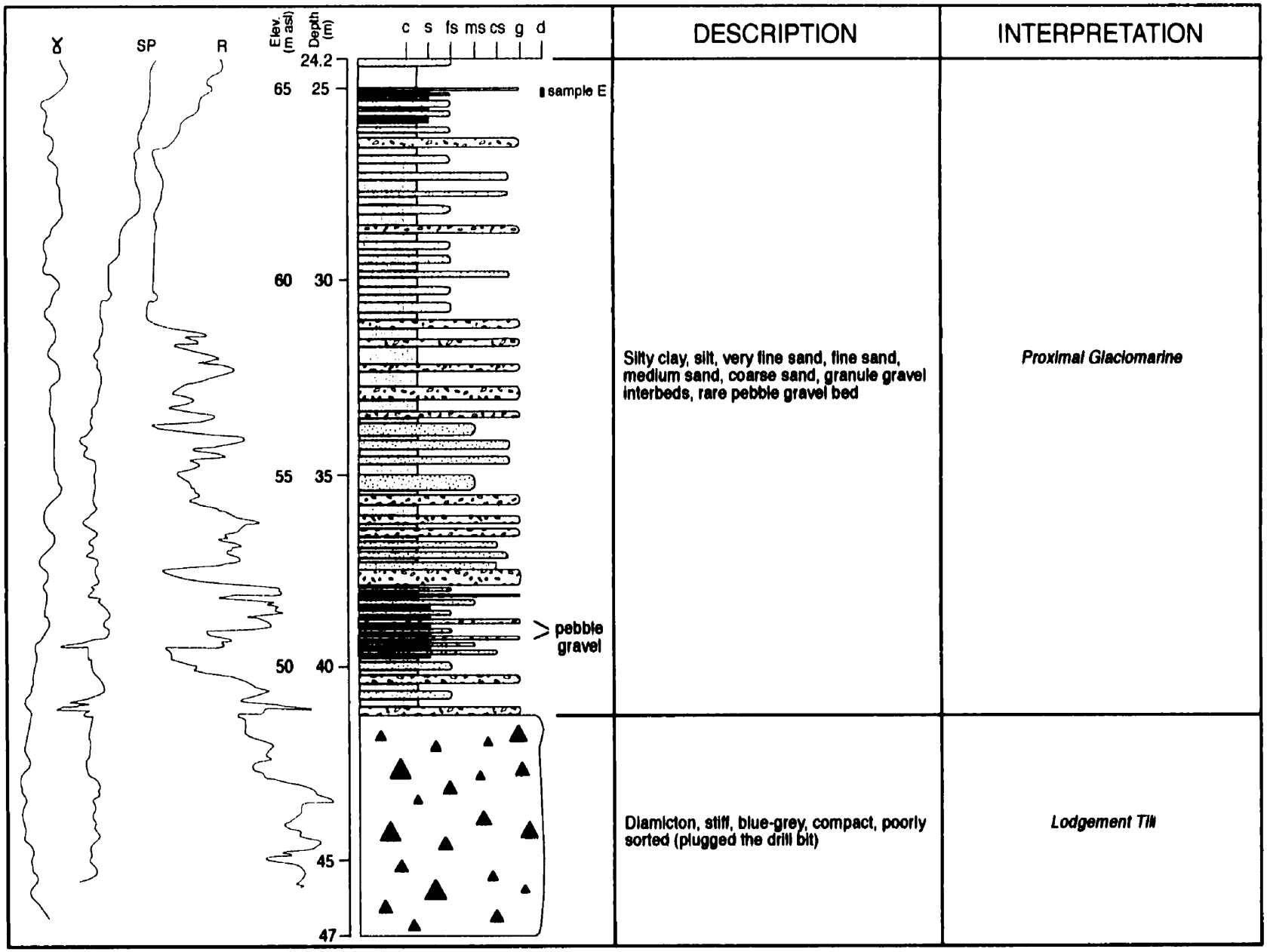


Figure 5.28. Lower half of Drillhole 98-6-1001, geophysical logs, lithological log, description and interpretation. Split spoon sample interval is shown with a black bar.

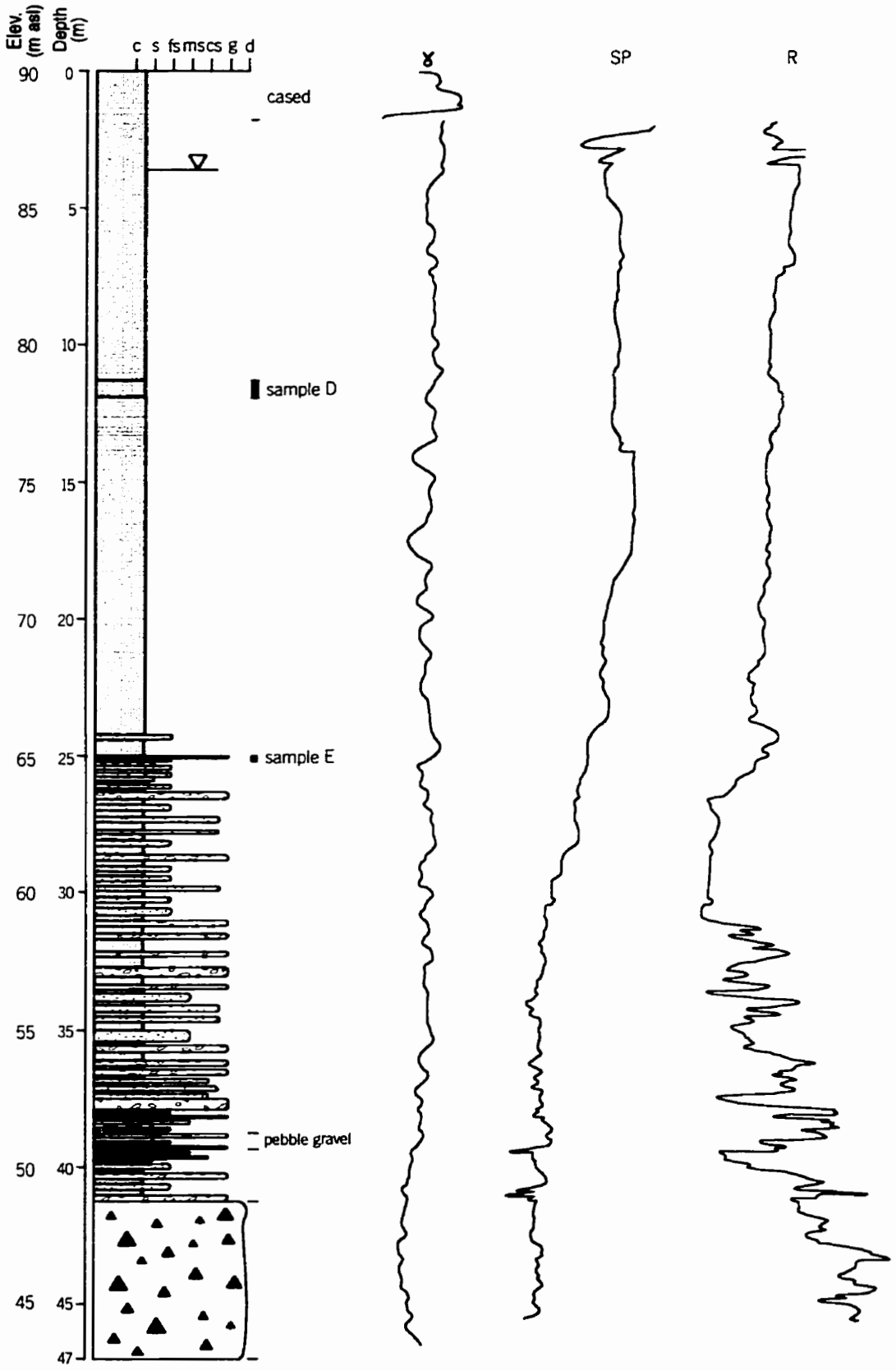


Figure 5.29. Complete lithologic and geophysical logs for Drill hole 98-6-1001.

Geophysical Log Description

The electric logs show the water table to be at 3.5 m. Slight deviations in the SP log and major deviations in the R log indicate a general upward fining trend from 41 to about 27 m, although it is not immediately apparent from the lithologic log (Figure 5.28). The R log shows a different peak pattern within the diamicton bed. The SP and R logs are also remarkably uniform throughout the homogeneous silty clay from 24.2 to 0 m. As with the other drill holes, the gamma log is not very informative, and possibly shows variations in illite concentration. Gamma radiation must not vary significantly in these siliciclastic sediments, possibly because they are all derived from the same source rocks or because clay minerals are rare.

Interpretation

The diamicton is interpreted as lodgement till due to its compactness, poor sorting, R log deflection and high matrix to clast ratio.

The area was below marine limit when ice retreated, but the ice margin was probably not far away when the interbedded sand, gravel and clay were deposited. These are considered proximal glaciomarine sediments deposited by subaqueous jets. The upward fining trend evident in the geophysical logs indicates that ice receded from this position as these sediments were laid down. It is also possible that meltwater output simply waned, but with the absence of any surficial evidence for a stable ice front (*e.g.* moraines or morainal sills), the former depositional environment is deemed more likely. The abrupt transition to silty clay deposition was possibly due to a rapid change to a distal depositional environment once the ice front retreated (cf. Stevens, 1990). The subglacial conduit providing all the debris must have switched locations, suddenly cutting off the supply of coarse sediment.

Distal glaciomarine silty clay deposition continued uninterrupted at the site for some time, but was slightly episodic, resulting in laminated silty clay in the early stages of deposition. This may indicate that this area was affected by variations in flow volumes at the ice front. This might mean it was not exceptionally distal, just far enough from the front not to contain any sediment flow deposits.

## Summary

*Stratigraphy*

From the section and drill hole data, a number of deposits were identified, and their relative stratigraphic position determined. The deposits, from oldest to youngest, comprise the following:

1) Flow till
2) Fluvial, lacustrine or deltaic deposits of Olympia Nonglacial age
3) Glaciofluvial sediments
4) 'Kwinatahl till' (mainly lodgement till, locally melt-out or deformation till)
5) Proximal glaciomarine sediments
6) Distal glaciomarine sediments
7) Retreat-phase glaciofluvial and glaciofluvial deltaic sediments
8) Alluvial fan sediments

The age of the early till (number 1) is unknown, so it could be either older or younger than the interstadial sediments of stratigraphic unit 2. The overlying glaciofluvial sediments may be advance- or retreat-phase deposits. 'Kwinatahl till' is a compact, very poorly sorted till that is most commonly found in the lodgement till form. Proximal glaciomarine sediments overlie the till and comprise interbedded deposits of silt, sand and gravel thought to be deposited by subaqueous jets. These deposits grade distally to massive or locally laminated silty clay deposits. Both types of glaciomarine sediments locally contain dropstones. Retreat-phase glaciofluvial deposits erosively overlie the glaciomarine sediments. Some of these deposits can be refined to braidplain type deposits by incorporating interpretations of mapped geomorphology. One possible glaciofluvial deltaic deposit associated with a mapped braidplain was identified. A Holocene alluvial fan overlies the Aiyansh lava flow and presumably other Holocene and Pleistocene deposits that underlie the flow.

*History*

In Olympia time, nonglacial fluvial or lacustrine environments existed. Lodgement till was deposited by glaciers either before or after this time. Glacial rivers formed after the full glacial period. Their deposits were overridden by ice, which deposited compact, clay-rich Kwinatahl till. Ice subsequently receded and marine water invaded the isostatically depressed landscape. In the Nass Valley, a major glacier retreated continuously, apparently experiencing no stillstands. Near the receding ice margin, subaqueous jets deposited alternating beds of silty clay, sand and gravel that fine distally. As ice continued its retreat, basinal areas farther down valley received only silty clay input, with or without local influx of slightly coarser-grained debris from fan deltas or subaqueous outwash. Subaqueous ice proximal deposition continued up valley at the ice margin. Glaciomarine sediments were thus deposited in a time transgressive (diachronous) manner, following the retreating ice front.

Ice eventually left the valley entirely and sea level dropped. The Nass and Aiyansh Braidplains were formed by rivers draining the melting glacier(s). These meltwater rivers incised into the exposed glaciomarine clays, and subsequently deposited gravel and sand over top of them. At least one delta formed at this time (at the terminal zone of the Aiyansh Braidplain). In Holocene time, alluvial fans formed.

# CHAPTER SIX

# SEISMIC STRATIGRAPHY

## Introduction

Shallow seismic reflection was used to investigate the subsurface geology of the Nass Valley basin fill in areas without any sections. The method works best in areas with wet clay at the surface. It was therefore undertaken in silty clay areas, although not all of the sites were water saturated. It was hoped that the seismic study would shed light on subsurface stratigraphy, and that the great penetration depths of the method would allow some significant stratigraphic interpretations to be made.

In total, 21 lines of varying lengths (from 150 m to 1400 m) were run in the upper Nass Valley. However, after extensive processing in the lab, only one of these produced a useable, interpretable profile. This was line 1001, which was shot in wet, silty clay. At this site, we did not have to add water to the auger holes for the buffalo gun because the water table was nearly at the surface. These conditions were not encountered at any of the other seismic line locations and this could be why the seismic data are so poor elsewhere. The field data were not exceptional, but they contained reflections, so it was not possible to ascertain the quality of the processed data in the field. Processing of the data in the field was not possible due to software bugs in an early version of Seismic Processing Workshop (SPW).

Another possible reason for the poor seismic results at other lines is that the geophones may have been too widely spaced for the target sediments. However, at most sites, both a 3 m and a 5 m spacing were tested. The majority of lines were run with a 3 m spacing. If spacing is the reason for poor data quality, it is suggested that perhaps a 1 or 2 m spacing would be advisable for future work in the area. Note that line 1001, the best line, was shot at a 2.5 m spacing.

The SPW program is explained in the Methods section (Chapter 3) and will not be discussed here. However, details of the processing flows for one of the seismic lines is outlined. Line 1001, the best seismic profile, is described below.

## Line 1001

This line was run from north to south along Sand Lake Road, 500 m northwest of the town of New Aiyansh. Its location with respect to Drill hole 98-6-1001 is shown in Figure 5.21. Geophone spacing was 2.5 m, and the shot offset was 20 m. The buffalo gun was used in 1 m deep auger holes that were naturally water filled due to a high water table. Velocities that vary with depth were determined during processing and were then used to determine actual depths. Velocities range from 1350 m/s at the top of the profile to 2860 m/s in the lower portions. Penetration was excellent (over 400 m, Figure 6.1). Unfortunately the top 25 m of the profile is not resolved due to interference from direct waves and refractions which were muted out during processing. The interpreted profile is shown in Figure 6.2.

Drill hole 98-6-1001 lies 200 m west of the line, at the 462 m mark on line 1001. The drill hole is also 10 m lower in elevation. The area outlined by a box in Figure 6.1 is blown up in Figure 6.3. The drill hole data is shown in the latter figure with reference to the seismic profile.

### *Seismic Facies Analysis*

#### Seismic Facies 1

The lowermost package (Seismic Facies 1) is dominated by north-dipping oblique clinoforms, only a few of which are tangential. They are evenly spaced, of low to moderate amplitude and low continuity. Some are wavy. They become more horizontal in the central portion of the profile (from about 300 to 400 m distance).

#### Seismic Facies 2

A major package of flat-lying reflections overlies the lowest package (Seismic Facies 2). These are horizontal, evenly spaced and moderately continuous to discontinuous. Amplitude is commonly low. Their reflection characteristics are quite different from those of Seismic Facies 1.

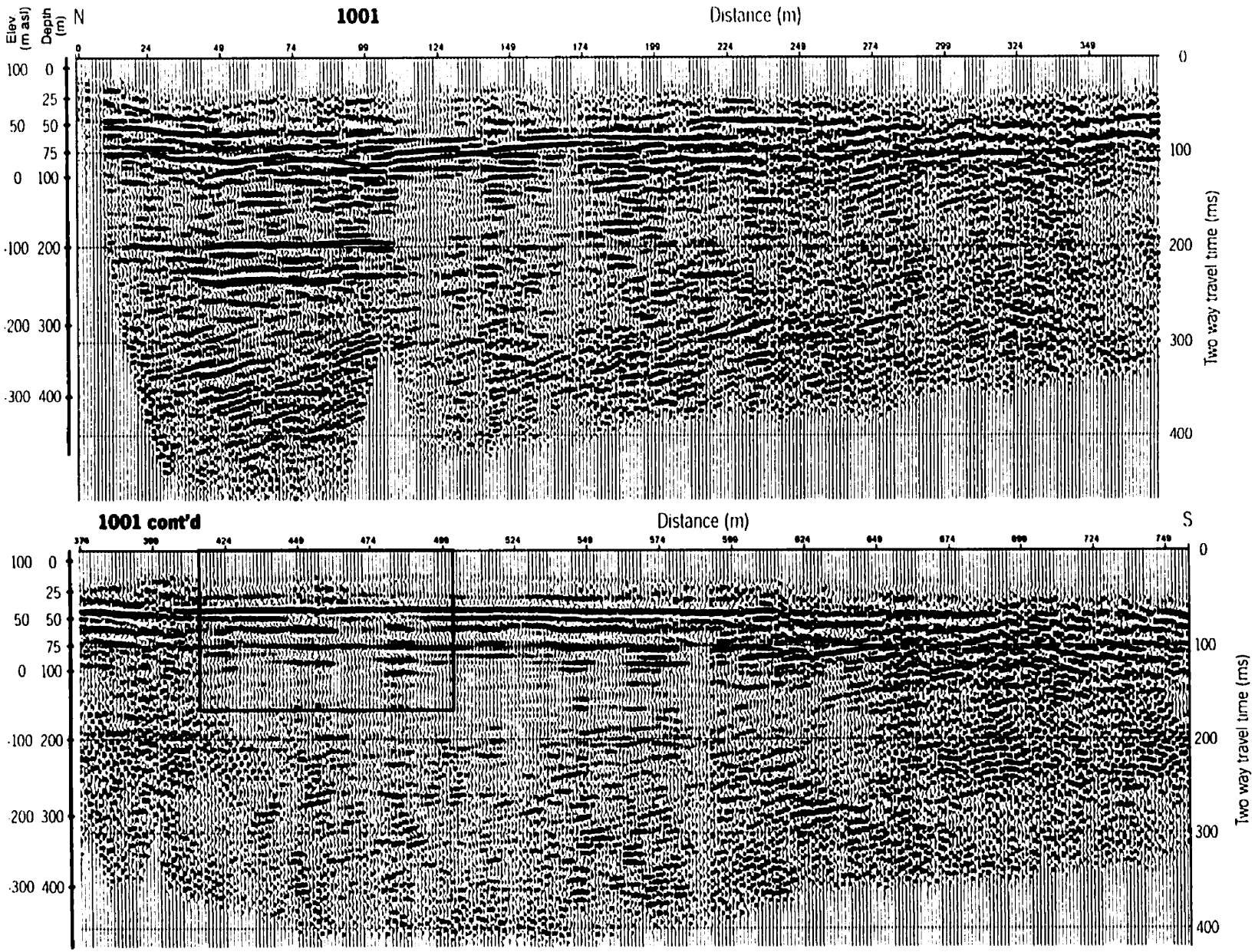


Figure 6.1. Seismic line 1001, uninterpreted profile. The lower profile is simply a continuation of the upper one. Area within box is shown in Figure 6.3.

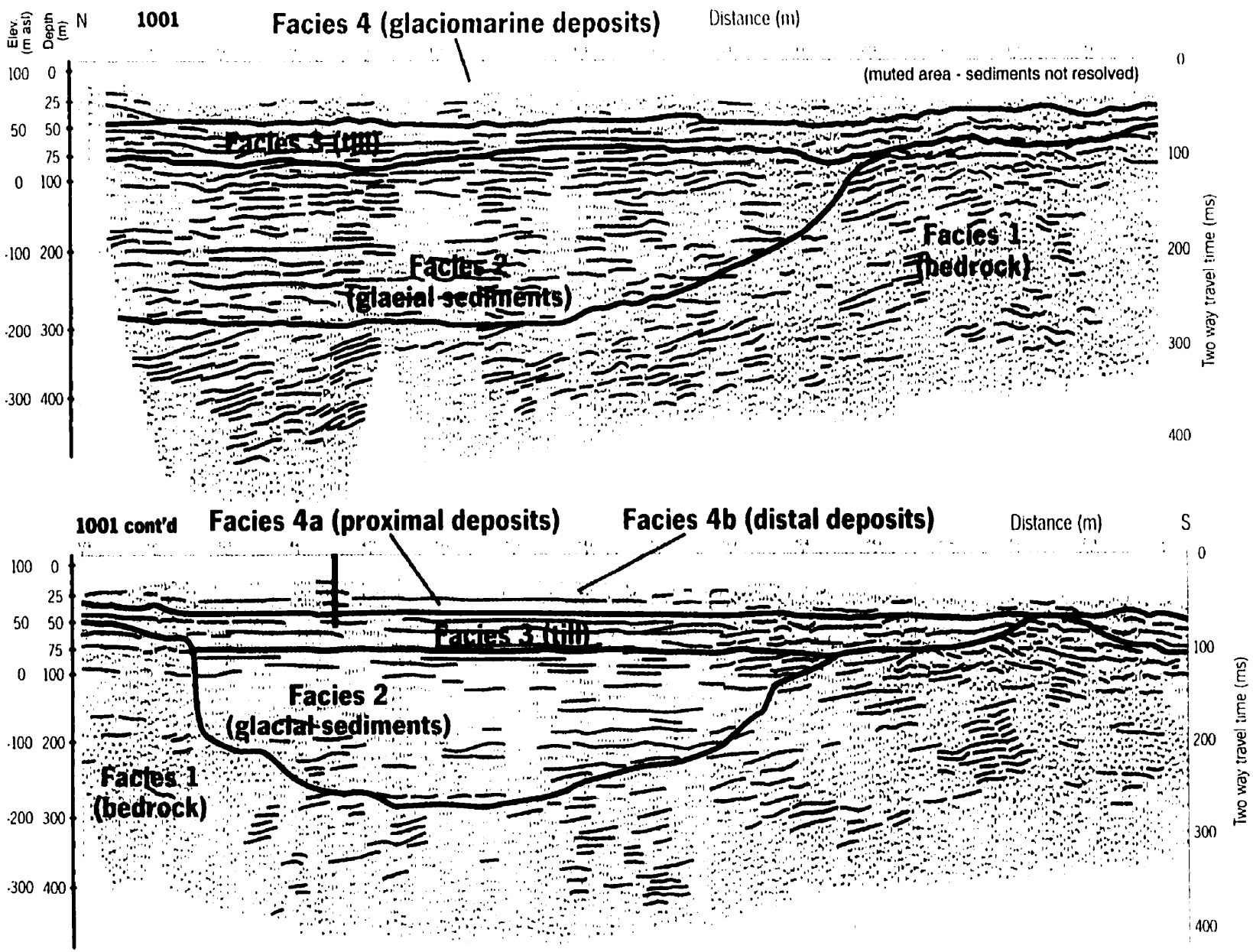


Figure 6.2. Seismic line 1001, interpreted profile. The vertical black bar is the location of Drill Hole 98-6-1001. A blown up view of the drill hole and seismic line is shown in Figure 6.6. The dashed line with two arrows within Seismic Facies 1 is a normal fault.

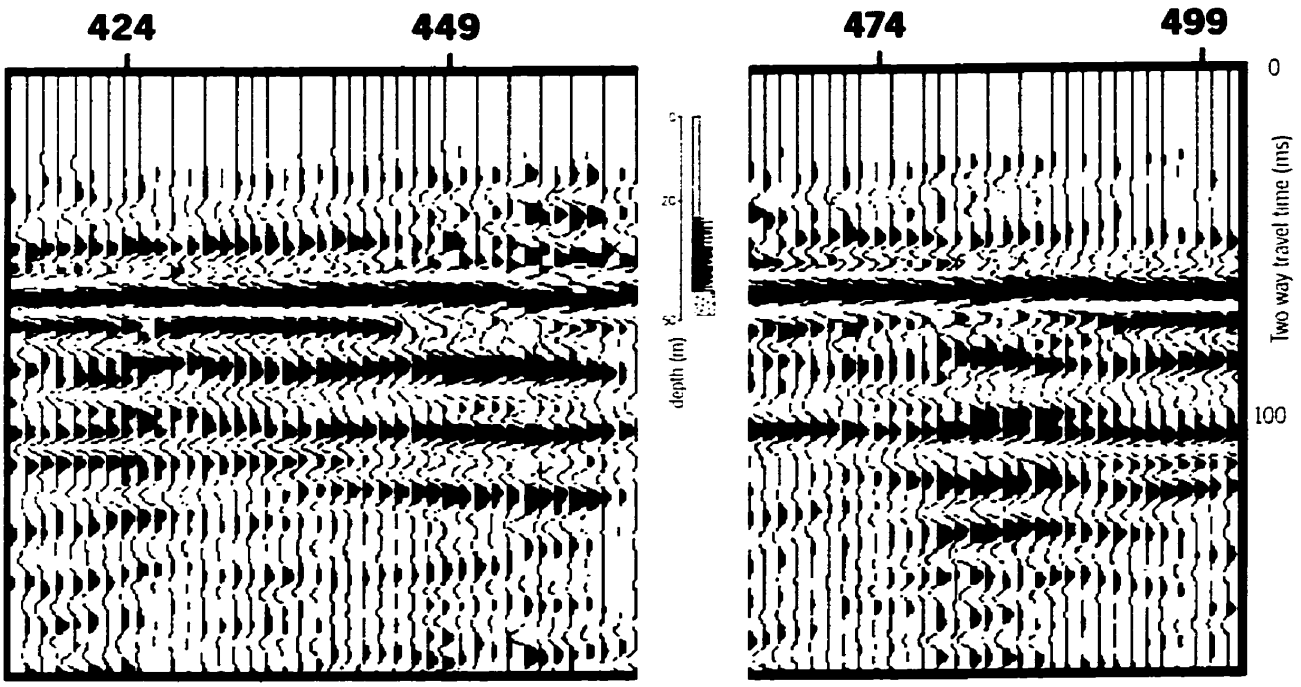


Figure 6.3. Relationship of drill hole 98-6-1001 to seismic line 1001, expanded view of part of line 1001. The hole was drilled at a location 9 m lower in elevation than the seismic line.

There are two discrete basins containing these packages. Some reflections are wavy, especially those at depth. The package appears to be conformable, although strong reflections at 200–240 m depth and 35–105 m distance may indicate some unconformities.

Seismic Facies 3

Seismic Facies 3 consists of subparallel horizontal reflections of high amplitude and high continuity. The reflections chosen as the lower boundary of this facies are quite continuous.

Seismic Facies 4

The upper part of the profile is characterized by parallel horizontal reflections of low amplitude and low to high continuity (Seismic Facies 4). The reflections are bounded below by a highly continuous, high amplitude horizontal reflection. The reflections of this facies are somewhat similar to those of seismic Facies 2, but they are more continuous in places (*e.g.* from 499 to 574 m).

*Seismic Facies Interpretation*

Seismic Facies 1: Bedrock

The lowermost succession is considered to be bedrock (Seismic Facies 1). The undulating nature of Seismic Facies 1 mirrors that of bedrock within the valley. The dipping clinoforms represent dipping beds of the low grade metamorphic rock. The transition to flat-lying beds in the central portion of the profile indicates that this area is part of a broad anticline, with one side of the fold dipping north. The lack of beds dipping the opposite way south of this area suggests that there may be fault at this location, but the lack of reflections here makes this area difficult to define. A second anticline is visible from 424 to 752 m, and the area between the two anticlines may be a syncline.

Seismic Facies 2: Glacial Sediments?

Seismic Facies 2 seems to rest on an erosional discontinuity. Horizontally bedded deposits of this facies are different in character from Seismic Facies 1. Unfortunately, Drill Hole 98-6-1001 did not penetrate far enough to conclusively confirm the deposit type (Figure 6.3). The similarity of the reflections to Seismic Facies 1 (*e.g.* between 424 and 574 m) suggests that the deposit is fine-grained. The change from wavy reflections at depth to flat-lying ones above may be a change from glaciofluvial to glaciomarine deposits, however, due to the uncertainty of the physical characteristics of Seismic Facies 2, it is interpreted only as glacial deposits. However, it is also possible that interstadial or interglacial deposits are present in the sequence.

Seismic Facies 3: Till

Seismic Facies 3 is interpreted as till, because till is found at the top of the package in the drill hole (Figure 6.3). The locally weak reflections, and their continuous, horizontal nature suggest that the till may be bedded. The strong uppermost reflection is probably a result of strong acoustic impedance at the till/gravel interface.

Seismic Facies 4: Glaciomarine Deposits

The uppermost package of weak reflections is defined by the drill hole results. It consists mostly of massive glaciomarine silty clay, underlain by gravel, sand and silty clay interbeds. The latter are proximal glaciomarine deposits (Seismic Facies 4a) and the former are distal glaciomarine deposits (Seismic Facies 4b). It is more difficult to distinguish 4a and 4b in the northern half of the profile, therefore, this area is simply interpreted as glaciomarine deposits (Seismic Facies 4).

## Summary

From seismic line 1001, the following seismic facies were identified:

Seismic Facies 1: Bedrock

Seismic Facies 2: Glacial Sediments?

Seismic Facies 3: Till

Seismic Facies 4: Glaciomarine Deposits

Slightly metamorphosed bedrock showing two major anticlines underlies thick glacial sediments. Seismic Facies 2 forms a horizontally bedded infill in two basins cut into the bedrock. The sediment type is uncertain, but it may be a glacial deposit. It may also contain or be completely made up of interstadial deposits. It is up to 200 m thick. Laterally extensive till overlies these glacial sediments and is 25 to 40 m thick. Glaciomarine deposits that overlie the till are even more laterally extensive and are up to 50 m thick. They can be subdivided into coarser-grained proximal deposits in the lower part of the facies, and finer-grained distal deposits in the upper part.

The two basins cut into bedrock (now infilled with glacial sediments) show that the Nass Valley had a medial ridge prior to the last glaciation. Its topography was probably somewhat similar to that of today, but perhaps with a different amount of valley fill.

# CHAPTER SEVEN
# RADAR STRATIGRAPHY

## Introduction

In the Nass Valley, ground penetrating radar (GPR) lines were run in areas where sand and gravel are exposed at the surface, the environments where GPR works best. The goal of this work was to delineate the structure and style of glaciofluvial deposition that characterized the Nass and Aiyansh braidplains in late glacial time.

A number of radar lines and test lines were run, but the test lines are not included in the thesis. For this reason, the radar line numbers are not perfectly consecutive.

Over 5 km of radar line data were acquired, including test lines. Of this, over 4 km of data are discussed in the thesis. The lines were located exclusively on the Nass and Aiyansh braidplains, which were identified by surficial geology mapping (discussed in Chapter 4). The locations of the lines with respect to the Aiyansh and Nass braidplains and surrounding glaciofluvial deposits are shown in Figure 7.1.

At a number of sites, evenly spaced, parallel horizontal reflections crosscut other reflections. In some areas, section evidence shows that these horizontal reflections are not real, and must be some kind of radar artifact (see lines NV113 to NV118). They appear in the better sorted sediments such as deltaic sand/gravel and silty clay deposits. The reason for their presence is unknown. In areas where there are only artifact reflections, the deposit is generally a structureless silty clay. Since these artifacts do not show real bedding, they are considered noise and are not interpreted in any of the profiles. Similar reflection artifacts are visible in GPR profiles from deltas in other studies (*e.g.* Figures 6, 8 and 10, in Jol and Smith, 1992), however, no explanation is given for their presence.

Boulder diffractions are common in the coarser grained deposits. These are not interpreted on the profiles because the diffraction hyperbolae detract from the depositional signature of the

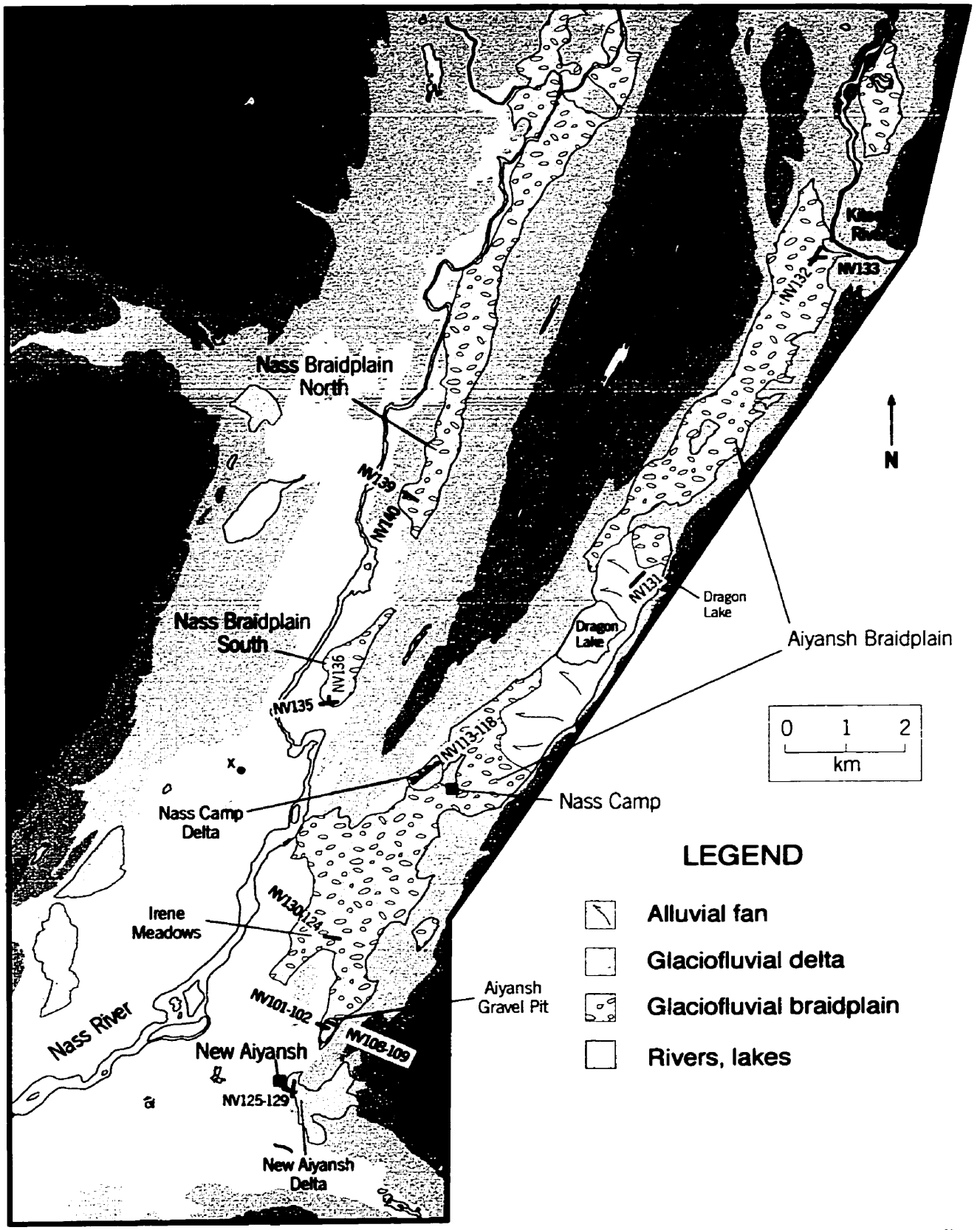


Figure 7.1. Location of radar lines with respect to the Nass and Aiyansh braidplains and the surrounding glaciofluvial deposits as they were originally mapped. Line lengths are exaggerated for greater visibility. Contours are shaded at 152 m intervals.

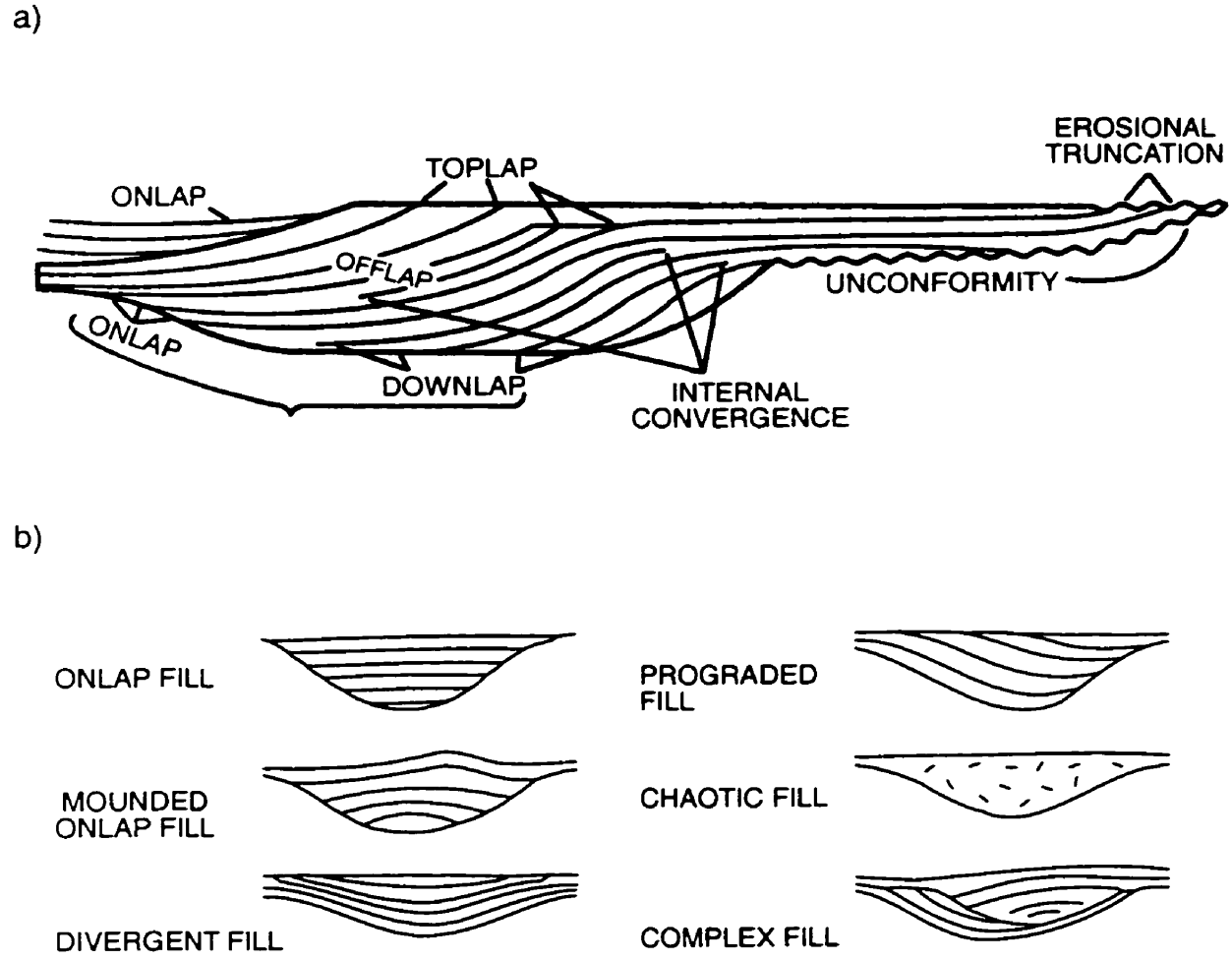


Figure 7.2. Reflector terminology for radar facies interpretations; a) offlap and onlap relationships. b) fill types (after Mitchum *et al.*,1977).

**1) Hyperbolic Facies**
overlapping hyperbolic reflectors, moderate continuity and amplitude, locally with high amplitude upper reflector

Bedrock

**2) Artifact Dominated Facies**
reflection-free, except for artifacts that are parallel to air and ground waves

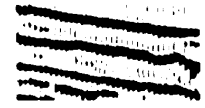

Glaciomarine Silty Clay

**3a) Dipping Clinoform Facies**
oblique clinoforms, straight, tangential or sigmoid, moderate continuity, moderate amplitude, parallel, evenly spaced, offlapping

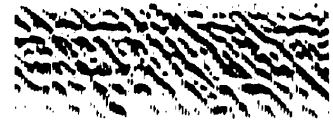

Glaciofluvial Braid Delta:
Foreset Beds

**3b) Horizontal, Discontinuous Facies**
horizontal, discontinuous, even to wavy, parallel, lower reflector of high amplitude and continuity

Glaciofluvial Braid Delta:
Topset Beds

**3c) Wavy, Irregular Facies**
irregular, moderate to high amplitude and continuity, even, subparallel horizontal reflectors, with some oblique clinoforms, small diffractions common

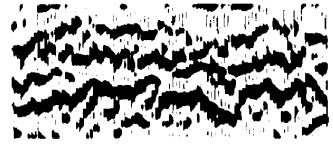

Glaciofluvial Braidplain:
Horizontally Bedded Deposits

**3d) Lens Facies**
same as 3c, but reflectors outline a lens with a flat, irregular or convex upper surface and a concave lower surface, fills may be onlapping, prograded or both

Glaciofluvial Braidplain:
Channel Deposits

**3e) Hummocky Facies**
moderate amplitude, moderate to high continuity, hummocky, commonly convex

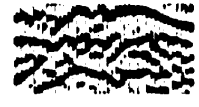

Glaciofluvial Braid Delta:
Slump Deposits

**4a) Wavy Facies**
wavy, moderate to high amplitude and continuity, even to hummocky, roughly parallel and horizontal, some diffractions

Alluvial Fan:
Horizontally Bedded Deposits

**4b) Lens and Ridge Facies**
same as 4a, but reflectors outline a flat-topped lens with a concave lower surface and steeply dipping clinoforms at each end of lens forming a ridge-like feature

Alluvial Fan:
Channel Deposits

Figure 7.3. Characteristics and visual examples of the radar facies. Interpreted depositional environments are listed on the right.

profiles. However, the diffractions do indicate the presence of boulders, and their presence is duly noted in the radar line interpretations.

## Radar Facies

The profiles are subdivided into radar facies, which are defined as a mappable sedimentary units, whose reflection characteristics differ from those of adjacent units (cf. Jol and Smith, 1991, Huggenberger, 1993). Reflections are described in this thesis on the basis of a number of factors defined by Brown and Fisher (1985): amplitude, frequency, continuity, terminations, transitions, geometry, parallelism and attitude. Offlap, onlap, toplap, downlap, fill types and erosional discontinuities are identified where possible (Figure 7.2). This is seismic reflection terminology, but it was found to be applicable to the scale of radar facies, with the exception of major unconformities, which probably cannot be identified at this scale.

After a study of all the radar profiles, a number of Radar Facies were identified. These are listed below. The facies were identified by analyzing the data set and do not necessarily parallel the findings of other workers. A summary of the characteristics of each Radar Facies, along with an example of each from the data set, is shown in Figure 7.3.

1) Hyperbolic Facies
2) Artifact Dominated Facies
3a) Dipping Clinoform Facies
3b) Horizontal, Discontinuous Facies
3c) Wavy, Irregular Facies
3d) Lens Facies
3e) Hummocky Facies
4a) Wavy Facies
4b) Lens and Ridge Facies

The GPR sites are described in the next part of the chapter. Examples of CMP surveys done for the radar lines are shown in Appendix C.

## Radar Line Descriptions and Interpretations

*Aiyansh Gravel Pit: Lines NV101 and NV102*

These lines were run at the lowest excavated level of the Aiyansh gravel pit to determine the location of the contact of overlying gravel with the silty clay unit (Figure 7.1). The pit is in the terminal area of the Aiyansh Braidplain. Section 97602-05 (Figure 5.15) shows the gravel pit deposits that stratigraphically overlie the profile. The line was run in the bottom of the gravel pit where there is no lithostratigraphic information at depth. The line begins at the pit bottom and moves westward across a gradational surface contact with finer sediments, into a flat area beyond the gravel pit (Figure 7.1). Gravel visible at the surface is gradually replaced by silty sand towards the end of line NV102. NV102 is simply a continuation of NV101. A velocity of 0.10 m/ns was determined by a CMP survey.

Radar Facies Description

Radar Facies 3a

Some oblique clinoforms (dipping reflections) are visible on the profile from 40 to 135 m (Figure 7.4), but penetration is poor – it does not go beyond a depth of 6 m. The clinoforms are somewhat continuous, of moderate amplitude, and indicate a dipping sheet-like geometry. They are parallel for the most part and their oblique offlap is suggestive of a progradational depositional environment. Dips of the clinoforms range from 5° to 10°.

From 140 to 270 m (Figure 7.4), penetration remains poor and reflections that show bedding features are lost, possibly because of the lateral fining observed at the surface. The disrupted area toward the end of the line is road fill (220-255 m). An artifact dominated zone in the silty sand area at the end of NV102 (145-272 m) is not surprising, since fine-grained sediments attenuate radar signals (Smith and Jol, 1995). The even horizontal artifact noise

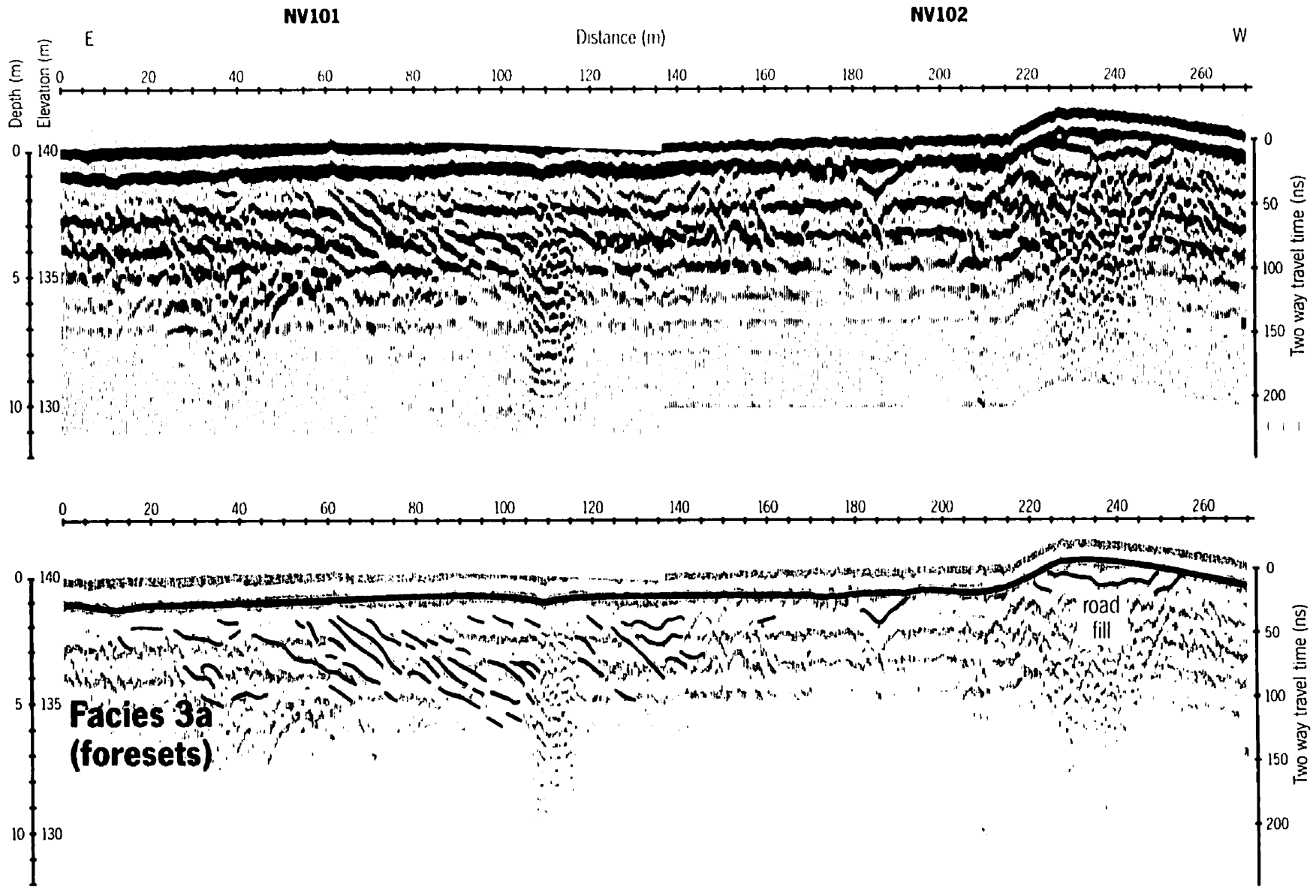


Figure 7.4. Radar lines NV101 and NV102, from Aiyansh Gravel Pit on left to silty clay area on right. NV102 is a continuation of line NV101. The disrupted reflections under the small hill are probably due to road fill. Diffractions between 140 and 160 m indicate that boulders are present at this location.

mentioned above is present throughout the profile and is discounted in this interpretation, as it is in subsequent profiles.

Radar Facies Interpretation

Radar Facies 3a: Braid Delta Foreset Beds

The radar reflections of these two profiles are interpreted as glaciofluvial braid delta foreset beds and related finer-grained deposits (Radar Facies 3a). Since the finer sediments at the surface at the end of NV102 are sandy, they are considered to be a finer-grained distal continuation of the same facies. The silty clay contact with overlying gravel was not identified. Signal is lost in the sandy facies, so it is not known exactly where the silty clay begins, if present, on the profile.

Dipping beds are not evident anywhere in the Aiyansh Gravel Pit exposures (Figure 5.15). These clinoforms, however, dip 5° - 10°. If these are indeed foreset beds, then the rest of the gravel pit must represent the flat-lying topset beds. It could be that other foreset beds have been mined out. The finer-grained sediments beyond the pit edge and beneath the dipping beds could be toeset beds, but this inference is inconclusive in the absence of reflections. It is thus concluded that this well sorted gravel pit is a raised delta, consisting mainly of topset beds that pass into clinoformal foresets in the subsurface.

*Aiyansh Gravel Pit: Lines NV108 and NV109*

These two lines were run in a southeast to northwest direction (the same direction as NV101-102) across the highest level of the Aiyansh gravel pit (Figure 7.1), to check radar data against pit section information (Figure 7.5). A mound of excavated fill was encountered at the end of line NV108 (at 81 m), so NV109 is a continuation of the same line in the same direction, but on the other side of the fill mound.

Section 97602-05 (Figure 5.15) is located at the end of line NV108 (at the 81 m position). The GPR profile shows reflections only to 10 m, and therefore covers the top third only of the sediments exposed in the pit.

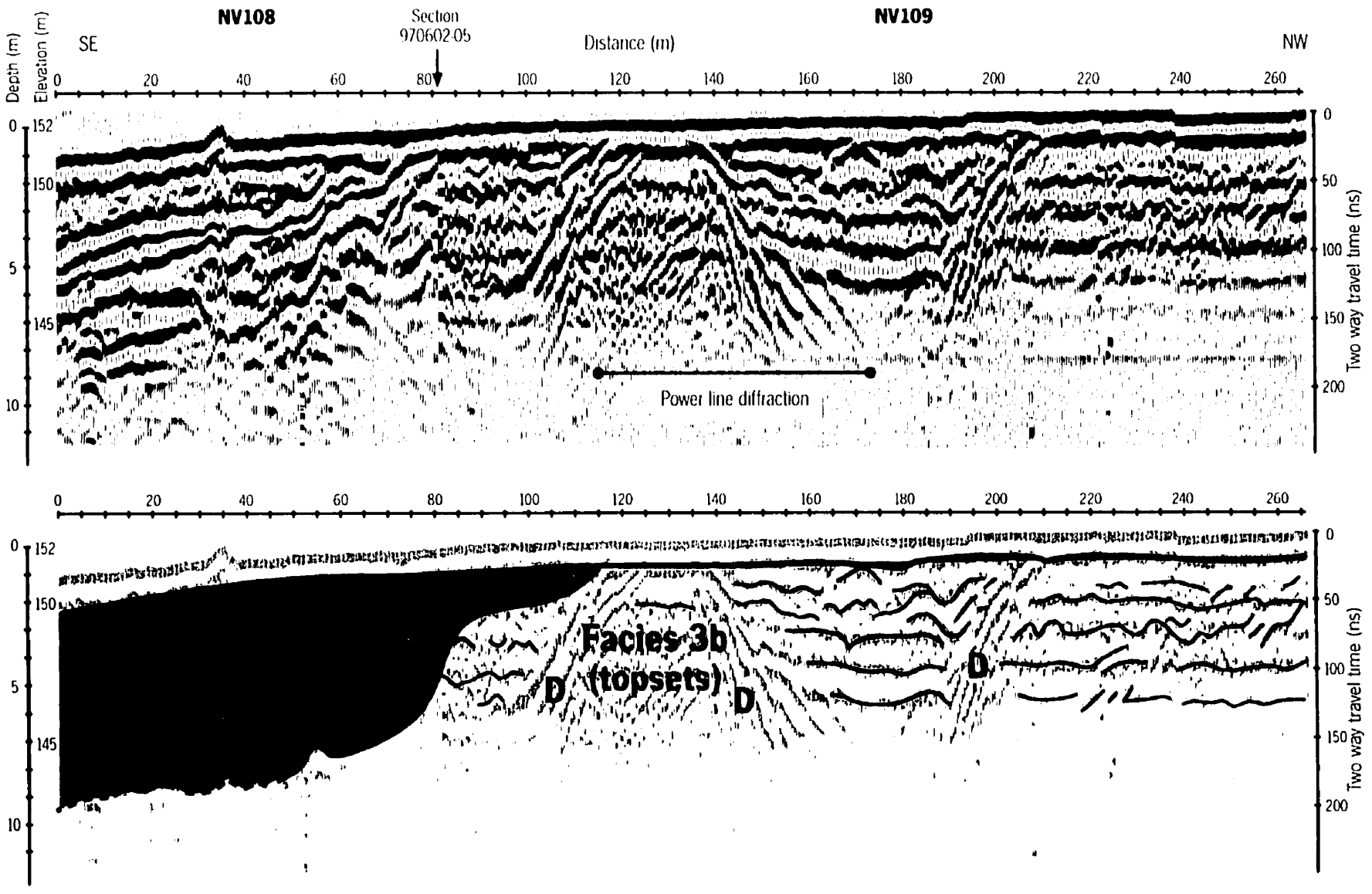


Figure 7.5. Radar lines NV108 and NV109, across the top of Aiyansh Gravel Pit. The extent of the power line diffraction is shown. Other diffractions are labelled 'D'.

Penetration is good at the start of the lines, but is reduced toward the end. There was a high tension power line at 135 to 145 m, shown by a diffraction at depth around this point (Figure 7.5). A velocity of 0.10 m/ns was used for these profiles, determined by the same CMP survey used for NV101-102. The CMP survey was run in the centre of the pit.

Radar Facies Description

Radar Facies 3d

The southeast end of the line shows southeastward-dipping, oblique clinoforms from 0-90 m. These high amplitude, subparallel reflections are highly continuous. Some reflections are wavy (*e.g.* 40-70 m), while others are even (*e.g.* 0-30 m). Some offlap is visible between 40 and 80 m. This combination of offlap and downlap can also be called a prograded fill (Figure 7.2). The dip of clinoforms at the southeast end is 1° - 3°. The steeper ones further northwest range from 5° to 11°. The geometry of this part of the line (from 0 to 80 m) is that of part of a large, flat-topped lens.

Radar Facies 3b

The northwest part of the line shows high amplitude, parallel, even to wavy, evenly spaced, continuous horizontal reflections (125-266 m). In this locality, they appear to be real reflections, rather than artifacts, because they are not perfectly horizontal and evenly spaced (*e.g.* 145-200 m), they don't all dissipate at exactly the same depth and they are not parallel to the air wave and ground wave. They are erosionally truncated at the boundary of the southeast facies at 80-90 m, which is inferred to be an erosional discontinuity. The other diffraction-like features have no known source, however, they could be diffractions from tree roots, since the small road is flanked by trees.

Radar Facies Interpretation

The strong reflections are indicative of a well sorted, coarse-grained deposit. The horizontal bedding is consistent with either a fluvial environment or deltaic topset beds. It is also consistent

with several other depositional environments, but the location of the profile at the terminal zone of a large braidplain (Nass Valley map), constrains the number of possible interpretations for this site. The profile is interpreted as Radar Facies 3, a glaciofluvial braidplain or delta. The thinning and fining-upward of the beds (Figure 5.15) was not identified by GPR. This is one of the limitations of the method.

Radar Facies 3d: Braidplain Channel Deposits

The oblique clinoforms define the edge of a prograded channel fill (Figure 7.2) in the former braidplain or delta surface. The 1° - 3° dipping clinoforms show the lower part of a prograded fill, while the steeper ones show the steeper offlap portion of a prograded fill. This unit is assigned to Facies 3d, and is interpreted as a braidplain channel deposit. In this chapter, channel deposits are shaded in the line interpretations to emphasize their morphology.

Radar Facies 3b: Braid Delta Topset Beds

From a previous GPR line (Figure 7.4), foreset beds appear to exist at a lower stratigraphic level. Thus, these horizontal beds probably comprise a thick sequence of topset beds. Alternatively, the Aiyansh Braidplain could have advanced over the delta. However, sediments deposited in a braidplain environment should have a high degree of lateral variability, with numerous cut and fill features. Only one large channel is seen in the profile and channel scours are rare in the section. The horizontal beds are laterally continuous over tens of metres. In addition, the pit is located at the southern terminus of the braidplain, a location where a delta is likely to have formed. The preferred interpretation is therefore deltaic topset beds, which further refines the environmental interpretation for the Aiyansh Pit Section (Chapter 5).

*Nass Camp Delta: Lines NV113 to NV118*

These lines were run across the top of a delta west of the small logging community of Nass Camp (Figure 7.1). This area was interpreted through mapping (air photo interpretation and field

checking) as a local delta at the edge of the Aiyansh Braidplain. Lines NV114 to NV118 are all perpendicular to line NV113; the line layout is shown in Figure 7.6.

Horizontal topset and tangential foreset beds are exposed in a road cut (Section 97708-01 on Figure 7.6) below the flat surface of the delta where the lines were run (Figure 7.7). The section provides lithological and structural (sedimentary) control for the GPR lines at this site. The beds in the exposed section consist of poorly sorted granule, pebble and boulder gravel, with either a silt/clay or granule/pebble matrix. The sand size fraction is absent. Clasts are blue grey to grey (oxidizing to yellow brown), unstriated, and subangular to well rounded. Foresets are generally finer-grained than topsets and commonly contain a gravel lag. Topset beds may be either clast- or matrix-supported, horizontally bedded and vaguely imbricate. Foresets occur below 3.8 m and many are tangential. Apparent dip is 23°. There is evidence of some slumping, indicated by a few wavy foreset beds. Apparent paleoflow direction is 320°.

On the northern side of the exposure, a large lens feature cuts the deposit, which is interpreted as a distributary channel. It cuts both the topset and the upper foreset beds. In the prodelta area of silty clay deposits to the northeast (see Nass Valley map), a number of clay coated boulders were found. They are interpreted to have rolled off the delta front into glaciomarine silty clay (J. Clague, pers. comm., 1995).

The GPR profiles achieved, on average, a penetration depth of 10 m. This is good, but not excellent; it does not extend beyond the 14 m deep section just described. Therefore, the loss of signal with depth is not due to the presence of fine sediment at depth, but is simply due to weakened signal with depth. The CMP data was ambiguous and difficult to interpret (Appendix C, approximately 0.06 m/ns). Several velocities were empirically tried in the radar program until the appropriate depths were achieved. A velocity of 0.13 m/ns was attained in this way for these profiles.

Radar Facies Description

In all of the profiles acquired at this site, the same reflection signatures are visible (Figures 7.8-7.11).

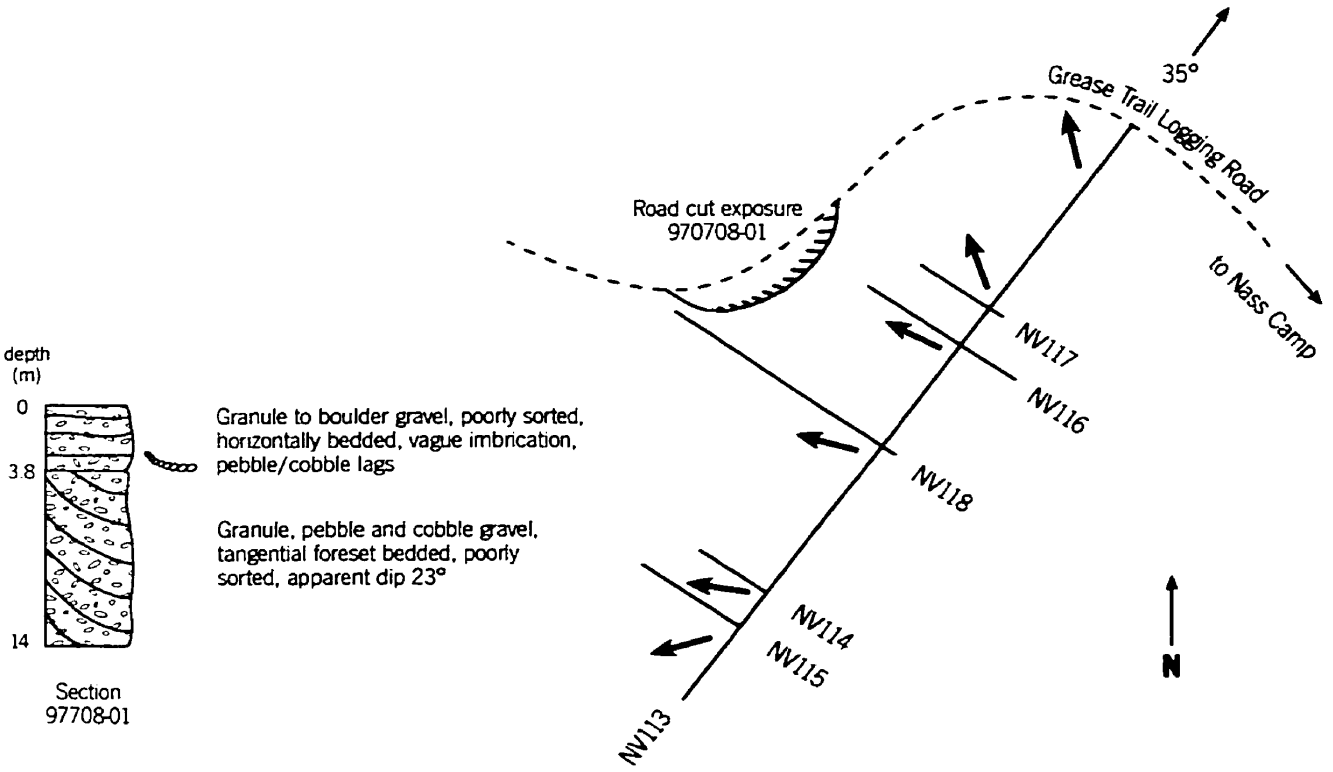


Figure 7.6. Nass Camp delta: radar lines and section location. Paleoflow direction (shown by heavy arrows) radiates from 255° to 350° (see fence diagram). Section 970708-01 is shown in more detail on the left.

Figure 7.7. Exposure 97708-01, view from logging road. Pole is 2.5 m long.. Note gravel lags at base of foreset beds (arrowed).

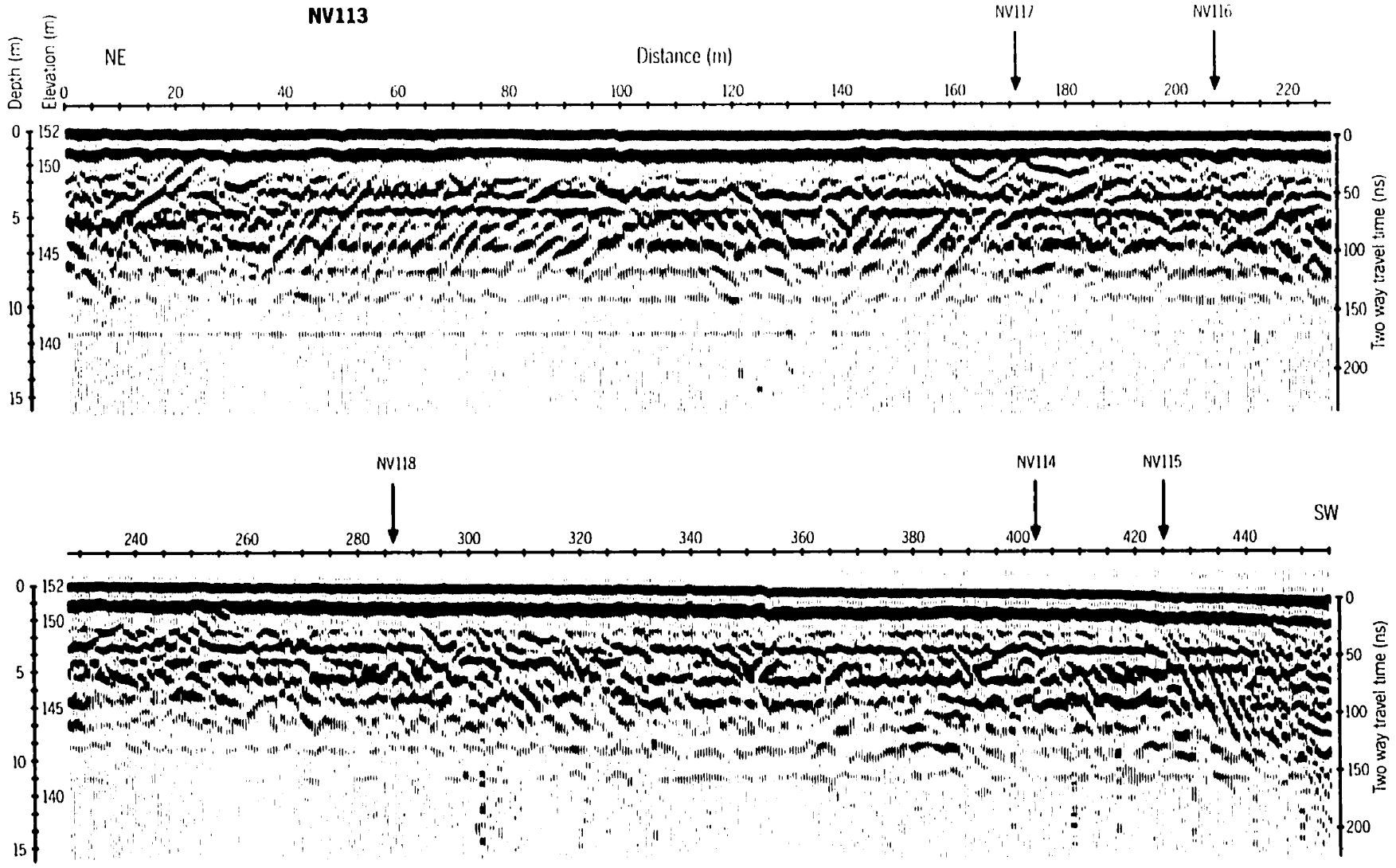


Figure 7.8. Line NV113, Nass Camp Delta, uninterpreted profile. Arrows show locations of intersecting radar lines (see Figures 7.10 and 7.11).

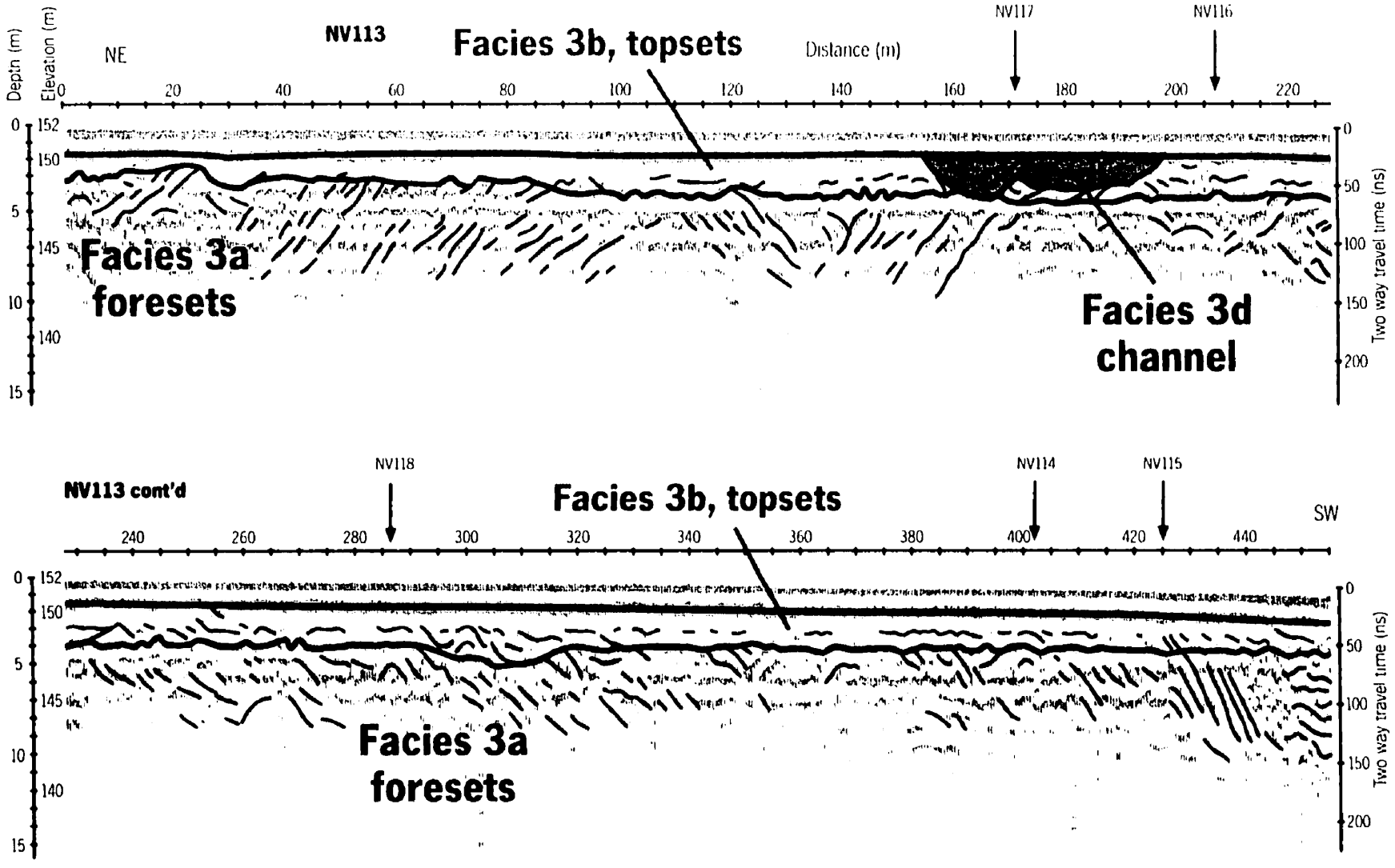


Figure 7.9. Line NV113, Nass Camp Delta, interpreted profile. Arrows show locations of cross-cutting radar lines (see Figures 7.10 and 7.11).

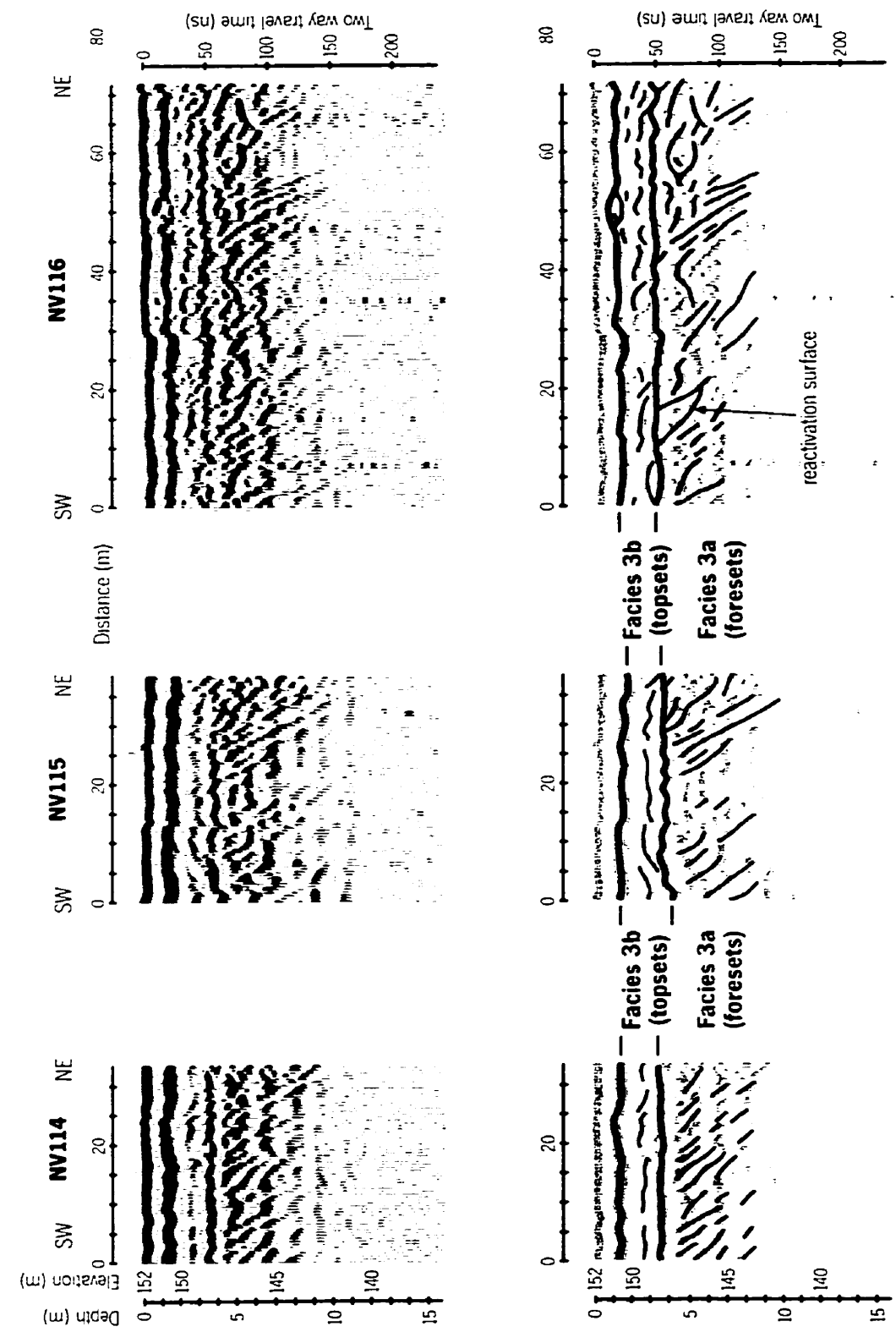


Figure 7.10. Radar lines NV114, NV115 and NV116, Nass Camp Delta, uninterpreted profiles above, interpreted profiles below. A diffraction is centered on the 30 m mark on line NV116.

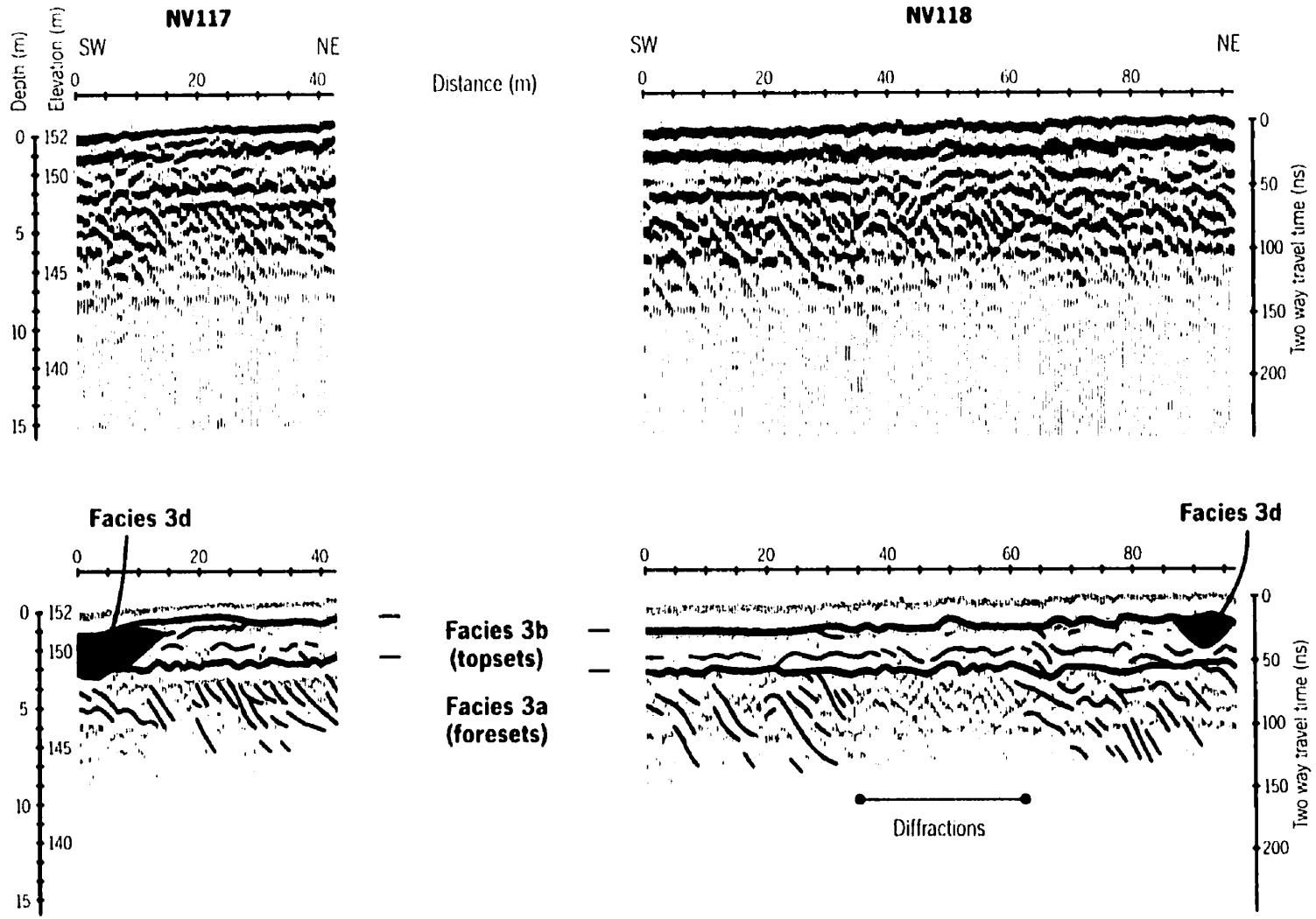


Figure 7.11. Radar lines NV117 and NV118, Nass Camp Delta, uninterpreted profiles above, interpreted profiles below. Note diffraction between 35 and 60 m on line NV118.

Radar Facies 3a

Below 4 m depth, oblique clinoforms, both straight (*e.g.* NV118, 75-90 m) and tangential (*e.g.* NV117, 30-40 m), are present. They are of moderate continuity and amplitude and toplap the overlying reflections. They are generally parallel, evenly spaced, and offlapping. The majority of these reflectors have a dip angle of 20° to 30°. Dips may be as low as 14°, but these lower angle reflections seem to be different types of surfaces (*e.g.* NV116, 10-20 m).

Radar Facies 3b

From a depth of 1.5 to 4 m, reflections are roughly horizontal, discontinuous, parallel and even to wavy (*e.g.* NV118, 0-40 m). The reflection immediately beneath the ground wave is low in amplitude, while the reflection beneath it is high in amplitude and highly continuous.

Radar Facies 3d

Some oblique reflections and reflections outlining flat-topped or convex-topped lenses are present within the upper package (*e.g.* NV113, 155-197 m).

The geometry is that of dipping sheets overlain by a large flat-lying sheet that is interrupted in places by a few lenses.

Radar Facies Interpretation

Radar Facies 3a and 3b: Braid Delta Foreset and Topset Beds

A glaciofluvial braid delta is found at this site. The toplapping and offlapping oblique clinoforms of low to moderate continuity are characteristic of deltas (Brown and Fisher, 1985). Facies 3b and Facies 3a are both present and are interpreted as topset beds and foreset beds, respectively (Figures 7.9, 7.10 and 7.11). The strong lower reflector of Facies 3b indicates the change from coarser-grained topset beds to finer-grained foreset beds (Figure 7.7). Foreset beds like those shown by clinoformal reflections on these profiles are common in braid delta

environments (McPherson *et al.*, 1987, Syvitski and Hein, 1991, Smith and Jol, 1997). The 20° to 30° dips are typical of foreset bed dips (Nemec, 1990, Smith and Jol, 1997). The deltaic interpretation of the surficial geology mapping is thus consistent with the radar interpretation (Figure 7.1).

Radar Facies 3d : Braidplain Channel Deposits

Several small channels can be seen within Facies 3b (*e.g.* Figure 7.9). These are interpreted as braidplain channel deposits and are assigned to Facies 3d. They are further interpreted as distributary channels of the delta top. In the Fraser Delta, distributary channels are also found within the topset beds or at the topset/foreset boundary (Roberts *et al.*, 1992).

Paleoflow

When the lines are assembled in a fence diagram, it is possible to visualize the delta in three dimensions (Figure 7.12). It becomes clear that the steeply dipping foreset beds illustrate radial paleoflow across the delta from 255° to 350°, or from west-southwest to north (Figure 7.6). A marine embayment is suggested to have existed to the northwest of the delta (Nass Valley map), so that a river flowing from the east was able to build this delta into the deeper marine waters. It changed direction periodically, presumably as distributary channels avulsed (illustrated by radial paleoflow). Clay-coated boulders identified in the silty clay sediments by surficial mapping indicate that oversteepening may have occurred, causing boulders from the delta to roll down the delta front into the finer-grained marine sediments. The edge of the mapped delta is therefore regarded as the true delta front at this location. The delta's surface elevation gives a former sea level stand of 152 m.

*Irene Meadows: Lines NV124 and NV130*

NV124 is a continuation of NV130. Both were run across a suspected topset bed location on Irene Meadows Road, east of the Nass River (Figure 7.1). The line is long and has been split into two segments for Figures 7.13 and 7.14. The radar lines were run across flat, even ground

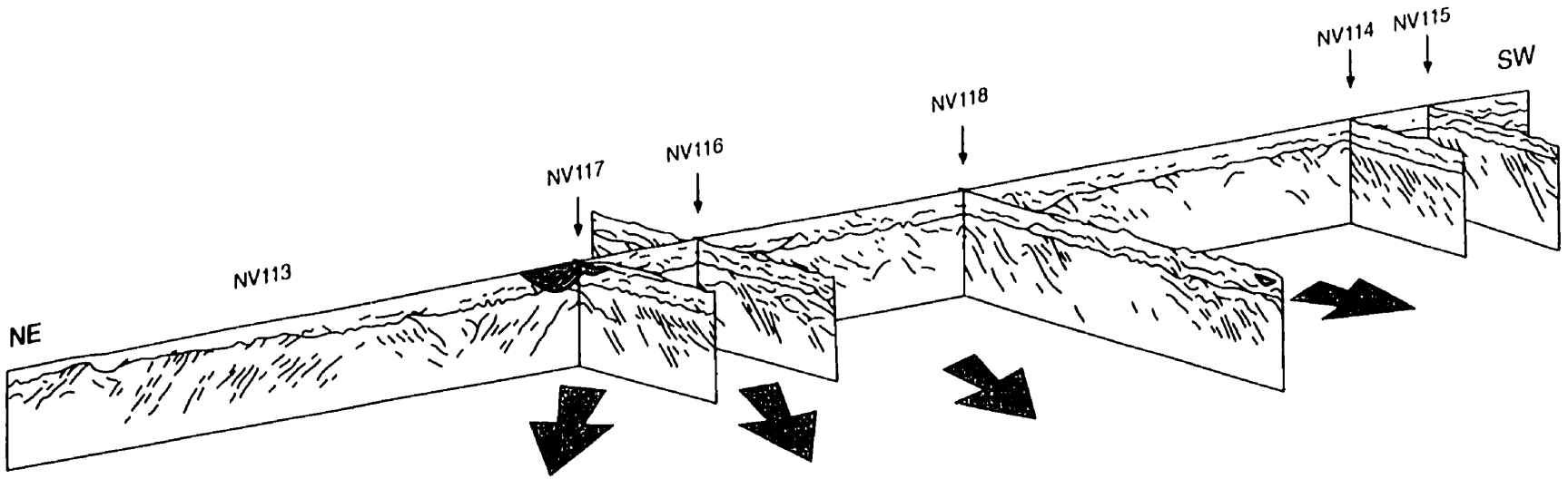


Figure 7.12. Fence diagram of radar lines NV113 to NV118. Foreset beds dip toward the viewer at the northeast end, and to the right of the page at the southeast end, reflecting a paleoflow pattern that radiates from WSW to NW. The elevation at the top of the topset beds is 152 m.

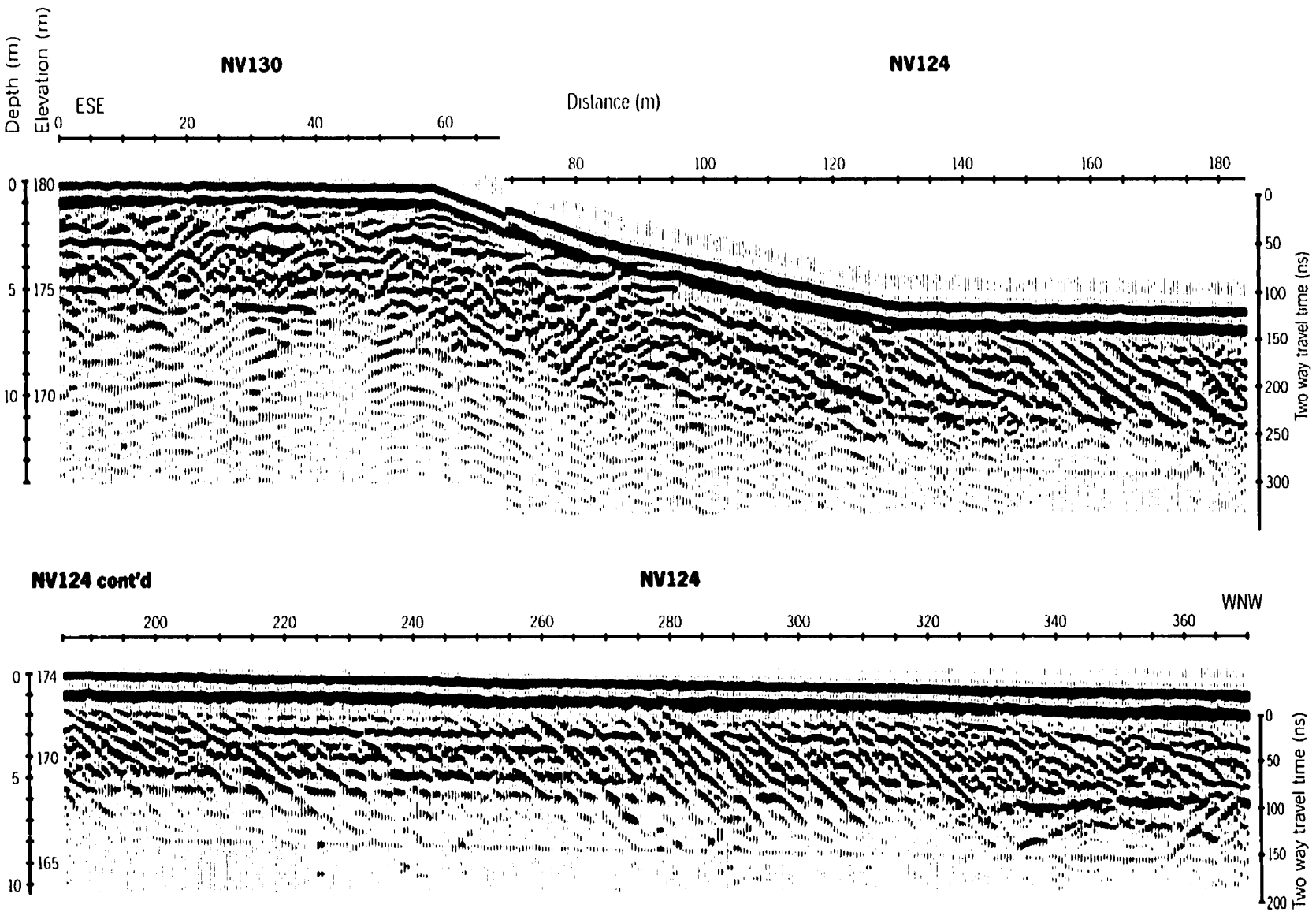


Figure 7.13. Radar lines NV130 and NV 124, Irene Meadows Road, uninterpreted profiles with topographic correction.

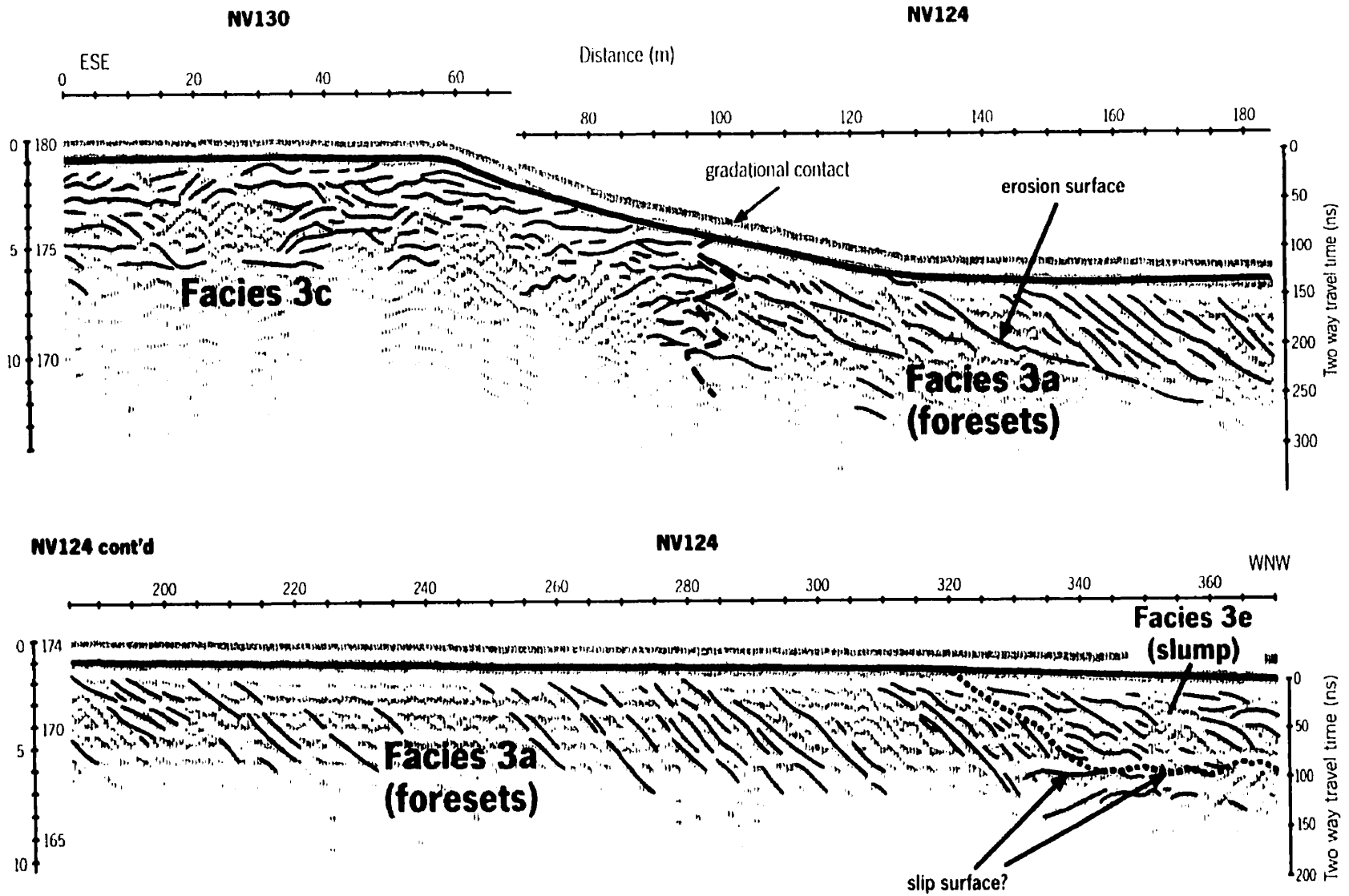


Figure 7.14. Radar lines NV130 and NV 124, Irene Meadows Road, interpreted profiles.

which then dips and flattens again, resembling the top and sloping surfaces of a delta. Penetration is not great, 7 - 8 m of well defined reflections over the whole profile, with some weaker reflections below 8 m from 0 - 70 m distance. A velocity of 0.11 m/ns was determined for this line from a CMP survey.

Radar Facies Description

Radar Facies 3a

NV124 is dominated by moderate amplitude, continuous to moderately continuous oblique clinoforms (Figure 7.13, *e.g.* 260-310 m), a few of which are tangential (*e.g.* continuous reflection from 105-125 m). They are parallel and offlapping. No toplap is evident. Between 123 and 170 m, a large tangential clinoform of lower dip (10°) is present within those of steeper dip (20°-30°).

Radar Facies 3c

In the upper part of NV130, reflections are of moderate continuity and amplitude, and a few are of high amplitude. They are roughly parallel, becoming hummocky and less continuous with depth. There is a gradual transition from the reflections of NV130 to the dipping reflections of NV124. Numerous boulder diffractions are also present at depth, indicating a much coarser-grained deposit.

Radar Facies 3e

Between 320 and 370 m on NV124, reflections are hummocky and lose their parallelism. Many are convex (*e.g.* 355-370 m). A horizontal reflection of high amplitude and continuity underlies this zone.

Radar Facies Interpretation

Radar Facies 3a: Braid Delta Foreset Beds

Facies 3a, deltaic foreset beds, are represented at this site, with an apparent dip of 20°-30° toward 285° (the road direction). Although toplap is not evident, the offlapping oblique clinoforms of moderate continuity are typical of foreset beds (Brown and Fisher, 1985, Smith and Jol, 1997). The lack of topset beds may be due to road grading, as this line was run down the centre of a gravel road. The 10° reflection is interpreted as an erosion surface or chute (Nemec, 1990), because it seems to truncate underlying reflections (or would if they are extended to meet it), and is less steep than overlying reflections.

Radar Facies 3c: Braidplain Horizontally Bedded Deposits

The hummocky to horizontal reflections of NV130 are assigned to Facies 3c and are interpreted as braidplain deposits. The numerous diffractions indicate a poorly sorted, bouldery deposit at depth, with little lateral continuity. The more continuous, boulder-free area above this section is interpreted as better sorted, horizontal beds. From 70 to 120 m, the horizontal beds of Facies 3c gradually dip and give way to the dipping clinoforms of Facies 3a. This gradual transition to foreset beds may mean that a braidplain - braid delta transition zone has been encountered. This implies that in a glacial setting (and possibly elsewhere) a braid delta does not necessarily have a distinct contact with its braidplain. However, the gradual transition zone may have formed by postdepositional slumping that has obscured the original relationship which may have been a more abrupt change from braidplain to delta.

Radar Facies 3e: Slump Deposits

Facies 3e (slump deposits) is present at the end of NV124. The foreset beds appear to have failed along the strong horizontal reflection, labelled as a slip surface in Figure 7.14. A contorted slump deposit with convex upward reflections is found above it. Similar convex reflections with convex upper surfaces have been interpreted in seismic profiles as slope failures

in the Fraser delta (Roberts *et al.*, 1992). This slump might even be the run out zone of the chute above in Facies 3a. The contact between Facies 3e and Facies 3a is dashed in Figure 6.14, as it is difficult to locate precisely. Slumping is common on oversteepened (>30° angle) prodelta slopes. An example of the chute and debris flow relationship is shown in Figure 7.15 (Nemec, 1990).

*New Aiyansh Delta: Lines NV125, 126, 128, 129*

These lines were run in the town of New Aiyansh, in an area mapped as glaciofluvial delta. This delta is separated from the terminal part of the Aiyansh Braidplain by a bedrock ridge (Nass Valley map; Figure 7.1). Since the delta is not attached to the Aiyansh Braidplain, it either represents a separate delta formed by a river flowing out of the Tseax Valley, or it is a remnant of the larger Aiyansh delta. If it is a remnant, then much of the delta would have to have eroded away during the Holocene.

The orientation of the four radar lines is shown in Figure 7.16. NV129 is a continuation of NV128 and NV126 is a continuation of NV125. Lines NV128-129 are reversed so they can be easily visualized with reference to Figure 7.16. Two sections are present, their locations are shown in Figure 7.16 and their lithologic logs are shown in Figure 7.17. The lines and their interpretations are shown in Figures 7.18-7.21. Penetration was good, but not excellent (up to 9 m). A velocity of 0.12 m/ns was determined from section information in the same manner as that outlined for the Nass Delta profiles (the CMP velocity of 0.06 was incorrect, as at NV113-118). A large transformer was encountered at 455 m on line NV129, which produced a major diffraction in the signal (Figure 7.20).

Two small sections are used as lithological controls, and to check depth calculations (Figures 7.16 and 7.17). Section 97602-04 is located at the start of line NV128. It consists of topset and foreset beds with a foreset dip of 35° to the northwest. This steep dip happens to be the maximum foreset dip angle for gravel deltas (Nemec, 1990) and is thus likely the true dip direction. Foreset beds are 8 m thick and topsets are 1 m thick. The topset beds are not visible on line NV128 due to interference at this elevation (150-152 m) by the air and ground waves.

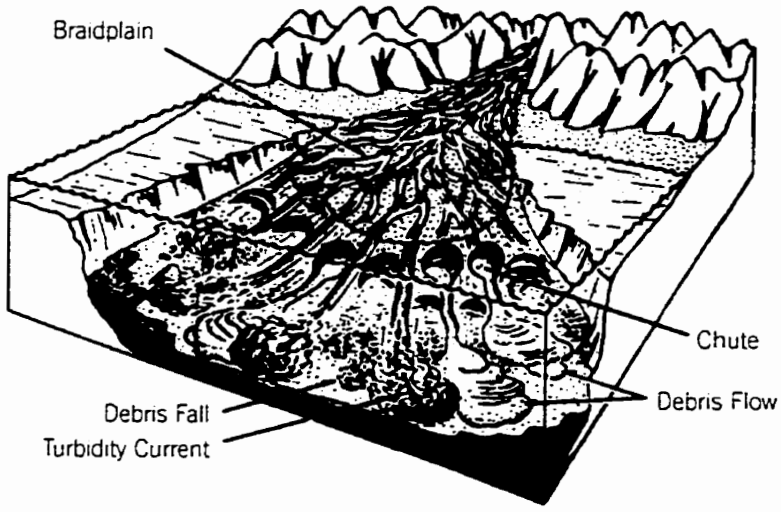


Figure 7.15. Slump activity on the prodelta slope of a braid delta (from Nemec, 1990).

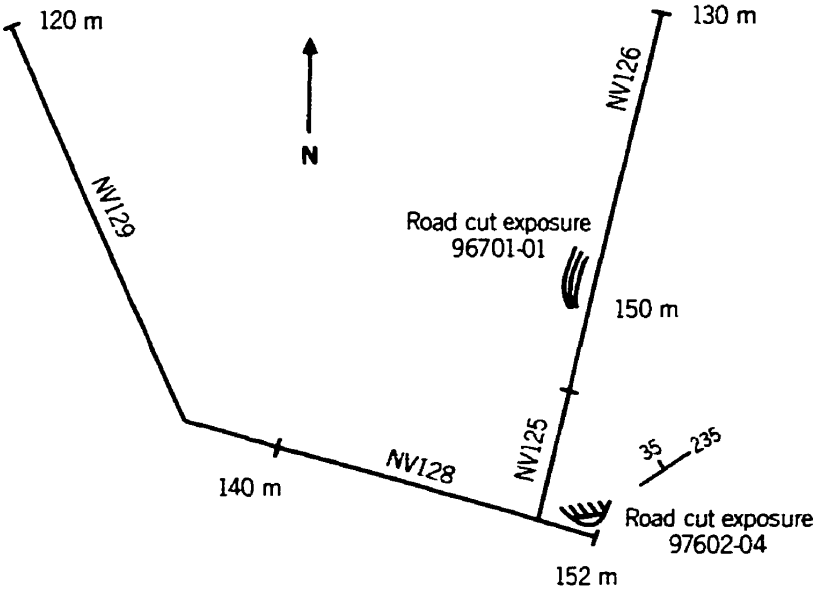


**Figure 7.16. Location of radar lines and sections in New Aiyansh. Strike and dip of foreset beds in section 970602-04 are given. Approximate elevations are shown in metres.**

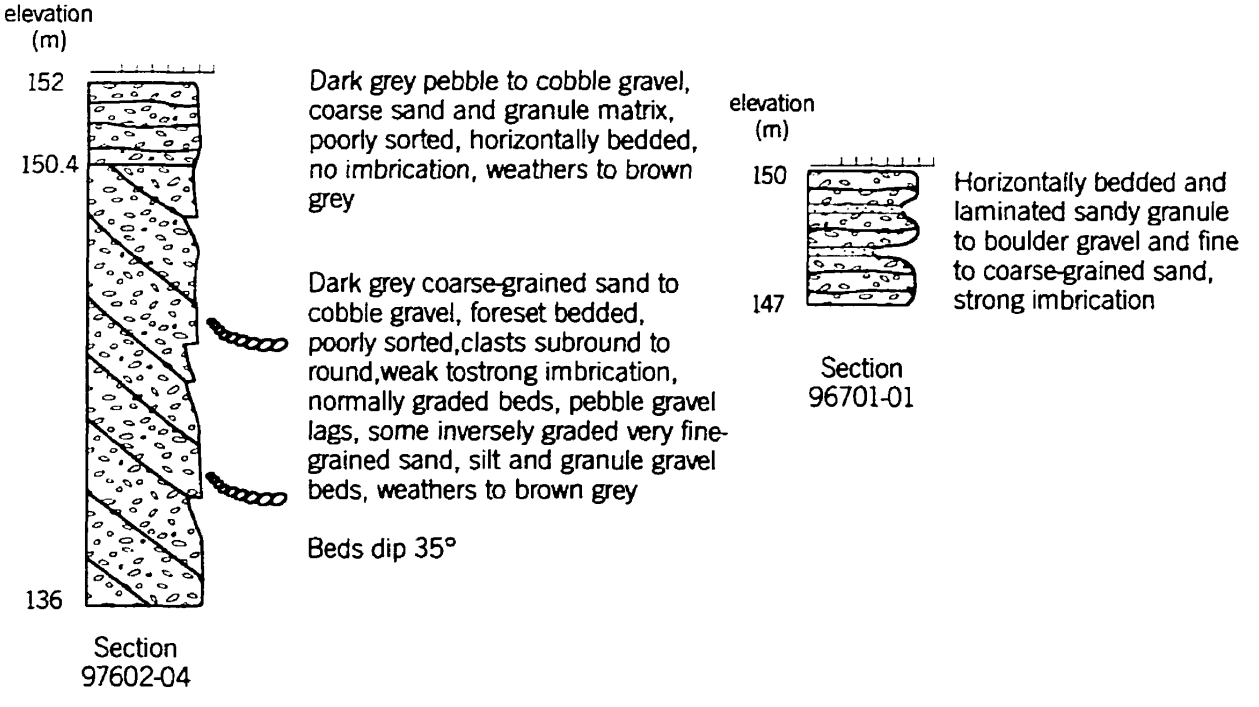


**Figure 7.17. Sections 97602-04 and 96701-01. They were measured within the road cut exposures above.**

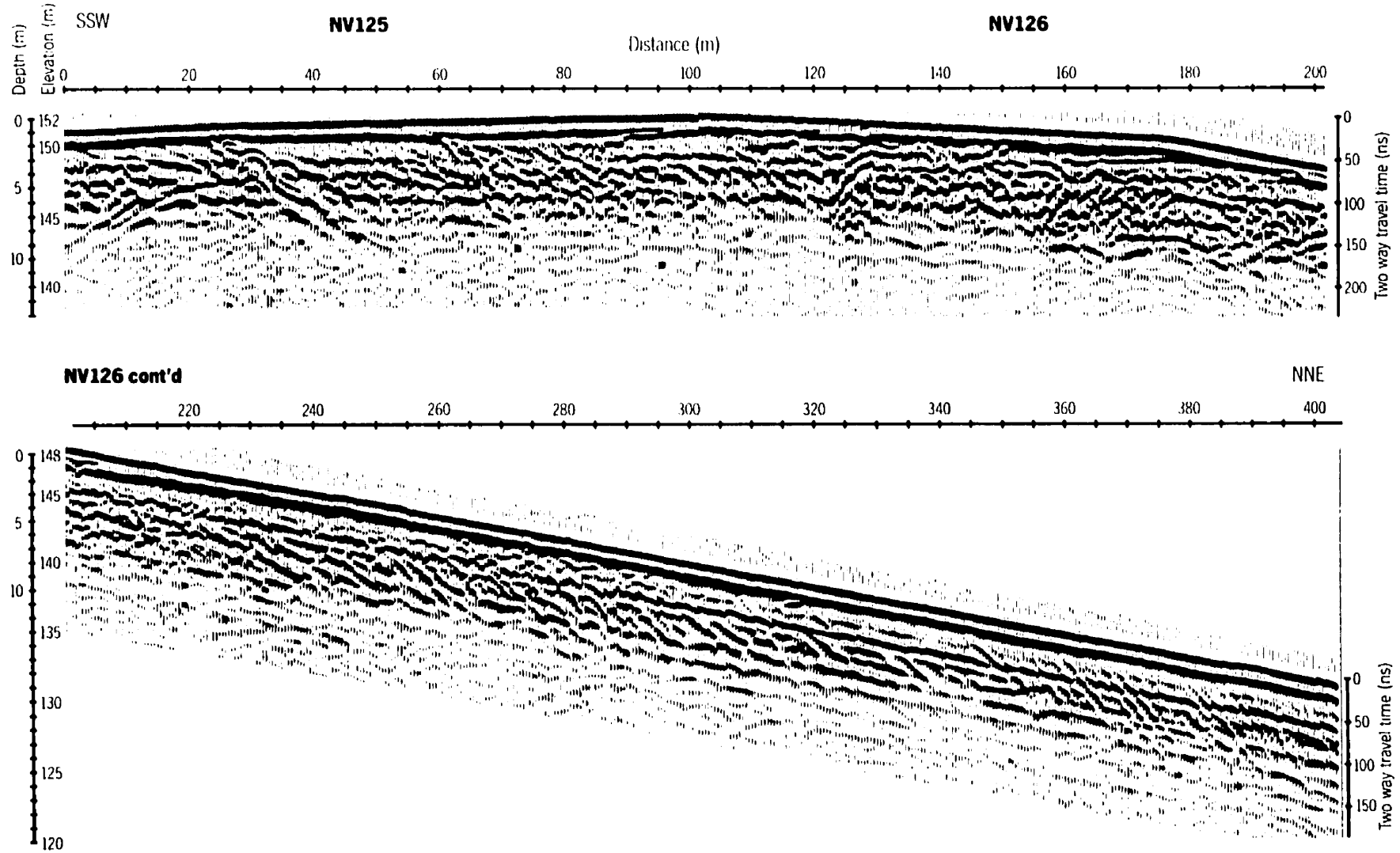


Figure 7.18. Radar lines NV125 and NV126, New Aiyansh Delta, uninterpreted profiles.

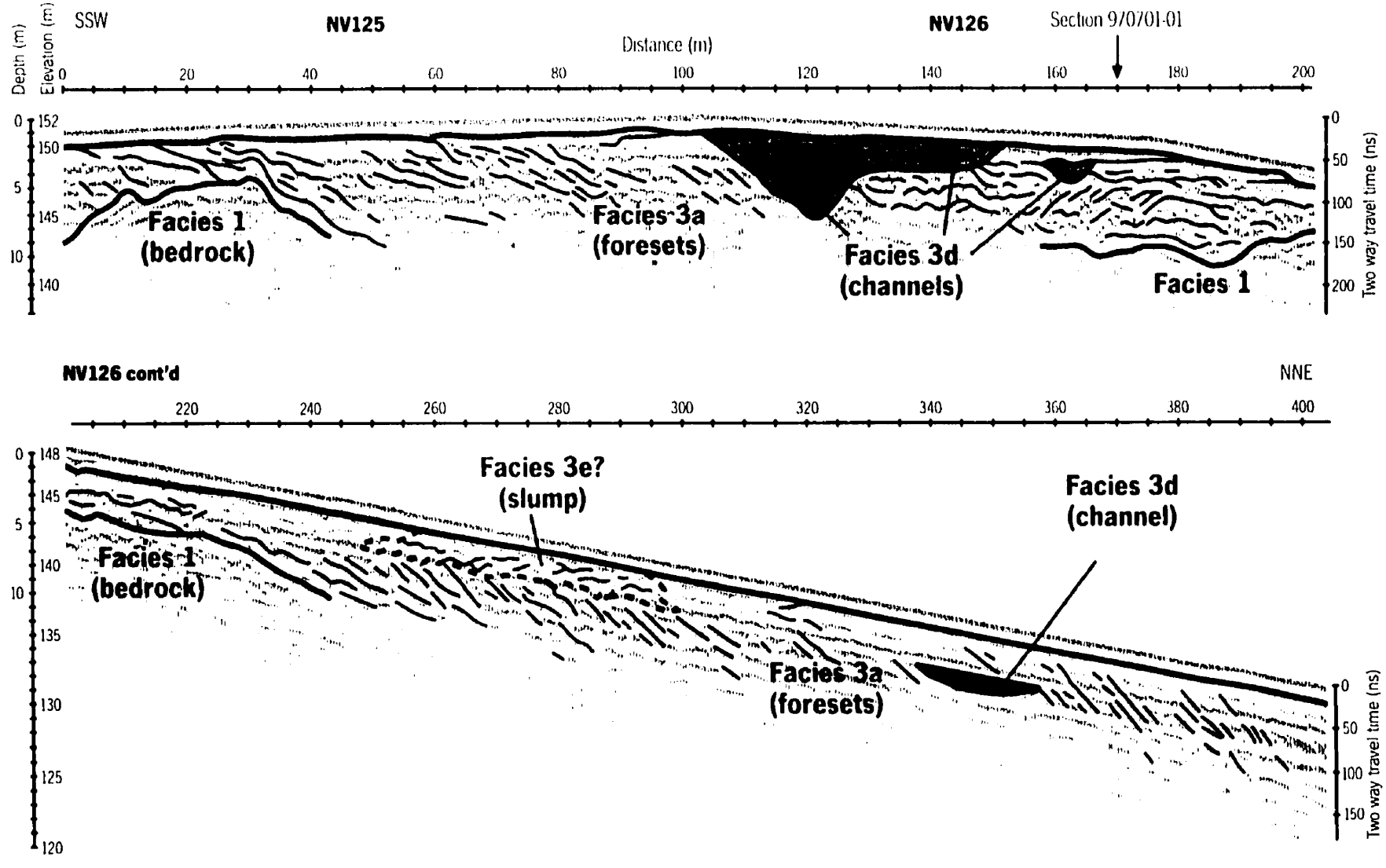


Figure 7.19. Radar lines NV125 and NV126, New Aiyansh Delta, interpreted profiles. The location of Section 970701-01 is shown.

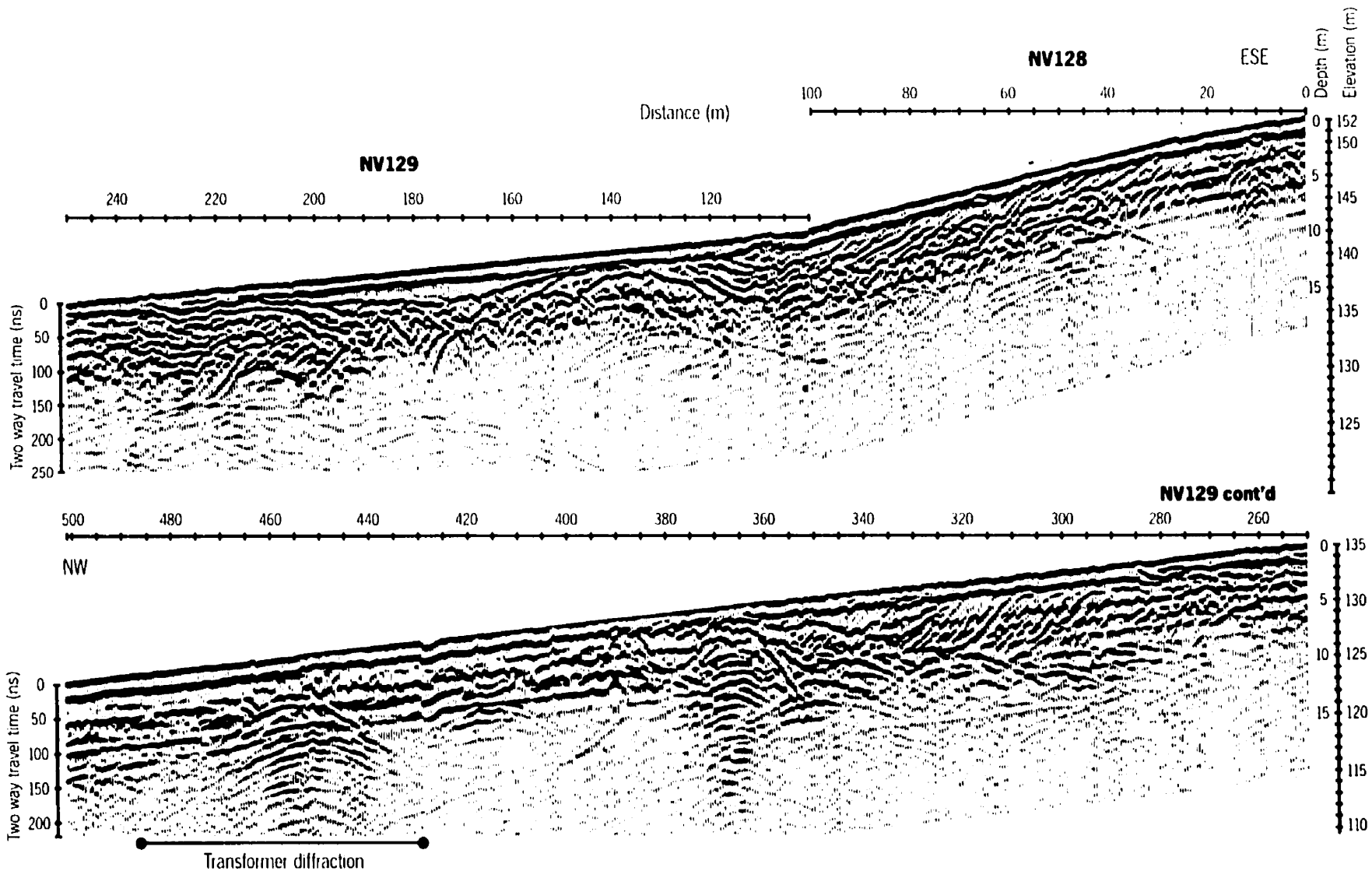


Figure 7.20. Radar lines NV128 and NV129, New Aiyansh Delta, uninterpreted profiles. The lines have been reversed so that their position on the radar line map shows the appropriate structure from left to right. The location of a power line transformer diffraction is shown.

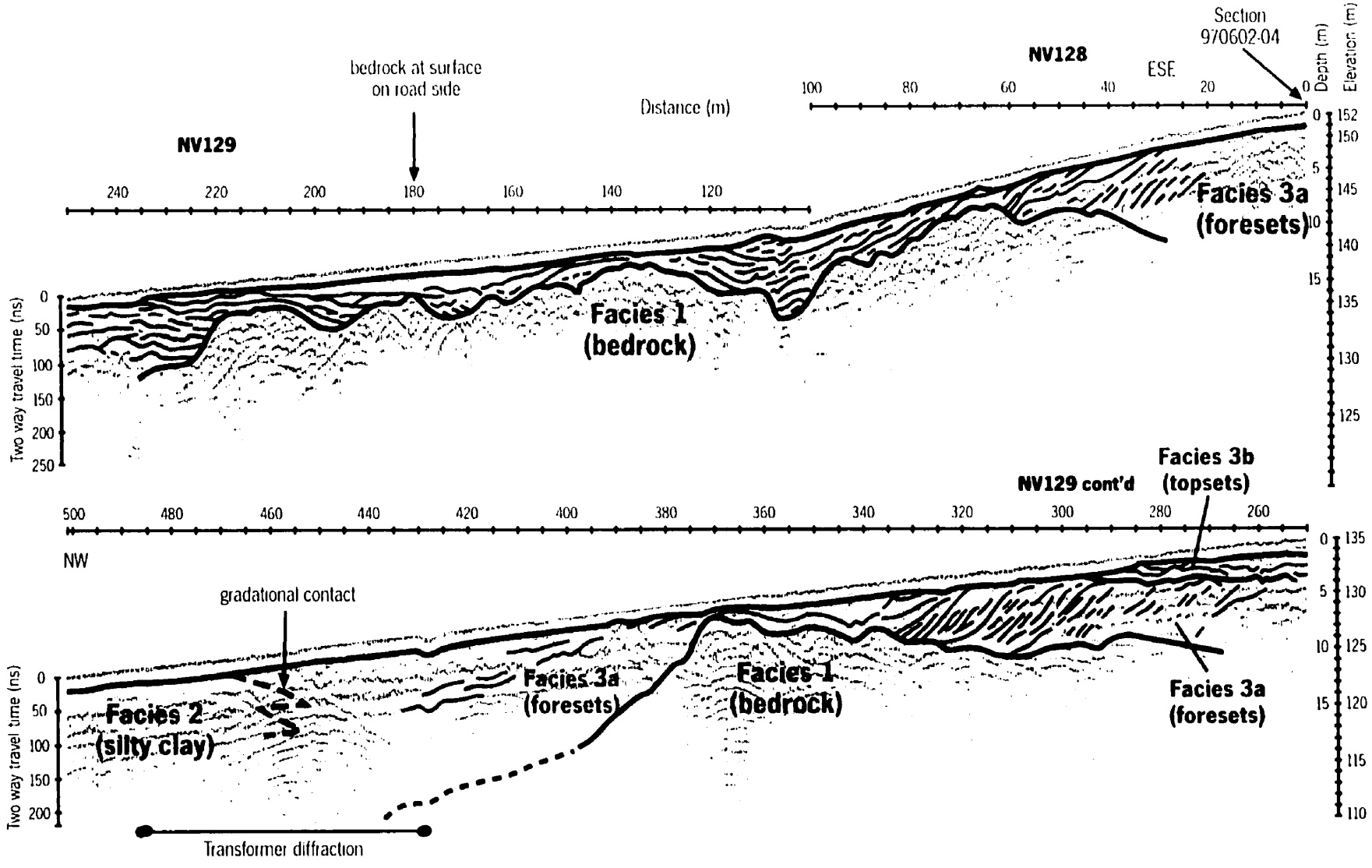


Figure 7.21. Radar lines NV128 and NV129, New Aiyansh Delta, interpreted profiles. Gravel and sand are exposed at the surface over most of the line, with the exception of bedrock that outcrops near 180 m and a gradation to silty clay from 440 to 480 m. The location of Section 970602-04 is also shown.

However, dipping beds from 150 to 136 m elevation are evident at the beginning of lines NV128 and NV125. Section 96701-01 comprises horizontally bedded and laminated fine-grained sand, coarse-grained sand, and granule, pebble and boulder gravel. It is poorly to moderately sorted. Clasts are strongly imbricate, unstriated and subangular to subround. Contacts are sharp and the lower contacts of coarser beds are erosive.

### Radar Facies Description

#### Radar Facies 1

A series of overlapping hyperbolic reflections are found in the lower part of NV128-129 (*e.g.* 145-220 m, Figure 7.21). They have moderate continuity and amplitude and commonly continue below the uppermost hyperbolic event (*e.g.* NV129, 355-375 m). On lines NV125-126 (0-45 m, 157-243 m, Figure 7.19), overlapping hyperbolic areas are also present but are less well defined.

#### Radar Facies 2

At the end of line NV129, data is lost entirely and only artifacts remain. The loss of detail from 430-500 m shows the transition to the glaciomarine silty clay which is evident at the surface (Figure 7.21).

#### Radar Facies 3a

The reflections overlying the hyperbolic reflections are variable. Some are dipping clinoforms (NV125, 0-50 m), some are sigmoid clinoforms (NV129, 290-330 m) and some are horizontal reflections (NV129, 129-250 m). They are of moderate amplitude, but the horizontal reflections are more continuous.

The oblique and sigmoid clinoforms are offlapping (NV125, 0-110 m, NV126, 225-405 m, NV128, 0-100 m, NV129, 260-335 m). They downlap onto the hyperbolic reflections, indicating that a discontinuity separates these two facies (NV128, 40-100 m, NV129, 290-335 m). Where

the hyperbolic facies approaches the surface, the clinoforms become horizontal reflections, which form a complex or divergent fill in hollows (NV126, 160-225 m, NV128-129, 70-250 m, 325-370 m). Toplap is evident on NV129 from 260 to 270 m, and on NV126 from 250 to 295 m.

Radar Facies 3b

Horizontal, moderately continuous reflections are seen in one area where the hyperbolic facies is further from the surface (NV129, 250-310 m).

Radar Facies 3d

Flat-topped lens geometries with divergent fill are also present (*e.g.* NV126, 105-153 m).

Radar Facies Interpretation

The overall interpretation of the New Aiyansh radar lines is that of an incipient braid delta deposited over an irregular bedrock surface. In some places the Gilbert-type delta is well developed, but in others, where bedrock is close to the surface, it has a different character.

Radar Facies 1: Bedrock

The hyperbolic reflections are inferred to represent bedrock. Bowser Lake Group bedrock was noted at the surface, about 5 m away from radar line NV129 at 180 m (Figure 7.21).

Radar Facies 2: Glaciomarine Silty Clay

Facies 3a grades laterally into Radar Facies 2 at the end of line NV129. This facies was identified at the surface (while surveying) as silty clay.

Radar Facies 3a: Braid Delta Foreset Beds

Radar Facies 3a unconformably overlies Radar Facies 1 and is interpreted as a deltaic foreset deposit. Oblique and sigmoid clinoformal reflections are interpreted as foresets that are

poorly developed in places due to the location of underlying bedrock. Although the steeply dipping beds flatten out over shallow bedrock and infill hollows, they are still considered a variety of the foreset facies 3a. Basin fills and onlapping horizontal beds form where bedrock is close to the surface.

Radar Facies 3b: Braid Delta Topset Beds

A second set of topset beds at 132 to 134 m asl on line NV129 (260-295 m distance), indicates a *second sea level highstand* at 134 m. The earlier stand is shown in section 97602-04, where topset beds give a sea level of 152 m. Clearly, some 'telescoping' of the delta has occurred due to sea level fall. As sea level dropped, the river incised into the existing delta, forming new topset/foreset beds at the 134 m level, when sea level stabilized for a time. This is the first evidence discovered of a 134 m marine limit. Lower delta sediments do not appear to overlie deposits of the earlier delta; at this location, the new delta is deposited directly over bedrock. Fluvial incision therefore must have eroded through the earlier delta to bedrock.

Radar Facies 3d: Braidplain Channel Deposits

Channels of Facies 3d are present locally. Since they occur in the foreset facies, they are not considered distributary channels of the 152 m delta. The channels may have formed after a drop in sea level, as feeders to the new deltas or they may have carried sediment flows down the delta front into deeper water.

Flat-lying gravel and sand beds at a distance of 170 m and an elevation of 148-150 m on lines NV125-126 are detailed at section 97701-01, and these are equivalent to parallel reflections visible near the surface. These do not appear to be topset beds, but rather disrupted infills due to the presence of bedrock 4 m below.

Line NV128 dips WNW, NV129 dips NW, and lines NV125-126 dip north-northeast, indicating an overall northwestward dip direction, which agrees with the dip of foreset bedding obtained from Section 97602-04 (Figure 7.17). The northwestern direction of dip indicates that this small delta was formed by a meltwater river flowing out of the Tseax Valley into the Nass

Valley. As it is not a remnant of the Aiyansh delta, no erosion occurred here and both deltas must have flowed into glaciomarine waters when sea level was about 150 m asl.

Given that a number of deltas graded to 152 m flowed coevally into glaciomarine waters, a line drawn on the 152 m contour would show the approximate extent of marine incursion at that time. This will be explored further at the end of this chapter.

*Dragon Lake: Line NV131*

This line was run along an alluvial fan just north of Dragon Lake (Figure 7.1), in order to compare an alluvial fan radar signature to the glaciofluvial signatures. The line started 40 m northeast of a small creek that flows to the northwest.

Penetration was good, reaching 10 m. The line's elevation of 230 m is not related to marine limit, as it was conducted on a Holocene feature that has accumulated on top of the Aiyansh Braidplain. A velocity of 0.12 m/ns was determined from a CMP survey.

Radar Facies Description

Radar Facies 4a

The reflections are wavy and generally continuous across the profile (Figure 7.22). Amplitudes are moderate to high and the horizontal artifacts that are so common in other profiles are notably absent. Boulder diffractions are present (e.g. 15-40 m), but not pervasive, suggesting that boulders are not an important part of this gravel deposit. Most of the reflections are evenly spaced and parallel (*e.g.* 40-75 m), becoming more hummocky (155-217 m) to the north-northeast.

Radar Facies 4b

Reflections outlining flat topped lenses are present in a few places. Two of these have steeply dipping clinoforms at each end (42-80 m, 107-128 m). A number of horizontal reflections are truncated by the lenses (*e.g.* 75-80 m), indicating that the base of the lenses and clinoforms are erosional discontinuities.

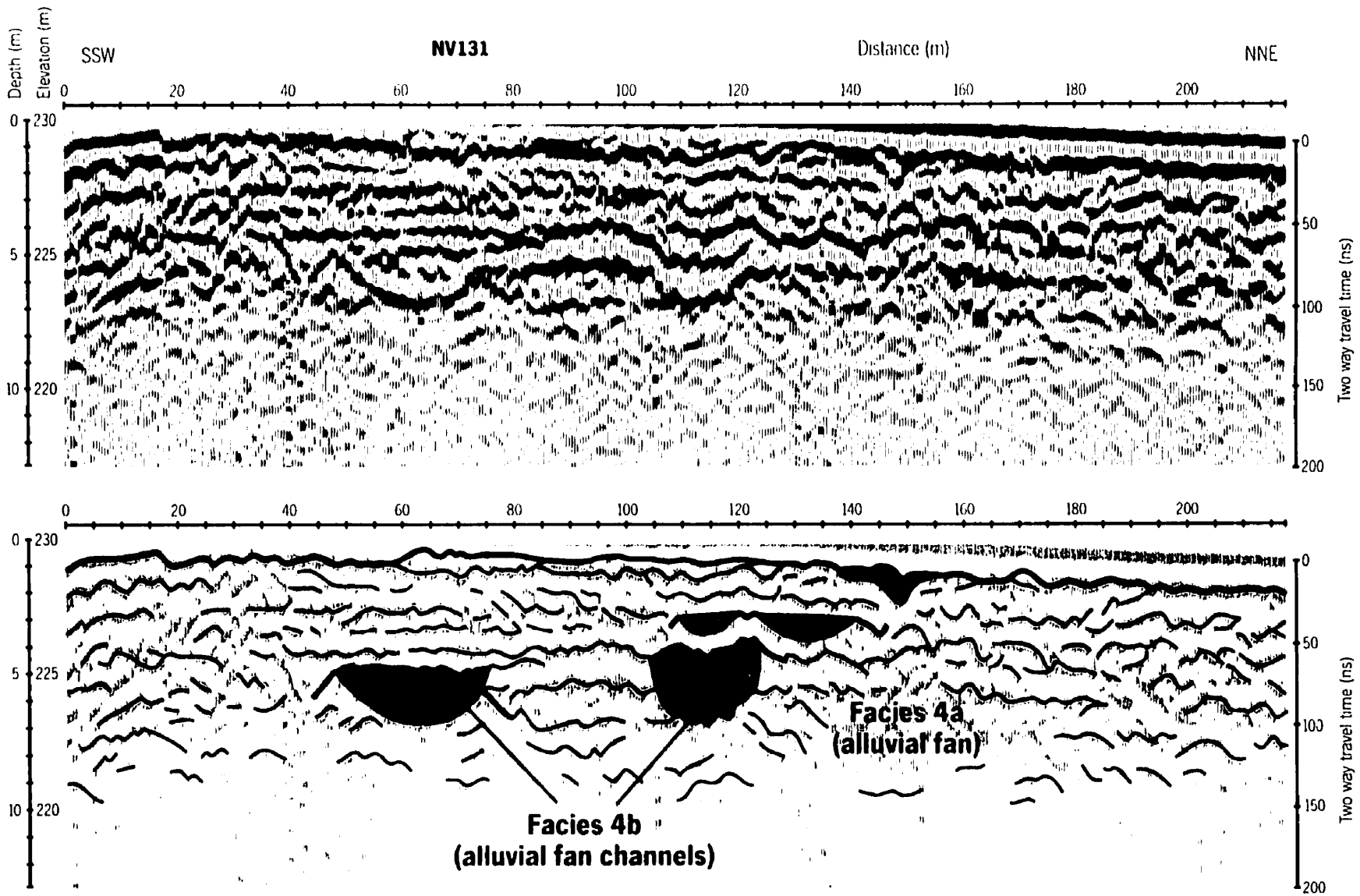


Figure 7.22. Radar line NV131, near Dragon Lake, uninterpreted profile above, interpreted profile below. The line is topographically corrected, but the air wave reflector has been truncated, due to technical problems with the field equipment (zero line drift during warm-up period). The 230 m elevation is not related to marine limit.

The overall geometry of the reflections is one of sheets that become less well defined to the north-northeast, and are interrupted locally by lenses. This is an aggradational, rather than a progradational fill, since beds are horizontal, rather than dipping (see Prograded Fill, Figure 7.2).

Radar Facies Interpretation

Radar Facies 4a and 4b: Alluvial Fan Horizontally Bedded and Channel Deposits

The horizontal reflections approximating sheet geometry are interpreted to represent fluvial or debris flow deposition, while the lenses show debris flow channels. The sharp base and sides of the lenses show erosive channelized deposits, while the steeply dipping clinoforms at either end of the channel forms represent large levees which are characteristic of the margins of debris flows. Radar Facies 4a and 4b, alluvial fan horizontally bedded and channel deposits, are represented here, consistent with the surficial geology mapping interpretation (Nass Valley map; Figure 7.1). The line displays data that shows how modern alluvial fans may be distinguished from glacial braided river deposits in some cases based on the type of lenses present (compare profile NV131 to NV132 and NV133, discussed next). Steeply dipping clinoforms at the end of lenses occur only on the alluvial fan profiles.

*Kiteen River: Lines NV132 and NV133*

These lines were run at the north end of the Aiyansh Braidplain near Kiteen River (Figure 7.1) to check the depositional signature of braidplain gravels. NV132 was run along the Nisga'a Highway, a major gravel road, and NV133 was run along a small logging road roughly perpendicular to it (Figure 7.23). Both were run in the centre of the road to avoid tree root diffractions. Cobble boulder gravel is visible at the edge of both roads on the surface. NV133 is a strike section across the braidplain, while NV132 is a dip section. Penetration is good for both lines. A velocity of 0.12 m/ns was determined.

A small road cut exposure is present at the start of NV132 and section 97519-04 was measured there (Figure 7.24). Nine metres of massive, poorly sorted, subround to well rounded, unstriated cobble/boulder gravel is exposed. The top 1 m of exposure is crudely horizontally

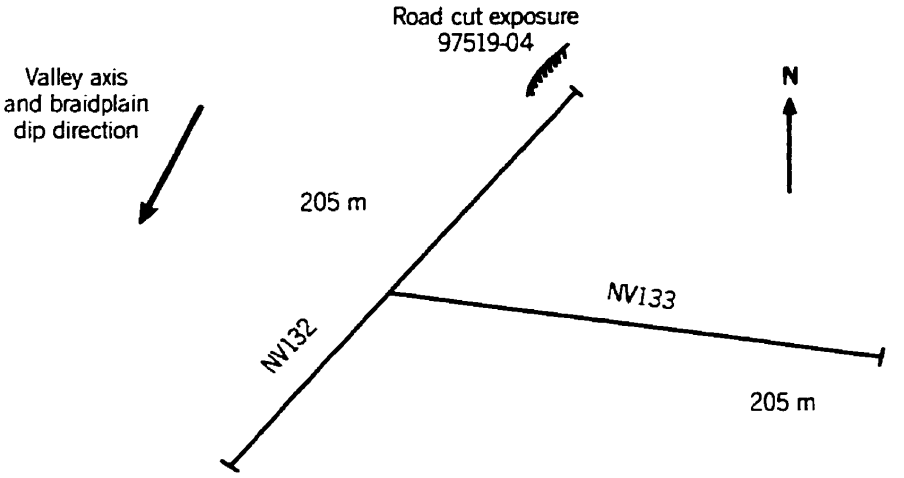


Figure 7.23. Location of radar lines and section near Kiteen River. Approximate elevation is shown in metres.

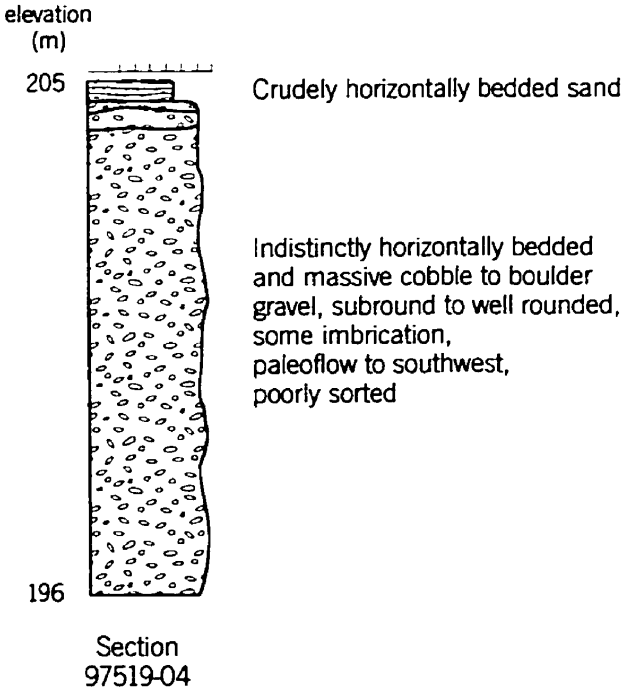


Figure 7.24. Section 97519-04. Its location at the start of radar line NV132 is shown in the above figure. Paleoflow indicated by imbrication is toward 225°, directly down valley.

bedded with weak imbrication hinting at a possible paleoflow direction to the southwest. The uppermost 20 cm is a weakly horizontally bedded, coarse-grained sand bed. 95% of clasts are of Bowser Lake Group lithologies, the remainder are granitic and volcanic.

Radar Facies Description

Radar Facies 3c

Throughout the profiles, these lines exhibit irregular, continuous to moderately continuous reflections interrupted by numerous small diffractions (Figures 7.25 and 7.26). Amplitudes of the major reflections are moderate to high. Both lines exhibit even, parallel horizontal reflections (NV132, 0-110 m, NV133, 40-265 m).

Radar Facies 3d

Oblique clinoforms (*e.g.* NV132, 135-200 m), oblique tangential clinoforms (e.g. NV133, 25-50 m) and clinoform sets are present locally (*e.g.* NV133, 155-180 m). Diverging continuous oblique clinoforms are evident on NV132 from 130 to 190 m. From 190 to 300 m, reflections are hummocky. This area appears to be part of a complex channel fill.

Lens geometries are common on NV133, but their upper surfaces are irregular or convex (*e.g.* 95-110 m, 205-265 m). These appear to be onlap fills (95-110 m) or a combination of prograded and onlap fills (0-45 m) (also known as complex fills, see Figure 7.2 for diagrams of this terminology).

The horizontal reflections at the northeast end of NV132 (0-110 m) may be truncated by the diverging ones, but this is difficult to tell. Similar reflections are truncated by lens geometries on NV133.

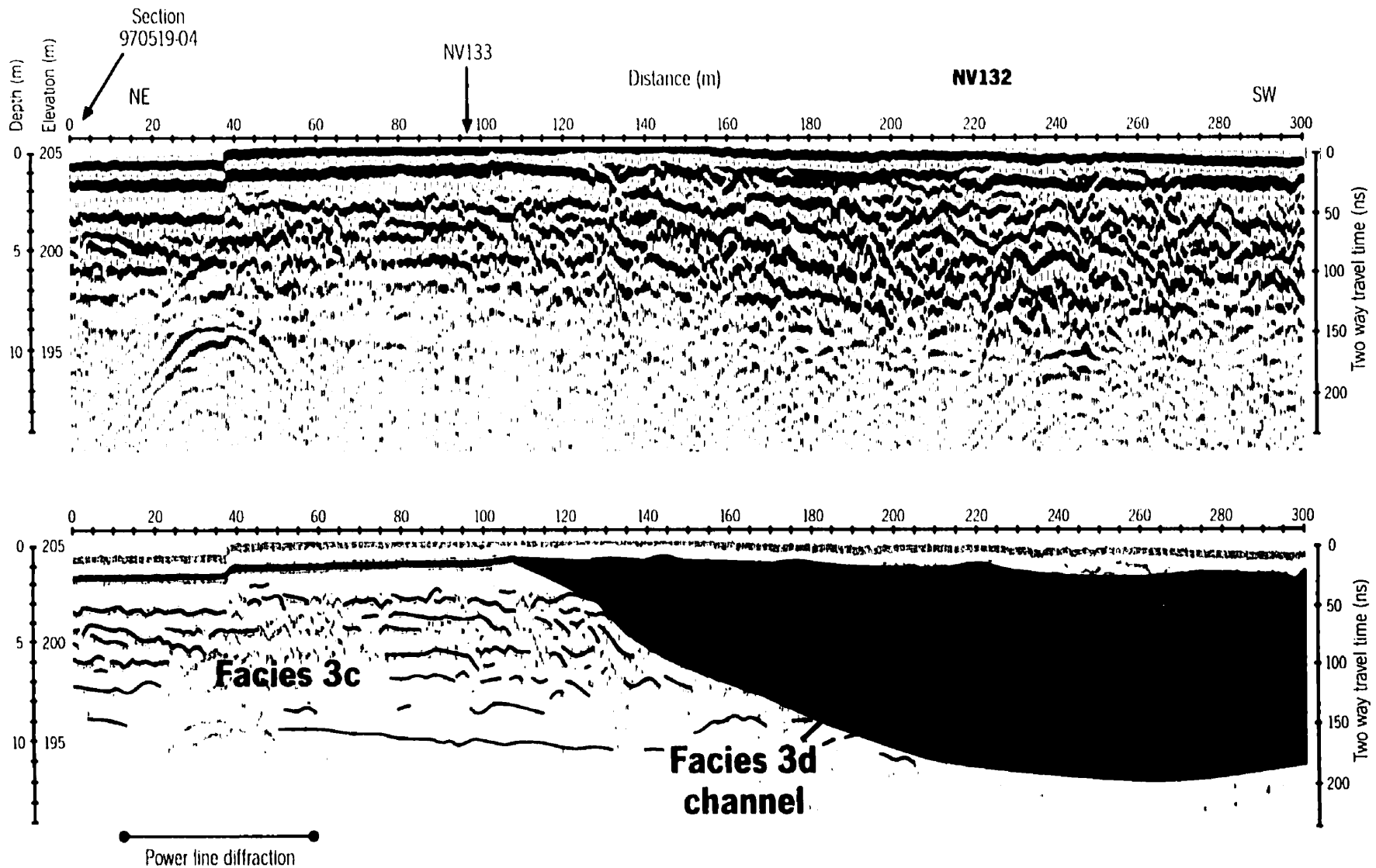


Figure 7.25. Radar line NV132, near Kiteen River, uninterpreted profile above, interpreted profile below. The location of Section 970519-04 and the starting point of line NV133 are shown with arrows. Small diffractions from large boulders are common, but are not interpreted. A diffraction centered on a hydro pole is visible at 35 m.

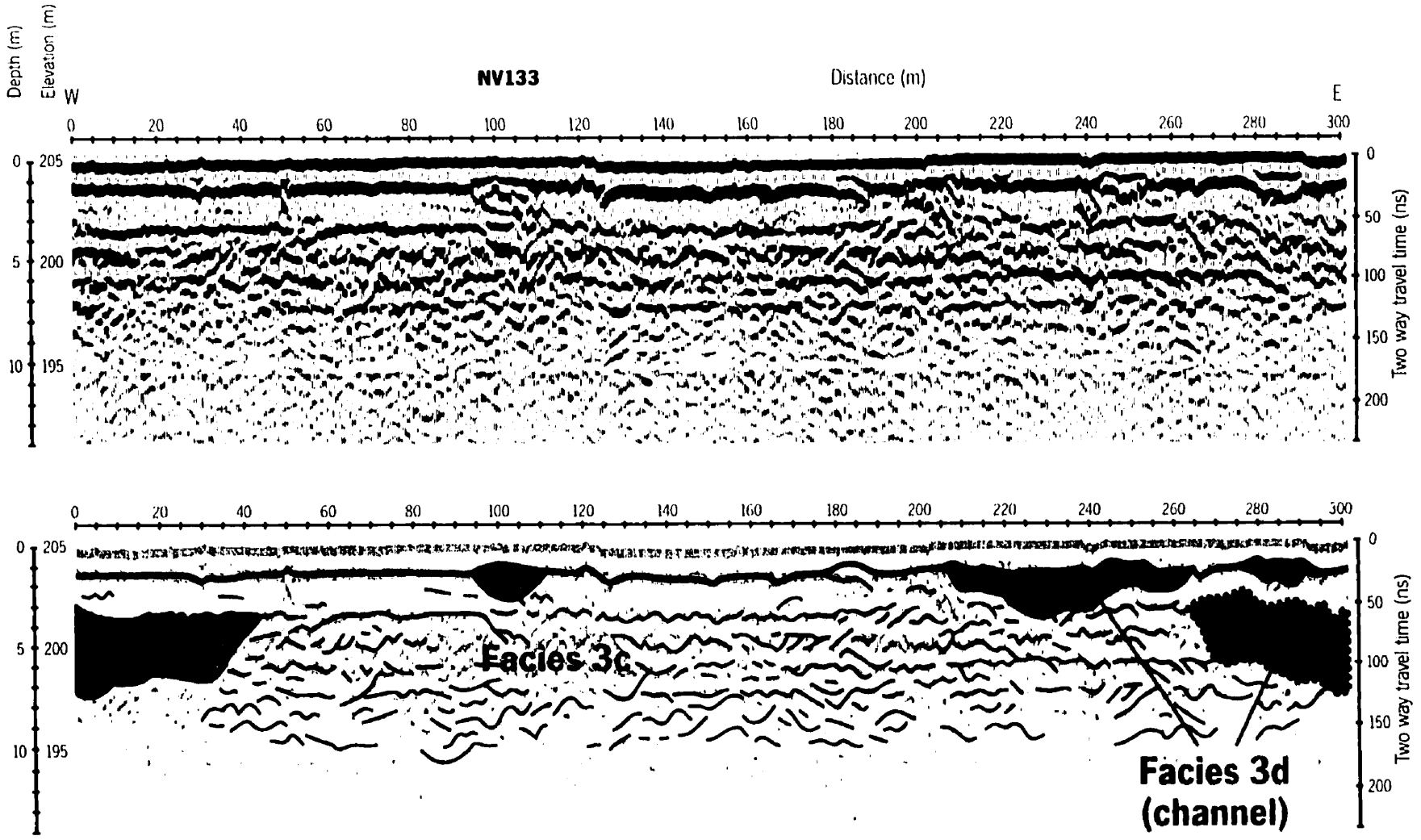


Figure 7.26. Radar line NV133, near Kiteen River, uninterpreted profile above, interpreted profile below. Several small boulder diffractions are present.

Radar Facies Interpretation

Radar Facies 3c: Braidplain Horizontally Bedded Deposits

At the surface and in section 97519-04, boulders are common. Diffractions on profiles NV132 (*e.g.* 40-7- m) and NV133 (*e.g.* 115-130 m) show that the deposit is also bouldery at depth. The wavy, roughly horizontal reflections represent the crude bedding seen in the section, and indicate fluvial aggradation. Subhorizontal and subparallel reflections and oblique and oblique tangential reflections are common in strike section profiles of braided glacial rivers (Huggenberger, 1993), and these are visible in NV133 (*e.g.* 0-40 m). The profile is thus interpreted as a horizontally bedded braidplain deposit.

Radar Facies 3d: Braidplain Channel Deposits

The lens features outline small channels (shaded areas on Figure 7.26) that were infilled by onlap (vertical aggradation) or a combination of both vertical aggradation and lateral progradation. These channels were cut into the horizontally bedded deposits as channels avulsed in a braided river environment and are only visible in the strike section.

The complex fill of NV132 shows the downflow infill of a large channel which was likely a major channel of a braided river. It is similar to the 'scour-infill' deposits of Huggenberger (1993), because it has a steeper upstream avalanche face and a less steep downstream area.

The upper Aiyansh Braidplain is thus a braided fluvial system consisting of Facies 3c and 3d. Channels of Facies 3d lie within the flat-lying beds of 3c. Paleoflow was to the southwest and the coarse deposits are at least 14 m thick. These braided river deposits are more complex than those identified in radar profiles by Jol and Smith (1991), because of the numerous channels that are present, many of which can only be seen in a strike orientation.

*Nass Braidplain South: Lines NV135 and NV136*

These lines are located on what is roughly the southern tip of the Nass Braidplain (Figure 7.1). The area is mapped as a glaciofluvial braidplain flanked by glaciomarine deposits to the west

and south, and by till and glaciofluvial veneer to the east (Nass Valley map). It was suspected that the area might have been deltaic, due to its location at the end of the Nass Braidplain.

NV135 is about 45° off a true strike section, while NV136 is about 15° off a true dip section (Figure 7.27). Fine- to medium-grained sand is visible at the surface at the start of line NV135. It grades to fine-grained sand toward the end of the line. Fine-grained sand was also seen at the surface on NV136. Line NV136 starts at the 50 m point on NV135. Penetration was good on both lines and a velocity of 0.12 m/ns was determined for depth calculations.

### Radar Facies Description

#### Radar Facies 1

One high amplitude, highly continuous reflection crosses the entire length of both lines at 5-10 m depth, and is interpreted to be an important discontinuity (Figures 7.28 and 7.29). Reflections beneath it are poorly resolved (NV135) or discontinuous and disrupted (NV136, 90-150 m). Diffractions are rare below this reflection. Some are present above it, below 5 m depth (*e.g.* NV135, 0-35 m).

#### Radar Facies 3c

The upper package of reflections is moderately continuous and of moderate amplitude (above the highly continuous reflector throughout the profiles). These parallel to subparallel reflections drape the lower facies (*e.g.* NV135, 70-150 m, NV136, 60-85 m), so it is an aggradational rather than an onlapping fill. A few oblique and oblique tangential reflections are present (*e.g.* NV135, 30-70 m), so this package resembles that of NV133.

#### Radar Facies 3d

Some flat-topped lenses occur near the top of Facies 3c (NV136, 0-12 m). They appear to be complex fills, both progradational and aggradational. On NV135 for example, the lens at 125-180 m seems to have prograded from east-southeast (bar deposition?), and then changed to an

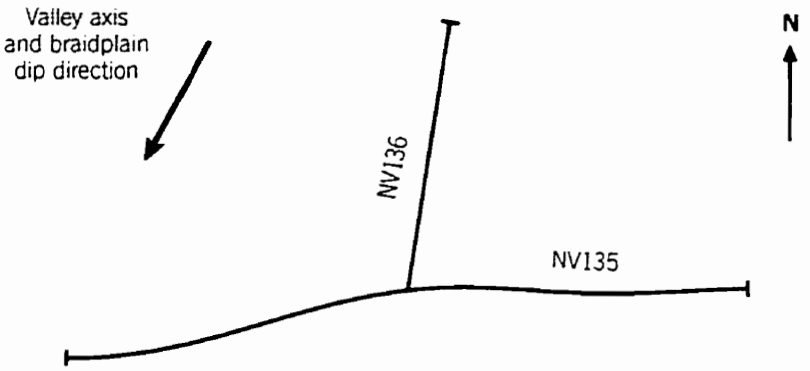


Figure 7.27. Orientation of radar lines NV135 and NV136.

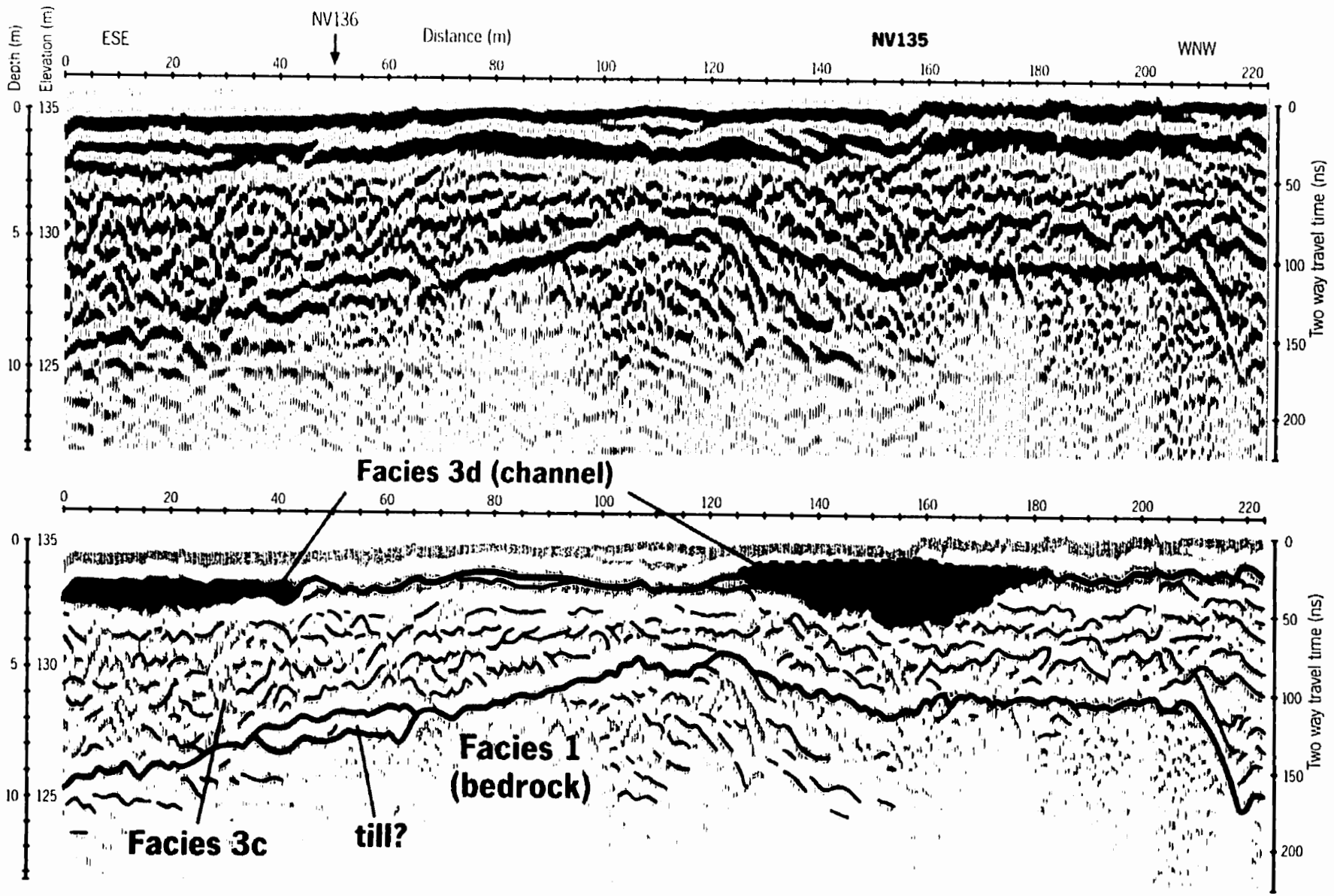


Figure 7.28. Radar line NV135, Nass Braidplain South, uninterpreted profile above, interpreted profile below. The starting point of line NV136 is shown with an arrow. Small diffractions from boulders are common.

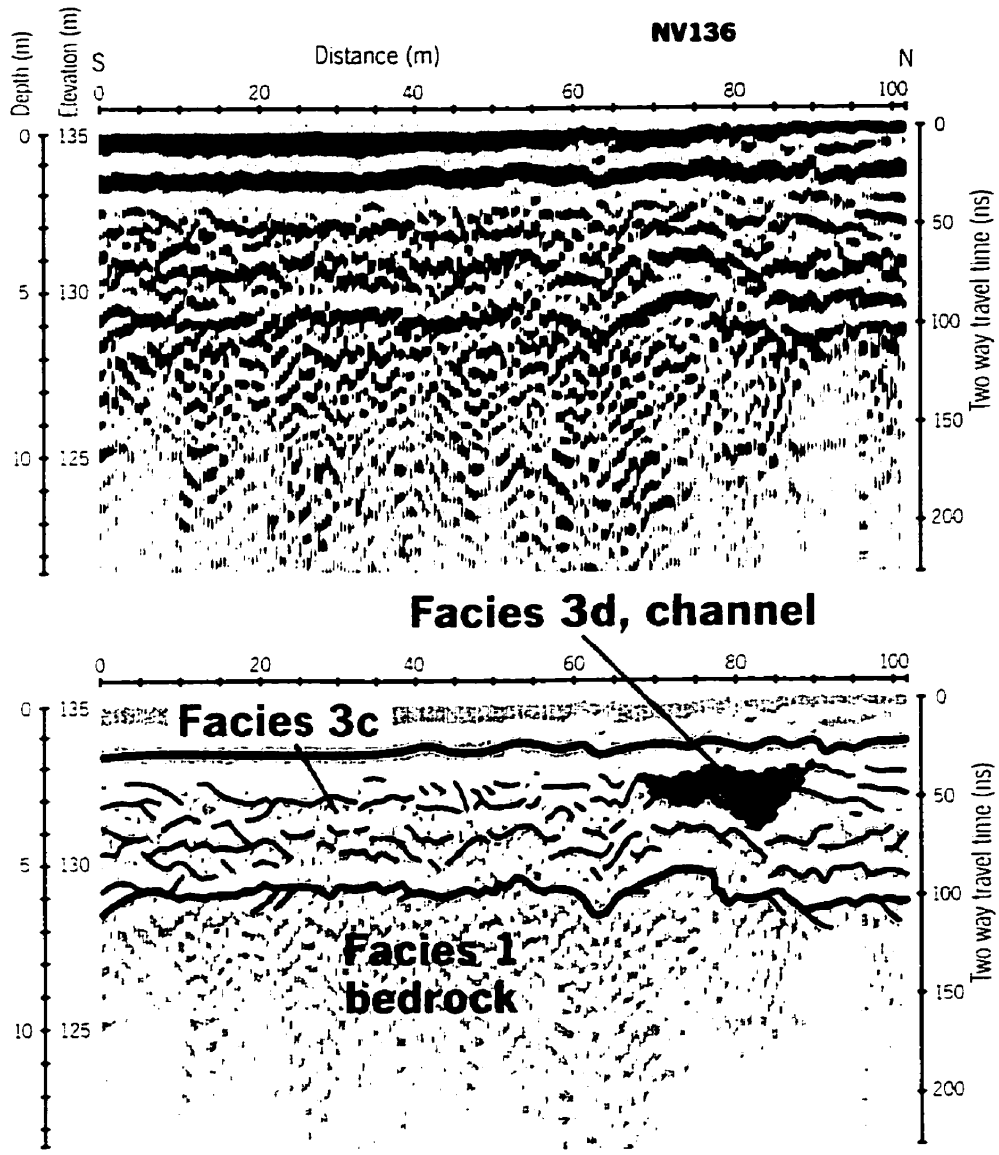


Figure 7.29. Radar line NV136, Nass Braidplain South, uninterpreted profile above, interpreted profile below.

aggradational fill. This lens is difficult to interpret, however, due to interference from the ground wave.

### Radar Facies Interpretation

#### Radar Facies 1: Bedrock

The lower unit is interpreted as bedrock, or Radar Facies 1. The major discontinuity is likely the bedrock/sediment interface, but in the absence of drilling, this is impossible to confirm. Although the reflections below the discontinuity do not show overlapping diffractions like those seen in lines NV128-129 (Figure 7.21), it may be that the bedrock beds here are flat-lying to slightly dipping, while bedding is more vertical in the New Aiyansh area. Possible horizontal bedrock beds can be seen near the start of NV135 (0-40 m), while dipping beds may be represented by dipping reflections from 90 to 145 m (Figure 7.28). Some diffractions are evident in the latter region (*e.g.* 120-130 m).

#### Radar Facies 3c and 3d: Braidplain Horizontally Bedded and Channel Deposits

The lack of horizontal reflections underlain by dipping ones shows that this is not a deltaic unit as was initially suspected. The upper unit appears to be an aggradational fill over the bedrock surface. It is bouldery at depth (diffractions), crudely horizontally bedded, and cut by channels. It is interpreted as a glaciofluvial braidplain deposit, by incorporating the surficial mapping interpretation with the radar analysis. Diffractions below 5 m seem to indicate that it is coarser at depth, while fine-grained sand at the surface may indicate a fining-upward trend.

This draped unit is inferred to be Radar Facies 3c, with channels of Facies 3d in its upper portions. It seems to be a braidplain that advanced over bare bedrock in this location. This indicates that a major erosional event occurred and a significant amount of time passed between the formation of the lower bedrock unit and the upper glacial deposit. The major discontinuity is thus a true unconformity.

*Nass Braidplain North: Lines NV139 and NV140*

These lines were run at the south end of the Nass Braidplain North (Figure 7.1). A sloping surface in this area resembles the sloping front of a delta (Figure 7.30). Radar lines were run part way down the slope in order to check that hypothesis. NV139 runs across the slope and is close to being a strike section, while NV140 goes down the slope, and is in a dip orientation (Figure 7.31). A CMP survey gave a velocity of 0.13 m/ns for these lines (Appendix C).

Radar Facies Description

Radar Facies 2

A high amplitude subhorizontal reflection overlying a reflection-free zone at 90 to 108 m on NV139 seems to indicate the presence of fine-grained sediments at depth (Figure 7.32). This reflection continues into line NV140, suggesting that fine-grained sediments continue in that direction as well. However, clinoforms continue as offlapping features right through the horizontal reflection, which turns upward at this point (10-30 m on NV140). This reflection cannot be the water table as it does not follow topography. It may simply indicate that the oblique clinoforms are part of a deposit that fines with depth. From 55-74 m on NV140, there is no non-artifact signal, so this area is considered reflection-free.

Radar Facies 3a

Offlapping oblique clinoforms of moderate amplitude and continuity are evident on both lines (Figure 7.32). They are steeper on line NV140, the dip section (0-40 m, 20°-35°). On NV139, they are ubiquitous and dip from 13°-20°.

Radar Facies 3e

From 30 to 55 m on NV140, clinoforms are wavy and irregular.

Figure 7.30. Sloping surface in logged area that resembles a delta front, looking west across Nass Valley. Flat ridge in middle distance is the valley central bedrock ridge.

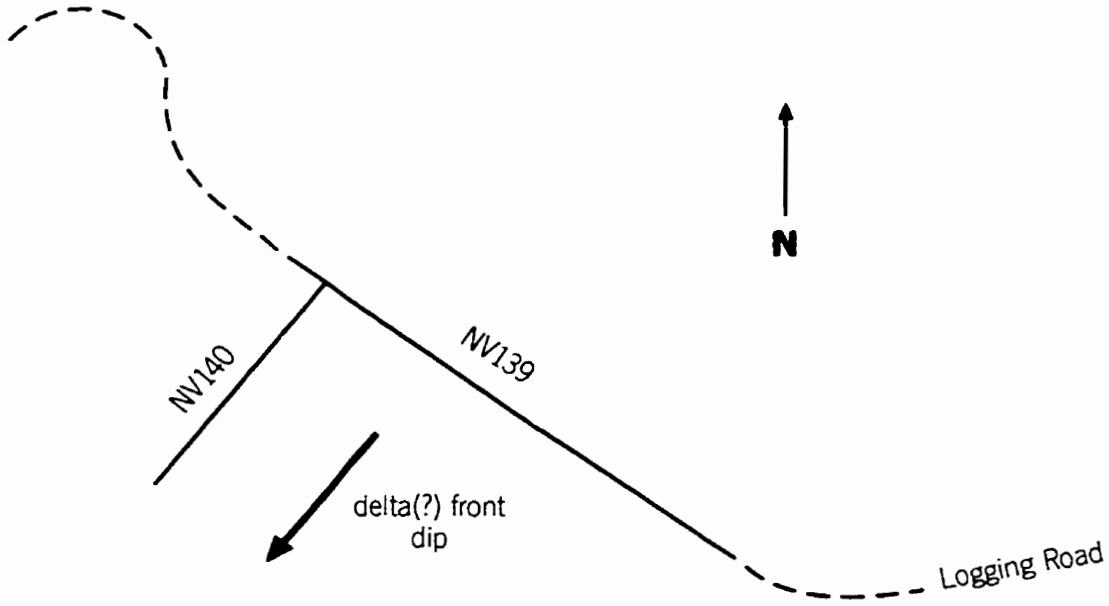


Figure 7.31. Orientation of lines NV139 and NV140 on the Nass Braidplain North. The dip direction of the possible delta front is shown.

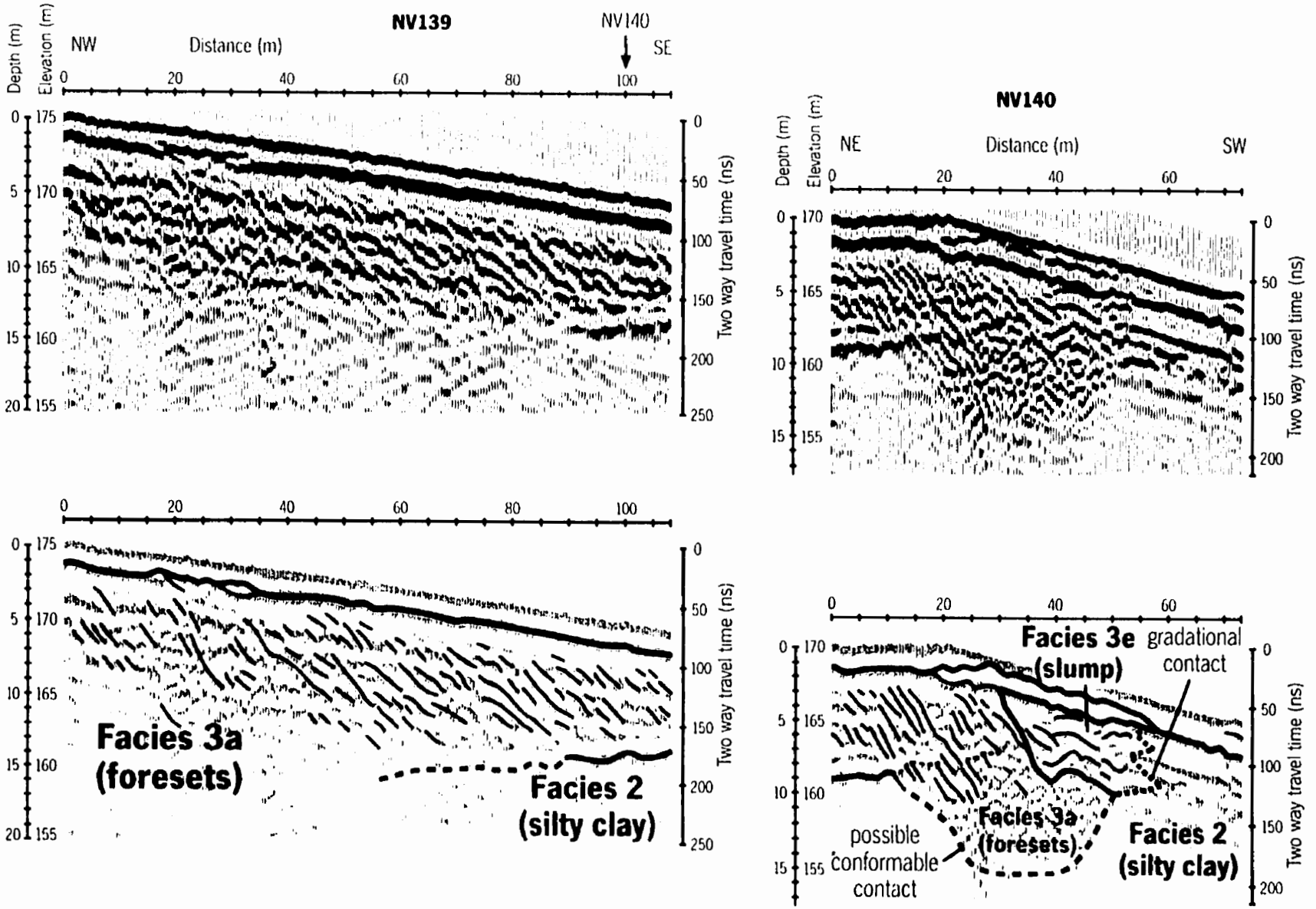


Figure 7.32. Radar lines NV139 and NV140, Nass Braidplain North, uninterpreted profiles above, interpreted profiles below. The starting point of line NV140 is shown with an arrow.

Radar Facies Interpretation

Radar Facies 2: Glaciomarine Silty Clay

Below the strong subhorizontal reflection and at the end of NV140, reflection-free zones are considered to be glaciomarine silty clay (Facies 2). This is supported by the fact that at the end of the line, silty clay was visible at the surface. The contact between 3a and 2 is gradational between 50 and 60 m, while at NV139 and the start of NV140, the basal contact appears to be sharp.

Radar Facies 3a: Braid Delta Foreset Beds

The sloping surface of Figure 6.33 is interpreted as a delta front. Dipping foreset beds (Facies 3a) are interpreted from the oblique clinoforms of both profiles. The 35° dip in NV140 is the maximum dip for a gravelly delta (cf. Nemec, 1990), which indicates that this line is probably the true dip direction (southwest). The offlapping clinoforms seem to show the progradation of a delta graded to 185 m, the elevation of the Nass Braidplain North just above the radar line locations. This is the first indication of a marine limit at 185 m.

Fine-grained sediments at depth may be indicated by the continuation of the high amplitude reflection into dipping beds of NV140. However, the downlapping aspect of toesets cannot be seen, so these are considered to belong to Facies 3a instead. Topset beds are not evident on NV139-140, nor are any channels, but this is due to their delta front location.

Radar Facies 3e: Slump Deposits

Disrupted reflections from 35-55 m on NV140 may indicate some prodeltaic failure, and are interpreted as the slump facies, Facies 3e.

## Radar Facies Summary

The surficial geology and geomorphology of the GPR sites were previously mapped, but exposures are rare and the mapping of some areas was considered tentative. The GPR provides a 2D (and locally 3D) look at the subsurface in these areas.

The most commonly found facies are those interpreted to reflect glaciofluvial environments. These include Radar Facies 3a, 3b, 3c and 3d. Less common are facies interpreted to represent bedrock, glaciomarine and alluvial fan environments (Radar Facies 1, 2, 4a, 4b, respectively).

The following is the environmental interpretation of the radar facies listed at the beginning of the chapter and shown in Figure 7.3:

*Interpreted Radar Facies*

1) Bedrock
2) Glaciomarine Silty Clay
3) Glaciofluvial Braidplain/Braid Delta
    - 3a) Braid Delta Foreset Beds
    - 3b) Braid Delta Topset Beds
    - 3c) Braidplain Horizontally Bedded Deposits
    - 3d) Braidplain Channel Deposits
    - 3e) Slump Deposits
4) Alluvial Fan
    - 4a) alluvial fan horizontally bedded deposits
    - 4b) alluvial fan channel deposits

The GPR signal was reasonable in all environments, with the exception of glaciomarine silty clay. Attenuation of electrical energy by clay particles caused a reflection-free signal in this type of

sediment. GPR is very useful, however, for determining small scale structures in braidplain, braid delta and alluvial fan environments.

Steeply dipping oblique and oblique tangential clinoforms were found to represent foreset beds. These are overlain by horizontal reflections interpreted as topset beds. Distributary channels within the topset beds are identified by lens-shaped reflections in several places. Locally, convex reflections are present. These are interpreted as prodelta slump deposits.

Horizontal, discontinuous wavy reflections with numerous boulder diffractions are interpreted as braidplain fluvial deposits. Lens geometries within this facies are inferred to be channels.

Alluvial fan deposits are similar to braidplain sediments in the profiles, except that some lenses have steeply dipping clinoforms at their edges. These are interpreted as debris flow levees.

Finally, a radar facies of overlapping hyperbolae is inferred to reflect bedrock. Bedrock underlies glaciofluvial deposits in all of the profiles where it was observed. Till was not definitively identified by GPR.

In the GPR study, braid delta environments were identified with radar data. A number of areas mapped as braidplain are therefore re-interpreted as deltaic (Figure 7.33), namely the Aiyansh Braidplain and Nass Braidplain North terminal zones. GPR has proven an effective tool for clarifying depositional environments in areas of restricted section exposure. The new delta locations have been incorporated into the Nass Valley map.

## Glacial History Summary

The 152 m (or approximately 150 m) position of sea level was an important sea level stand. If the 152 m contour is placed on the map of the upper Nass Valley (Figure 7.34) some interesting insights are obtained. The following numbered paragraphs describe the numbered features on Figure 7.34.

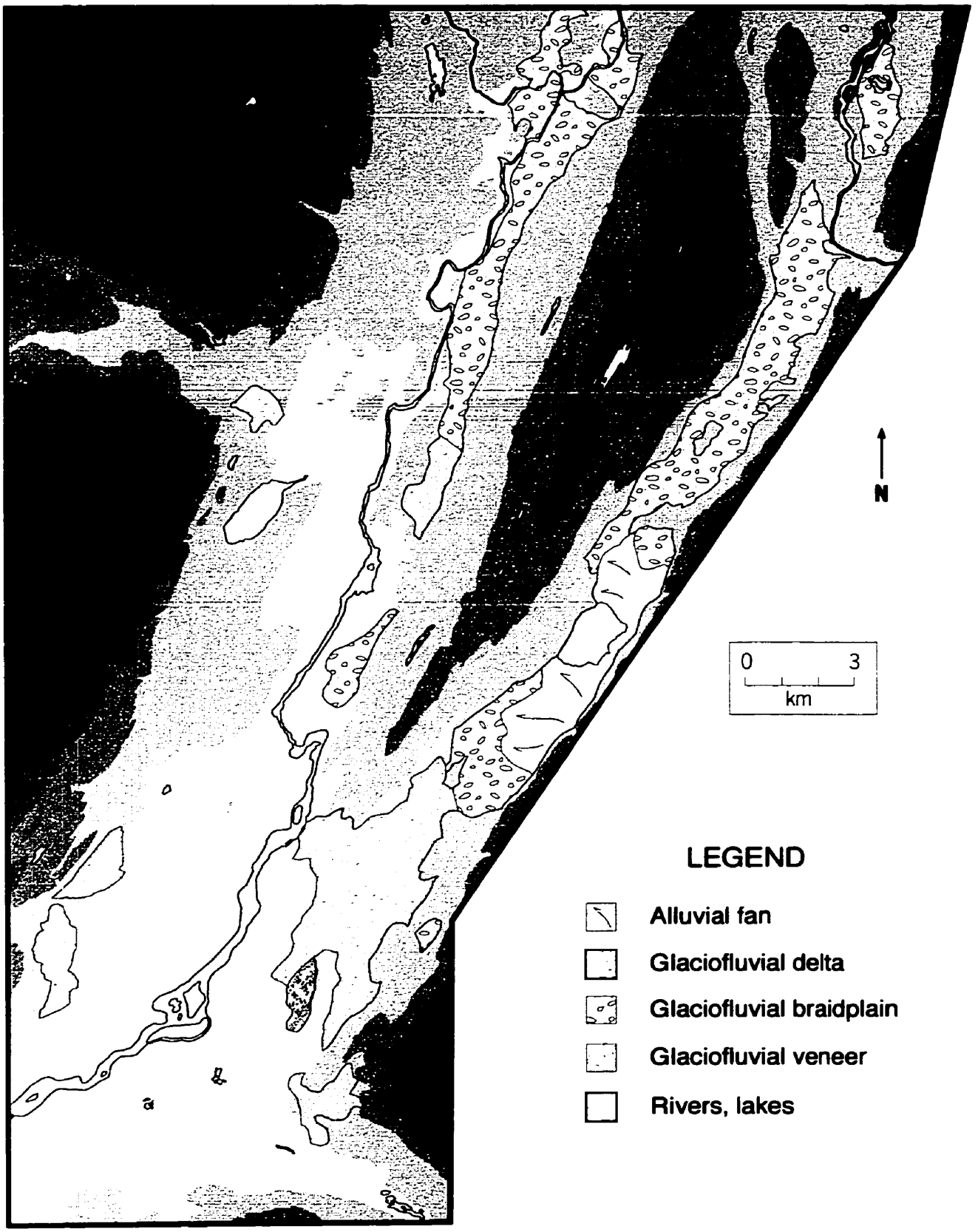


Figure 7.33. The location of deltas as re-interpreted from GPR data.

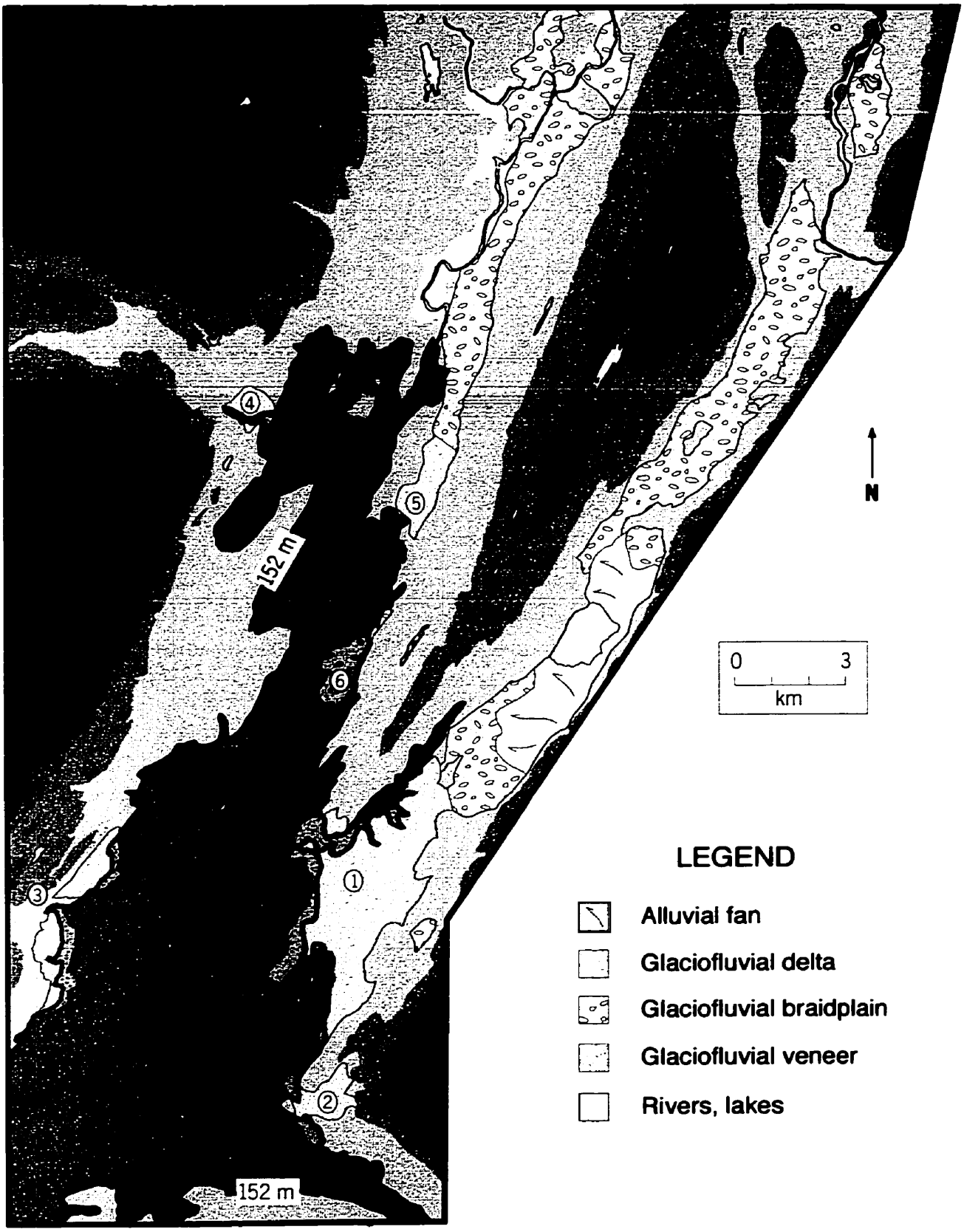


Figure 7.34. Location of 152 m contour with respect to glaciofluvial deposits. Note the location of deltaic deposits with respect to marine limit. Numbered areas are discussed in the text.

1) The 152 m contour is an almost perfect match defining the edge of the Aiyansh Braid Delta. The contour is inferred to show the approximate location of marine water when the delta formed. Therefore, the delta as it exists today has not been modified at all since deposition. This is consistent with the west to northwest radiating paleoflow into a marine embayment inferred for radar profiles NV113- NV118.
2) The small delta at the town of New Aiyansh is a separate entity, unrelated to the Aiyansh Braidplain/delta. This fact, coupled with its northwestern paleoflow direction, shows that this delta was formed by a meltwater river flowing from the Tseax Valley into the Nass Valley.
3) A delta from a river flowing out of Shumal Valley also formed when sea level was at 152 m. The 152 m shoreline is again an excellent match for the edge of the delta.
4) This feature's genesis was determined indirectly by GPR. It is a glaciofluvial feature at the mouth of Kwinatahl Valley that had been mapped as a possible braidplain. Re-evaluation suggests, however, that it too is a delta that formed at this sea level stand, although the match with the shoreline is not as good as elsewhere. This feature has since been incised by Kwinatahl River, which has cut terraces into it.
5) The delta of the Nass Braidplain North lies above the 152 m limit, at 185 m, therefore, it formed prior to features 1 to 4.
6) The Nass Braidplain South lies below the 152 m limit, at 135 m. It is therefore regarded as a separate braidplain from a lower sea level stand. Deltaic sediments that may have existed at its terminus may have been eroded away by the modern Nass River.

From this set of sedimentological and geomorphic features, a late deglacial history of the valley can be reconstructed. The proto-Nass meltwater river initially flowed down the west side of the medial bedrock ridge, when sea level was 185 m. The river incised glaciomarine deposits and formed a braidplain/braid delta system. The braidplain deposits formed at this time are in excess of 40 m thick in places. Glaciofluvial deposits at 183 m asl at the top of the Shumal Creek Section, Figure 5.3, may also be related to this sea level stand.

Sea level subsequently fell to 150 m. The river switched to the other side of the bedrock ridge and formed the large Aiyansh Braidplain/Braid Delta. Its deposits are at least 28 m thick. Numerous other braidplains and deltas also formed at this time, both in the Nass fiord and in other fiords (Anyox and Donahue Creek deltas, Sutton and Kshwan Valley braidplains). This highstand must therefore have been relatively long-lived. A slight readvance of a nearby ice margin may have been responsible for the change of river location. The lack of moraines indicating a stillstand lends some doubt to this supposition. However, the relatively long-lived sea level stand may have been caused by a regional ice readvance that is simply not recorded in the Nass Valley (or elsewhere). Another possible explanation for the switch is that the thick deposits of the Nass Braidplain North blocked the river's flow path as sea level dropped. The lowest, easiest water flow path may have been down the Aiyansh side of the ridge.

Sea level later dropped to 135 m, and a small braidplain, and probably its delta, formed just southwest of the Nass Braidplain North. The river had switched back to its original position, possibly because of thick fluvial deposits (or ice) that blocked its lowered flow path on the other side of the ridge. By this time, ice may have receded a considerable distance from the area. The Tseax meltwater river incised its own delta, eroded down to bedrock, and formed new deltaic deposits at the 135 m sea level. The thickest deposits formed at this time were approximately 10 m thick.

The river remained on this side of the ridge and evolved into the modern Nass River, which incises two of its own former deposits, the Nass Braidplain North and South. The Aiyansh Braidplain has remained largely unmodified since its formation.

# CHAPTER EIGHT
# ICE FLOW AND SEA LEVEL HISTORY

## Ice Flow History

Two distinct ice flow histories were identified from field evidence: early regional southwestward flow and later flow directed along major valleys and fiords (Figure 8.1).

Approximately 90% of the ice flow indicators used to make these determinations were striations. Striations were found to be best preserved on Bowser Lake Group rocks whose bedding planes had low dip angles. Granitic rocks are more likely to host grooves (large striations) and, less commonly, chattermarks. Gabbro and basalt dykes within otherwise granitic regions are also good host rocks for striations. Chattermarks are most common in the Hastings Arm/Observatory Inlet area, at sites near sea level and at sites on rounded mountain peaks.

### *Early Ice Flow*

Striations, grooves, chattermarks and roches moutonnées measured at numerous sites in the study area show a consistent trend of 210° to 230° regardless of topography for the early phase of flow. These early ice flow indicators can be well preserved at high elevations (Figure 8.2), although frost shattering and extensive felsenmeer development commonly remove them. There are a total of 28 high elevation early ice flow sites shown on the two maps (recall that ten striae were measured at each site). Early flow indicators are present at lower elevations as striations or grooves in bedrock facets that were not eroded by subsequent ice flow. Less commonly, early southwesterly flow is indicated at low elevations by crosscutting relationships between striations and/or grooves, where the early direction is always toward the southwest. In this case, the larger grooves are crosscut by younger, finer striations. An example can be seen in the White River area of the Kitsault Valley map. Early ice flow striae are also preserved on Larcom Island, Hastings Arm (Nass Valley map). This suggests that regional ice flowed *across* valleys and lowlands in many areas at the glacial maximum.

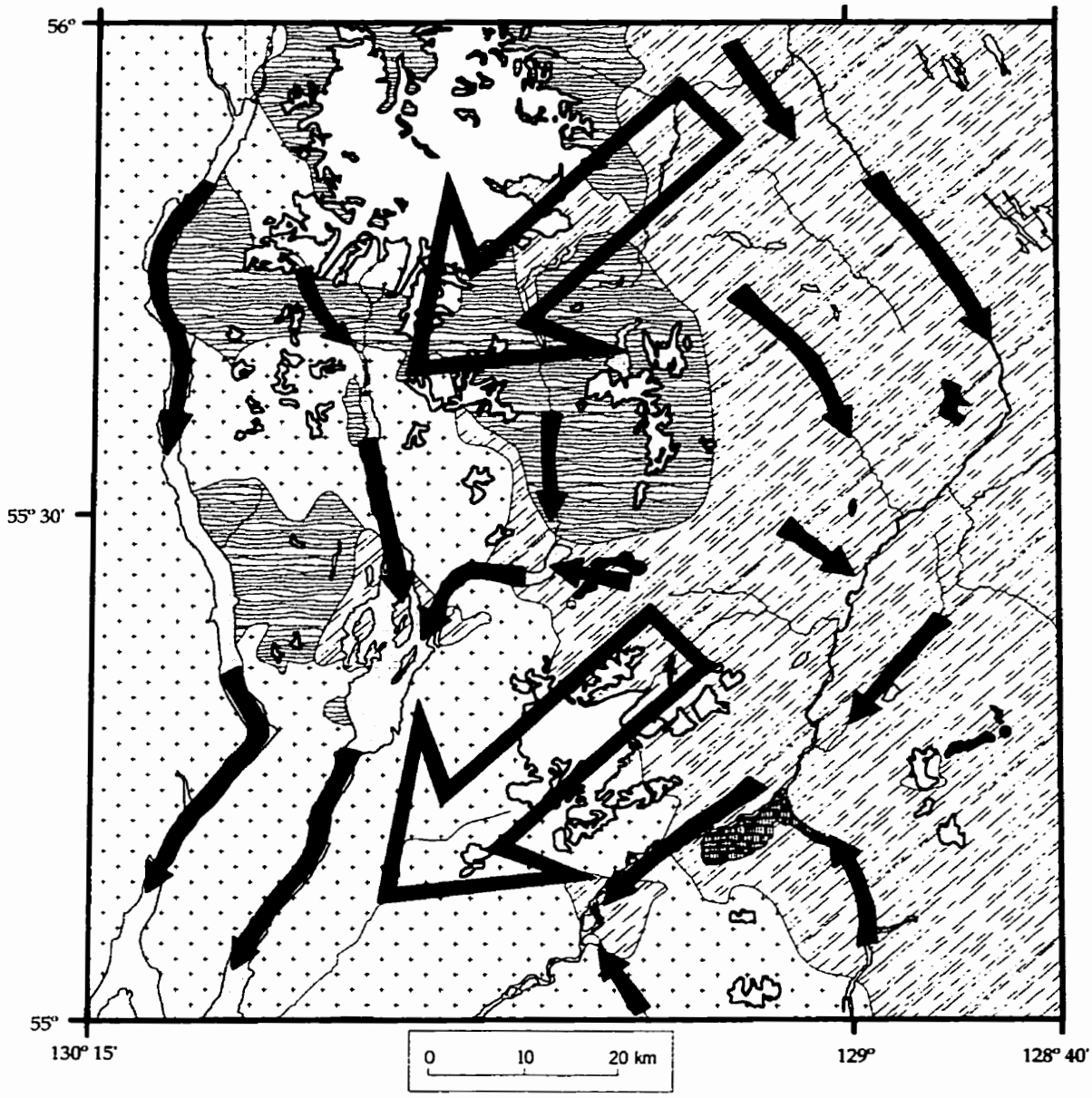


Figure 8.1. Ice flow directions superimposed on bedrock geology. Large open arrows indicate the early phase of ice flow, while smaller arrows show late phase flow directed down valleys and fjords.

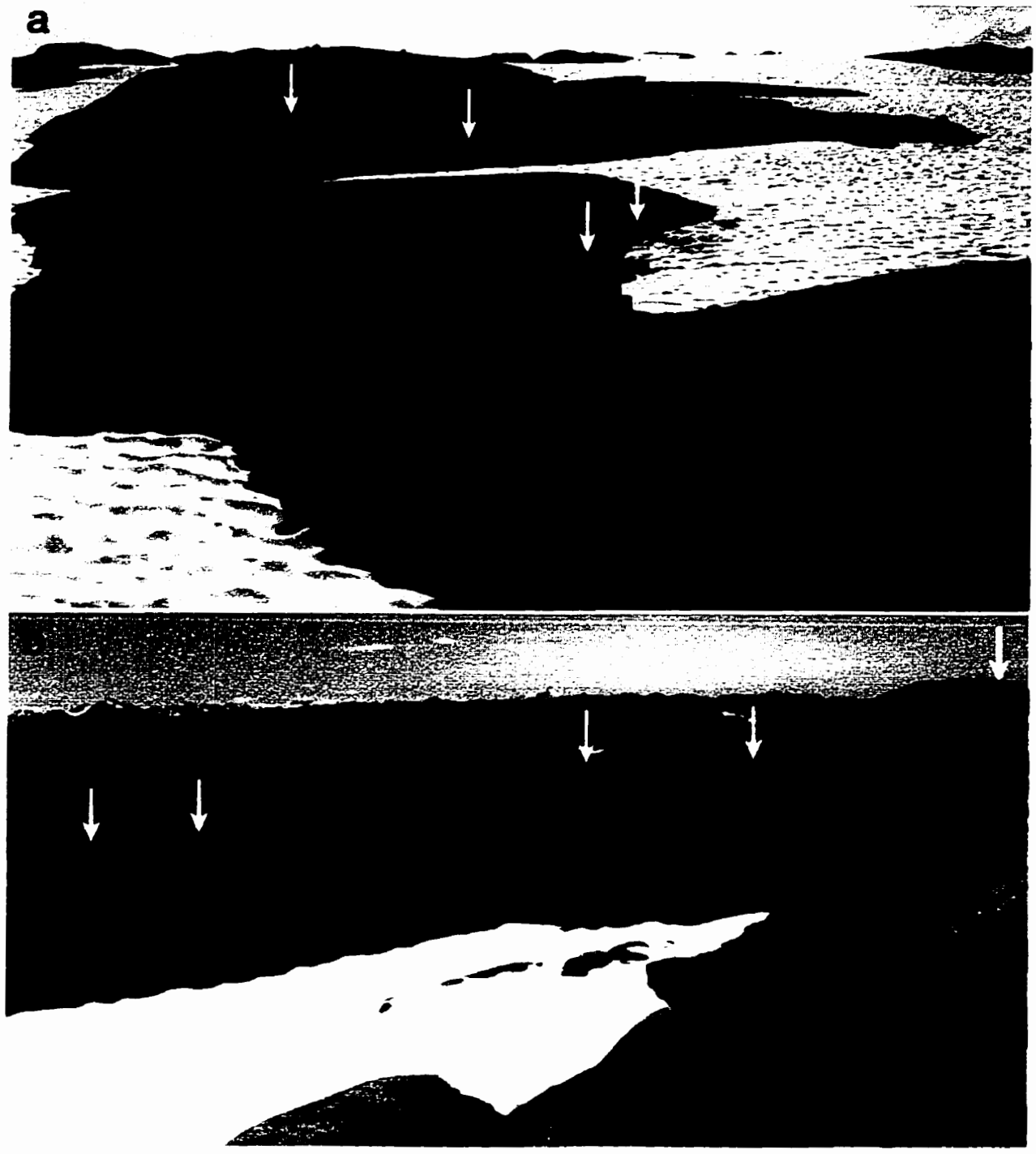


Figure 8.2. High elevation early ice flow indicators. a) Crescentic fractures and grooves, Campbell Ridge, looking south (1405 m asl). Flow was from left to right (231°) and bedrock lee sides are plucked (arrowed). A 60 cm high backpack is present for scale. b) Roches moutonnées on mountain ridge west of Kincolith Valley, near mouth of Nass River, looking south toward Kitimat Ranges (1200 m asl). Flow was from lower left to upper right. Note plucked lee sides (arrowed). Grooves with identical stoss and lee relationships cover the surfaces of the features.

There is no definitive evidence that nunataks were present during the early flow event, as there are no visible moraine ridges circling any of the mountain peaks. However, since lower ridges are rounded and higher ones are sharp, nunataks were probably present.

*Late Ice Flow*

Late ice flow was controlled by topography and ice was limited to fiords and valleys. Late ice flow generally erased evidence of the earlier flow direction. Late ice flow indicators are common at low elevations and on valley walls.

*Streamlined Bedrock Features*

Valley sides exhibit streamlined bedrock ridges that have variously been called rock drumlins and whalebacks. Unfortunately, it is only possible to view them in clear cut areas. Many ridges are steep sided, and have either steeper stoss ends or a humped appearance, where the highest point is the centre of the ridge. Their irregular crests are often jagged compared to the smoother shapes characteristic of drumlins in the area, and are generally subparallel to each other and to the valley axis (Figure 8.3). They are generally elongate features oriented somewhat parallel to late ice flow, so they are considered 'streamlined' despite their lack of smooth upper surfaces. Their orientations are strongly influenced by bedrock structure. For these reasons, they are considered to be ice formed. Only ice flow would allow bedrock structure to exert so much control over orientation, and the features are not smoothly curving in the way that fluvially scoured ridges typically are. Additionally, in many areas, grooves and striae are exactly parallel to the streamlined bedrock, which is overlain by till. However, at sites east of the Nass River and southwest of the lava flow, these ridges are covered in glaciofluvial veneer. In this location water flow may have contributed to their formation, however, their extremely rough surfaces suggest that they too were formed predominantly by ice (Figure 8.3c). The ridges, in general, are roughly parallel to the valleys in which they are found, suggesting that they are probably late phase ice flow features. However, they are not used as directional indicators for ice flow.

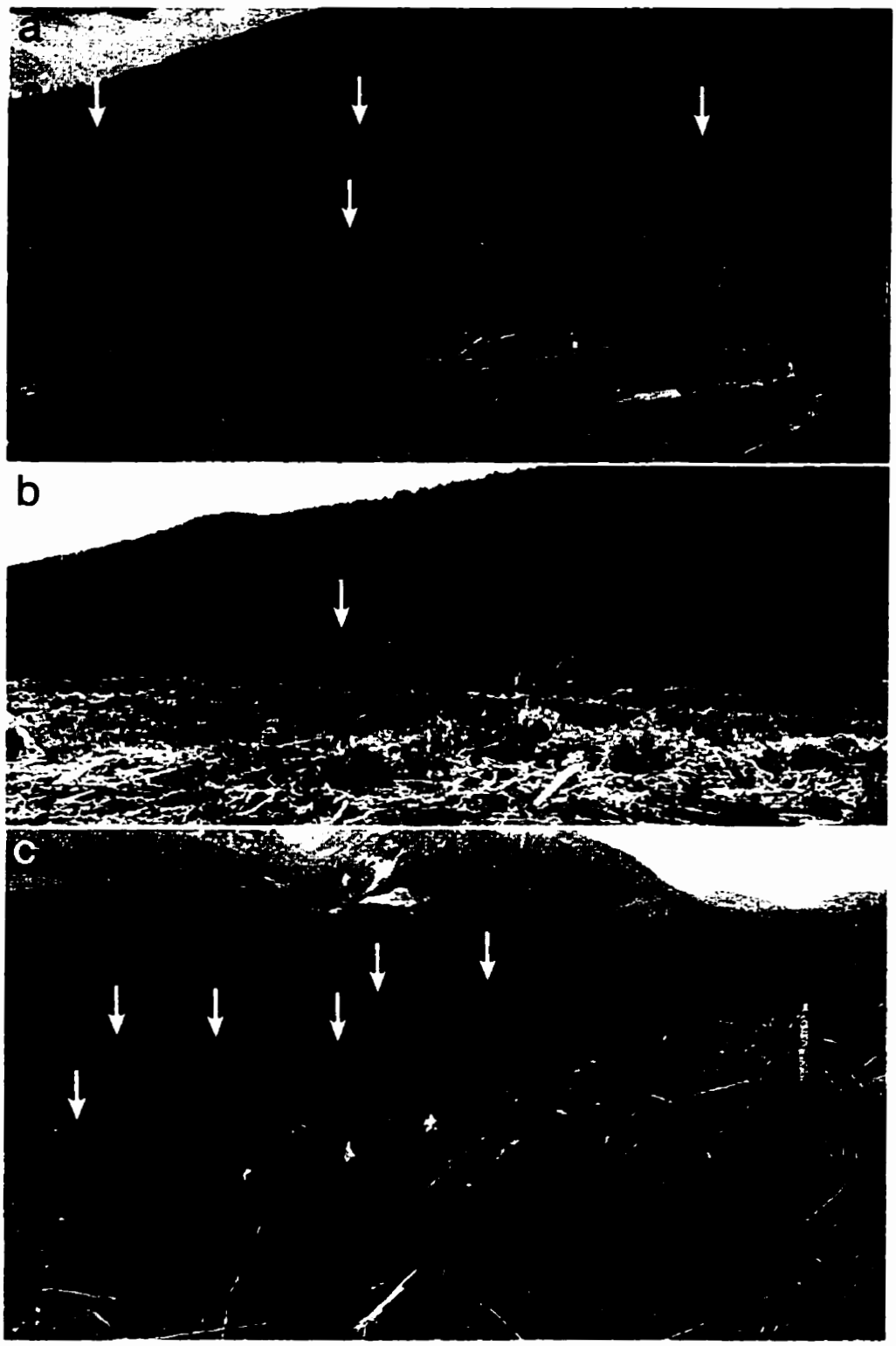


Figure 8.3. Streamlined bedrock ridges. a,b) Streamlined ridges, flow to left. Note angularity of crests (arrowed). c) Angular crested ridges in the Nass Valley that are veneered with glaciofluvial deposits; flow to lower left. Angular crests are arrowed.

Roches moutonnées are rare, and occur mainly at high elevations. They have plucked lee sides and their surfaces commonly also have grooves, chattermarks and striae parallel to the roches moutonnées themselves. At one site, 1220 m above the mouth of the Nass River, the surface of a group of roches moutonnées is grooved and chattermarked (Figure 8.2b). Grooves at this site have micro-scale stoss and lee relationships in the same orientation as the roches moutonnées (early ice flow direction). On a peak south of the southwest end of the Aiyansh Lava Flow, grooves are parallel to the roches moutonnées (also early flow direction) at 1710 m asl (Nass Valley map). Low elevation roches moutonnées showing late flow directions are rare.

*Very Early Ice Flow*

It is possible that an alpine glacial advance preceded the full glacial phase, as this occurred in the Stikine area (Ryder and Maynard, 1991). Most of the evidence of pre-climax flow from local ice centres such as the Cambria Ice Field appears to have been completely obliterated by erosion during the regional ice advance. At one site on Campbell Ridge, however, a cirque shows evidence of the regional southwesterly flow (see Nass Valley map, ridge east of Hastings Arm). Sculpted bedrock with good stoss and lee relationships indicates ice flow upward along the cirque wall (Figure 8.4). Therefore, the cirque formed prior to the early ice flow event.

*Summary*

In conclusion, ice flow during the climax of the last glaciation was dominated by regional southwesterly flow, presumably from the Cordilleran Ice Sheet. This is the same regional flow direction as in areas to the north (Kerr, 1934, Ryder and Maynard, 1991) and east (Levson *et al.*, 1997). The Skeena Mountains therefore may have been the major ice source area at the glacial maximum. The Skeena and Hazelton Mountains are also considered to be a source area for southeast flowing ice in the Nechako Plateau (Plouffe, 1997). Ice must have been quite thick for it to have flowed independently of topography. In fact, the highest elevation at which southwest ice flow indicators were found is 1840 m, from striation measurements on a mountain southwest of Kinskuch Lake and east of Kitsault River (see Kitsault Valley map for location). A Bowser Lake

Figure 8.4. Stoss and lee relationships showing ice flow up the wall of a cirque on Campbell Ridge. Flow direction is shown with an arrow. Although the bedrock is jointed, smoothed stoss surfaces (s) with plucked lee sides (l) show the ice flow direction.

Group erratic was observed resting on Tertiary granitic rock west of Kshwan River at 1590 m asl by Carol Evenchick of the Geological Survey of Canada (pers. comm., 1998). Clearly, ice was able to move debris at these high elevations. The highest elevation striations that record late flow were found on a peak just northeast of Ksedin Creek at 1450 m (Nass Valley map).

Since there is some minor evidence of very early alpine glaciation, an intense alpine phase likely preceded the continental ice sheet phase of the Cordilleran Ice Sheet (Kerr, 1936, Davis and Mathews, 1944) which was dominated by southwesterly flow in this region. Any evidence of an intervening mountain ice sheet phase where piedmont and thick valley glaciers formed between nunataks (Davis and Mathews, 1944), has probably been removed by subsequent glacial erosion. At the glacial maximum, the ice sheet likely far exceeded 1840 m in thickness (1840 m being the highest early flow striation elevation). Since ice thickness greatly exceeded relief, and flow was controlled by an ice divide in the Skeena Mountain area (as opposed to being controlled by topography), the continental ice sheet phase of Kerr (1936) and Davis and Mathews (1944) was reached.

Ice retreat following the reverse order of the above (Davis and Mathews (1944) model for deglaciation) is represented in its entirety within the study area. Continental ice was reduced to the mountain ice sheet phase, which was topographically controlled. Continued melting shifted it to the intense alpine phase of valley glaciation with ice sources in local mountains. Finally, the alpine phase, a nonglacial period with only alpine glaciation, was reached in the Holocene and persists today. There is no evidence for regional ice stagnation.

Although the thesis data fits nicely with the Davis and Mathews model, it contradicts other studies that suggest that the Late Wisconsinan event (Fraser Glaciation) reached only the mountain ice sheet phase (Clague, 1981; Fulton, 1991; Ryder *et al.*, 1991). It may be that more extensive ice cover was present in northern B.C. due to its latitude and/or the presence of central mountain ranges. If that is the case, then the continental phase of glaciation may have been reached in all of northern B.C. However, the near coastal location of the study area may mean that a moist climate contributed to the thickness of the ice sheet. In that case, the continental phase may have been reached only in northern areas of B.C. along the Coast Mountains.

Late Wisconsinan (?) ice flow in the region reflects an early southwest flow event followed by flow along valleys and fiords. Since early ice flow directions were southwest across the entire region at the climax of Wisconsinan (Fraser) Glaciation, it appears that Figure 2.2 (Ryder and Maynard, 1991) is not entirely correct. The ice flow directions shown are actually those of the late ice flow phase, not the glacial maximum phase. Kerr (1934) also detected southwest flow across the Coast Mountains. It is suggested that this flow direction may have occurred at the Fraser Glacial maximum, and that the ice flow directions shown in Figure 2.2 for the Iskut, Stikine and Taku River regions are in fact those of the deglacial phase of the last glaciation.

This re-examination of ice flow directions implies that there was indeed an ice divide in the Skeena Mountain/Williston Lake area at the glacial maximum, and it may have extended southeastward (Figure 8.5). To confirm this hypothesis, future research should include more detailed ice flow studies at high altitudes in northern B.C., focussing mainly on the Coast Mountains (for example, the study by Clague, 1984b, in the Terrace region, did not record high elevation information). A recent study including high elevation sites southeast of the study area shows southwestward and westward ice flow from a major divide during the last glacial maximum, (Stumpf *et al.*, in press). This information has been incorporated into Figure 8.5, and it supports the inference that ice flowed coastward from a major interior ice divide.

The fiords of the Nass River area were likely carved into a preglacial fluvial landscape (Roberts and Rood, 1984) that was controlled by bedrock structure. The great length, width and depth of the fiords, particularly the Nass Valley, were further excavated by glacial ice. The Nass Valley was large enough to drain a significant portion of the Cordilleran Ice Sheet, even at the height of glaciation. The Nass glacier may have behaved as an ice stream during deglaciation, given the size and morphology of the fiord and its highly abraded, till covered floor. However, the valley's great size may simply be due to repeated abrasion in the same ice flow direction for the entire duration of one or more glaciations.

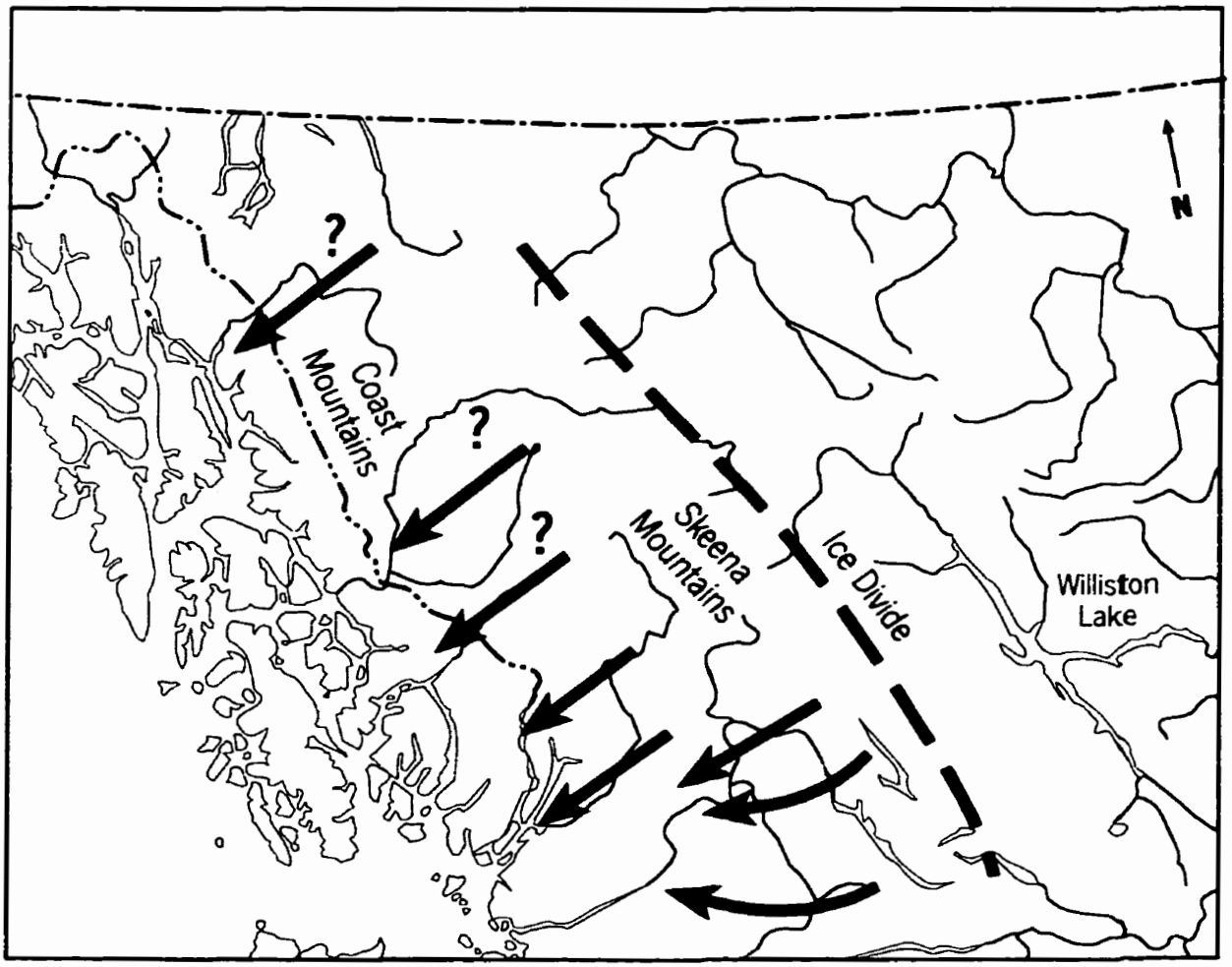


Figure 8.5. Revised ice flow directions for the glacial maximum in northwestern B.C., after Stumpf *et al.* (in press) and this thesis. Ice flowed to the southwest and west across the Coast Mountains from the Skeena Mountian area, without any topographic control. An ice divide must have been located in the Skeena Mountain/Williston Lake area. One possible position for this divide is shown. Ice flow directed down valleys, as in Figure 2.2, is omitted as it is considered to represent ice flow during deglaciation only. Possible southwestward flow to the north of the study area is postulated, based on Kerr's (1934) identification of southwesterly flow in the Taku, Iskut and Stikine regions.

## Till Fabric Analysis

Till fabrics are used to detect ice flow directions. When extension occurs during flow, clast a-axes are aligned parallel to ice flow, with a-b planes dipping shallowly (Boulton, 1971). In areas of compressive flow, clast a-b planes dip steeply up ice, while a-axes are transverse to flow directions (Boulton, 1971). Thus, a-axes both parallel and transverse to flow are expected. A-axes can also be parallel to ice movement along a zone of shear. However, variability is known to occur, even within-site, so some caution must be exercised in the interpretation of till fabrics.

A total of 24 till fabric analyses were carried out in various locations. The fabric data are summarized in Table 8.1. Sample numbers indicate Kwinatahl till with "kw" and Kinskuch till with "kk".

Fabrics were analyzed for statistical significance using the computer program Spheri-Stat. Data are represented on Schmidt equal area stereonets, using the eigenvalue method (Mark, 1973) to examine data mathematically. Eigenvector 1 (the principal eigenvector) marks the direction of maximum clustering. Eigenvector 3 points in the direction of minimum clustering and S2 is the intermediate eigenvector. The eigenvalues listed show the degree of clustering around each eigenvector, such that $S1 \geq S2 \geq S3$. In a spherically uniform sample, $S1=S2=S3=0.33$. If $S1>S2\equiv3$, there is a cluster, while $S1\equiv S2>3$ means a girdle (Woodcock and Naylor, 1983). In all samples except A4 and C3, the first (cluster) relationship is true (Table 8.1). The S1/S2 value graph (Woodcock and Naylor, 1983) was used to get the statistical significance or randomness of each sample at various confidence levels (Figure 8.6). All samples except A4 were found to be significant at >99% confidence levels (Table 8.1).

*White River area*

In the White River area, drumlins trend 150° to 165°, and five striation measurements from the area trend 158°, 158°, 160°, 171° and 212° (Figure 8.7). The 212° striation, found at the same site as a 158° striation, is likely an early flow indicator. The striations are interpreted to show

| SAMPLE | S1 | S2 | S3 | S1/S3 | CONFIDENCE LEVEL | S1 TREND | S1 PLUNGE |
|---|---|---|---|---|---|---|---|
| 967083kw | 0.66 | 0.20 | 0.14 | 4.71 | >99% | 146 | 13 |
| 968149kw | 0.67 | 0.20 | 0.13 | 5.15 | >99% | 335 (155) | 5 |
| 975214kw | 0.73 | 0.20 | 0.06 | 12.17 | >99% | 290 (110) | 23 |
| 985271kk | 0.56 | 0.31 | 0.14 | 4.00 | >99% | 203 | 17 |
| 985271kw | 0.57 | 0.37 | 0.06 | 9.50 | >99% | 205 | 2 |
| A1kk | 0.65 | 0.24 | 0.11 | 5.91 | >99% | 331 (151) | 26 |
| A2kw | 0.57 | 0.30 | 0.13 | 4.38 | >99% | 348 (168) | 23 |
| A3kk | 0.60 | 0.33 | 0.07 | 8.57 | >99% | 355 (175) | 27 |
| A4kk | 0.42 | 0.39 | 0.19 | 2.21 | >97.5% | 56 | 17 |
| B1kk | 0.58 | 0.31 | 0.11 | 5.27 | >99% | 199 | 8 |
| C1kk | 0.53 | 0.34 | 0.12 | 4.42 | >99% | 159 | 1 |
| C2kk | 0.59 | 0.26 | 0.15 | 3.93 | >99% | 0 (180) | 17 |
| C3kk | 0.45 | 0.42 | 0.13 | 3.46 | >99% | 342 (162) | 22 |
| D1kw | 0.54 | 0.31 | 0.15 | 3.60 | >99% | 219 | 7 |
| D2kw | 0.56 | 0.30 | 0.14 | 4.00 | >99% | 11 (191) | 10 |
| E1kk | 0.49 | 0.37 | 0.14 | 3.50 | >99% | 231 | 1 |
| F1kw | 0.61 | 0.28 | 0.11 | 5.54 | >99% | 112 | 21 |
| G1kw | 0.57 | 0.27 | 0.15 | 3.80 | >99% | 73 (253) | 5 |
| G2kk | 0.53 | 0.35 | 0.11 | 4.82 | >99% | 283 (103) | 5 |
| H1kw | 0.49 | 0.36 | 0.16 | 3.06 | >99% | 43 (223) | 4 |
| JJS12 | 0.52 | 0.36 | 0.12 | 4.33 | >99% | 99 | 3 |
| JJS12B | 0.65 | 0.23 | 0.12 | 5.42 | >99% | 213 | 3 |
| KITEENkk/kw | 0.61 | 0.25 | 0.14 | 4.35 | >99% | 149 | 13 |
| TSEAXkk | 0.59 | 0.27 | 0.14 | 4.21 | >99% | 254 | 11 |

Table 8.1. Till fabric data. Kwinatahl tills are indicated with 'kw', Kinskuch tills with 'kk'. Drumlins are lettered. Bracketed S1 trends are 180° from the S1 data, but are the actual flow directions based on all striation and fabric evidence.

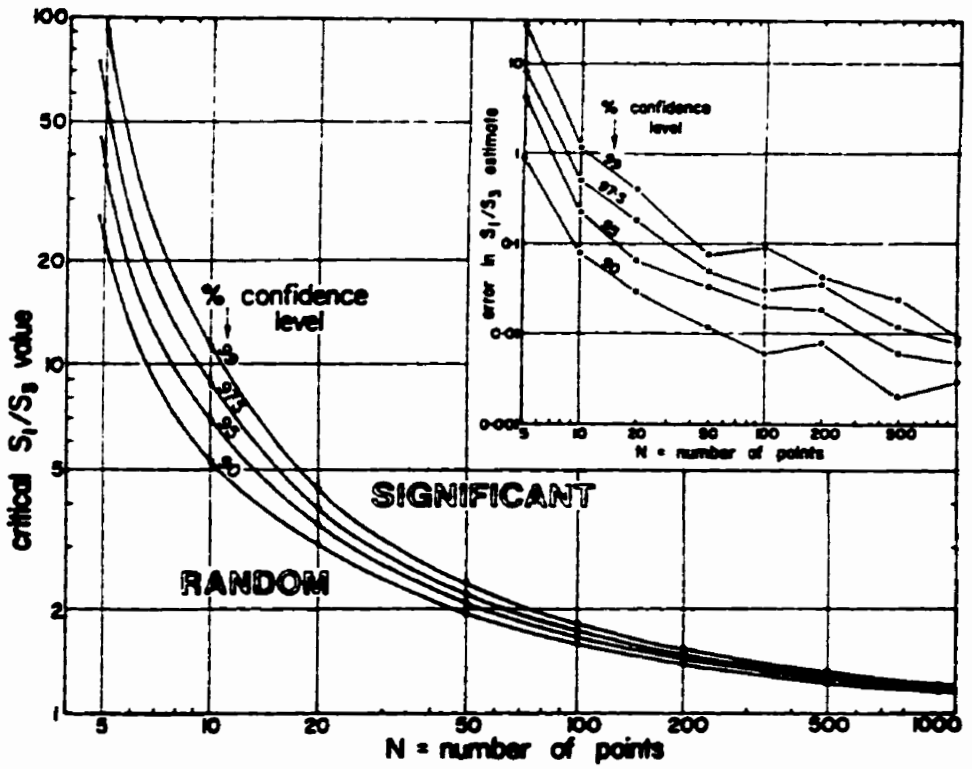


Figure 8.6. Confidence levels for S1/S3 values of till fabrics. All samples in this study had 50 point values measured (from Woodcock and Naylor, 1983).

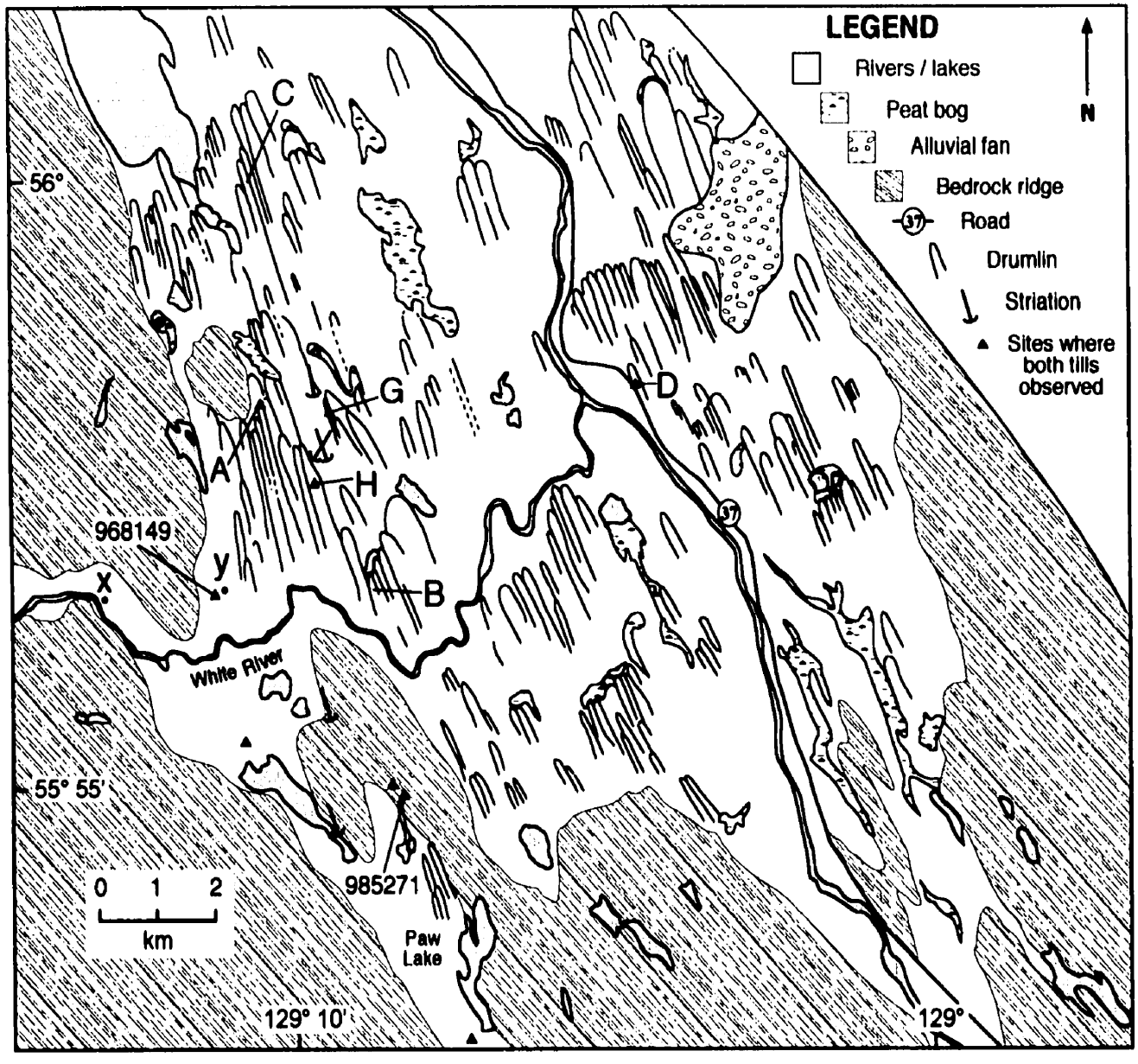


Figure 8.7. Location of drumlins in White River area, with respect to bedrock ridges, lakes, rivers and bogs. Sites x and y are discussed in the text.

southwest ice flow (212°) during the early phase of glaciation and south-southeast ice flow (about 160°) parallel to the valley during the late phase of glaciation (Figure 8.7).

Three till fabrics from two sections in this area are shown in Figure 8.8. None of these fabrics are from drumlins. Sections 968149 and 985271 exposed both Kinskuch and Kwinatahl tills, however, Kinskuch till at the former section was too thin and too weathered to permit a fabric measurement. Both of these till fabric sites are shown on Figure 8.7.

Only one of the fabrics (968149kw) shows the Nass Depression parallel trend of 155° and it is from Kwinatahl till. The strong fabric (S1 = 0.67, Table 9.1) and the S1 trend of 335° (up-ice clast dip) reflect lodgement by southeast flowing ice. The slight spread of the fabric suggests that lodgement was followed by deformation. This is another site where there is evidence of continued Kwinatahl deposition after ice flow changed to a late phase ice flow direction.

The other two fabrics from this area are weaker, with S1 values of 0.56 and 0.57 (Table 8.1). Fabrics 985271kw and 985271kk trend southwest. The physical characteristics of the tills indicate deposition by lodgement (see Chapter 4), but the poor fabrics seem to indicate that deformation or flow has occurred. These fabrics come from a thick till pocket on a bedrock ridge, within a till veneer area. It is possible that local ice flow deflections or shear zones could have occurred here. Alternatively, both may have been reworked by downhill flow, as topography dips southwest at this location. It is unlikely that 98527kk is a lodgement or melt-out till showing a southwest ice flow direction because the fabric is poor and the till contains volcanic clasts from a northwestern source area.

*Kinskuch/Nass Valley area*

Four fabrics were measured in the Kinskuch/Nass Valley area (Figure 8.9) and their locations are shown in Figure 8.10.

Fabric 967083kw was measured because striation evidence was lacking in Kinskuch Valley. The sample is from the Tchitin River area and shows a Kwinatahl till with a fabric that is parallel to the valley. This Kwinatahl till, therefore, was also deposited during late phase ice flow, another indication that there was no hiatus between the deposition of the two tills. Ice changed directions

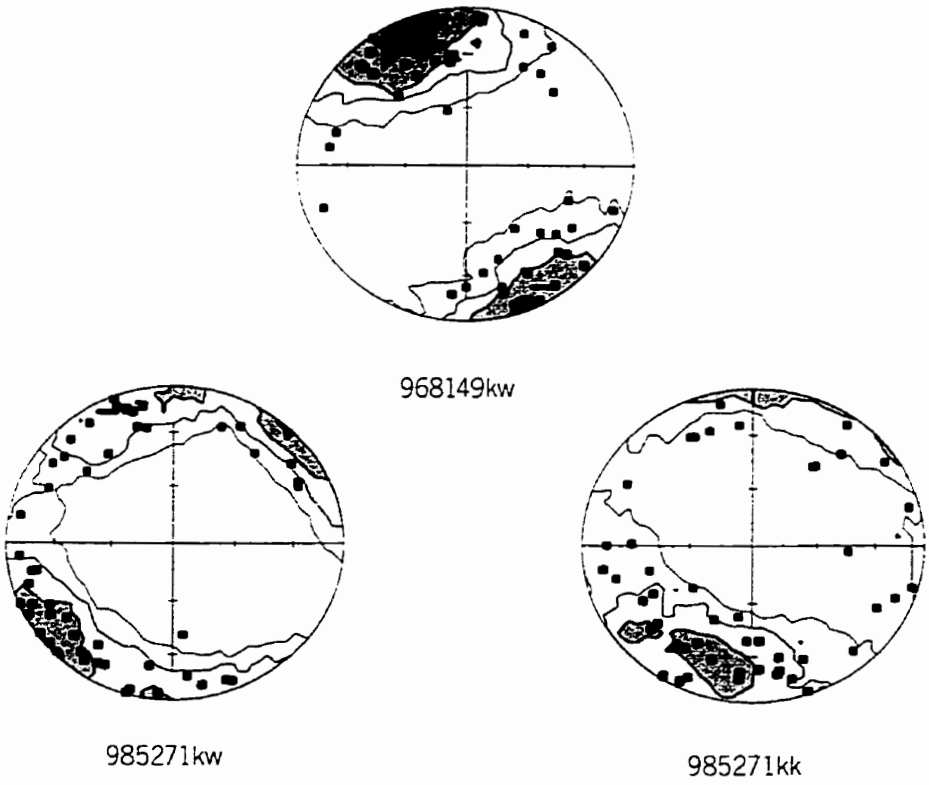


Figure 8.8. White River area till fabrics, non-drumlin areas. kk = Kinskuch till, kw = Kwinatahl till. Kinskuch till is present at site 968149, but was too thin and too weathered for a fabric measurement.

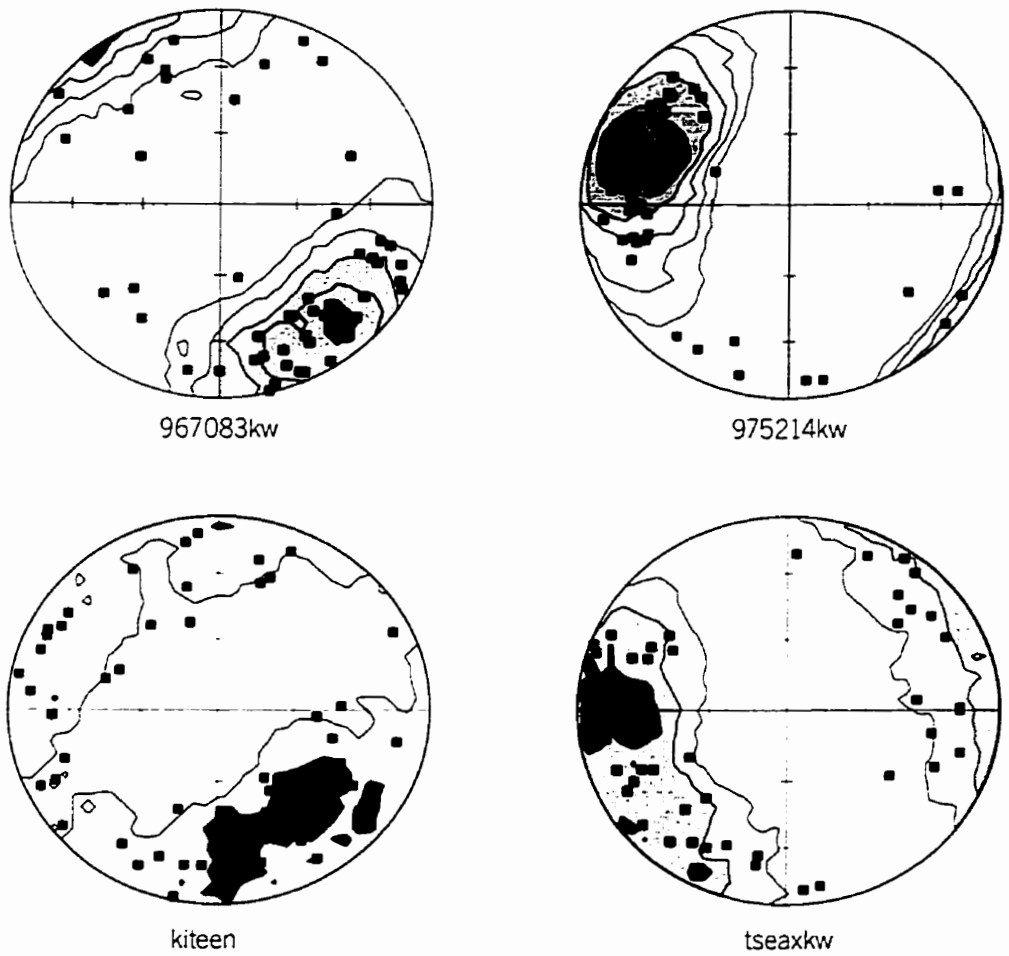


Figure 8.9. Till fabrics from various localities. See Figure 8.5 for locations.

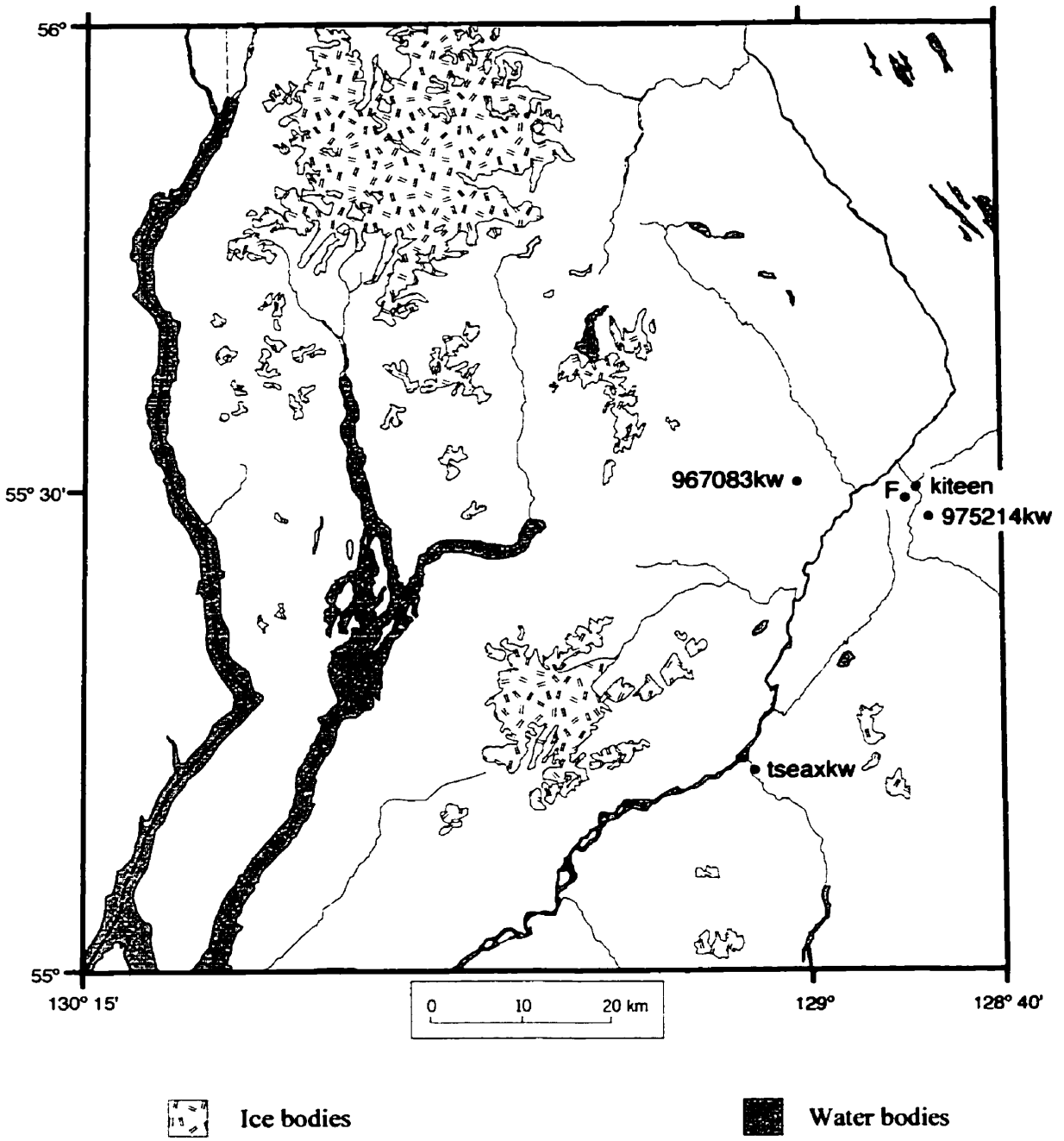


Figure 8.10. Locations of various till fabric sites and drumlin F.

and it took time for the till to reflect its new source area. Till at depth may show the southwest early ice flow direction, but exposures excavated by a backhoe would be required to confirm this. The strong but spread out fabric suggests that till at this location is a deformed lodgement till or a deformation till.

Fabric 975214kw is from a Kwinatahl till in the drumlinized area near Kiteen River in the Nass Valley and the fabric is perpendicular to the Nass Valley. It has the highest S1 value (0.73) (Table 8.1). This area is a narrow constriction where compressive flow would be expected, so this may actually be a transverse fabric indicating ice flow down the Nass Valley (to the southwest). The southeast fabric is unlikely to be due to southeastern ice flow from Kinskuch Valley, since ice would have to have first flowed northeast, then southeast to this location. The strong fabric rules out the possibility that the till flowed down the drumlin flank. However, its spread out nature suggests deformation of what may have been a lodgement till.

Kiteen is from the Kiteen River section (Figure 5.9). This till is considered to be older than both Kwinatahl and Kinskuch till. Its very poor fabric suggests that it is a flow till or a deformation till. Since the lower contact is draped, it must be a flow till. (It is not a debris flow deposit because clasts are heavily striated).

The fabric of Tseaxkw is more pronounced, but not exceptionally strong, and seems to show ice flow roughly to the southwest, parallel to the Nass Valley. This sample is from the Tseax River Section (Figure 5.17) and shows considerable spread, so it may be a deformation till.

In summary, Kwinatahl till was deposited by deformation or by lodgement followed by deformation mainly during early southwesterly flow, but also during late phase ice flow parallel to the Nass Depression and other valleys. It took some time for re-oriented ice flow to pick up clasts of new source areas and create Kinskuch till. The one Kinskuch till fabric is poor, and may show topographically controlled flow reworking.

*Drumlins*

Air Photo Interpretation

Drumlin fields occur in the Kinskuch and upper Nass Valleys and the Nass Depression. The drumlins are elongate and spindle shaped but with flat tails (Figures 8.7 and 8.11). They resemble drumlins in the Prince George region that Shaw (1994) terms 'hairpin erosional marks' or other drumlins termed Beverleys (Shaw, 1996). However, noticeable furrows wrapped around their stoss ends and sides are evident in only a few places. Very subdued lower elevation areas separate the drumlins (visible as straight lines on air photos). Unlike Beverleys and hairpin scours, lateral 'furrows' do not run into the stoss ends of down flow drumlins (*cf.*, Shaw, 1996). They do not cluster down flow of escarpments, but there is a poorly developed en echelon pattern in a few areas. The drumlins appear to be randomly distributed for the most part, but they only occur in areas of thick till between bedrock ridges (see Kitsault Valley map) and tend toward clustering (Figures 8.7 and 8.11). Lengths vary from 300 to 2000 m and heights range from 10 to 40 m. Some are irregularly shaped. There are no parabolic or transverse asymmetrical drumlins.

There is no overall pattern to the drumlins - no orderly grouping, no asymmetry, no regular change of shape from one area to another (when present, these are common features of subglacial fluvial erosional drumlins). The drumlin fields are not marked by signs of fluvial activity: there are no tunnel valleys, no eskers and very few other glaciofluvial sediments that are not parts of braidplains. "Comma form lakes" are not evident either, although a pseudo "comma form lake" is visible in the centre of Figure 8.11 and something that might be called a "comma form bog" is present in the lower central portion of Figure 8.7. There are also meltwater channel features adjacent to the drumlin fields (see both maps).

Bogs are common in drumlinized areas, as they are elsewhere. Bedrock surfaces, where exposed, are flat or sloping and heavily striated. Sichelwannen, muschelbruche, furrows and other fluvial scour indicators are not evident on bedrock surfaces between drumlins, but these bedrock exposures are relatively small.

Streamlined bedrock ridges do not possess the same morphology as drumlins. Their axial crests are sharp and irregular and stoss ends much steeper (as explained earlier in this chapter).

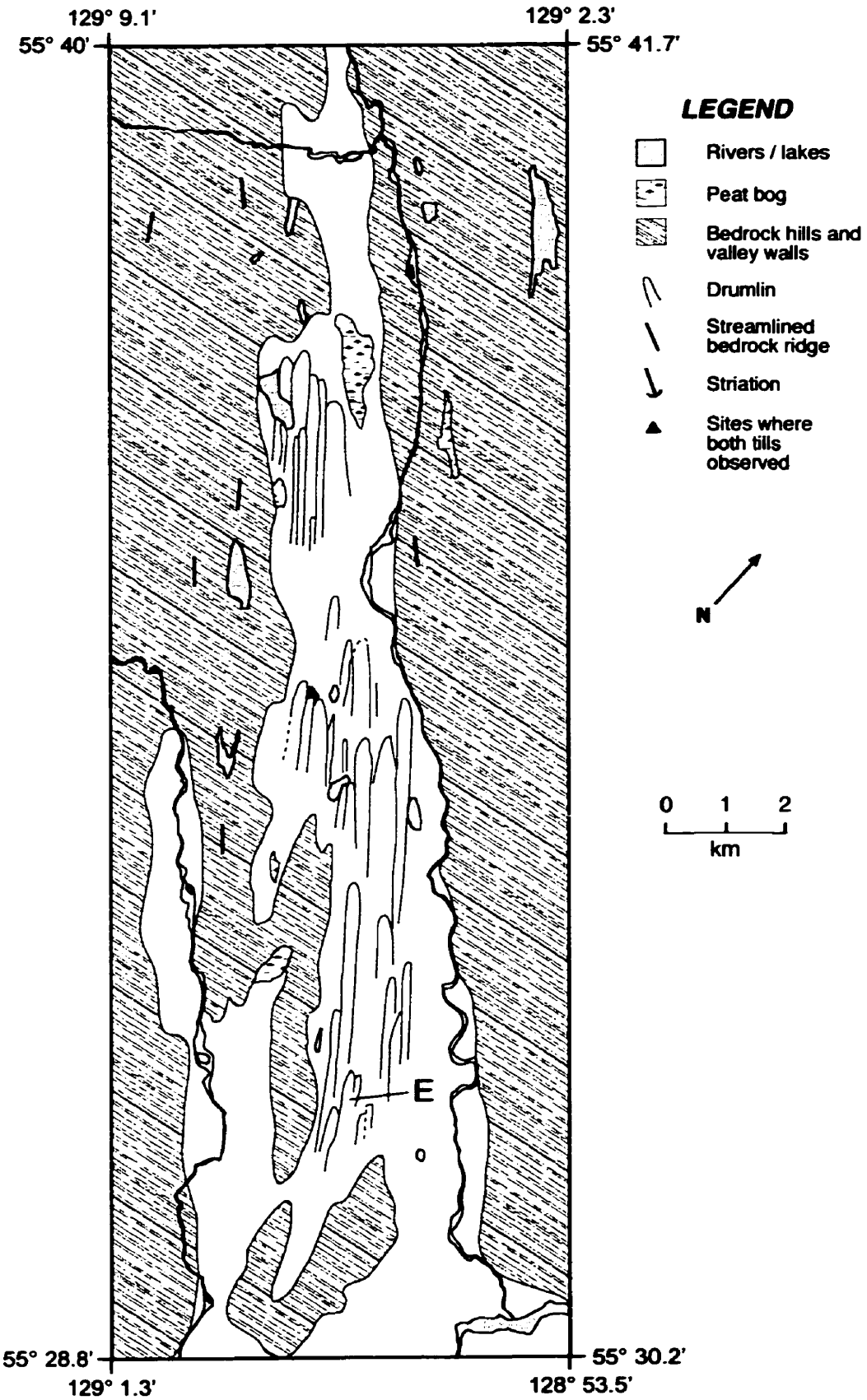


Figure 8.11. Locations of drumlins, streamlined bedrock and bedrock ridges in Kinskuch Valley.

Commonly, the central part of a bedrock ridge crest is the highest part of the feature. Drumlins are much more elongate and tend to be more subdued in comparison. In addition, streamlined bedrock ridges are not always perfectly parallel, because they commonly reflect bedrock structure, whereas in contrast, the parallel nature of drumlins is striking (Figure 8.11).

Till Fabric Analysis

A number of drumlins were analyzed in detail for clues as to their genesis. Nass Depression and Kinskuch Valley drumlins were all found to be cored by a succession of Kwinatahl till overlain by Kinskuch till. Kinskuch till comprises the inter-drumlin areas. Nass Valley drumlins consist of Kwinatahl till only.

Although Kinskuch till makes up the inter-drumlin areas, two small glaciolacustrine or glaciofluvial deposits were found near fabric site 968149 (x and y on Figure 8.7). These are discussed under Glaciolacustrine Deposits in Chapter 4. The proximity of both deposits to White River suggests that this river may have been a more extensive glacial meltwater river at one time. In fact, glacial braidplain deposits are present upriver, supporting this hypothesis (Kitsault Valley map).

Due to the shallow depth and limited breadth of drumlin sections and the variable type of contact (irregular or gradational) between Kinskuch and Kwinatahl tills, it is difficult to say whether the relationship of Kinskuch to Kwinatahl till in drumlinized areas is erosive or draped (Figure 8.12). However, since Kinskuch till comprises the interdrumlin areas and coats the entire tops and flanks of the drumlins, it is probably draped. At sites 968149 and 985271 (Figure 8.7), both tills are present. It is evident then, that both tills comprise the interdrumlin areas as well, supporting a draped relationship (because Kinskuch till is never more than 5 m thick).

Till fabric analyses were carried out on eight drumlins: six in the White River area, one in lower Kinskuch Valley and one in the Kiteen River area, to provide some understanding of the genesis of the two tills, as well as their relationship, if any, to drumlin orientation. The drumlins sampled are labelled A to H (Figures 8.7, 8.10 and 8.11), and till fabrics taken at each one are numbered (*e.g.* A1, A2). The fabric data are summarized in Table 8.1. Kwinatahl and Kinskuch tills

a) Erosive Relationship

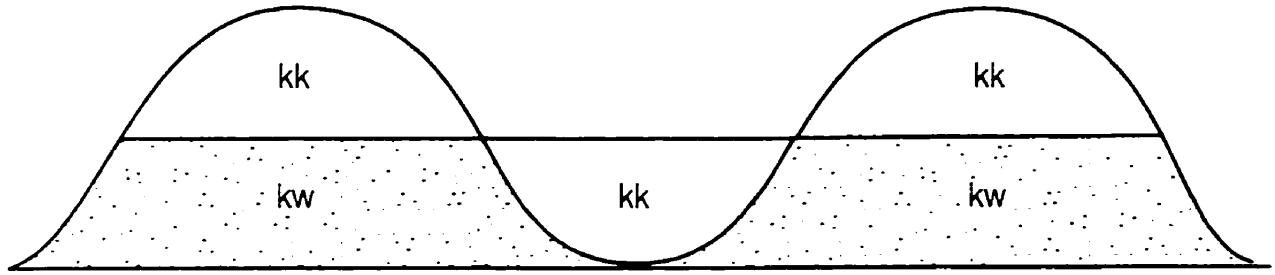


b) Draped Relationship

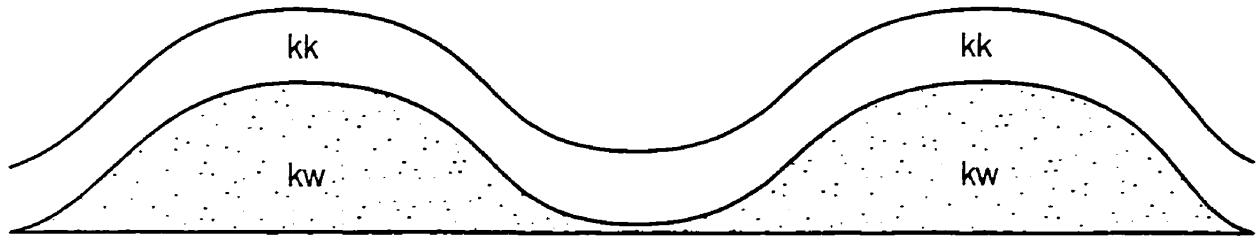


Figure 8.12. Possible relationships of Kinskuch till (kk) to Kwinathl till (kw) in drumlinized terrain.

are identified using the kw and kk nomenclature described previously. Only two drumlins actually exposed both tills well enough for both to be analyzed (Drumlins A and G).

Drumlin A is a large drumlin trending 165° (Figures 8.7 and 8.13). It is part of a drumlin cluster that has formed over a small hill. Kinskuch till coats the drumlin, drumlin tail and interdrumlin areas. Trees on the drumlin have been removed by logging and a small road cut exposes part of the drumlin snout. At this exposure, three fabrics were measured in Kinskuch till (A1, A3, A4) and one in the stratigraphically lower Kwinatahl till (A2). However, it was not possible to delineate the complete contact as much of the exposure was obscured by large stumps. The same trend as the drumlin axis is visually evident in all fabrics (Table 8.1, Figure 8.13), but fabrics A3 and A4 exhibit weak and strong transverse elements, respectively. A1 and A3 have strong fabrics, A2 has a moderately strong fabric and A4 has a weak one (A4 was a true girdle fabric statistically, so no ice flow inferences can be made from it). Thus, fabric strength in the Kinskuch till is variable, while it is moderately strong in the Kwinatahl till. A1, A2 and A3 have slightly spread fabrics.

One exposure of Kinskuch till was found at drumlin B (Figures 8.7 and 8.14). The weak fabric trend at this location is southwest (199°), but not perfectly perpendicular to the drumlin. Kinskuch till is also found at the crest of the drumlin's tail area and in the somewhat boggy interdrumlin areas.

Drumlin C is located just north of the map area (Figures 8.7 and 8.15), south of a small, flat, glaciofluvial braidplain. The whole drumlin is boulder rich and the crest portion of the drumlin is highly weathered. We were not able to penetrate to unweathered till in this area, so no fabrics were taken on the crest. The tail and interdrumlin areas consist of Kinskuch till. Pits were dug at locations where it was possible to do so. This drumlin had been sprayed with herbicide, which restricted vegetative growth, but rooted stumps left over from logging activities impeded pit location in many places. Kinskuch till was penetrated at three sites. Fabrics C1 and C3 are weak, while C2 is strong, but spread (Figure 8.15). Again, Kinskuch till shows variable strength - from a near girdle fabric at C1 to a strong fabric at C2. All are oriented approximately parallel to the drumlin, as at Drumlin A.

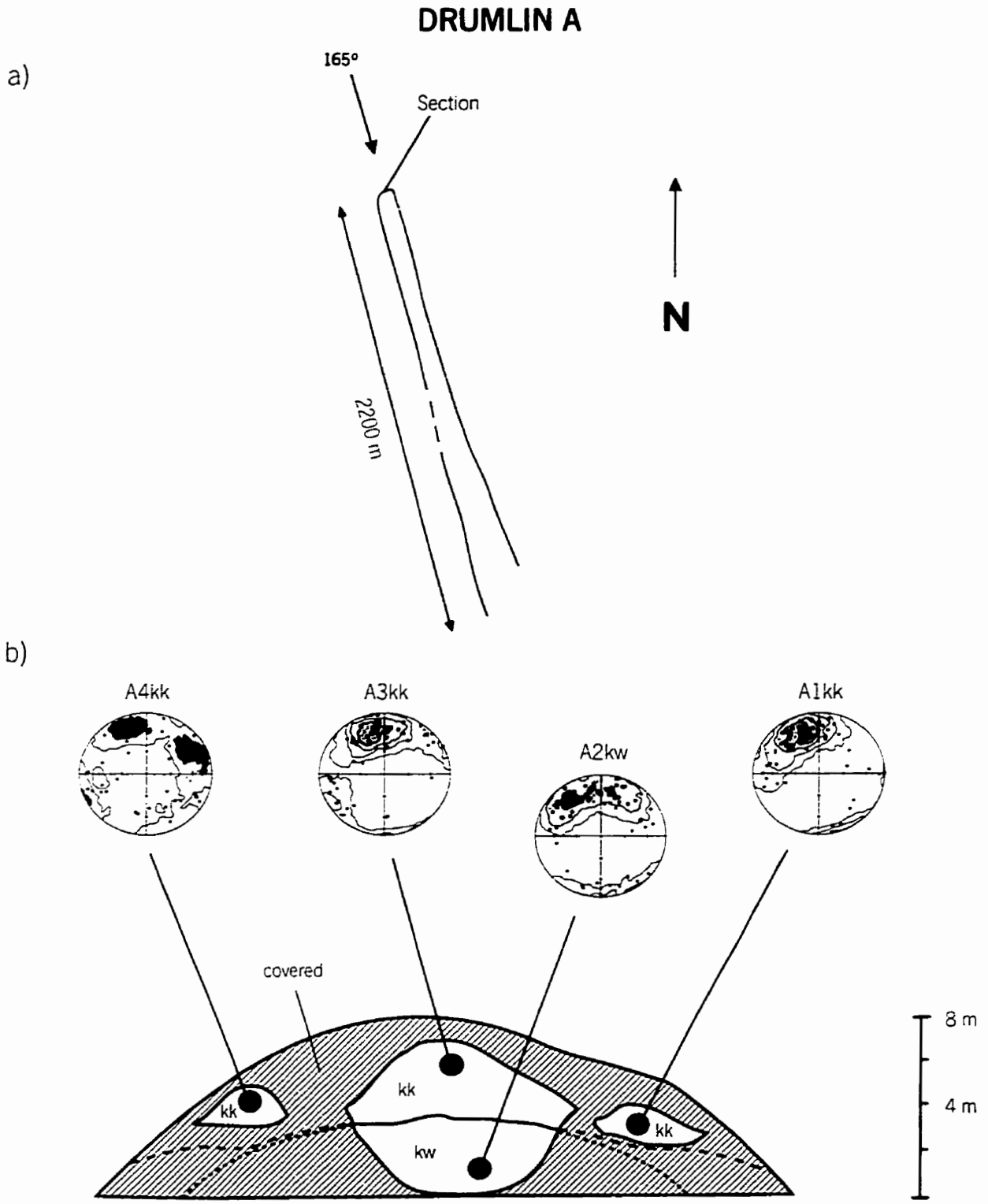


Figure 8.13. Drumlin A: 12 m high drumlin with 8 m high section at north end, a) plan view of drumlin, b) cross-section of sampled exposure, showing fabric locations. Two possible contact configurations are shown with dashed lines.

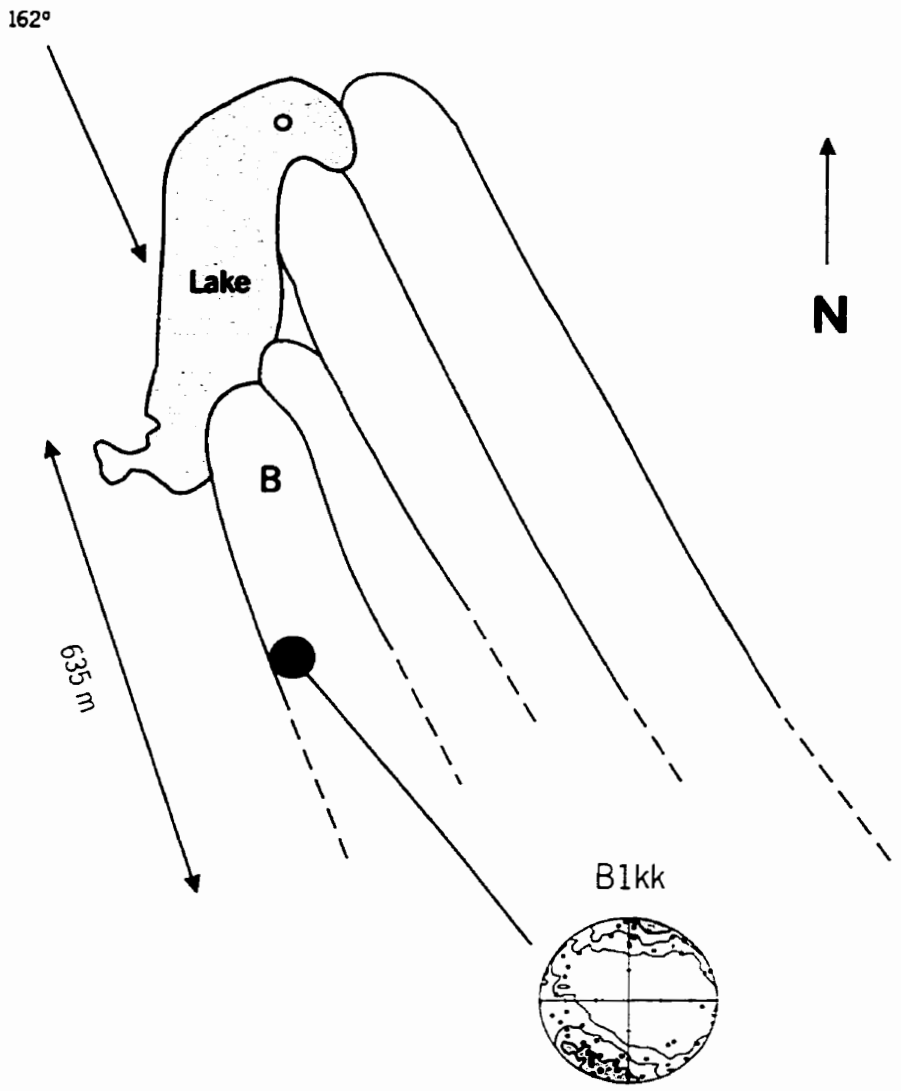


Figure 8.14. Drumlin B: Plan view showing fabric location in a small exposure near the surface of a small, 8 m high, drumlin south of a lake. Sample is from 1 m below surface.

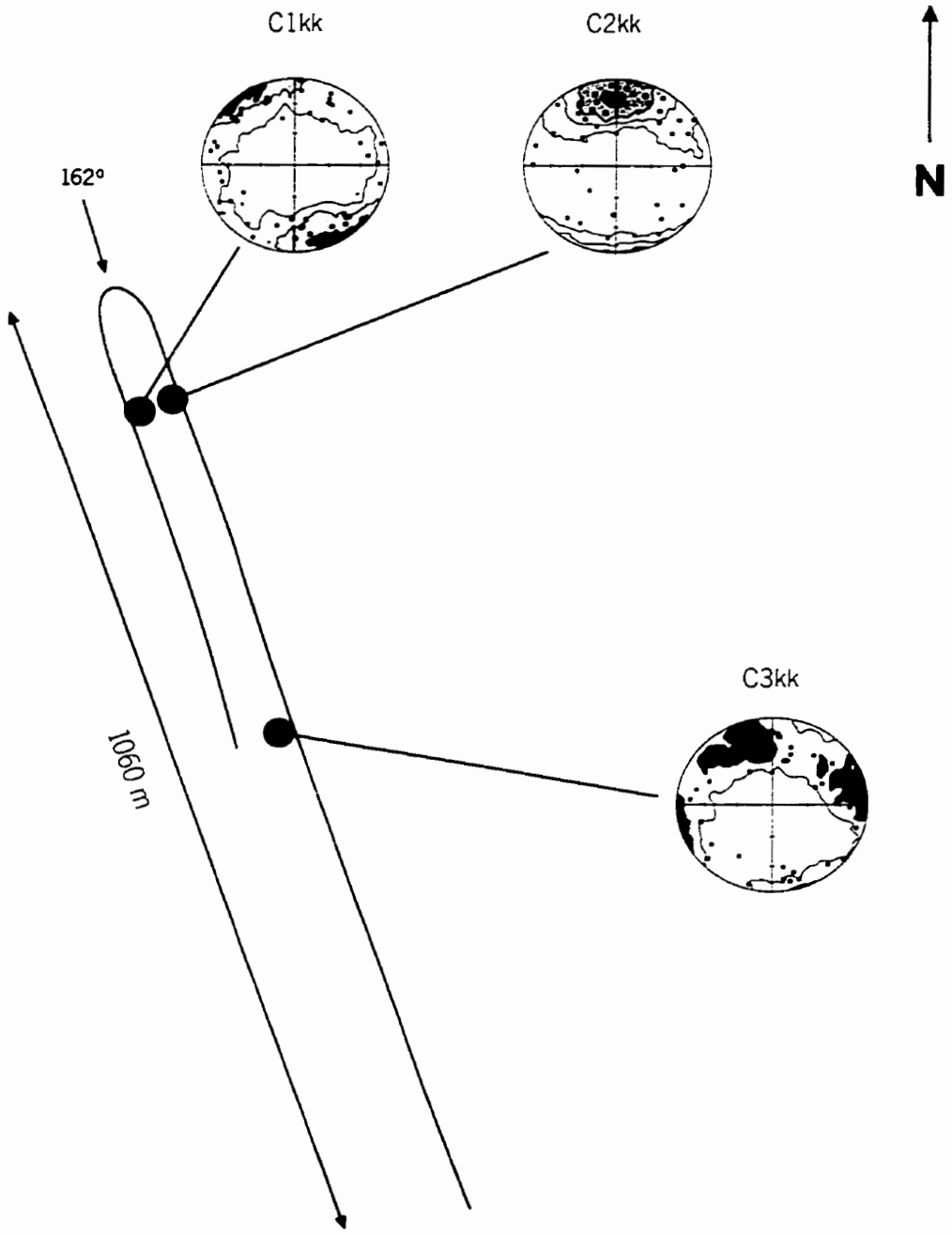


Figure 8.15. Drumlin C: plan view of 12 m high drumlin, showing location of fabrics from 1 to 1.5 m deep pits dug in surface.

Drumlin D is exposed along a highway road cut (all others are small logging roads) (Figures 8.7 and 8.16). Two fabrics were taken from Kwinatahl till containing heavily striated clasts. Kinskuch till was not present, although a thin, weathered layer in which a soil had developed may have originally been Kinskuch till. The fabrics are of low to moderate strength, very spread out and are oriented in a southwest direction. The interdrumlin area is forested and wet, and a thick organic soil made glacial sediment identification impossible.

Drumlin E is an oddly shaped drumlin with a small drumlinoid extension on its flank (Figures 8.11 and 8.17). The exposure here is small (about 1.5 m high), and only Kinskuch till is exposed. It is a typical Kinskuch till, with clasts that are heavily striated. Some boulders exhibit parallel striae on a faceted face (indicative of lodgement). Others have randomly oriented striations, indicative of possible deformation (clasts rolled within the till). The till has a poor fabric that is almost a girdle fabric.

Drumlin F is a drumlin in the northern Nass Valley that is at least 12 m high (Figures 8.10 and 8.18). It is located at 511140E, 6151625N which is just beyond the map area. Only Kwinatahl till is present. The fabric is strong, slightly spread and perpendicular to the drumlin and the valley, as at 975214kw. This area may also have been affected by compressive flow so this fabric may actually indicate valley and drumlin parallel ice flow. A few large, angular erratics are present within the forest on the drumlin surface. One such boulder (2 m in diameter) has striations on its upper and lower surfaces, but few on its sides.

Drumlin G is a small drumlin flanking three larger ones in the White River area (Figures 8.7 and 8.19). A small section was exposed in a logging road cut, but the contact between the two tills was difficult to make out after the section had been cleaned. This could mean the contact is gradational, but this is difficult to determine. The Kwinatahl till (G1kw) shows a moderately strong, spread out southwest fabric trend of 253° (Figure 8.19). The Kinskuch till has a weaker fabric with a trend of 103°.

Both tills are present in a road cut section in Drumlin H. The Kinskuch till is too thin, however, for a fabric measurement. The Kwinatahl till fabric is poor, but shows a southwest trend of 223° (Figure 8.20).

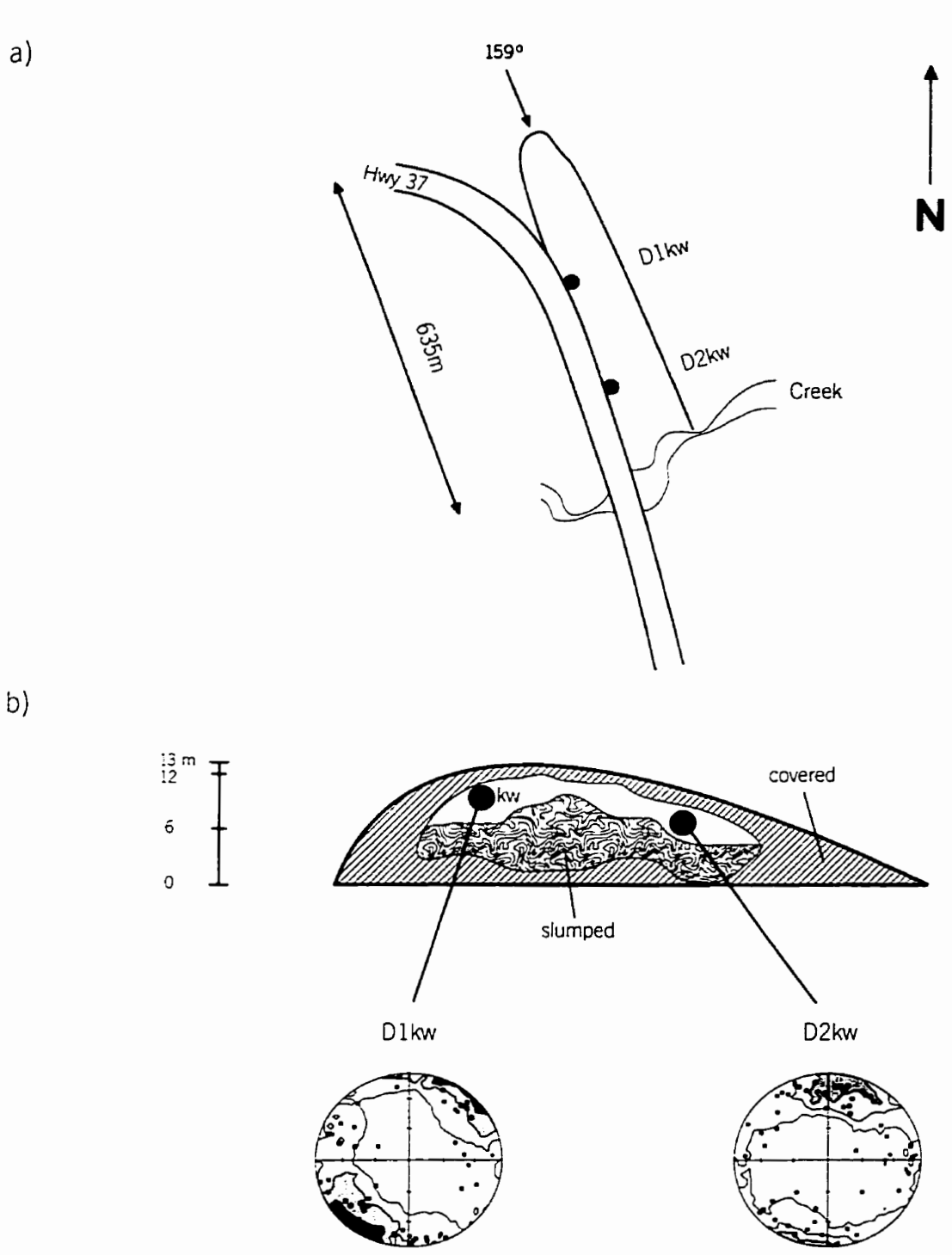


Figure 8.16. Drumlin D: till fabrics from Kwinatahl till in drumlin exposure along Highway 37; a) plan view of highway cut through drumlin, b) section view showing fabrics and locations. There is no exposure at the creek crossing. The upper part of the section is highly weathered; Kinskuch till may be present but it is difficult to tell.

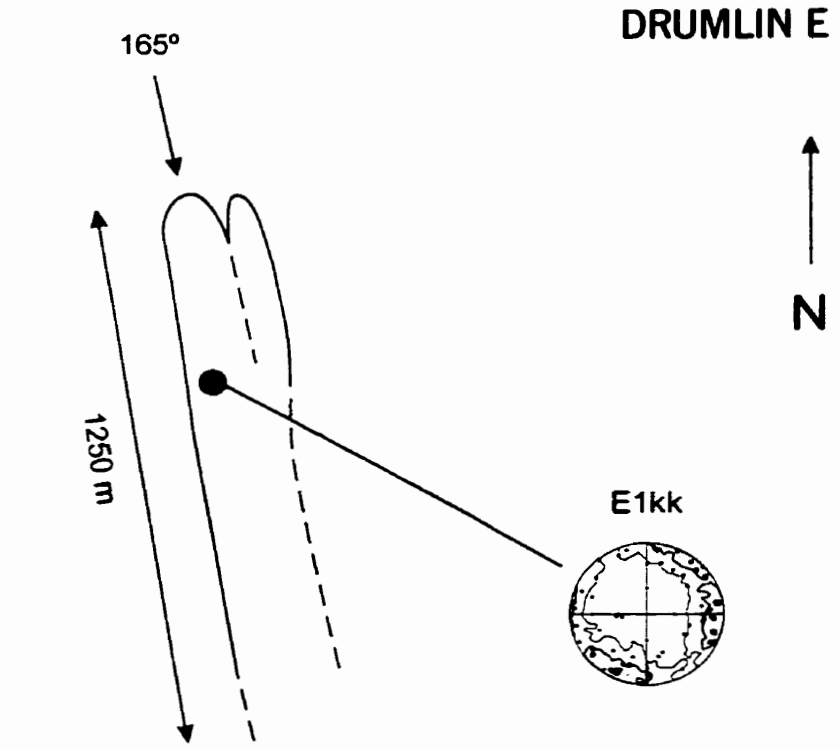


Figure 8.17. Drumlin E: plan view of fabric location from an exposure near the surface of a large drumlin, south Kinskuch Valley. Sample is about 1.5 m below surface.

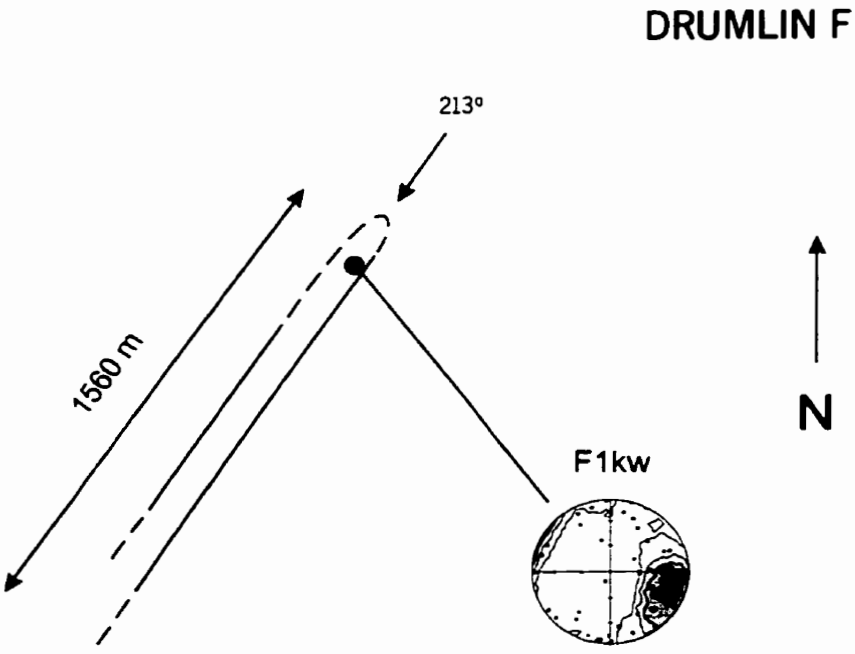


Figure 8.18. Drumlin F: plan view of fabric location from an exposure near the surface of a large drumlin, west of Kiteen River. Sample is about 2 m below surface.

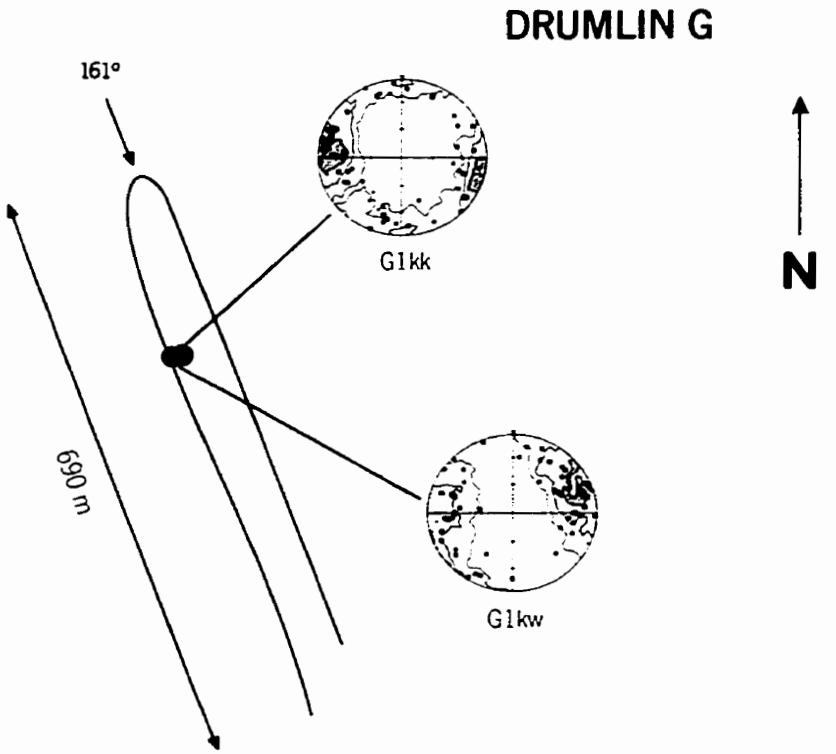


Figure 8.19. Drumlin G: till fabrics from a small exposure in a logging road cut. Both tills are present and the irregular contact is indistinct when exposed.

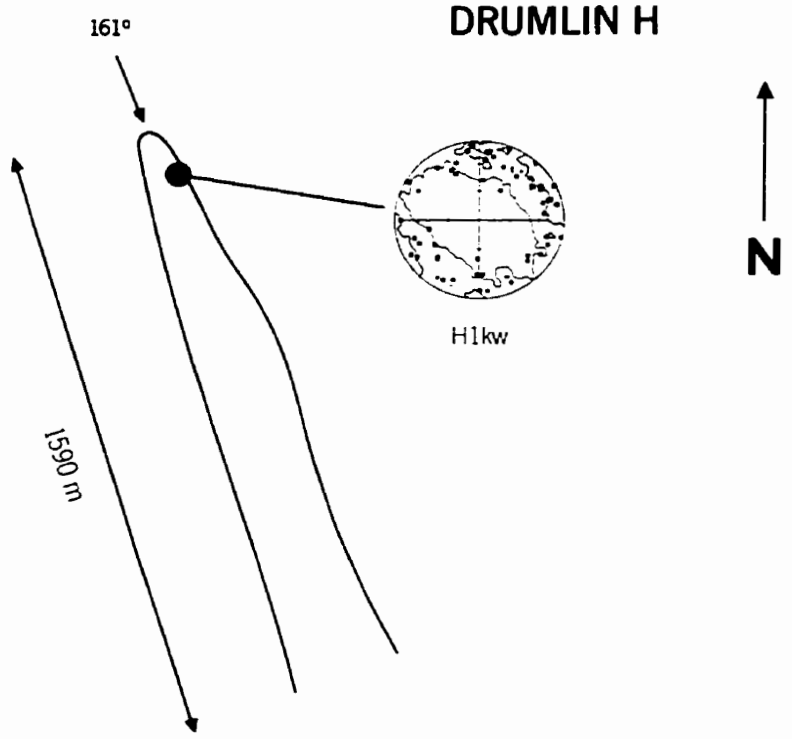


Figure 8.20. Drumlin H: till fabrics from a small exposure in a 5 m high logging road cut. Both tills are present, but Kinskuch till is too thin to measure at this exposure.

In summary, Kwinatahl tills in drumlins typically have stronger fabrics that are spread, while fabrics of Kinskuch till are variable and tend to be weaker. Kwinatahl till fabrics indicate both a southwest ice flow direction (early phase) and valley and drumlin parallel flow (late phase). The inference made earlier that this till was deposited during both phases of ice flow is again supported. The strong but spread out fabrics suggest that Kwinatahl till is a deformed lodgement or a deformation till, despite the lack of deformation structures within it.

Kinskuch tills have weaker fabrics. They can either trend parallel to valleys and drumlins or be roughly perpendicular. They may be interpreted as deformation tills as they show variable fabrics: both strong but spread fabrics and weak fabrics. The weak fabric trends all seem to show a drumlin flank dip orientation, which suggests that the tills may have flowed down the drumlin flanks postglacially in some areas. Kwinatahl till may have also been reworked by flow in a few places (*e.g.* H1kw).

Kwinatahl till formed by deformation or lodgement followed by deformation in the early and late phases of ice flow, while Kinskuch till is considered a deformation till formed during late phase ice flow. Kinskuch till is commonly reworked by secondary flow down the drumlin flank. This process is less common in the underlying Kwinatahl till.

Kinskuch till is quite thin at drumlins D and H and at site 968149 but not elsewhere. Its variability suggests that it does not show a consistent thickness trend *(e.g.* thicker over drumlin crests or in interdrumlin areas).

Drumlin Genesis Theories

There are several theories of drumlin formation, and no single theory is yet able to explain the genesis of all drumlins. Various theories are discussed and some discarded, based on the constraining factors of the study area. Recent drumlin genesis theories that can be ruled out based on the information presented here are subglacial fluvial cavity-fill (Shaw, 1983), as all drumlins are till covered and till cored, and shearing due to contrasting bed rheology (Boulton and Hindmarsh, 1987), because the same bedrock and the same two tills underlie the whole area. It is not possible to see deformation structures in either till, so there is no supporting evidence at the

exposure level for squeezing of sediments into cavities (Bluemle *et al.*, 1993, van der Meer, 1997) or basal shear, although both may have occurred.

The fact that drumlins only occur between bedrock ridges has been considered an unimportant factor in determining drumlin genesis (Patterson and Hooke, 1995). However, in this study it seems to play an important role. Perhaps the presence of thick sediment, not evident on bedrock ridges, was required for the formation of the drumlins. The drumlins in this study certainly formed during deglaciation, under thin ice, as have many other drumlin fields (Patterson and Hooke, 1995), although some of their Kwinatahl till cores formed earlier. They must have formed coevally with or after the deposition of Kinskuch till, which formed during late phase ice flow (because there was apparently no hiatus between Kwinatahl and Kinskuch till deposition). They are not associated with separate fluvial deposits, such as eskers, that would indicate subglacial drainage after drumlin formation.

From the preceding fabric discussion, Kinskuch till is considered to be a deformation till deposited in an ice flow direction that is parallel to drumlin orientation. Locally poor fabrics show that the till may have flowed postdepositionally in some places.

The deformational hypothesis of drumlin formation describes till streaming and deformation around older sediments (Boyce and Eyles, 1991), or other obstructions (Hart, 1997; Eyles and Boyce, 1998). This process requires a deforming bed, which is postulated to occur beneath fast moving thin ice. The evidence presented here is in line with this theory, with the more competent Kwinatahl till or perhaps fluvial debris acting as the core obstruction. Kinskuch till fabrics parallel to drumlins show that Kinskuch till could be considered the deforming layer. However, the interface between the two tills is not erosional, as is called for by the theory (Hart, 1997).

The drumlin shapes are roughly 'hairpin'. These shapes have been described in sheared diamicton surfaces where one surface passes over another that has harder clasts projecting above its surface. 'Crescentic grooves' wrap around the clasts and continue parallel to them (Eyles and Boyce, 1998). These features are formed by the shearing that occurs as two surfaces pass over each other, as in a fault. Associated bedrock features include crescentic fractures,

striated bedrock and nail head striations, of which the latter two are present in the drumlinized areas.

The deformational theory does not explain the abundant rounded debris within Kinskuch till. The rounded debris is so widespread that both subglacial conduits and floods could have contributed the rounded clasts. (Recall that there was no hiatus between the deposition of Kwinatahl and Kinskuch tills, so the rounded clast source must be subglacial).

The fluvial erosional hypothesis (Shaw, 1994, 1996) is another possibility for the drumlin forming process. In this theory, drumlins are considered to be erosional remnants formed by large subglacial floods that scour around an obstruction and up into the ice. The core sediments and their fabrics are irrelevant in this case. This theory is based on the apparent similarity between hairpin drumlin shapes and of 'hairpin erosional marks', formed by rapidly flowing water that encounters an obstacle (Figure 8.21, Shaw, 1994). Associated features include grooves which become shallower downflow, and contain little or no striation due to heavy fluvial scour (Shaw, 1994). These erosional marks are thought to represent a short-lived subglacial flood event.

There are problems with applying the fluvial erosion theory to the study area as well. A group of striations just north of drumlin G (Figure 8.7) *are* located in a groove flanking a drumlin. The bedrock surface in the groove is heavily striated. The drumlins formed during deglaciation (valley-parallel orientation, Kinskuch till) and abundant meltwater was present at or before this time (fluvial material in Kinskuch till). The lack of eskers and other stagnation features, along with the presence of heavily striated bedrock in a few locations, suggest that ice flowed actively until it disappeared. A subglacial meltwater flood would have had to occur immediately before ice disappeared, or the drumlins would have been removed or remoulded by subsequent ice flow. Since the Nass Valley was a depositional basin at this time, flood deposits would be expected. However, there are no such deposits (see glaciomarine deposit discussions, Chapter 4). A flood would therefore have had to occur before marine incursion. Ice would have to be clean, in order to preserve the drumlins throughout the ongoing ice flow. The abundant glaciomarine sediments in the Nass Valley show that ice was, in fact, not clean. Waning catastrophic floodwater flow carrying abundant debris might also leave a depositional signature in the vicinity of the drumlins

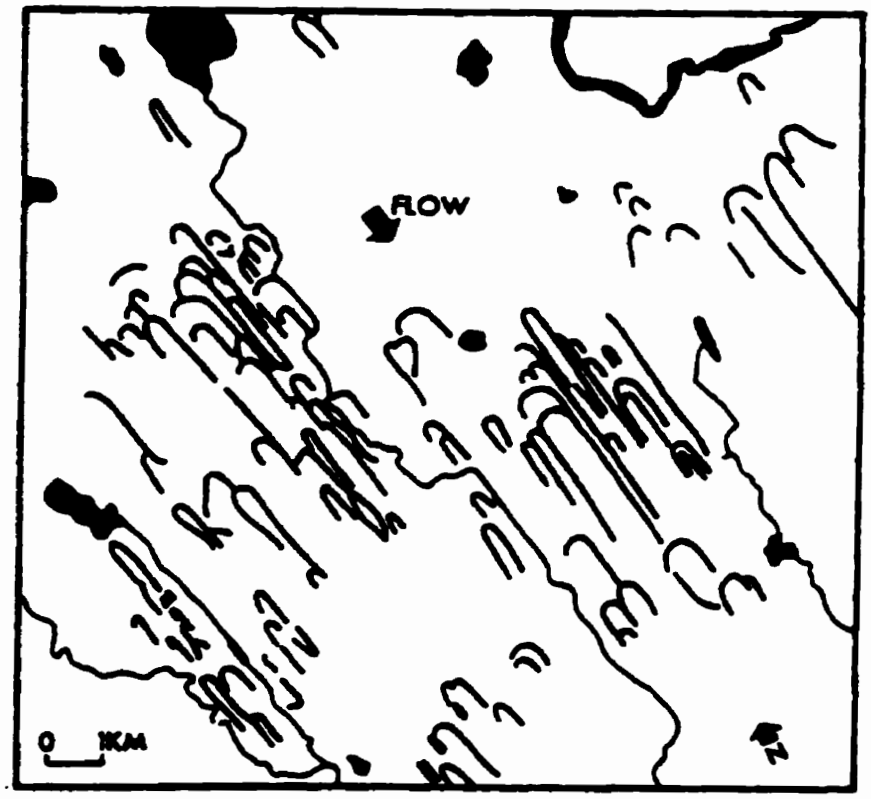


Figure 8.21. Hairpin erosional marks (from Shaw, 1994).

and elsewhere. There is no evidence of such fluvial deposition on top of or in the lee of drumlins, however, and there are very few glaciofluvial deposits in the vicinity of the drumlin areas. There are no associated tunnel channels and eskers, which may form in such environments when flood flow wanes to channelized flow (Brennand and Sharpe, 1993). Glaciofluvial gravels in the Nass Valley (Chapter 7) and flanking the Nass River near Highway 37 were subaerially deposited after retreat.

If the Nass and Kinskuch Valleys are considered tunnel valleys despite their wide, shallow cross sections, then fluvial scour features should be present. These features are not found within drumlin areas and are uncommon elsewhere. Bedrock surfaces are heavily striated and locally faceted on valley floors and walls. Since streamlined bedrock features are not perfectly parallel, can have ragged crests and are somewhat influenced by bedrock structure, it is suggested that these are ice-moulded features, formed on a more resistant substrate.

The deformational hypothesis is thought to be the most applicable theory to describe the formation of the drumlins in the study area. The streaming that formed the drumlins could also have been responsible for the complete destruction of any subglacial fluvial deposits, as well as the formation of Kinskuch till. Reworked glaciofluvial material and angular clasts of local derivation both comprise Kinskuch till. This complex Kinskuch till streamed over and around obstructions in Kwinatahl till, forming drumlins and infilling interdrumlin areas. The deglacial ice was thin and was not powerful enough to streamline the much harder adjacent bedrock to the same degree. There may have also been less debris at higher elevations in the ice, so that bedrock ridges were subject to less abrasion than valley floors.

It is a definite possibility that a meltwater flood provided the initial drumlin form and left behind a rich deposit of rounded debris. Potential esker material from subglacial channels could have been added and all of this material might have been remobilized by active ice flow. The fluvial debris would have been reworked into Kinskuch till, the deforming layer over which ice flowed rapidly. One way to confirm this idea would be to look for evidence of flood deposition offshore.

The drumlins can be adequately explained by the deformational theory without invoking a meltwater flood, if subglacial channel deposits were the sole source of rounded debris. The abundance of coarse-grained proximal glaciomarine sediments certainly supports the contention that there were copious quantities of subglacial channel debris produced by these glaciers. However, the lack of an erosional interface between the two tills is still problematic.

In conclusion, the subglacial deformation theory best explains drumlin genesis. Since ice flow appears to have moulded the drumlins, at least in the later phases of their development, they can be used as ice flow direction indicators in this area.

## Sea Level History

As outlined in Chapter 2, sea level fell rapidly during deglaciation in many parts of coastal northwestern B.C. and Alaska. Marine inundation due to isostatic depression caused sea levels to be as high as 230 m above present sea level (Miller, 1972) at the start of deglacial time. The Nass River area preserves a great deal of evidence of this marine incursion and provides more details about sea level change in northwestern B.C.

Marine inundation occurred in the Nass region during deglaciation due to eustatic sea level rise during the slow isostatic recovery period. The higher relative sea level probably caused calving, which would have accelerated the retreat of tidewater glaciers. The highest and earliest marine limit is given by two deltas: one at the town site of Kitsault and another that is a delta remnant in the southern part of the Nass Valley northeast of Ksedin Creek (Nass Valley map). Both are graded to 230 m asl. Deltas at Anyox (Observatory Inlet), Greenville, Shumal Creek (Nass Valley) and Donahue Creek (Portland Canal), as well as raised braidplains in Sutton and Kshwan valleys (south of Cambria Ice Field) are graded to a later shoreline of 150 m (Figure 8.22, both maps). In their terminal zones, Sutton Valley and Kshwan Valley braidplain elevations range from 150 to 160 m. The Aiyansh braid delta (determined by GPR) and the small delta in the town of New Aiyansh are also graded to about 150 m. The 150 m highstand must have been quite long-lived, for so many large features to have formed at that time. The Aiyansh Braidplain, in particular,

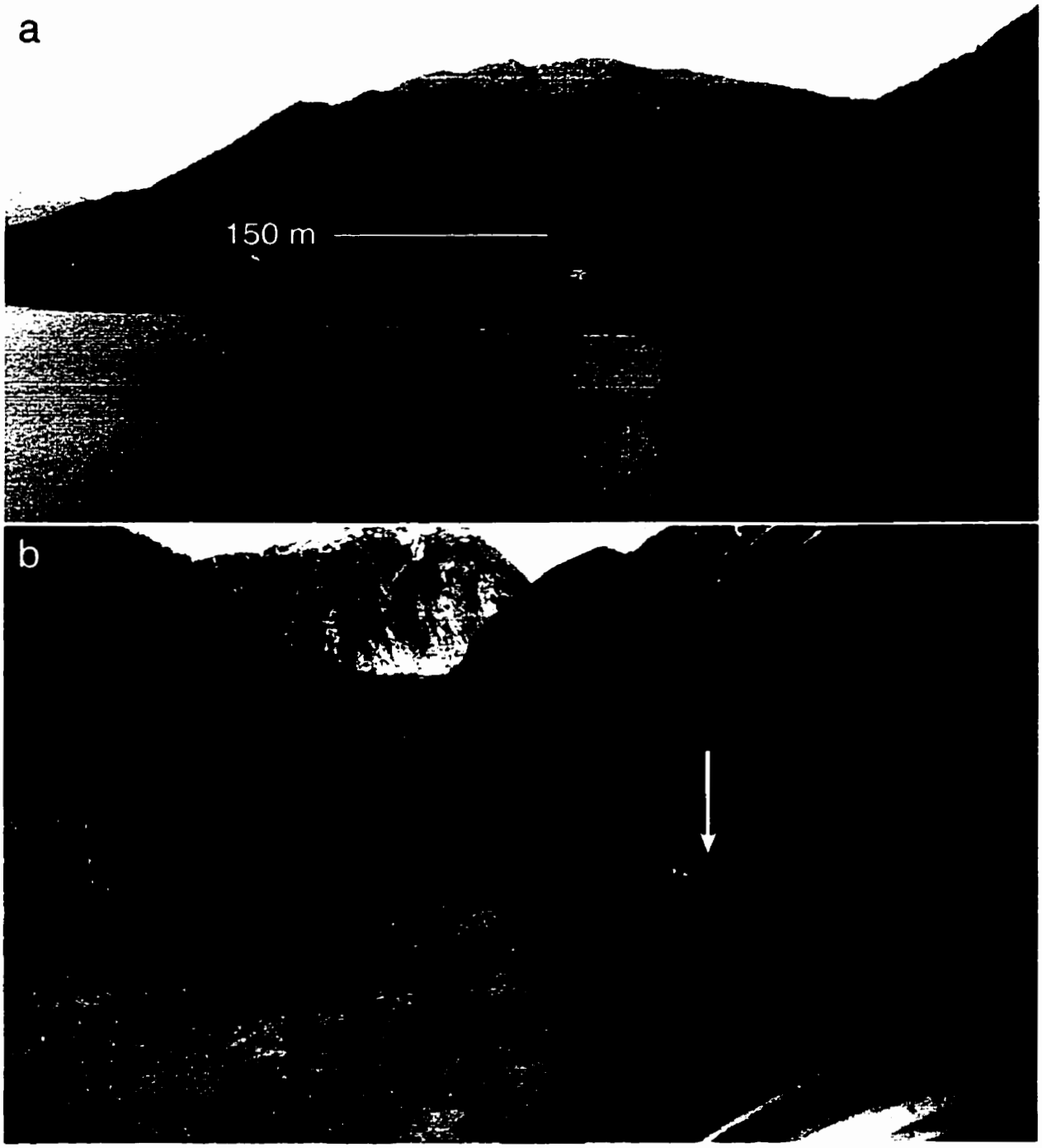


Figure 8.22. a) Raised delta on Portland Canal at Donahue Creek. This large delta is graded to 150 m asl. b) Raised braidplain in Kshwan Valley. The braidplain dips gently in a downvalley direction to a terminal zone graded to 160 to 150 m asl. Kshwan River (arrowed) incises the deposit, but no exposures are available due to heavy forest cover. The boggy areas in the foreground and in the distance may indicate that till or glaciomarine deposits underlie braidplain gravels, forming an aquitard.

is an extensive landform. Radar evidence indicates two more minor highstands, one at 185 m and one at 135 m.

The various sea level highstands imply that sea level was stable at these levels for sufficient periods of time to form the various features, with possible rapid drops in between (Figure 8.23). The timing of these stable periods is not known. The stable periods may be due to regional glacial readvances or stillstands that are not well recorded in the Nass River region. There might also be some kind of tectonic control.

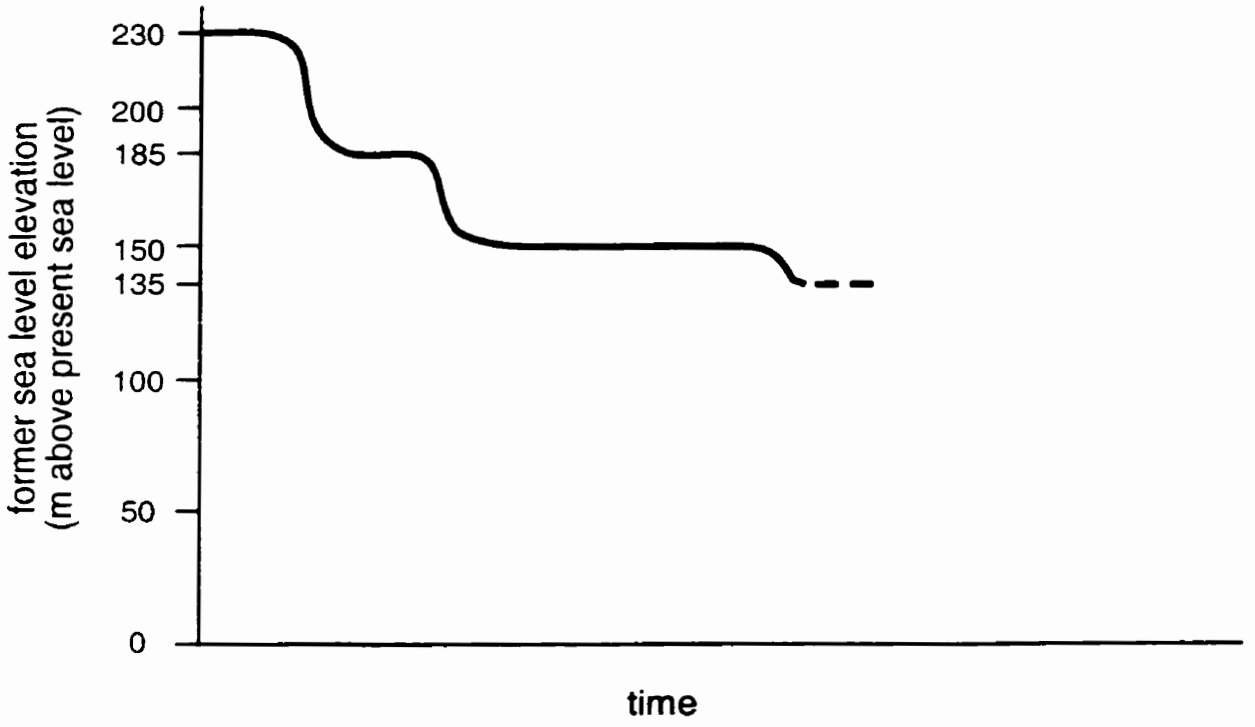


Figure 8.23. Apparent changes in sea level over time.

# CHAPTER NINE

# SUMMARY AND CONCLUSIONS

A number of different methods were used to investigate the Quaternary geology and glacial history of the Nass River region. Information from ten sections, six drill holes, one seismic line, twenty ground penetrating radar profiles and from surficial geology mapping work was combined to determine the stratigraphic succession and depositional history of the region, and particularly of the Nass Valley. Till fabric analyses, radiocarbon dating and micropaleontological analyses helped to further elucidate glacial history.

## Quaternary Stratigraphy

Surficial geology of the region was mapped. The Kitsault Valley and Nass Valley maps are found in the map pocket of the thesis. However, they give only a two dimensional view of regional Quaternary deposits. Stratigraphic information is required to determine the relationships of the units and the sequence in which they were deposited. The following is the stratigraphic succession determined for the region. The units are found throughout the study area, but they are most completely preserved in the Nass Valley (with the exception of Kinskuch till, which is found mainly in the northeastern part of the study area).

Lithostratigraphic Units and Stratigraphic Sequence, from oldest to youngest:

1) Bedrock (generally pre-Pleistocene)

2) Older sediments (Pleistocene)

   2a) Melt-out or flow till

   2b) Fluvial or lacustrine sediments of Olympia age

   2c) Glaciofluvial deposits

3) Till of the last glaciation (Pleistocene)

   3a) Kwinatahl till

   3b) Kinskuch till

4) Retreat-phase glaciomarine sediments (Pleistocene)

   4a) Interbedded proximal deposits

   4b) Distal silty clay deposits

   4c) Fan delta deposits

5) Retreat-phase glaciofluvial sediments (Pleistocene)

   *(these deposits are contemporaneous)*

   5a) Braidplain deposits

   5b) Braid delta deposits

6) Postglacial sediments (Holocene)

   *(these deposits are contemporaneous)*

   6a) Neoglacial deposits

   6b) Alluvial deposits

   6c) Colluvial deposits

   6d) Alluvial fan deposits

Sediments that pre-date the last glaciation are rare. They include fluvial or lacustrine gravel, sand and clay of Olympia age, till and glaciofluvial gravel deposits. There may be up to 200 m of

older deposits underlying till in the Nass Valley (determined by seismic reflection). However, the actual sediment type of these deposits is not known.

Sediments deposited during the last (Fraser) glaciation include the informally named 'Kwinatahl' and 'Kinskuch' tills. Kwinatahl till is found throughout the study area and can be up to 50 m thick. Kinskuch till is found only in the northeastern part of the study area and is about 4 m thick, on average. Differing compositions of the tills are interpreted as being due to deposition during different ice flow phases of the last glaciation. Both tills are predominantly lodgement tills, although Kinskuch till exhibits locally poor fabrics that may indicate flow till facies.

Retreat-phase sediments include glaciomarine, glaciofluvial and glaciolacustrine deposits. Glaciolacustrine deposits are extremely rare. Glaciomarine sediments that are up to 50 m thick overlie Kwinatahl till. Proximal deposits comprise interbedded silt, sand and gravel thought to be deposited by subaqueous jets. These deposits grade distally to massive or locally laminated silty clay deposits. Both types of glaciomarine sediments locally contain dropstones. These sediments are devoid of fossils, possibly because sedimentation rates were high and the water was too turbid for life forms. Local beds of sand within the silty clay deposits are inferred to be due to sediment flows from fan deltas or from subaqueous jets.

Retreat-phase glaciofluvial deposits erosively overlie the glaciomarine sediments. They include sandy pebble, cobble and boulder gravel that often forms braidplain-braid delta geomorphic units. Braidplain deposits are horizontally bedded and cut by numerous channels. Braid deltas are found at terminal zones of braidplains and commonly display Gilbert-type topset and foreset beds, with channels found locally within the topset beds. Deltas without associated braidplains are common as well. These formed at the mouths of small, steep valleys.

Postglacial deposits include sandy Neoglacial till of local provenance, alluvial sediments, colluvial deposits and alluvial fan or fan delta deposits. Colluvium is abundant, occurring most commonly as a thin veneer on slopes. Alluvial fans overlie bedrock or glacial sediments and fan deltas are common in fiords. The Aiyansh Lava Flow is also a postglacial feature.

## Glacial History

In Olympia time, nonglacial fluvial or lacustrine environments existed. Lodgement till was deposited by glaciers either before or after this time. Glacial rivers formed some time after the deposition of the till, but before the last glaciation.

At the height of the last glaciation, ice from the Cordilleran Ice Sheet flowed southwestward over the Nass River region, rounding and smoothing many of the Coast Mountains. The ice was over 1840 m thick and flowed from an ice divide in the Skeena Mountain/Williston Lake area. The ice sheet incorporated large quantities of soft metasedimentary rocks from the Bowser Lake Group and deposited them in all parts of the map area as a compact, clay-rich till (Kwinatahl till). This event must have been highly erosive, as very little evidence of earlier glaciations was found.

During retreat, ice thinned and became restricted to fiords and valleys. Retreat was accomplished by calving, thinning and frontal wastage, but ice flowed actively during deglaciation. Kinskuch till was deposited over Kwinatahl till in the northeastern portion of the study area at this time. It is of more local provenance than Kwinatahl till and occurs in an area of drumlinized terrain. The transition from one type of till to the other is gradational, the change possibly having occurred as ice gradually became valley confined during deglaciation. The drumlins are believed to have formed by subglacial deformation of Kinskuch till, which incorporated fluvial sediments from subglacial channel and possibly flood deposits that were abundant during deglaciation.

Ice subsequently receded and marine water invaded the isostatically depressed landscape. This sea level rise probably caused rapid retreat in fiords. Marine sediments were laid down in fiord areas below marine limit (230 m asl). In the Nass Valley, a major glacier retreated continuously, apparently experiencing no stillstands. Near the receding ice margin, subaqueous jets deposited alternating beds of silty clay, sand and gravel that fine distally. As ice continued its retreat, basinal areas farther down valley received only silty clay input, with or without local influx of slightly coarser-grained debris from fan deltas or subaqueous outwash. Subaqueous ice proximal deposition continued up valley at the ice margin. Glaciomarine sediments were thus deposited in a time transgressive manner, following the retreating ice front.

Sea level fall and rapid retreat eventually resulted in glaciers becoming grounded on land. Meltwater rivers draining the retreating glaciers deposited glaciofluvial gravel and sand, most commonly as extensive braidplains and deltas. Small glacial lakes formed locally, but were relatively uncommon.

Sea level dropped to 185 m, and the Nass Braidplain North formed in the Nass Valley, west of a bedrock rise. The meltwater river that formed it incised into earlier glaciomarine deposits. By the time sea level dropped to 150 m, the meltwater river had moved to the opposite side of the bedrock ridge, forming the extensive Aiyansh Braidplain/Braid Delta complex northeast of New Aiyansh. Sea level remained at 150 m for a relatively long time, allowing the formation of a number of glaciofluvial deltas in the Nass Valley, Observatory Inlet and Portland Canal areas. Two braidplains also formed at the north end of Hastings Arm at this time. Sea level subsequently dropped to 135 m, and a small braidplain formed just southwest of the Nass Braidplain North, as the meltwater river had returned to its original position. The river stayed in this general location throughout the Holocene, and evolved into the modern Nass River, which incises two of its own former deposits, the Nass Braidplains North and South. The Aiyansh Braidplain has remained largely unmodified since its formation.

Colluvium, alluvium, alluvial fan, fan delta and bog deposits formed on top of glacial deposits during the Holocene. Earthflows formed in the upper part of the Nass Braidplain North as rivers incised into the underlying unstable glaciomarine silty clay deposits.

The region's glacial history conforms to Kerr's (1936) and Davis and Matthews' (1944) model of Cordilleran glaciation. An intense alpine phase of glaciation was followed possibly by a mountain ice sheet phase and definitely by a continental ice sheet phase, where ice flowed independently of topography. During deglaciation, the mountain ice sheet phase was reached when glaciers became confined to valleys and fiords. Intense alpine glaciation, with valley glaciers only, followed and the modern situation of alpine glaciation was eventually reached.

## Comparison Of Regional Glacial History To Other Parts Of British Columbia

*Pleistocene Deposits*

The lower till at the Kiteen River Section is the only evidence of pre-Fraser glaciation. Pollen from the Olympia-age clay of Kinskuch Valley shows that the area was a spruce forest just prior to Fraser Glaciation.

The thick accumulations of advance-phase glaciofluvial sediments so common elsewhere are extremely rare. The only example of such a deposit is the unit interpreted as glaciofluvial at the Kiteen River Section, and even this may actually be a retreat-phase deposit from an earlier glaciation. Other locations where advance-phase glaciofluvial sediments are found include coastal southwestern B.C. (Quadra Sand, Clague 1981, 1986), the Kamloops area (Fulton, 1975, Ryder *et al.*, 1991), the Fraser-Chilcotin area (Eyles and Clague, 1991), Quesnel area (Eyles, 1987), Bulkley River and Terrace-Kitimat area (Clague, 1984b), Stikine River area (Ryder and Maynard, 1991) and the Fort St. John region (Clague, 1981). Their rarity in the study area may be due to vigourous, highly erosive ice flow.

Unlike some other parts of B.C., the continental ice sheet phase appears to have been reached in this northern coastal region. This implies that montane ice was overridden by Cordilleran ice and flow directions were locally reversed.

Kwinatahl till is comparable to till deposited elsewhere during the mountain and intense alpine phases of Fraser Glaciation. Other tills deposited at this time include the Vashon till of Vancouver (Clague, 1981), Kamloops drift till (Fulton, 1975), reworked till in the Skeena Valley (Clague, 1984), lodgement till in Bulkley Valley (Clague, 1984) and lodgement till near Quesnel. One difference is that Kwinatahl till was also deposited in the study area during the continental ice sheet phase.

Restriction of ice to valleys occurred in the study area during deglaciation. This was also a common feature during deglaciation in the Terrace-Kitimat region (Clague, 1984b), Stikine area (Ryder and Maynard, 1991), and the Babine Lake region (Levson *et al.*, 1997).

Glaciomarine sediments in the study area are correlative to glaciomarine deposits in the Terrace-Kitimat region (Clague, 1986). However, subaqueous fans of the Nass Valley were not able to grow into ice contact deltas as they did to the south, probably because there were no long-lived stillstands of the Nass Glacier. The Kitsault Delta did evolve in this way, but by the time the delta stage was reached, ice had retreated from the area. Nass region glaciomarine sediments are broadly correlative with the Capilano sediments of southwestern B.C. (Armstrong, 1981).

The ice stagnation that occurred in interior regions (*e.g.* in the Kamloops area; Fulton, 1975) did not occur at all in this coastal transition zone. Major glacial lake sediments that are common in the interior are also lacking.

The extensive glaciofluvial braidplains and deltas are similar to thick fluvial retreat sequences elsewhere: the Fort Langley Formation, southwestern B.C., channel deposits near Quesnel (Eyles, 1987) and braidplains in northern B.C. (Ryder and Maynard, 1991). They are different from the Terrace region braidplains (Clague, 1984b) in that they are not ice-contact features that formed at the highest marine limit. However, minor ice contact deltas at 100-130 m, that were built in the Terrace (Thornhill) area a few hundred years after the 200 m deltas formed (Clague, 1984b), may correlate roughly to the 135 m braidplain of the Nass Valley. The deltas that formed at the Nass area's marine limit of 230 m likely correlate to the 200 m ice contact braidplains and braid deltas of the Terrace region (Clague, 1984b).

*Sea Levels*

Sea level rise during early deglaciation probably caused rapid glacier retreat in the Nass and other fiord valleys. The marine limit of 230 m is the highest recorded to date in B.C., but it is comparable to a 230 m limit in Juneau (Miller, 1973). It is also close to the 200 m marine limit reached in Kitimat between 13 and 11 ka BP (Clague *et al.*, 1982b), and near Terrace at 10.5 ka (Clague, 1984b). Sea level fell from this elevation to 115 m in less than 1000 years (Clague, 1983). A rapid sea level drop also occurred in the Prince Rupert region (Barrie and Conway, 1998, Clague *et al.*, 1982b).

As Kitsault and New Aiyansh are approximately the same distance inland from the coast as Terrace, and since Terrace is the closest dated location to New Aiyansh, the 230 m sea level in the study area was likely reached at some time around 10.5 ka BP. Rapid sea level fall ensued, as at Kitimat and Prince Rupert, however, important stalls occurred at 185, 150 and 135 m asl. The 150 m highstand was particularly long-lived. Glaciers had retreated from marine areas by this time, so retreat must have been more rapid than in Terrace (due to uninterrupted retreat?). Highstands of 185 and 150 m were also interpreted from units at Juneau (Miller, 1972); the former are older than 9.3 ka BP. However, Juneau is quite far from the Nass River region and is not inland from the coast, so the date and the sea level highstands are not comparable.

Sea level dropped to 120 m in the Terrace area by 10.1 ka BP and to 35 m by 9.3 ka BP. Present sea level was reached by 8-8.5 ka BP (Clague, 1984b). These dates may be correlative to the study area, so the 135 m limit was probably reached around 10.1 ka, and present day sea level by about 8 ka. If these dates are correct, then sea level fell rapidly, the drop from 230 to 135 m being accomplished in a few hundred years.

## Recommendations for Future Work

Emphasis should be placed on high elevation studies of the Coast Mountains, especially in northern B.C. Ice flow directions should be determined in these areas to confirm whether or not Figure 8.5 is correct.

Cosmogenic dating, especially of the rounded ridge areas, would be a good way to get a better understanding of the timing of glacial events, since there is little radiocarbon datable material in the area.

More drilling in areas of proximal glaciomarine sedimentation might be able to reveal the positions of subaqueous fans (morainal banks) that may exist beneath glaciomarine clay in the Nass Valley. Alternatively, seismic work and drilling in the fiords might be capable of identifying morainal sills, as well as possible meltwater flood deposits.

A more in depth landform-sediment analysis of the drumlin fields, preferably with access to a backhoe, might yield some interesting results regarding drumlin genesis.

## REFERENCES


Armstrong, J.E. (1981). Post-Vashon Wisconsin glaciation, Fraser Lowland, British Columbia. *Geological Survey of Canada Bulletin* 322, 34 p.

Armstrong, J.E. and Tipper, H.W. (1948). Glaciation in north central British Columbia. *American Journal of Science* 246, 283-299.

Barrie, J.V. and Conway, KW. (1998). Late Quaternary glaciation and post-glacial sea level response on the Northern Pacific margin of Canada. *Abstract Volume, Joint meeting GAC, MAC, APGGQ, IAH, CGU, May 18-20, 1998, Quebec City*, A10.

Barrie, J.V. and Conway, KW. (1999). Late Quaternary glaciation and post-glacial stratigraphy of the Northern Pacific margin of Canada. *Quaternary Research* 51, 113-123.

Berglund, B.E. (1986). *Handbook of Holocene Palaeoecology and Palaeohydrology*, Wiley, Toronto, 869p.

Berry, R.W. and Torrance, J.K. (1998). Mineralogy, grain-size distribution and geotechnical behavior of Champlain clay core samples, Quebec. *The Canadian Mineralogist* 36, 1625-1636.

Blaise, B., Clague, J.J. and Mathewes, R.W. (1990). Time of maximum Late Wisconsin glaciation, west coast of Canada. *Quaternary Research* 34, 282-295.

Bluemle, J.P. Lord, M.L. and Hunke, N.T. (1993). Exceptionally long, narrow drumlins formed in subglacial cavities, North Dakota. *Boreas* 22, 15-24.

Bornhold, B.D. (1983). Sedimentation in Douglas Channel and Kitimat Arm. *Canadian Technical Report, Hydrographic Ocean Science* 18, 88-114.

Boulton, G.S. (1971). Till Genesis and Fabric in Svalbard, Spitsbergen. In *Till; a Symposium* , Ohio State University Press, Columbus, 41-72

Boulton, G.S. and Hindmarsh, R.C.A. (1987). Sediment deformation beneath glaciers: rheology and geological consequences. *Journal of Geophysical Research* 92, 9059-9082.

Boyce, J.I. and Eyles, N. (1991). Drumlins carved by deforming till streams below the Laurentide Ice Sheet. *Geology* 19, 787-790.

Brennand, T.A. and Sharpe, D.R. (1993). Ice-sheet dynamics and subglacial meltwater regime inferred from form and sedimentology of glaciofluvial systems: Victoria Island, District of Franklin, Northwest Territories. *Canadian Journal of Earth Sciences* 30, 928-944.

Brown, L.F., Jr. and Fisher, W.L. (1985). *Seismic Stratigraphic Interpretation and Petroleum Exploration, Continuing Education Course Note Series 16*, American Association of Petroleum Geologists, Tulsa, 56p.

Carter, N.C. and Grove, E.W. (1971). Geological compilation of the Stewart, Anyox, Alice Arm, and Terrace areas, *British Columbia Ministry of Energy, Mines and Petroleum Resources, Preliminary Map 8*, 1:250 000.

Clague, J.J. (1978). Terrain hazards in the Skeena and Kitimat River basins, British Columbia. In *Current Research, Part A, Geological Survey of Canada, Paper 78-1A*, 183-188.

Clague, J.J. (1981). Late Quaternary geology and geochronology of British Columbia. Part 2: Summary and discussion of radiocarbon-dated Quaternary history. *Geological Survey of Canada, Paper* 80-35, 29p.

Clague, J.J. (1983). Glacio-isostatic effects of the Cordilleran Ice Sheet, British Columbia, Canada. In Smith, D.E. and Dawson, A.G. (eds.), *Shorelines and Isostasy,* Academic Press, London, 321-343.

Clague, J.J. (1984a). Deglaciation of the Prince Rupert-Kitimat area, British Columbia. *Canadian Journal of Earth Sciences* 22, 256-265.

Clague, J.J. (1984b). Quaternary geology and geomorphology, Smithers-Terrace-Prince Rupert area, British Columbia. *Geological Survey of Canada, Memoir 413,* 71p.

Clague, J.J. (1986). The Quaternary stratigraphic record of British Columbia--evidence for episodic sedimentation and erosion controlled by glaciation. *Canadian Journal of Earth Sciences* 23, 885-894.

Clague, J.J., Harper, J.R., Hebda, R.J. and Howes, D.E. (1982a). Late Quaternary sea levels and crustal movements, coastal British Columbia. *Canadian Journal of Earth Sciences* 19, 597-618.

Clague, J.J., Mathewes, R.W., and Warner, B.G. (1982b). Late Quaternary geology of eastern Graham Island, Queen Charlotte Islands, British Columbia. *Canadian Journal of Earth Sciences* 19, 1786-1795.

Cowan, W.A., Jinkui, C., Powell, R.D., Clark, J.D., and Pitcher, J.N. (1997). Temperate glacimarine varves: an example from Disenchantment Bay, southern Alaska. *Journal of Sedimentary Research,* 67, 536-549.

Davis, J. L. and Annan, A. P. (1989): GPR for high-resolution mapping of soil and rock stratigraphy. *Geophysical Prospecting* 37, 531-551.

Davis, N.F.G. and Mathews, W.H. (1944). Four phases of glaciation with illustrations from southwestern British Columbia. *Journal of Geology* 52, 403-413.

Dawson, G.L. and Alldrick, D.J. (1986). Geology and mineral deposits of the Kitsault Valley. In *Geological Fieldwork, 1985, British Columbia Ministry of Energy, Mines and Petroleum Resources, Paper 1986-1,* 219-224.

Evenchick, C.A. and Holm, K. (1997). Bedrock geology of the Anyox pendant and surrounding areas, Observatory Inlet (103P/5) and parts of Hastings Arm (103P/12) and 103O/9 map areas, British Columbia. In *Current Research 1997-A, Geological Survey of Canada,* 11-20.

Evenchick, C.A. and Mustard, P.S. (1996). Bedrock geology of north-central and west-central Nass River map area, British Columbia. In *Current Research, Part A, Geological Survey of Canada, Paper 96-1A,* 45-55.

Evenchick, C.A., Alldrick, D.J., Currie, L.D., Haggart, J.W., McCuaig, S., McNicoll, V. and Woodsworth, G.J. (1997). Status of research in the Nass River multidisciplinary geoscience project, British Columbia. In *Current Research 1997-A, Geological Survey of Canada,* 21-30.

Evenchick, C.A., Mustard, P.S., Porter, J.S. and Greig, C.J. (1992). Regional Jurassic and Cretaceous facies assemblages, and structural geology in Bowser Lake map area (104A), B.C.. *Geological Survey of Canada, Open File 2582,* 17p.

Eyles, N. (1987). Late Pleistocene debris-flow deposits in large glacial lakes in British Columbia and Alaska. *Sedimentary Geology* 53, 33-71.

Eyles, N. and Boyce, J.I. (1998). Kinematic indicators in fault gouge: tectonic analog for soft-bedded ice sheets. *Sedimentary Geology* 116, 1-12.

Eyles, N. and Clague, J.J. (1991). Glaciolacustrine sedimentation during advance and retreat of the Cordilleran Ice Sheet in central British Columbia. *Géographie physique et Quaternaire* 45, 317-331.

Farley, A.L. (1979). *Atlas of British Columbia, people, environment and resource use.* University of British Columbia Press, Vancouver, 136 p.

Foged, N. (1981). *Diatoms in Alaska*, Strauss and Cramer, Hirschberg, 317p.

Fulton, R.J. (1975). Quaternary geology and geomorphology, Nicola-Vernon area, British Columbia. *Geological Survey of Canada, Memoir* 380, 50 p.

Fulton, R.J. (1971). Radiocarbon geochronology of southern British Columbia. *Geological Survey of Canada Paper 71-37.*, 28 p.

Fulton, R.J. (1991). A conceptual model for growth and decay of the Cordilleran Ice Sheet. *Géographie physique et Quaternaire* 45, 281-286.

Geertsema, M. (1998). Flowslides in waterlain muds of northwestern British Columbia, Canada. In *8th International IAEG Congress, v. 3*, Balkema, 1913-1921.

Geertsema, M. and Schwab, J. (1995). The Mink Creek earthflow; Forest Sciences, Prince Rupert Forest Region, Extension Note 4, 5 p.

Greig, C.J. (1992). Fieldwork in the Oweegee and Snowslide Ranges and Kinskuch Lake area, northwestern British Columbia. In *Current Research, Part A, Geological Survey of Canada, Paper 92-1A*, 145-155.

Greig, C.J. and Gehrels, G.E. (1995). U-Pb zircon geochronology of Lower Jurassic and Paleozoic Stikinian strata and Tertiary intrusions, northwestern British Columbia. *Canadian Journal of Earth Sciences*, 32, 1155-1171.

Haggart, J.W. (1998). *Geology, Kiteen River, British Columbia (103P/7)*, Geological Survey of Canada Open File 3668, 1:50 000 scale map.

Hanson, G. (1921). Upper Kitsault Valley, British Columbia. *Geological Survey of Canada, Summary Report, Part A*, 7-21.

Hanson, G. (1935). Portland Canal area, British Columbia. *Geological Survey of Canada, Memoir 175*, 30-34.

Hart, J.K. (1997). The relationship between drumlins and other forms of subglacial glaciotectonic deformation. *Quaternary Science Reviews* 16, 93-107.

Hartley, B. (1996). *An atlas of British diatoms*, Biopress Ltd., Bristol, 601 p.

Henoch. W.E.S. (1967). *Glacier map of northern British Columbia and southeastern Alaska*, Glaciology Section, Inland Waters Branch, Department of Energy, Mines and Resources, Ottawa.

Huggenberger, P. (1993). Radar facies: recognition of facies patterns and heterogeneities within Pleistocene Rhine gravels, NE Switzerland, In Best, J.L. and Bristow, C.S. (eds.), *Braided Rivers*, Geological Society Special Publication 75, 163-176.

Hunter, J.A., Pullan, S.E., Burns, R.A., Gagne, R.M. and Good, R.L. (1984). Shallow seismic reflection mapping of the overburden-bedrock interface with the engineering seismograph – some simple techniques. *Geophysics* 49, 1381-1385.

Huntley, D.H., Stumpf, A., Levson, V.M. and Broster, B.E. (1996). Babine porphyry belt project: Quaternary geology and regional till geochemistry sampling in the Old Fort Mountain (93M/01) and Fulton Lake (93L/16) map areas, British Columbia. In Grant, B. and Newell, J.M. (eds.), *Geological Fieldwork 1995, British Columbia Ministry of Energy, Mines and Petroleum Resources, Paper 1996-1*, 45-53.

Hutchinson, I. (in press). Neotectonics and relative sea-level change in the Pacific Northwest. *Encyclopaedia of Quaternary Science*, Kluwer.

Jol, H.M. and Smith, D.G. (1991). Ground penetrating radar of northern lacustrine deltas, *Canadian Journal of Earth Sciences*, 28, 1939-1947.

Jol, H.M. and Smith, D.G. (1992). Geometry and structure of deltas in large lakes: a ground penetrating radar overview. In Hanninen P. and Autio, S. (eds.), *4th International Conference on Ground Penetrating Radar, Geological Survey of Finland Special Paper 16*, 159-168.

Jol, H. M., Young, R., Fisher, T.G., Smith, D. G. and Meyers, R.A. (1996). Ground penetrating radar of eskers, kame terraces, and moraines: Alberta and Saskatchewan, Canada. *Proceedings, 6th International Conference on Ground Penetrating Radar*, 439-443.

Josenhans, H., Fedje, D.F., Conway, K.W. and Barrie, J.V. (1995). Postglacial sea levels on the western Canadian continental shelf: evidence for rapid change, extensive subaerial exposure, and early human habitation. *Marine Geology* 125, 73-94.

Josenhans, H., Fedje, D.F., Pienitz, R. and Southon, J. (1997). Early humans and rapidly changing Holocene sea levels in the Queen Charlotte Islands - Hecate Strait, British Columbia, Canada. *Science* 277, 71-74.

Kerr, F.A. (1934). Glaciation in northern British Columbia. *Proceedings and Transactions of the Royal Society of Canada* 28, 17-32.

Kerr, F.A. (1936). Quaternary glaciation in the Coast Range, northern British Columbia and Alaska. *Journal of Geology* 44, 681-700.

Kirkbride, M. and Spedding, N. (1996). The influence of englacial drainage on sediment-transport pathways and till texture of temperate valley glaciers. *Annals of Glaciology* 22, 160-166.

Kor, P.S.G., Shaw, J. and Sharpe, D.R. (1991). Erosion of bedrock by subglacial meltwater, Georgian Bay, Ontario: a regional view. *Canadian Journal of Earth Sciences* 28, 623-642.

Kowall, R. and Daykin, P. (1981). British Columbia Geological Survey terrain maps: 103O/,9,16, 103P/5,6,11-14.

Levson, V.M., Stumpf, A., Meldrum, D.G., O'Brien, E.K. and Broster, B.E. (1997). Quaternary geology and ice flow history of the Babine copper porphyry belt, British Columbia (NTS 93L/NE, M/SE). In Lefebure, D.V., McMillan, W.J. and McArthur, J.G. (eds.), *Geological Fieldwork 1996, British Columbia Ministry of Employment and Investment, Energy and Minerals Division, Geological Survey Branch, Paper 1997-1*, 427-438.

Lian, O.B. (1997). *Quaternary Geology of the Fraser Valley Area, Big Bar Creek to Pavilion, South-central British Columbia*, unpublished Ph.D. thesis, University of Western Ontario, London.

Mann, D.H. and Hamilton, T.D. (1995). Late Pleistocene and Holocene paleoenvironments of the north Pacific coast. *Quaternary Science Reviews* 14, 449-471.

Mark, D.M. (1973). Analysis of axial orientation data, including till fabrics. *Geological Society of America Bulletin* 84, 1369-1374.

Mathews, W.H. (1986). Physiography of the Canadian Cordillera; *Geological Survey of Canada Map* 1701A.

McCann, S.B. and Kostaschuk, R.A. (1987). Fjord sedimentation in northern British Columbia. In Fitzgerald, D.M. and Rosen, P.S. *Glaciated Coasts*, Academic Press Inc., San Diego, 33-49.

McConnell, R.G. (1913). Portions of Portland Canal and Skeena Mining Divisions, Skeena District, B.C. *Geological Survey of Canada, Memoir 32*, 21-22.

McCuaig, S.J. (1997). Quaternary geology of the Nass River region, British Columbia. *Current Research 1997-A, Geological Survey of Canada,* 183-189.

McCullagh, J.B. (1918). *Ignis, a parable of the great lava plain in the valley of 'eternal Bloom'.* Mission Press, Aiyansh, 20p.

McPherson, J.G., Shanmugan, G. and Moiola, R.J. (1987). Fan-deltas and braid deltas: varieties of coarse-grained deltas. *Geological Society of America Bulletin* 99, 331-340.

Menzies, J. (1996). *Past Glacial Environments: sediments, forms and techniques.* Butterworth Heinemann, Oxford, 598p.

Miall, A.D. (1977). A review of the braided-river depositional environment. *Earth Science Reviews* 13, 1-62.

Miller, R.D. (1972). Surficial geology of the Juneau urban area and vicinity, Alaska: with emphasis on earthquake and other geological hazards. *United States Geological Survey Open File Report*, United States Government Printing Office, Washington, 108 p.

Miller, R.D. (1973). Gastineau Channel Formation, a composite glaciomarine deposit near Juneau, Alaska. *United States Geological Survey Bulletin 1394-C*, United States Government Printing Office, Washington, 20p.

Mitchum, R.M. Jr., Vail, P.R. and Sangree, J.B. (1977). Part 6, Stratigraphic interpretation of seismic reflection patterns in depositional sequences. In Payton, C.E. (ed.), *Seismic stratigraphy; applications to hydrocarbon exploration*, American Association of Petroleum Geologists, Memoir 26, 117-133.

Molnia, B.F. (1983). Subarctic glacial-marine sedimentation: a model. In Molnia, B.F. (ed.), *Glacial-Marine Sedimentation,* Plenum, New York, 95-143.

Moorman, B.J., Judge, A.S. and Smith, D.G. (1991). Examining fluvial sediments using ground penetrating radar in British Columbia. *Current Research, Part A. Geological Survey of Canada, Paper 91-1A*, 31-36.

Nemec, W. (1990). Aspects of sediment movement on steep delta slopes. In Colella, A. and Prior, B. (eds.), *Coarse-Grained Deltas, International Association of Sedimentologists, Special Publication 10,* Blackwell Scientific Publications, Boston, 29-73.

Østrem, G. (1972). Height of the glaciation level in northern British Columbia and southeastern Alaska. *Geografiska Annaler* 54, 39-47.

Paterson, W.S.B. (1994). *The Physics of Glaciers, third edition*, Pergamon, Oxford, p. 375-376.

Patrick, R. and Reimer, C.W. (1975). *The diatoms of the United States; exclusive of Alaska and Hawaii*, Academy of Natural Sciences of Philadelphia, Philadelphia, v. 1, 213 p, v. 2, 688 p.

Patterson, C.J. and Hooke, R.L. (1995). Physical environment of drumlin formation. *Journal of glaciology* 41, 30-38.

Patterson, R.T. and Cameron, B.E. (1993). Holocene foraminiferal faunas from cores collected on the Fraser River delta, British Columbia. *Current Research Paper 93-1A, Geological Survey of Canada*, 245-254.

Patterson, R.T. and Luternauer, J.L. (1991). Paleoenvironmental significance of the foraminiferal biofacies succession in the late Quaternary sediments of the Fraser River delta, British Columbia. *Journal of Foraminiferal Research* 21, 228-243.

Plouffe, A. (1997). Ice flow and late glacial lakes of the Fraser Glaciation, central British Columbia. In *Current Research 1997-A, Geological Survey of Canada,* 133-143.

Powell, R.D (1981). A model for sedimentation by tidewater glaciers. *Annals of Glaciology* 2, 129-134.

Powell, R.D and Molnia, B.F. (1989). Glacimarine sedimentary processes, facies and morphology of the south-southeast Alaska shelf and fjords. *Marine Geology*, 85, 359-390.

Pullan, S.E. and MacAulay, H.A. (1987). An in-hole shotgun source for engineering seismic surveys. *Geophysics* 52, 985-996.

Pullan, S.E. and Hunter, J.A. (1999). Land-based shallow seismic methods. In Gilbert, R. (ed.), *A Handbook of Geophysical Techniques for Geomorphic and Environmental Research, Geological Survey of Canada Open File* 3731, Ottawa, 31-55.

Roberts, M.C. and Rood, K.M. (1984). The role of the ice contributing area in the morphology of transverse fjords, British Columbia. *Geografiska Annaler* 66A, 381-393.

Roberts, M.C., Pullan, S.E. and Hunter, J.A. (1992). Applications of land-based high resolution seismic reflection analysis to Quaternary and geomorphic research. *Quaternary Science Reviews* 11, 557-568.

Round, F.E., Crawford, R.M., Mann, D.G., (1996). *The Diatoms: Biology and Morphology of the Genera.*, Cambridge University Press, Cambridge, 747 p.

Rust, B.R. (1978). Depositional models for braided alluvium. In Miall, A.D. (ed.), *Fluvial Sedimentology*, Canadian Society of Petroleum Geologists, Memoir 5, Calgary, 605-625.

Rust, B.R. and Koster, E.H. (1984). Coarse alluvial deposits. In Walker, R.G., (ed.), *Facies Models, Second Edition*, Geoscience Canada Reprint Series 1, Kitchener, 53-69.

Ryder, J.M. (1970). The stratigraphy and morphology of para-glacial alluvial fans in south-central British Columbia. *Canadian Journal of Earth Sciences* 8, 279-298.

Ryder, J.M. and Maynard, D. (1991). The Cordilleran Ice Sheet in northern British Columbia. *Géographie physique et Quaternaire* 45, 355-363.

Ryder, J.M., Fulton, R.J. and Clague, J.J. (1991). The Cordilleran Ice Sheet and the glacial geomorphology of southern and central British Columbia. *Géographie physique et Quaternaire* 45, 365-377.

Sharp, R.J. (1980). *The geology, geochemistry, and sulfur isotopes of the Anyox massive sulfide deposits.* Unpublished M.Sc. thesis, University of Alberta, Edmonton, 5-6, 28.

Shaw, J. (1977). Sedimentation in an alpine lake during deglaciation, Okanagan Valley, British Columbia, Canada. *Geografiska Annaler* 59, 221-240.

Shaw, J. (1983). Drumlin formation related to inverted melt-water erosional marks. *Journal of Glaciology* 29, 461-478.

Shaw, J. (1994). Hairpin erosional marks, horseshoe vortices and subglacial erosion. *Sedimentary Geology* 91, 269-283.

Shaw, J. (1996). A meltwater model for Laurentide subglacial landscapes. In McCann, S.B. and Ford, D.C. (eds.), *Geomorphology Sans Frontières,* John Wiley and Sons, Ltd., West Sussex, 181-236.

Smith, D. G. and Jol, H. M. (1995). Ground penetrating radar: antenna frequencies and maximum probable depths of penetration in Quaternary sediments. *Journal of Applied Geophysics* 33, 93-100.

Smith, D. G. and Jol, H. M. (1997). Radar structure of a Gilbert-type delta, Peyto Lake, Banff National Park, Canada, *Sedimentary Geology.*113, 195-209.

Spooner, I.S., Osborn, G.D., Barendregt, R. and Irving, E. (1996). A Middle Pleistocene (isotope stage 10) glacial sequence in the Stikine River valley, British Columbia. *Canadian Journal of Earth Sciences* 33, 1428-1438.

Steeples, D.W. and Miller, R.D. (1990). Seismic reflection methods applied to engineering, environmental and groundwater problems. In Ward, S. H. (ed.), *Geotechnical and Environmental Geophysics I, Tutorial,* Society of Exploration Geophysicists, Tulsa, 1-30.

Stevens, R. L. (1990). Proximal and distal glacimarine deposits in southwestern Sweden: contrasts in sedimentation. In Dowdeswell, J.A. and Scourse, J.D. (eds); *Glacimarine Environments: Processes and Sediments,* Geological Society Special Publication 53, 307-316.

Stumpf, A.J., Levson, V.M. and Broster, B.E. (in press). Which way did the glaciers really flow? New evidence of a major Fraser Glacial Maximum westerly ice-flow event in central British Columbia, Canada. *Canadian Journal of Earth Sciences .*

Sutherland Brown, A. (1969). Aiyansh lava flow, British Columbia. *Canadian Journal of Earth Sciences* 6, 1460-1468.

Syverson, K.M. (1995). The ability of ice-flow indicators to record complex, historic deglaciation events, Burroughs Glacier, Alaska. *Boreas* 24, 232-244.

Syvitski, J. P. M. (1993). Glaciomarine environments in Canada: an overview; *Canadian Journal of Earth Science* 30, 354-371.

Syvitski, J. P. M. and Hein, F.J. (1991). Sedimentology of an Arctic basin: Itirbilung Fiord, Baffin Island, Northwest Territories. *Geological Survey of Canada Paper 91-11*, 66p.

Syvitski, J. P. M., Burrell, D.C. and Skei, J.M. (1986). *Fjords: processes and products*. Springer-Verlag, New York, 379p.

Torrance, J.K. (1988). Mineralogy, pore-water chemistry, and geotechnical behaviour of Champlain Sea and related sediments, In Gadd, N.R. (ed.), *The Late Quaternary Development of the Champlain Sea Basin: Geological Association of Canada, Special Paper 35,* Ottawa, 157-167.

van der Meer, J.J.M. (1997). Short-lived streamlined bedforms (annual small flutes) formed under clean ice, Turtmann Glacier, Switzerland. *Sedimentary Geology* 111, 107-118.

Vanderburgh, S. and Roberts, M.C. (1996). Depositional systems and seismic stratigraphy of a Quaternary basin: north Okanagan Valley, British Columbia. *Canadian Journal of Earth Sciences*, 33, 917-927.

Vold, T. (1980). British Columbia Geological Survey terrain maps: 103O/1, 103P/3,4.

Warner, B.G., Mathewes, R.W., and Clague, J.J. (1982). Ice-free conditions on the Queen Charlotte Islands, British Columbia at the height of late Wisconsin glaciation. *Science*, 218, 675-677.

Woodcock, N.H. and Naylor, M.A. (1983). Randomness testing in three-dimensional orientation data. *Journal of Structural Geology* 5, 539-548.

# APPENDIX A

# GEOCHEMISTRY

Geochemical information was obtained on a number of till samples, a requisite part of mapping for the Geological Survey of Canada. This was not a drift prospecting study, but the results are reported here for those who might be interested (Figure A.1).

| Lab Number | Sample ID | Ag | Cu | Pb | Zn | Mo | Ni | Co | Cd | Bi | As | Sb | Fe | Mn | Te | Ba | Cr | V | Sn | W |
|---|---|---|---|---|---|---|---|---|---|---|---|---|---|---|---|---|---|---|---|---|
| 1810001 | 96JJS-01 | 0.3 | 83 | 28 | 345 | 4 | 156 | 23 | 1.4 | 6 | -5 | -5 | 7.18 | 1537 | -10 | 106 | 112 | 70 | -20 | |
| 1810002 | 96JJS-02 | 0.2 | 68 | 15 | 192 | 3 | 152 | 27 | -0.2 | -5 | -5 | -5 | 6.14 | 1163 | -10 | 148 | 105 | 62 | -20 | |
| 1810003 | 96JJS-03 | -0.2 | 66 | 19 | 181 | 4 | 141 | 27 | -0.2 | 6 | -5 | -5 | 6.19 | 1029 | -10 | 143 | 94 | 63 | -20 | |
| 1810004 | 96JJS-04 | -0.2 | 59 | 16 | 167 | 3 | 126 | 24 | 0.3 | 7 | -5 | -5 | 7.29 | 1137 | -10 | 146 | 94 | 78 | -20 | |
| 1810005 | 96JJS-05 | 0.3 | 89 | 17 | 247 | 3 | 136 | 32 | 0.4 | 6 | -5 | -5 | 7.39 | 2378 | -10 | 153 | 90 | 78 | -20 | |
| 1810006 | 96JJS-06 | 0.3 | 88 | 16 | 216 | 4 | 114 | 25 | 0.3 | 10 | -5 | -5 | 7.64 | 1680 | -10 | 118 | 78 | 77 | -20 | |
| 1810007 | 96JJS-07 | -0.2 | 110 | 24 | 247 | 4 | 142 | 41 | 0.5 | 7 | -5 | -5 | 7.7 | 3069 | -10 | 125 | 88 | 70 | -20 | |
| 1810008 | 96JJS-08 | 1.4 | 144 | 39 | 359 | 8 | 181 | 45 | 0.9 | 8 | -5 | -5 | 7.47 | 1507 | -10 | 162 | 114 | 85 | -20 | |
| 1810009 | 96JJS-09 | -0.2 | 80 | 18 | 212 | 4 | 153 | 28 | 0.6 | -5 | -5 | -5 | 7.57 | 1290 | -10 | 240 | 110 | 87 | -20 | |
| 1810010 | 96JJS-10 | 1.7 | 1277 | 25 | 1100 | 7 | 58 | 50 | 3.9 | 11 | -5 | -5 | 10 | 937 | 11 | 84 | 75 | 153 | 22 | |
| 1810011 | 96JJS-11 | 0.5 | 127 | 22 | 184 | 6 | 53 | 40 | 0.6 | 10 | -5 | -5 | 10 | 916 | 10 | 97 | 83 | 218 | 26 | |
| 1810012 | 96JJS-12 | 0.3 | 89 | 16 | 216 | 3 | 144 | 30 | 0.3 | 7 | -5 | -5 | 7.91 | 1940 | -10 | 144 | 102 | 81 | -20 | |
| 1810013 | 96JJS-13 | -0.2 | 65 | 14 | 233 | 3 | 79 | 24 | 0.3 | 8 | -5 | -5 | 7.78 | 1975 | -10 | 100 | 64 | 76 | -20 | |
| 1810014 | 96JJS-14 | 0.8 | 179 | 32 | 279 | 9 | 399 | 60 | 1.4 | 9 | 48 | -5 | 8.68 | 1160 | -10 | 126 | 142 | 83 | 21 | |
| 1810015 | 96JJS-15 | -0.2 | 51 | 32 | 263 | 5 | 19 | 20 | 1.1 | -5 | -5 | -5 | 8.46 | 2163 | -10 | 514 | 26 | 182 | 24 | |
| 1810016 | 96JJS-16 | -0.2 | 83 | 17 | 205 | 4 | 141 | 28 | 0.5 | 8 | -5 | -5 | 6.84 | 1482 | -10 | 125 | 101 | 75 | -20 | |
| 1810017 | 96JJS-17A | 0.4 | 90 | 17 | 211 | 4 | 154 | 29 | 0.8 | 6 | -5 | -5 | 7.13 | 1776 | -10 | 126 | 103 | 73 | -20 | |
| 1810018 | 96JJS-17B | 0.6 | 91 | 14 | 250 | 5 | 133 | 19 | 0.6 | 10 | -5 | -5 | 7.77 | 1905 | -10 | 134 | 99 | 80 | -20 | |
| 1810019 | 96JJS-18 | -0.2 | 81 | 13 | 223 | 4 | 118 | 26 | 0.5 | 10 | -5 | -5 | 6.95 | 1779 | -10 | 116 | 83 | 71 | -20 | |
| 1810021 | 96JJS-19 | 0.3 | 92 | 16 | 242 | 4 | 160 | 30 | 0.5 | 9 | -5 | -5 | 7.28 | 1987 | -10 | 115 | 105 | 83 | -20 | |
| 1810022 | 96JJS-20 | -0.2 | 77 | 15 | 206 | 4 | 132 | 23 | 0.8 | 8 | -5 | -5 | 6.61 | 1445 | -10 | 135 | 98 | 76 | -20 | |
| 1810023 | 96JJS-21 | -0.2 | 89 | 15 | 217 | 3 | 146 | 29 | 0.5 | 6 | -5 | -5 | 6.87 | 2072 | -10 | 138 | 110 | 85 | -20 | |
| 1810024 | 96JJS-22 | 2 | 231 | 34 | 347 | 11 | 94 | 61 | 2.8 | 11 | 39 | 9 | 8.84 | 3016 | -10 | 361 | 65 | 122 | -20 | |
| 1810025 | 96JJS-23 | 1.9 | 128 | 48 | 173 | 9 | 69 | 82 | 1.3 | 9 | 8 | -5 | 9.61 | 8688 | -10 | 137 | 117 | 68 | -20 | |
| 1810026 | 96JJS-24 | -0.2 | 171 | 24 | 179 | 5 | 83 | 37 | 0.7 | 8 | -5 | -5 | 8.29 | 2435 | -10 | 242 | 86 | 153 | -20 | |
| 1810027 | 96JJS-25 | 0.4 | 327 | 28 | 322 | 5 | 66 | 64 | 2.1 | 12 | 5 | -5 | 9.43 | 4805 | -10 | 324 | 32 | 107 | -20 | |
| 1810028 | 96JJS-26 | 0.3 | 286 | 18 | 69 | 7 | 48 | 97 | 0.5 | 14 | -5 | -5 | 10 | 11532 | 10 | 493 | 10 | 47 | -20 | |
| 1810029 | 96JJS-27 | 0.3 | 95 | 24 | 252 | 4 | 95 | 32 | 0.6 | 5 | -5 | -5 | 6.77 | 3051 | -10 | 166 | 63 | 75 | -20 | |
| 1810030 | 96JJS-28 | -0.2 | 144 | 16 | 201 | 3 | 86 | 34 | 0.5 | 6 | -5 | -5 | 6.35 | 3039 | -10 | 127 | 74 | 75 | -20 | |
| 1810031 | 96JJS-29 | -0.2 | 1070 | 26 | 137 | 2 | 3 | 7 | 0.4 | -5 | -5 | -5 | 2.88 | 857 | -10 | 184 | 4 | 57 | -20 | |
| 1810032 | 96JJS-30 | 0.3 | 71 | 12 | 187 | 3 | 106 | 22 | 0.7 | 6 | -5 | -5 | 5.55 | 1144 | -10 | 117 | 63 | 55 | -20 | |
| 1810033 | 96JJS-31 | -0.2 | 15 | 53 | 41 | 80 | 9 | -1 | 0.3 | 9 | -5 | -5 | 9.19 | 133 | 12 | 37 | 29 | 169 | 40 | |
| 1810034 | 96JJS-32 | 0.3 | 63 | 26 | 202 | 95 | 53 | 15 | 0.4 | -5 | -5 | -5 | 6.06 | 640 | -10 | 126 | 55 | 100 | -20 | |
| 1810035 | 96JJS-33 | 0.7 | 136 | 17 | 359 | 3 | 181 | 54 | 0.7 | 8 | 13 | -5 | 6.33 | 1276 | -10 | 173 | 89 | 60 | -20 | |
| 1810036 | 96JJS-34 | 0.8 | 104 | 23 | 232 | 3 | 182 | 36 | 0.4 | 6 | -5 | -5 | 5.94 | 786 | -10 | 229 | 107 | 66 | -20 | |
| 1810037 | 96JJS-35 | 0.3 | 47 | 23 | 91 | 2 | 64 | 8 | -0.2 | -5 | -5 | -5 | 2.29 | 92 | -10 | 438 | 79 | 70 | -20 | |
| 1810041 | 96JJS-36 | 0.6 | 84 | 22 | 163 | -1 | 146 | 25 | -0.2 | -5 | -5 | -5 | 4.42 | 293 | -10 | 583 | 104 | 90 | -20 | |
| 1810042 | 96JJS-37 | 0.3 | 80 | 32 | 136 | 6 | 81 | 27 | 0.6 | -5 | -5 | -5 | 6.53 | 1948 | -10 | 179 | 79 | 92 | -20 | |
| 1810043 | 96JJS-38 | 0.8 | 53 | 75 | 229 | 4 | 24 | 16 | 2.4 | -5 | -5 | -5 | 6.07 | 2714 | -10 | 433 | 25 | 61 | -20 | |
| 1810044 | 96JJS-39 | 0.8 | 83 | 26 | 136 | 6 | 46 | 7 | 0.4 | 6 | -5 | -5 | 7.51 | 418 | -10 | 62 | 55 | 88 | -20 | |
| 1810045 | 96JJS-40 | -0.2 | 96 | 25 | 94 | 5 | 95 | 15 | 0.3 | 6 | -5 | -5 | 6.55 | 408 | -10 | 94 | 301 | 106 | -20 | |
| 1810046 | 96JJS-41 | 0.9 | 110 | 29 | 183 | 3 | 36 | 27 | 1.3 | 6 | -5 | -5 | 7.13 | 2091 | -10 | 743 | 32 | 118 | -20 | |
| 1810047 | 96JJS-42 | 0.5 | 97 | 27 | 56 | 7 | 16 | 7 | 0.6 | 7 | -5 | -5 | 7.88 | 517 | -10 | 75 | 32 | 120 | -20 | |
| 1810048 | 96JJS-43 | -0.2 | 152 | 22 | 277 | 4 | 193 | 41 | 0.4 | 6 | -5 | -5 | 7.47 | 1233 | -10 | 131 | 85 | 79 | -20 | |
| 1810049 | 96JJS-44 | 0.4 | 85 | 10 | 184 | 3 | 123 | 23 | 0.8 | -5 | -5 | -5 | 6.41 | 1042 | -10 | 150 | 83 | 70 | -20 | |
| 1810050 | 96JJS-45 | -0.2 | 57 | 14 | 245 | 3 | 20 | 20 | 1.4 | 9 | -5 | -5 | 9.55 | 2177 | 11 | 194 | 12 | 186 | -20 | |
| 1810051 | 96JJS-46 | 0.3 | 72 | 10 | 164 | 2 | 136 | 21 | -0.2 | 7 | -5 | -5 | 6.26 | 1452 | -10 | 157 | 121 | 71 | -20 | |
| 1810052 | 96JJS-47 | 0.2 | 94 | 12 | 174 | 2 | 130 | 26 | 0.6 | 5 | -5 | -5 | 6.18 | 1726 | -10 | 255 | 94 | 73 | -20 | |
| 1810053 | 96JJS-48 | -0.2 | 84 | 11 | 171 | 3 | 141 | 24 | 0.4 | 6 | -5 | -5 | 6.67 | 1608 | -10 | 189 | 106 | 76 | -20 | |
| 1810054 | 96JJS-49 | -0.2 | 88 | 11 | 157 | 2 | 124 | 21 | 0.3 | 6 | -5 | -5 | 6.87 | 1332 | -10 | 137 | 98 | 80 | -20 | |
| 1810055 | 96JJS-50 | -0.2 | 112 | 12 | 199 | 3 | 156 | 26 | 0.8 | 7 | -5 | -5 | 6.92 | 1690 | -10 | 331 | 102 | 84 | -20 | |
| 1810056 | 96JJS-51 | -0.2 | 83 | 12 | 178 | 3 | 138 | 22 | 0.3 | 8 | -5 | -5 | 6.47 | 1747 | -10 | 286 | 107 | 83 | -20 | |
| 1810057 | 96JJS-52A | 0.5 | 87 | 10 | 194 | 2 | 130 | 16 | 0.4 | 8 | -5 | -5 | 7.15 | 1407 | -10 | 174 | 100 | 86 | -20 | |
| 1810058 | 96JJS-53 | -0.2 | 93 | 12 | 182 | 3 | 141 | 25 | 0.5 | 7 | -5 | -5 | 6.47 | 1829 | -10 | 159 | 100 | 83 | -20 | |
| 1810059 | 96JJS-54 | 0.3 | 124 | 13 | 227 | 4 | 161 | 34 | 0.9 | 9 | -5 | -5 | 7.34 | 2399 | -10 | 220 | 107 | 90 | -20 | |
| 1810061 | 96JJS-55 | 0.4 | 91 | 11 | 202 | 3 | 145 | 19 | 0.6 | 7 | -5 | -5 | 7.24 | 1507 | -10 | 143 | 109 | 85 | -20 | |
| 1810062 | 96JJS-56 | -0.2 | 88 | 9 | 163 | 3 | 140 | 24 | 0.4 | 8 | -5 | -5 | 6.96 | 1625 | -10 | 193 | 110 | 87 | -20 | |
| 1810063 | 96JJS-57 | -0.2 | 107 | 10 | 176 | 2 | 146 | 24 | 0.5 | 5 | -5 | -5 | 7.14 | 1281 | -10 | 214 | 110 | 86 | -20 | |
| 1810064 | 96JJS-58 | 0.2 | 107 | 12 | 185 | 3 | 135 | 23 | 0.9 | 7 | -5 | -5 | 6.76 | 1628 | -10 | 152 | 104 | 81 | -20 | |
| 1810065 | 96JJS-59 | -0.2 | 101 | 14 | 168 | 3 | 132 | 23 | 0.3 | 6 | -5 | -5 | 6.74 | 2240 | -10 | 140 | 96 | 84 | -20 | |
| 1810066 | 96JJS-60 | -0.2 | 92 | 12 | 170 | 3 | 125 | 17 | -0.2 | 7 | -5 | -5 | 6.69 | 1628 | -10 | 143 | 96 | 84 | -20 | |
| 1810067 | 96JJS-61 | -0.2 | 107 | 14 | 193 | 3 | 129 | 23 | 0.3 | 6 | -5 | -5 | 7.14 | 2255 | -10 | 188 | 98 | 85 | -20 | |
| 1810068 | 96JJS-62 | -0.2 | 84 | 14 | 166 | 3 | 124 | 15 | 0.3 | 7 | -5 | -5 | 6.15 | 1387 | -10 | 138 | 102 | 86 | -20 | |
| 1810069 | 96JJS-63 | 0.3 | 92 | 13 | 211 | 4 | 123 | 19 | 0.4 | 8 | -5 | -5 | 7.27 | 2144 | -10 | 230 | 97 | 78 | -20 | |
| 1810070 | 96JJS-64 | -0.2 | 103 | 8 | 212 | 3 | 116 | 17 | 0.3 | -5 | -5 | -5 | 7.33 | 1369 | -10 | 205 | 84 | 70 | -20 | |
| 1810071 | 96JJS-65 | 0.2 | 96 | 9 | 222 | 4 | 133 | 24 | 0.7 | 6 | -5 | -5 | 7.05 | 2097 | -10 | 206 | 98 | 77 | -20 | |
| 1810072 | 96JJS-66 | 0.3 | 140 | 22 | 212 | 5 | 139 | 34 | 0.9 | 7 | -5 | -5 | 7.87 | 3174 | -10 | 152 | 106 | 88 | -20 | |
| 1810073 | 96JJS-67 | 0.7 | 138 | 15 | 250 | 4 | 159 | 24 | 0.6 | 7 | -5 | -5 | 6.67 | 2756 | -10 | 203 | 115 | 90 | -20 | |

PROJECT 23397-5-0107 #SAMPLES: 90 REFERENCE: S.O. 23397-5-107-SS

IS: Insufficient Sample

-9: No Value Recorded

Values above the upper limit

Values below the lower limit

Figure A.1. Till geochemistry and UTM locations of samples.

| Ba | Cr | V | Sn | W | La | Al | Mg | Ca | Na | K | Sr | Y | Ga | Li | Nb | Sc | Ta | Ti | Zr | Easting | Northing |
|---|---|---|---|---|---|---|---|---|---|---|---|---|---|---|---|---|---|---|---|---|---|
| 106 | 112 | 70 | -20 | -20 | 6 | 3.21 | 2.67 | 0.32 | 0.25 | 0.25 | 23 | 9 | 4 | 39 | 1 | 8 | -10 | 0.03 | -1 | 469271 | 6144869 |
| 148 | 105 | 62 | -20 | -20 | 4 | 3.03 | 2.47 | 0.28 | 0.18 | 0.21 | 26 | 7 | 5 | 44 | -1 | 6 | -10 | 0.02 | 3 | 479650 | 6144410 |
| 143 | 94 | 63 | -20 | -20 | 6 | 3.12 | 2.33 | 0.25 | 0.22 | 0.24 | 33 | 7 | 5 | 48 | 1 | 6 | -10 | -0.01 | 3 | 490790 | 6142090 |
| 146 | 94 | 78 | -20 | -20 | 4 | 3.76 | 2.33 | 0.23 | 0.30 | 0.15 | 22 | 7 | 6 | 44 | 1 | 7 | -10 | -0.01 | 6 | 473259 | 6100735 |
| 153 | 90 | 78 | -20 | -20 | 4 | 3.40 | 2.54 | 0.25 | 0.21 | 0.26 | 37 | 6 | 4 | 47 | 1 | 8 | -10 | 0.02 | 3 | 478425 | 6095050 |
| 118 | 78 | 77 | -20 | -20 | 7 | 3.70 | 2.55 | 0.33 | 0.20 | 0.23 | 31 | 6 | 4 | 52 | 1 | 7 | -10 | 0.02 | 3 | 479163 | 6103796 |
| 125 | 88 | 70 | -20 | -20 | 7 | 4.18 | 2.23 | 0.12 | 0.30 | 0.18 | 17 | 7 | 3 | 41 | 1 | 7 | -10 | 0.02 | 3 | 496657 | 6112456 |
| 162 | 114 | 85 | -20 | -20 | 9 | 5.23 | 2.35 | 0.18 | 0.59 | 0.23 | 50 | 15 | 6 | 74 | 1 | 13 | -10 | -0.01 | 8 | 498572 | 6106309 |
| 240 | 110 | 87 | -20 | -20 | 7 | 3.93 | 3.08 | 0.36 | 0.20 | 0.29 | 55 | 6 | 6 | 47 | 1 | 7 | -10 | 0.04 | 4 | 498572 | 6106309 |
| 84 | 75 | 153 | 22 | -20 | 19 | 5.80 | 3.05 | 0.81 | 0.58 | 0.30 | 37 | 10 | 8 | 25 | 2 | 11 | -10 | 0.04 | -1 | 447720 | 6143320 |
| 97 | 83 | 218 | 26 | -20 | 13 | 6.04 | 4.02 | 1.12 | 0.42 | 0.29 | 34 | 5 | 12 | 26 | 2 | 12 | -10 | 0.15 | 3 | 447610 | 6143630 |
| 144 | 102 | 81 | -20 | -20 | 5 | 3.55 | 2.61 | 0.27 | 0.27 | 0.21 | 30 | 6 | 4 | 41 | 1 | 8 | -10 | 0.03 | 2 | 481283 | 6109023 |
| 100 | 64 | 76 | -20 | -20 | 9 | 3.88 | 2.58 | 0.63 | 0.19 | 0.20 | 36 | 6 | 6 | 66 | 1 | 6 | -10 | 0.02 | 1 | 481279 | 6104082 |
| 126 | 142 | 83 | 21 | -20 | 17 | 3.90 | 2.72 | 0.29 | 0.34 | 0.23 | 33 | 15 | 7 | 45 | 2 | 11 | -10 | 0.01 | -1 | 473100 | 6142950 |
| 514 | 26 | 182 | 24 | -20 | 15 | 5.27 | 3.29 | 1.63 | 0.35 | 2.05 | 91 | 5 | 12 | 40 | 1 | 12 | -10 | 0.35 | 4 | 449490 | 6155910 |
| 125 | 101 | 75 | -20 | -20 | 4 | 3.28 | 2.55 | 0.29 | 0.18 | 0.19 | 30 | 6 | 5 | 46 | -1 | 7 | -10 | -0.01 | 3 | 497810 | 6154625 |
| 126 | 103 | 73 | -20 | -20 | 6 | 3.30 | 2.48 | 0.26 | 0.20 | 0.22 | 29 | 7 | 4 | 46 | 1 | 7 | -10 | -0.01 | 2 | 496325 | 6157750 |
| 134 | 99 | 80 | -20 | -20 | 6 | 3.54 | 2.47 | 0.25 | 0.25 | 0.21 | 28 | 7 | 5 | 53 | 1 | 8 | -10 | -0.01 | 2 | 496325 | 6157750 |
| 116 | 83 | 71 | -20 | -20 | 4 | 3.08 | 2.21 | 0.23 | 0.21 | 0.21 | 25 | 6 | 4 | 48 | 1 | 8 | -10 | -0.01 | 2 | 497150 | 6163675 |
| 115 | 105 | 83 | -20 | -20 | 6 | 3.38 | 2.53 | 0.31 | 0.19 | 0.19 | 28 | 7 | 4 | 47 | 1 | 8 | -10 | -0.01 | 3 | 490476 | 6172366 |
| 135 | 98 | 76 | -20 | -20 | 5 | 3.20 | 2.46 | 0.42 | 0.17 | 0.22 | 38 | 7 | 5 | 46 | -1 | 7 | -10 | 0.01 | 3 | 488114 | 6174399 |
| 138 | 110 | 85 | -20 | -20 | 5 | 3.44 | 2.62 | 0.39 | 0.19 | 0.21 | 34 | 7 | 5 | 47 | 1 | 7 | -10 | -0.01 | 3 | 485725 | 6178475 |
| 361 | 65 | 122 | -20 | -20 | 12 | 3.10 | 2.49 | 0.44 | 0.44 | 0.26 | 51 | 9 | 2 | 33 | 2 | 11 | -10 | -0.01 | -1 | 443310 | 6194350 |
| 137 | 117 | 68 | -20 | -20 | 14 | 6.48 | 1.21 | 0.09 | 1.16 | 0.17 | 7 | 26 | -2 | 21 | 3 | 12 | -10 | 0.04 | 29 | 463190 | 6172480 |
| 242 | 86 | 153 | -20 | -20 | 16 | 3.75 | 2.91 | 1.00 | 0.32 | 0.26 | 45 | 10 | 4 | 41 | 1 | 12 | -10 | 0.07 | 5 | 463900 | 6171478 |
| 324 | 32 | 107 | -20 | -20 | 16 | 2.80 | 1.89 | 0.87 | 0.37 | 0.34 | 49 | 13 | -2 | 28 | 2 | 17 | -10 | 0.01 | 2 | 464490 | 6171460 |
| 493 | 10 | 47 | -20 | -20 | 15 | 2.07 | 1.20 | 0.21 | 0.41 | 0.20 | 15 | 20 | 11 | 23 | 2 | 22 | -10 | -0.01 | -1 | 462310 | 6174220 |
| 166 | 63 | 75 | -20 | -20 | 11 | 4.38 | 1.75 | 0.02 | 0.44 | 0.30 | 6 | 6 | 5 | 52 | 2 | 6 | -10 | 0.01 | 11 | 463133 | 6174192 |
| 127 | 74 | 75 | -20 | -20 | 10 | 4.09 | 1.67 | 0.03 | 0.52 | 0.22 | 4 | 5 | 3 | 49 | 1 | 9 | -10 | -0.01 | 4 | 472233 | 6161210 |
| 184 | 4 | 57 | -20 | -20 | 7 | 1.99 | 1.60 | 0.93 | 0.20 | 0.34 | 21 | 3 | 3 | 21 | -1 | 8 | -10 | -0.01 | 2 | 477725 | 6167860 |
| 117 | 63 | 55 | -20 | -20 | 11 | 2.57 | 1.73 | 0.31 | 0.21 | 0.26 | 31 | 6 | 4 | 54 | -1 | 6 | -10 | 0.01 | 2 | 478390 | 6190580 |
| 37 | 29 | 169 | 40 | -20 | 39 | 2.65 | 0.24 | 0.02 | 1.45 | 0.11 | 5 | 6 | 112 | 8 | 57 | -5 | -10 | 0.26 | 20 | 454188 | 6155006 |
| 126 | 55 | 100 | -20 | -20 | 22 | 6.08 | 1.95 | 0.17 | 0.54 | 0.26 | 14 | 11 | 13 | 48 | 4 | 7 | -10 | 0.17 | 10 | 453889 | 6154653 |
| 173 | 89 | 60 | -20 | -20 | 8 | 3.04 | 1.99 | 0.17 | 0.28 | 0.29 | 37 | 7 | 6 | 55 | 1 | 8 | -10 | -0.01 | 1 | 488897 | 6145851 |
| 229 | 107 | 66 | -20 | -20 | 13 | 3.59 | 2.06 | 0.27 | 0.43 | 0.23 | 23 | 6 | 9 | 78 | 1 | 9 | -10 | 0.01 | 4 | 484896 | 6146214 |
| 438 | 79 | 70 | -20 | -20 | 5 | 3.78 | 1.03 | 0.24 | 0.64 | 0.20 | 220 | 6 | 9 | 63 | 1 | 8 | -10 | -0.01 | 4 | 488370 | 6148737 |
| 583 | 104 | 90 | -20 | -20 | 7 | 3.74 | 1.61 | 0.21 | 0.36 | 0.14 | 47 | 4 | 8 | 66 | -1 | 8 | -10 | -0.01 | 1 | 488799 | 6148711 |
| 179 | 79 | 92 | -20 | -20 | 15 | 5.83 | 1.68 | 0.06 | 0.66 | 0.16 | 8 | 7 | 8 | 27 | 2 | 6 | -10 | 0.12 | 5 | 467572 | 6140034 |
| 433 | 25 | 61 | -20 | -20 | 34 | 2.45 | 1.72 | 0.38 | 0.94 | 0.49 | 52 | 14 | 9 | 36 | -1 | 7 | -10 | 0.06 | -1 | 465760 | 6129920 |
| 62 | 55 | 88 | -20 | -20 | 17 | 6.80 | 1.03 | 0.11 | 1.00 | 0.14 | 8 | 6 | 13 | 19 | 12 | -5 | -10 | 0.09 | 24 | 444462 | 6127940 |
| 94 | 301 | 106 | -20 | -20 | 15 | 6.74 | 2.13 | 0.20 | 0.51 | 0.21 | 13 | 8 | 15 | 27 | 14 | -5 | -10 | 0.14 | 20 | 434317 | 6184277 |
| 743 | 32 | 118 | -20 | -20 | 21 | 3.58 | 2.52 | 1.33 | 0.61 | 0.28 | 130 | 8 | 9 | 34 | 1 | 7 | -10 | 0.1 | 3 | 444000 | 6177350 |
| 75 | 32 | 120 | -20 | -20 | 16 | 8.77 | 0.71 | 0.09 | 1.26 | 0.16 | 8 | 8 | 9 | 12 | 9 | 5 | -10 | 0.14 | 49 | 447620 | 6162079 |
| 131 | 85 | 79 | -20 | -20 | 15 | 6.35 | 1.89 | 0.05 | 0.51 | 0.27 | 9 | 5 | 9 | 57 | 2 | -5 | -10 | 0.04 | 1 | 480500 | 6098815 |
| 150 | 83 | 70 | -20 | -20 | 11 | 3.00 | 1.85 | 0.30 | 0.25 | 0.26 | 41 | 6 | 5 | 44 | -1 | 7 | -10 | 0.03 | 1 | 487890 | 6122700 |
| 194 | 12 | 186 | -20 | -20 | 24 | 4.32 | 2.70 | 1.03 | 0.30 | 0.24 | 52 | 8 | 10 | 48 | 1 | 10 | -10 | 0.09 | 3 | 474292 | 6202950 |
| 157 | 121 | 71 | -20 | -20 | 14 | 3.19 | 2.12 | 0.30 | 0.22 | 0.20 | 29 | 6 | 7 | 51 | -1 | 5 | -10 | 0.03 | 4 | 490810 | 6199675 |
| 255 | 94 | 73 | -20 | -20 | 11 | 3.09 | 2.05 | 0.38 | 0.23 | 0.19 | 55 | 7 | 6 | 46 | -1 | 6 | -10 | 0.01 | 2 | 487210 | 6138950 |
| 189 | 106 | 76 | -20 | -20 | 12 | 3.44 | 2.23 | 0.34 | 0.17 | 0.19 | 44 | 6 | 7 | 47 | -1 | 6 | -10 | 0.01 | 4 | 484610 | 6137990 |
| 137 | 98 | 80 | -20 | -20 | 14 | 3.65 | 2.19 | 0.48 | 0.24 | 0.20 | 41 | 6 | 7 | 47 | -1 | 6 | -10 | 0.03 | 1 | 493710 | 6118175 |
| 331 | 102 | 84 | -20 | -20 | 10 | 3.77 | 2.13 | 0.30 | 0.29 | 0.18 | 34 | 7 | 7 | 37 | -1 | 8 | -10 | -0.01 | 2 | 499710 | 6182350 |
| 286 | 107 | 83 | -20 | -20 | 10 | 3.30 | 2.18 | 0.37 | 0.21 | 0.21 | 49 | 7 | 8 | 50 | -1 | 6 | -10 | -0.01 | 3 | 496750 | 6181875 |
| 174 | 100 | 86 | -20 | -20 | 11 | 3.41 | 2.10 | 0.50 | 0.28 | 0.21 | 34 | 7 | 7 | 45 | -1 | 7 | -10 | 0.02 | 3 | 489790 | 6201695 |
| 159 | 100 | 83 | -20 | -20 | 10 | 3.18 | 2.19 | 0.39 | 0.18 | 0.20 | 40 | 7 | 6 | 46 | -1 | 6 | -10 | -0.01 | 3 | 487900 | 6199610 |
| 220 | 107 | 90 | -20 | -20 | 11 | 3.48 | 2.31 | 0.30 | 0.26 | 0.21 | 37 | 7 | 6 | 47 | 1 | 8 | -10 | 0.01 | 3 | 490916 | 6196841 |
| 143 | 109 | 85 | -20 | -20 | 11 | 3.36 | 2.17 | 0.32 | 0.28 | 0.19 | 27 | 7 | 7 | 45 | 1 | 7 | -10 | 0.01 | 3 | 492308 | 6192874 |
| 193 | 110 | 87 | -20 | -20 | 11 | 3.56 | 2.30 | 0.47 | 0.21 | 0.19 | 44 | 7 | 7 | 45 | -1 | 7 | -10 | 0.01 | 4 | 495262 | 6189628 |
| 214 | 110 | 86 | -20 | -20 | 12 | 3.71 | 2.28 | 0.40 | 0.26 | 0.18 | 31 | 7 | 8 | 41 | -1 | 7 | -10 | -0.01 | 3 | 499990 | 6185210 |
| 152 | 104 | 81 | -20 | -20 | 11 | 3.48 | 2.17 | 0.41 | 0.27 | 0.18 | 28 | 7 | 7 | 39 | -1 | 7 | -10 | 0.01 | 2 | 494050 | 6203200 |
| 140 | 96 | 84 | -20 | -20 | 11 | 4.09 | 1.91 | 0.04 | 0.29 | 0.21 | 7 | 4 | 6 | 40 | 1 | 6 | -10 | 0.02 | 1 | 489961 | 6202382 |
| 143 | 96 | 84 | -20 | -20 | 9 | 4.14 | 1.87 | 0.02 | 0.29 | 0.19 | 6 | 3 | 6 | 43 | 1 | 6 | -10 | -0.01 | 1 | 488902 | 6201826 |
| 188 | 98 | 85 | -20 | -20 | 11 | 3.90 | 1.86 | 0.07 | 0.29 | 0.18 | 10 | 5 | 6 | 41 | 1 | 8 | -10 | 0.02 | 1 | 488524 | 6197414 |
| 138 | 102 | 86 | -20 | -20 | 8 | 4.52 | 1.91 | 0.02 | 0.32 | 0.17 | 4 | 5 | 8 | 50 | 1 | 6 | -10 | -0.01 | 3 | 492308 | 6192874 |
| 230 | 97 | 78 | -20 | -20 | 9 | 3.50 | 1.83 | 0.15 | 0.41 | 0.21 | 28 | 5 | 6 | 54 | 1 | 8 | -10 | -0.01 | 2 | 498125 | 6159850 |
| 205 | 84 | 70 | -20 | -20 | 10 | 3.11 | 1.68 | 0.25 | 0.29 | 0.22 | 32 | 5 | 5 | 50 | -1 | 8 | -10 | -0.01 | 2 | 497185 | 6163750 |
| 206 | 98 | 77 | -20 | -20 | 11 | 3.06 | 1.93 | 0.28 | 0.31 | 0.20 | 35 | 7 | 5 | 47 | -1 | 8 | -10 | -0.01 | 2 | 488710 | 6173350 |
| 152 | 106 | 88 | -20 | -20 | 12 | 4.34 | 1.80 | 0.04 | 0.41 | 0.21 | 7 | 15 | 6 | 45 | 1 | 12 | -10 | 0.01 | 4 | 486438 | 6176651 |
| 203 | 115 | 90 | -20 | -20 | 11 | 4.85 | 1.87 | 0.08 | 0.49 | 0.20 | 16 | 11 | 7 | 59 | -1 | 9 | -10 | -0.01 | 6 | 485775 | 6178475 |

Values above the upper limit are shown as +uplimt

Values below the lower limit are shown as -lolmt (ie not detected)

# APPENDIX B

## WEIGHT DROP

This appendix contains the plans for making a weight drop device (Figures B.1 and B.2). The weight drop device is rather heavy and must be moved with a heavy duty hand cart.

A few problems were encountered with the prototype. A handle attached to the base broke off due to metal fatigue and the base of the pipe eventually broke due to the strain of being lifted on to the hand cart. The pipe was welded during the field season, but broke again at the weld. Modifications to the design were done in the fall of 1997, and included a solid steel shank fit inside the pipe at the base, and lugs on the base instead of a handle (Figure B.1). Rope can be threaded through the lugs for lifting the device onto and off of the hand cart.

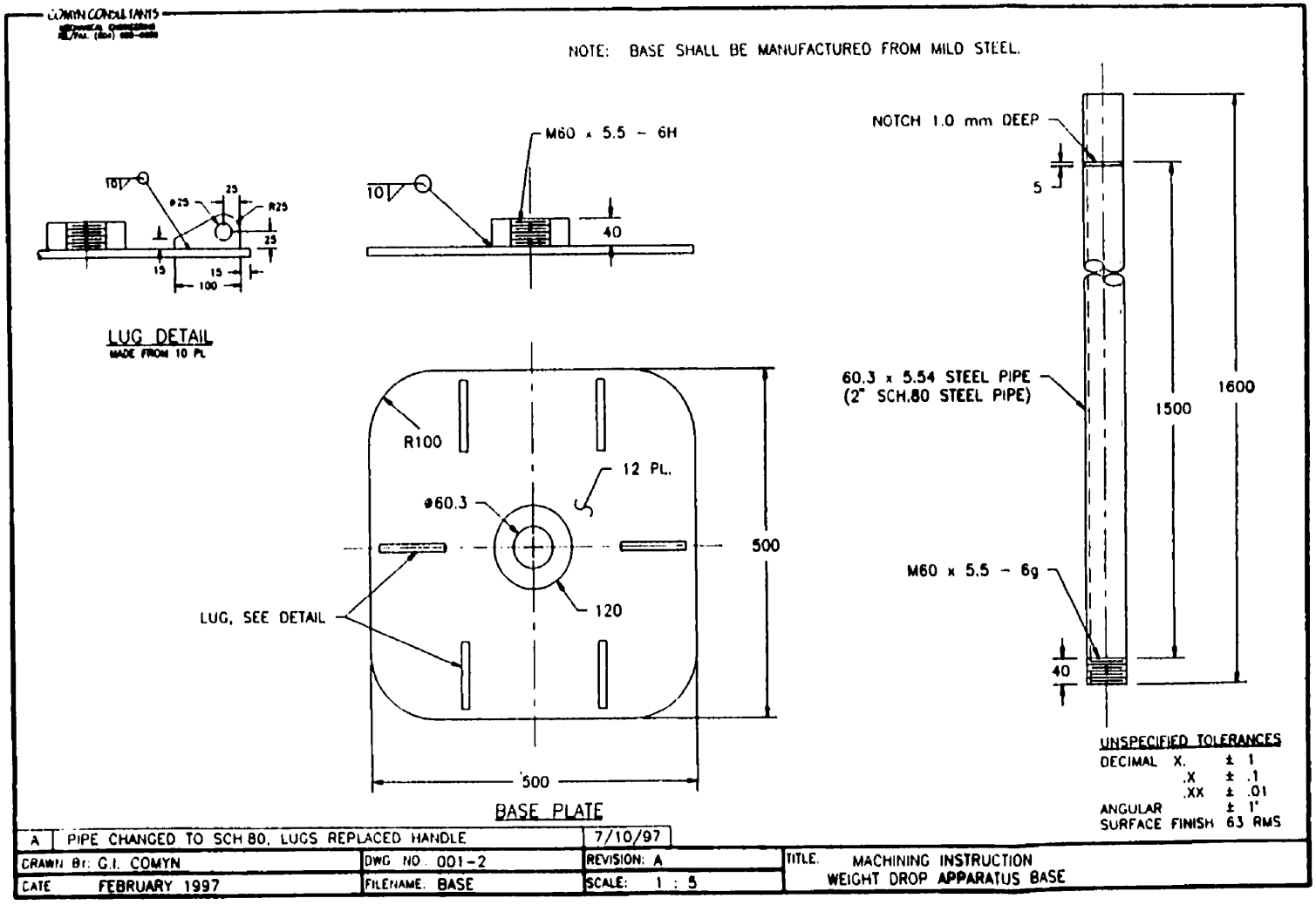


Figure B.1. Machining instructions for the weight drop device. The handle which broke off due to metal fatigue is here replaced with metal lugs through which ropes can be threaded for lifting the device onto a hand cart.

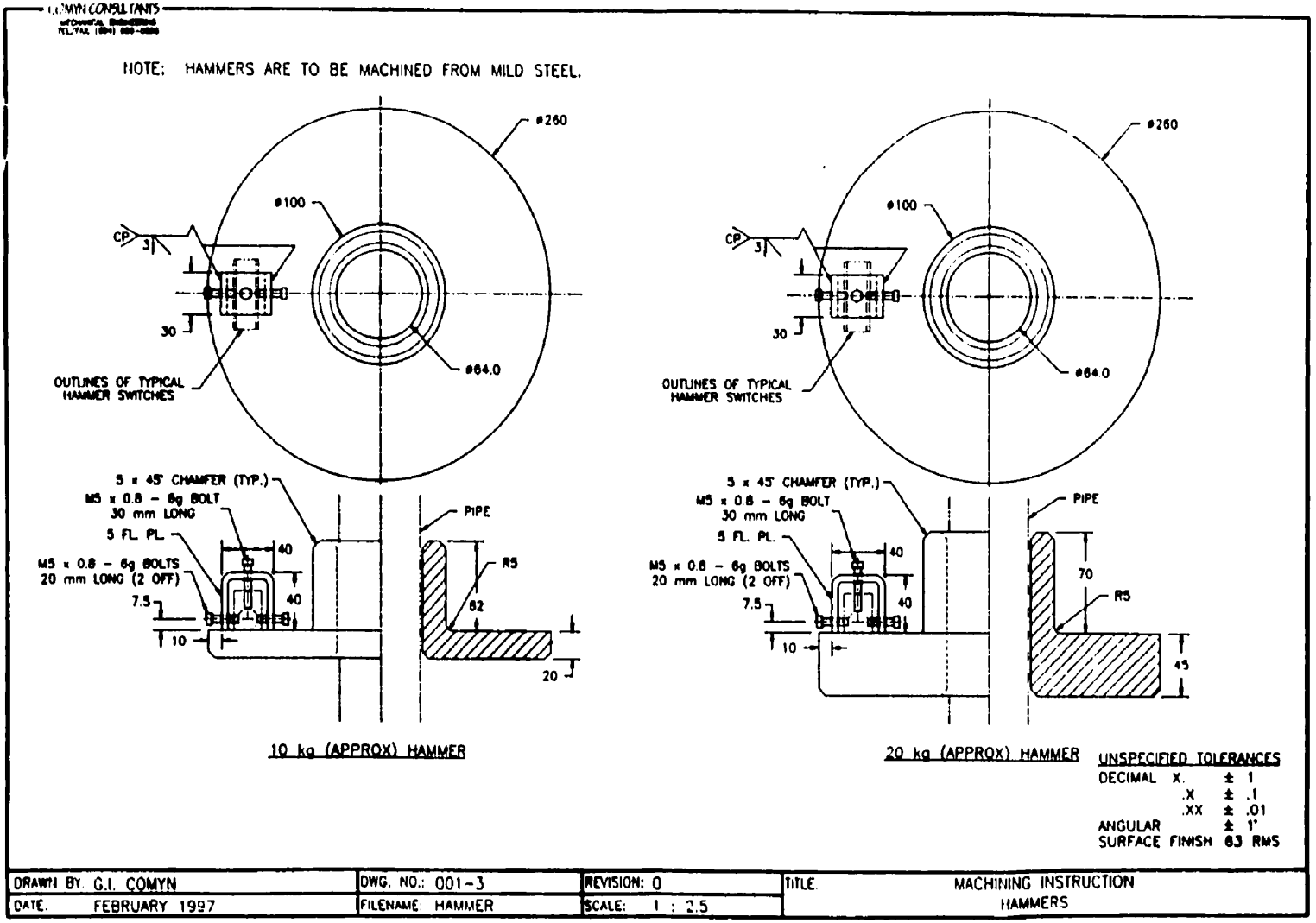


Figure B.2. Machining instructions for the weight drop weights. The seismograph trigger is wrapped with electrical tape and is then attached to the weight with screws. Impact is thus perpendicular to switch length, allowing proper trigger function.

APPENDIX C
CMP DATA

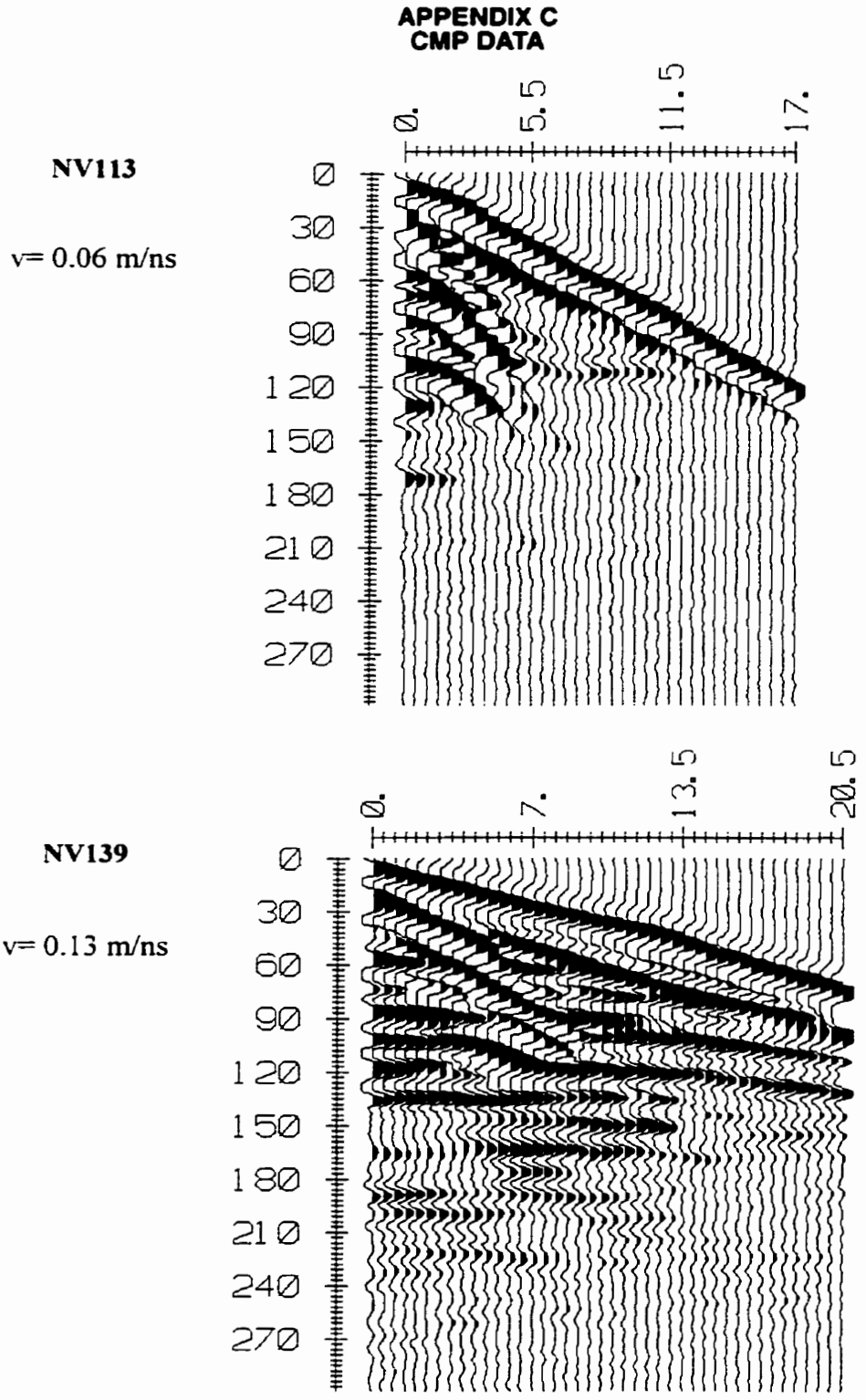


Figure C.1. Examples of CMP (common mid-point) data. The upper cmp survey, which applies to lines NV113-118, is difficult to interpret. Section evidence was used to determine a more accurate velocity. The lower cmp survey applies to lines NV139-140.

# APPENDIX D

# APPLICATIONS

## Engineering Properties of Glacial Sediments

Till and bedrock are the best substrates for building foundations, however till has poor drainage qualities.

Glaciomarine clays make poor building sites because their low bearing strengths, tendency to liquefy, poor drainage and propensity for water expulsion under load result in subsidence and downslope movement.

The abundant gravelly glaciofluvial deposits are well drained, easy to excavate and have a high bearing capacity (can hold a significant weight without subsiding). However, in areas where these deposits overlie thick glaciomarine clay that is undercut by rivers (*e.g.* earthflow area in northeast part of Nass Valley map), their stability is questionable. Other sites where earthflows have not occurred may still be problematic building sites because the weight of a structure may cause underlying glaciomarine sediments to fail as they did during the construction of the Alcan smelter in Kitimat (Clague, 1984b). An example of such an area is the Nass Braidplain North Delta (number 5 in Figure 7.34).

Although alluvial and colluvial fans are coarse-grained and have high bearing strengths, building is not advised due to the danger of future debris flows, rock falls or other catastrophic events in their vicinity.

## Groundwater

Glacial sediments in the Nass valley are abundant; some make excellent aquifers, some do not.

Interbedded proximal glaciomarine gravel and sand, make excellent aquifers. As these deposits are commonly overlain by clay, it is possible for artesian conditions to exist, but that

depends on the attitude of the proximal deposit. If it tilts toward the surface and becomes recharged by rainfall, then downslope artesian conditions could conceivably occur. However, no artesian conditions were encountered in any of our drill holes. If a well is drilled in surface clay, it would be wise to attempt to hit the proximal glaciomarine deposits that may exist at depth. If till is encountered directly beneath the clay (which is highly possible), the well will be very poor and drilling should be tried elsewhere.

Braidplain and braid delta deposits act as unconfined aquifers because they rest on impermeable deposits such as glaciomarine clay or till. The position of the water table is highly dependent on weather.

Fan deltas, alluvial fans and colluvial fans are aquifers of intermediate quality due to their limited recharge areas and variable underlying deposits. In addition, limited lateral continuity of permeable (non-diamicton) sediments limits groundwater flow in these types of deposits.

Till almost invariably overlies bedrock and is an extremely poor groundwater source. Once till has been encountered by drilling, there is no point in drilling further.

## Aggregate Resources

The Nass Valley is especially rich in glaciofluvial deposits. The rounded gravel and sand of these units are a good source of aggregate for road building, for fill, and for use in concrete and asphalt. In some parts of B.C., such deposits are commonly not available due to coverage by urban sprawl. This is not the case in the Nass Valley, so aggregate or concrete production may be viable industries there. Forests could be replanted in the underlying glaciomarine clay after gravel removal to minimize the environmental impact of such operations.

Glaciofluvial deposits are relatively scarce in other parts of the study area. Alluvial fans can be used as aggregate resources, but they contain much more fine-grained material that would have to be sieved out.

## Potential Hazards

The high precipitation levels, seismic activity and mountainous nature of the area predispose it to landslides, debris flows, snow avalanches and earthflows.

Slumps and landslides in till and glaciofluvial sediments are common where they are undercut by river flow or road construction. Till can hold a steeper face than gravel and is less susceptible to slumping than gravel, but it is still a problem as it also fails (Figure D.1).

The numerous debris flows and landslides on mountain slopes show that sudden catastrophic failure is very common in this region. Debris flows will likely occur again in areas of past activity (marked on maps by debris flow tracks), particularly when heavy autumn rains and storms cause oversaturation of slope sediments. Rock slides and rock avalanches may be triggered by earthquakes, so their future locations are less predictable, although they are more likely to occur on mountain sides where bedrock fractures and faults dip in a downslope direction.

Avalanche tracks are also shown on the maps. Snow avalanches can be serious road and logging hazards.

Flowslides or earthflows have occurred in glaciomarine clays overlain by glaciofluvial gravel in the Nass Valley and at Kitsault. The Kitsault slide occurred at the edge of the 230 m delta (see Deltas, Chapter 4), where gravel overlies silty clay. The base of the clay is subject to wave erosion in Alice Arm. Part of a trailer park succumbed to the slide and the area is currently fenced off. The Nass Valley earthflows are shown on Nass Valley map. All have occurred because of fluvial incision into gravel and clay. Undercutting by streams into steep glaciomarine clay banks seems to be an important mechanism in earthflow generation. Another important factor is that the glaciomarine clay is likely a sensitive clay, or one prone to this type of failure (see SEM Analysis, Appendix E). Similar earthflows have occurred in glaciomarine sediments near Terrace (Clague, 1978, Geertsema and Schwab, 1995).

Given the status of earthflows that have already occurred, areas of predicted future instability are those where glaciomarine clay is undercut by stream or wave action. Overlying glaciofluvial gravels are probably not necessary for sliding to occur, they are simply a common

Figure D.1. Debris slide from till slope adjacent to logging road. Figure for scale is circled.

overlying deposit in the region. Areas of possible future instability (see both maps for locations) include the following: 1) the Kitsault Delta area, 2) the Anyox delta area, 3) the Donahue Creek delta, 4) the Sutton and Kshwan braidplains, 5) the Greenville delta area, 6) parts of the Aiyansh Braidplain that have been strongly undercut (*e.g.* Kiteen River area, Seaskinnish Creek mouth area), 7) the Shumal Creek area (upstream of alluvial fan) and 8) all areas of glaciomarine blanket or glaciofluvial blanket/braidplain/delta that are subject to wave or river erosion.

Areas where the glaciomarine clay is not thick (*e.g.* the Tseax Creek Section) or where glaciofluvial deposits are underlain by bedrock (*e.g.* New Aiyansh delta) should be reasonably stable.

At Kitsault, the slide deposit may protect the surrounding area because it keeps wave action away from the unaffected glaciomarine sediments. However, areas adjacent to it are at risk. Damming of the river at Anyox may have reduced the potential for sliding there. The creek at Greenville does not seem to be eroding into marine sediments (because it is rip-rapped?), so it is safe there for the moment, however, a watch should be kept on it and buildings should be kept away from Greenville Creek. Gitwinksilkw's glaciomarine deposits appear to be mainly proximal gravelly deposits, so sliding is unlikely there. Earthflows have occurred recently on the Aiyansh Braidplain at the Kiteen River section (Figure D.2), and more can be expected in this area. The Kiteen bridge is an area that is now incised to bedrock, but a change in direction of the river could cause problems on the braidplain just to the northeast. Seaskinnish Creek is also incised into bedrock near its mouth, but upstream areas may be susceptible to sliding.

All of the earthflows in the Nass Valley at the north end of Nass Valley map are inactive because streams are currently incised into bedrock. However, upstream areas that are incised into clay are likely still hazardous.

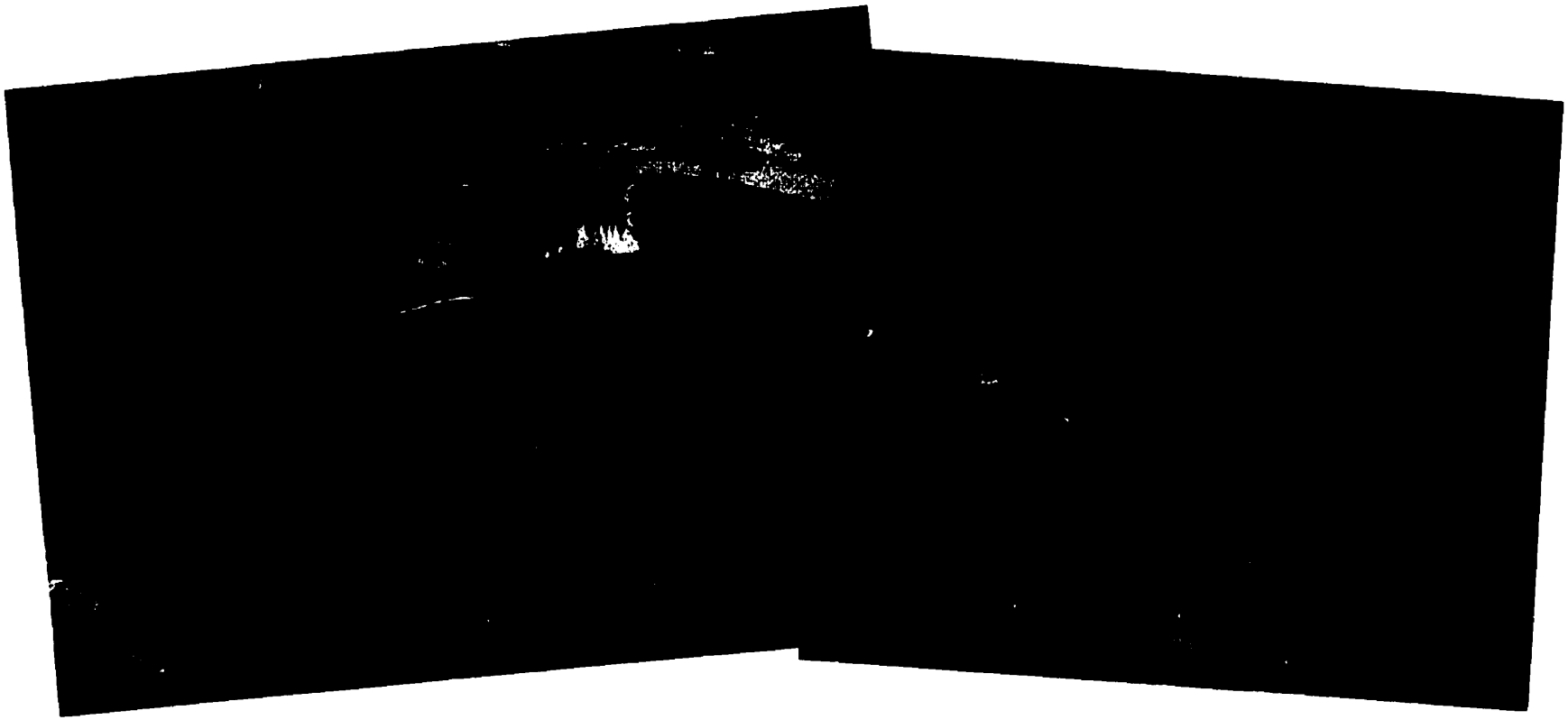

Figure D.2. Earthflow in glaciomarine sediments overlain by glaciofluvial gravels, Kiteen River. The Kiteen River Section is visible in the background.

# APPENDIX E

# RADIOCARBON DATING AND MICROPALEONTOLOGICAL ANALYSES

## Radiocarbon Dating

A number of organic samples were radiocarbon dated to determine the timing of glacial events. Their locations are shown in Figure E.1 and the dates are listed in Table E.1. Bulk dates were done at the Geological Survey of Canada (lab numbers starting with GSC) and Accelerator Mass Spectrometry (AMS) dates were done at IsoTrace Labs (TO) and Beta Analytic (Beta).

| Sample | Easting | Northing | Material | Lab Number | Age (years BP) |
|---|---|---|---|---|---|
| R1 | 469728 | 6103111 | deciduous bark | GSC-6161 | modern |
| R2 | 476514 | 6096501 | leaf fragment | TO-6352 | modern |
| R5 | 481279 | 6104082 | woody detritus | GSC-6164 | 1960 ± 50 |
| R7 | 496875 | 6164400 | terrestrial moss | TO-6354 | 27 130 ± 280 |
| R7 | 496875 | 6164400 | *Equisetum* sp. | Beta-124778 | 30 080 ± 170 |
| R8 | 464060 | 6097250 | deciduous wood (*Salix?*) | GSC-6147 | 590 ± 60 |
| R12 | 492038 | 6118953 | deciduous wood | GSC-6150 | 280 ± 50 |
| R13 | 506910 | 6137750 | peat | Beta-130442 | 2830 ± 40 |

Table E.1. Radiocarbon dates.

The two modern dates, R1 and R2, were derived from samples collected from a Holocene alluvial fan and a glaciolacustrine deposit. The alluvial fan sample (R1) was overlain by 50 cm of horizontally and cross-laminated very fine- to medium-grained sand, and another 50 cm of cobble gravel. The section was incised down to 4.5 m by the modern stream channel. Evidently the aggradation and incision all occurred in recent times. The glaciolacustrine sample (R2) was found at an elevation of 350 m, was enclosed in clay, and was overlain and underlain by glaciofluvial gravel, sand and silt. This deposit cannot be modern, so the leaf fragment must have been a

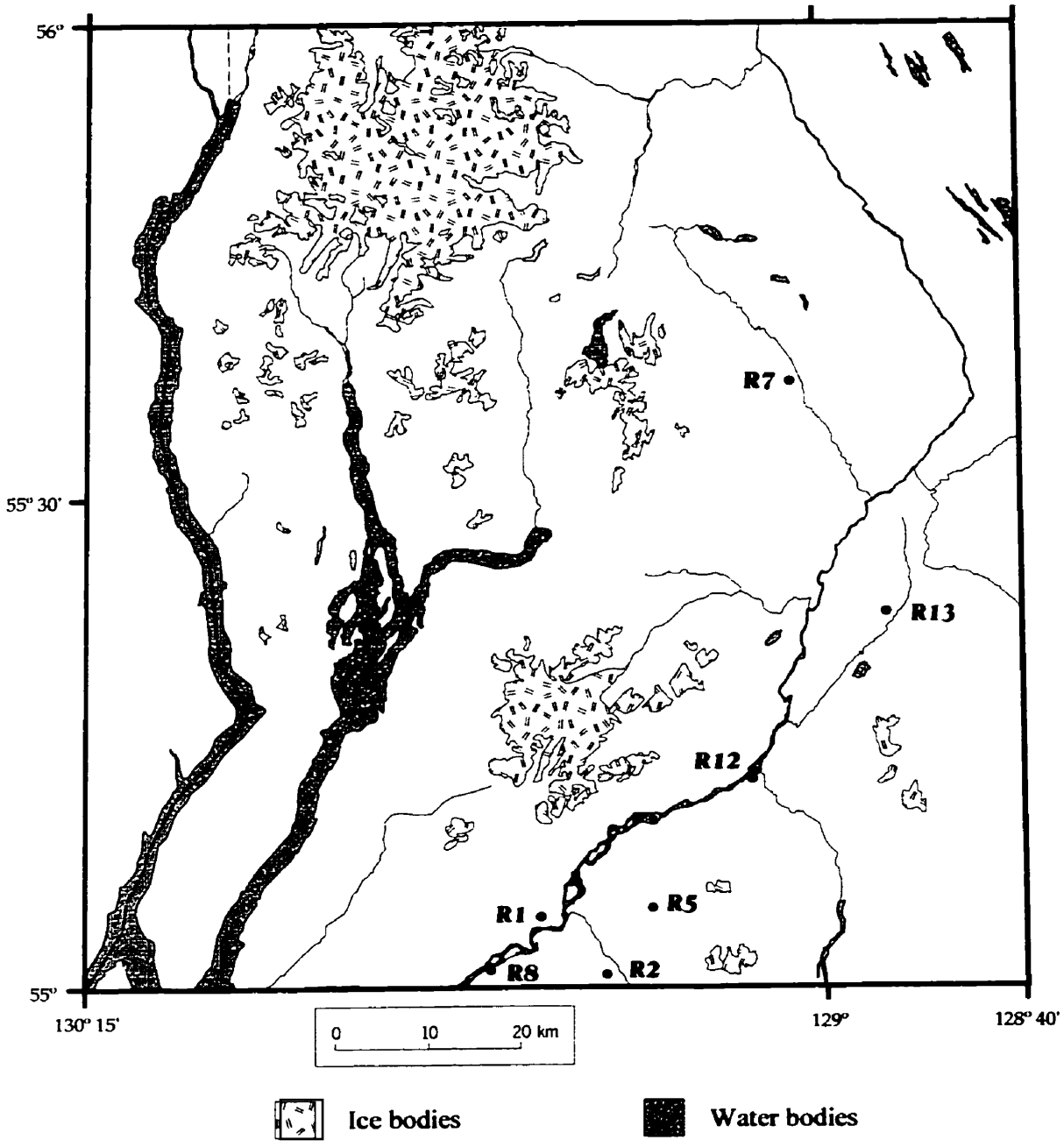


Figure E.1. Locations of various samples taken for radiocarbon dating.

contaminant introduced into the sample. It is not known how this happened, as only horizontally bedded clay was sampled, after removal of the slumped outer surface of the section.

Sample R5 is from a high elevation (640 m) organic mat overlying till that was formerly a bog. The bog is of late Holocene age and it drained sometime after 2000 years ago.

Sample R7 was taken from a road cut in Kinskuch Valley. It is the same sample as 97723-31, Kinskuch Valley Section, Figure 5.7. The organic sample was actually taken a year before the section was described, hence the different sample number. Terrestrial moss (identified by R. Mathews, Biological Sciences Dept., SFU) was initially AMS dated (TO-6354). It was considered *in situ* as it formed mats of a single species. When this age turned out to be interstadial, a second age was obtained from flattened stems of *Equisetum* sp. in the same sample (Beta-124778). This age is slightly older, possibly due to the different labs at which the samples were dated. The site is interglacial, correlative to the Olympia Nonglacial Interval of southern B.C.

R8 was a large wood sample from a bank of the Nass River. It was overlain and underlain by 1.1 m and 0.4 m of massive grey clay, respectively, and overlain at the surface by 40 cm of horizontally bedded, imbricate pebble-cobble (fluvial) gravel. It was thought that the clay might be glaciomarine, but the young age shows that this is a fluvial deposit of the Nass River, possibly an abandoned channel.

R12 was a sample of wood from the Aiyansh lava flow. It came from a lava-encased tree trunk in growth position (Figure E.2). Moss growing on the top of the stump was avoided when sampling. Since 8 cm of trunk was missing at the edge of the tree mould and there was an average of 5 rings/cm in the sample collected, the date is about 40 years too old. As this was a bulk date - several rings were pulverized - it is probably another 10 years older. The calendar dates for the 280 ± 50 radiocarbon years BP date are 1526-1557 or 1629-1663 A.D. Subtracting 50 years, the new calendar ages are 1476-1507 or 1579-1613 A.D.

R13 is a bog bottom sample from a large bog on the Aiyansh Braidplain. It was hoped that a limiting age for deglaciation could be obtained from this sample. Unfortunately, the bog appears to have formed in late Holocene time.

Figure E.2. Tree trunk in growth position (arrowed) within a lava flow tree mould, looking down into vertical cylindrical hole. Radiocarbon sample R12 was taken from the base of the trunk, where there was no moss.

In conclusion, no limiting ages for deglaciation were acquired from these samples.

## Micropaleontological Analyses

Clay samples were taken for a number of microanalyses. Their locations are shown in Figure E.3.

### *Diatom Analysis*

Diatoms are phytoplankton that live in fresh water and marine environments. Their frustules are generally well preserved because they are made of silica, a substance resistant to both physical and chemical weathering. Intricate details can be made out under the microscope, enabling identification to species level in most cases. Where the exact species is not known, the environment of deposition can still be determined from taxonomy texts.

The results of diatom analysis by the author on various clay samples are listed in Table E.2. No more than one individual of each species was found in any sample. Most samples are from the Nass Valley (marked NV in Table E.2); others are from various parts of the Nass River region. The habitats of each species are listed in Table E.3.

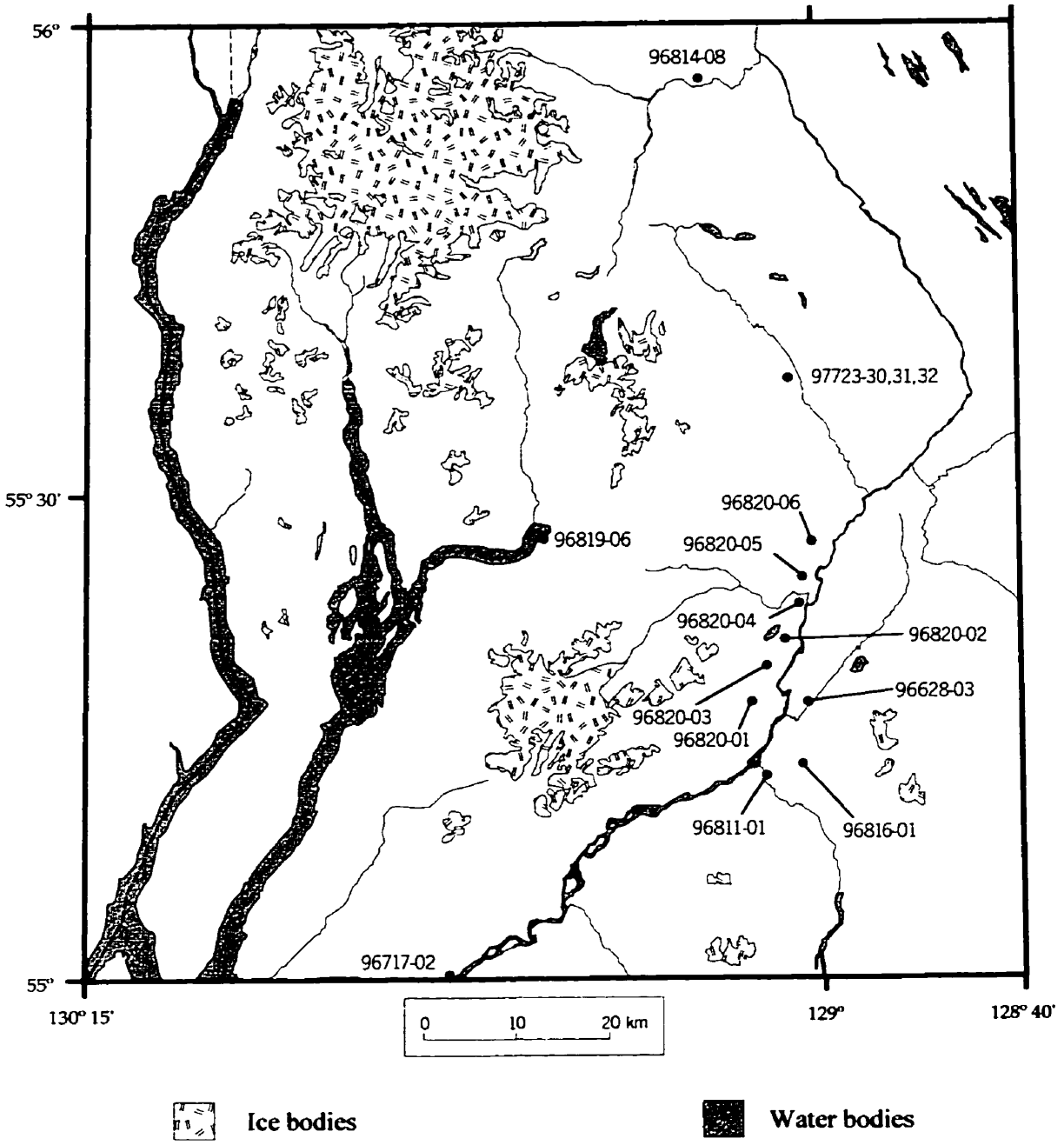


Figure E.3. Location of clay samples for micropaleontological analyses.

| Sample Number | Species | Easting | Northing | Context |
|---|---|---|---|---|
| 96628-03a | barren | 498923 | 6127156 | NV: fresh clay near small delta section |
| 96628-03b | *Amphora libyca* | 498923 | 6127156 | NV: weathered clay near small delta section |
| 96811-01 | barren | 493710 | 6118175 | NV: Tseax section |
| 96814-08 | *Pinnularia subcapitata* | 488108 | 6199641 | inland GL clay, 1 km north of White River |
| 96816-01 | barren | 497900 | 6119400 | NV: Aiyansh gravel pit |
| 96819-06 | barren | 469950 | 6146025 | Kitsault flowslide |
| 96820-01 | barren | 492910 | 6127125 | NV: 3 km northwest of Old Aiyansh |
| 96820-02 | barren | 496182 | 6134209 | NV: just east of Kwinamuck Lake |
| 96820-05 | barren | 494585 | 6131029 | NV: 2 km south of Kshadin Creek |
| 96820-06 | barren | 497975 | 6141102 | NV: 2.5 km north of Kshadin Creek |
| 97723-30 | barren | 496875 | 6164400 | clay at 640 cm, Kinskuch section |
| 97723-31 | *Neidium septentrionale* | 496875 | 6164400 | organic bed, at 660 cm, Kinskuch section |
| | *Pinnularia sudetica* | | | (also 14C sample JJS-R7: 27 ka BP) |
| | *Pinnularia sp.* | | | |
| 97723-32 | barren | 496875 | 6164400 | fine-grained sand, 680 cm, Kinskuch section |
| Sample E | barren | 494290 | 6118410 | drill hole 98-6-1001, 25 m depth |

Table E.2. Locations and results of diatom analyses.

| Sample Number | Species | **Ecology** (Foged, 1981, Hartley, 1996, Patrick and Reimer, 1975) |
|---|---|---|
| 96628-03b | *Amphora libyca* | alkaline, standing or slowly flowing fresh water |
| 96814-08 | *Pinnularia subcapitata* | fresh water of neutral pH, low mineral content |
| 97723-31 | *Neidium septentrionale* | fresh water |
| | *Pinnularia sudetica* | fresh water sphagnum bog |
| | *Pinnularia sp.* | fresh water |

Table E.3. Diatom ecology.

As evident from Table E.3, all of the samples are nearly or completely devoid of diatoms. Only five individual diatoms are present out of 78 prepared slides. This indicates that the depositional environment was not conducive to diatom communities. One *Pinus* pollen grain was

found in sample E, and a few unidentified pollen grains were noted in other barren samples. Pollen, though not completely absent, is also extremely rare.

Five individuals, all of different fresh water species, were identified (Tables E.2 and E.3). Three of these are from sample 97723-31 (also called sample R7), which is the Olympia age organic deposit from the Kinskuch Valley section (Figure 5.7). *Equisetum sp.* and terrestrial moss present in this deposit indicate that it was a peat bog in Olympia time. The freshwater diatoms are consistent with this interpretation.

All of the samples from the Nass Valley, except 96628-03b, are barren. Sample 96628-03b is from a section near the Nass Camp Delta, where fluvial input was obviously a factor, so the *Amphora libyca* diatom is likely allochthonous. The diatom of 96814-08 is autochthonous, since it is from a glaciolacustrine clay well above marine limit. The Kitsault sample was also barren, despite the presence of foraminifera in it (see Foraminiferal Analysis).

Weathering of the Nass Valley clays was not a problem for preservation, since the weathered sample of 96628-03 yielded one diatom, while the unweathered sample had none. Dissolution is unlikely as all diatoms were well preserved.

It is considered unlikely that the Nass Valley and Kitsault fiords were chemically unable to support diatoms. The bedrock is a siliciclastic turbidite sequence, which, if anything, should have been conducive to silicic frustule development. There is no evidence for excessively acidic conditions in these areas, nor for repeated drying out episodes. Hypersaline conditions in a cold glacial environment are unlikely.

In short, diatoms should have been able to live in the Nass Valley fiord. Since they did not, the problem must have been one of light transmission, rapid sedimentation, or both. There may not have been enough light getting through the water column possibly because the system was too turbid or because ice was present. In turbid modern fiords of B.C. and Alaska, less than 1% of daily sunlight penetrates the first metre of surface water during periods of high discharge (Syvitski *et al.*, 1991). These conditions could have been easily achieved during deglaciation. Rapid sedimentation might cause dilution of diatom communities, so that a very large quantity of clay

would have to be sampled in order to get reasonable concentrations of diatoms for analysis. However, if sedimentation exceeds 20 cm/a, organisms cannot exist (Syvitski *et al.*, 1986).

An ice shelf environment is a possibility, but none exist in present day temperate fiords due to active calving at tidewater fronts. Also, since there are three deltas and braidplains graded to various sea levels in the Nass Valley, open water conditions must have existed for a long time. The ice shelf option is thus ruled out.

The lack of diatoms does not lend insights into the silty clay depositional environment of the Nass Valley or Kitsault areas. Turbidity and rapid sedimentation rates may have combined to prohibit photosynthesis, or abundant sediment supply alone may have swamped diatom production.

Rare freshwater diatoms in the White River and Kinskuch areas are considered autochthonous in the glaciolacustrine and interglacial peat bog environments in which they were found, although their paucity remains unexplained.

*Foraminiferal Analysis*

The results of foraminiferal analyses are presented in Table E.4.

| Sample | Easting | Northing | Forams present? | comments |
|---|---|---|---|---|
| R2 | 476514 | 6196501 | no | |
| R3 | 447720 | 6143320 | no | |
| R7 | 496875 | 6164400 | no | very peaty |
| R8 | 464060 | 6097250 | no | very peaty |
| 96717-02 | 459610 | 6095200 | no | abundant peaty organics |
| 96811-01 | 493710 | 6118175 | no | carbonized organics |
| 96814-08 | 488108 | 6199641 | no | |
| 96816-01 | 497900 | 6119400 | no | |
| 96819-06 | 469950 | 6146025 | yes | abundant peat |
| 96820-01 | 492910 | 6127125 | no | carbonized organics |
| 96820-02 | 496182 | 6134209 | no | carbonized organics (root |
| 96820-05 | 494585 | 6131029 | no | carbonized organics |
| 96820-06 | 497975 | 6141102 | no | carbonized organics |

Table E.4. Locations and results of foraminiferal analyses on clay samples and clay from radiocarbon samples.

T. Patterson of Carleton University analyzed the foraminifera. The peat in sample 96819-06 may be a contaminant introduced into the clay by mass movement, as this sample was retrieved from an earthflow at Kitsault. The following is paraphrased from his February 2, 1997 report on the samples:

Foraminifera were only recovered from sample 960819-06, and that fauna consisted of only a few specimens of *Cassidulina reniforme*, *Cribroelphidium excavatum*, and *Entosolenia lineata*. However, two of these species characterize very distinct environments and can thus provide data important to the paleoenvironmental interpretation of the unit.

*Cassidulina reniforme* is associated with ice proximal glaciomarine environments today and has been reported from similar late glacial environments in eastern Canada and British Columbia.

*Cribroelphidium excavatum* is widely distributed at shallow depths in temperate and polar seas in the present day, and is common in late Pleistocene glaciomarine deposits, where it commonly constitutes 50-80% of the foraminiferal fauna. In temperate environments its presence indicates a salinity below that of standard sea water. Although several forms of *C. excavatum* exist, the *'clavatum'* variant is the only one collected from the sample, as is the case with specimens observed in Fraser Delta deposits dating from the early postglacial (Patterson and Cameron, 1991, Patterson and Luternauer, 1993). This form is indicative of either cold, normal marine waters (sometimes described as a 'warm ice margin fauna') or of water characterized by slightly reduced salinities. The dominance of the *'clavatum'* form suggests that the water temperature and/or salinity in the area were somewhat lower than normal marine values.

Since the sample with foraminifera is from clay overlain by the 230 m glaciofluvial delta at Kitsault, the interpretation of an ice proximal glaciomarine delta that evolved into an ice distal delta (Chapter 4) is supported. All clay deposits below 230 m are therefore interpreted to be glaciomarine in origin.

*Palynological Analysis*

The results of this analysis (done by M. Pellatt, Biological Sciences Dept., SFU) are presented in Table E.5.

| Sample Number | Pollen Present? | Easting | Northing | Context |
|---|---|---|---|---|
| 96628-03a | No | 498923 | 6127156 | NV: fresh clay near small delta section |
| 96820-05 | No | 494585 | 6131029 | NV: 2 km south of Kshadin Creek |
| 97723-27 | Yes | 496875 | 6164400 | Kinskuch Valley section |
| 97723-27 | Yes | 496875 | 6164400 | Kinskuch Valley section |
| 97723-27 | Yes | 496875 | 6164400 | Kinskuch Valley section |

Table E.5. Locations and results of pollen and palynomorph analysis.

It appears that the glaciomarine clay is barren of pollen, dinoflagellates or acritarchs, which is unusual. Since it has been suggested that there was no ice cover over the glaciomarine environment of the Nass Valley, sedimentation rates must have been extremely high for wind-borne pollen to not be present. A number of factors now point to extremely rapid and turbid marine sedimentation during deglaciation.

The samples taken from the Kinskuch Valley section (Figure 5.7) are dominated by spruce pollen (Table E.6). This means that a spruce-dominated forest existed in the region during the Olympia Nonglacial Interval. This type of forest has no modern analogue and indicates that climate at that time was cooler than present.

| Pollen Species | 97723-27 (%) | 97723-29 (%) | 97723-31 (%) |
|---|---|---|---|
| *Picea* | 85.4 | 97.2 | 83.3 |
| *Pinus* - Diploxylon | 0 | 0.4 | 1.0 |
| Chenopodiiae | 0.5 | 0 | 0 |
| *Lycopodium* | 0 | 0 | 0.7 |
| *Selaginella selaginoides* | 0 | 1.2 | 13.5 |
| *Cedrus* (reworked) | 14.1 | 1.2 | 1.5 |

Table E.6. Percentages of pollen types found at the Kinskuch Valley section.

## X-Radiography

X-radiography was conducted on drill core samples to obtain a better idea of the mode of sedimentation in the cores. A variety of x-ray settings were tested on sample D from Drill Hole 98-6-1001, the only sample with lamination visible to the naked eye. The laminations in the sample are less than 1 mm thick and they were not detected by x-radiography. No dropstones were detected either, but this was not surprising, as none are visible in the sample. Laying the sample in a box filled with fine-grained sand to enhance the x-ray contrast did not improve the results. Either the features are too fine for detection or the x-ray device available at SFU is not powerful enough to pick them up. Since laminations were not highlighted in the laminated sample, only one massive sample was checked for structure and possible dropstone content (with the same results) and then x-radiography was discontinued.

## SEM and XRF Analysis

SEM (Scanning Electron Microprobe) analysis was used to look at grain shapes within the silty clay and XRF (x-ray fluorescence) was used for elemental analysis on sample E from Drill Hole 98-6-1001. The SEM-XRF machine of the Dept. of Physics, SFU, was used.

No NaCl was found. For certain silt grains, the atomic percentage of each element is listed in Table E.7, along with the mineralogical interpretation. Feldspars are expressed in the Or-Ab-An system, showing the relative percentage of orthoclase, albite and anorthite or K, Na and Ca.

| Silt Grain | Na | Mg | Al | Si | K | Ca | Ti | Fe | O | | |
|---|---|---|---|---|---|---|---|---|---|---|---|
| bulk clay | 0.17 | 1.90 | 17.75 | 69.69 | 5.34 | 3.44 | 1.19 | 0.53 | 0.00 | | |
| A1 | | | | | | | | | | | |
| A2 | 5.12 | 0.00 | 14.34 | 80.17 | 0.31 | 0.07 | 0.00 | 0.00 | 0.00 | albite | NaAlSi3O8 |
| Q1 | | | | | | | | | | | |
| L | 6.08 | 0.00 | 19.10 | 70.88 | 0.31 | 0.16 | 3.48 | 0.00 | 0.00 | labradorite | (Na,Ca)(Al)1.2(Si)3.2O8 |
| L | | | | | | | | | | | |
| BG | 0.00 | 0.00 | 20.73 | 71.42 | 4.39 | 1.98 | 0.98 | 0.50 | 0.00 | biotite/glauconite | (K,Ca,Ti)Fe3(AlSi3O10)(OH)2 |
| Q1 | | | | | | | | | | | |

Table E.7. Atomic percentage of elements identified by XRF, with postulated mineral formula and mineral identification.

In Figure E.4a, an SEM photograph, the larger grains are silt-sized (10 - 20 μm) and are subangular to subround. The clay fraction is more difficult to see, but grains are also subangular to subround and appear somewhat, but not completely, flaky.

A bulk analysis on the clay (within black dashed square) revealed mostly Si and Al, with minor amounts of Na, Mg, Fe, K, and Ca. A very small amount of Ti is present (Table E.7). The grain labelled $A_1$ is the sodium feldspar albite ($Or_2Ab_{93}An_5$). Fe is present as in impurity. Grain $A_2$ is also albite ($Or_0Ab_{99}An_1$) and grain $Q_1$ is quartz (96% Si; O is not identified with XRF), with impurities. Quartz may be one source of the titanium (rutilated quartz?) in the bulk clay. Grain L is labradorite ($Or_2Ab_{62}An_{36}$). Feldspars appear to be a common constituent of the silt-sized fraction.

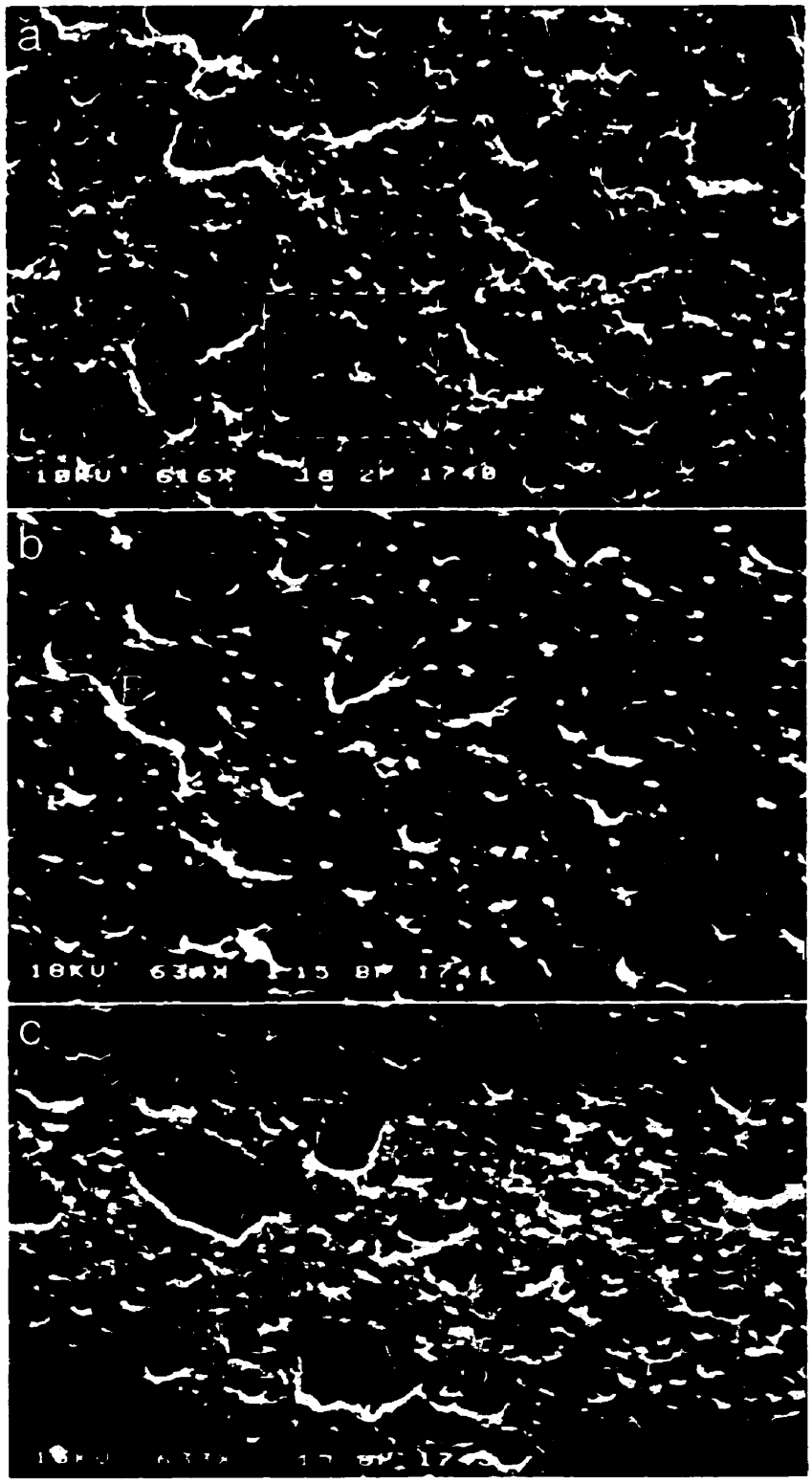


Figure E.4. Scanning electron microprobe analyses from Sample E, Drill Hole 98-6-1001, 25 m depth. a) Silt and clay with grain identifications. Scale bar (wide black bar) is 16.2 mm. Bulk clay analysis was done within the white dashed box. b) Another portion of the slide, with grain identifications. Scale bar is 15.8 mm. c) Near the edge of the slide, with grain identifications. The pale area in grain O is where the XRF sampled the grain. Scale bar is 15.8 mm.

Figure E.4b also contains angular and subangular silt grains with flaky and granular clay-sized particles. $Q_2$ and $Q_3$ are quartz, while $A_3$ and $A_4$ are albite. The latter four elemental concentrations were not calculated, as they were immediately recognized by the peak signatures of the XRF. Grain BG (the white grain) is slightly different, with a lower Si to Al ratio than the feldspars (2.4 compared to 4 or 5) and a noticeable presence of Fe and some Ti. A 2:1 ratio of K : Ca, with no Na, means it cannot be a feldspar. It is interpreted as biotite or glauconite with Ca and Ti substituting for some of the K. This is another source of titanium in the bulk clay. P is obviously pyrite, with a 2:1 ratio of S to Fe.

Figure E.4c is another section of the slide. The paler areas in grain O are where the XRF analysis was done. This grain is orthoclase ($Or_{100}Ab_0An_0$) (potassium feldspar). Grain $A_5$ is albite and $Q_4$ is quartz, both determined solely from XRF peaks on the screen.

Geertsema (1998) found the silt size fraction of a Nass Valley clay sample to be quartz, feldspar, chlorite and illite, and the clay size fraction to be the same except that it lacked feldspar.

In summary, the glaciomarine silty clay of the Nass Valley consists mainly of feldspar and quartz, with minor biotite/glauconite, pyrite, chlorite and illite. Expandable clay minerals that would prevent sensitive clay development (Berry and Torrance, 1998) are not present. The presence of silicates and non-swelling clay minerals such as illite predispose these silty clays to earthflows. They allow the liquid limit and remoulded shear strength to drop when salt is removed, setting the stage for failure.

# NOTE TO USERS

**Oversize maps and charts are microfilmed in sections in the following manner:**

## LEFT TO RIGHT, TOP TO BOTTOM, WITH SMALL OVERLAPS

**This reproduction is the best copy available.**

UMI

Natural Resources Canada | Ressources naturelles Canada

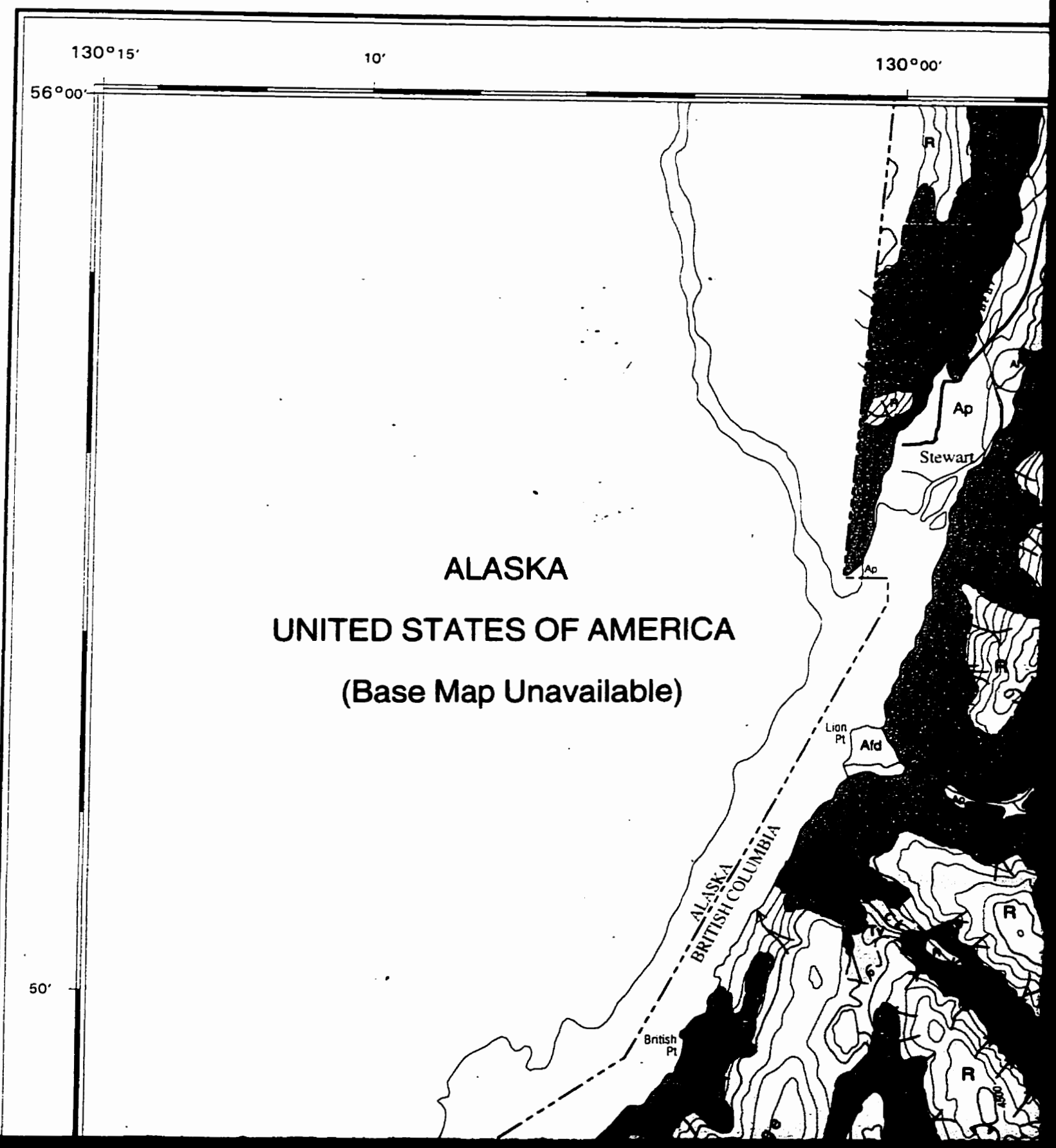

GEOLOGICAL SURVEY OF CANADA

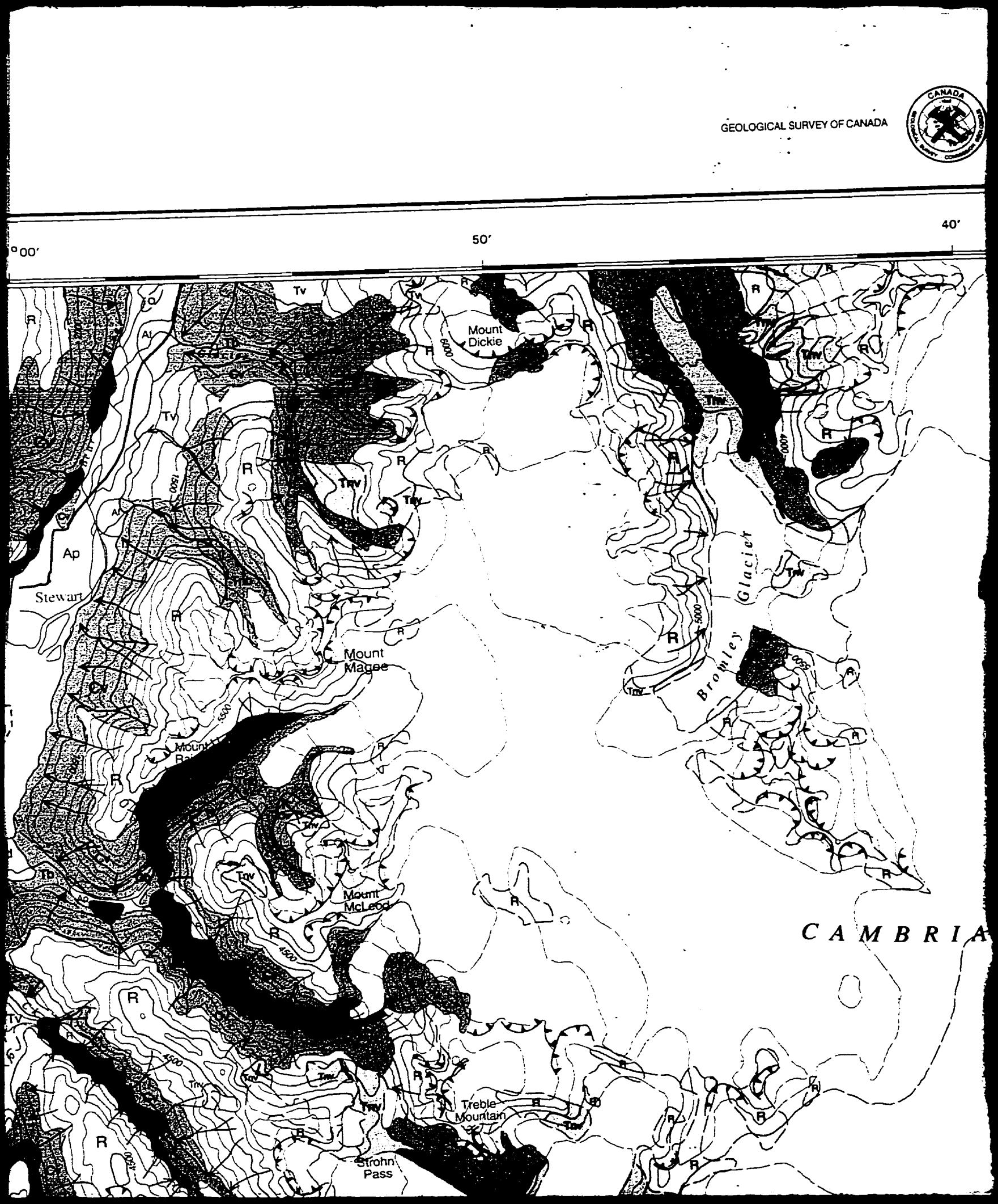

GEOLOGICAL SURVEY OF CANADA COMMISSION GÉOLOGIQUE DU CANADA

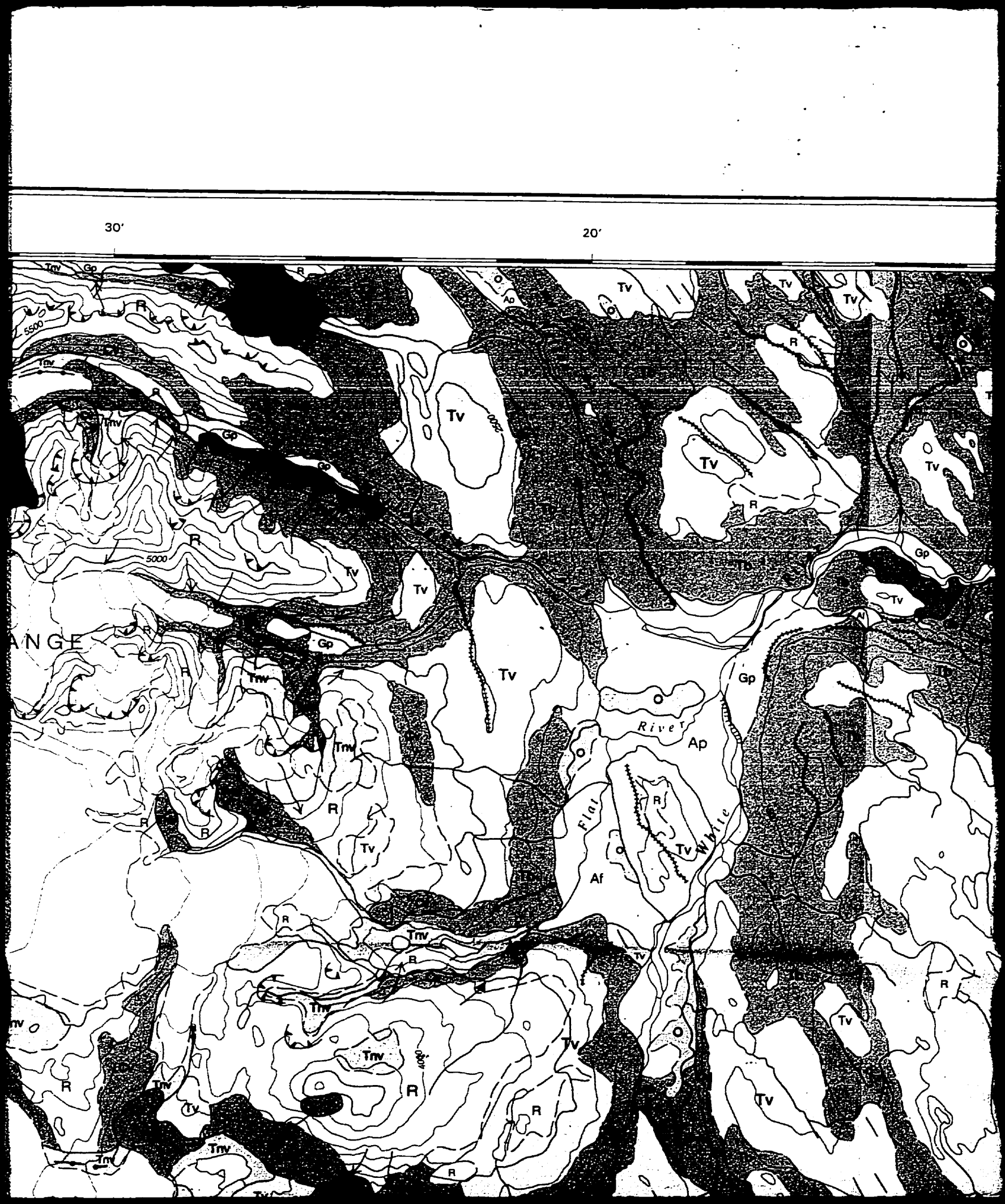
30′
20′
ANGE
River
Flat
White
Tv
Tnv
Gp
R
Ap
Af
5500
5000
4000

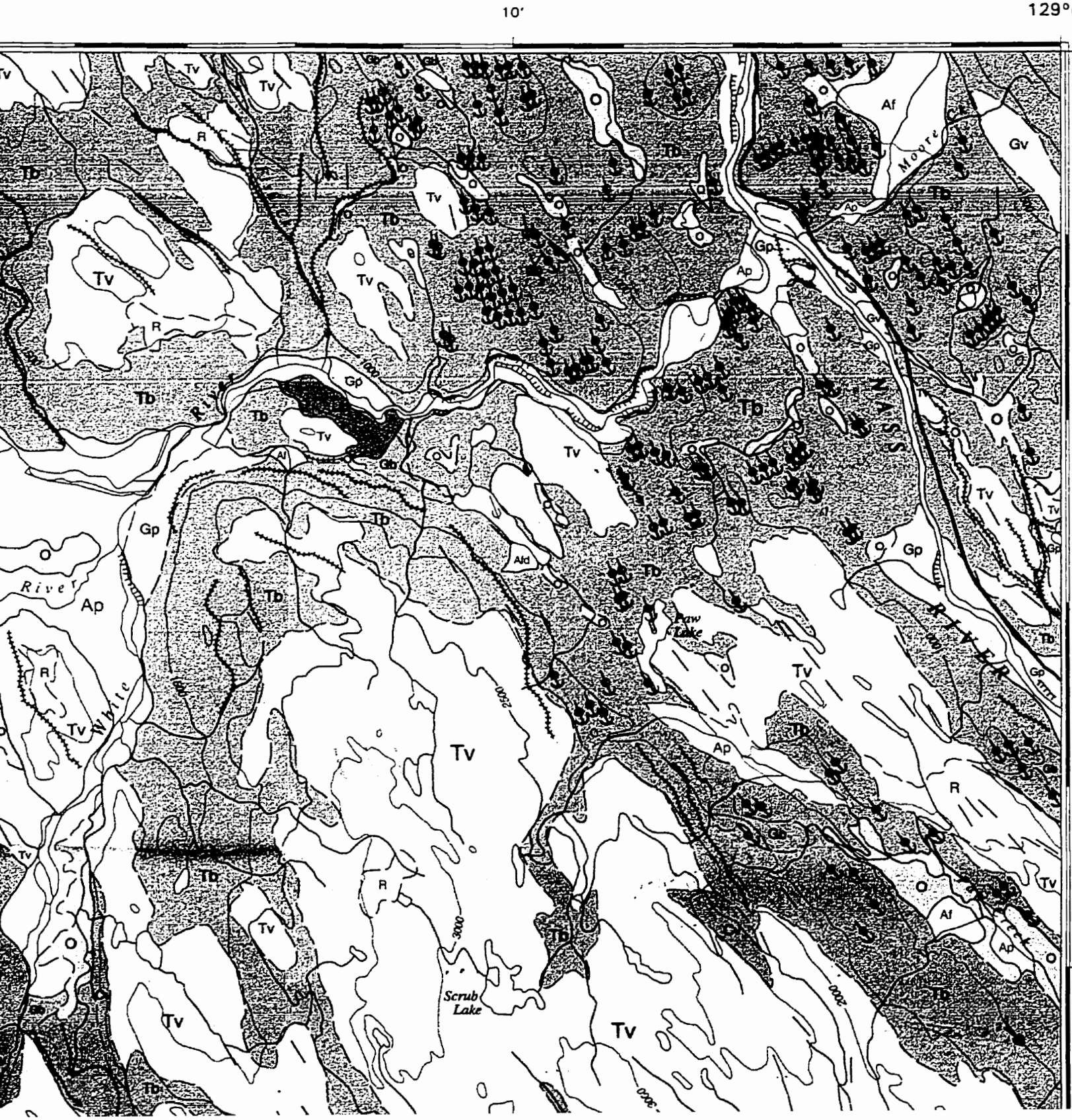
10'
129°00'
56°
50'
Tv
Tb
Gp
Ap
Af
Gv
Gb
Afd
R
O
Moore
NASS
RIVER
White
River
Paw Lake
Scrub Lake
1000
2000
2500
3000

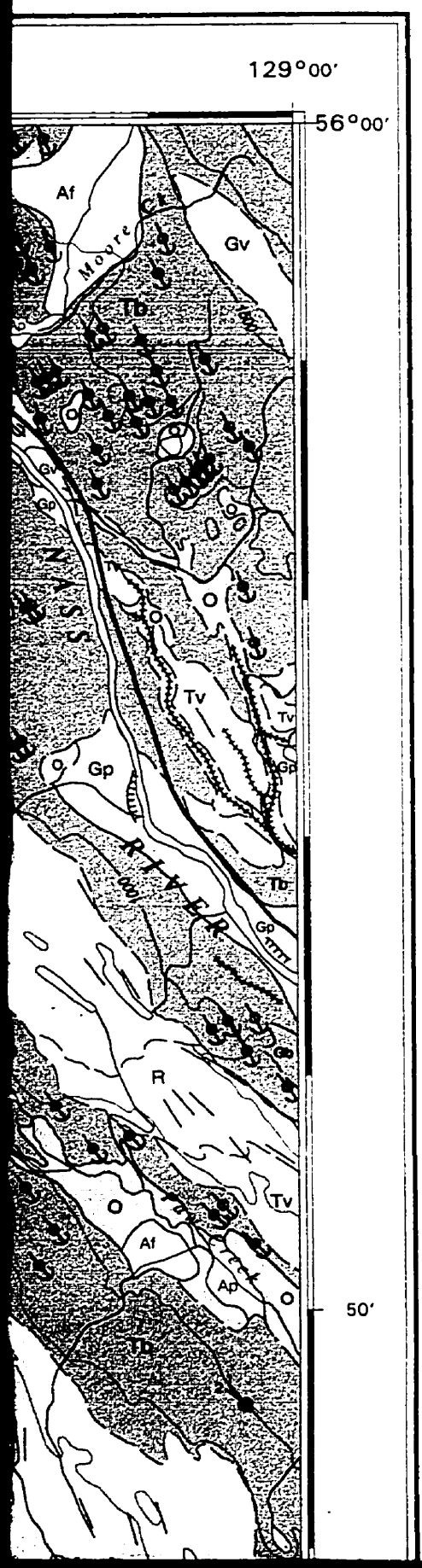


*POST-FRASER GLACIATION*

*Organic Deposits:*

**Organic Deposits:** *peat and organic-rich silt; water saturated; formed predominantly by the accumulation of plant material in bogs, fens, and swamps; thickness > 2 m*

*Colluvial Deposits: bouldery gravel with clay to sand size matrix; loose, very poorly sorted, massive; dominated by subangular to angular clasts of local bedrock; texture dependent on source sediments; forms by gravitational processes such as debris flow, rockfall, earthflow and snow avalanche*

**Colluvial Blanket:** *diamicton; generally found on valley floors; thickness > 2 m*

**Colluvial Apron:** *bouldery diamicton; forms a talus apron or sheet at foot of steep slope; little or no vegetation where active; thickness > 2 m, thickening toward base of slope*

**Colluvial Fan:** *bouldery diamicton with a sandy matrix; forms steep fan or cone shaped bodies at foot of steep bedrock slopes; deposited by debris flow and rock avalanche; thickness up to 10 m near fan midpoint*

**Landslide Sediments:** *bouldery diamicton; mainly silty clay if accompanied by earthflow symbol; forms hummocky terrain; little or no vegetation if recent; thickness 3-20 m*

**Colluvial Veneer:** *diamicton; takes form of underlying surface; discontinuous cover with numerous areas of exposed bedrock; thickness 1 to 2 m*

**Undivided Colluvial Sediments:** *mixture of colluvial blanket, apron, fan, landslide and veneer, which cannot be subdivided at this map scale, thickness > 2 m*

*Alluvial Deposits: gravel and sand, with minor silt; moderately to well sorted; clasts generally subrounded to well rounded; deposited by rivers either within channels or as overbank deposits*

Ap — **Alluvial Plain:** *gravel and sand; massive to stratified; moderately to well sorted; locally overlain by peat and organic-rich silt deposited in abandoned channels and on floodplain surface; forms flat plains occupied by single or multiple channel rivers; includes deltas at mouths of major rivers; thickness 2 to 10 m, > 10 m in deltaic settings*

Af — **Alluvial Fan:** *diamicton, gravel and sand; matrix supported, massive to weakly stratified, poorly sorted; interbedded with moderately to well sorted, clast supported, bedded fluvial gravel and sand; forms fan shaped bodies where rivers enter larger valleys; deposited by debris flows and streams; thickness up to 10 m at fan midpoint*

Afd — **Fan Delta:** *diamicton, gravel and sand; massive to stratified; subaerial facies same as alluvial fans, subaqueous facies consisting of interbedded silt, clay, sand and gravel; beach facies predominantly pebble-cobble gravel, with boulder concentration at high tide line; forms where alluvial fans meet marine water; thickness 3 to 15 m*

*GLACIAL DEPOSITS*

*Neoglacial Deposits: diamicton (till): grey, massive, matrix supported; subangular to angular, striated granule to boulder sized clasts set in silty sand or sand matrix; loose to slightly compact, commonly unweathered; formed by melt-out from ice and found surrounding modern alpine glaciers and ice fields; deposited during Holocene glaciation*

**Neoglacial Till Blanket:** *till; locally forming flights of recessional moraines; thickness 2 to 40 m*

Tnv — **Neoglacial Till Veneer:** *till; discontinuous cover with numerous areas of exposed bedrock; takes form of underlying surface; thickness 1 to 2 m*

*FRASER GLACIATION (Wisconsinan)*

*PROGLACIAL DEPOSITS*

40'
UNITED STATES OF AMERICA
CANADA
PORTLAND CANAL
White Pt
Blue Pt
Miner Pt
Round Pt
Afd
Tv
Gv
Gp
R
3000
3500
4000
4500
Mount Brown
Ashwood Lake
CARR RIDGE
HANGE

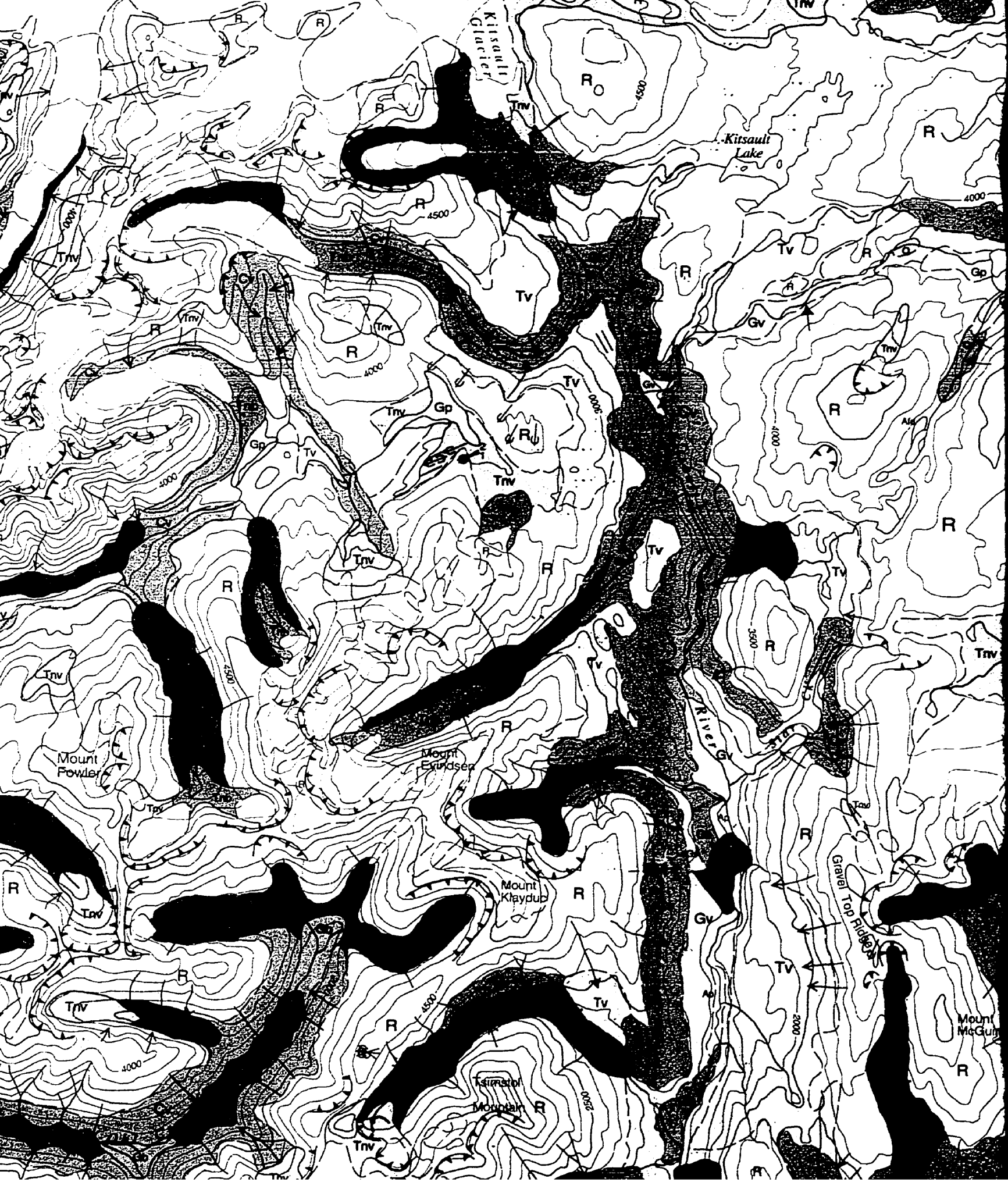
Kitsault Glacier
Kitsault Lake
Mount Fowler
Mount Evindsen
Mount Klaydup
Tsimstol Mountain
Gravel Top Ridge
River
Tnv
Tv
Gp
Gv
R
4500
4000
3500
3000
2500
2000

Jade Lake
Kinskuch Lake
Lavender Peak
Gravel Top Ridge
Mount McGuire
Tchitin Peak
Illiance Mountain
4000
5000
4500
2500
3000
Tv
R
Cv
Gv
Gb
Gp
Afd
Tnv
Tnb
Af
Ap
Gd

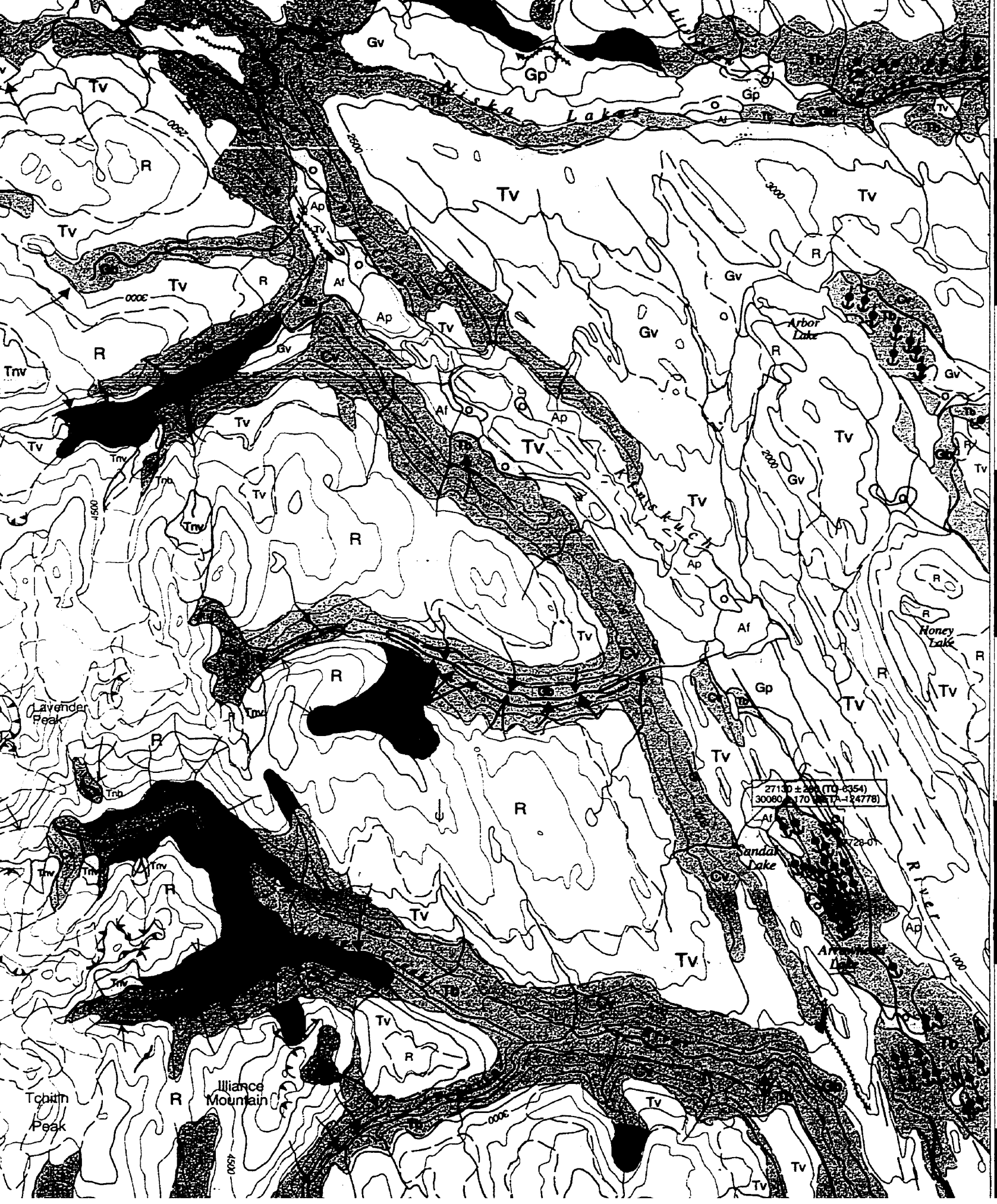

Niska Lakes
Arbor Lake
Honey Lake
Sandal Lake
Lavender Peak
Tchitin Peak
Illiance Mountain
River
Tv
R
Gv
Gp
Af
Ap
Tb
Cv
Tnv
Tnb
2500
3000
2000
4500
1000

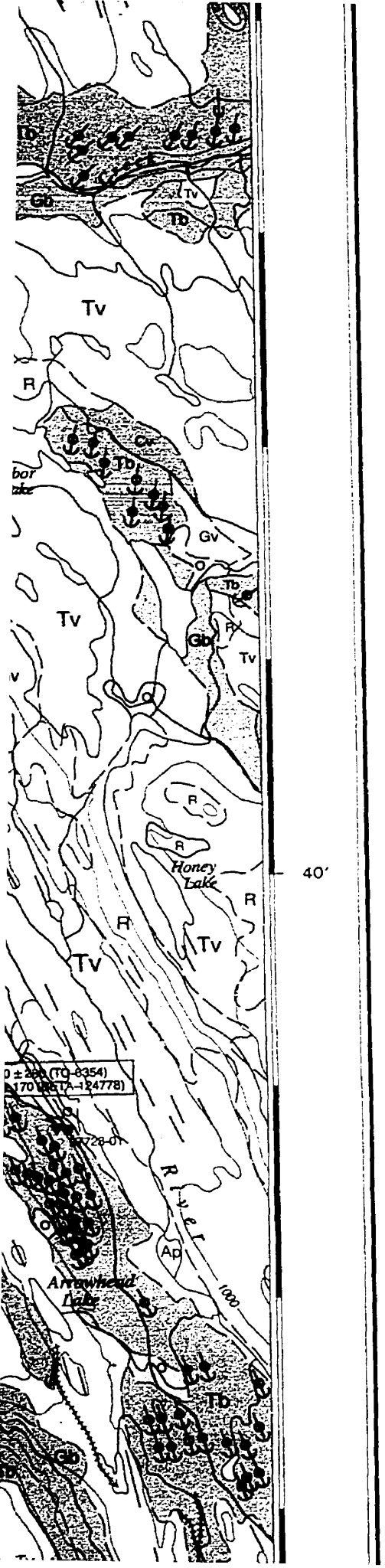


*Glaciolacustrine Deposits: laminated silt, clay and minor sand deposited in lakes ponded by glacial ice; well sorted; dropstones common, macrofossils absent*

**Glaciolacustrine Blanket:** *silt, clay, minor sand; irregular or conforms to underlying surface; thickness > 2 m*

*Glaciomarine Deposits: massive blue-grey or grey silty clay with minor silt, sand and granule gravel; rarely weakly laminated; locally containing dropstones; found in coastal areas below marine limit; coarser proximal deposits are horizontally bedded and well sorted; distal deposits are dominated by massive silty clay that is weathered to pale brown at the surface and may contain salt crusts; marine macrofossils are absent*

**Glaciomarine Blanket:** *massive silty clay with minor sand, silt and granule gravel; irregular surface; thickness > 2 m*

My

**Glaciomarine Veneer:** *massive silty clay with minor sand, silt and granule gravel; discontinuous cover with numerous areas of exposed bedrock; takes form of underlying surface; thickness 1 to 2 m*

*Glaciofluvial Deposits: gravel, sand, minor silt and clay; poorly to well sorted; deposited by meltwater flowing away from or in contact with glacial ice; including deltas graded to former sea levels; rarely faulted; clasts commonly rounded and of more local provenance than underlying till*

Gp

**Glaciofluvial Plain:** *gravel and sand; massive to weakly horizontally bedded; forms flat surfaces; consists of former outwash plains; bogs common on plain surface; thickness 2 to 50 m*

Gd

**Glaciofluvial Delta:** *gravel, sand and silt; poorly to moderately sorted, angular to well rounded clasts; forming flat surfaces; deposited as proglacial marine deltas, often forming terminal regions of glaciofluvial braidplains; thickness up to 230 m*

Gb

**Glaciofluvial Blanket:** *gravel and sand; massive to weakly horizontally bedded; forms irregular surface; thickness 2 to 20 m*

Gv

**Glaciofluvial Veneer:** *gravel and sand, massive to vaguely horizontally bedded; discontinuous cover with large areas of exposed bedrock and locally, colluvial veneer; takes form of underlying surface; thickness 1 to 2 m*

Gu

**Undivided Glaciofluvial Sediments:** *glaciofluvial gravel and sand, with till and glaciolacustrine clay, undifferentiated at this scale of mapping; forms irregular or rolling terrain; thickness 2 to 20 m*

*GLACIAL DEPOSITS*

*Glacial Deposits: diamicton (till), granule to boulder size clasts in a silt to silty clay matrix; massive, very compact, very poorly sorted, with angular to subrounded striated clasts; commonly blue-grey or grey; dominant clast lithologies are Bowser Lake Group sandstone, siltstone and mudstone; deposited directly by glacial ice or by gravity flow from glacial ice*

Tb

**Till Blanket:** *till; conforms to and locally obscures underlying topography; thickness 2 to 20 m*

Tv

**Till Veneer:** *till; discontinuous cover with numerous areas of exposed bedrock and locally, colluvial veneer; takes form of underlying surface; thickness 1 to 2 m*

*BEDROCK*

*Pre-Quaternary*

R

*Triassic-Jurassic volcanic and sedimentary bedrock of island arc origin, slightly metamorphosed, and Cretaceous igneous intrusions; includes minor colluvial and till veneer, but > 75% of unit is bedrock*

## SYMBOLS

*Boundary (defined, approximate, assumed)*

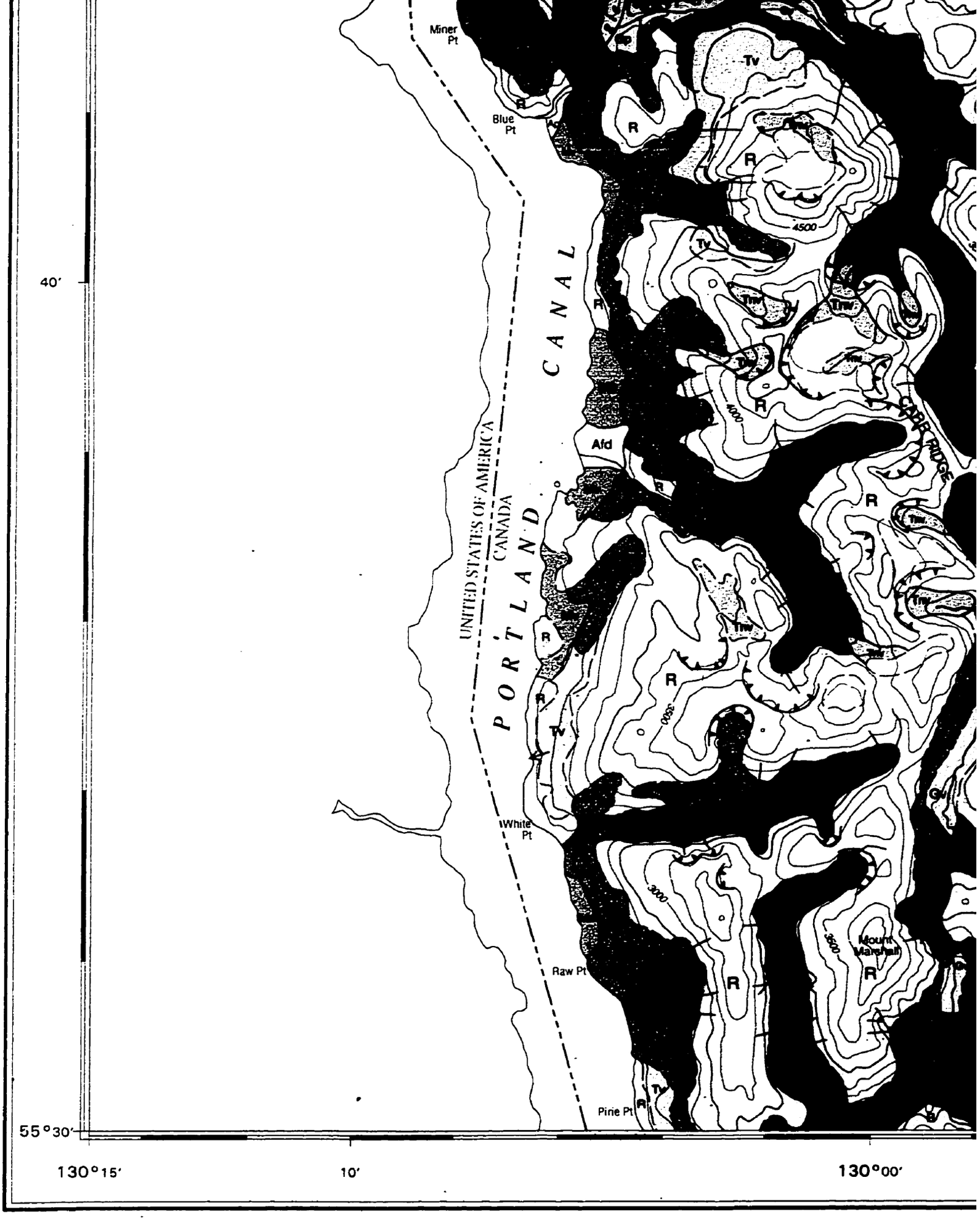

Miner Pt
Blue Pt
Tv
R
4500
Tv
Trw
Trw
Trw
R
4000
CARR RIDGE
Afd
R
R
Trw
Trw
R
R
3500
Tv
White Pt
3000
3500
Mount Marshall
R
R
Raw Pt
Tv
R
Pirie Pt
PORTLAND CANAL
UNITED STATES OF AMERICA
CANADA
40′
55°30′
130°15′
10′
130°00′

130°00′ 50′

OPEN F

OPEN FILE XXX1

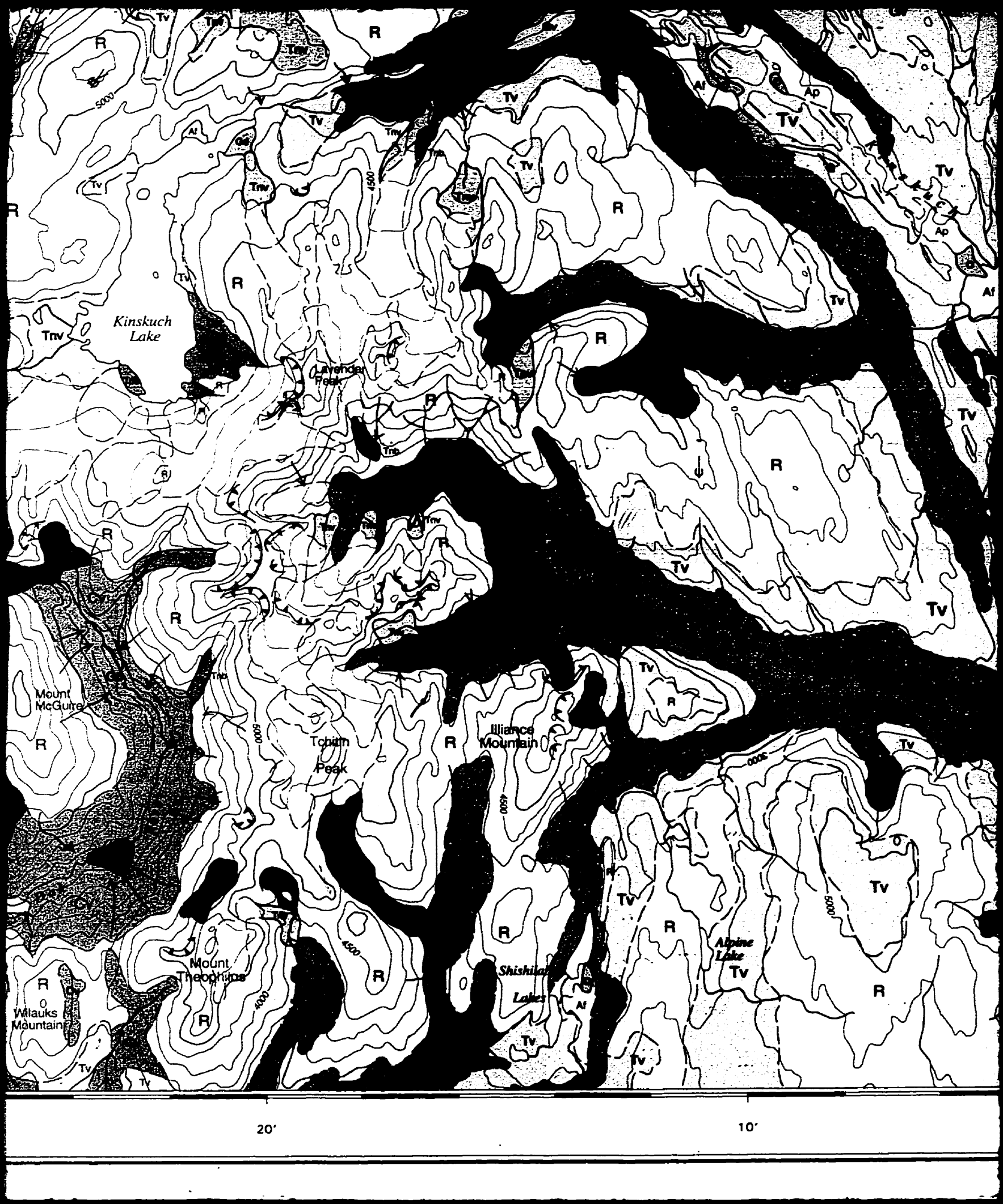
Kinskuch Lake
Lavender Peak
Mount McGuire
Tchitin Peak
Illiance Mountain
Mount Theophilus
Shishilak Lakes
Alpine Lake
Wilauks Mountain
5000'
4500
4000
20'
10'

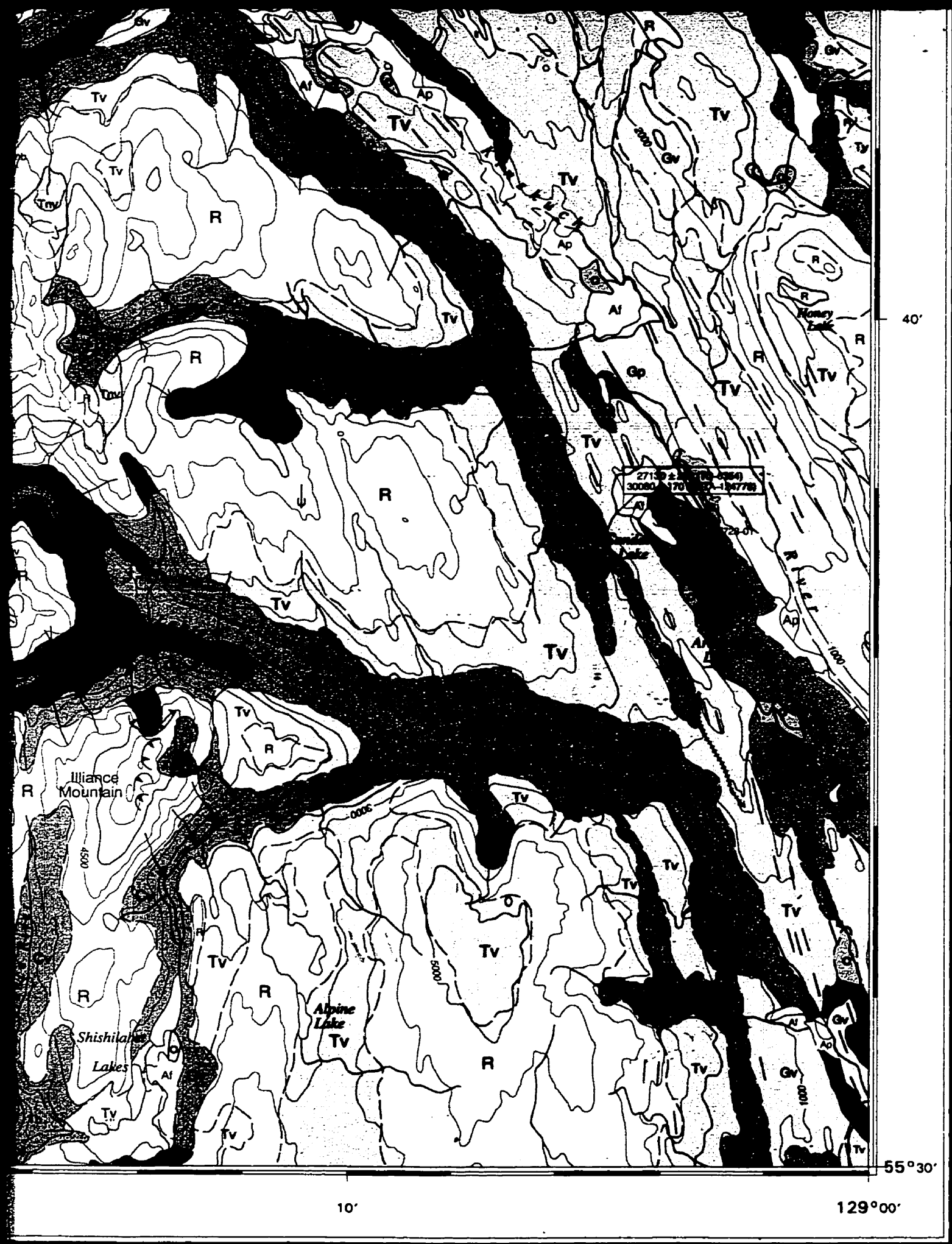


Unit
Avali
Debr
Terra
Cirqu
Meltw
Drum
Mora
Linea
Roch
Striat
n
Strati
Radi
Glac

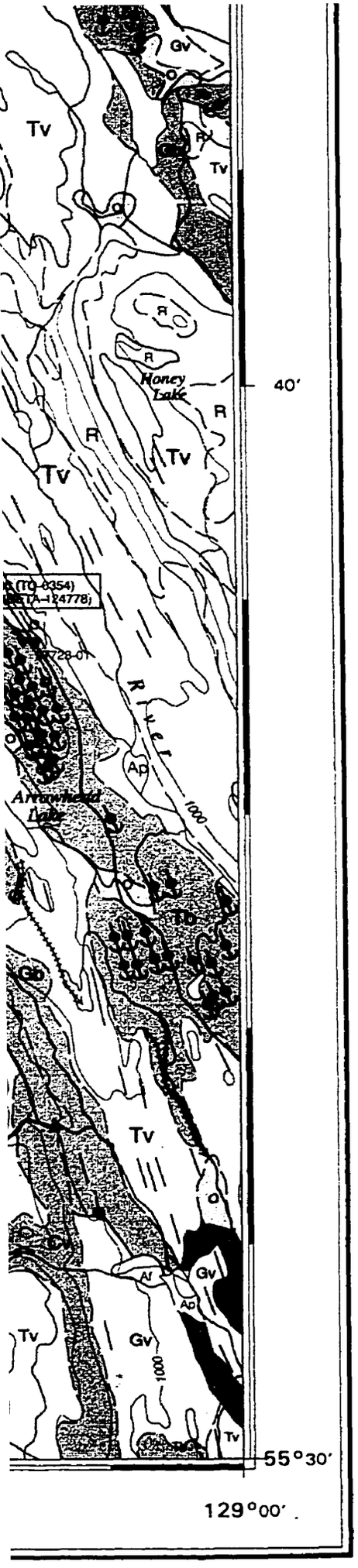


*Glaciofluvial Deposits: gravel, sand, minor silt and clay; poorly to well sorted; deposited by meltwater flowing away from or in contact with glacial ice: including deltas graded to former sea levels; rarely faulted; clasts commonly rounded and of more local provenance than underlying till*

**Gp** — ***Glaciofluvial Plain:*** *gravel and sand; massive to weakly horizontally bedded; forms flat surfaces; consists of former outwash plains; bogs common on plain surface; thickness 2 to 50 m*

**Gd** — ***Glaciofluvial Delta:*** *gravel, sand and silt; poorly to moderately sorted, angular to well rounded clasts; forming flat surfaces; deposited as proglacial marine deltas, often forming terminal regions of glaciofluvial braidplains; thickness up to 230 m*

***Glaciofluvial Blanket:*** *gravel and sand; massive to weakly horizontally bedded; forms irregular surface; thickness 2 to 20 m*

**Gv** — ***Glaciofluvial Veneer:*** *gravel and sand, massive to vaguely horizontally bedded; discontinuous cover with large areas of exposed bedrock and locally, colluvial veneer; takes form of underlying surface; thickness 1 to 2 m*

***Undivided Glaciofluvial Sediments:*** *glaciofluvial gravel and sand, with till and glaciolacustrine clay, undifferentiated at this scale of mapping; forms irregular or rolling terrain; thickness 2 to 20 m*

*GLACIAL DEPOSITS*

*Glacial Deposits: diamicton (till), granule to boulder size clasts in a silt to silty clay matrix; massive, very compact, very poorly sorted, with angular to subrounded striated clasts; commonly blue-grey or grey; dominant clast lithologies are Bowser Lake Group sandstone, siltstone and mudstone; deposited directly by glacial ice or by gravity flow from glacial ice*

***Till Blanket:*** *till; conforms to and locally obscures underlying topography; thickness 2 to 20 m*

**Tv** — ***Till Veneer:*** *till; discontinuous cover with numerous areas of exposed bedrock and locally, colluvial veneer; takes form of underlying surface; thickness 1 to 2 m*

*BEDROCK*

*Pre-Quaternary*

**R** — *Triassic-Jurassic volcanic and sedimentary bedrock of island arc origin, slightly metamorphosed, and Cretaceous igneous intrusions; includes minor colluvial and till veneer, but > 75% of unit is bedrock*

## SYMBOLS

*Unit Boundary (defined, approximate, assumed)*

*Avalanche track*

*Debris flow track*

*Terrace scarp*

*Cirque*

*Meltwater channel (small, large)*

*Drumlin (long drumlins shown by two or more symbols)*

*Moraine*

*Linear bedrock ridge*

*Roche moutonnée*

*Striation (ice flow direction known; unknown; older = 1, younger = 2, no numbers = age relationship unknown)*

96805-10

*Stratigraphic section*

*Radiocarbon date*

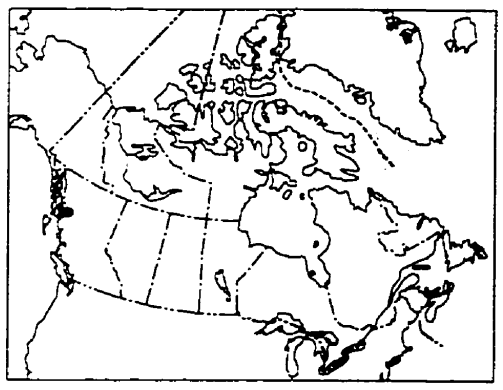

LOCATION MAP

*Geology by S. McCuaig, Geological Survey of Canada a*

*Digital cartography by S. McCuaig and K. Shimamura, G*

*Any revisions or additional geological information would be welcomed by the Geological Surv*

Canada

130°00′ 50′

*Cuaig, Geological Survey of Canada and Simon Fraser University*

*by S. McCuaig and K. Shimamura, Geological Survey of Canada*

*ons or additional geological information known to the user*
*d be welcomed by the Geological Survey of Canada*

**KITS**

**B**

**Scal**

kilometres 2 0

Universal Transverse Mercator Pr
North American Datum 198
©Her Majesty the Queen in Right of C

UNDER FINAL REVIEW –T

OPEN FILE XXX1

SURFICIAL GEOLOGY

# KITSAULT VALLEY

## BRITISH COLUMBIA

Scale 1:100 000 – Échelle 1/100 000

kilometres 2 0 2 4 6 8 kilomètres

Universal Transverse Mercator Projection
North American Datum 1983
©Her Majesty the Queen in Right of Canada, 2000

Projection transverse universelle de Mercator
Système de référence géodésique nord-américain, 1983
©Sa Majestéla Reine du chef du Canada, 2000

FINAL REVIEW –TO BE RELEASED AS AN OPEN FILE

*Digital base map from data compiled by Geomatics Canada, modified by the Terrain Sciences Division*

*Mean magnetic declination (2000), 24 ° 07' E, decreasing 9.3' annually. Readings vary from 23 ° 59' E in the SW corner to 24° 14' E in the NE corner of the map*

*CONTOUR INTERVAL 500 FEET*

N OPEN FILE

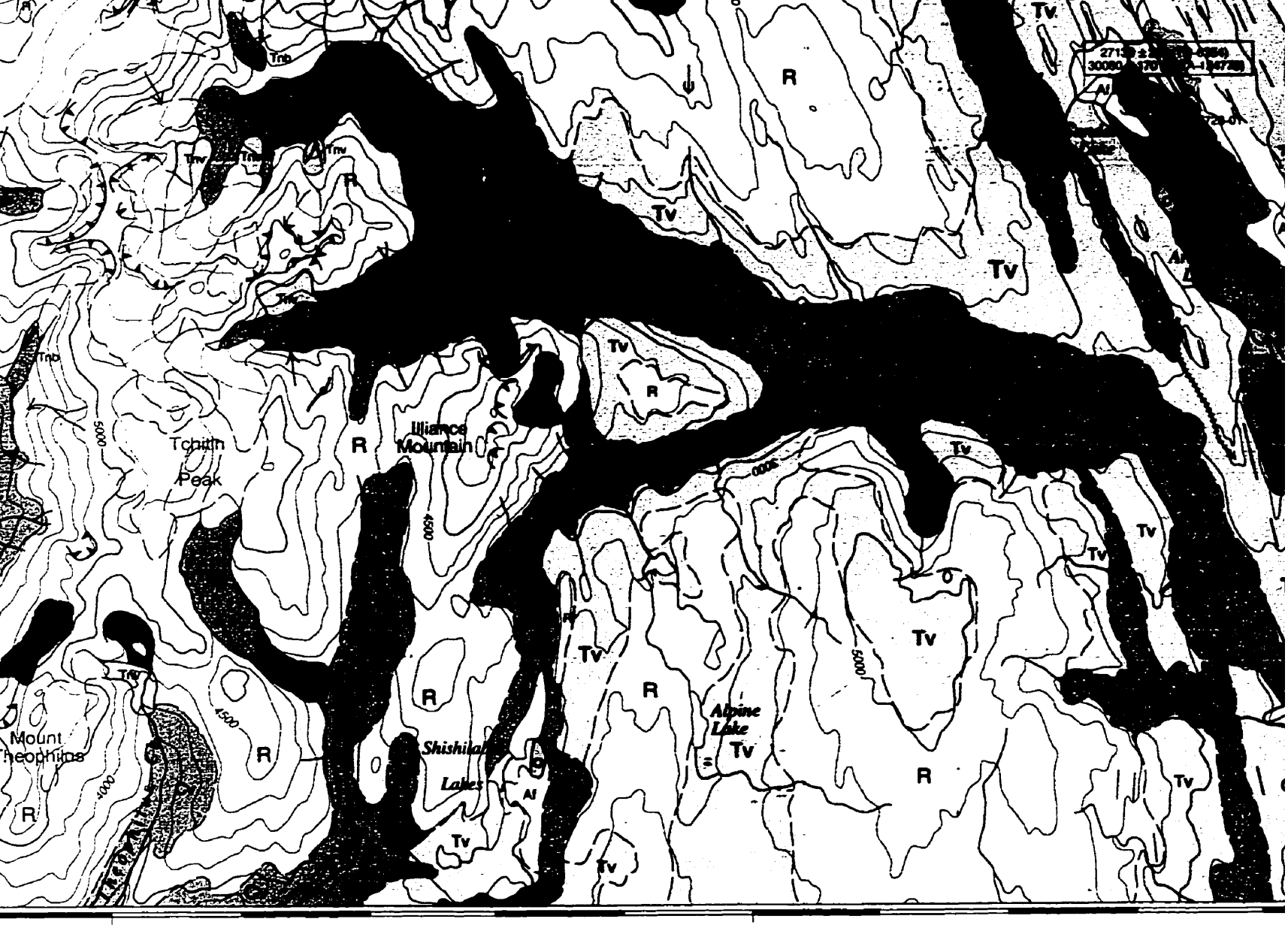


data compiled by Geomatics Canada, modified by the Terrain Sciences Division

declination (2000), 24 ° 07' E, decreasing 9.3' lings vary from 23 ° 59' E in the SW corner to 14' E in the NE corner of the map

ONTOUR INTERVAL 500 FEET

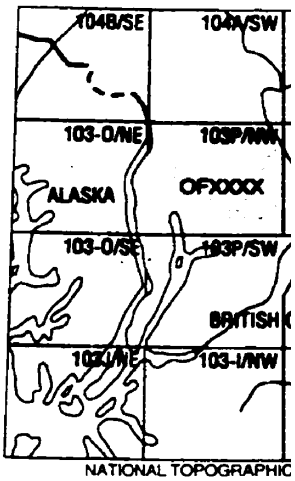


NATIONAL TOPOGRAPHIC

*GLACIAL DEPOSITS*

*Glacial Deposits: diamicton (till), granule to boulder size clasts in a silt to silty clay matrix; massive, very compact, very poorly sorted, with angular to subrounded striated clasts; commonly blue-grey or grey; dominant clast lithologies are Bowser Lake Group sandstone, siltstone and mudstone; deposited directly by glacial ice or by gravity flow from glacial ice*

**Till Blanket:** *till; conforms to and locally obscures underlying topography; thickness 2 to 20 m*

Tv

**Till Veneer:** *till; discontinuous cover with numerous areas of exposed bedrock and locally, colluvial veneer; takes form of underlying surface; thickness 1 to 2 m*

*BEDROCK*

R

*Pre-Quaternary*
*Triassic-Jurassic volcanic and sedimentary bedrock of island arc origin, slightly metamorphosed, and Cretaceous igneous intrusions; includes minor colluvial and till veneer, but > 75% of unit is bedrock*

## SYMBOLS

*Unit Boundary (defined, approximate, assumed)*

*Avalanche track*

*Debris flow track*

*Terrace scarp*

*Cirque*

*Meltwater channel (small, large)*

*Drumlin (long drumlins shown by two or more symbols)*

*Moraine*

*Linear bedrock ridge*

*Roche moutonnée*

*Striation (ice flow direction known; unknown; older = 1, younger = 2, no numbers = age relationship unknown)*

1 2

*Stratigraphic section*

96805-10

*Radiocarbon date*

*Glaciers*

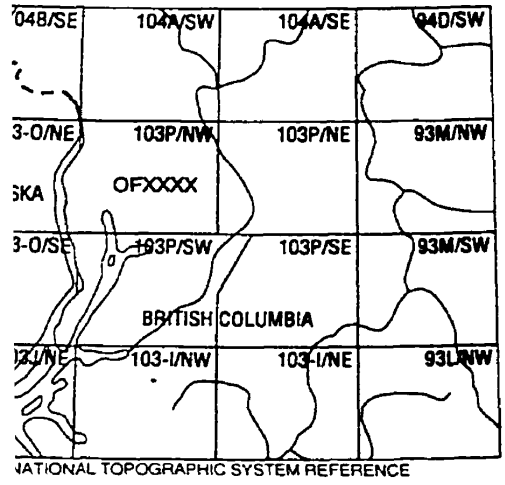


**OPEN FILE**
**DOSSIER PUBLIC**
**XXX1**

GEOLOGICAL SURVEY OF CANADA
COMMISSION GÉOLOGIQUE DU CANADA
OTTAWA

05/2000

Recommended citation:
Section diagrams accompanies this map, Open File XXX3
**McCuaig, S.**
2000: Surficial geology, Kitsault Valley, British Columbia; Geological

# NOTE TO USERS

**Oversize maps and charts are microfilmed in sections in the following manner:**

## LEFT TO RIGHT, TOP TO BOTTOM, WITH SMALL OVERLAPS

**This reproduction is the best copy available.**

**UMI**

Natural Resources Canada | Ressources naturelles Canada

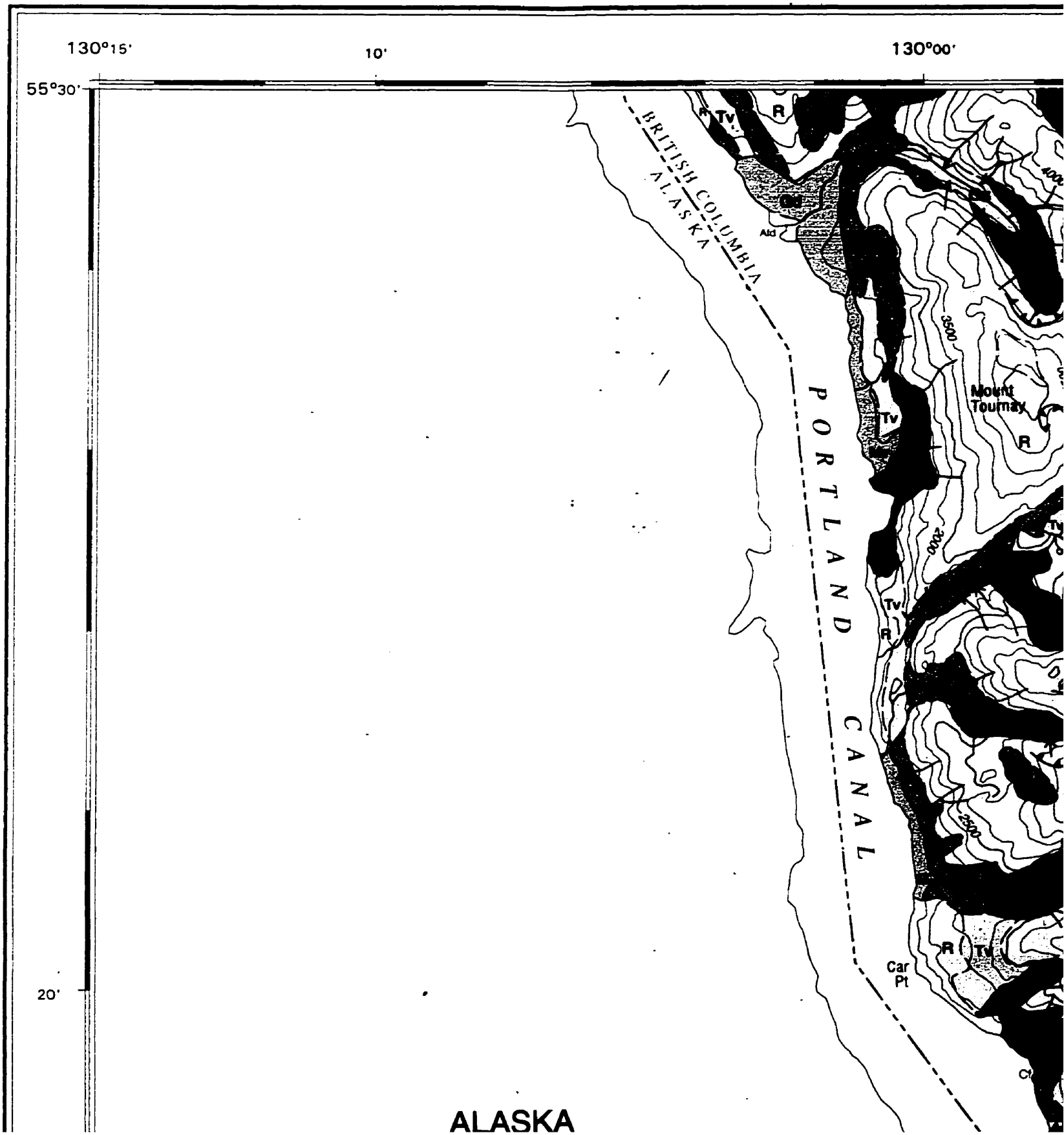


ALASKA

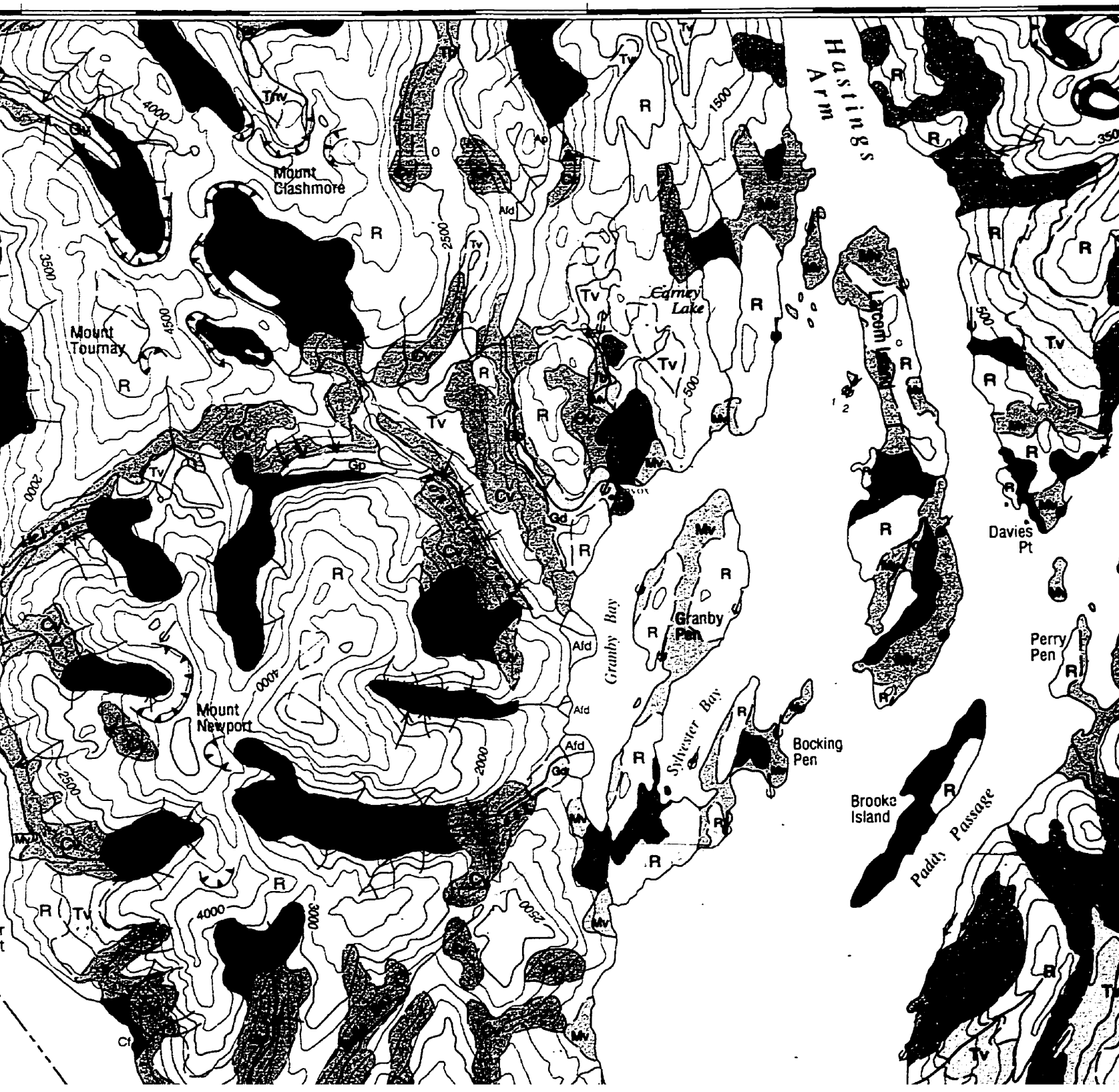
30°00'
50'
Hastings Arm
Mount Clashmore
Mount Tournay
Carney Lake
Larcom Island
Davies Pt
Granby Bay
Granby Pen
Perry Pen
Mount Newport
Sylvester Bay
Bocking Pen
Brooke Island
Paddy Passage
4000
3500
4500
2500
2000
1500
500
3000
R
Tv
Tnv
Cv
Gp
Gd
Afd
Mv
Cf

GEOLOGICAL SURVEY OF CANADA

COMMISSION GÉOLOGIQUE DU CANADA

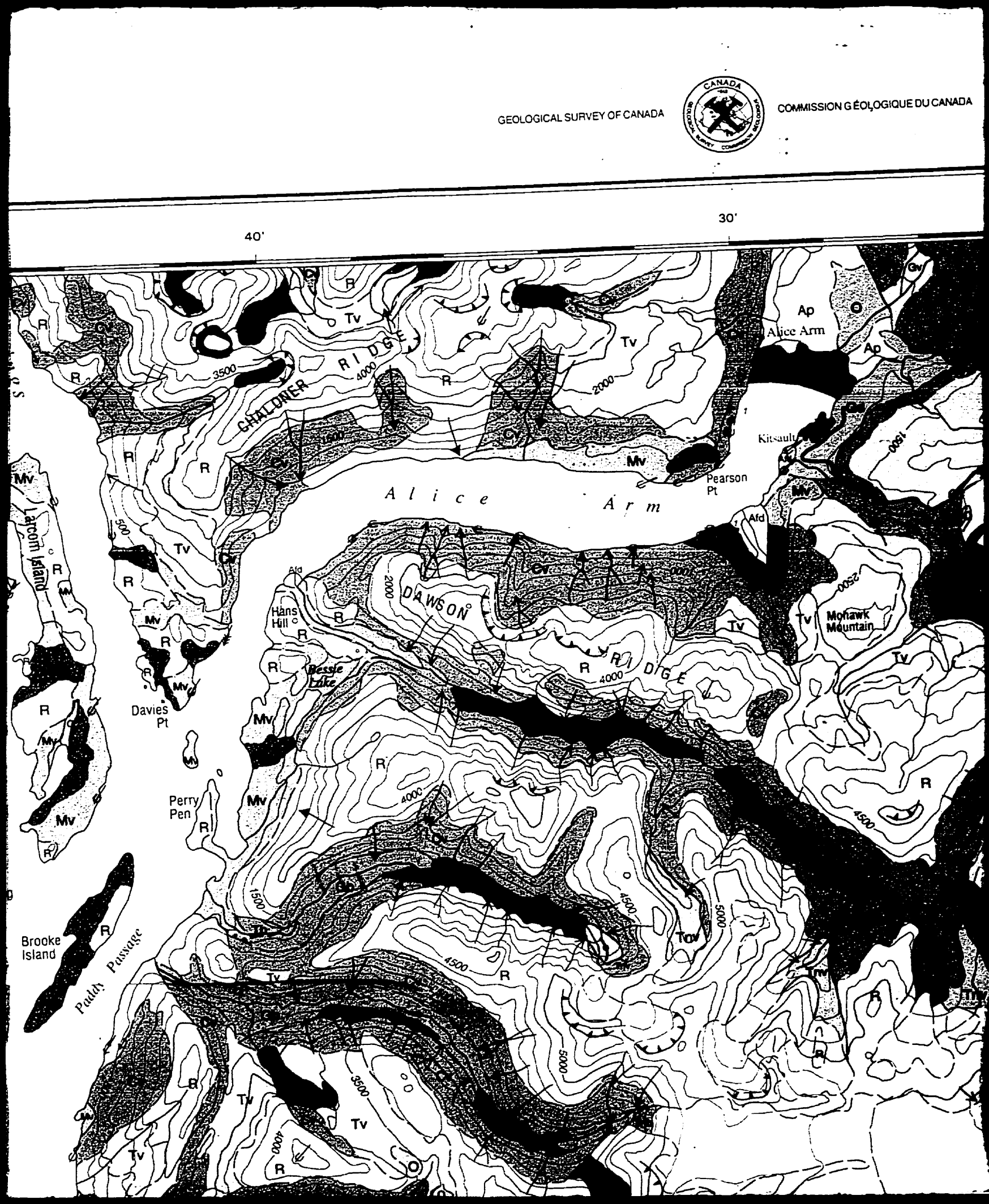

COMMISSION GÉOLOGIQUE DU CANADA

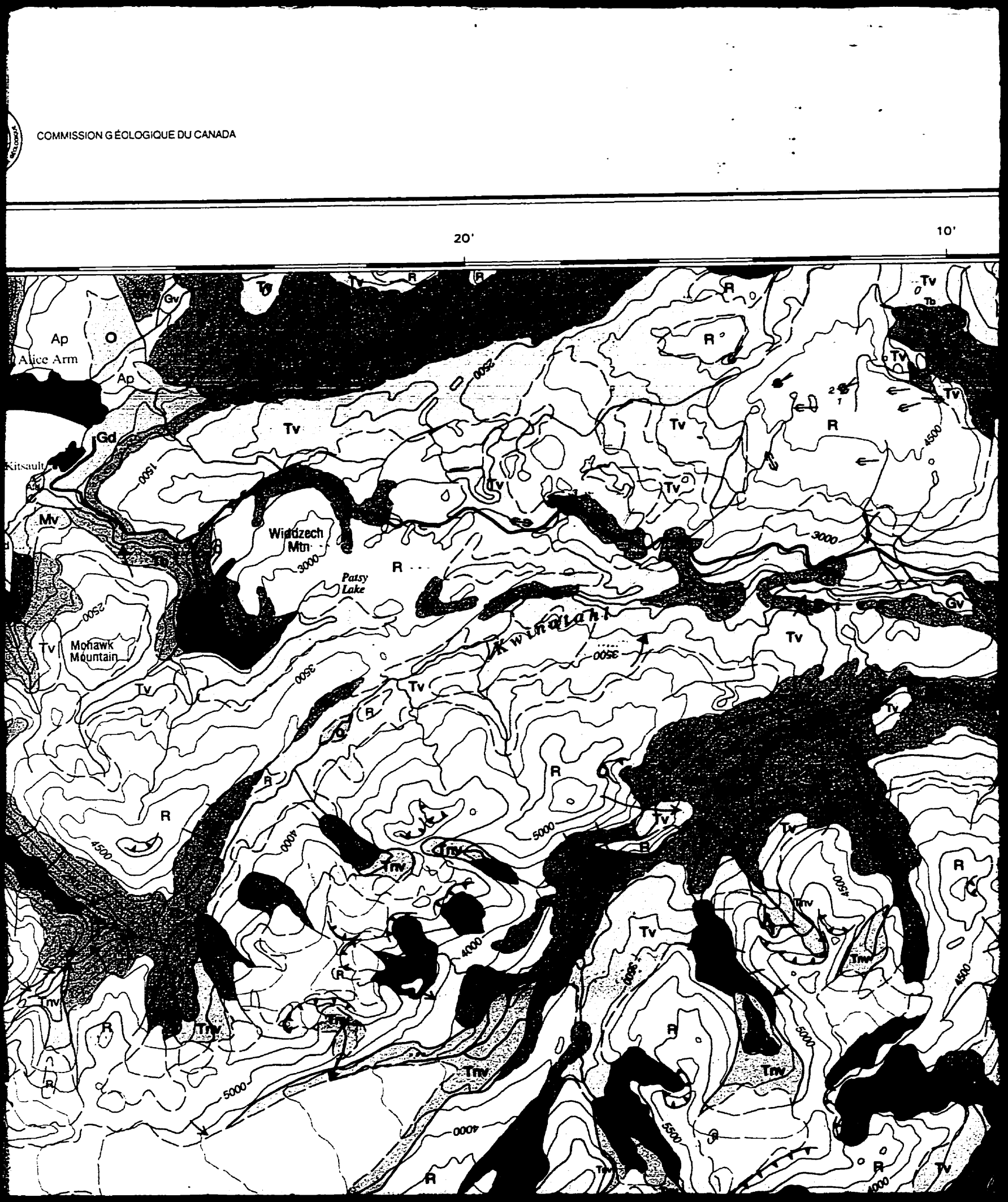

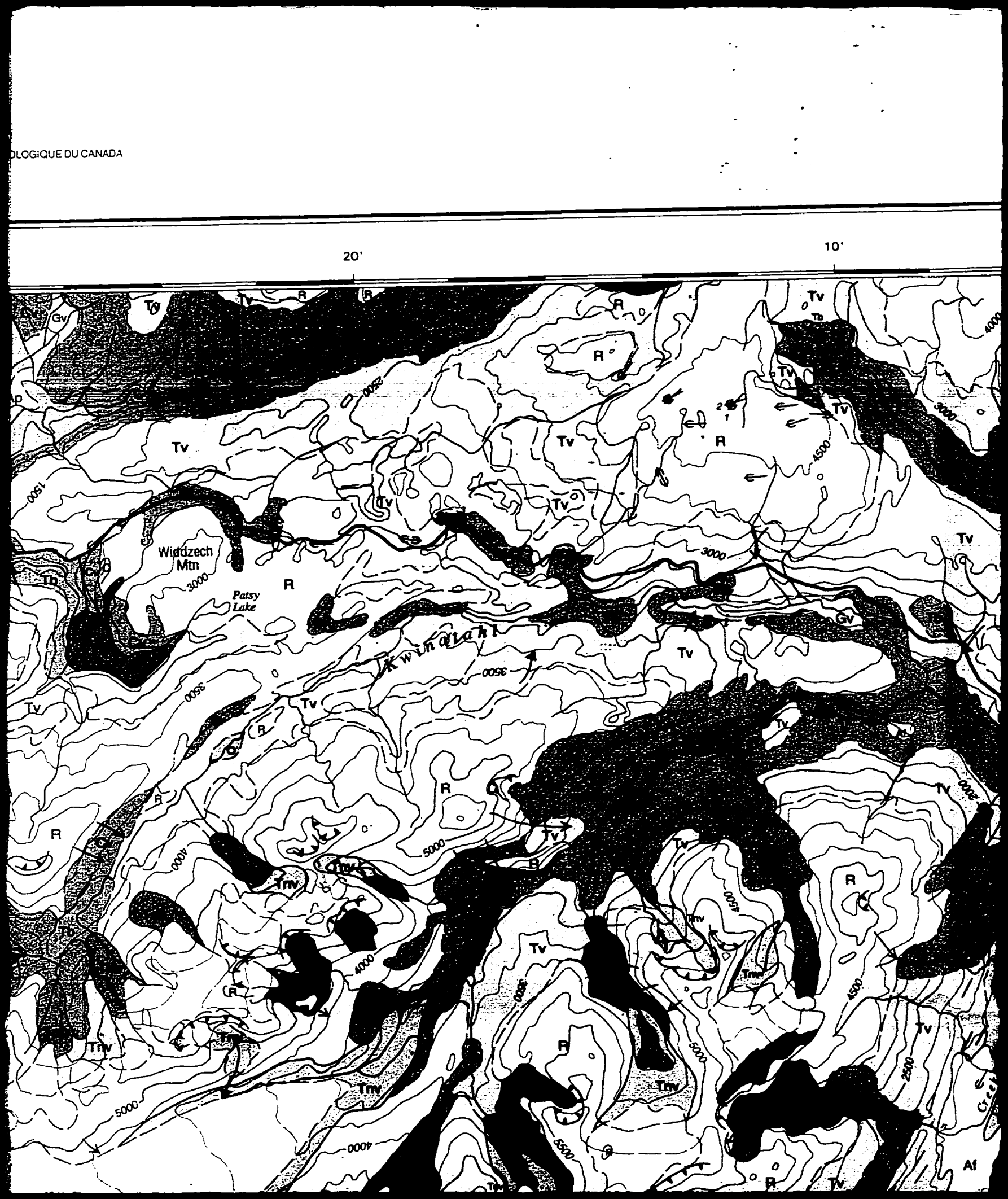

OLOGIQUE DU CANADA
20'
10'
Widdzech Mtn
Patsy Lake
Kwinatahl
Tv
R
Gv
Tb
Tnv
Af
3000
3500
4000
4500
5000
5500
2500
1500

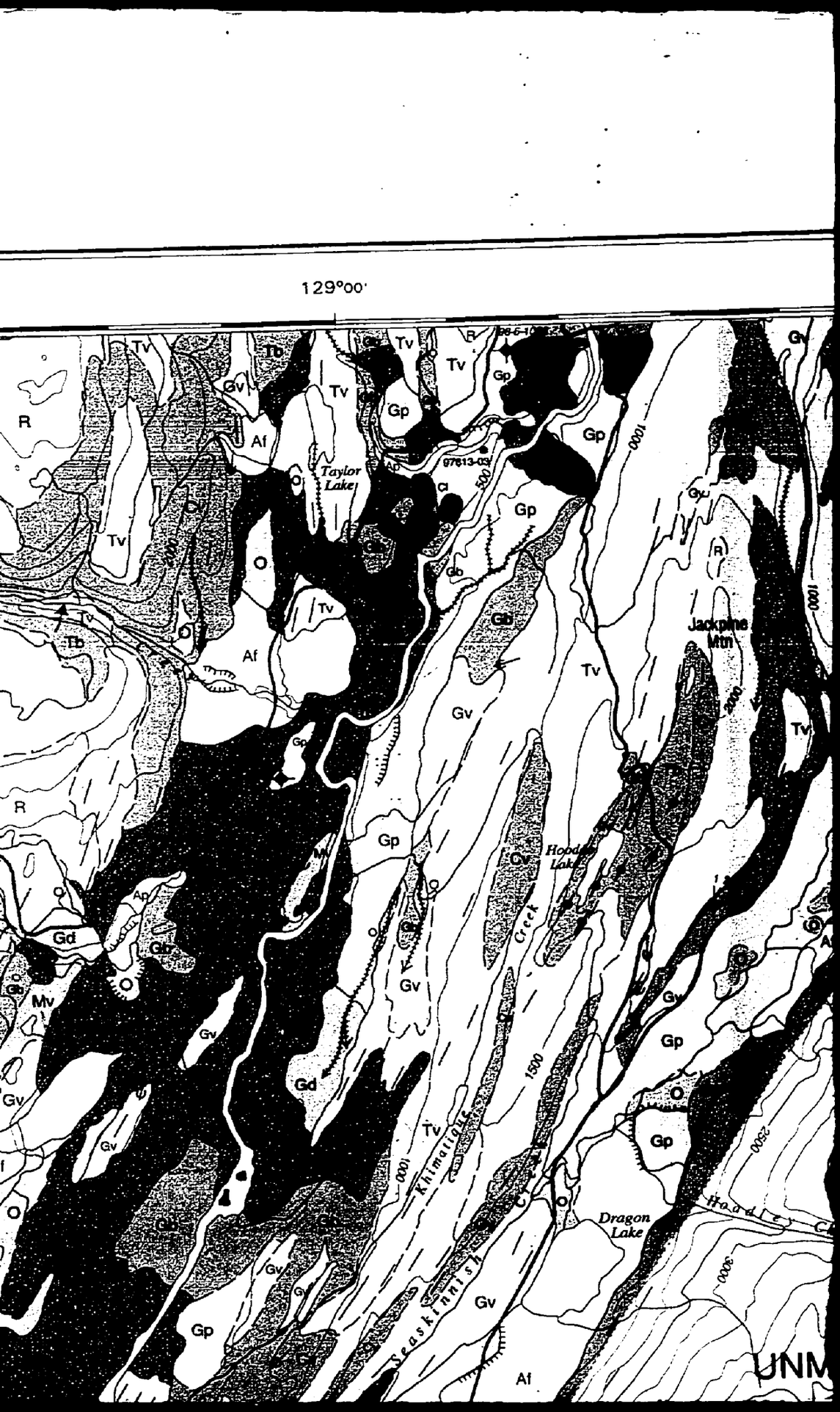
129°00'
Taylor Lake
Jackpine Mtn
Hoodley Lake
Dragon Lake
Khimatique Creek
Seaskinnish
Hoadley Cr
UNM

## LEGEND

*POST-FRASER GLACIATION*

*Artificial Deposits:*

***Made Land:*** *artificial fill and mine waste*

*Organic Deposits:*

***Organic deposits:*** *peat and organic-rich silt; water s the accumulation of plant material in bogs, fens, and*

*Colluvial Deposits: bouldery gravel with clay to sand s sorted, massive; dominated by subangular to angular dependent on source sediments; forms by gravitation flow, rockfall, earthflow and snow avalanche*

***Colluvial Blanket:*** *diamicton; generally found on va*

***Colluvial Apron:*** *bouldery diamicton; forms a talus slope; little or no vegetation where active; thickness slope*

***Colluvial Fan:*** *bouldery diamicton with a sandy mat bodies at foot of steep bedrock slopes; deposited by thickness up to 10 m near fan midpoint*

***Landslide Sediments:*** *bouldery diamicton; mainly earthflow symbol; forms hummocky terrain; little or n 3-20 m*

***Colluvial Veneer:*** *diamicton; takes form of underly with numerous areas of exposed bedrock; thickness*

***Undivided Colluvial Sediments:*** *mixture of colluv veneer, which cannot be subdivided at this map sca*

*Marine Deposits:*

***Marine Tidal Flat:*** *silt and clay, forming tidal flat in rivers; thickness 2 to 10 m*

*Alluvial Deposits: gravel and sand, with minor silt; n generally subrounded to well rounded; deposited by as overbank deposits*

Ap — ***Alluvial Plain:*** *gravel and sand; massive to stratifi overlain by peat and organic-rich silt deposited in a floodplain surface; forms flat plains occupied by sin includes deltas at mouths of major rivers; thickness settings*

Af — ***Alluvial Fan:*** *diamicton, gravel and sand; matrix : stratified, poorly sorted; interbedded with moderat bedded fluvial gravel and sand; forms fan shaped valleys; deposited by debris flows and streams; thi*

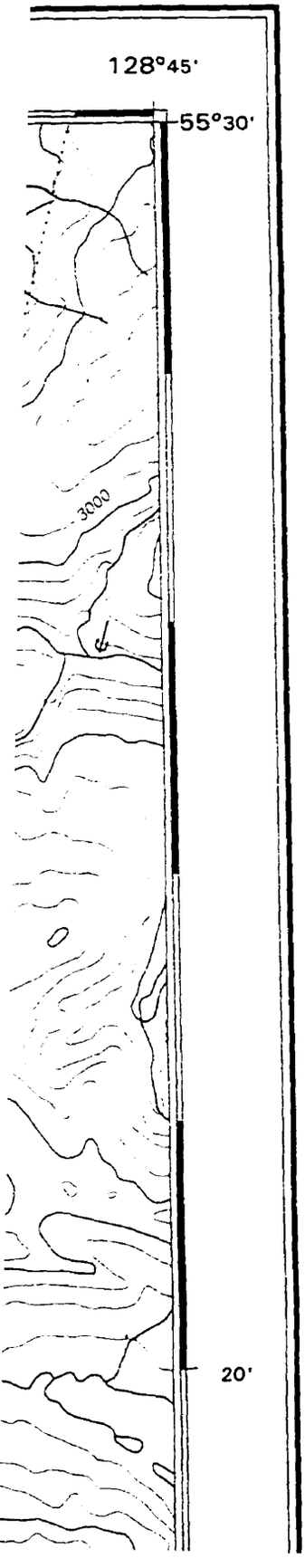


# LEGEND

*POST-FRASER GLACIATION*

*Artificial Deposits:*

***Made Land:*** *artificial fill and mine waste*

*Organic Deposits:*

***Organic deposits:*** *peat and organic-rich silt; water saturated; formed predominantly by the accumulation of plant material in bogs, fens, and swamps; thickness > 2 m*

*Colluvial Deposits: bouldery gravel with clay to sand size matrix; loose, very poorly sorted, massive; dominated by subangular to angular clasts of local bedrock; texture dependent on source sediments; forms by gravitational processes such as debris flow, rockfall, earthflow and snow avalanche*

***Colluvial Blanket:*** *diamicton; generally found on valley floors; thickness > 2 m*

***Colluvial Apron:*** *bouldery diamicton; forms a talus apron or sheet at foot of steep slope; little or no vegetation where active; thickness > 2 m, thickening toward base of slope*

***Colluvial Fan:*** *bouldery diamicton with a sandy matrix; forms steep fan or cone shaped bodies at foot of steep bedrock slopes; deposited by debris flow and rock avalanche; thickness up to 10 m near fan midpoint*

***Landslide Sediments:*** *bouldery diamicton; mainly silty clay if accompanied by earthflow symbol; forms hummocky terrain; little or no vegetation if recent; thickness 3-20 m*

***Colluvial Veneer:*** *diamicton; takes form of underlying surface; discontinuous cover with numerous areas of exposed bedrock; thickness 1 to 2 m*

***Undivided Colluvial Sediments:*** *mixture of colluvial blanket, apron, fan, landslide and veneer, which cannot be subdivided at this map scale; thickness > 2 m*

*Marine Deposits:*

***Marine Tidal Flat:*** *silt and clay, forming tidal flat in brackish water at mouths of major rivers; thickness 2 to 10 m*

*Alluvial Deposits: gravel and sand, with minor silt; moderately to well sorted; clasts generally subrounded to well rounded; deposited by rivers either within channels or as overbank deposits*

Ap — ***Alluvial Plain:*** *gravel and sand; massive to stratified; moderately to well sorted; locally overlain by peat and organic-rich silt deposited in abandoned channels and on floodplain surface; forms flat plains occupied by single or multiple channel rivers; includes deltas at mouths of major rivers; thickness 2 to 10 m, > 10 m in deltaic settings*

Af — ***Alluvial Fan:*** *diamicton, gravel and sand; matrix supported, massive to weakly stratified, poorly sorted; interbedded with moderately to well sorted, clast supported, bedded fluvial gravel and sand; forms fan shaped bodies where rivers enter larger valleys; deposited by debris flows and streams; thickness up to 10 m at fan midpoint*

# ALASKA

# UNITED STATES OF AMERICA

(Base map unavailable)

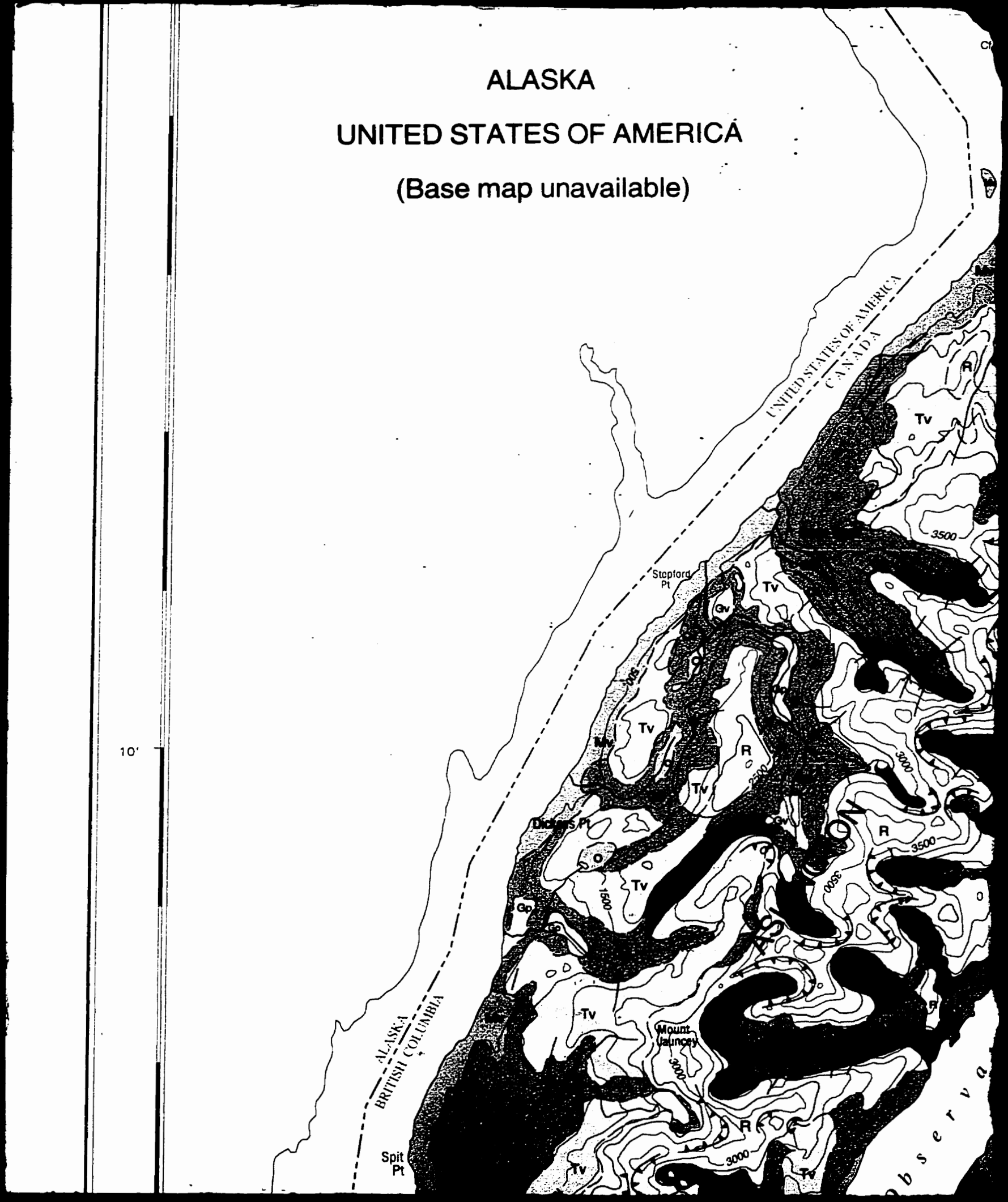

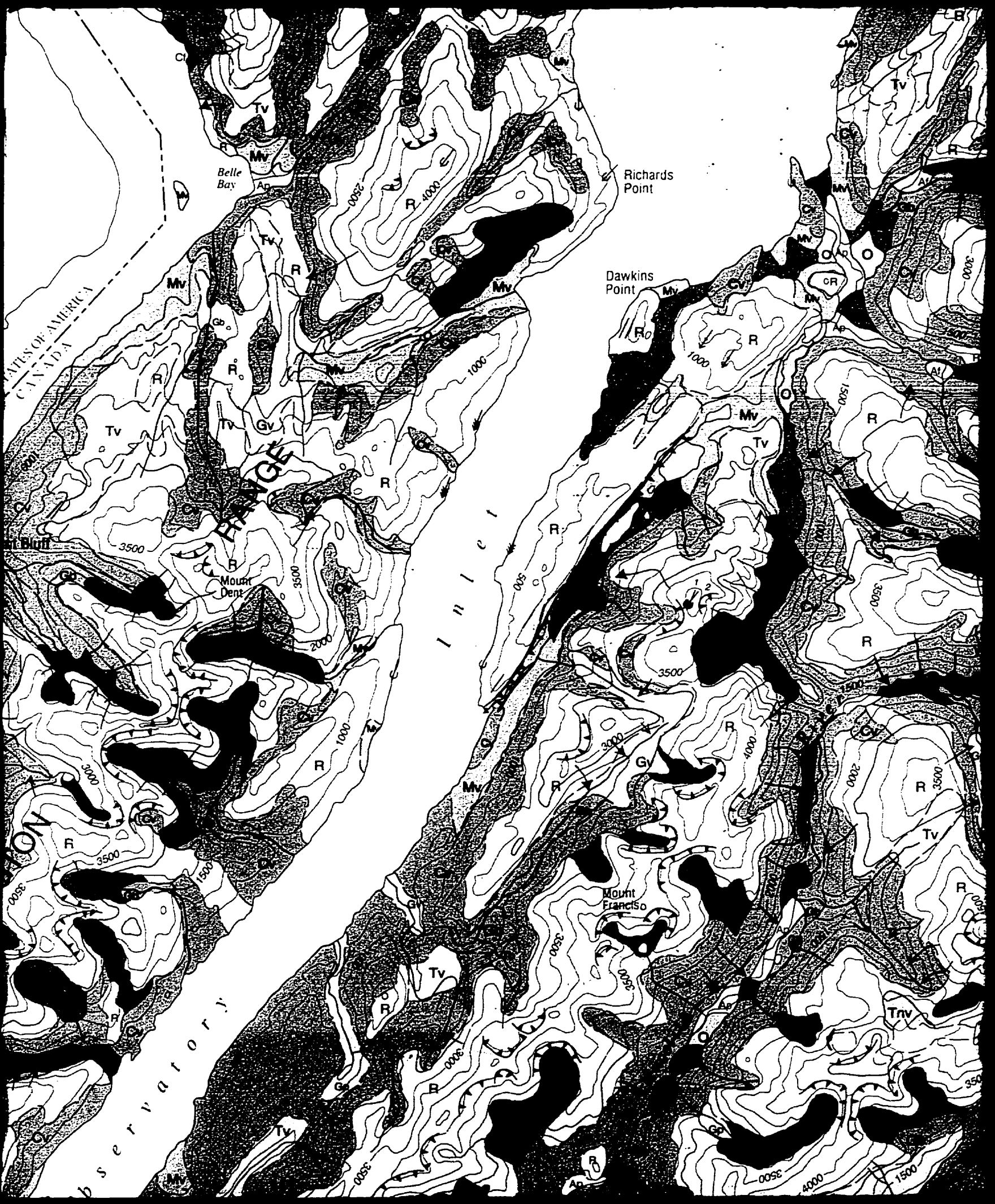

Belle Bay
Richards Point
Dawkins Point
Mount Dent
Mount Francis
Inlet
RANGE
CANADA

Richards Point
Dawkins Point
Mount Huntingdon
Mount Francis
Tv
Cv
Mv
R
O
Gb
Gp
Tnv
Af
Ap
1000
1500
2000
2500
3000
3500
4000
4500
5000

Mountain Peak
Creek
Gulch
Gb
Gp
Gv
Qa
Qc
Qt
Af
Ap
Mv
Tlv
Tv
R
O
5000
4500
4000
3500
2500
2000
1000

Tnv
Tv
Af
Gp
Gv
Gd
Tb
Cv
Mv
Ap
O
R
NASS
KITIMAT
Zolzap
Creek
Vetter Peak 6000

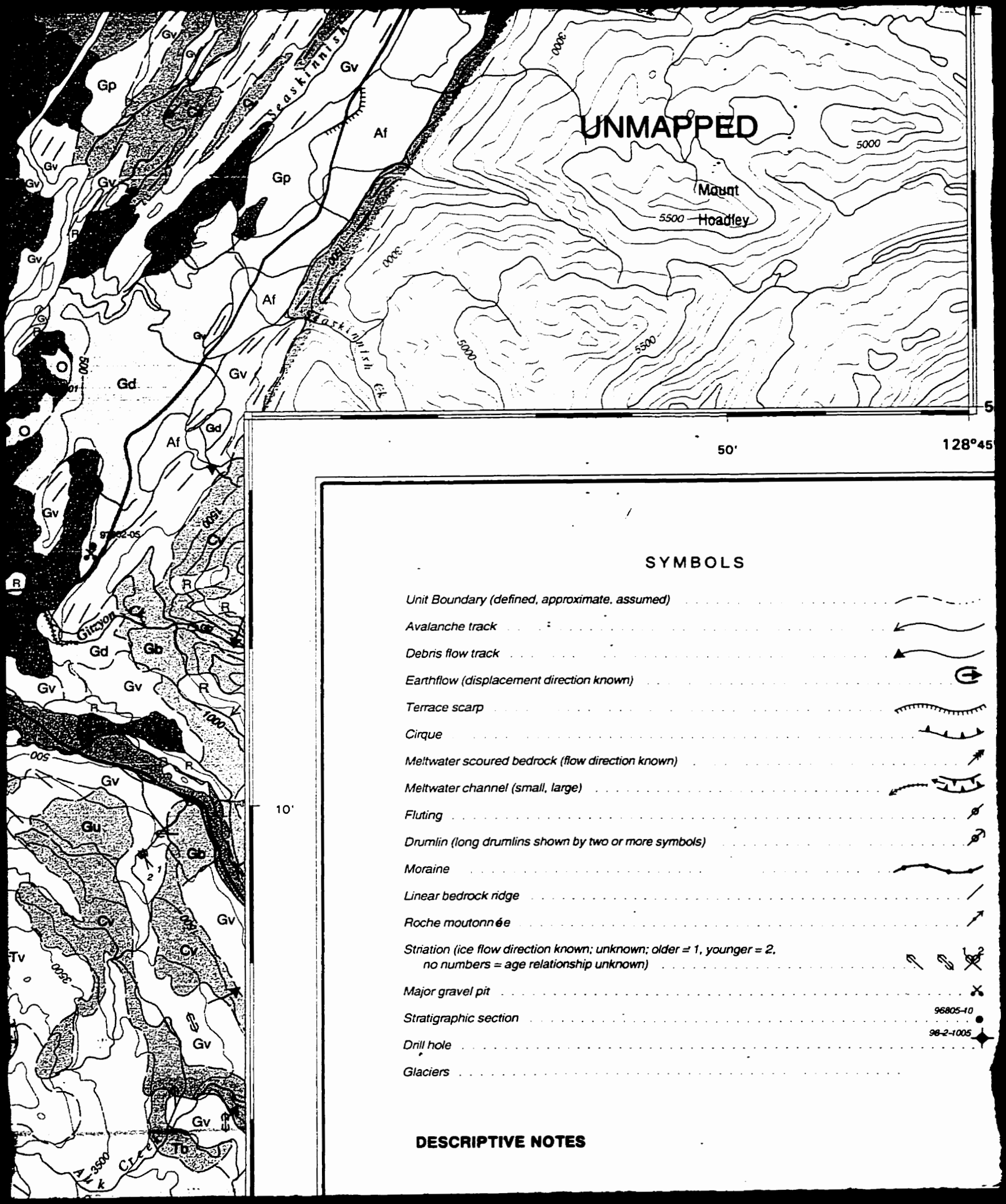


## SYMBOLS

- *Unit Boundary (defined, approximate, assumed)*
- *Avalanche track*
- *Debris flow track*
- *Earthflow (displacement direction known)*
- *Terrace scarp*
- *Cirque*
- *Meltwater scoured bedrock (flow direction known)*
- *Meltwater channel (small, large)*
- *Fluting*
- *Drumlin (long drumlins shown by two or more symbols)*
- *Moraine*
- *Linear bedrock ridge*
- *Roche moutonnée*
- *Striation (ice flow direction known; unknown; older = 1, younger = 2, no numbers = age relationship unknown)*
- *Major gravel pit*
- *Stratigraphic section* — 96805-10
- *Drill hole* — 98-2-1005
- *Glaciers*

## DESCRIPTIVE NOTES

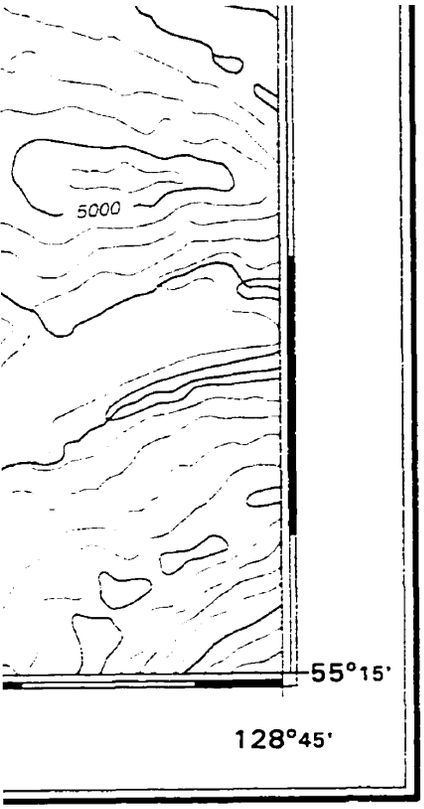


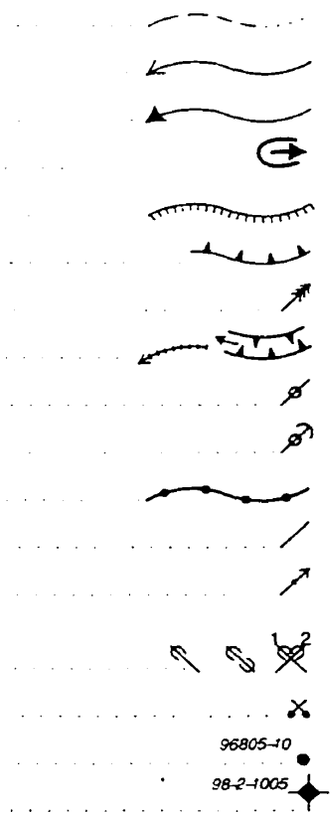


*includes deltas at mouths of major rivers; thickness 2 to 10 m, > 10 m in deltaic settings*

Af — ***Alluvial Fan:*** *diamicton, gravel and sand; matrix supported, massive to weakly stratified, poorly sorted; interbedded with moderately to well sorted, clast supported, bedded fluvial gravel and sand; forms fan shaped bodies where rivers enter larger valleys; deposited by debris flows and streams; thickness up to 10 m at fan midpoint*

Afd — ***Fan Delta:*** *diamicton, gravel and sand; massive to stratified; subaerial facies same as alluvial fans, subaqueous facies consisting of interbedded silt, clay, sand and gravel; beach facies predominantly pebble-cobble gravel with boulder concentration at high tide line; forms where alluvial fans meet marine water; thickness 3 to 15 m*

*GLACIAL DEPOSITS*

*Neoglacial Deposits: diamicton (till); grey, massive, matrix supported; subangular to angular, striated granule to boulder sized clasts set in silty sand or sand matrix; loose to slightly compact, commonly unweathered; formed by melt-out from ice and found surrounding modern alpine glaciers and ice fields; deposited during Holocene glaciation*

***Neoglacial Till Blanket:*** *till; locally forming flights of recessional moraines; thickness 2 to 40 m*

Tnv — ***Neoglacial Till Veneer:*** *till; discontinuous cover with numerous areas of exposed bedrock; takes form of underlying surface; thickness 1 to 2 m*

*FRASER GLACIATION (Wisconsinan)*

*PROGLACIAL DEPOSITS*

*Glaciolacustrine Deposits: laminated silt, clay and minor sand deposited in lakes ponded by glacial ice; well sorted; dropstones common, macrofossils absent*

***Glaciolacustrine Blanket:*** *silt, clay, minor sand; irregular or conforms to underlying surface; thickness > 2 m*

*Glaciomarine Deposits: massive blue-grey or grey silty clay with minor silt, sand and granule gravel; rarely weakly laminated; locally containing dropstones; found in coastal areas below marine limit; coarser proximal deposits are horizontally bedded and well sorted; distal deposits are dominated by massive silty clay that is weathered to pale brown at the surface and may contain salt crusts; marine macrofossils are absent*

***Glaciomarine Blanket:*** *massive silty clay with minor sand, silt and granule gravel; irregular surface; thickness > 2 m*

Mv — ***Glaciomarine Veneer:*** *massive silty clay with minor sand, silt and granule gravel; discontinuous cover with numerous areas of exposed bedrock; takes form of underlying surface; thickness 1 to 2 m*

*Glaciofluvial Deposits: gravel, sand, minor silt and clay; poorly to well sorted; deposited by meltwater flowing away from or in contact with glacial ice; including deltas graded to former sea levels; rarely faulted; clasts commonly rounded and of more local provenance than underlying till*

Gp — ***Glaciofluvial Plain:*** *gravel and sand; massive to weakly horizontally bedded; forms flat surfaces; consists of former outwash plains; bogs common on plain surface; thickness 2 to 50 m*

Gd — ***Glaciofluvial Delta:*** *gravel, sand and silt; poorly to moderately sorted, angular to well rounded clasts; forming flat surfaces; deposited as proglacial marine deltas, often forming terminal regions of glaciofluvial braidplains; thickness up to 230 m*

***Glaciofluvial Blanket:*** *gravel and sand; massive to weakly horizontally bedded; forms irregular surface; thickness 2 to 20 m*

Gv — ***Glaciofluvial Veneer:*** *gravel and sand, massive to vaguely horizontally bedded; discontinuous cover with large areas of exposed bedrock and locally, colluvial veneer; takes form of underlying surface; thickness 1 to 2 m*

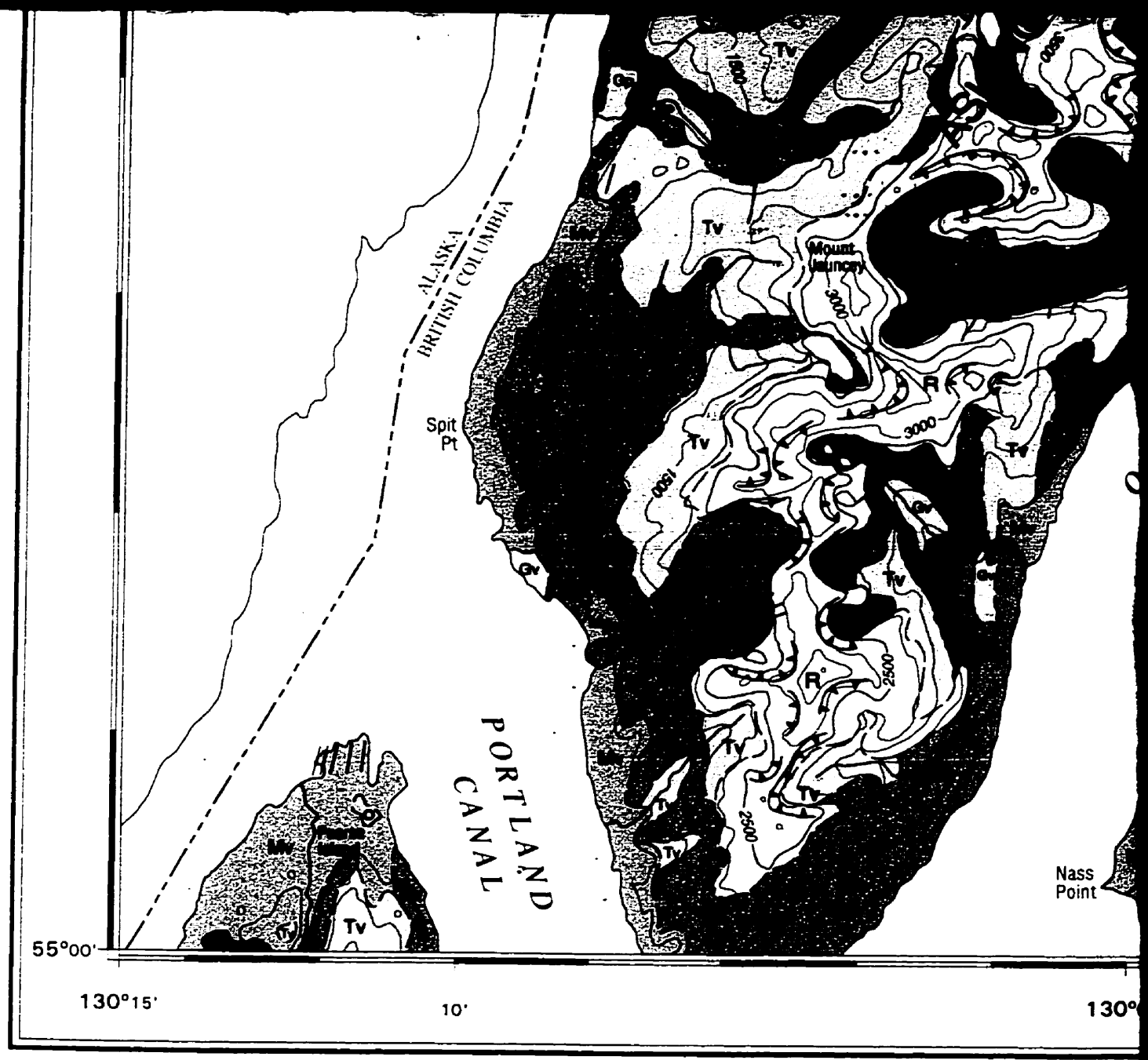


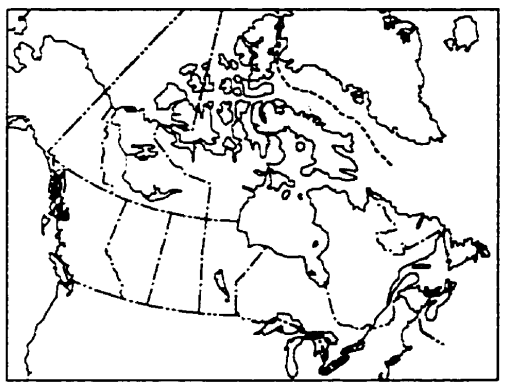

LOCATION MAP

Canada

130°00'

50'

*Geology by S. McCuaig, Geological Survey of Canada and Simon Fraser University, 1999*

*Digital cartography by S. McCuaig and K. Shimamura, Geological Survey of Canada*

*Any revisions or additional geological information known to the user would be welcomed by the Geological Survey of Canada*

40'

30'

OPEN FILE XXX2

SURFICIAL GEOLOGY

# NASS VALLEY

## BRITISH COLUMBIA

Scale 1:100 000 – Échelle 1/100 000

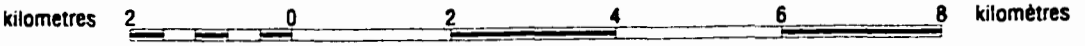


Universal Transverse Mercator Projection
North American Datum 1983
©Her Majesty the Queen in Right of Canada, 2000

Projection transverse universelle de Mercator
Système de référence géodésique nord-américain, 1983
©Sa Majesté la Reine du chef du Canada, 2000

UNDER FINAL REVIEW –TO BE RELEASED AS AN

30'

20'

)PEN FILE XXX2

FICIAL GEOLOGY

# S VALLEY

ISH COLUMBIA

)0 000 – Échelle 1/100 000

2 4 6 8 kilomètres

Projection transverse universelle de Mercator
Système de référence géodésique nord-américain, 1983
!000 ©Sa Majestéla Reine du chef du Canada, 2000

# BE RELEASED AS AN OPEN FILE

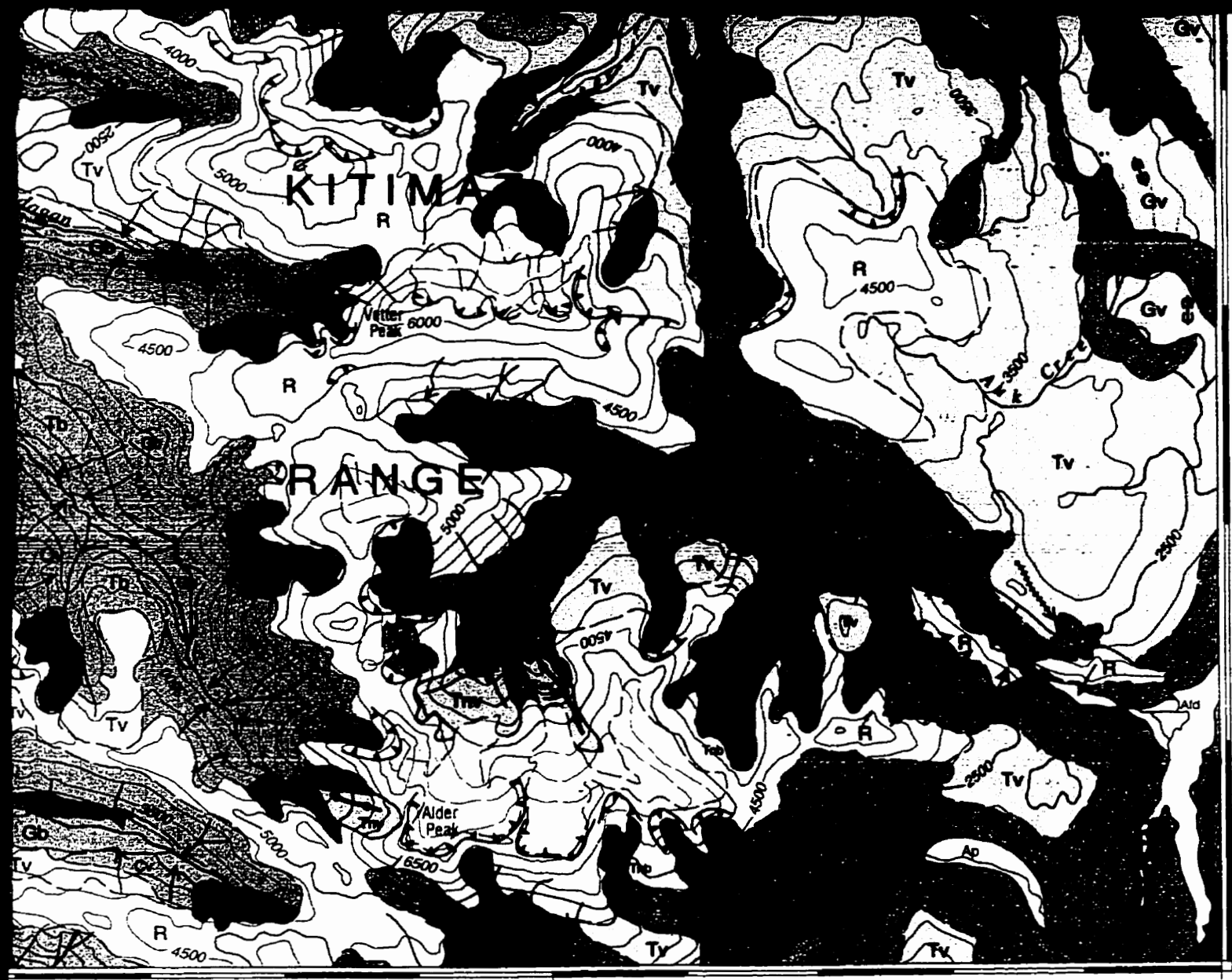


*Digital base map from data compiled by Geomatics Canada, modified by the Terrain Sciences Division*

*Mean magnetic declination (2000), 23 ° 48' E, decreasing 9.1' annually. Readings vary from 23 ° 41' E in the SW corner to 23° 54' E in the NE corner of the map*

*CONTOUR INTERVAL 500 FEET*

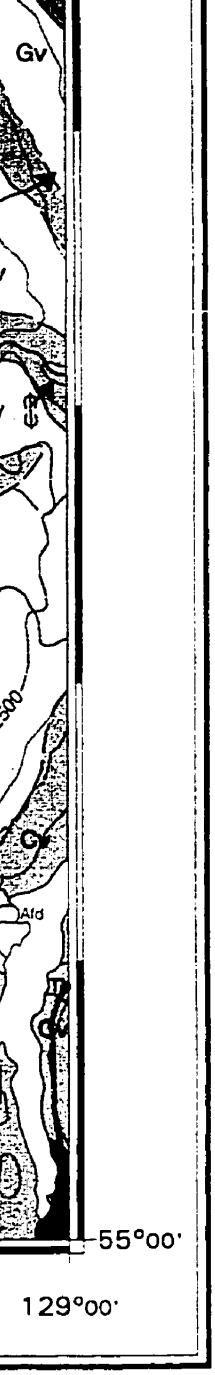


*Linear bedrock ridge* . . . . . ↗

*Roche moutonnée* . . . . . ↗

*Striation (ice flow direction known; unknown; older = 1, younger = 2, no numbers = age relationship unknown)* . . . . . ↖ ↘ 1 2

*Major gravel pit* . . . . . ✕

*Stratigraphic section* . . . . . 96805-10 ●

*Drill hole* . . . . . 98-2-1005 ✦

*Glaciers* . . . . . ▭

## DESCRIPTIVE NOTES

### GLACIAL HISTORY OF THE NASS RIVER REGION (Maps 103P/NW and 103P/SW)

Surficial geology mapping, shallow seismic reflection, ground penetrating radar and drilling were used to determine the stratigraphy of the Nass Valley and the glacial history of the Nass River region.

At the height of the last glaciation, ice flowed southwest over the entire region. It deposited a compact till called 'Kwinatahl Till'. This till is dominated by Bowser Lake Group metasedimentary rocks which outcrop in the eastern part of the map area. Kwinatahl Till deposits can be more than 50 m thick.

As ice thinned during deglaciation, it became confined to valleys and fiords. 'Kinskuch Till', a till containing rounded clasts and volcanic material, formed in the northeastern part of the study area at this time (map 103P/NW). Kinskuch Till overlies Kwinatahl Till and occurs in an area of drumlinized terrain.

Sea level rise at the start of deglaciation caused calving and rapid retreat of glaciers in fiord areas. The maximum marine limit was 230 m above present sea level. This sea level is thought to have been achieved around 10 200 years BP, and was followed by rapid deglaciation and rapid sea level fall.

Interbedded gravel, sand and silt were deposited subaqueously at this time in ice-proximal glaciomarine environments. These deposits grade distally to massive silty clay. Apparently, there were no stillstands; proximal to distal depositional environments migrated as the ice margins retreated. Distal silty clay deposits in the Nass Valley can be up to 25 m thick.

Eventually, ice became grounded as valley glaciers retreated and sea level dropped. Extensive meltwater braidplains formed in front of the glaciers, terminating in marine water and forming large deltas. These deltas and braidplains record sea levels of 185, 150 and 135 m, of which the 150 m highstand was the longest lived.

In the upper Nass Valley, one such braidplain formed during the 185 m highstand. This was succeeded by an extensive braidplain that formed northeast of the town of New Aiyansh when sea level had dropped to 150 m. The meltwater river then moved back to its original location (further west) when sea level was at 135 m, forming a small braidplain southwest of the 185 m braidplain. Sea level then fell to is current level. The meltwater river evolved into the modern Nass River and assumed its current course, which incises the 185 m and 135 m braidplains.

The most complete Quaternary stratigraphic sequence is found in the Nass Valley. Less complete sequences occur elsewhere in the study area. From oldest to youngest, the region's stratigraphy comprises bedrock, till, glaciomarine proximal deposits, glaciomarine distal deposits and glaciofluvial braidplain/braid delta deposits. Holocene peat bogs, colluvium and alluvium overlie all of these units.

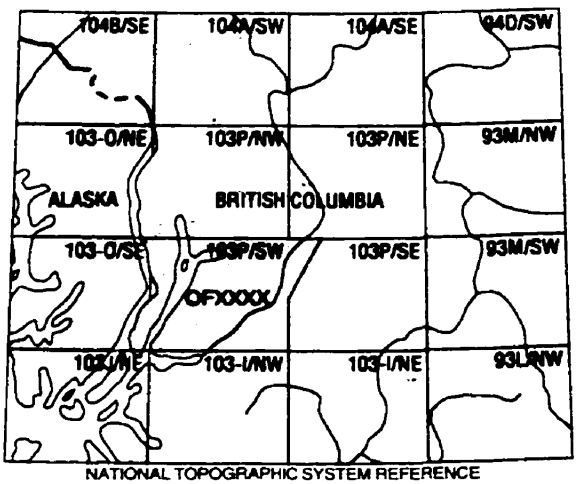


NATIONAL TOPOGRAPHIC SYSTEM REFERENCE

more local provenance than underlying till

Gp — **Glaciofluvial Plain:** gravel and sand, massive to weakly horizontally bedded, forms flat surfaces, consists of former outwash plains, bogs common on plain surface, thickness 2 to 50 m

Gd — **Glaciofluvial Delta:** gravel, sand and silt, poorly to moderately sorted, angular to well rounded clasts, forming flat surfaces, deposited as proglacial marine deltas, often forming terminal regions of glaciofluvial braidplains, thickness up to 230 m

**Glaciofluvial Blanket:** gravel and sand, massive to weakly horizontally bedded, forms irregular surface, thickness 2 to 20 m

Gv — **Glaciofluvial Veneer:** gravel and sand, massive to vaguely horizontally bedded, discontinuous cover with large areas of exposed bedrock and locally colluvial veneer, takes form of underlying surface, thickness 1 to 2 m

**Undivided Glaciofluvial Sediments:** glaciofluvial gravel and sand, with till and glaciolacustrine clay, undifferentiated at this scale of mapping, forms irregular or rolling terrain, thickness 2 to 20 m

GLACIAL DEPOSITS

Glacial Deposits: diamicton (till), granule to boulder size clasts in a silt to silty clay matrix, massive, very compact, very poorly sorted, with angular to subrounded striated clasts, commonly blue-grey or grey, dominant clast lithologies are Bowser Lake Group sandstone, siltstone and mudstone, deposited directly by glacial ice or by gravity flow from glacial ice

Td — **Till Blanket:** till, conforms to and locally obscures underlying topography, thickness 2 to 20 m

Tv — **Till Veneer:** till, discontinuous cover with numerous areas of exposed bedrock and locally colluvial veneer, takes form of underlying surface, thickness 1 to 2 m

BEDROCK

Holocene

Basaltic flows, forming ridged and blocky valley fill, little vegetation due to recent activity, thickness 3-15 m

R — Pre Quaternary
Triassic-Jurassic volcanic and sedimentary bedrock of island arc origin, slightly metamorphosed, and Cretaceous igneous intrusions, includes minor colluvial and till veneer, but > 75% of unit is bedrock


OPEN FILE
DOSSIER PUBLIC
XXX2
GEOLOGICAL SURVEY OF CANADA
COMMISSION GÉOLOGIQUE DU CANADA
OTTAWA
05/2000



Recommended citation:
Section diagrams accompanies this map, Open File XXX3
**McCuaig, S.**
2000: Surficial geology, Nass Valley, British Columbia; Geological Survey of Canada, Open File XXX2, scale 1:100 000.



94D/SW
93M/NW
93M/SW
93L/NW